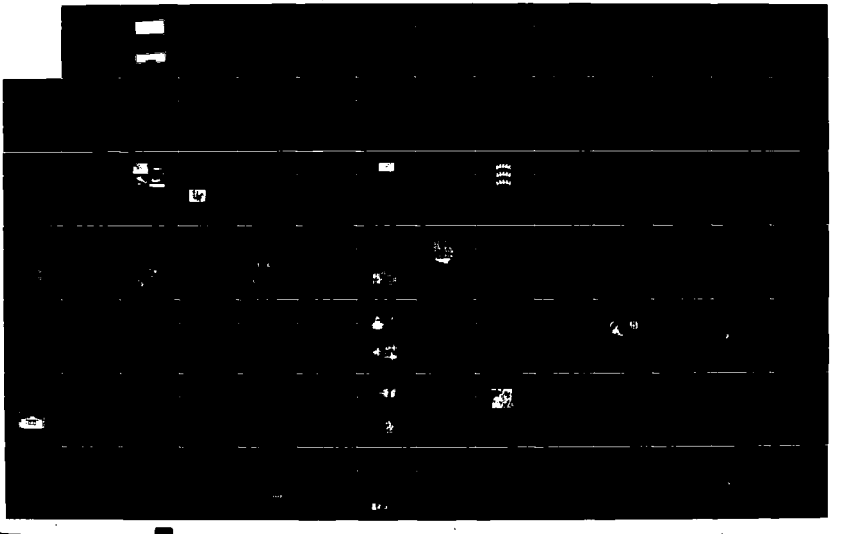
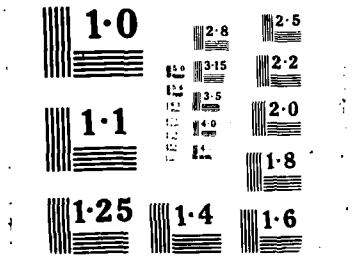
AD-A152 673 GEARS AND POWER TRANSMISSION SYSTEMS FOR HELICOPTERS AND TURBOPROPS: CONF. (U) ADVISORY GROUP FOR AEROSPACE RESEARCH AND DEVELOPMENT NEUILLY.. JAN 85 AGARD-CP-369 1/3

UNCLASSIFIED F/G 21/5 NL




1·0
1·1
1·25
2·8
3·15
3·5
4·0
4·5
2·5
2·2
2·0
1·8
1·4
1·6

AD-A152 673

AD-A152 673
AGARD-CP-369

AGARD

ADVISORY GROUP FOR AEROSPACE RESEARCH & DEVELOPMENT

7 RUE ANCELLE 92200 NEUILLY SUR SEINE FRANCE

AGARD CONFERENCE PROCEEDINGS No.369

Gears and Power Transmission Systems for Helicopters and Turboprops

NORTH ATLANTIC TREATY ORGANIZATION

REPRODUCED BY
NATIONAL TECHNICAL
INFORMATION SERVICE
U.S. DEPARTMENT OF COMMERCE
SPRINGFIELD, VA. 22161

DISTRIBUTION AND AVAILABILITY
ON BACK COVER

DTIC FILE COPY

This document has been approved for public release and sale; its distribution is unlimited.

REPRODUCED BY
NATIONAL TECHNICAL
INFORMATION SERVICE
U.S. DEPARTMENT OF COMMERCE
SPRINGFIELD, VA. 22161

83 04

2

REPORT DOCUMENTATION PAGE

1. Recipient's Reference	2. Originator's Reference	3. Further Reference	4. Security Classification of Document
	AGARD-CP-369	ISBN 92-835-0372-4	UNCLASSIFIED

5. Originator Advisory Group for Aerospace Research and Development
North Atlantic Treaty Organization
7 rue Ancelle, 92200 Neuilly sur Seine, France

6. Title GEARS AND POWER TRANSMISSION SYSTEMS FOR HELICOPTERS AND TURBOPROPS

7. Presented at the Propulsion and Energetics Panel 64th Symposium, held in Lisbon, Portugal, 8–12 October 1984.

8. Author(s)/Editor(s)	9. Date
Various	January 1985
10. Author's/Editor's Address	**11. Pages**
Various	396

12. Distribution Statement This document is distributed in accordance with AGARD policies and regulations, which are outlined on the *Outside Back Covers of all AGARD publications.*

13. Keywords/Descriptors

Gears	Transmission systems
Power transmission systems	Drive trains
Helicopters	Roller bearings
Turboprops	Tribology
Tooth failures	Lubrication

14. Abstract

The Conference Proceedings contain 32 papers presented at the Propulsion and Energetics 64th Symposium on Gears and Power Transmission Systems for Helicopters and Turboprops, which was held 8–12 October 1984 in Lisbon, Portugal.

The Technical Evaluation Report is included at the beginning of the Proceedings. Questions and answers of the discussions follow each paper. The Symposium was arranged in seven sessions: Review of Current Transmission Technology (4); Helicopter and Turboprop Transmission Technology Needs and Design (4); Component Design Technology and Manufacturing Considerations (8); Tribological Aspects of Transmission Components (6); Diagnostics, Measurements, and Noise (5); Problems and Failures in Gearing Application (3); and Qualification Standards and Specifications (2).

The purpose of the Symposium was to exchange and disseminate information on research and development conducted on gears and transmission systems in order to introduce new technologies for improvements in weight, performance, and life-cycle costs. The achievements were listed in the Technical Evaluation Report. The Symposium could not cover the whole area; the gaps left will be discussed in an AGARDograph to be published in 1987.

AGARD-CP-369

NORTH ATLANTIC TREATY ORGANIZATION

ADVISORY GROUP FOR AEROSPACE RESEARCH AND DEVELOPMENT

(ORGANISATION DU TRAITE DE L'ATLANTIQUE NORD)

AGARD Conference Proceedings No.369

GEARS AND POWER TRANSMISSION SYSTEMS FOR HELICOPTERS AND TURBOPROPS

Papers presented at the Propulsion and Energetics Panel 64th Symposium,
held in Lisbon, Portugal, 8—12 October 1984.

THE MISSION OF AGARD

The mission of AGARD is to bring together the leading personalities of the NATO nations in the fields of science and technology relating to aerospace for the following purposes:

- Exchanging of scientific and technical information;
- Continuously stimulating advances in the aerospace sciences relevant to strengthening the common defence posture;
- Improving the co-operation among member nations in aerospace research and development;
- Providing scientific and technical advice and assistance to the North Atlantic Military Committee in the field of aerospace research and development;
- Rendering scientific and technical assistance, as requested, to other NATO bodies and to member nations in connection with research and development problems in the aerospace field;
- Providing assistance to member nations for the purpose of increasing their scientific and technical potential;
- Recommending effective ways for the member nations to use their research and development capabilities for the common benefit of the NATO community.

The highest authority within AGARD is the National Delegates Board consisting of officially appointed senior representatives from each member nation. The mission of AGARD is carried out through the Panels which are composed of experts appointed by the National Delegates, the Consultant and Exchange Programme and the Aerospace Applications Studies Programme. The results of AGARD work are reported to the member nations and the NATO Authorities through the AGARD series of publications of which this is one.

Participation in AGARD activities is by invitation only and is normally limited to citizens of the NATO nations.

The content of this publication has been reproduced directly from material supplied by AGARD or the authors.

Published January 1985

Copyright © AGARD 1985
All Rights Reserved

ISBN 92-835-0372-4

Printed by Specialised Printing Services Limited
40 Chigwell Lane, Loughton, Essex IG10 3TZ

RECENT PUBLICATIONS OF THE PROPULSION AND ENERGETICS PANEL

Conference Proceedings

Testing and Measurement Techniques in Heat Transfer and Combustion
AGARD Conference Proceedings No.281, 55th A Meeting, May 1980

Centrifugal Compressors, Flow Phenomena and Performance
AGARD Conference Proceedings No.282, 55th B Meeting, May 1980

Turbine Engine Testing
AGARD Conference Proceedings No.293, 56th Meeting, September/October 1980

Helicopter Propulsion Systems
AGARD Conference Proceedings No.302, 57th Meeting, May 1981

Ramjets and Ramrockets for Military Applications
AGARD Conference Proceedings No.307, 58th Meeting, October 1981

Problems in Bearings and Lubrication
AGARD Conference Proceedings No.323, 59th Meeting, May/June 1982

Engine Handling
AGARD Conference Proceedings No.324, 60th Meeting, October 1982

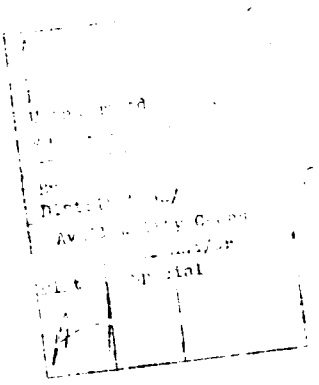
Viscous Effects in Turbomachines
AGARD Conference Proceedings No.351, 61st A Meeting, June 1983

Auxiliary Power Systems
AGARD Conference Proceedings No.352, 61st B Meeting, May 1983

Combustion Problems in Turbine Engines
AGARD Conference Proceedings No.353, 62nd Meeting, October 1983

Hazard Studies for Solid Propellant Rocket Motors
AGARD Conference Proceedings No.367, 63rd A Meeting, May 1984

Engine Cyclic Durability by Analysis and Testing
AGARD Conference Proceedings No.368, 63rd B Meeting, May/June 1984



Working Group Reports

Aircraft Fire Safety
AGARD Advisory Report No.132, Vol.1 and Vol.2. Results of WG 11 (September and November 1979)

Turbulent Transport Phenomena
AGARD Advisory Report No.150 (in English and French). Results of WG 09 (February 1980)

Through Flow Calculations in Axial Turbomachines
AGARD Advisory Report No.175. Results of WG 12 (October 1981)

Alternative Jet Engine Fuels
AGARD Advisory Report No.181 Vol.1 and Vol.2. Results of WG 13 (July 1982)

Suitable Averaging Techniques in Non-Uniform Internal Flows
AGARD Advisory Report No.182 (in English and French). Results of WG 14 (June/August 1983)

Lecture Series Publications

Non-Destructive Inspection Methods for Propulsion Systems and Components
AGARD Lecture Series 103 (April 1979)

The Application of Design to Cost and Life Cycle Cost to Aircraft Engines
AGARD Lecture Series 107 (May 1980)

Microcomputer Applications in Power and Propulsion Systems
AGARD Lecture Series 113 (April 1981)

Aircraft Fire Safety
AGARD Lecture Series 123 (June 1982)

Operation and Performance Measurement of Engines in Sea Level Test Facilities
AGARD Lecture Series 132 (April 1984)

Ramjet and Ramrocket Propulsion Systems for Missiles
AGARD Lecture Series 136 (September 1984)

Other Publications

Airbreathing Engine Test Facility Register
AGARD AGARDograph 269 (July 1981)

THEME

Because of rapidly growing technology demands for potential new and advanced helicopter and turboprop transmissions, a need for broad discussions of power transfer systems has become apparent. New research results have dictated that more attention be given to possibilities for improvement in weight, performance, and life-cycle costs. In 1981, and again in 1982, the Panel addressed only small portions of the wide range of topics necessary to cover these critical areas. With that concern in mind, and in keeping with interests of the host nation (Portugal), the Panel has selected this subject for its 1984 Fall Symposium. Included were sessions on current aircraft transmissions, technology voids and needs, design and manufacturing considerations, performance predictions, tribological aspects, noise and vibration, and specification standards. Interest in these subjects includes topics of concern to all manufacturers of aircraft as well as specialists in the fields of research on mechanical components for transmissions.

• • • •

La demande croissante en matière de technologie permettant de réaliser des transmissions potentielles, nouvelles ou de conception avancée, pour hélicoptères et turbopropulseurs, a mis en évidence la nécessité de procéder à des entretiens de nature générale sur les systèmes de transmission d'énergie. Les résultats de recherches récemment effectuées ont montré qu'un surcroît d'efforts devait être consacré aux possibilités d'amélioration de poids, de performances, et de coûts de cycle de vie. En 1981, et à nouveau en 1982, le Panel n'a traité qu'une petite partie des points extrêmement nombreux qui entrent dans le cadre de ces domaines critiques. C'est en songeant à ce problème et aussi pour répondre à l'intérêt exprimé par le pays hôte, le Portugal, que le Panel a choisi ce sujet comme thème de son Symposium de l'automne 1984. Les diverses séances ont été consacrées aux transmissions actuellement utilisées sur les aéronefs, aux lacunes et aux besoins de la technologie, à des considérations sur la conception et la fabrication, aux prédictions de performances aux aspects tribologiques, au bruit et aux vibrations, et aux normes en matière de cahier des charges. L'intérêt pour ces différents sujets est partagé par tous les constructeurs d'avions ainsi que par les spécialistes de la recherche sur les composants mécaniques des systèmes de transmission.

REPRODUCED AT GOVERNMENT EXPENSE

PROPULSION AND ENERGETICS PANEL

Chairman: Professor Ch.Hirsch
Vrije Universiteit Brussel
Dienst Stromingsmechanica
Pleinlaan 2
1050 Brussel, Belgium

Deputy Chairman: Professor Ir. H.Wittenberg
Delft University of Technology
Dept. of Aerospace Engineering
Kluyverweg 1
2629 HS Delft, Netherlands

PROGRAMME COMMITTEE

Mr J.Acurio (Chairman)
Director, Propulsion Laboratory
US Army Research & Technology Labs (AVSCOM)
Cleveland, Ohio 44135, US

Professor D.Dini
Università degli Studi
Istituto di Macchine
Via Diotisalvi 3
56100 Pisa, Italy

Dr D.K.Hennecke
Fachgebiet Flugantriebe
Technische Hochschule Darmstadt
Petersenstrasse 30
6100 Darmstadt, Germany

Dr W.L.Macmillan
National Defence Headquarters
CRAD/DST (OV)
101 Colonel By Drive
Ottawa, Ontario K1A 0K2,
Canada

Mr N.A.Mitchell
Rolls Royce Ltd
PO Box 3
Filton, Bristol BS12 7QE, UK

Professor M.N.R.Nina
CTAMFUTL
Instituto Superior Tecnico
Avenida Rovisco Pais
Lisboa 1096 Codex, Portugal

M. l'Ing. de l'Armement P.Ramette
Direction des Recherches, Etudes
et Techniques – SDR/G 72
26 Boulevard Victor
75996 Paris Armées, France

HOST NATION COORDINATOR

Professor M.N.R.Nina

PANEL EXECUTIVE

Dr-Ing. E.Riester,
AGARD-NATO
7 rue Ancelle
92200 Neuilly sur Seine
France

ACKNOWLEDGEMENT

The Propulsion and Energetics Panel wishes to express its thanks to the Portuguese National Delegate for the invitation to hold this meeting in Lisbon, Portugal, and for the facilities and personnel which made the meeting possible.

CONTENTS

	Page
RECENT PUBLICATIONS OF PEP	iii
THEME	v
PROPULSION AND ENERGETICS PANEL	vi
TECHNICAL EVALUATION REPORT by B.Sternlicht	xi
	Reference
SESSION I – REVIEW OF CURRENT TRANSMISSION TECHNOLOGY	
OVERVIEW ON POWER TRANSFER TECHNOLOGY by B.Sternlicht	1
SUMMARY OF DRIVE-TRAIN COMPONENT TECHNOLOGY IN HELICOPTERS by G.J.Weden and J.J.Coy	2
SYSTEMES DE TRANSMISSION ACTUELS par R.François	3
HELICOPTER TRANSMISSION LUBRICANTS by H.A.Spikes	4
SESSION II – HELICOPTER AND TURBOPROP TRANSMISSION TECHNOLOGY NEEDS AND DESIGN	
SPECIAL POWER TRAIN REQUIREMENTS FOR THE NEXT GENERATION OF ROTARY-WING AIRCRAFT by R.J.Drago and J.W.Lenski, Jr	5
Paper 6 withdrawn	
A STATE OF THE ART ASSESSMENT OF TURBOPROP TRANSMISSION TECHNOLOGY AND PROJECTED NEEDS FOR THE NEXT GENERATION by R.J.Willis, Jr	7
ADVANCED GEARBOX TECHNOLOGY IN SMALL TURBO PROPELLER ENGINES by C.Brownridge and D.Hollingworth	8
THE HELICOPTER TRANSMISSION DESIGN PROCESS by R.Battles	9
SESSION III – COMPONENT DESIGN TECHNOLOGY AND MANUFACTURING CONSIDERATION	
LOGICIEL DE CONCEPTION DES DENTURES D'ENGRENAGES POUR REDUCTEURS ET BOITES DE VITESSE par L.Faure et A.Borrien	10
FINE FILTRATION – AN ATTRACTIVE ROUTE TOWARDS LOWER HELICOPTER OPERATING COSTS by P.B.Macpherson	11
DESIGN, TECHNOLOGY AND MANUFACTURING OF A NON-CONVENTIONAL HELICOPTER MAIN ROTOR MAST* by A.Garavaglia	12
LOAD CAPACITY OF CAGES OF ROLLER BEARINGS FOR PLANET WHEELS by F.Jarchow and P.G.Hoch	13

* Not available at time of printing.

Reference

LOAD CARRYING CAPACITY OF DOUBLE CIRCULAR ARC GEARS
by M.A.K.Fahmy and R.E.Jonckheere 14

MANUFACTURING PERSPECTIVE IN THE DESIGN OF BEVEL GEARING
by A.J.Lemanski, H.K.Frint and W.D.Glasow 15

MANUFACTURING CONSIDERATIONS RELATED TO AIRCRAFT GEARBOXES
by J.N.McDade and G.B.Collin 16

POSSIBLE TECHNOLOGICAL ANSWERS TO NEW DESIGN REQUIREMENTS FOR POWER TRANSMISSION SYSTEMS
by L.Battezzato and S.Turra 17

CASE DEPTH ON FLANKS OF GEARS FOR HELICOPTER GEARBOXES
by A.Watteeuw 18

Paper 19 withdrawn

SESSION IV – TRIBOLOGICAL ASPECTS OF TRANSMISSION COMPONENTS

TRANSMISSION EFFICIENCY MEASUREMENTS AND CORRELATIONS WITH PHYSICAL CHARACTERISTICS OF THE LUBRICANT
by J.J.Coy, A.M.Mitchell and B.J.Hamrock 20

THE CHARACTERISTICS OF SURFACE ROUGHNESS IMPORTANT TO GEAR AND ROLLING BEARING PROBLEMS
by R.S.Sayles and M.N.Webster 21

PARAMETRES SIGNIFICATIFS DU COMPORTEMENT ET DES AVARIES DE SURFACE DU CONTACT HERTZIEN LUBRIFIE. APPLICATION AUX ENGRENAGES
par D.Berthe et L.Flamand 22

PROBLEMS OF ELASTIC HYDRODYNAMIC LUBRICATION OF HELICOPTER TRANSMISSION GEARS
by D.Dini 23

CHEMICAL-MECHANICAL INTERACTION IN GEARS
by E.Saibel 24

REDUCTION DE L'USURE PAR LES LUBRIFIANTS DANS LES CONTACTS ETROITS
par Ph.Kapsa et M.Belin 25

SESSION V – DIAGNOSTICS, MEASUREMENTS, AND NOISE

ROOT STRESSES IN CONFORMAL GEARS – STRAIN GAUGE AND PHOTOELASTIC INVESTIGATIONS
by D.G.Astridge, B.R.Reason and D.Bathe 26

TRANSMISSION OF GEAR NOISE TO AIRCRAFT INTERIORS: PREDICTION METHODS
by A.Berman 27

EVOLUTION OF THE DESIGN TECHNIQUES FOR HELICOPTER MAIN TRANSMISSION GEARBOXES
by G.Bensi and L.Tarricone 28

CONDITION MONITORING OF HELICOPTER GEARBOXES USING AUTOMATIC VIBRATION ANALYSIS TECHNIQUES
by P.Gadd and P.J.Mitchell 29

GEAR NOISE ORIGINS
by W.D.Mark 30

Reference

SESSION VI – PROBLEMS AND FAILURES IN GEARING APPLICATION

THE OBSERVATION AND INTERPRETATION OF GEAR TOOTH FAILURES
by B.A.Shotter 31

PROBLEMS REGARDING THE PRACTICAL EVALUATION OF EFFICIENCY OF WORM GEARS
by F.A.P.Da Silva 32

TRANSMISSION ERROR MEASUREMENTS IN GEARBOX DEVELOPMENT
by J.D.Smith 33

SESSION VII – QUALIFICATION STANDARDS AND SPECIFICATIONS

DO NEW AIRCRAFT NEED NEW TECHNOLOGIES AND CERTIFICATION RULES?
by J.Hartmann and W.Jonda 34

ESTABLISHMENT AND MAINTENANCE OF CERTIFICATION STANDARDS FOR HELICOPTER AND TURBOPROP POWER TRANSMISSION SYSTEMS
by H.W.Ferris 35

TECHNICAL EVALUATION REPORT

by

Dr Beno Sternlicht
Mechanical Technology Incorporated
Latham, New York 12110, USA

PREVIOUS PAGE IS BLANK

INTRODUCTION

The Propulsion and Energetics Panel 64th Symposium on Gears and Power Transmission Systems for Helicopters and Turboprops was convened at the Gulbenkian Foundation in Lisbon, Portugal on October 8—12, 1984. The purpose of the meeting was to exchange and disseminate information on R & D being conducted on the above subject in the NATO countries and to identify future technology needs based on new requirements.

The participants were engineers and management engaged in R & D, manufacturing, testing, certification, and education. The five day symposium was divided into seven sessions in which 33 invited papers were presented. Each paper was followed by lively discussion. The seven sessions are listed below:

I Review of Current Transmission Technology
II Helicopter & Turboprop Transmission Technology Needs and Design
III Component Design Technology and Manufacturing Consideration
IV Tribology Aspects of Transmission Components
V Diagnostics, Measurements, and Noise
VI Problems and Failures in Gearing Applications
VII Qualification Standards and Specifications

CONTENTS OF THE MEETING

It is clear that helicopters and turboprops are gaining wide acceptance but at the same time they are becoming more complex. The requirements for these aircraft are increasing and the performance is stretching the current state of technology so that today transmissions represent the weakest link in the system.

Two papers (Refs. 34 and 35)* in Session VII dealing with certification clearly indicated the rapidly increasing cost for helicopter qualification. One hundred million dollars was cited by Mr H W Ferris of FAA as the present cost for certification of one helicopter. This clearly indicated that a significant, well funded, and continuing R & D effort is required to meet the future needs of military and civilian helicopters and turboprop aircraft. It would have been valuable to have the papers in Session VII presented very early in the program so as to put the limited R & D effort in proper perspective. It also would have been valuable to present or summarize a recent report of the Helicopter Air Worthiness Review Panel (HARP) which dealt with this very important subject and made eleven specific recommendations.

TABLE I

KEY FACTORS

1 Cost — Acquisition (First Cost)
— Maintenance
— Energy (function of efficiency)
2 Life
3 Reliability
4 Availability
5 Time Between Overhaul (TBO)
6 Mean Time Between Repair (MTBR)
7 Noise
8 Vulnerability/Fail Safe
9 Weight
10 Size

The 33 invited papers covered a wide range of subjects relevant to transmission systems for helicopters and turboprops

*References are listed in the Contents, pages VII—IX

BEARINGS

In today's Army helicopters many types of bearing are used. Bearings are heavily loaded, the design of these mechanical elements is highly refined, and the design limits are known with reasonable accuracy. Deep groove bearing are used in accessory drives. Spherical double row bearings are used in planetary gear supports for their ability to withstand misalignments imposed by offset loads on the planet carrier posts. Bevel gears, being sensitive to misalignment problems induced by loads and thermal distortions, are rigidly mounted in bearings. Several arrangements are found. Triplex mounted angular contact bearings and a straight cylindrical roller bearing in a straddle mount have been used. Recent step improvements have been made, transitioning to more advanced bearings for gear shaft support. One example is the Boeing-Vertol CH-47A (1960), CH-47C (late 1960's) and CH-47D (mid 1970's). In this application materials evolved from 52100 to CEVM M50 and from standard ball and roller designs to out-of-round (for skidding control) roller bearings with integral spaces (ref. 14). Also there has been a transition to integral bearing raceway/shaft designs in many designs in order to reduce parts count and reduce fretting wear. The Sikorsky UH-60 Blackhawk incorporates tapered roller bearings for gear shaft support for the input main bevels, combining bevel and tail rotor drive take-off.

Ball bearings are used in high speed turbine engine shaft supports and with this severe application as a driving force have achieved very high speed capability: speeds as high as $3x10^6$ DN have been demonstrated. The parameter DN is defined as the product of diameter in millimeters and speed in revolutions per minute. Roller bearings are more limited in speed because of higher heat generation. This is partially due to intentional out-of-roundness or "pinch" that is sometimes put on the raceways to control skidding at high speeds and light loads. Tapered roller bearings have good load capacity for combined axial and radial loads such as when reacting spiral bevel gear loads. However tapered roller bearings are used on the slower speed shafts because of heat generation at the roller ends. Conventional (inner cone ribs) tapered roller bearings are limited to $0.5x10^6$ DN which is compatible with a cone rib velocity of 36 m/s (7000 ft/min). However, work done in the 1970's (refs. 15 to 18) has improved the high speed performance up to $3x10^6$ DN for pure thrust loads and $2.4x10^6$ DN for combined thrust and radial loads. Of course, this technology has not yet been input to current helicopter transmissions.

SEALS, CLUTCHES, COUPLINGS

Typically, seals on the input and output shafts are spring loaded lip, elastomeric types. For high speed and more critical requirements spring-loaded carbon type seals may be used.

Clutches most widely used in helicopter free-wheel units are the sprag type (fig. 16) and the roller/ramp type. The OH-58 and the Hueys use the former and the UH-60 the latter. Roller type clutches are somewhat heavier than sprag-types but they do not have a possibility of "rollover" failure. Rollover is where, the torque level being too high, the sprag rolls over and positive engagement is is lost.

A study of the technology of clutches has been made (ref. 19). The overrunning clutches should be on the highest speed shafts, giving lightest weight. A spring type clutch is an attractive candidate for speeds up to 27,000 rpm. Sprags that will not roll over have been developed (fig. 17). The positive continuous engagement type sprag, when overloaded abuts its neighbor sprags, limiting the amount of roll-over. Applications up to 20,000 rpm or 50 m/s (10,000 ft/min) are suitable for sprag clutches. Roller/ramp clutches are limited to 12,000 rpm. The highest Hertz contact stress occurs at the nonconforming inner race contact. Industry practice is to not exceed 3.5 GPa (500,000 psi) contact stress (refs. 1 and 2).

Couplings are used in helicopter drive lines to accommodate shaft misalignments which are caused by airframe flexibilities. Past experience has shown that, for reliable operation, much attention should be given to the coupling design. One important parameter is the torsional stiffness. This affects drive line dynamics. Space and weight considerations are also important and affect the selection of coupling type. There are two main types of coupling in use. The gear coupling is most prevalent (fig. 18). The UH-1 and OH-58 use this type. It is able to carry the torque loads with 3 degrees of continuous misalignment and transient conditions up to 6 degrees of misalignment. Speeds up to 20,000 rpm are possible. Grease with an extreme pressure additive is used as lubricant for lower speeds, and forced oil flow for better cooling at high speeds. Rotor/transmission/pylon systems with soft mounts require the large misalignment capability of gear type couplings. The gear coupling is normally limited by its thermal capacity. The usual failure mode is overheating followed by plastic shearing of the gear teeth and/or local welding of the gear teeth.

Another popular coupling is the flexible element type. There are several similar types in this category: the flexible ring type or Thomas Coupling (fig. 19); the flexible diaphragm type or Bendix Coupling (fig. 20); and the axially loadable straight element type (Kaman K-Flex Coupling), (fig. 21). The first two need to be used in conjunction with a spline for axial motions. These types of coupling are usually found on the larger helicopters where they have a weight advantage over geared couplings. They are simple, light, and don't require lubrication. However the Thomas and Bendix types may carry only up to 1 degree misalignment. The Kaman type may carry up to 0.5 degree per plate element. With these types, the failure problems are flexural fatigue and

LIFE AND RELIABILITY

Achievement of long-lived, reliable power transfer systems can be difficult to achieve and today's helicopters are one of the most severe applications of this technology. Helicopters (sometimes referred to as flying fatigue machines) present the ultimate test of materials and designs for reliability. The many failure mechanisms for bearing and gears must be weighed against anticipated loads which are not know with certainty. In addition to known classical modes of failure, such as pitting, scoring, and bending fatigue, there are unanticipated events that can ground helicopters. Things like sudden leaks producing low oil levels, undetected contamination of lubricant, and poor maintenance practices can severly lower the reliability of the mechanical components of the transmission. There is no way to anticipate the exact effect and typical experience has been that there has to be a suffering through the debugging phase of new designs. Generally, today's flying helicopters have been achieving 500 to 1200 hr time-between-overhaul (TBO) for main transmissions with tail rotor gearbox TBO's up to 1600 hrs. Design calculations often indicate much greater reliability. This is because all the various reasons for failure are not accounted for in those calculations, and there has been no sensible way to calculate the effects of unknown or unanticipated causes. Indeed, it has been found that in overhaul and unscheduled removal operations only about ten percent of failed bearings exhibit classical failure modes. Gears are even less likely to fail, giving rise to the speculation that current gear design practice is more conservative than bearing design practice.

Current practice is to calculate bearing and gear life using AGMA (American Gear Manufacturer's Association) and AFBMA (Antifriction Bearing Manufacturer's Association) standards for pitting fatigue life. Many aircraft companies have established their own data base for bearing and gear reliability from which designs are extrapolated. Experience has shown that subsurface initiated fatigue life is distributed according to the Weibull probability distribution. This holds for gears as well as bearings. As for sensitivity factors, the Weibull slope is one to two for bearings and two to three for gears, where the slope is measured on special coordinates defined by the Weibull distribution. The ordinate is the log-log of the reciprocal of probability of survival graduated as the statistical percent of specimens failed. The abscissa is the log of time to failure or system life. Load also affects life. For gears, life is inversely proportional to the 4.3 power of load and the cube of load for bearings. There are other factors such as material, lubrication, processing and speed which can have an effect and data is in hand (ref. 10) to provide reasonable guidance in estimating surface fatigue life.

There has always been some confusion about the proper relation between individual gear or bearing life and total system life. Moreover, the exact relation that exists between the average system failure rate, TBO, and MTBF has not always been understood. However these figures of merit can and should be rigorously related through proper application of mathematical statistics with an adequate match of circumstances to the basic assumptions of the theory. For example, laboratory measured life distributions for components may determine an average life. But under service conditions in a fleet this circumstance (laboratory condition) does not apply. This is because in a fleet operation, components are repaired or replaced periodically and after a time the fleet is comprised of a mixture of ages for the components. This circumstance fits the classical "renewal theory" assumptions, and the distribution in the limit approaches the exponential distribution instead of the Weibull distribution (ref. 11). It is for the exponential distribution that MTBF is defined. It is precisely this transition of conditions from laboratory to field, with the attendant problems of overhaul and repair record keeping that makes it difficult to correlate the theoretical or design predictions for life with field experience.

Recent publications have documented a life prediction methodology for gears and bearings as applied to an entire transmission (refs. 12 and 13). In reference 12 a current turboprop gearbox (fig. 13) was analyzed using the life prediction methodology developed at the NASA Lewis Research Center. The turboprop gearbox is strikingly similar to a helicopter gearbox if the turboprop input spur gear stage were changed to spiral bevel gear pair. The NASA analysis of the turboprop gearbox is summarized on a Weibull plot (fig. 14). Each gear and bearing life distribution is shown relative to the ten percent life of the entire transmission. The single weakest component, according to the analysis, was the planet bearing.

In reference 13 a similar study was done for a typical planetary gear set such as found in a turboprop or helicopter reduction gear stage. The study was done for a three planet system with an output of 150 kW (200 hp) at 300 rpm. The gears were AISI 9310 Vacuum Arc Remelt steel with face width 51 mm (2.0 in.), module 4.23 mm (diametral pitch 6 $in.^{-1}$), and 20° pressure angle. The tooth numbers were sun, 24; ring, 96; and planet, 36. The planet bearings were 75-02 cylindrical roller bearings with a width of 25 mm (1 in.) and outside diameter of 130 mm (5-1/8 in.). The life distribution of the system and the most critical elements, sun and planet bearing are shown in the Weibull plot (fig. 15). In contrast to the turboprop example, the sun gear is the weakest element according to the analysis.

WEIGHT

The specific weights for current main rotor gearboxes range from 0.30 to 0.50 lb/hp. A summary showing the total drive system weight is given in table II. The total drive specific weight ranges from 0.4 to 0.6 lb/hp on the basis of input power to the drive train. The helicopters considered here are plotted with weight trends in figure 8. Housing assemblies are usually made of low density materials such as cast magnesium and forged aluminum for the load bearing members. This is important because housings comprise 20 to 60 percent of total transmission weight in current helicopters. The gears themselves increase in weight according to the quare of the ratio. Therefore high ratio reductions in a single stage are not common. The order of weights from lightest to heaviest (for equal gear ratios) is planetary, parallel axis, spiral bevel, and it is beneficial to take higher reductions nearest to the final output. This will trade-off number of stages against overall weight. Current designs reflect this, as the bevel stages usually take the less reduction at the higher speed. These rules may not apply if weight distribution and the effect on helicopter center of gravity are overriding factors.

EFFICIENCY

The current helicopter transmissions transfer power from engine to rotor in an highly efficient manner. Transmission efficiencies range from 97 to 99 percent in today's flying helicopters. The power losses arise from windage losses inside the case, bearing losses, seal sliding friction losses, pumping losses, with the main contributor being the sliding losses in the gear teeth. For a single spiral bevel or a spur mesh there is approximately 0.50 percent loss; for a planetary stage, a 0.75 percent loss. These figures apply only to a fully loaded transmission. At part load, the efficiency decreases significantly. Figure 9 shows a plot of measured efficiency for the OH-58 transmission. Efficiency at maximum speed and torque is 98.4 percent. The effect of decreasing torque is characteristic of all transmissions. The gear teeth need to be loaded to their capacity for the given size and properly lubricated. Also the effect of speed is shown on this figure. As the speed is halved at full torque, a 1/10 percent increase in efficiency is noticed. This is the sensitivity to windage. Efficiency of power transfer is extremely important to the overall operation envelope of the helicopter. For example, in a 3000 hp helicopter, such as the Blackhawk, a one percent decrease in efficiency would consume an additional 30 hp. A medium helicopter suffers a useful payload reduction of 100 to 200 lb with a one percent power loss. In addition, the added 30 hp would have to be dissipated, requiring a larger oil cooler which would be heavier and more vulnerable. Therefore, any new designs, in order to be viable, must be at least as efficient as current designs or they must be much lighter, if not as efficient, in order to compensate for loss of payload and increased cooling system weight.

NOISE

Transmissions are the main source of noise in today's helicopter interiors. The noise is predominantly pure tone multiples of gear mesh frequencies. The frequencies range from several hundred hertz to beyond hearing range. The source of noise is the gear mesh as an impact exciter, with sound transmitted to the listener through structural and airborn pathways. There is currently no universally satisfactory treatment. Current analytical tools are only now being refined and they may be useful to design the next generation of helicopters. Current remedies are spot treatments using damping material around the passenger compartments and friction damping rings on the gear blanks. Sound treatments in use today have the disadvantage of weight and cost penalty and increased maintenance man hours due to the need for removal of noise abatement materials for airframe and component inspection. Moreover, the materials may never be replaced subsequent to an airframe maintenance inspection. Experience has shown that higher frequencies are easier to treat, and that for equal pitch line velocities, helical gears are the most quiet, followed in order by, spur and bevel gears. Generally, higher contact ratio and finer pitch give quieter gears, but fine pitch gears are not as strong as their more course counterparts. This requires a trade-off study.

A study of interior noise levels of current helicopters has been completed recently (ref. 8). The findings, obtained by averaging the measurements from two microphones placed near the pilot's and copilot's heads, were as follows: OH-58A, 107 dB; UH-1H, 113 dB; AH-1S, 120 dB; UH-60A, 115 dB and CH-47C, 118 dB. These measurements are for overall sound pressure levels at cruise conditions. There were significant variations in frequency content from aircraft to aircraft. Costs of noise treatments for cabin interiors have been assessed (ref. 9). For the Bell Jet Ranger III (fig. 10) which is civil version of the OH-58 a speech interference level of 84 dB at cruise conditions can be achieved with a kit supplied by a third party for under $4000. For larger helicopters the costs are proportional to helicopter size and noise severity. Single rotor helicopters have the transmission closer to the passenger compartment, whereas tandem rotor aircraft have the forward transmission very near the cockpit. Transmission location determines the type of noise treatment because of the varied noise paths between the two types of aircraft.

Figure 11 shows that over the past two decades transmissions have steadily become noisier. Figure 12 shows that in the same period the transmissions have steadily become lighter. The result is that in order to meet military noise specification MIL-A-8806A, soundproofing treatments resulted in heavier packages when the combination of main gearbox and sound proofing weights are added together (fig. 12).

FATIGUE AND RESIDUAL STRESS

In the manufacturing process there are many factors which affect the residual stress in transmission components. Most prominent of these are the type machinery involved in the cutting, speed of the machine, machining lubricants, shape of the part, surface finish, heat-treat processes and handling. The resulting residual stress can be either beneficial or detrimental to the fatigue strength of the part. Parts with surface tension stresses could have shortened life since any applied tension fatigue stress would be additive. Whereas parts with compressive stresses could have beneficial effects as the compressive stress would subtract from applied tension fatigue stresses and inhibit crack initiation or growth.

One method used by the helicopter companies to eliminate the residual stress is through shot peening. Shot peening has long been used as a method for improving the bending strength of gears. However, until recently it had not been considered to be a factor in extending fatigue life. Studies conducted on residual stresses in rolling-element bearings at NASA Lewis Research Center have shown that increased residual compressive stress increases rolling-element (surface) fatigue life (refs. 5 and 6). In addition, an investigation was conducted to determine the effect of shot peening of gear teeth on surface fatigue life (ref. 7). Gear surface fatigue endurance tests were conducted on two groups of carburized and hardened AISI 9310 steel spur gears, manufactured from the same heat of material. One group was subject to an additional shot peening process on the gear tooth surface and root radius. The test results are shown in table I (ref. 7). Basically, the shot peened gears exhibited fatigue lives 1.6 times the life of standard gears without shot peening (ref. 7).

Thus, it can be seen that shot peening provides an increase in fatigue life in addition to improving bending strength.

GEAR STEEL

The most commonly used gear material in U.S. helicopter transmission is AISI 9310. However, the Boeing Vertol Company changed to VASCO X-2, modified in the CH-47D. Other materials such as CBS 600, CBS 1000 and Carpenter X53, are being evaluated by industry and government laboratories. The shift to VASCO X-2 stems from a desire for a steel with improved high-hot-hardness characteristics which would enable gears to carry higher loads without the surface distress that was becoming a limiting factor with AISI 9310. In addition, survivability was of concern to the military and the capability to get home in case of damage to the lubrication system.

Boeing Vertol with support from the Army and Navy developed VASCO X-2 in the early seventies. It now is used on the CH-47D transmission in all the highly loaded gears which had potential for scoring/scuffing using AISI 9310. In comparative tests between VASCO X-2 and AISI 9310, VASCO X-2 has shown superior resistance to scuffing and scoring which limit the load capability under conditions of thin-film lubrication (lightweight synthetic oils), figure 9 (ref. 4). In tests of the bending fatigue endurance limit VASCO X-2 and AISI 9310 were essentially the same (ref. 4). VASCO X-2 has a somewhat improved capacity over AISI 9310 in contact (Hertzian) capacity (ref. 4). In fracture mechanics property tests, AISI 9310 has higher impact strength and fracture toughness, while VASCO X-2 and AISI 9310 have equivalent fatigue crack propagation rates and threshold values (ref. 4). Before this material could be utilized it was necessary to develop a thorough understanding of the material chemistry and heat treatment in addition to the processing variables and quality control. This was accomplished after a great deal of effort by Boeing Vertol and VASCO X-2 now is firmly established as a gear material.

GEAR PARAMETERS

The majority of the current helicopter transmissions have spur-gear contact ratios (average number of teeth in contact) less than two. The contact ratios range from 1.3 to 1.6 so that the number of teeth in engagement is either one or two. Basically, the load is shared by two teeth during the entrance and exit phases of engagement while one pair of teeth carries the load the remaining time. Many gears use a pressure angle of 20 to 25° and operate with a contact ratio of approximately 1.?. Pressure angles up to 28° have been used successfully. This provides improved tooth strength, however, at the same time it increases noise and may cause lower pitting fatigue life.

Allowable stresses vary with gear material to be used and the maximum temperature to be endured. Most designs are based on maximum gear body temperature under 400 K (approx. 250° F). The AGMA (American Gear Manufacturers Association) standards for aircraft gearing are used to calculate both Hertz contact stress and bending stresses. In today's helicopters designs are limited to about 1.1 GPa (160,000 psi) for Hertz Stress, thus allowing for leeway in case of misalignments induced by case flexibility and manuever-imposed loads. Total loads rarely exceed 1.5 GPa (220,000 psi) for Hertz stress in gears. For bending, 0.4 GPa (60,000 psi) is rarely exceeded. Bevel gear limits are lower than for spur and helical gears.

Pitch line velocity in current transmissions for high speed bevel gears is approximately 50 to 100 m/s (10,000 to 20,000 ft/min). These limits were necessary because of the need to limit lubrication churning power loss, as well as to prevent high dynamic loads.

to 7:1 for a single stage (sun gear input, ring gear fixed, cage output). In current practice the planetary seldom has a reduction ratio greater than 4.7:1 when fitted with five planet pinions (refs 1 and 2).

There are times when two planetaries are used in series (CH-47 and UH-1) to obtain higher reduction ratios. A wide variety of reduction ratios is available with two planetaries and the designer has the choice of reduction ratio for each stage to attain a specific overall ratio.

TYPICAL CONFIGURATIONS

The OH-58 has a single main rotor transmission which represents current design practice in light helicopters (fig. 3). There are four reduction stages between the engine and main rotor shaft. The engine output speed of 35,350 rpm is reduced in two stages of helical gears to 6060 rpm at the input of the main gearbox. The helical gears provide an offset between the engine and bevel pinion axis and allow power to be extracted from the final helical gear for the tail rotor. The first-stage gearing in the transmission is spiral bevel (19/71 reduction) and provides a speed of 1622 rpm to the sun gear of a fixed-ring planetary unit. The planetary unit provides the final reduction of 4.67:1 and gives a speed of 347.5 rpm to the planet carrier and main shaft.

Noteworthy features of this design include the use of self-aligning bearings in the planet pinions, a radially flexible ring gear and a cantilever support for the bevel gear which was used to reduce the overall height.

Stepping up to the larger size single rotor helicopter, we find the UH-1 and UH-60. Both are in the utility class, however, only the UH-60 will be addressed since the UH-1 drive-train configuration even with an additional planetary stage is similar to the OH-58. The UH-60 main transmission has five separate, interchangeable modules (fig. 4). They are the main module, two engine input modules and two accessory modules. The power train has two spiral bevel gear meshes (17.3:1 reduction and a spur gear planetary system with five pinions (4.67:1 reduction). Three additional spiral bevel meshes provide power take-off for the accessory modules and tail rotor while four spur gear meshes drive the accessories and lubrication pumps. This drive-train configuration provides an overall reduction ratio of 80:1 and reduces the input speed from 20,900 to 258 rpm at the main rotor. The continuous rating of transmission is 2828-hp with a single engine rating of 1560 hp.

While the OH-58 is representative of the single rotor main transmission, the CH-47 has transmissions typical of tandem rotor design. The CH-47 has engine and combining transmissions in addition to forward and aft main rotor transmissions. Each engine gearbox changes the direction of axis from the power plant to the combining transmission and reduces the speed. The gearing is spiral bevel with a reduction ratio of 1.23:1. The power rating of the gearbox is 3750 hp. A clutch is located at the output shaft to allow autorotation without drag from the engine and gearbox.

The combining transmission takes the input from the two engine gearboxes and has two outputs to drive the forward and aft transmissions. The combining transmission has spiral bevel gearing with a reduction ratio of 1.7:1 and a power rating of 6000-hp.

Power from the combining gearbox is transmitted through synchronizing shafts to the forward and aft transmissions, which are similar in design (fig. 5). The first-stage gearing in the transmission is spiral bevel, followed by two simple spur gear planetary units with a common ring gear. This configuration provides a reduction ratio of 30.73 in both the forward and aft transmissions. They are rated at 3600 hp with an input speed of 7465 rpm and 243 rotor rpm.

QUALITY OF MATERIALS

Major advances have been made in the past two decades which improve the quality of bearing and gearing materials for transmissions. These advances involve improved processing and cleanliness and greater control on material chemistry and heat treatment. The largest and most significant improvement is related to the use of double-vacuum-melt steel instead of single-vacuum-melt. This process involves the use of Vacuum-Induction-Melt (VIM) in combination with Vacuum-Arc-Remelt (VAR). The processing techniques provide a very homogenous material with reduced nonmetallic inclusions, entrapped gases, and trace elements.

The first benefit of the improved cleanliness of the material is an increase in fatigue life. An example of the exceptional long fatigue life that can be obtained with VIM-VAR AISI M-50 is presented in reference 3. A group of 120-mm-bore, angular contact ball bearings was endurance tested at three million DN (D is bore diameter in millimeters and N is speed in rpm) and a thrust load of 22,200-N (5000 lb). The ten percent fatigue life obtained was over 100 times the predicted AFBMA life. This long life includes lubrication effects which are beneficial to life at these high speeds, so that the improvement attributed to VIM-VAR AISI M-50 was a factor of 44 (ref. 3).

A second benefit gained through the use of double-vacuum-melt over single-vacuum-melt steel is the improvement in the threshold stress allowables and in fractur toughness characteristics. Tests conducted by Boeing Vertol indicate a substantial improvement in threshold stress as shown in figure 6 (ref. 4). For these reasons, the Army now is specifying VIM-VAR on critical transmission components.

SUMMARY OF DRIVE-TRAIN COMPONENT TECHNOLOGY IN HELICOPTERS

Gilbert J. Weden and John J. Coy
Propulsion Laboratory
AVSCOM Research and Technology Laboratories
Lewis Research Center
Cleveland, Ohio 44135

ABSTRACT

A review of current helicopters was conducted to determine the technology in the drive-train systems. This paper highlights the design features including reliability, maintainability and survivability characteristics, in transmission systems for the OH-58, UH-1, CH-47 and UH-60 helicopters. In addition, trade-offs involving cost, reliability and life are discussed.

INTRODUCTION

With the advent of the gas turbine engine and its application to helicopters in the late fifties and early sixties, there was a significant change in the design and technology of helicopter transmissions. Drive system input speeds increased from 2500 to 20,000 rpm and power to be absorbed tripled. These challenges were met by the helicopter industry. In the seventies and early eighties there have been other challenges: requirements for reduced weight, reduced noise, increased survivability, increased safety and lower life-cycle costs.

In most cases the technology to meet these challenges has been paced by military interests, in particular the U.S. Army (refs 1 and 2). This being the case, a review was made of the drive system technology in the Army's OH-58, UH-1, CH-47 and UH-60 (Fig. 1). These helicopters represent a range from light observation to medium-lift cargo. With the exception of the UH-60, they became operational in the sixties and have continued in service through several versions (A, B, C and D series) with the latest models expected to be in the Army inventory through 1990. Many are being built under licensee agreements. Their evolution has been characterized by improved range and speed and by constantly improving reliability and safety. New or improved drive systems have been developed for the latest models with the objective of step improvements in maintainability and reliability.

The UH-60 is a relatively new helicopter; first production deliveries began in 1979. It is used extensively by the Army and Navy and is designed primarily to carry eleven fully equipped troops plus a crew of two. The gearbox represents current state-of-the-art design for helicopter transmissions.

DESIGN APPROACH

The design of the transmission system is dictated by the configuration of the helicopter. Two configurations are in general use: (1) a single main rotor with a tail rotor and (2) a tandem configuration with twin contrarotating rotors of equal size and loading so that the torques of the rotors are equal and opposing. A typical drive train configuration for the single-rotor machine is shown in figure 2 with the main variations occurring in the location and configuration of the engines.

In both configurations, single and tandem rotor, the transmission loads are a function of power and speed. The engine power is determined from the maximum performance requirements of the mission, such as hover at 4000 ft (out-of-ground-effect) at 95° F. The input speed to the transmission is fixed by the output speed of the engine, while the rotor speed is determined by the top speed of the rotor blade. Thus the overall drive train reduction ratio can be determined for a given rotor diameter. Trade-off studies are conducted to evaluate different configurations for splitting the reduction ratio among the various transmission components (epicyclic bevel gear set, spur set, etc.) and achieving a design with minimum weight. Consideration also must be given to the transmission housing.

Finally, a thorough aerodynamic analysis is conducted on the helicopter mission in order to obtain complete spectra of the rotor loads and moments as well as the maneuver loads and transients for maximum transmission reliability. This analysis is compared with known load-life relations on similar components to achieve maximum transmission reliability and minimum weight.

OVERALL ARRANGEMENT

Current helicopter main transmission systems have a reduction ratio in the region of 80:1 to 100:1 to reduce the gas-turbine engine speed to the main rotor. This ratio is achieved in either three or four stages of gearing, where each stage is either an epicyclic gear assembly, a spiral bevel gear pair or a helical gear pair. The predominant configuration in current designs is the planetary gear train. The trend to planetary gear trains is well established as it provides maximum torque in a lightweight and compact gear reduction. In the planetary design, practical reductions vary from 2.15:1

The overall experience in reliability, availability, and life of U.S. manufactured equipment, not just military equipment, leaves much to be desired. Our recent experience with U.S. made automobiles has shown great lack in these areas as compared to other foreign manufactured products. Our whole quality control and inspection programs have been challenged.

Because these problems are much more important to the military, they have considerably more to gain in solving them. Thus, reliability and maintainability improvements in military equipment is beginning to receive considerably more attention and should have a very positive impact on our commercial and industrial products. This area represents another technology "spinoff" resulting from military development efforts that will have positive effect on a great variety of products.

It is expected that in the free world about 30,000 helicopters will be built in the 1980's. Approximately 30% of these will be for military use. This corresponds to approximately a thirty billion dollar business, approximately half of it in the U.S.A. Most of the civil advances are expected to come from the military developments very similar to the aircraft experience. It is, therefore, very important that the military continues to make the necessary technology advances. This represents another reason for continued commitment to the advances of this technology.

In reviewing the variety of papers on transmissions, which also include this symposium, I found that the sessions could have been divided into the following broad categories:

		No. of Paper in this Conference
1.	Future Requirements	4
2.	Component Technology I	11
3.	Component Technology II (Emphasis on Tribology)	7
4.	System Technology	6
5.	Design	5
6.	Manufacturing	4
7.	Certification	2

I offer this observation because this breakdown might help me in preparing the Technical Evaluation Report. I would, therefore, like to request that each author identifies the classification of his paper along the above seven categories. Some of the papers may actually cover two or more categories. I would also like to request that each author clearly identifies technological gaps and points out the possible payoff resulting from the advances he is making. I hope that the authors will spend most of the allotted time on raising issues, projecting future trends, and providing forum for lively discussions. In technical sessions and symposia, I have found that lively discussions and diverse points of view are often much more valuable and informative than the paper itself.

In summary, I am sure that all of us will learn something new. We are bound to gain better understanding of the current status of this technology. For some of us, the symposium will spark new ideas for technology advances; for others, it may provide answers to existing problems. Thus, I am sure that all of us will derive value out of these sessions.

added to the analytical complexity, but the high speed, high storage capacity computer was able to cope with this.

In the case of transmissions, the analyses are much more difficult primarily because they are made up of a large number of components and there is considerably more interaction between the various parameters. This is especially true in military applications where weight, reliability, and noise are important factors that must be considered. For example, when we reduce weight, we tend to get more deflection, higher stresses, greater noise, poorer elasto-hydrodynamics lubrication, lower reliability, etc.

Today we are on the threshold of a new computer advance which will help us to analyze complex systems. It is the emergence of CAD/CAM technology. These new tools will enable us to study design changes and help us to see their effects. Thus, we can study deflections, stress, lubrication, and heat transfer and extend it to vibration and noise. We can quickly assess dimensional changes on the performance of components and systems. These dimensional changes not only affect lubrication, vibration, and noise, but also system weight. The added advantage of this tool is that it can be used in a man-machine interactive mode, and thus an experienced designer can rapidly see the effects of the change. I, therefore, believe that this relatively new design and manufacturing tool will greatly help to speed up the development process and give us a much better chance to optimize complete transmissions and propulsion systems. The CAD technology is expected to contribute to system analyses in the eighties in a similar way that the high speed, high storage capacity computers did in component analyses during the fifties and sixties.

Another very important advance in the past decade has been the development of microchips which have been very effectively used not only in computers, but also in signal analyses. Processing equipment using microelectronics can be coupled to a variety of of miniature sensors and transducers to accurately give us experimental and diagnostic data that we were unable to get before. These will be used to improve reliability, life, and maintainability of power drive systems.

Thus, complex three-dimensional problems of lubrication, elasticity, and energy can be analyzed today for complex geometries very quickly and at relatively low cost. This is very important, especially in the assessment and development of a variety of military transmissions such as planetary, hybrid, traction, and split torque.

It is well recognized that weight reduction is very important in aircraft and space equipment. Over a relatively short period of time, transmission weight has been reduced from 0.4 lbs/HP to 0.3 lbs/HP. Considerable effort has been directed to weight reduction, and split torque transmissions for helicopters of around 0.2 lbs/HP are now being investigated. Weight recuctions are often related to higher speed, reduced lubrication volume, use of new materials, etc. Unfortunately, some of the weight reduction efforts have also had some negative effects on life by causing higher stresses and poor lubrication which resulted in premature failures. Inadequate analytical tools and understanding are the prime causes of these failures.

I am reminded of the development of the Vulcan gun at the General Electric Company. During its illustrious history, I was exposed to three independent teams of Value Analysts whose assignment was to reduce cost through weight reductions. It was a very noble objective, but one that resulted in serious problems. Each time the modifications resulted in failures, and it was concluded that the weight reduction caused excessive deflections which resulted in a host of performance problems. In each case, the structure finally had to be beefed up. If easy to use analytical tools were available, these problems would probably have been avoided.

This rather poor experience in no way should imply that weight reductions are not possible. In fact, CAD/CAM has been very effectively used for this purpose in weight reductions of automobiles, and it can be applied to transmissions and propulsion systems. During the past two decades, there have also been very significant developments of new alloys (e.g., EX-53) and processes (e.g., shot peening, growth of large single crystals, etc.). Also, there have been significant advances in ceramics and composites. These new materials, with a number of very desirable properties, will result in some very significant weight, cost, noise, and vibration reductions. For instance, shafting that uses composite materials offers considerable advantages both in weight reduction and rotor dynamics. It is, therefore, hoped that many of these new advances in materials and analyses will quickly find their way into the power drive systems.

Another area that deserves discussion is that of reliability, TBO, MTBR, and cost. We recognize that these are very important factors, especially in military applications where the cost of maintenance tends to be very high. Helicopter and turboprop aircraft are highly vulnerable to transmission failures. Studies have shown that over 50% of helicopter maintenance cost is attributed to mechanical drive systems. Rolling element bearing fatigue, spalling, spline wear, fretting, gear track fatigue, and tapered roller lubrication failures are just a few examples. MTBR of about 1,000 hours is very short, and obviously there is a need to significantly increase this number. It should be remembered that transmissions are made up of a large number of components whose lives have to be an order of magnitude higher. (For MTBR of 1,000 hours with 20 components, each must have a life of $1{,}000 \times 20 = 20{,}000$ hrs.) These short lives are often attributed to poor design, inadequate analytical tools, poor lubrication, poor materials resulting from inadequate development, poor correlation between theory and experiment, etc. Artificial Intelligence (AI) will become a very important diagnostic tool in failure analyses. Adapting AI and expert systems to transmission analyses should result in significant payoff.

OVERVIEW OF POWER TRANSFER TECHNOLOGY

Dr. Beno Sternlicht - Technical Director
Mechanical Technology Incorporated
968 Albany Shaker Road, Latham, N.Y., 12110, U.S.A.

When I was asked by Mr. John Acurio to be the technical evaluator of this symposium, my first reaction was negative. This was primarily because I did not consider myself to be an expert in this field. I felt that I would contribute little to this group of experts. Then, with a little more persuasion from John, whom I learned to respect, I finally accepted this invitation. I would like to share with you some of the reasons for my acceptance:

1. MTI, since its founding, has been one of the leading technology groups working in bearings, seals, gears, and transmissions. During our history, we have been engaged in the development of mechanical transmissions covering such areas as design, troubleshooting, and also applying them to our products. This symposium, I felt, would provide me with a good opportunity to learn what others were doing.

2. I have had personal experience in several technology areas common to this field. In the past, I have found that an expert in one technical area can often provide an objective assessment of a related field because he has no ax to grind.

3. The purpose of a symposium is to disseminate information and to spark new ideas for R&D. I have always believed that technology is only valuable when it is effectively disseminated and applied. This symposium would provide an important avenue for dissemination of information.

4. I strongly felt that the AGARD meeting provided an opportunity for the leading experts in NATO to exchange scientific and technical information, provide consulting services and, all in all, find new research directions which are likely to result in significant impact.

These factors finally convinced me to accept this challenge. Here I am, hoping that all of us are going to have a productive and educational meeting, one in which we will openly present both our accomplishments and failures. I have found that well documented failures are often just as important as successes, for they spark new ideas and provide new research directions.

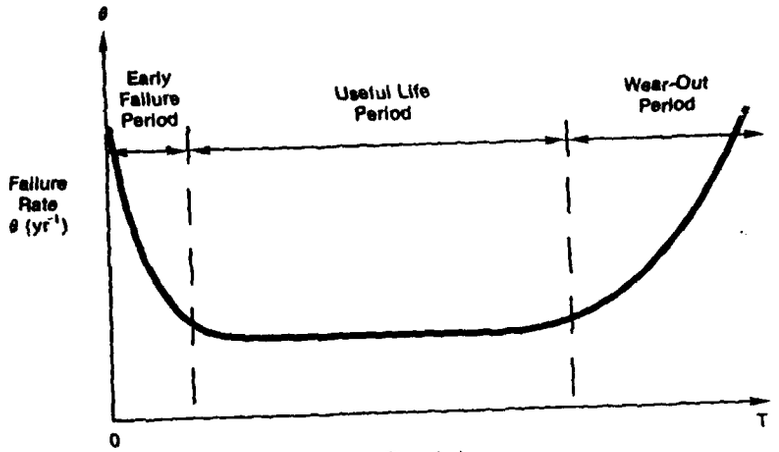
To get rapidly up to speed in this area of technology, I took several steps. I conducted a library search of papers on aircraft transmissions that were published in the last decade. I then laboriously pored through these and selected about fifty papers which I reviewed in more detail. Most of these, because of time restraint, were by American authors. One compendium of papers that proved to be very valuable was the Advanced Power Transmission Technology conducted by NASA-Lewis on June 9-11, 1981. I also telephoned several transmission experts to learn what R&D they were doing and to identify areas which they felt were important.

Based on this study, I have concluded that we are on the threshold of getting a much better understanding of the various parameters influencing transmission design. Thus, in the next few years, we should be able to make significant contributions to transmission design and performance. Why do I feel that we are on the threshold of some significant breakthroughs in this area? To answer this observation, I would like to contrast this area of technology to one with which I am considerably more familiar.

In the fifties and sixties there were very significant strides made in the field of fluid film bearings (hydrodynamics and hydrostatics). This was due to the advent of high speed computers which enabled us to use finite element methods to solve complex partial differential equations. A number of technologists used these tools to similtaneously solve Reynolds and energy equations for a variety of bearing geometries. These analyses eliminated the need for approximations and the use of empirical correction factors. During the same period, with the aid of more accurate film thickness and temperature measurements, experimentalists showed very good correlation between theory and practice. In the late sixties and early seventies, theory was extended to elasto-hydrodynamics and thermo-elasto-hydrodynamics (a word coined by me). Thus, we were able to better understand the process of lubrication and traction in rolling element bearings, gears, traction drives, and seals. Through this effort, major strides were made in increasing life, speed, and DN value of rolling element bearings. During the same period, theory was also extended to compressible fluids, and this enabled many companies to develop gas bearings and apply them to a variety of products ranging from turbochargers to computers. The theory was also extended to bearing rotor dynamics which gave us better insight into stability, critical speeds, balancing and vibration of the complete machinery systems.

Thus, the high speed, high storage capacity computers enabled us to analyze a variety of machine elements and systems. In fluid film bearings, often the analyses could be two-dimensional and for the low speed and light loads, the energy consideration could be neglected. In the case of high shear, the energy equations had to be included. For rolling element bearings and gears, hydrodynamic, elasticity, and energy equations often had to be solved simultaneously. In the case of rotor dynamics, the spring and damping functions of the bearings had to be included in the analyses. This, of course, significantly

MORTALITY CURVE



Failure Rate Characteristics
(The "Bath-Tub" Curve)

Figure 1

FAILURE RATE DISTRIBUTION OF MALES IN ENGLAND AND WALES BETWEEN 1960 AND 1962

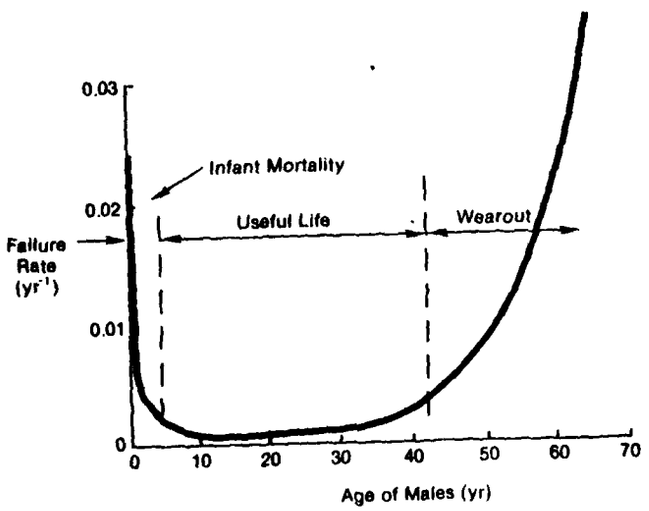


Figure 2

- Involute vs. conformal with regard to cost, noise, availability, vulnerability and weight.

(4) Revolutionary changes where the improvements are at least a factor of two.

CONCLUSIONS

(1) The symposium presented an excellent forum for dissemination of R & D information conducted in this very important area of technology.

(2) The R & D effort seems to be evolutionary and not revolutionary and seems to be receiving inadequate emphasis and funding.

(3) The power train represents the weakest link in helicopters. The TBO and MTBR is very short and needs to be significantly increased.

(4) New tools are now available which can have significant impact on transmission design and performance.

(5) Transmission technology needs to receive greater professional recognition. This will require stronger interaction with professional societies and universities.

RECOMMENDATIONS

(1) Prepare AGARDographs covering such subjeccts as:

(a) Future transmission needs – (past 1995)

(b) Cost/benefit analyses

(c) Critical comparisons of:
Involute vs. conformal gears
Advanced revolutionary transmission concepts
Integral design vs. *stacked design*
Engine/transmission integration vs. present coupled system.

(d) Artificial intelligence – failure modes

(e) Two lubricants (engine & transmission) vs. one common lubricant

(f) CAD/CAM manufacturing to increase life
lower noise
lower cost

(g) Materials and structures (including composites)

(h) Health monitoring technologies

(2) During the meetings, longer time should be allocated to discussions. (It would be valuable to arrange for some prepared discussions, especially if those can present an opposite point of view to that of the author.)

(3) Panels of experts should be considered to discuss or debate a controversial topic.

(4) R & D funding should be significantly increased in this important area of propulsion.

Artificial intelligence, failure mode analyses, trend and statistical analyses should be employed in the generation of the "bath tub" mortality curve for any new transmission design. It is interesting to point out that there is great similarity between the mortality curves for products, e.g. transmissions, and humans (Figures 1 & 2). Accurate predictions of mortality curves can have a very important payoff as illustrated by the performance of insurance companies.

In the USA, insurance companies that employed advanced analytical tools, especially statistical methods, made a lot of money in the 1950s and 60s for they were able to accurately predict the mortality curve. Then, based on trend analyses, they were able to project future mortality curves and thus set their insurance rates. European insurance companies went broke at the turn of this century because they did not predict the high death rate resulting from World War I. It is difficult and very expensive to get life insurance in Israel because of the unpredictability of deaths by terrorists. Now let's look at the similarities:

HUMAN	TRANSMISSIONS
Infant Mortality	
• Health of parents	Design & Manufacturing { capability competence
• Environment-cleanliness	Cleanliness & filtration
• Early nutrition — vitamins — low viscosity food	Use of additives { Cutting lubricants/fluids break in lubricants
Useful Life (reliability analyses)	
• Inheritance	• Materials
• Nutrition	• Lubrication
• Environment — water & air quality recently — noise	• Dirt & chemical decomposition Surface finish
Wear Out (cause of death very large body of statistical data)	• Failure modes
Heart — massive heart attack, stroke, seizure, heart failure	Fatigue (break, massive crack, surface-plucking, pitting, spalling)
Cancer — various forms	Wear (scpuring, scuffing)
Various therapies e.g., by-pass valve, heart transplant, radiation, chemotherapy	

Our objective with manufactured systems is to limit the failure rate during infant mortality and shorten the time for infant mortality. By far, the most important objective is to increase useful life of equipment.

The symposium did not address the following issues:

(1) What are the future transmission needs, e.g. in mid-90s?

(2) What is the cost/benefit of transmission R & D?

- What will be the $ saving in fuel cost if the transmission weight is halved?
- What will be the increase in TBO, MTBR and life by using separate transmission lubricant?
- What is the ratio of transmission acquisition cost vs. maintenance cost?
- What are the advantages of integral design from the standpoint of cost, availability, vulnerability and noise?

The above need to be quantified.

(3) Critical comparison of various areas, e.g.,

- Planetary vs. split torque vs. hybrid vs. traction

TABLE II

Session		Paper #	Future Req.	Comp. Tech. I	Comp. Tech. II (Tribology)	Sys. Tech.	Design	Mfg.	Certif. Qualif.	Remarks
I	Introduction	1								Introduction
	Review of Current Transmission Technology	2	x			x				Technology status and trade-offs
		3		x			x			Safety, reliability & noise
		4			x					Tribology
II	Helicopter & Turboprop Transmission Technology Needs and Design	5	x	x						Future requirements, technology needs
		6								Not presented
		7		x			x			Technology status and needs
		8		x			x			Weight considerations in small turboprop engines TPE
		9					x	x	x	Design process including mfg. & testing
III	Component Design Technology and Manufacturing Considerations	10					x			Gear tooth computer design software CADOR
		11			x					Filtration to increase TBO
		12					x			Weight, integral design of bearing
		13			x					Cages
		14		x						Load capacity of DCA gears
		15						x		Metrology of spiral bevel teeth CAD/CAM
		16						x		Quality cost reliability (QCR)
		17		x		x	x			Technology to meet system needs
		18						x		Case depth
		19								No paper
IV	Tribology Aspects of Transmission Components	20			x	x				Transmission eff. with II lubricants
		21		x	x		x	x		Influence of surface roughness and topography
		22			x					Tribology and reliability
		23			x					Elastohydrodynamic lubrication
		24			x					Chemical-mechanical interaction
		25			x					Tribology and surface reaction
V	Diagnostics Measurements and Noise	26		x	x					Conformal vs. involute, photoelastic stress analyses of gears
		27				x				Noise analyses
		28					x			Design selection using several factors
		29				x				Gear vibrication health monitoring
		30				x				Gear noise origins
VI	Problems & Failures in Gear Applic.	31		x						Gear tooth failures
		32		x						Worm gears
		33				x				Error measurements and noise
VII	Qualification Standards & Specifications	34		x					x	Certification, technology advances
		35							x	Certification
			2	11	10	7	9	5	3	

Several papers discussed more than one topic. The symposium, as a whole, covered a wide spectrum of subjects ranging from:

- Future Requirements to Certification
- Design to Manufacturing
- Component to System Technologies
- Diagnostic systems — wear to vibration
- Measurements of surface topography, tooth profile, vibration and noise
- Lubricants, filtration, surface finish, topography, chemical adhesion
- Experimental Analyses — photoelasticity, strain gauging, error measurements

As technical evaluator, I have taken the subject matter presented in the 33 papers and have categorized the papers along seven somewhat different subject headings as illustrated in Table II. By doing this, it became clear that more than half of the papers dealt with component technologies, primarily with gear stresses and various aspects of tribology.

The important subject of increasing TBO and MTBR was discussed by various authors. It was pointed out that a large number of factors influence these two very important design parameters, e.g.:

(a) Materials (Refs. 2, 5, 13, 18)
(b) Lubricant properties (Ref. 4)
(c) Use of two lubricants (one for the engine and the other for transmission)
(d) Filtration (Ref. 11)
(e) Surface topography and roughness (Ref. 21)
(f) Elastohydrodynamics (Ref. 23)
(g) Chemical — mechanical interaction (Ref. 24)
(h) Tooth geometry (conformal vs. involute) (Ref. 26)
(i) Diagnostics (Refs. 29, 31, 34, 35)

The subject of weight reduction was treated only superficially. Three papers briefly touched on:

(a) Weight reduction of components
(b) Weight reduction of transmission casing (resulting from the use of new materials, e.g., magnesium and composites)

Nowhere was the subject treated on a comparative basis discussing various designs, transmission types, and configurations that result in the lowest weight (Lb./HP) without sacrificing other important design objectives.

Three papers dealt with the subject of transmission noise. One of these (Ref. 27) discussed the complexity of the analysis. The second paper (Ref. 30) discussed the origins of gear noise. None of the papers gave theoretical or experimental comparisons of noise for various transmissions nor did they present guidelines or approaches for noise reduction and attenuation. The R & D effort needed in this technology area was not well defined.

The subject of gear profile received very little attention. Ref. 26 made only limited comparisons between conformal and involute gears. Several papers briefly discussed integral gear/bearing design, but there was no data given on life, cost, or weight comparisons.

Vulnerability and fail safe, while mentioned as highly desirable and important considerations in design (Ref. 17), were not covered in other papers. Yet vulnerability and safety as indicated (Refs. 34, 35) are the key reasons for the very high cost associated with certification. Health monitoring of transmissions will have to play a much greater role in the future and requires considerably more R & D effort.

As Technical Evaluator of the meeting, I was left with the following general impressions:

(1) the R & D effort in transmissions is evolutionary and not revolutionary.
(2) The level of funding for the R & D effort in transmissions is very low.
(3) Transmission R & D is not receiving the emphasis that it deserves.
(4) The air frame and engine manufacturers view transmissions as an auxiliary and not as a vital link in the system design.
(5) Health monitoring of transmissions must receive considerably more attention.

Thus, transmission R & D is receiving rather low priority. This obviously needs to be corrected in the light of the importance of transmissions and the history and cost of both maintenance and failures.

The papers and discussions at the meeting confirmed my introductory remarks that we are on the threshold of major technological breakthroughs in transmission development. Some of the papers discussed the use of CAD/CAM (Refs. 10, 15, 16). Others mentioned the use of microelectronics for measurements and diagnostics (Refs. 26, 29, 33). The use of composite materials for shafting and transmission casing was also mentioned as offering the twofold advantage of both weight reduction and noise attenuation. In several of the discussions the subject of artificial intelligence for both design and failure analysis was mentioned. The high cost of transmissions, maintenance, and certification clearly indicates the need for more R & D. The reliability and life of transmissions need to be greatly increased.

fretting at the bolted connections. The Thomas type is used on the UH-60 Blackhawk main transmission input, the CH-47 synchronizing shaft, and the OH-58 tail rotor drive. An advantage is that when failure occurs by flexural fatigue in one of the flexible elements, it is easily seen and the failure is progressive so that catastrophic breakage is not the case. So far, the Kaman coupling has been given experimental trials on UH-1's at Ft. Rucker. Based on that experience, the Army is now retrofitting the K flex couplings on UH-1's.

CONCLUDING REMARKS

This has been an overview of some of the current drive train concepts that are used in the U.S. Army helicopters that are flying today. The history of rotary wing aircraft has seen evolutionary change in component technology that has brought in lightweight reliable drive trains. The current concepts have been reviewed for bearings, gears, seals, clutches, materials and overall design arrangements. The implications of materials and treatments have been reviewed. Performance indices such as power to weight relations, efficiency, and reliability have been discussed. Indeed, in the past 30 years several generations of rotary wing aircraft have been brought into the military scene, and it is certainly expected that more refinements and new concepts will be introduced.

Trends for future developments that are expected will be in the areas of improved reliability, quieter drive trains, better materials for high temperature components, better materials for corrosion resistance and high fracture toughness. Mean time between overhaul and/or removal will increase and operating envelopes will be extended in the future as a result of component technology that is being researched, developed, and experimentally verified at the present time. Better design techniques will be brought in with the advent of modern computer analysis techniques that will enable design optimizations to be run by the transmission designers. Finite element analyses will become cheaper and faster to run because of work that is being done on pre- and post-processors that are being developed especially for gears.

It has been the intention of this paper to briefly, review current technology and to provide some background from the U.S. Army's viewpoint for the papers that follow in this symposium. The following papers will add more detail to the topic of drive trains for rotary wing and turboprop aircraft, and the pertinent research and developments that can be factored into the next generation of flying aircraft. Today's, rotary wing aircraft are wonders of technology, and the challenge is to make tommorrow's even better.

REFERENCES

1. Engineering Design Handbook. Helicopter Engineering. Part One. Preliminary Design. AMCP-706-201, US Army Materiel Command, 1974. (AD-A002007).

2. Engineering Design Handbook. Helicopter Engineering. Part Two. Detail Design. AMCP-706-202, US Army Materiel Command, 1976. (AD-A033216).

3. Bamberger, E. N.; Zaretsky, E. V.; and Signer, H.: Endurance and Failure Characteristic of Main-Shaft Jet Engine Bearing at $3x10^6$ DN. J. Lubr. Technol., vol. 98, no. 4, Oct. 1976, pp. 580-585.

4. Binder, S.; and Mack, J. C.: Advanced Technology Applied to the CH-47D Drive System. SAE Paper 781040, Nov. 1978.

5. Zaretsky, Erwin V.; et al.: Effect of Component Differential Hardnesses on Residual Stress and Rolling-Contact Fatigue. NASA TN D-2664, 1965.

6. Zaretsky, Erwin V.; Parker, R. J.; and Anderson, W. J.: Component Hardness Differences and Their Effect on Bearing Fatigue. J. Lub. Technol., vol. 89, no. 1, Jan. 1967, pp. 47-62.

7. Townsend, Dennis P.; and Zaretsky, Erwin V.: Effect of Shot Peening on Surface Fatigue Life or Carburized and Hardened AISI 9310 Spur Gears. NASA TP-2047, 1982.

8. Clevenson, S. A.; Leatherwood, J. D.; and Hollenbaugh, D. D.: Operational Military Helicopter Interior Noise and Vibration Measurements with Comparisons to Ride Quality Criteria. AIAA Paper 83-2526, Oct. 1983.

9. Barber, J. J.: Designing the Quiet Cabin: Noise Needn't Ride Inside, Rotor and Wing International, Oct. 1983, pp. 48-51.

10. Bamberger, E. N.; et al.: Life Adjustments Factors for Ball and Roller Bearings. An Engineering Design Guide. American Society of Mechanical Engineers, 1971.

11. Coy, John J.; Zaretsky, Erwin V.; and Cowgill, Glenn R.: Life Analysis of Restored and Refurbished Bearings, NASA TN D-8486, 1977.

12. Lewicki, D. G.; et al.: Fatique Life Analysis of a Turboprop Reduction Gearbox, AIAA-84-1384, June 1984.

13. Savage, M.; Knorr, R. J., and Coy, J. J.: Life and Reliability Models for Helicopter Transmissions. AHS-RWP-16, Nov. 1982. (NASA TM-82976, ABRADCOM TR 82-C-15)

14. Drago, Raymond J.; and Lenski, Joseph W., Jr.: Developments in the Design, Analysis, and Fabrication of Advanced Technology Transmission Elements, Paper AHS-RWP-12, Nov. 1982.

15. Lemanski, A. J.; Lenski, J. W., Jr.; and Drago, R. J.: Design Fabrication, Test, and Evaluation of Spiral Bevel Support Bearings (Tapered Roller). USAAMRDL-TR-73-16. Boeing Vertol Co., 1973, (AD-769064).

16. Parker, R. J.; and Signer, H. R.: Lubrication of High-Speed, Large Bore Tapered-Roller Bearings, J. Lubr. Technol., vol. 100, no. 1, Jan. 1978, pp. 31-38.

17. Orvos, P. S.; and Dressler, G. J.: Tapered Roller Bearing Development for Aircraft Turbine Engines. AFAPL-TR-79-2007, Timken Co., 1979. (AD-A069440).

18. Parker, R. J.; Pinel, S. I.; and Signer, H. R.: Performance of Computer-Optimized Tapered-Roller Bearings to 2.4 Million DN. J. Lubr. Technol., vol. 103, no. 1, Jan. 1981, pp. 13-20.

19. Kish, Jules G.: Advanced Overrunning Clutch Technology, USAAMRDL TR-77-16, Dec., 1977, (AD-A052635).

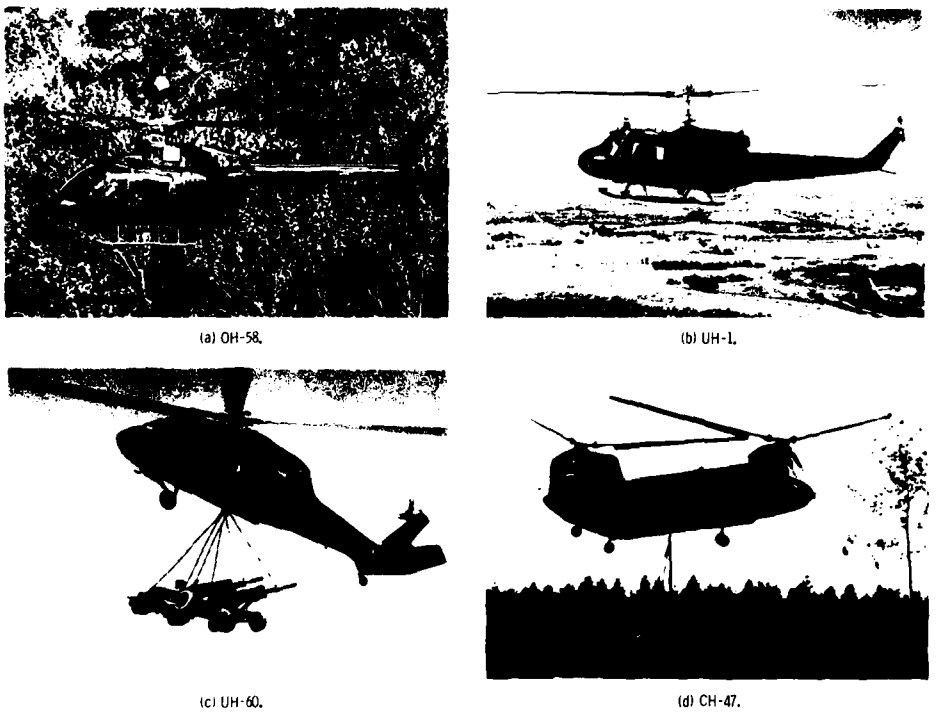
TABLE I. - FATIGUE RESULTS WITH AISI 9310 STANDARD AND SHOT-PEENED TEST GEARS

Gears	10-Percent life, cycles	50-Percent life, cycles	Slope	Failure index[a]	Confidence number,[b] percent
Standard	19×10^6	46×10^6	2.1	18/18	----
Shot peened	30	68	2.1	24/24	83

[a]Indicates number of failures out of total number of tests.
[b]Probability, expressed as a percentage, that the 10-percent life with the baseline AISI 9310 gears is either less than, or greater than, that of the particular lot of gears being considered.

TABLE II. - WEIGHTS FOR CURRENT DRIVE SYSTEMS

Helicopter type	Engines	Drive train			
		Input, hp	Gearboxes rotor shafts, lb	Drive shafts, lb	Total weight, lb
Bell OH-58A "KIOWA"	1-ALLISON 25-C18A	300	153	21	174
Bell UH-1H "HUEY/IROQUIS"	1-LYCOMING T53-L-13	1400	512	66	578
Bell AH-1J "HUEY COBRA"	1-PRATT WHITNEY T400-CP-400	1250	576	69	645
HUGHES AH-64 "APACHE"	2-GENERAL ELECTRIC T700[c]	1900	1175	92	1267
SIKORSKY UH-60 "BLACKHAWK"	2-GENERAL ELECTRIC T700[c]	3000	1368	95	1463
BOEING-VERTOL CH-47C "CHINOOK"	2-LYCOMING T55-L-11[c]	4500	3401	282	3683
BOEING-VERTOL CH-47D "CHINOOK"	2-AVCO LYCOMING T55-L-712[c]	5000	4178	281	4459



(a) OH-58.

(b) UH-1.

(c) UH-60.

(d) CH-47.

Figure 1. - Representative US Army helicopters.

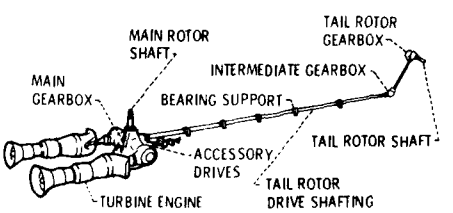
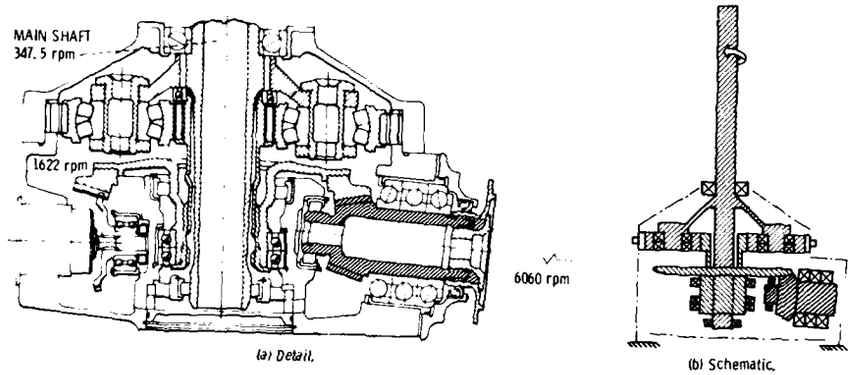


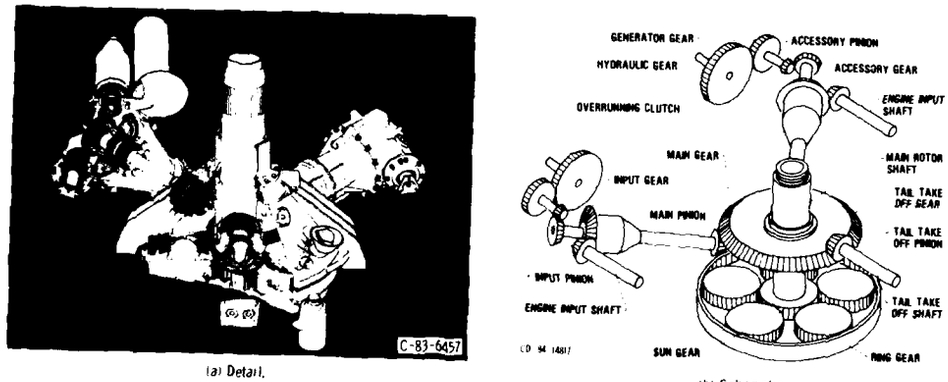
Figure 2. - Typical transmission system in single-rotor helicopter.



(a) Detail.

(b) Schematic.

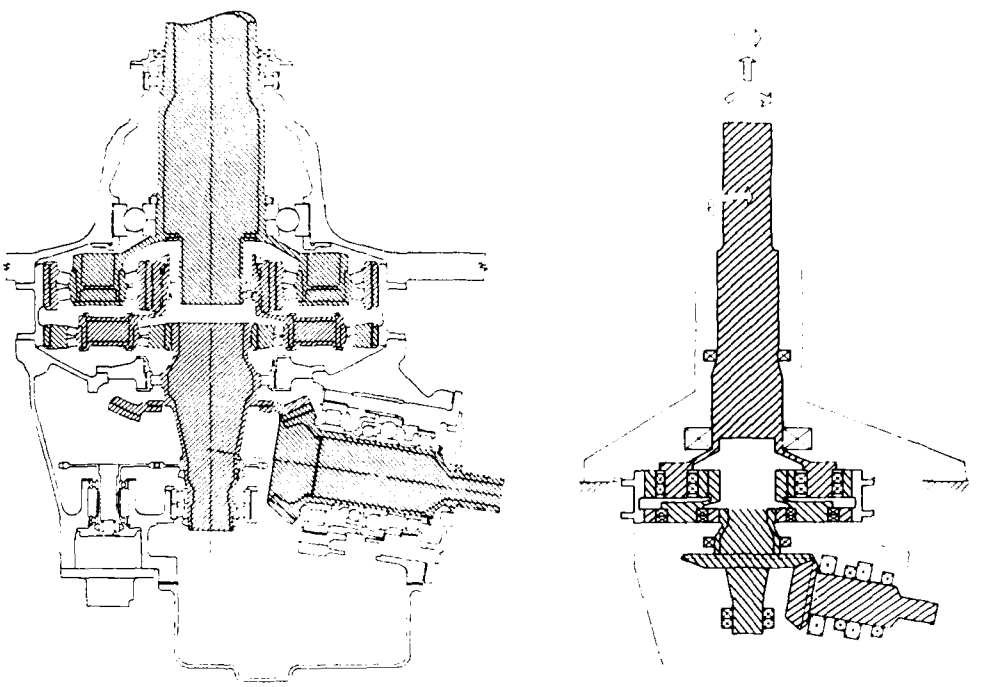
Figure 3. - OH-58 main transmission.



(a) Detail.

(b) Schematic.

Figure 4. - UH-60 Blackhawk main transmission.



(a) Detail

(b) Schematic

Figure 5. CH47 forward transmission.

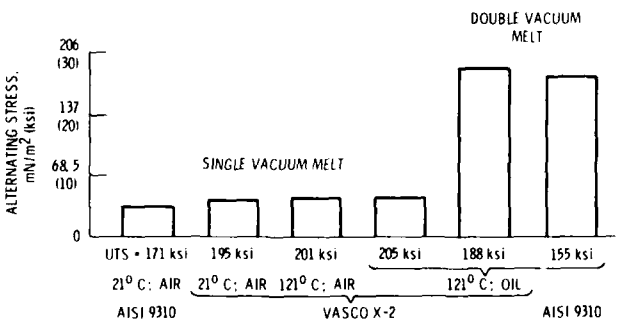
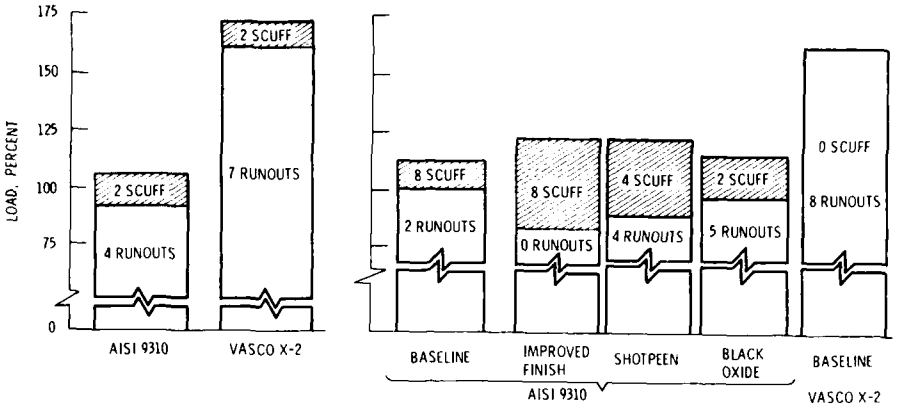


Figure 6. - Effect of multiple remelting (ref. 4).



(a) Spiral bevel test results.

(b) Spur gear test results.

Figure 7. - Scoring and scuffing tests indicate improvement in load capacity (ref. 4).

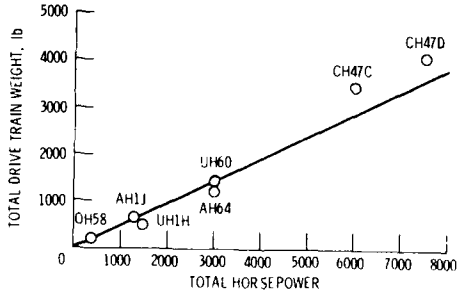


Figure 8. - Weight trends for current helicopter drive trains.

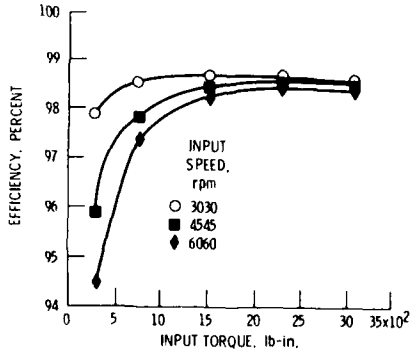


Figure 9. - OH 58 helicopter transmission efficiency, 3-planet assembly, Mobil Jet II (180° F oil inlet).



Figure 10. - Bell Jet Ranger.

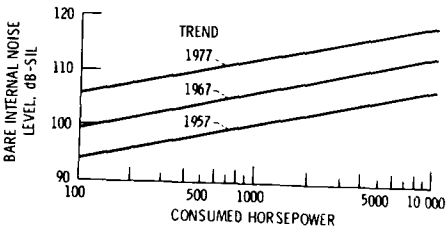


Figure 11. - Transmission noise has increased 6 dB per decade.

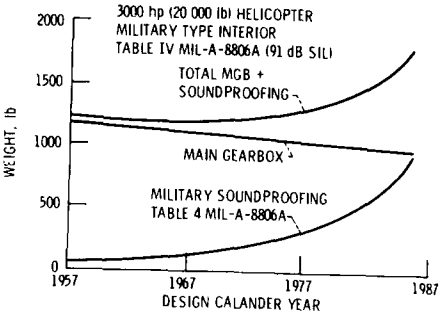


Figure 12. - Gearbox weight technology gain offset by acoustic treatment weight penalty.

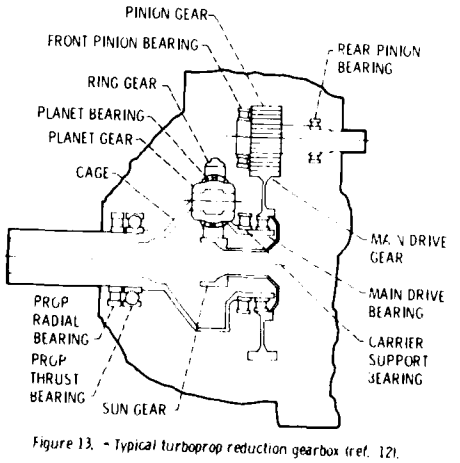


Figure 13. - Typical turboprop reduction gearbox (ref. 12).

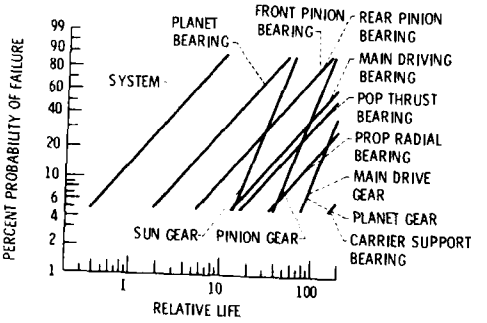


Figure 14. - Calculated theoretical system and component pitting fatigue mission lives (ref. 12).

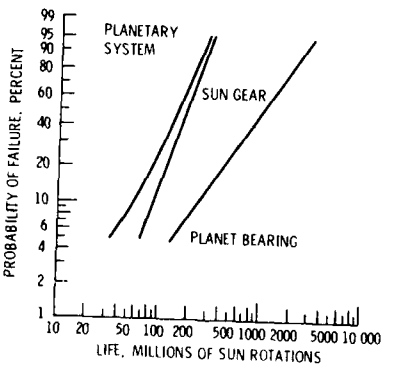


Figure 15. - Calculated theoretical life distributions for planetary drive (ref. 13).

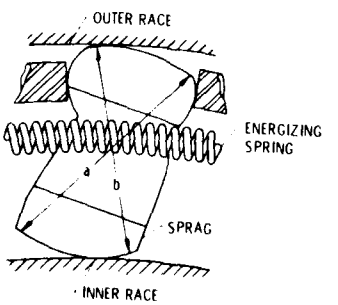
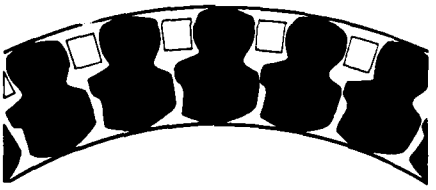


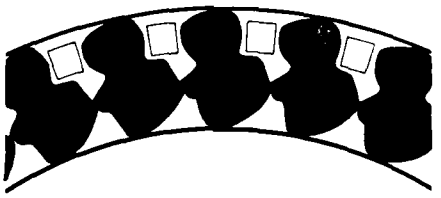
Figure 16. - Sprag overrunning clutch detail (ref. 1).



(a) Normal overrunning position.



(b) Driving under normal load.



(c) Driving with extreme overload.

Figure 17. - Sprags resistant to roll over (ref. 1).

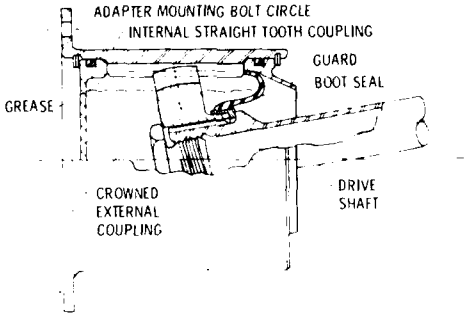


Figure 18. - Gear coupling (ref. 2).

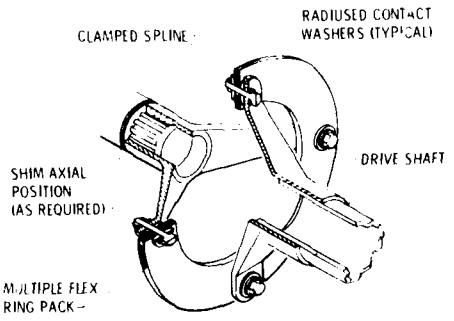


Figure 19. - Typical laminated ring coupling (ref. 1).

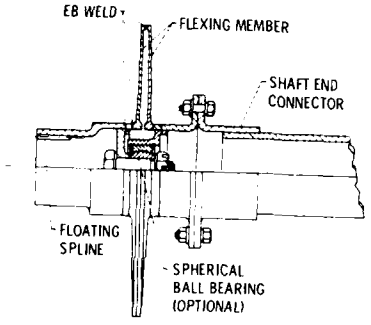


Figure 20. - Typical flexible disk coupling (ref. 1).

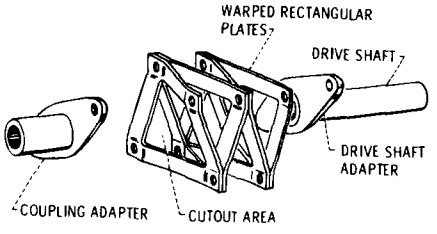


Figure 21. - Kaman Kaflex coupling (ref. 2).

DISCUSSION

A.Watteenuw, Be

1. Are all pinions and internal ring gear shot peened?
2. Are the pinions shot peened on the flanks and in the root?

Author's Reply

1. The current practice with army helicopter has been to shot peen carburized gears and *not* the nitrided gears.
2. The total pinion gear is shot peened. Shot peening is not limited to the tooth.

Rh.Ramette, Fr

How do you measure the noise of the transmission systems, and how do you separate it from the other sources of noise, in particular from the motor noise?

Author's Reply

Noise measurements were made at the main transmission. Measurements were made at several different locations and the noise levels mentioned in the presentation represent the average noise level. There was no attempt to screen out noise contributions from the engine.

SYSTEMES DE TRANSMISSION ACTUELS

R.FRANCOIS, CHEF DU SERVICE D'ETUDE DES TRANSMISSIONS

SOCIETE NATIONALE INDUSTRIELLE AEROSPATIALE

B.P. 13 - 13725 MARIGNANE CEDEX FRANCE

RESUME :

Après une brève description des systèmes de transmission equipant la nouvelle generation d'helicoptères Ecureuil, Dauphin et Super-Puma produite en serie par la Societe Nationale Industrielle Aerospatiale, une analyse comparative des options techniques les plus significatives est faite, mettant en evidence les progrès accomplis dans le domaine de la securité, de la fiabilité et du bruit des réducteurs et transmissions de ces helicoptères :

- Sécurité : La démonstration effective des marges de sécurite est evoquée, ainsi que les systèmes redondants de lubrification de la boite de transmission principale.
- Fiabilité : On montre que, grâce à un effort de simplicite de conception et en faisant appel à des aciers et traitements thermiques plus performants pour les engrenages et roulements, un progrès sensible est obtenu.
- Bruit : Le choix des caracteristiques géométriques des dentures en tenant compte du critère de bruit est commenté.

SYSTEMES DE TRANSMISSION ACTUELS

1. INTRODUCTION

Au cours des 15 dernières années la Société Nationale Industrielle Aérospatiale a renouvelé sa gamme d'hélicoptères légers et moyens, mettant à profit, dans le domaine des transmissions l'expérience acquise sur ses hélicoptères de la génération précédente et les résultats alors disponibles des programmes de recherche et développement.

Nous procéderons en premier lieu à un survol des systèmes de transmission utilisés sur Ecureuil, Dauphin et Super-Puma dont une description de la technologie et des principales caractéristiques sera faite.

Ensuite une analyse comparative mettant en valeur les progrès réalisés dans le domaine de la sécurité, de la fiabilité et du bruit, sera conduite.

2. PRESENTATION DES SYSTEMES DE TRANSMISSION DES HELICOPTERES DE LA NOUVELLE GENERATION

Ecureuil AS.350 monomoteur et bi-moteur AS.355.

Ces 2 hélicoptères ont en commun les éléments de transmission tels que la partie centrale de la boîte de transmission principale (BTP), le tronçon principal de la transmission arrière et la boîte de transmission arrière (BTA).

On notera sur la figure 1 qu'il n'y a pas de boîte de transmission intermédiaire (BTI) et que le ventilateur (repère 10) de refroidissement d'huile moteurs et BTP est entraîné par l'arbre de transmission arrière (repère 9), dans le cas du bi-moteur.

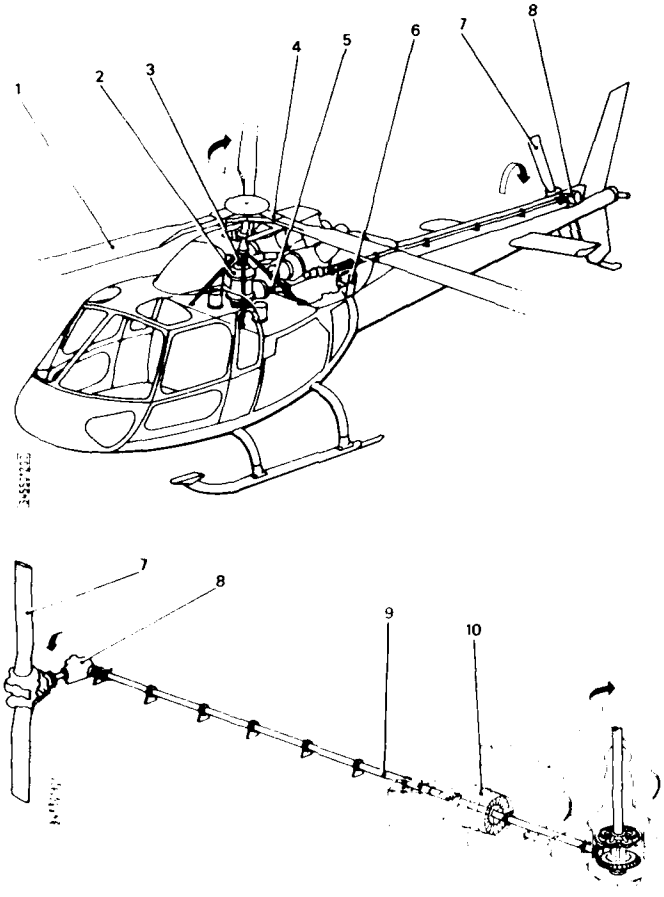


FIGURE 1 - SYSTEME DE TRANSMISSION ECUREUIL AS.350 - 355

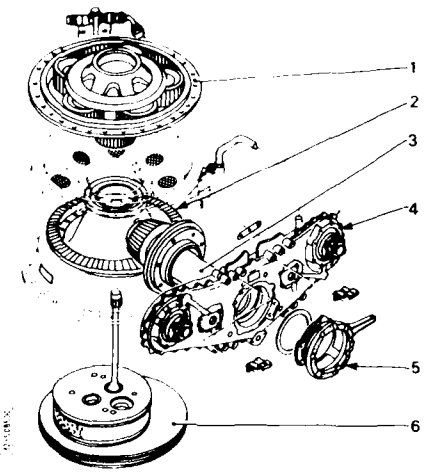


FIGURE 2 - P.T.P. ECUREUIL

La BTP schématisée sur la figure 2, est de conception modulaire : vous noterez les 3 modules, conique (repère 2), épicycloïdal (repère 1), et pompe à huile (repère 6). Le module (repère 4) est un étage d'addition des couples des 2 moteurs et n'est ajouté évidemment que dans la version bi-moteur, il contient 5 pignons hélicoïdaux.

L'arbre de transmission arrière est constitué respectivement de 3 ou 2 tronçons, selon la version bi-moteur ou monomoteur ; le tronçon principal arrière (repère 9) est commun aux 2 versions et se compose d'un tube de section constante en alliage d'aluminium monté sur 6 paliers à roulement. (Voir figure 1)

La BTA (repère 8) est un simple renvoi d'angle (1 couple spiro-conique).

L'arbre de liaison (figure 3 repère 12) entre le(s) moteur(s) et la BTP est contenu dans un tube articulé (repère 11) réalisant un attelage des moteurs à la boîte. Grâce à cette solution, commune aux 3 types d'hélicoptères, la masse des moteurs est associée aux ensembles centraux dans leur mouvement alterne, et participe à la filtration des vibrations induites par le rotor principal.

Tous les accouplements élastiques utilisés sur les arbres de transmission, sont du type flector.

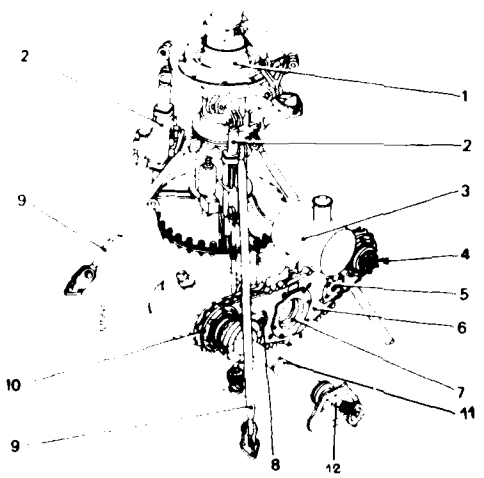


FIGURE 3 - ARBRE DE LIAISON (Repère 12)

Fretting Performance

A third common form of damage in helicopter transmissions is spline fretting. It has been shown by Ku (17) that fretting performance is controlled in part by lubricant composition. Oxidation inhibitor additives have been shown to reduce fretting in splines (18). Interestingly, in helicopter transmission development work, the author has found that an oil with excellent scuff-preventing properties also proved very successful at reducing fretting (5). This may reflect the ability of protective chemical films to form on rubbing surfaces.

The work cited above, by Ku (17) and Newley (18) has demonstrated the effectiveness of spline fretting tests. Such tests could usefully be included in helicopter transmission oil specifications. Not only would this ensure reasonable fretting performance, but it might also generate more research in this very neglected area of the influence of lubricant chemistry on fretting.

NEW LUBRICANTS FOR HELICOPTER TRANSMISSIONS

From a knowledge of the requirements of helicopter transmissions and the limitations of existing oils it is possible to speculate on the broad composition of improved helicopter transmissions lubricants in the future.

Base Stock

Up till now, esters and mineral oils have been the favoured base stocks in helicopter transmissions, for reasons discussed earlier.

It is generally agreed that a maximum viscosity of about 150000cS at -40°F or lower is desirable, to avoid the necessity for changing the lubricant in cold climates. The choice of viscosity at normal running temperatures is more contentious. A low viscosity is more suited to the high speed end of the transmission and vice versa. In previous helicopter oil development work a viscosity of 7½cS at 100°C was selected, based on the viscosity of ENG RD 2487 fluids (5). Currently, somewhat higher viscosities of 8-10cS at 100°C are being evaluated, to increase specific film thicknesses and damping at high temperatures. The above viscosities imply a viscosity index in the range 140 to 150. This, together with low pour point and adequate thermal and hydrostatic stability suggest likely base oils as

- thickened esters
- synthetic hydrocarbons

These are available, well explored and have good additive response. Most pure esters are not viscous enough to meet the 100°C viscosities suggested above. However, if extreme temperature stability is not a target, esters can be thickened with polymeric esters or glycols to give fluids of suitable viscosity.

Additives

Currently, additives in helicopter transmission oils vary depending on the oils' original intended use. Gas turbine oil derived products are based around high temperature stability. They have at least one and often two powerful oxidation inhibitors in high concentrations. Normally included also are small quantities of copper corrosion inhibitor and foam inhibitor. Some anti-wear additives are included, usually quite large concentrations of stable, relatively unreactive phosphorus additives, so as not to destabilize the lubricant at high temperatures. Gear oil derived products by contrast are based about extreme pressure requirements. They tend to contain standardised extreme pressure packages, containing a balanced mixture of sulphur-phosphorus extreme pressure additives, oxidation inhibitors, corrosion, rust and foam inhibitors.

In my view, as explained earlier, future oils are more likely to concentrate of powerful mixtures of phosphorus anti-wear additives, to achieve reliable performance in the range of gears found in a helicopter transmission. If freed from the ultra high temperature stability requirement of gas turbine oils, these would be more reactive and thus powerful than those currently employed in gas turbines. A modicum of extreme pressure additive might also be included. Some oxidation inhibitors are likely to be required, not only for thermal stability but also to improve fretting performance. The same degree of corrosion and foam inhibition as currently found in gas turbine oils is likely to be required.

The possible problem lies in the area of rust inhibitors. A degree of anti-rusting is required in helicopter transmission oils since quite large quantities of water are known, on occasions, to be present in oil. Rust inhibitors have been used in some lubricants for helicopter transmissions (20). It would be highly desirable if the required degree of rust inhibitors could be provided by the base stocks and anti-wear additives. The alternative is to use specially added rust inhibitors, but such additives are commonly found to interfere quite severely with the action of extreme pressure and possibly anti-wear additives. This complicates the whole oil formulation process.

CONCLUSION

This paper has examined briefly the lubricants currently used in helicopter transmissions and has tried to explain their origins and weaknesses. It has concluded that significant performance improvements are likely to be achievable if firstly the requirement for a common engine, transmission oil is lifted and secondly if specialised lubricants are designed specifically for helicopter transmissions. Perhaps we shall see the day when a "common" helicopter oil means a tailor-made transmission oil common to both of NATO helicopters rather than one shared between engine and transmission.

The benefits of lubricant improvements should be to increase TBO's and generally to meet the existing requirements of the generation of helicopters now entering production. A likely reason for

The standard gear tests such as the IAE or Ryder have fewer limitations than simple [illegible] tests, but even they do not usually overcome (c) and (d) above, though some gear tests permit a step-wise increase of load during running. However gear tests are not suited to innovative lubricant development work since tests are both costly and, due to inevitable variations in gear profile, give results with high scatter.

It is thus the author's view that for the continuously severe conditions found in helicopter transmissions, more emphasis needs to be put on lubricants which prevent scuffing in an "anti-wear" manner than on those that recover from a scuff by an "extreme pressure" response. A further implication is that the successful design of such lubricants requires a test sequence closer to the metallurgy and operating conditions found in helicopter transmissions than standard gear oil tests provide.

A sequence of tests used by the author [4] is that shown in Figure 1. It has, effectively, three levels of scuffing test depending on the level of realism and cost appropriate. The simplest level uses a four-ball type of rotating arrangement but employs specimens of the intended gear steel immersed in test lubricant. Such specimens are most conveniently made from bar and are generally not available as balls. This implies a crossed cylinders geometry to give a simple non-conforming contact. The actual cone and cylinder arrangement used, shown in Figure 2, is a variant on crossed cylinders, arranged for ease of support and alignment. The upper cone is rotated against the lower cylinders.

The test procedure involves successively increasing load in stages without halting the rig whilst continuously monitoring friction. Bulk temperature can be controlled and the lubricant jet insulated when required. Typical friction traces are shown in Figure 3. Both initial seizure and, at a later stage, final seizure performance can be gauged

This type of test has been shown to grade helicopter lubricant scuffing performance, in a similar order to disc machine tests for a range of lubricants and operating temperatures. It has proved valuable in screening work in the early stages of helicopter transmission oil development and also in providing rapid assessment of candidate oils for helicopter use.

The next stage of testing, giving more realism at approximately 15 times the cost, uses a scuffing disc machine. Here two discs of the intended gear steel are hydraulically loaded and run under a slide-roll ratio appropriate to the gears being modelled. Oil temperature is controlled and, again, the load is increased in stages and friction monitored until scuffing occurs. Friction traces very similar in form to those in figure 3 are obtained.

This type of test has been shown to correlate with helicopter gearbox tests and has proved useful as an intermediate proving stage in lubricant development and also to explore the response of helicopter lubricants to temperature, etc (10).

The highest level of testing involves a four square test stand with a tail rotor helicopter gear box. This is clearly the most realistic stage, but tests cost approximately 10 times those of the disc machine.

It should be noted that at each stage conditions are such as to ensure that realistic scuffing performance as discussed above can be measured i.e.

(i) Gear steels of the appropriate metallurgy are used
(ii) The test temperature is controlled at an appropriate level
(iii) The tests are continuous and of reasonable duration thus allowing lubricant chemical films to develop, where possible, before scuffing conditions are reached.

Contact Fatigue Performance

A lubricant can influence pitting in at least three different ways. Firstly the viscosity and the pressure viscosity coefficient of the lubricant determine the specific film thickness, i.e. the ratio of EHD film thickness to composite surface roughness. Fatigue life is critically depended on specific film thickness (11). As well as this, however, different base stocks and additives have also been shown to influence fatigue lives independently of EHD film thickness (12) (13). No specific guidelines have yet emerged. It is the author's experience that "anti-wear" type lubricants, that form protective scuff-preventing films on surfaces tend also to extend fatigue life. Extreme pressure additives, which react only in emergencies and which are corrosive might be considered as far less likely to inhibit fatigue. It has been shown that the friction or traction properties of helicopter gear lubricants can vary quite widely (4), but this has not yet been related to fatigue performance.

A third way in which lubricants may influence fatigue is by containing dissolved water. Very small amounts of dissolved water, less than 0.01% have been shown to cause dramatic reductions in fatigue life (14). Some synthetic lubricants such as esters and polyglycols dissolve at least ten times as much water as hydrocarbon oils under similar conditions. There is as yet insufficient work to indicate whether this is likely to be important in practice, though work is proceeding.

Since gear pitting is one of the more common forms of damage in helicopter transmissions it would appear suprising that pitting tests so rarely form part of helicopter lubricant specifications. Disc machines have been used successfully to test for the pitting performance of helicopter lubricants at an intermediate stage of oil development and the results obtained correlated well with helicopter gear box tests (5). The influence of vibration and filtration on pitting using gear steels has also been investigated using disc machines (15) (16). The superior repeatibility and economy of such disc machine tests compared to gear tests might well make them suitable in type approval tests for pitting resistant helicopter gear oils.

HELICOPTER TRANSMISSION LUBRICANT PERFORMANCE

A major problem both in developing and in assessing helicopter transmission lubricants, and one that needs to be overcome before new lubricants can be designed, is the lack of suitable testing procedures for scuffing, pitting, and fretting.

This paucity can be seen by examining typical helicopter lubricating oil specifications. Thus even recent gas turbine oils such as MIL-L-23699B and ENG RD 2497 each contain only a single relatively undemanding gear oil load carrying test. No pitting or fretting assessment is required at all. Similarly the only quality assurance test demanded of DTD 5810 lubricants, referred to in Table 1, is a mean Hertz load 4-ball test.

In this section the ways in which helicopter lubricants can control scuffing, pitting and fretting will be discussed, and reference will be made to how these properties can be measured.

Scuffing Performance

The scuffing performance of helicopter gear lubricants, like other gear oils, is controlled by the inclusion of additives which react with hot, rubbed steel surfaces. Without such reactions, heavily loaded gears with significant sliding would scuff very rapidly.

Two anti-scuff additives are commonly differentiated, "extreme pressure" and "anti-wear" additives and both are to be found in oils currently used in helicopter transmissions. The distinction is somewhat arbitrary and diffuse, but broadly speaking extreme pressure additives react by checking the development of incipient scuffing whereas anti-wear additives prevent scuffing from arising at all.

Extreme pressure additives are chosen to react very quickly with the torn and excessively hot metal surfaces produced when scuffing begins. The resultant reacted layer is significantly abraded but, being weak, friction is lowered and the process of scuffing is checked at the expense of heavy wear. This type of scuffing resistance is directly measured in 4-ball tests, which rub a series of metal samples together at a succession of loads for short periods, to find the maximum load survivable without welding. Those helicopter gear lubricants which derive from automotive or industrial gear oils normally contain extreme pressure additives.

Anti-wear additives, by contrast, are designed to build up a protective low friction film on rubbing surfaces under normal running conditions. Because these films are not high iron content corrosion products they do not result in significant loss of sliding material - hence anti-wear. Although such steady film formation at normal operating temperatures is traditionally named "anti-wear" it can also be very effective in raising the scuffing load of a gear system. It has been known for sometime that quite thick chemical films grow on rubbed surfaces (6),(7),(8) but recent work suggests that these may be more substantial and protective than previously recognised (9). Helicopter lubricants derived from gas turbine oils tend to contain anti-wear additives. Extreme pressure additives would destabilise the lubricant and cause excessive corrosion at the high temperatures prevelant in an engine.

Gear lubricants are normally developed using a combination of simple, standardised scuffing tests such as the 4-ball or Timken test for screening work, followed by gear rig tests such as the IAE , FZG or Ryder at later stages of development. It makes some sense to develop a helicopter lubricant for good scuffing performance in the first instance, even if pitting is a commoner mode of failure in practice. There is no doubt that helicopter transmissions often operate close to their scuffing limit. Also scuffing tests are quickly and easily carried out in screening work, whereas pitting tests are time consuming and show high scatter. It is also the author's experience that a lubricant with good antiscuff performance in gears tends to show good contact fatigue properties (5).

A problem with screening tests for scuffing when applied to helicopter oils is that most such tests were designed to measure the scuffing resistance of automotive hypoid gears and thus tend to concentrate on the extreme pressure type of scuffing prevention outlined above.

The use of 4-ball and most other simple tests has, thus in the authors opinion, tended to lead to the development of gear oils with extreme pressure characteristics, i.e. the ability to survive the immediate application of extremely high sliding loads by a process of recovery from incipient scuffing.

This may be appropriate to the negligible oil film thickness, low speed-high torque conditions of an automotive hypoid gear but is less so to the continously demanding, high load, mixed EHD regimes of a helicopter transmission. What is really needed for these systems are scuff-preventing, anti-wear type films. Most simple scuffing tests do not adequately measure the ability of a lubricant to develop such scuff-preventing films since:

(a) the tests last too short a time (15 seconds for 4-ball test)
(b) they often start immediately from a high load situation, which is too severe for such films to start to develop
(c) the bulk temperatures used are often not sufficiently high
(d) the metallurgy used is unrealistic of the gears for which the lubricant is intended

The latter two points are important since it appears that the formation of protective anti-wear or "scuff-preventing" films is more sensitive to bulk temperature and metal type than normal extreme pressure reactions, where the enormously high surface temperatures formed after scuffing starts overwhelm anything else.

Some wear tests use extended runs at controlled temperatures, fulfilling some of the requirements listed above, but they tend not to explore the scuffing limits of lubricants, but rather to stay at a single, lower load.

From the operational point of view, a requirement, common to aircraft and helicopters, is that the helicopter lubricant must be effective over a wide range of external temperatures, from -40°C to +120°C. A final constraint often imposed for logistic convenience is that the oil be common to both gas turbine engine and transmission. Military operators prefer a common oil, and, where possible, this has been achieved.

The operating constraints outlined above are, to a great extent, contradictory in the demands that they put on the lubricant.

The high and low speed ends of the transmission impose rather different requirements. A high speed transmission able to cope with a wide temperature range suggests a low pour point, high VI fluid with moderately low viscosity at 100°C to reduce churning losses and to ensure provision of the lubrication where required. However low speeds, high tooth stresses indicate a viscous oil, capable of generating an EHD film between gear teeth even at low speeds. Such an oil will also provide a degree of vibration damping. For the transmission generally, a high degree of chemical activity is implied, to provide the required boundary lubrication involved in a low specific film thickness, heavily loaded, high sliding system with probable misalignment.

Far more contradictory than the demands of the different parts of the transmission system, however, is the clash between gas turbine engine and transmission requirements. Gas turbine oils are necessarily low viscosity, very chemically stable products, able to cope with the extremely high temperatures in the engine without coking or other degradation. Their intrinsic boundary lubrication needs are small which is just as well since the addition of active anti-wear and extreme pressure additives generally tend to limit high temperature stability. By contrast low speed, heavily loaded transmissions need both high viscosity and reactive additives to cope with the mixed EHD-boundary lubrication conditions involved.

The features of an oil which will meet the requirements for a transmission system as outlined above will be discussed later, but it should be noted that the oils listed in Table 1, and currently used to lubricate helicopters, are not ideal. The mineral oils do not meet the required low temperature characteristics, 8cS at 100°C implying a minimum operating temperature of -30°C and 17.5cS a minimum temperature of -15°C. In the case of the heavier oil this means, in practice, change to a lighter oil for cold conditions which is a most undesirable feature. Also the additive packages used in conventional gear-box lubricants do not provide continuous protection over the intermediate 80°C to 90°C bulk oil temperature range often found in helicopter transmissions (3).

The esters have low viscosities and tend to give low EHD film thicknesses. This is compensated for, to some extent, by anti-wear additives and one or two commercial products are quite effective (3). Unfortunately those products which give the best transmission performance tend to give the most problems in engines, due to the trade-off between chemical reactivity and stability.

It should be clear from the above that the helicopter lubricants currently used do not match the specific requirements of helicopter transmissions. Clearly they work, or helicopters would not fly, but the inadequacies of existing helicopter lubricants is illustrated by generally low TBO's (3), with life limited usually by either bearing failure or gear pitting. Micropitting is frequently found at overhaul and, less frequently, scuffing. Further evidence that current helicopter lubricants are operating near their limits is their tendency to scuff when other transmission problems arise. These inadequacies, in the author's view, reflect the use of oils developed for other purposes, which have not been designed to the particular needs of helicopter transmissions.

As well as low TBO's and extensive replacement at overhaul, a secondary effect of using indifferent lubricants is the barrier it puts on new transmission design. There is a natural reluctance to design for higher stresses or gearbox temperatures when it is recognised that current lubricants are already close to the limits of their performance.

It is the author's opinion that substantial improvements in helicopter transmission lubricants can be made, but only if

(i) The necessity for a common engine, transmission oil is discarded
(ii) Lubricants are designed specifically for helicopter transmission systems rather than merely being modified from existing lubricants.

The requirement of a common oil is not actually widely observed, but is ingrained deep in UK and, particularly US military thought. One reason for this is the apparent success of the common engine/transmission oil, MIL-L-2104C in military vehicles. It is the contention of the author that gas turbine and helicopter requirements are so different that the inevitable weaknesses of a common oil outweigh the advantages of commonality.

The advantages of a separate, specially designed helicopter transmission lubricant were first recognised in the UK some twelve years ago and, with the support of the Ministry of Defence, have led to the development of an experimental helicopter transmission lubricant (5). Some of the thinking and method involved in this development will be discussed later in this paper. Significantly, during the last 18 months a similar development program has been initiated in the US.

It is unsuprising that such initiatives have come from the Services and from helicopter manufacturers rather than from lubricant suppliers. The small quantities of oil involved coupled with the very high costs of lubricant validation in helicopters makes the development work involved unappetising for the major oil companies.

HELICOPTER TRANSMISSION LUBRICANTS

by
H.A. Spikes
Tribology Section
Department of Mechanical Engineering
Imperial College
Exhibition Road
London, SW7 2BX

SUMMARY

This paper outlines the problems associated with the lubrication of helicopter transmissions. It then discusses how helicopter lubricants are likely to change over the next decade.

For many years, helicopter transmission reliability has suffered both in the UK and the USA from the requirement that the oil be common to both the transmission and the gas turbine. In practice, certainly in the UK, most helicopters do not, in fact, use a common oil. The UK helicopter industry is in sympathy with the logistic advantages of minimizing the number of oils stocked but feels that this could be more successfully achieved by adopting a single transmission oil for all NATO helicopters. It now appears that this is now being considered as a practical alternative on both sides of the Atlantic. In the UK, the MOD has funded the successful development of a helicopter transmission oil in anticipation of such a move. The USA after many years of being antagonistic towards separate gearbox and engine lubricants is about to embark on a relevant oil development program.

Another likely change over the next few years is the move towards a higher temperature transmission oil, as the amount of external cooling is progressively removed. The British helicopter industry, supported by the MOD is actively engaged in developing new oils to meet this requirement.

INTRODUCTION

The last 30 years has seen the use of a wide variety of helicopter transmission lubricants. The earliest types of helicopter in this period were powered with piston engines and thus generally employed a mineral oil-based piston engine oil in their transmission systems (1).

The introduction of gas turbines in the late 1950's led to a considerable degree of divergence. Some helicopters adopted a common gas turbine engine, transmission oil. They thus used mineral oil, and later, synthetic type I ester-based gas turbine oils in both engine and transmission. Others continued to employ mineral oil-based gear lubricants but, with the piston engine compatability lifted, were able to choose from a wider viscosity range.

Problems of oil loss in combat conditions in the late 1960's led to the development of greases for consideration as transmission lubricants in small, non-circulating gear boxes (2). These greases did not, however, become at all widely used. In the 1960's high performance gas turbines were introduced, the operating temperatures of which required the use of 5cS hindered ester gas turbine oils. In some helicopters these lubricants were made common to both engine and transmission systems. Recently 3cS gas turbine oils have been used by French operators in a few gearboxes (3).

There is thus now an enormous diversity of helicopter lubricants in use. Table 1 shows the lubricants currently employed in the transmissions of just one UK based helicopter manufacturer (3).

A feature of all the oils listed in Table 1, and similar lists compiled by other authors (4), is that none has been specifically developed with a helicopter transmission in mind. As shown in Table 1, all were designed initially for a different role and were later adopted in helicopter transmissions with, at the most, minor modifications. There are, broadly, two types, conventional mineral oil-based gear lubricants and ester-based gas turbine oils.

This paper examines the problems associated with helicopter transmission lubricants and relates these problems to the rather ad-hoc way in which helicopter transmission lubricants have derived. It suggests how the situation is changing and looks forward to specifically designed and improved helicopter lubricants.

REQUIREMENTS OF HELICOPTER TRANSMISSION LUBRICANTS

Helicopter transmissions provide particularly exacting conditions as far as the lubricant is concerned. Overall weight control in helicopters is stringent, which means, firstly, that transmission power/mass ratios are high while, secondly, the structure in which the transmission is supported is quite flexible. Localised tooth stresses are thus severe, variable and somewhat unpredictable. Some degree of misalignment is inevitable.

Another feature of helicopter transmissions is that the overall reduction ratio is large, approaching 100 to 1. Typical reductions are from 20000rpm to 600rpm although sometimes the 1st stage reduction is in the engine. Such a wide range of speed conditions would ideally be met by using more than one lubricant, but this is not generally a practicable solution. The use of [illegible] gears in some helicopters has led to continuous high sliding speeds in the [illegible]. Typical gear-box temperatures are 70 to 90°C, but reach 130°C in warmer climates.

A insonorisation égale, la prise en compte de l'objectif de réduction du bruit dès la conception de la BTP a permis, sans aucun doute, de rendre la gêne auditive des passagers moins grande sur les hélicoptères de nouvelle génération. Le résultat suivant en témoigne : dans la cabine de l'Ecureuil faiblement insonorisée, le niveau de bruit est de 79 dB SIL en vol de croisière et de 73 dB SIL en vol stationnaire.

5. CONCLUSION

Au cours des dix dernières années, la conception des systèmes de transmission a connu une évolution favorable se traduisant sur la nouvelle famille d'hélicoptères que l'Aérospatiale a mis en service, par une plus grande sécurité, une fiabilité accrue et une amélioration du confort. Les résultats des travaux actuels de recherche laissent déjà présager que d'autres progrès interviendront dans ces domaines.

DISCUSSION

J.Godston, US

You mentioned that synthetic oils are used in your transmission systems. Why?

Is the oil (lubrication system) separate from the motor and from the engine?

What will be the future for synthetic oils if, in fact, the systems are separated?

Author's Reply

1. Why do we utilize synthetic oils in the transmission system?
   The synthetic oils are utilized because they are available everywhere in the world. In addition, they have the qualities required in turbine oils (stable, with unstable temperatures from $-40°C$ to $+50°C$). But, they also have their defects: their weak load capacity in gear mesh and rolling element applications. From this point of view, mineral oils with additives are much better for transmission boxes.

   It will be desirable for the future to develop a synthetic oil which combines the qualities of good stability and good load capacity.

2. Are separate lubrication systems used for the transmission boxes and the motor?
   Yes, for reasons of security and accessibility.

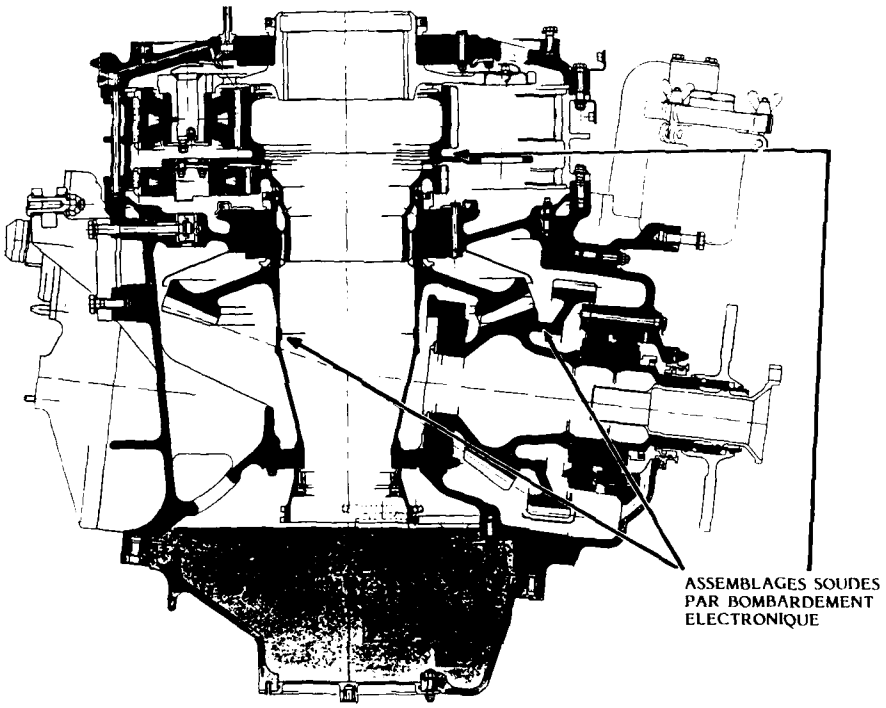


FIGURE 12 - B.T.P. SUPER-PUMA

La figure 12 est un exemple significatif de recherche de réduction du nombre d'assemblages majeurs par boulons et pions de cisaillement, appliqué à la BTP Super-Puma. Par rapport à la BTP Puma d'architecture similaire, 3 liaisons ont été supprimées grâce à l'utilisation de la soudure par faisceaux d'électrons. Ce procédé est maintenant bien maîtrisé et permet des soudures dont l'épaisseur peut atteindre 10 mm dans des zones chargées.

Cette solution apporte un gain de masse important par rapport aux types classiques de liaison, en plus d'une amélioration incontestable de la fiabilité en service.

En ce qui concerne les engrenages et les roulements, leur fiabilité prévisionnelle a été améliorée dès la conception, par une baisse volontaire des charges, et par l'emploi de l'acier M50 VIM VAR pour certains roulements, et de l'acier nitruré 32 CDV 13 plus pour certains engrenages.

Ces aciers apportent une augmentation importante de la durée de vie B10 des roulements (facteur en vigueur à AS : 3), et de la résistance aux avaries superficielles des dentures (pression de Hertz maxi admissible améliorée de 20 %). La combinaison de la réduction des charges et de l'emploi de matériaux plus performants évite la perte de masse.

4.3. Bruit

Depuis plus de 10 ans une importance croissante est accordée à la réduction du bruit interne ; il est généré en partie par la BTP dont certains engrènements produisent des raies assez peu filtrées 500 à 3000 Hz dans leur cheminement jusqu'à la cabine, lorsqu'il n'y a pas d'insonorisation additionnelle.

Les caractéristiques des engrènements et plus particulièrement celles des couples spiro-coniques des BTP Ecureuil, Dauphin et Super-Puma, ont été choisies de telle sorte que les rapports de recouvrement soient largement supérieurs à 2. Nous avons ainsi obtenu une réduction sensible des émergences sonores. Par ailleurs un résultat favorable a été atteint récemment sur Dauphin grâce à la mise en service d'une denture de train epicycloïdal dont le rapport de conduite est supérieur à 2.

FIGURE 10 - COMPARAISON DES CHAINES CINEMATIQUES ECUREUIL ET ALOUETTE

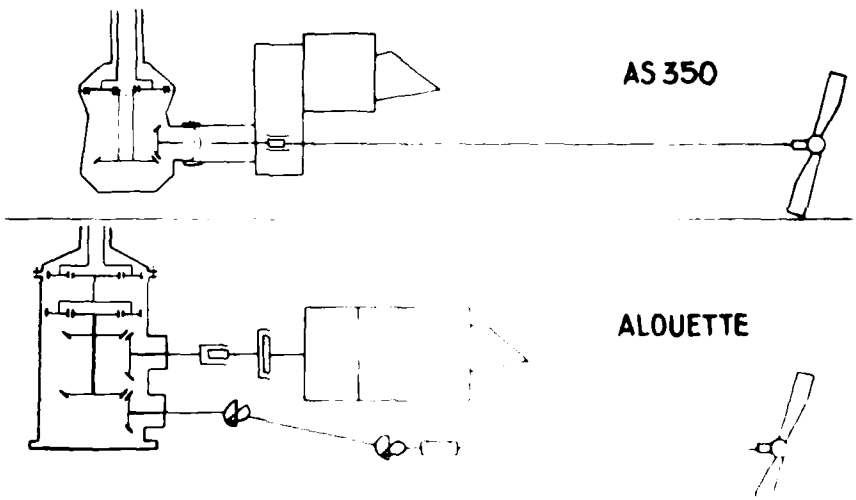
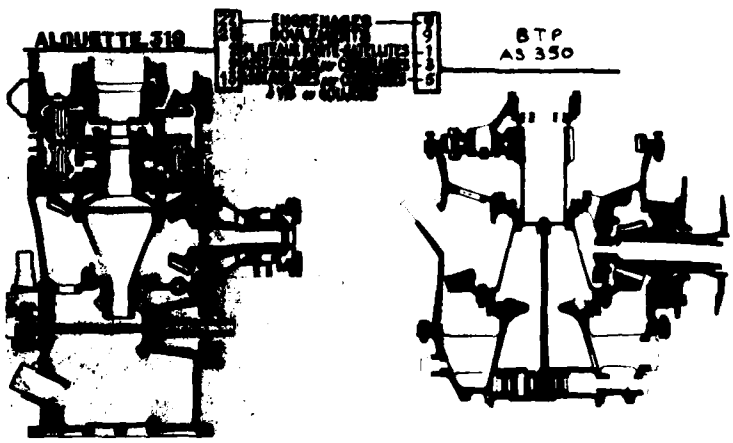


FIGURE 11 - B.T.P. - COMPARAISON DU NOMBRE D'ELEMENTS PRINCIPAUX



Il comporte notamment 2 pompes, l'une alimentant le circuit de refroidissement, l'autre alimente un circuit restant à l'intérieur de la BTP et qui rejoint directement le filtre d'entrée BTP sans passer par un échangeur de refroidissement.

En fonctionnement normal la pompe de secours n'alimente pas le circuit de graissage, du fait d'un clapet anti-retour installé dans le filtre et de la supériorité de la pression délivrée par le circuit principal, de l'autre côté de ce clapet.

Le niveau d'aspiration de l'huile dans le fond de boite est plus bas pour la pompe de secours que pour la pompe principale.

Un système d'obturation commandé par la pression de sortie de la pompe principale est monté à l'entrée de la pompe de secours, et ouvre l'aspiration de celle-ci en cas de baisse de pression sur le circuit principal.

Ce double circuit couvre, de par sa conception et ses moyens de surveillance (Voir figure 9), les cas de pannes suivants :

- panne de pompe principale ou secours
- fuite d'huile sur le circuit extérieur de refroidissement
- fuite d'huile lente aux joints dynamiques de la BTP.

Dans tous les cas, sauf la panne de pompe de secours, on perd le refroidissement par échangeur.
Nous avons démontré sur un banc avec rotors que cette perte ne remet pas en cause le bon fonctionnement de la boite pendant 5 heures au moins, malgré la température assez élevée atteinte par l'huile (200 à 250°C). Par ailleurs, il se trouve que pendant cet essai de simulation, une fuite d'huile aux joint dynamique d'une entrée grande vitesse s'est produite, entrainant une chute progressive de la pression BTP, du fait de la perte d'huile. Ceci n'a pas compromis le fonctionnement et a rendu l'essai encore plus démonstratif de la tolérance du système de lubrification aux divers cas de pannes.

Un résultat tout aussi favorable a été obtenu sur un hélicoptère Dauphin attaché au sol.

Il est clair que ces doubles circuits de lubrification apportent un avantage important par rapport aux BTP d'hélicoptères de l'ancienne génération dont les circuits sont uniques. Néanmoins, le cas de panne le plus sévère de perte totale d'huile n'est pas couvert.

Nous nous sommes souciés de cette panne dès la conception des différentes BTP en utilisant notamment pour la fabrication des engrenages et roulements les plus critiques, des aciers et traitements thermiques dont les caractéristiques mécaniques sont conservées pour des températures élevées :

- 500°C pour les engrenages nitrurés en acier 32 CDV13
- 400°C pour les roulements en acier rapide M50 VIM VAR.

Ces matériaux ont apporté une amélioration sensible : les essais de simulation de perte d'huile ont donné d'excellents résultats, le meilleur ayant été obtenu sur BTP Ecureuil bi-moteur : elle a fonctionné correctement pendant 2 heures sans huile.

Dans ce cas extrême comme pour les autres défaillances évoquées précédemment, on peut mesurer le progrès significatif accompli.

4.2. Fiabilité

Les éléments déterminant en grande partie la fiabilité d'une BTP sont : les roulements, les engrenages, les liaisons par cannelures ou boulonnées et les joints d'étanchéité dynamique. Alors que, pour ces derniers, on peut généralement tolérer une performance médiocre car l'échange de joint est faisable sans dépose de la boite, la défaillance des autres éléments est beaucoup plus pénalisante car elle implique bien souvent une dépose prématurée de la BTP.

Lors de la conception des BTP de la nouvelle génération, nous avons considérablement favorisé l'objectif de fiabilité en recherchant la simplicité par la réduction du nombre d'ensembles mécaniques, de roulements, d'engrenages et de liaisons, et en adoptant des matériaux et traitements plus performants pour les engrenages et les roulements.

L'architecture du système de transmission de l'Ecureuil AS.350 (figure 10) et la BTP sont 2 exemples illustrant notre recherche de simplicité. On note en comparaison avec l'Alouette que dans la chaine cinématique Ecureuil il n'y a pas d'embrayage, ni arbre de transmission arrière à cardan, ni couple conique de renvoi arrière dans la BTP.

Le nombre de pièces majeures et assemblages est 2,5 fois plus faible dans une BTP Ecureuil, en comparaison avec la boite Alouette (Voir figure 11).

4. LES PROGRES REALISES PAR RAPPORT A LA GENERATION PRECEDENTE D'HELICOPTERES

4.1. Sécurité

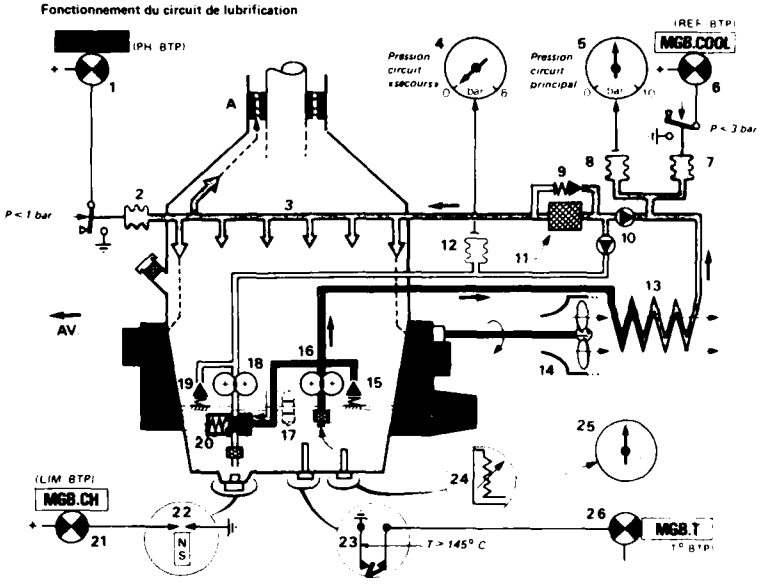
Nous savons tous que la fonction remplie par les systèmes de transmission est vitale à divers degrés et implique que les marges de sécurité soient parfaitement maîtrisées, en ce qui concerne les engrenages et les arbres de transmission .

Dans ce but toutes les boîtes décrites précédemment ont été soumises à des essais de fatigue sur bancs de mise en charge, à un niveau de puissance égal à 1,4 fois la puissance maxi en utilisation bi-moteur et monomoteur, pour une durée correspondant à 2 mégacycles sur le pignon le plus lent.

Les arbres de puissance et les porte-satellites des trains épicycloïdaux ont eux aussi été soumis à des essais de fatigue vibratoire et/ou temporaire, justifiant des marges de sécurité de 2 par rapport à la limite de fatigue moyenne.

Il est tout aussi notoire pour des spécialistes que la sécurité est mise en cause assez rapidement par la défaillance du système de lubrification de la BTP.

La figure 9 montre le double circuit de lubrification de la BTP Super-Puma. Un système semblable a été développé pour la BTP Dauphin.



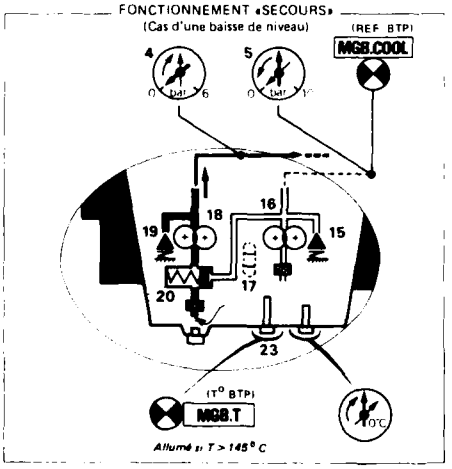


FIGURE 9 - DOUBLE CIRCUIT DE LUBRIFICATION SUPER-PUMA

Les figures 7 et 8 illustrent le système de transmission du *Super-Puma AS.332* et l'architecture interne de la BTP.

On remarque que les moteurs sont devant la BTP et entraînent directement la boîte à la vitesse de rotation de la turbine libre 22840 t/mn.

Après le premier étage cylindrique hélicoïdal "haute vitesse", sont placées les roues libres, puis l'étage cylindrique hélicoïdal d'addition des 2 couples moteurs.

On trouve ensuite dans la chaîne commune, un couple spiro-conique Gleason et 2 étages épicycloïdaux à couronne fixe.

Le porte-satellites du 2ème étage entraîne l'arbre rotor principal.

On note aussi 2 pompes de lubrification au fond de la boîte qui fait office de réservoir d'huile.

Deux tables accessoires droite et gauche sont placées à l'arrière et assurent l'entraînement des pompes hydrauliques, alternateurs et ventilateur de refroidissement d'huile BTP.

Cette boîte peut être équipée sur la chaîne gauche d'un système original de décrabotage modifiant la fonction roue libre et autorisant ainsi la rotation du moteur et des accessoires gauches sans entraînement des rotors.

La roue d'addition des couples moteurs entraîne directement l'arbre horizontal de transmission arrière.
Une boîte de transmission intermédiaire et une BTA assurent ensuite les changements de la direction et de la vitesse de rotation, nécessaires à l'entraînement du rotor arrière.

L'arbre de transmission arrière est constitué de 8 tronçons (7 horizontaux et 1 oblique) séparés entre eux par des accouplements flexibles type "flector".

Le système de liaison entre la boîte et les moteurs est conçu suivant le même principe que ceux du Dauphin et de l'Écureuil (tube anticouple articulé), les accouplements flexibles, situés à la sortie moteur et à l'entrée BTP sont à diaphragmes.

3. RECAPITULATIF DES CARACTERISTIQUES PRINCIPALES DES TRANSMISSIONS

HELICOPTERE	MASSE MAXI KG	Puissance maxi à l'entrée BTP KW	Vitesses t/mn — Entrée BTP		Rapport de réduction moteur/rotor principal	Nombre d'étages de réduction BTP	MASSE BTP KG
			Rotor principal	Rotor arrière			
ECUREUIL AS.350 MONOMOTEUR	1900	395	6000		15,5	2	68
			386	2043			
ECUREUIL AS.355 BI-MOTEUR	2400	480	6016		15,3	3	105
			394	2088			
DAUPHIN AS 365N	4000	970	6000		17,1	3	190
			350	4706			
SUPER-PUMA AS.332	8600	2250	22841		86,2	5	330
			265	1280			

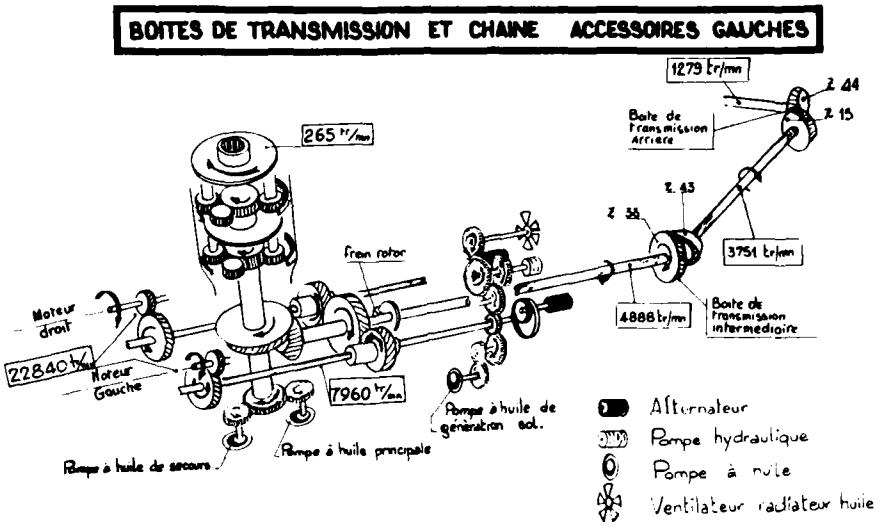


FIGURE 7 - CHAINE CINEMATIQUE SUPER-PUMA

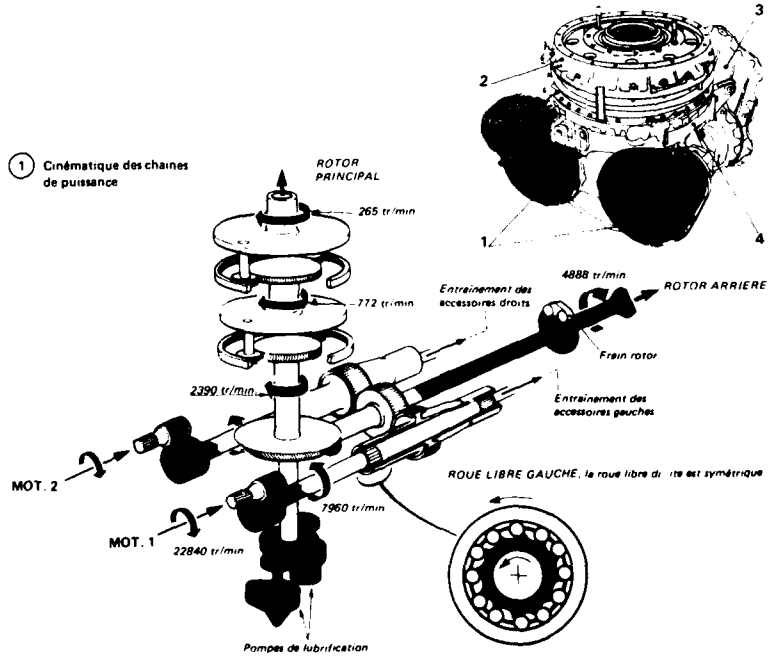


FIGURE 8 - B.T.P. SUPER-PUMA

Une représentation simplifiée de la chaine cinématique de la BTP est donnée par la figure 5. La boîte comporte en allant des moteurs vers la sortie au rotor principal, 2 roues libres (repère 5 et 16), dont le principe de fonctionnement apparait dans les schémas de droite, 2 étages spiro-coniques, la roue du deuxième réalisant l'addition des couples des moteurs. Un train épicycloïdal (repère 2) assure le complément de réduction de vitesse et constitue l'étage de sortie ; l'arbre rotor principal est entraîné directement par le porte-satellite du train épicycloïdal à couronne fixe par l'intermédiaire de cannelures.

En dessous du plan défini par les axes des 2 entrées (repères 4 et 1) se trouve un couple spiro-conique multiplicateur dont le pignon (repère 8) assure l'entrainement de l'arbre de transmission arrière. La roue menante est fixée sur l'arbre de roue conique principale d'addition.

On notera également les diverses prises de mouvement accessoires : A l'avant, les prises de pompes hydrauliques (repères 6 et 15), d'alternateurs (repères 14 et 7), de ventilateur de refroidissement d'huile boîte et moteurs et du disque de frein rotor (repères 13 et 12) ; dans la partie inférieure, en latéral, l'entrainement des pompes de lubrification (repères 9 et 11) ; vers l'avant, une prise pour génératrice tachymétrique.

Une coupe horizontale de la BTA apparait sur la figure 6 et illustre son environnement et sa conception spécifique au rotor caréné fenestron.

On remarque plus particulièrement l'arbre rotor très court et l'ensemble plateau de commande d'incidence associé aux tiges de commande tournante et fixe, contenues dans l'arbre rotor.

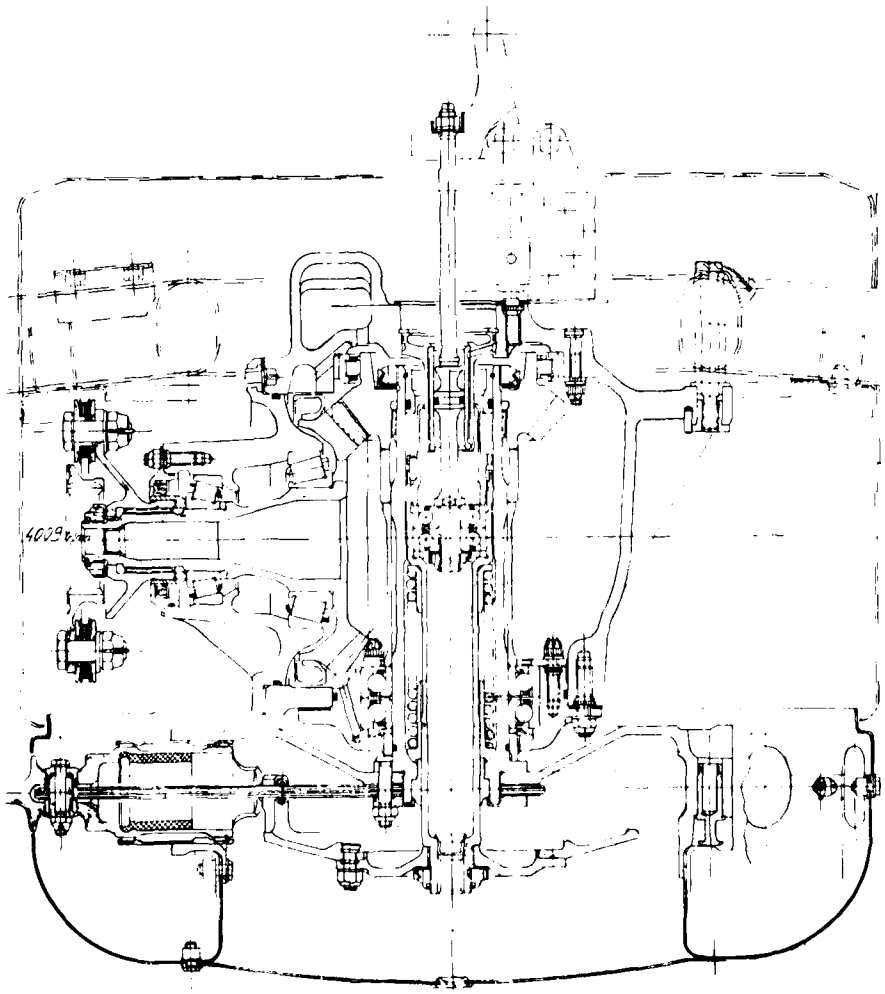


FIGURE 6 - BTA ET MOYEU ROTOR ARRIERE DAUPHIN

Dauphin bi-moteur AS.365N

La figure 4 montre l'architecture du système de transmission.

On distingue les éléments principaux suivants :

- liaison moteur-BTP (repère 1) avec tube articulé anticouple, de même principe que sur Ecureuil
- la BTP (repère 2)
- l'arbre de transmission arrière (repère 4), de conception voisine de celle de l'hélicoptère AS.355
- la BTA (repère 5) assure l'entraînement du rotor arrière caréné
- le groupe de refroidissement d'huile moteur et BTP, à l'avant (repère 3).

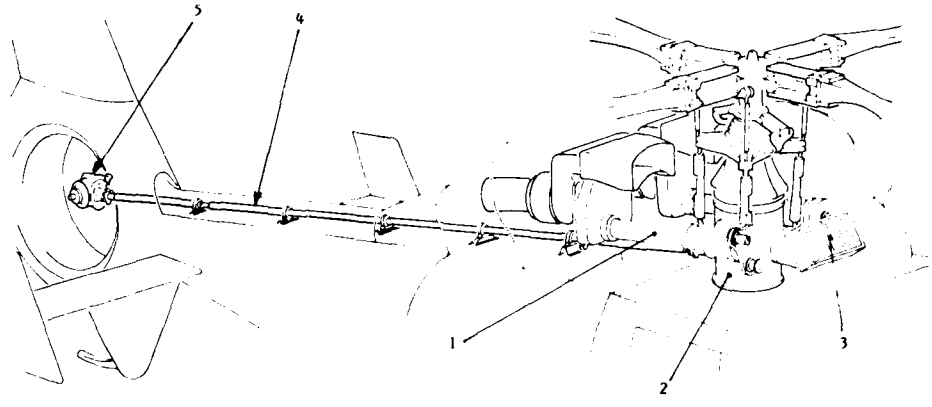


FIGURE 4 - SYSTEME DE TRANSMISSION DAUPHIN

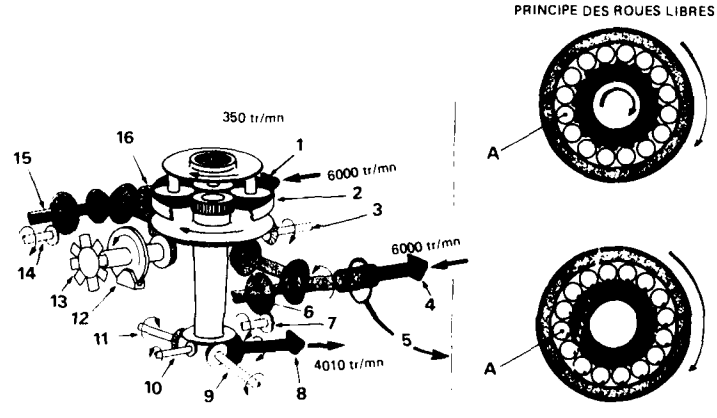


FIGURE 5 - CINEMATIQUE DE LA BTP DAUPHIN

the lack of systematic helicopter transmission oil development by the major oil companies is the low volume of lubricant required. By the same token however, even if better oils were to cost significantly more, this would be negligible compared to replacement and overhaul costs.

A second motive for seeking significantly improved lubricants stems from likely design changes in the next generation of helicopters. It is probable that this generation will have significantly hotter bulk oil temperatures, around 130°C (3). This will require reasonable stable synthetics with powerful anti-wear performance over the whole temperature range, up to 160°C. A program has been recently established in the UK to develop such a lubricant.

When helicopters and lubricant designers start to work closely together, and the lubricant is seen as an integral component in the design, then the possibilities are enormous. A long term possibility is the removal of external cooling entirely from helicopter transmissions, to be partially replaced by improved cooling through the gearbox housing. This would result in probable bulk oil temperatures of 200°C. Such a gearbox is clearly some years away but, with specially designed lubricants, it is conceivable.

REFERENCES

1. Conboy J.D. "State of the Art Review of Helicopter Transmissions, Turboprop Gearboxes and Lubrication Thereof", Naval Air Engineering Center, Philidelphia PA, Rep 02.1967, Feb. 1967.

2. Christian, J.B. and Simmons, B.R. "Grease Lubrication of Helicopter Transmissions", Lubrication Engineering, (1984), 30, p340-350.

3. Macpherson, P.B. "Future Requirements for a Helicopter Transmission Lubricant", ASME/ASLE Conference, Washington, October 1982.

4. Mitchell, A.M. and Coy, J.J. "Lubricant Effects on Efficiency of a Helicopter Transmission", American Helicopter Society Specialists. Meeting on Rotary Wing Propulsion Systems, Williamsburg, Nov 1982.

5. Spikes H.A. and Macpherson, P.B. "The Design, Formulation and Testing of a New Type of Lubricant for Helicopter Gearboxes", Performance and Testing of Gear Oils and Transmission Fluids I.P. Symposium, Oct 1980.

6. Feng, I.M., Perilstein, W.L. and Adam, M.R. "Solid Film Deposition and Non-Sacrificial Boundary Lubrication", Trans. ASLE, 6, p60 (1963).

7. Georges, J.M. "Mechanism of Boundary Lubrication with Zinc Dithiophosphate", Wear, 53, p9, (1979).

8. Watkins, R.C. "The Anti-Wear Mechanism of ZDDP's Part 2", Tribology Int., 15, p3, (1982).

9. Fowles, P.E., Jackson, A. and Murphy, W.R. "Lubricant Chemistry in Rolling Contact Fatigue. The Performance and Mechanism of One Anti Fatigue Additive", ASLE Trans., 24, p107, (1981).

10. Macpherson, P.B. "Pitting of Hardened Steels", Proc. Int. Symp. on Rolling Contact Fatigue, Institute of Petroleum (1976).

11. ASME Engineering Design Guide. "Life Adjustment Factors for Ball and Roller Bearings", (1971).

12. Fisher, M.T. "Lubricant Additive Effects Upon Bearing Metal Fatigue", U.S. Army Weapons Command Tech. Report, No. 66-1293, (1966).

13. Parker, R.J. and Zaretsky, E.V. "Effect of Lubricant Extreme Pressure Additives on Rolling-Element Fatigue Life", NASA TN D-7383, (1973).

14. Spikes, H.A. and Macpherson, P.B. "Water Content of Helicopter Gear Oils", ASME 80-[illegible]-12.

15. Smith, A.G.D. "The Effect of Industrial Loading on Gear Scuffing", PhD University of London, (1976).

16. Bhachu, R., Sayles, R.S. and Macpherson, P.B. "The Influence of Filtration on Rolling Element Bearing Life", MPPG/Nat. Bur. of Standards Meeting, Washington, April 1981.

17. Weatherford, W.D., Valtierra, M.L. and Ku, P.M. "Mechanisms of Wear in Misaligned Splines", ASME, J. Lub. Tech., (1968), p42.

18. Newley, R.A., Spikes, H.A. and Macpherson, P.B. "Oxidative Wear in Lubricated Contact", ASME J. Lub. Tech., (1980), p539.

19. Brown, C. and Feinberg, F. "Development of Corrosion Inhibited Lubricants for Gas Turbine Engines and Helicopter Transmissions", Lubrication Engineering, (1981), 37, p138.

YEAR INTRODUCED	HELICOPTER	OIL TYPE	OIL SPEC.	VISC cSt at 100°C	
58	Whirlwind	Mineral	D.ENG.RD.2479/1	9.1	Very early mineral gas turbine
59	Wessex	Ester	D.ENG.RD.2487	7.7	Gas turbine oil (Type 1)
62	Scout	Mineral	DTD 900/4981	17.5	Modified back axle oil
64	Sea King	Ester	MIL-L-23699B	5.25	Gas turbine oil (Type 2)
67	Gazelle	Mineral	DTD 581C	8.2	Aircraft oil
67	Puma	Mineral	DTD 581C	8.2	Aircraft oil
67	Lynx	Mineral	DTD 900/4981	17.5	Modified back axle oil
80	W.30	Mineral	DTD 900/4981	17.5	Modified back axle oil

Table 1 Typical Main Gearbox Lubricants in Current Use

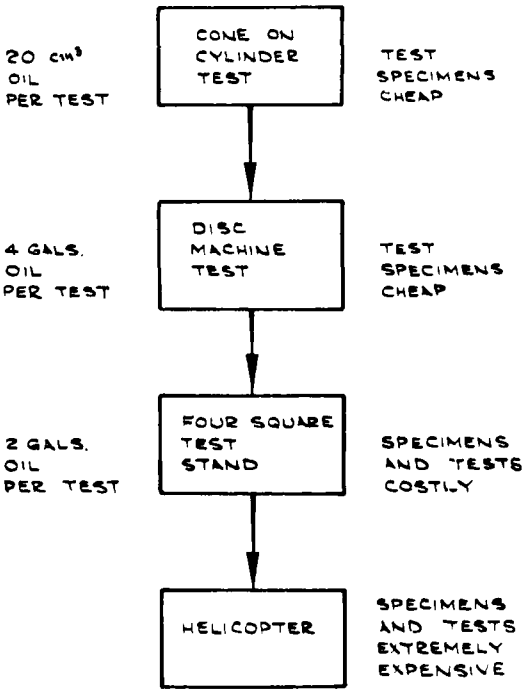


FIG.1. HELICOPTER OIL DEVELOPMENT SEQUENCE.

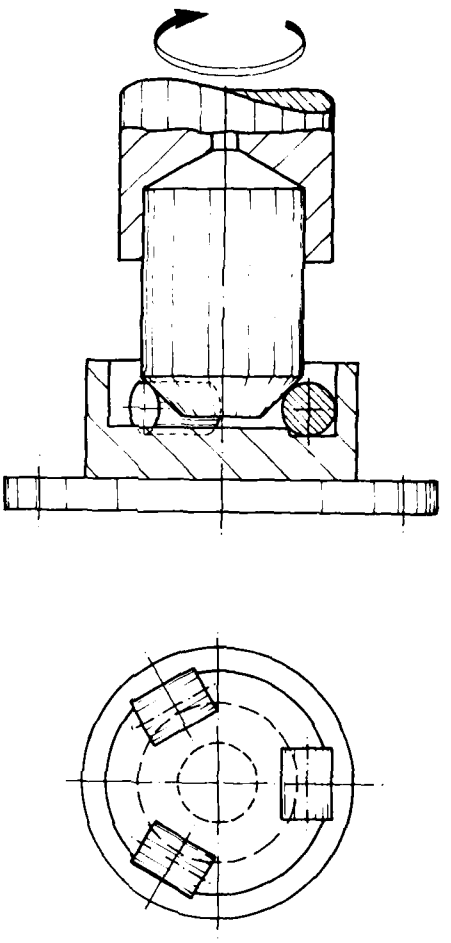


FIG.2. CONE ON CYLINDER GEOMETRY.

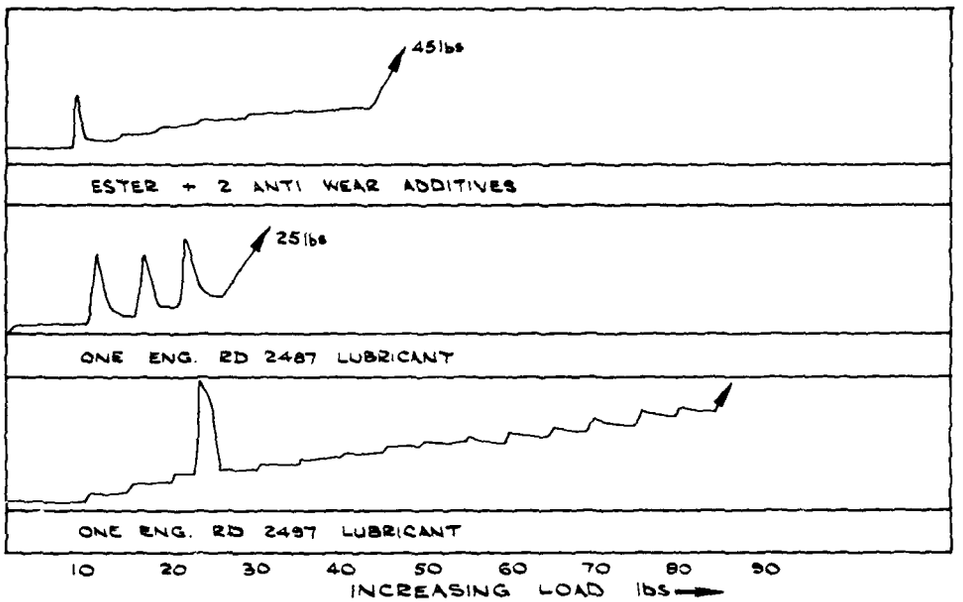


FIG.3. CONE ON CYLINDER TESTS ON THREE OILS.

DISCUSSION

Rh.Ramette, Fr

Have you evaluated the effects of different lubricants on performance and life of some helicopter transmission systems?

Author's Reply

In developing a lubricant for helicopter transmission, as mentioned in my paper, the first and most lengthy stage was to design an integrated series of tests of lubricant performance, ranging from simple screening tests to actual helicopter gearbox tests. The requirement was that these tests correlated with each other in that they gave the same lubricant response to scuffing, pitting, etc. in the whole range of tests.

In setting up this sequence, several currently used helicopter lubricants were fully evaluated to provide benchmarks of performance. There were striking differences in lubricant performance, especially relating to scuffing, between different lubricants approved for the same specification.

E.Saibel, US

There is a human factor consideration, personnel cannot be trusted to get different oils in the right places. It is necessary to develop one oil for both places.

Author's Reply

Such an oil would not be the best for gas turbine lubrication or the best possible transmission oil. It is simply a question of whether we are prepared to accept short lives, reduced reliability and constraints on transmission design for the sake of the principle of a common oil.

J.Godston, US

What is the chemical composition of the oil?

What are details of "proof of concept" program for the acceptability of the lubricant?

How do you determine through testing the efficiency (performance), improved durability of the new lubricant compared to the present or old lubricants?

Author's Reply

The lubricants developed so far have been based on ester and ester/polyglycol based fluids. They include a mixture of non-conventional phosphor-containing anti-wear additives. Also present are concentrated oxidation, corrosion and foam inhibitors. Thus far, the main candidate oil has had many hundreds of hours evaluation in spiral bevel tail rotor gearboxes. It has also been run for 250 hours at 40% overload in a helicopter main box.

No specific investigations of efficiency have been made. Input and output torques in gearbox tests have been measured and indicate an increase in efficiency, but the losses lay within the large inaccuracy of the strain gauge measurements. Running with the best candidate oil did give steady state oil temperatures of 7°C less than using standard oils, suggesting higher efficiencies.

Comment: P.J.Mitchell, UK

Our view on specially formulated transmission lubricants is that they would be very well worthwhile if we can get longer TBO's and MTBR's by using them, despite increasing the range of lubricants we have to carry.

B.Sternlicht, US

Have you included shear effect on viscosity and its effect on pitting and scuffing?

Author's Reply

There is no doubt that the friction properties of a lubricant in EHD can influence pitting and scuffing. In principle, this is one effect to be taken into account in developing new oils. In practice, however, film thicknesses and chemical effects have much greater effect. We have tended, in developing new oils, to use existing, tested and proven synthetic base oils rather than look at exotics. We have accepted the limitations of these base oils and concentrated on additives to mitigate pitting and fatigue. This is the most practical medium-term approach, though in the very long term, base oils with specially chosen lubricant properties may be developed.

SPECIAL POWER TRAIN REQUIREMENTS FOR THE NEXT GENERATION OF ROTARY-WING AIRCRAFT

Raymond J. Drago and Joseph W. Lenski, Jr.
Senior Engineers
Boeing Vertol Company
P.O. Box 16858
Philadelphia, Pennsylvania 19142

ABSTRACT

The omnipresent rotary-wing drive system requirements for minimum weight with maximum reliability will be compounded in the future by additional restrictions on size, damage tolerance, cost, and ease of assembly and maintenance. The authors present their view of the form of these restrictions and provide some broad insight into possible approaches designed to improve the performance of rotary-wing drive systems. We also provide specific examples of extensions of current technology and some speculation about potential applications.

INTRODUCTION

Many advances ir technology across a broad interdisciplinary front will be required over the next decade if the design of rotary-wing power train systems is to keep pace with improvements in place or with those anticipated for future aircraft. New concepts such as the tiltwing or tiltrotor require even more basic changes in both design philosophy and techniques. In this paper we present our view of some of these primary areas of power train system development.

A summary of several current applications of advanced-technology concepts is presented in Reference 1. Future developments will be the logical next-step advance in each of these areas.

GEARING

Materials and Processing

The development of high hot hardness materials, such as VASCO X2M, has permitted substantial improvements in both durability and scoring capacity. The next step in this area will be an improvement in the case hardening process used for such parts. Vacuum carburizing, for example, has been used recently for some commercial applications. Research is now under way (Reference 2) to evaluate the use of high-temperature vacuum-carburizing techniques with an integral quench sequence to reduce both the cost and time required to produce aircraft-quality gears while improving their load capacity. The reduction in cycle time (and thus energy usage and total cost) for a typical gear is substantial, Figure 1. Additionally, the preoxidizing step currently required for VASCO would be eliminated.

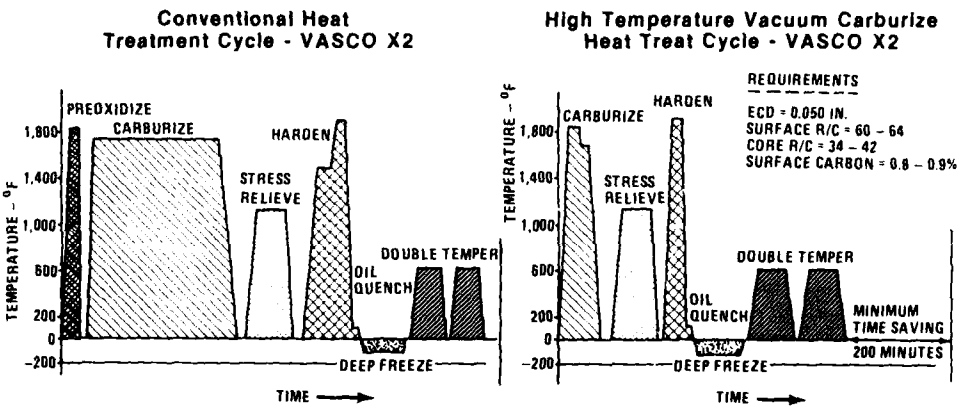


Figure 1. Typical Conventional and High-Temperature Vacuum-Carburizing Cycles

Analytical Techniques

The application of three-dimensional finite-element methods (FEM) to the analysis of complex spur, helical, and spiral bevel gears has progressed rapidly in the last few years. Pre- and postprocessing programs have been developed (Reference 3) which permit the rapid and accurate preparation of FEM models such as that shown in Figure 2. The next step in this effort will be the linking toge her of fully generated models of mating gear sets so that their interactions, particularly load distribution among the teeth in contact and along the instant lines of contact, can be studied. The concept of load distribution

has received limited study with simple models, but more advanced study with large, complex models has been restricted by computer size and speed limits. The new supercomputers (such as the Cray) have the potential of removing these limits.

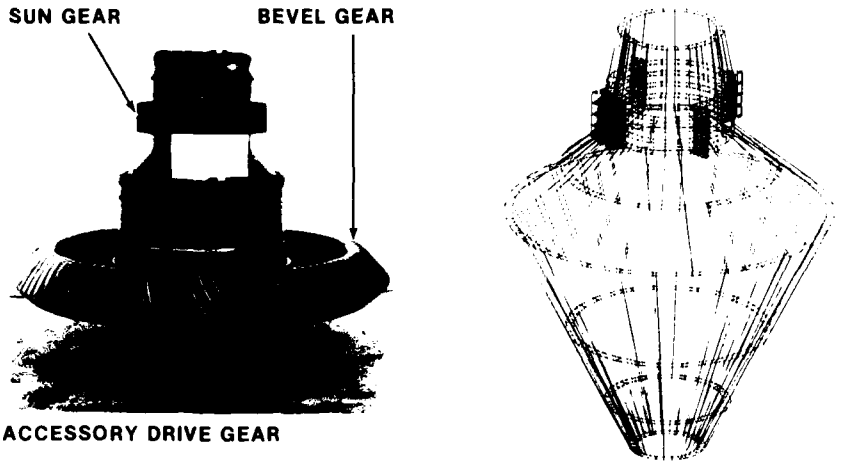


Figure 2. FEM Model of Typical Complex Bevel Gear

Integrated Design

The problems associated with assembling gears to their shafts with keys, splines, or bolted-flange arrangements have prompted the use of EB (electron beam) welding to provide an integral shaft and gear configuration in some applications. The design of the CH-47D (Reference 4) and CH-46E transmissions carries this concept even further by using advanced computer analysis and graphic techniques to permit simultaneous optimization of gear and shaft geometry while also considering the gear cutting and grinding tooling requirements. This results in integral gear and shaft configurations of a complex nature with no welding required. The resultant parts are, as Figure 3 and Table I show, lighter and more reliable. Although some simple cylindrical bearing races are included in these integration efforts, the maximum benefit will be obtained by truly integrating the entire gear-shaft-bearing system (Reference 5) (Figure 4). This is the next logical level of integration and will yield further improvements in weight, overall size, and, especially, reliability.

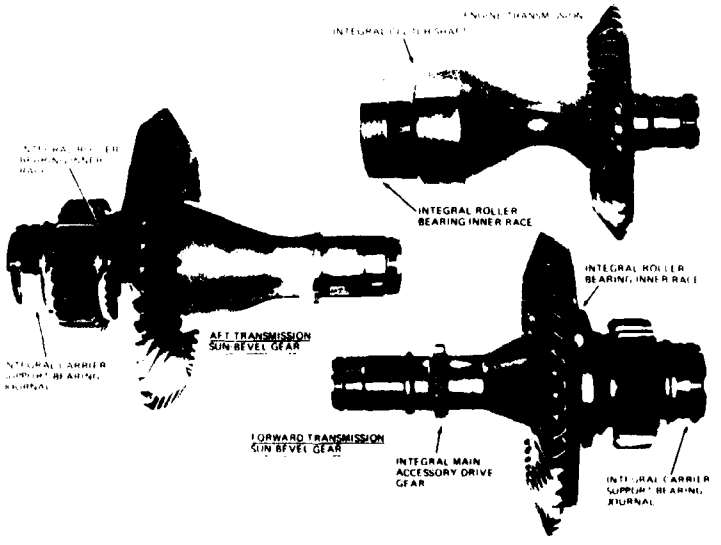


Figure 3. Representative Integral Spiral Bevel Gears for the CH-47D Helicopter

TABLE I. RELATIVE WEIGHTS OF CH-47C BOLTED-FLANGE AND CH-47D INTEGRAL BEVEL GEARS

Transmission	CH-47C (6,000-hp System) (hp/lb)	CH-47D (10,000-hp System) (hp/lb)	Percent Improvement
Forward	89	102	15
Aft	96	105	10
Mix	123	147	20
Engine	175	209	20

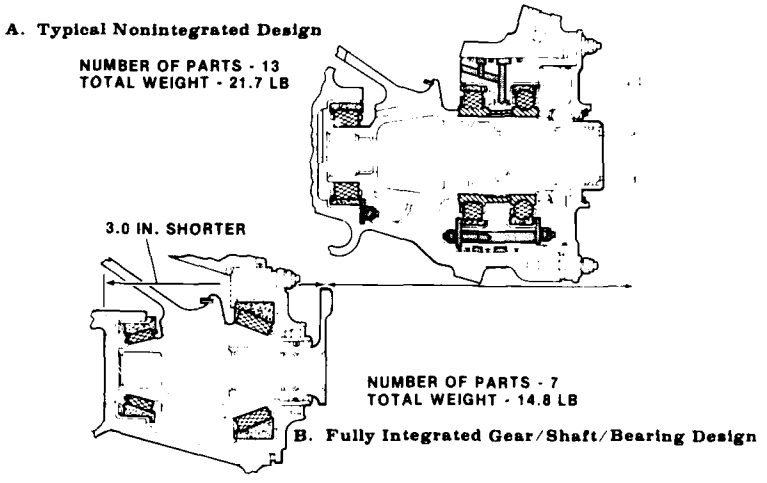


Figure 4. Comparison of Typical Nonintegrated and Fully Integrated Designs

Tooth Form

Many different tooth forms, varying from involute-based, high-profile-contact-ratio spur gears to completely noninvolute concepts such as the conformal gear (used on the Westland Lynx) and the maximum conjugative concept (being evaluated for low-noise automotive applications), have been evaluated for aircraft applications. Unfortunately, these approaches have taken the form of a solution looking for a problem. Future efforts in this area should center on the reverse approach--identifying a specific form-related problem and following a line of investigation to a solution. Similar to the recent NASA-sponsored test program (Reference 6) in which a noninvolute, constant-relative-curvature tooth form was evaluated. As Figure 5 shows, the surface durability life of the advanced tooth form test gears is approximately five times that of the standard baseline gears. Their scoring-load capacity (Figure 6) is, however, lower than the baseline. The future of tooth-form development will center on optimizing different properties of specific forms to accomplish specific objectives.

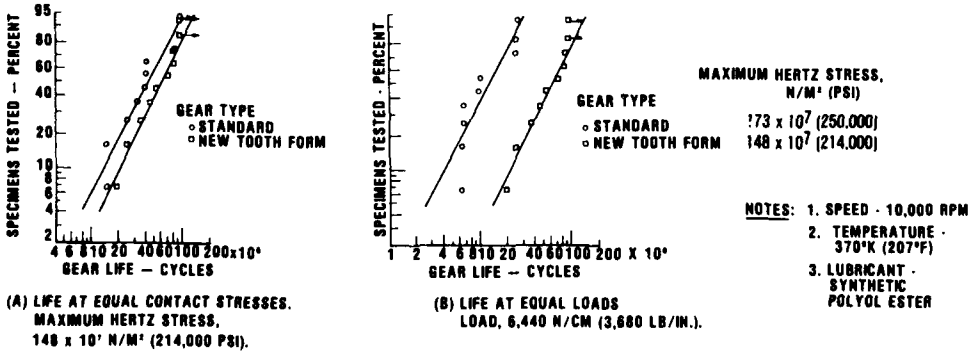


Figure 5. Pitting Fatigue Lives of Spur Gears With Standard and New Tooth Form

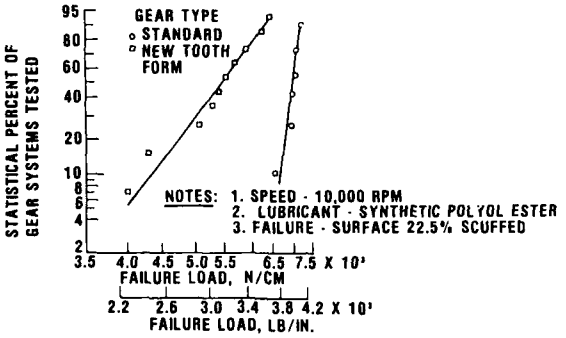


Figure 6. Scoring Failure Load of Spur Gears With Standard and New Tooth Form as Function of Percentage of Specimens Tested

LUBRICATION

Currently a common oil is used in both the engines and transmissions of virtually all U.S. military helicopters. This provides significant logistic advantages, but they are only attained by compromising the optimization of the oil for either system. Since the oils used are basically engine oils and not gear oils, the transmissions suffer the severest penalties.

Recent research (References 7 and 8) yields strong evidence that a specially developed, dedicated transmission lubricant can provide substantial improvements in the next generation of transmission systems. Many factors were considered in both studies. We will treat only two aspects here to provide insight into the potential benefits associated with the development of a new gear oil for rotary-wing aircraft use.

Higher Viscosity

An oil with a higher viscosity (in the range of 10 cs at 210°F) will improve bearing life due to an increase in lubricant film thickness. Considering two typical existing helicopter bearings will provide some insight into the magnitude of the improvements we can expect. As Figure 7 shows, the probability of lubricant-related surface distress occurring decreases with increasing percentage of film formation. For a typical moderate-speed helicopter transmission bearing (Reference 7), the percentage of full EHD (elasto-hydrodynamic) film formation increases from 62 percent, which is barely out of the "region of possible surface distress...," to 94 percent, practically full development. On the other hand, a typical low-speed helicopter transmission bearing (Reference 8) shows a percentage film formation with MIL-L-23699 oil of virtually zero. Changing the oil will bring this bearing to approximately the same percentage of full film as the moderate-speed bearing with MIL-L-23699 oil. For both bearings, an improvement in life, as shown in Table II, can be expected due to the new oil.

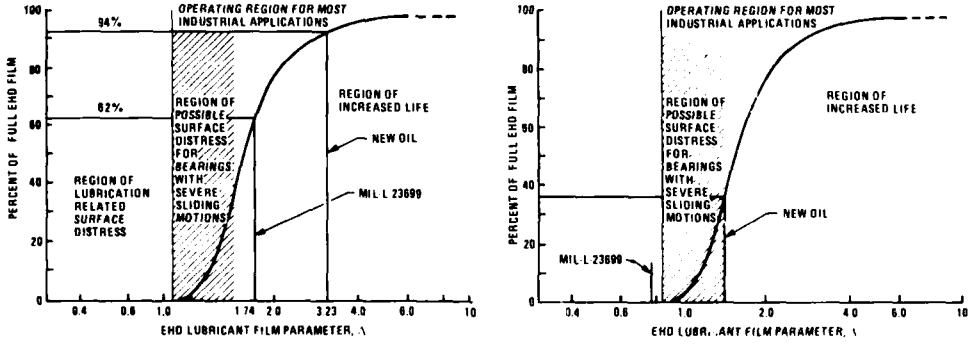


Figure 7. Percent of Full Elastohydrodynamic Film Development as a Function of Lambda

TABLE II. BEARING LIFE IMPROVEMENT DUE TO NEW OIL

Bearing	Oil	Expected Life Increase (percent)
Moderate speed	MIL-L-23699	--
	New	46
Low speed	MIL-L-23699	--
	New	500

Improved Corrosion Protection

At this time, corrosion is the leading single cause for transmission parts rejection at overhaul for the U.S. Navy CH-46 helicopter. The latest cumulative overhaul records indicate that over 40 percent of the gears and bearings examined at overhaul are discarded or reworked due to corrosion alone. In general, the primary problem which results from corrosion is replacement at overhaul. To show the magnitude of the cost savings which can be obtained through the use of an oil with improved corrosion protection, we have reviewed the overhaul records for the CH-46 and CH-47 military fleets as well as data from commercial operations using the same aircraft with different lubricants. This experience, summarized in Table III, indicates that the occurrence of corrosion in gearboxes lubricated with MIL-L-23699 oil is far greater than that with either of the two other oils used. The projected cost of corrosion per flight hour, with the CH-46 fleet as a basis for comparison, was calculated using the rejection rates shown in Table III for each lubricant. Bearing costs were calculated by averaging the cost of bearings and multiplying by the number of bearings in each transmission. It was further assumed that only half of the corroded parts would require replacement while the remainder would be reworked and reinstalled--a conservative cost approach since it is seldom possible to rework a bearing (bearings account for 75 percent of main parts rejected due to corrosion) while it is often possible to rework a corroded gear. Only the cost of replacement was considered; no rework costs were included in the analysis. The resultant projected costs are summarized in Table IV. The cost impact of using a lubricant with improved corrosion resistance is quite apparent.

TABLE III. CORROSION EXPERIENCE FOR THREE LUBRICANTS

	Percent of Parts Corroded		
Lubricant	MIL-L-23699	MIL-L-7808	MIL-L-6082
Gears	10	2	1
Bearings	31	7	1

TABLE IV. PROJECTED COST OF REPLACING CH-46 GEARS AND BEARINGS DUE TO CORROSION FOR THREE LUBRICANTS

Lubricant / Gearbox	1982 Dollars per Flight Hour		
	MIL-L-23699	MIL-L-7808	MIL-L-6082
Forward	1.82	0.29	0.16
Aft	4.45	0.54	0.29
Mix	3.94	0.62	0.30

In terms of the CH-46 fleet alone, a total cost saving of over 20 million dollars would accrue during the projected remaining life of these aircraft (about 17 years) if an oil with the corrosion-resistant properties of MIL-L-6082 were used.

BEARINGS

Several areas of rolling-element bearing technology are advancing rapidly. We will touch on only two in this paper to demonstrate the overall effect.

Improved Material for Bearings

In many helicopter applications, consumable-electrode vacuum-melted AISI 52100 and 9310 steels provide satisfactory performance for gears and bearings operating at less than 300°F. As the operating temperatures of bearings exceed 300°F (bulk and/or contact temperature), both of these steels exhibit a loss of hardness and load carrying capacity. Figure 8 shows the hot hardness characteristics of these steels and indicates that 9310 drops below Rc 58 at approximately 300°F and that 52100 will reach the same hardness at a slightly higher temperature. To overcome this factor in bearings, many bearings have been fabricated from consumable-electrode vacuum-melt M-50 steel which has demonstrated excellent load-carrying capacity, fatigue life, and stable operation up to and exceeding 650°F. With the ever-increasing use and demand for this material, problems of increased expense for both the material and processing and a low tolerance for crack propagation have resulted in the demand for a new replacement material.

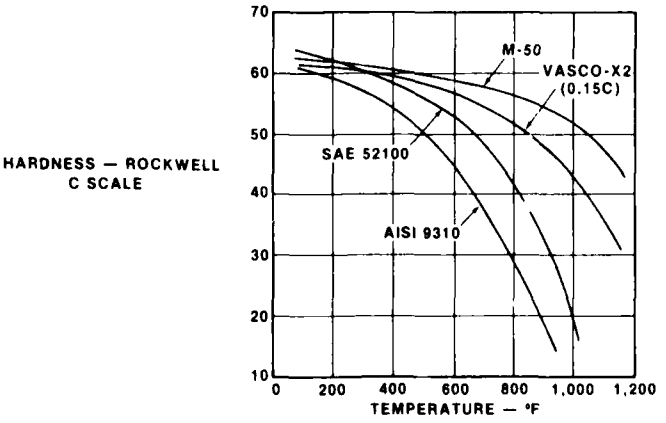


Figure 8. Hot-Hardness Characteristics of Common Bearing Steels

Based upon the expected requirement for future helicopter transmission bearings, the following material characteristics will be required of future bearing materials:

- Increased fatigue life (material factor greater than 6)
- Increased scoring resistance
- Slow crack propagation after initial failure
- Stability during reduced oil flow operation
- Hot hardness better than Rc 58 at elevated temperatures (> 350°F)

Boeing Vertol experience has shown that a modified version of case-carburized steel has the potential to achieve all these requirements. The material that can achieve these goals is VASCO-X2 steel. This material has the excellent characteristic of retaining hardness at elevated temperatures coupled with excellent rolling-contact fatigue properties. When comparing through-hardened versus case-carburized materials, experience has shown that cracks propagating from a fatigue spall are stopped by the soft core (Rc 40) of case-carburized steel bearings, while rapid unstable crack extension occurs in through-hardened bearings. Failure of this type results in the loss of the structural integrity of the bearing as shown in Figure 9.

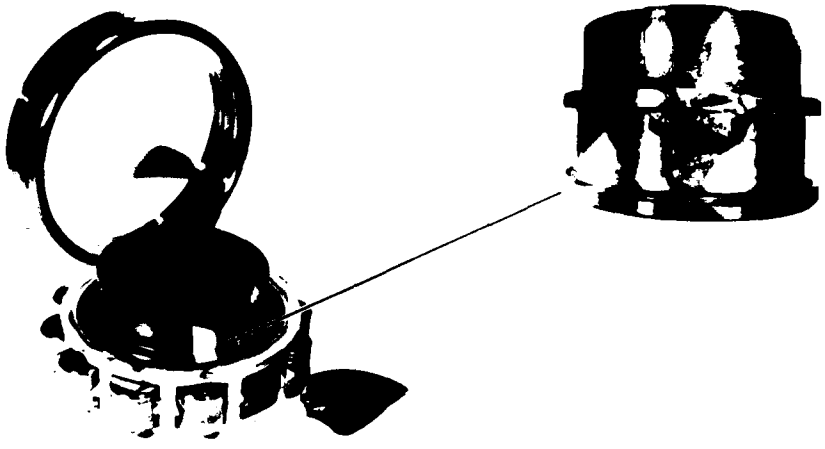


Figure 9. Typical Fracture Failure of Through-Hardened No. 50 Steel

In addition to meeting the needs of rolling-element bearings, the same material should be suitable for fabrication of gears and shafts. The use of a common material offers many advantages to the design integration of gear and bearing components. This is further expanded in the following section.

Integrated Design

The simple configuration possible with an integrated gear/bearing system design (Figure 4) will result in fewer individual component parts, reduction in the number of fretting surfaces, and a significant reduction in system weight. The risk of replacement of an integrated gear/bearing assembly is present due to damage to one of many critical surfaces, but the net effect is that of a more reliable, less costly, and increased-service-life component.

The need of an integrated gear/bearing system design has evolved over the years. The initial design, (Figure 10, A), shows that standardized parts are used resulting in many simple components and associated faying surfaces. Experience demonstrates that transmission removals from service are due to fretting of the mating surfaces and rotation of the outer races in the housings. These designs were modified to include keying of the outer race and integrating the inner spacers as part of the bearing inner race, (Figure 10, B). This modification improved the service experience but did not correct all the problems. The next-generation drive systems that entered service in the early 1980s (Figure 10, C) continue to integrate components. This includes tabs on the outer race for antirotation, integrated spacers on the inner and outer races, elimination of finger-type oil jets, and the use of an inner-race centrifugally operated oil lubrication system. This approach has eliminated many of the nuisance problems that plague helicopter transmissions. This is a significant step in the right direction, but further work will be required to achieve a fully integrated gear/bearing system as proposed in Figures 10, D and 4.

High-Speed, Cup-Ribbed, Integral Shaft/Race, Tapered-Roller Bearings

Typical helicopter transmission spiral bevel gears are supported by rolling-element bearings in either an overhung or straddle configuration. Each of these designs can be supported by ball, cylindrical, spherical, or tapered-roller bearings. The final design selection is usually based upon system loads and speeds, life requirements, and available space. Bearings which support spiral bevel gears are required to react combined radial, thrust, and moment loads. For this type of application, tapered-roller bearings appear to have the greatest load capacity for a given envelope and total bearing weight. The widespread use of tapered-roller bearings in such applications has been restricted to lower operating speeds.

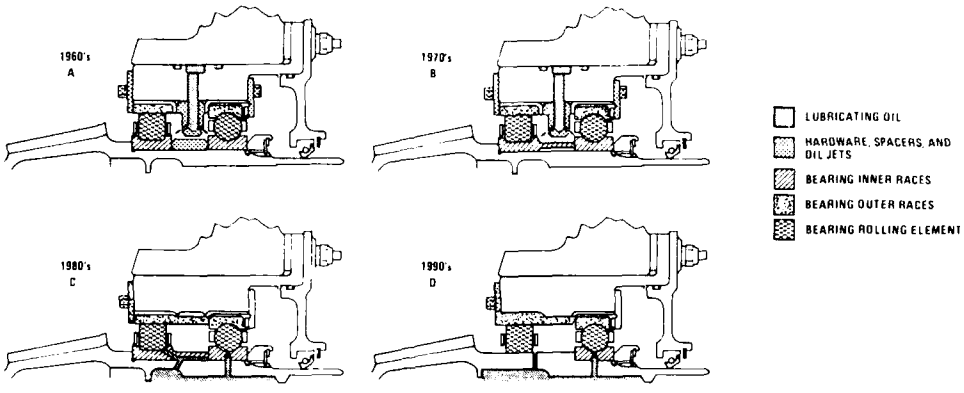


Figure 10. Integrated Bearing and Gear Design

In the late 1960s work was initiated to develop high-speed tapered-roller bearings. Rapid advances were made to increase the limiting speeds of tapered-roller bearings from 5,000 ft/min cone rib velocity to over 20,000 ft/min (Reference 9). This was done by optimizing the internal geometry of the bearing and by supplying secondary lubrication to the cone rib area. This work was successfully incorporated in a helicopter drive system during the HLH/ATC program (Reference 10). In less than 7 years, the potential high-speed operation of tapered-roller bearings was demonstrated. Although testing was successful at high speeds, there still remain three major restraints on complete acceptance of tapered-roller bearings in high-speed aircraft applications:

- Sensitivity to oil interruption
- Sensitivity to mounted end play or preload
- Integration of inner race and gear shaft.

The first restraint--oil interruption and/or oil-off operation--is perhaps the most serious. Much development work has been done in the helicopter industry to achieve limited oil-off operation. Generally, cylindrical roller bearings can operate without oil for extended periods of time. Ball thrust bearings provide a more difficult challenge but can still achieve desired goals. Because of limited development, tapered-roller bearings are not yet successfully operating without oil at high speeds.

Tests and analysis demonstrate that the inner race (cone) rib which guides the roller ends quickly deteriorates under oil interruption conditions. High-speed photography (Reference 9) shows that as speed increases the natural path of the oil is the outer raceway. To overcome this problem, the bearing was modified by adding many lube holes in the inner race to provide a second oil path to the critical cone rib/roller end contact zone. This makes it possible to increase the speed limit of tapered-roller bearings by more than eight times. The main disadvantages are the increased manufacturing cost and complexity with no improvement in sensitivity to oil interruption.

Further review of the tapered-roller bearing indicates that the area of the cup/roller end is a logical location for the placement of the most critical contact of the bearing. This area provides the best oil wetting under marginal oil flow conditions and the space to trap residual oil under zero oil flow and startup conditions. Locating the race rib on the cup not only improves the lubrication of the bearing, but it also relaxes the third major restraint: difficulty of fabrication of the integral inner race and shaft; the geometric feature to be incorporated as part of the gear shaft becomes a simple cone. The difficult rib area is still part of the bearing supplied by the bearing manufacturer. With these advances incorporated, the use of the cup rib design for advanced transmission concepts shows significant promise.

Design studies show that a direct bearing mount (face-to-face) on a spiral bevel gear can provide many advantages. By comparison with conventional bearing mounting (ball and cylindrical roller bearings), a less complex and smaller envelope design is able to support a spiral bevel gear (Figure 4). Although this type of bearing system may not result in the smallest bearings, there are many other significant advantages such as elimination of the inner race components, locknuts, and most outer race retention hardware. The overall advantage of this type of gear support is a significant reduction in weight and parts count.

In addition, the final restraint on tapered-roller bearings is overcome with this type of mounting arrangement. With tapered-roller bearings in a direct mount, the cups can be used to apply the desired preload or axial setting. By providing a floating cup and a spring at one end of the shaft, it is possible to minimize the sensitivity to the as-mounted end play. The preload spring maintains a uniform bearing preload over a wide range of operating conditions, resulting in higher fatigue life and reducing the risk of excessive preloading.

Finally, as noted earlier, this design allows for the direct incorporation of the bearing inner races as part of a high-precision gear. Initially this may not seem to be the correct approach for reducing drive system costs. Damage or failure of any bearing or gear will result in the replacement of an expensive item. Although the initial cost of the gear may be slightly higher, total system cost will be offset by lower overall life-cycle costs. Also, service history of integral designs shows that elimination

of fretting surfaces can greatly increase the service life of transmission components. Secondary damage such as fretting corrosion and handling and assembly damage are the major contributing factors in reduced service life. We can significantly improve life and reliability by applying high-speed, cup-ribbed, tapered-roller bearings to helicopter transmission systems.

Improved Bearing Corrosion Protection

As our discussion of lubrication has already demonstrated, bearing corrosion is a serious problem. Recent research indicates that new floating technologies which permit the deposit of very thin, dense, chrome coatings on bearing surfaces have the potential for reducing corrosion significantly while improving wear resistance and fatigue life. Detailed, independently verified test data are not yet available (the authors are, however, currently pursuing such data), but Figure 11 (from Reference 11) provides insight into the potential advantages of such techniques.

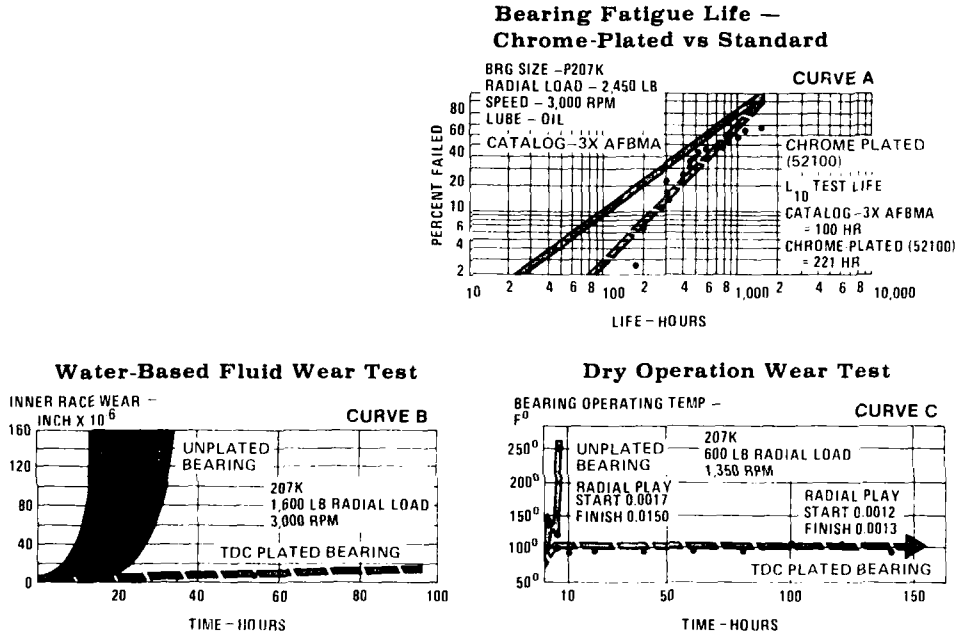


Figure 11. Potential Advantages of Corrosion-Resistant Coatings for Bearings

Forty-eight hour salt-spray tests which compared coated 52100 steel bearings with 440C stainless bearings showed in a 50 to 70-percent surface corrosion rate on the stainless bearings and only minor corrosion on the coated 52100 steel bearings. Considering the corrosion damage figures cited earlier, this improvement alone can yield substantial savings.

COMPOSITE APPLICATIONS

The main focus of most recent composite developments is on their use as structural airframe members. The next generation of rotary-wing aircraft will use composites in the drive system as well, not only in static applications but also as rotating, dynamic load-carrying members.

The application of fiber-reinforced-resin composites to selected areas of the helicopter drive system will produce weight and cost savings as well as improvements in reliability and safety. These improvements which have been demonstrated in airframe applications can be transferred to structural components in the drive system. Major structures like the rotor shafts and transmission housings provide the opportunity to realize advantages which include:

- Inherent failsafety through slow failure progression
- Corrosion resistance
- Simplified tooling with lower costs and lead times
- Minimum machining through net-shape forming
- Elimination of critical materials and machine tools in the processing.

We will treat two ongoing programs (one of which has already reached production status) as indicators of the future potential of such materials. Our discussion addresses the design, fabrication, and testing of two drive system components. The use of composites in these areas furthers a technology that can be directly applied to similar drive system components in advanced rotary-wing aircraft.

Composite Shafting

We have been investigating the use of composite drive shafts since the mid-sixties. Fabrication and testing show graphite T300 filament-wound tubes of 4 to 6-inch diameter with thin walls (0.08 to 0.12 inch) to be very damage-sensitive. Based upon this early experience, handling-damage criteria were developed and additional tubes with heavier wall thicknesses were fabricated. The new tubes are capable of surviving the low-velocity impact of tool drops and other handling damage. Testing shows no decrease in fatigue life after damage testing. Design studies indicate that a major weight reduction (30 percent) can be obtained through the use of graphite tubes due mainly to increased bending stiffness as compared to that of conventional aluminum tube shafting. Shaft spans (between bearing supports) are determined by critical speed requirements and can be lengthened, resulting in fewer coupling and bearing supports.

In addition to drive shafting, fatigue life of main rotor shafts is being increased by substituting a composite structure for existing aluminum components. Although increased fatigue life is the main objective of the composite rotor shaft, studies indicate other benefits will also accrue. These benefits include weight, cost, and reliability.

A weight saving of 25 percent is expected as compared to equivalent metallic structures--a reduction due to the inherent high stiffness of composites essential to a main rotor shaft design.

The tooling costs for composite shaft fabrication are significantly lower than for metallic equivalents. A simple tube mandrel suffices for most shafting; a main rotor shaft requires only diameter machining of selected areas, and other diameters remain net from the winding mandrel.

Corrosion protection of steel rotor shafts is a continuing problem, and corrosion of mating steel surfaces represents a significant cause for removal, rework, or rejection. Graphite and glass shafts with proper dielectric separators and the use of selected corrosion-resistant steels for fasteners make the composite structure essentially corrosion-proof. The inclusion of S-glass in the torque path of the rotor shaft provides an expected improvement in failure modes as compared to steel or aluminum. The composite shaft has a soft failure mode which is detected by a slow change in stiffness rather than a total loss of load-carrying capability.

A thick-wall composite tube was evaluated for the center section of a 3-piece CH-47 rotor shaft assembly (Figure 12). The composite section was designed to an unlimited fatigue life goal to replace the life-limited metallic center section now in use. The composite section was also sufficiently strong to withstand multiple handling damage defined by the criterion of a 2-pound ball dropped from 6 feet. The composite tube is connected by several rows of radial pins to the upper and lower steel splined shafts. Some outstanding operational requirements of the composite rotor shaft assembly include:

Torque (fatigue)	1.11 x 10 ± 0.133 x 10 in.-lb
Torque (ultimate)	2.33 x 10 in.-lb
Torsional stiffness	GJ = 2,180 x 10 lb-in.
Bending stiffness	EI = 2,180 x 10 lb-in.
Bending moment (at upper joint)	± 425,000 in.-lb
Desired life	10,000 hours

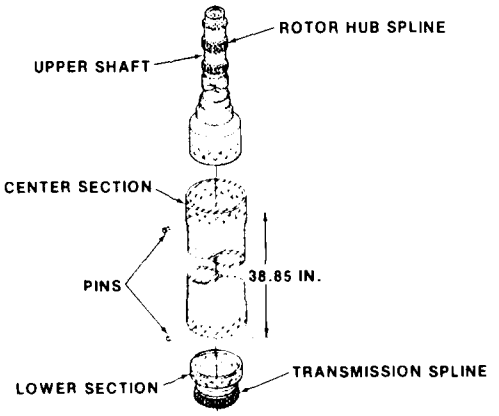


Figure 12. CH-47 Aft Rotor Shaft Assembly

Analysis of this design indicated that a major proportion of the composite tube would be graphite in order to achieve the desired stiffness to match the dynamic properties inherent in the current aluminum tube. The final weight of this section is 85 pounds; by comparison the limited-life aluminum tube is 80 pounds, and a steel tube with unlimited life was designed weighing 110 pounds. The composite rotor shaft section was fabricated by filament-winding techniques using a rotating mandrel. The mandrel shape forms the inside diameter of the tube to net dimensions; radial holes are machined to suit the upper and lower drive pins, and final assembly is completed.

12. FUTURE NEEDS

The need for high temperature gear oils and their market potential should be identified in order to stimulate activity in this area. For over twenty-five years high temperature operational capabilities of gear materials have lain dormant due to the absence of compatible lubricants. It should be determined whether their availability would result in a worthwhile gain in overall operational efficiency and whether or not the total development and system costs can be repaid by performance gains.

There should be a purposeful effort to remove gear design from empiricism by means of synthesis and optimization techniques. Their application is simpler when there are no constraints on the system such as spacial relationships. Usually the constraints of high power turboprop drive systems are relatively simple and may be met by a number of different gear arrangements. What follows is an example of what might be initiated by making use of state-of-the-art technology as the framework of a design synthesis methodology:

- Comparison of gear arrangements with selection of ideal arrangements by weighted logic.
- Sizing of gears to mission requirements and growth factor.
- Selection of number of teeth based upon optimization techniques for maximum load capacity. Includes Fourier Series analysis to minimize dynamic load effects.
- Optimization of conjugate gear tooth form to suit application.
- EHD analysis by modified TELSGE program.
- Dynamic analysis by modified GRDYN program.
- Selection of bearings.
- Life analysis of gears and bearings as a total system.
- Torsional vibration analysis of complete power transmission system.

Caution must be exercised when departing from traditional design practices. It is apparent that the growth inherent in a number of existing gearboxes was there because of empiricism and implicit conservatism in the initial design that was used to advantage as load increases were desired. In the future new designs will be targeted at a predetermined growth factor coupled with mission requirements needed by the potential applications envisioned for the machine. Designing machines to material properties and weighted load life will result in smaller and lighter units, but they will have less growth potential than was available in the past.

It is of the utmost importance to achieve design simplicity in order to meet future reliability, maintainability and economic goals. To this end it is essential that the propeller pitch change mechanism be an integral part of the overall design of the gearbox. The speed reduction gearbox may be viewed as a dedicated mechanism which provides power to and controls the propeller. Ideally, it will be a self-contained entity that will initially provide for its own lubrication, cooling and monitoring. Eventually, a "smart" gearbox may emerge which will monitor and control its environment according to operating conditions in real time.

rationale and logic of a gear tooth synthesis modeling methodology and a computer program flow chart. The program merges three models: the first concerns conjugate profiles and Hertz contact pressure; the next is a bending strength model which adjusts pitch line tooth thickness and profile curvature; and the third is a search routine which provides for the maximum capacity of the gearset. A balance is reached which makes the most efficient use of the given pitch line space width. A referenced report is noted which deals with the manufacture and testing of synthesized gears based on quiet running conditions. This is an area which should be exploited rapidly to explore its potential and its degree of correlation.

10. STRUCTURAL

The large general-purpose structural computer programs such as NASTRAN and ANSYS are a boon to designers and have been responsible for expanding design capabilities and machine performance. They are relatively simple to apply to engine components such as turbine wheels and compressor casings which are axi-symmetrically loaded. Gears, on the other hand, are considered to be point-loaded and this makes modeling considerably more difficult. In order to model gear loads it is necessary to express them in terms of a Fourier series. This is both time consuming and expensive and, because of the extra mathematical manipulations required, the results become subject to error accumulation.

Finite Elements Methods (FEM) have been developed for application to the gear tooth form, but presently the amount of operator time and computer time required is discouraging. Two and three dimensional finite element analyses of symmetric and asymmetric gear tooth forms were reported in 1972(34). The accuracy of the two dimensional calculated stress data was compared with data from a photoelastic model. Predicted stresses ranged from a fraction of one percent to twenty percent lower than those predicted by conventional methods. The work was applicable to spur, helical and bevel gears, and included a substructuring routine which reduced the computer time required. A preprocessing computer program is under development(12) which automatically creates a finite element model of spur, helical and spiral bevel gears.

11. TRACTION DRIVES

The latest proposed applications of aerospace traction drives are for hybrid arrangements where the final speed reduction is accomplished by a multiplicity of externally toothed pinions, rather than rollers, driving a common ring gear.

A turboprop application which is intended for use as a speed reduction component in an advanced propeller pitch change mechanism(Fig. 5) is presently in the design stage. This as a truly unique application which capitalizes on the characteristics of the traction drive:

- It can achieve a very large speed reduction in a very small volume.
- The creep experienced by the traction drive does not affect performance since position control is the final function.
- Input power is relatively low so that a 6% power loss is acceptable.

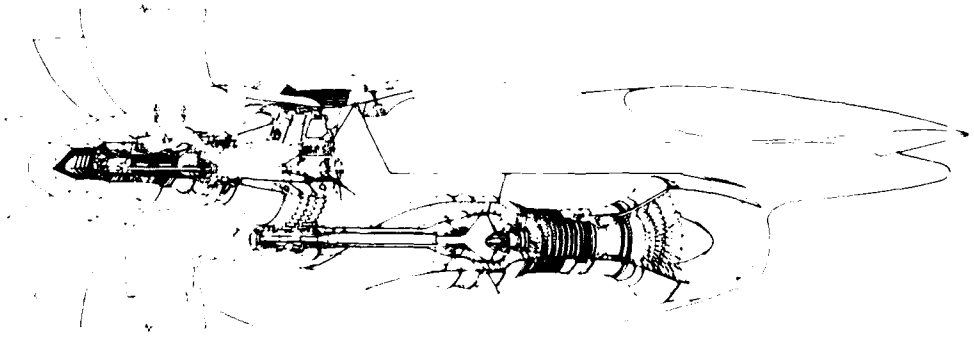


Figure 5
Traction Drive Propeller Pitch Change Mechanism

most useful to program users since they are difficult to obtain. This is a powerful and useful analytical tool that can be used for design purposes or for comparing the effects of varying lubricants and/or operating conditions of existing machines. The program should be modified to accept any conjugate tooth form to meet potential future requirements.

Actual power transmission systems are being used as test vehicles to advance the state of the art in actual flying scenarios. Monitoring systems are being developed for use on helicopter power transmission systems which will offer application advantages to future turboprops. A U.S. Army program concerned with debris monitoring and fine filtration effects utilized an initial test fleet of fifty UH-1 helicopters to gather statistically significant data. Thirty-eight were modified by having their 38 micron oil filters and splash-type chip detectors replaced with three micron oil filters and full-flow burn-off chip detectors. Recommended oil service life has been increased from 300 hours to 1000 hours in the transmission and average filter life has increased from about 400 hours to 1000 hours as the systems became cleaner(23). In the same genre, Westland Helicopter has been actively developing a Health and Usage Monitoring program which includes vibration analysis, wear sensors, torque monitoring and oil analysis.

The ground test vehicles of helicopter main transmissions are being used in progressive test programs where components of advanced design and/or advanced materials and lubricants are evaluated, and their reliability at elevated temperatures predicted(24). In another series of tests an OH58A transmission rated at 500 H.P. was mounted on a regenerative test stand to determine its efficiency with each of eleven different lubricants(25). The results indicated that the efficiency of the test transmission ranged from 98.3 to 98.8 percent dependent upon the lubricant used. This variation in efficiency represents a 50 percent difference in transmission losses.

There are operational requirements where it is impossible to develop the value of specific film thickness necessary to achieve gear tooth separation and the load is shared by the surface asperities. In this mode the composite surface roughness is most certainly not that specified on the gear drawings nor that which exists on newly manufactured gear teeth. Theory suggests that gears which have been run-in have had the slopes of their asperities reduced, thus providing more contact area(26). A realistic value of specific film thickness is difficult to determine due to the uncertainty of actual operational surface roughness. As a result, the value of specific film thickness which is calculated as existing in the boundary lubrication regime is open to question.

A methodology has been developed(27,28), utilizing published test data which considers the elastohydrodynamic film thickness and the composite surface roughness as two separate parameters. Although the work was done with data from bearing tests, the basic theory should be applicable to gears as well. The theory should be tested and, if confirmed, should be used to modify present EHD computer programs. It does seem to be good practice to relate to the surface topography of gears and bearings in an as-run condition rather than in an as-manufactured condition.

There is a concern that the Ryder Gear Test (ASTM-D-1947) has reached the limits of its usefulness. Published papers refer to an "imprecision problem." What is required is a test machine which will give statistically repeatable results quickly and economically by means of test specimens that duplicate the sliding/rolling motions found in the gearmesh. The ability to screen lubricants and to define load-carrying capacity with precision may be critical in the development of high-temperature gear oils.

The drive for increased installed efficiency requires the development of high temperature gear lubricants. These may be based upon existing synthetic stocks by increasing viscosity and adding additives, or by going to synthetic hydrocarbon-based stocks. In any event, their performance in the gearmesh environment must be evaluated and a rationale developed which allows for engineering predetermination of their usefulness in an application. This may require combining the results of Disk and Ryder tests with EHD programs to account for boundary lubrication. A fundamental understanding of the physical and chemical interactions between the lubricant and the gears is lacking at this time, and this is a goal that must be given more emphasis.

In addition to the technical aspects of lubrication it follows that in order to secure its maximum effectiveness; i.e., maximum penetration for cooling and EHD film development, the lubricant must be put into the mesh zone properly(29-31)and removed from the gearbox with the minimum amount of energy transferred to it.

9. DESIGN SYNTHESIS

The open literature contains very little concerning gear synthesis and gear arrangements. Yet, these are the rationales that, in combination with gear lubrication and stress analysis, will make a truly complete gear design synthesis program possible. A methodology related to involute gearing which synthesized both gear arrangement and design to predetermined stress levels was published in 1963(32). It has the virtue of simplicity which eases reduction to a computer program format.

During September of 1982 a paper was presented at an ASME conference which may have significant potential in the area of dedicated gear drives(33). The paper presents the

should be a valuable tool for assaying the planetary gears in existing helicopters and turboprop gearboxes. It may even serve as a guide of how to improve them. It has the potential of being transformed into a design tool for comparing planetary gears with the same overall ratio, but with varying numbers of planet gears and gear teeth. This would give the designer the opportunity of comparing the effects of different combinations of tooth numbers which result in hunting ratio, common factors and simultaneous meshing. There is the capability of expressing the numbers of gear teeth which are used in the equations in terms of overall ratio, and further generalizing, so that all types of the epicycle differential gear may be examined.

Dynamic Analysis

A number of mathematical models have been proposed to resolve the dynamic loads which result from the effects of tooth spacing errors, wear, profile variations, tooth tip relief, and variations in stiffness of the individual tooth pairs as the location of their mutual line of contact changes during operation(15-18). With NASA-Lewis sponsorship, a methodology was developed and incorporated into a computer program named, "Gear Dynamics" (GRDYN), which will handle both low- and high-contact-ratio gearing(19).

A review of the literature reveals that from a vibration and dynamic viewpoint, the gearbox is being addressed as an isolated entity rather than as a component of a larger and more complex power transmission system by most of the investigators. A few have recognized the influence of all of the other components involved(20,21). Displacement and/or torsional excitations can provide a stimulus which may act upon the drive system to induce unwanted torsional vibrations. This includes the characteristics of the prime mover, the load, the mount system and the vehicle which supports the drive system.

8. LUBRICANTS AND LUBRICATION

In the United States the demands of logistics require that the lubricant for turboprop power transmissions be MIL-L-7808 and/or MIL-L-23699. Neither of these oils has additives which are beneficial to the gearmesh. There is a specific commercially available brand of oil which meets the MIL-L-23699 specification that does contain additives; however, the gear designer is not permitted to specify it. Presently, both the engine and gear train are served by a common lube oil source whose bulk temperature is normally given as a range of 175°F to 225°F. To assure meeting design requirements, it is assumed that operation is with the less viscous oil at its maximum bulk temperature. This places obvious constraints upon gear design options.

Experience with the T64 gearbox, which has been developed from 1600 to 3500 horsepower, indicates that tooth breakage is not a gear failure mode. An effective growth limit based on lubricant properties exists which does not allow for gear root stress capability to be exploited. Higher power levels have been achieved at lower bulk oil temperatures. The suggestion is that the specified lubricants are the barrier to increased performance.

There appears to be three viable paths available to immediately increase gear capabilities and two development areas to consider for the future. These are:

- To separate the gearbox lube oil system from the engine lube system and to supply the gears with a gear oil.
- To seek out the potential increased capabilities claimed for the Conformal gear tooth form.
- To examine the potential of involute gear teeth with larger than standard pressure angles in the double helical configuration.
- To develop high temperature gear oils.
- To develop and test "synthesized" gears.

The unexpected appearance of a lubricant which would meet present oil specification requirements, maintains sufficient gearmesh film thickness and contained additives to improve boundary lubrication conditions when needed would not eliminate any of the items just noted.

NASA has sponsored a computer program, "Thermal Elastohydrodynamic Lubrication of Spur Gears", (TELSGE)(22) which has been correlated with T64 operating data. The program utilizes both temperature and pressure viscosity relationships in evaluating lubricant performance. The line of action is divided into fifty equal divisions on both sides of the pitch point and a solution is arrived at for each of the one hundred points. It is dedicated to the elastohydrodynamic lubrication regime. It does not account for the additional load-carrying effects of additives nor does it consider boundary lubrication. The output is available in either numeric or graphic form; the latter making ideal permanent records to substantiate design decisions. A periodic publication of a compilation of viscosity coefficients as they become available would be

5. GEARBOX MATERIALS

The light metal alloys, aluminum and magnesium, have been the primary materials used for helicopter transmission and turboprop gearbox housings. The suppliers of these materials have been improving their performance with regard to modulus and strength at temperatures above 300°F, but they face fierce competition from ferrous alloys and composites. The composite structure of the Lear Fan aircraft and its engine power transmission shafts is perhaps the ultimate example of the potential of composites.

Boeing Vertol has a composite CH-47 aft rotor shaft torque tube and an engine-mounted nose bevel-gearbox housing under development(12). The composite torque tube section, designed for unlimited life, is approximately 23% lighter than an equivalent steel tube. The composite nose gearbox has been static load tested to 120% single-engine power. It is approximately 80% lighter than the present magnesium housing, can tolerate operation at 450°F, and has the potential of significant noise reduction.

The potential of higher gearbox operating temperatures has resulted in a move away from light-alloy housings to a stainless steel fabricated main housing by Sikorsky(2). A lighter weight and less costly housing is claimed. A close matching of the coefficients of thermal expansion between the housing, bearings and gearshafts are substantial aids in operational and cost performance. Other noted advantages are the virtual elimination of corrosion, fewer required machining operations and the elimination of bearing liners, studs and inserts.

6. BEARINGS

It would be expected that bearing life and reliability would meet system design requirements. This confidence level is based upon the continuing development of bearing materials with improved fatigue and impact properties, the analytic capabilities of present computer programs and the ability of bearing manufacturers to produce precision products.

Presently, VIM-VAR M-50 is a premium bearing material which has not proven itself to be suitable for the gear environment. The steels which are of interest to gear designers are those which will tolerate increased operating temperatures and excel in operation functioning as gears and bearings. This has come about by the effort to increase the load capacity of gears which results in smaller gear sizes for a given torque load. Unfortunately, smaller gear sizes translate into larger bearing loads. The potential fretting problem between the inner race and shaft journal may be avoided by making use of integral inner races. When this is done, the bearing load capacity is usually increased since a larger diameter rolling element may normally be used.

It appears that the U.S. helicopter manufacturers are working to reduce the number of bearings required to support the bevel gears in their main transmissions. Boeing Vertol has chosen the tapered roller bearing for this purpose(12). They have relocated the cone back-face rib to the cup front-face and made the cone integral with the gearshaft. The new location of the rib traps oil for improved roller-to-rib lubrication. Also, the use of tapered roller bearings in this application reduces the number of bearings required per gearshaft from three to two. This has decreased the length of the gearshaft and the overall size and weight of the bevel nose gearbox. Sikorsky Aircraft is developing a hybrid roller bearing with the object of increasing its thrust capacity and thereby eliminating the need for a ball thrust bearing. This bearing was incorporated into a proof-of-principle main transmission and run at full speed and load.

There are ongoing programs to prove ball bearing geometry and materials at high DN values; i.e., two million DN and three million DN. It is feasible to consider that a bearing for an aircraft gas turbine gas generator may run at these DN values, however, such a requirement will probably not be necessary for a turboprop gearbox.

Modern computer programs are available for designing and evaluating bearings of many different types for use in a variety of applications. A gearshaft-bearing assembly may be analyzed as an interacting system subjected to a complex load-speed-time duty cycle. Items such as bearing internal geometry and clearances, elastohydrodynamic lubrication; the centrifugal field, materials, temperature, etc., are involved in the rationale. Life multipliers are constantly being correlated with field experience. As a result, the anticipated life and reliability of all of the bearings in a complex drive system, as well as the overall system reliability, may now be predicted with increased confidence.

7. LIFE ANALYSIS

Basic research relating to the surface fatigue life of gears has been reported on by NASA-Lewis investigators(13).This work has been expanded to include a reliability model for planetary gear trains(14). The model is based on the Weibul distribution of the individual reliabilities of the gears and bearings which make up the machine. This

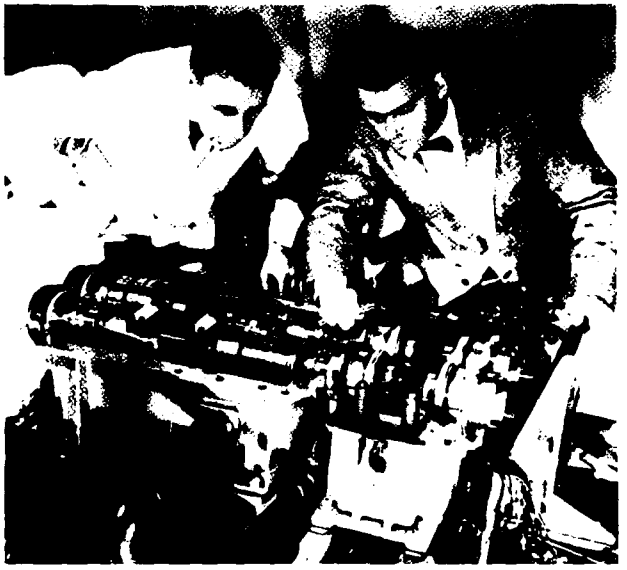


Figure 4
High-Temperature Gear Lube Test Stand

There are steels with hot-high hardness strength from which gears have been manufactured and incorporated into helicopter ground test vehicles. The steels of primary interest are CBS600, VASCO-X2 and Carpenter EX-00053. The former two are considered to be good bearing steels so the option of designing gearshafts with integral bearing races exists. However, testing(9) indicates that CBS600 and VASCO-X2 do not display statistical gains over AISI 9310 in bending fatigue life. Moreover, they exhibit a potential for a surface fatigue spall which acts as a nucleus for a tooth fracture failure. Their advantage is their ability to maintain hardness and strength at temperatures that render AISI 9310 useless.

Another steel which exhibits high hot-hardness strength and is being tested as a candidate material for gas turbine main shaft bearings is a modified AISI M50 designated M-50NIL(10). It is among a new generation of materials being developed which will provide improved fracture toughness and corrosion resistance. Tests conducted with bearings made of a carburizing grade of AISI M-50 showed no tendency toward fracture nor an indication of incipient fracture although the bearings had spalled. It has not yet been determined whether the favorable characteristics exhibited in bearing tests will carry over into the gear environment.

The importance of developing steels that perform well in both gear and bearing applications cannot be overemphasized. In addition to the size and weight benefits gained by gearshafts with integral bearing inner races there is the avoidance of fretting to be considered.

With aerospace gears the final stages of the manufacturing process may vary after hardening. Some gears are protuberance hobbed so that the final grinding operation does not affect the root. Gears with ground and unground roots have had their roots shot-peened to increase bending fatigue life. Whether shot-peening has been extended to the tooth flanks to improve pitting fatigue life in operation is unknown. Had the researches of Townsend and Zaretsky(11) been published earlier, no doubt the process would have been qualified for production gears.

3. GEAR TOOTH FORMS

Ongoing projects and studies relative to gear tooth forms may have a significant impact upon future power transmission systems. The involute tooth form, the Wildhaber-Novikov tooth form and a potential synthesized gear tooth form are being examined. The former two are undergoing serious development in the analytic and hardware stages while the synthesized tooth form exists as a computer program. A number of involute gear tooth form modifications have been developed and are undergoing test in the United States in association with advanced helicopter transmission programs. A similar activity is taking place in England, except that the tooth form is "Conformal." In both countries the goal is to improve load carrying capabilities. The involute modifications are essentially related to high contact ratio gearing. The effort is being carried out by Boeing Vertol, Bell and Sikorsky under contract with NASA-Lewis and the U.S. Army Research and Technology Laboratories.

Sikorsky Aircraft has developed a high-contact-ratio involute tooth form which has a standard 20° pressure angle on the drive side and a 25° pressure angle on the coast side which they have chosen to call a "buttressed" tooth form(1). The planetary gearset of a development Black Hawk transmission was made up with buttressed tooth form gears and ran at full load in a test transmission. Published test results(2) claim an increase in gear fatigue life of 65:1 over that of a standard involute tooth form due to the reduction of gear tooth bending stresses inherent in the high-contact-ratio design. It is expected that an increase in load capacity is achievable for the modified transmission. It was also noted that the high-contact-ratio gearsets have increased lube oil temperature differentials when compared to standard involute gearing.

Bell Helicopter published the results of engineering calculations which predicted the results of a series of tests which were to be run in a common planetary arrangement(3). Standard spur gears, high-contact-ratio spur gears and double-helical gears were to be evaluated. Planetary gears made up of each tooth form were to be run sequentially in the same gearbox, under similar test load conditions. At the time of writing, the results of the tests were not yet made public; however, calculated test results indicated that the double-helical gears would be the most efficient and have the lowest lube oil temperature rise.

Another variation of the basic involute was designed and manufactured by the Boeing Vertol Company and designated as the New-Tooth-Form (NTF)(4).This tooth form was a high-contact-ratio spur gear with large profile modifications at both the addendum and dedendum. The profile radius of curvature was reduced at the addendum and increased at the dedendum in an effort to reduce sliding. Test results indicate an increase in pitting fatigue life, decreases in scoring and bending capabilities, and an increase in operating temperature as compared to standard involute low-contact-ratio gears(5).

In England, Westland Helicopter is utilizing gears which have circular-arc tooth forms for the last reduction stage in the main transmission of their Lynx helicopter(6). The tooth form has been derived from the Wildhaber-Novikov tooth system which Westland has designated as Conformal. The tooth profiles are basically circular arcs, the pinion having a convex surface and the gear a concave form. Theoretically, the Conformal has a point contact as opposed to the line contact of an involute; however, in practice an elliptical contact pattern exists. It is claimed that their load capacity is 50% greater than involute capacity for case hardened and ground gears and that they experience slightly lower losses(7). Early test reports stated that they were sensitive to center distance variation. If so, that problem is evidently susceptible to detailed engineering analysis and profile modification. There are compromises to make in its application; a relatively long face width is required since it drives through its helix and its performance improves as the ratio increases. The Conformal tooth form allows for a pinion with an extraordinarily low number of teeth to be made for use in a power transmission gearset. The result is the ability of a pair of gears to achieve a large speed ratio.

4. GEAR & BEARING MATERIALS

One approach to increasing overall aircraft performance is to decrease the heat rejection rate of the installed machinery. In order to achieve this goal the operating temperature must be increased. The idea of operating gears at higher temperatures is not a new one. Almost thirty years ago a high temperature gear test stand(Fig.4) was put into operation and testing conducted(8). Gear materials that could function at elevated temperatures, up to 600°F, were identified. Lubricants were not.

The vast majority of turboprop gears have been made of AISI 9310 steel. As the quality has improved from premium quality air-melt to Consumable-Electrode-Vacuum Melted (CEVM) and to Vacuum Induction Melted-Vacuum Arc Remelted (VIM-VAR), it has been incorporated into the product. However, the material improvements due to cleanliness have not affected the tempering temperature of approximately 300°F, thus present gearboxes are temperature limited. Moreover, there has been no incentive to use high, hot-hardness gear steels in the past due to the inability of lubricants to maintain a sufficient film thickness at elevated temperatures.

investment and life cycle costs. Future turboprop gearboxes will feature the absolute minimum number of gears required to perform the desired function consistent with what advances in materials, lubricants, gear tooth form and bearings will allow.

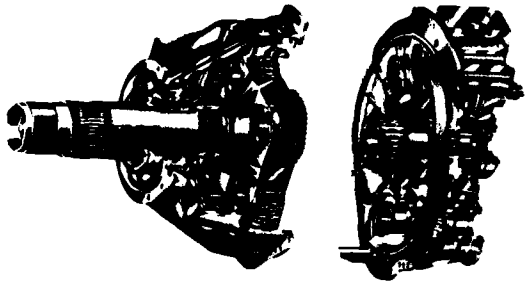


Figure 1
Turboprop Planetary Gear

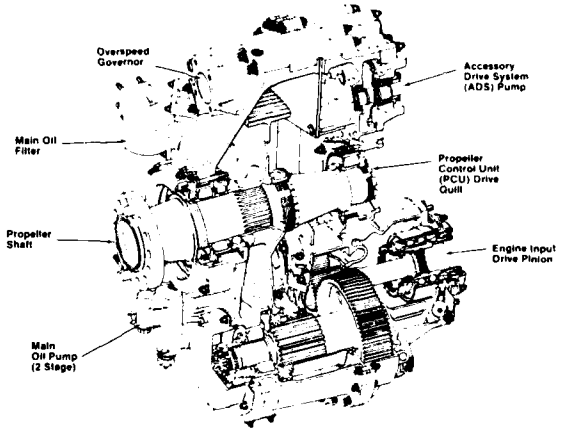


Figure 2
Turboprop Double-Reduction Double Branch Offset Gearbox

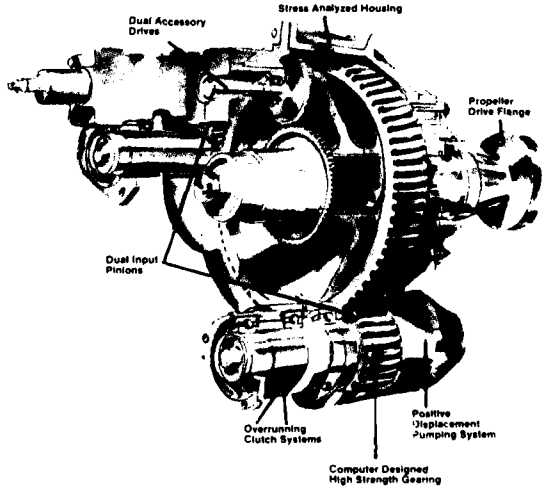


Figure 3
Western Gear/Lear Fan Propeller Gearbox

A STATE OF THE ART ASSESSMENT OF TURBOPROP TRANSMISSION TECHNOLOGY AND PROJECTED NEEDS FOR THE NEXT GENERATION

by
Robert J. Willis, Jr.
Principal Engineer - Gear Systems
General Electric Company
1000 Western Avenue
Lynn, Massachusetts 01910, U.S.A.

The major share of power transmission research and development during the past twenty years has been expended on the improvement of helicopter main rotor drives. Fortunately, most of the advanced technology features resulting from these efforts are directly applicable to turboprop transmissions. The technology base is made up of a number of interacting disciplines whose application is tempered by economics as well as the engineering state of the art at any given time. Modern computers are playing an ever increasing role in the design process and promise to be the means of removing gear design from its empirical background.

1. INTRODUCTION

The increase in the price of fuel as a percentage of direct operating costs has stimulated interest in the turboprop engine as a potential replacement for turbofan engines. Although popular immediately following World War II, it was soon displaced on large transport aircraft by increasingly improved turbofan engines which allowed for higher cruise speeds and eliminated the speed-reducing gearbox by having a direct drive between the power turbine and the fan. In areas where economics or high thrust capability at low velocities were the governing criteria, rather than speed, the turboprop held its own as evidenced by its many applications in military and general aviation aircraft. With the exception of the CT7 and the PW100 series engines, plus the engine/gearbox combination powering the Lear Fan, all of the major turboprop engines were certified prior to 1968. Twenty years or more have passed since the initiation of their designs. In that interim the helicopter was found to be a most attractive machine in a broad application/utilization area and attention was given to its development. In the meantime, dedicated turboprop transmissions have experienced increased load capabilities by means of continuing product improvement programs. These include the qualification and use of improved materials, as they become available, and design changes within the constraints of an existing product.

Historically, turboprop and helicopter gear arrangements have favored some form of the epicyclic differential gear for the last reduction stage. The gear teeth have been of the involute tooth form and engine oil has been specified for the gearbox to satisfy the demands of logistics. Recently, there has been a trend to use other types of gear systems. For example, neither the CT7, PW100 nor the Lear Fan/Western Gear turboprop gearboxes utilize epicyclic gearsets. This also applies to the power transmission system of the Westland Lynx helicopter. In addition, conformal gears rather than involutes are used in its last reduction stage, and it has its own lubrication system. A gear oil is specified rather than an engine oil so as to not compromise the gears.

The state of the art in gearing is largely based upon empiricism. However, some of the accomplishments of recent years, aided by the enormous high-speed computational capability of modern computers, have increased our knowledge and understanding of fundamentals and suggest that further advances may be made.

2. GEAR ARRANGEMENT

A review of turboprop engines listed in several volumes of "Jane's All the World's Aircraft," with regard to gear arrangement, illustrates the popularity of the epicyclic differential gearset for this application(Fig.1). Of twenty older engines surveyed, fully eighteen of them incorporated some form of this type of gearset in their propeller drive trains. This popularity exists for single and dual gas turbine engine drives and for counter-rotating and single rotation propellers. The exceptions are the Bristol Coupled Proteus and the Napier Naiad.

The latest turboprop engines to appear in North America have abandoned this trend(Fig.2). The CT7 and the PW100 series engines both make use of double-reduction, double-branch offset layouts which have simple geometries and fewer parts than comparable epicyclic gearsets. The gearbox designed and developed by Western Gear for the new Lear Fan aircraft has dual inputs and a single output which drives a pusher propeller mounted at the rear of the fuselage(Fig.3). It is different in that a spiral bevel "V" drive with 7° shaft angles is used for the drive gears. All of these gearboxes stress overall design and manufacturing simplicity and a minimum number of parts. A new trend which extols simplicity appears to have begun. This is no doubt a reflection of the increasing emphasis placed upon reliability, maintainability, initial

(Speaker not identified)
Do you use MSO in gears also?

Author's Reply
No, we use Vasco X2.

DISCUSSON

G.Kreselmeier, Ge

Did you make comparison tests between tapered roller bearings and ball cylindrical roller bearings in the case of oil-off?

What results did you get?

Author's Reply

We have conducted a considerable number of oil-off and minimal oil flow tests on systems with all three types of bearings, but no one-on-one comparisons within a fixed system. In general, tapered roller bearings fared much more poorly in both cases due to rapid failure at the rib. When supplied with minimal oil, however, performance, while not optimum, was good.

L.Battezzato, It

Literature shows that by adding reinforcing elements to MG alloy, we obtain a good increase of UTC and YS. The elongation instead is expected to become very low or, in other words, the structure becomes very fragile. Can you comment on this and show which type of reinforcement allows a better characteristic as far as the fragility is concerned?

Author's Reply

Much work is currently being done using MG FP metal matrix composites. After much development, it has been our experience that rigidity is *very* much improved but with no appreciable penalty on impact resistance. The fibres themselves, in the uncompounded state, are fragile, but not so in the cast MMC state. Programs are under way but no further documentation is available at this time.

B.A.Shotter, UK

Do you see any problems associated with the optimization of the lubricant when associated with the new gearing materials and with T.D.C. coatings on bearings?

Author's Reply

Preliminary tests show no problem with 23699 or 7808 or Shell 555, etc. I see no real problem with future oils.

J.Godston, US

Housing materials — what are the properties for composites dealing with stability for clearance control (what about long time stability)?

When will the technology be available for production products?

With gear and bearing material advances pointing toward temperature in the 300 to 400 + capabilities, composite materials need to have this capability. What is being done to provide this capability?

What is the program and what is the plan to put this in the world engineering community?

Author's Reply

Early tests showed some long term creep problems, but more recent designs have shown only minimal problems.

At higher temperatures, conventional epoxy/fiber glass probably will not work. Best potential solution appears to be metal matrix composites.

Much research is under way on MMC, but it is "sensitive".

R.François, Fr

What is considered as being the minimum life (for bearing races or gear teeth) for TAE integrated designed parts?

Author's Reply

1. Fully integrated spiral bevel/tapered roller bearings are not in production yet. Next generation will use such design.
2. Current production uses some cylindrical races as integral parts of the gear. Such parts are normally removed "on-condition" only, thus no minimum life is specified.
3. For future requirements (which is the topic of this paper), design life of bearings may well be, for fully integrated design, 5,000 to 20,000 hrs., probably higher on an "on-condition" basis. This is true because most current failures are not actually real B-10 type failures but may be traced to secondary forces. By minimizing potential secondary sources, actual life will be extended.

2. Army Mechanics and Materials Research Center, DAA646-81-0196; AIRCRAFT QUALITY HIGH TEMPERATURE VACUUM CARBURIZING; Watertown, Massachusetts.

3. Drago, R.J.; RESULTS OF AN EXPERIMENTAL PROGRAM UTILIZED TO VERIFY A NEW GEAR TOOTH STRENGTH ANALYSIS; American Gear Association, Washington, DC, Fall Technical Meeting, October 1983.

4. Drago, R.J.; ON THE DESIGN AND MANUFACTURE OF INTEGRAL SPIRAL BEVEL GEARS FOR THE CH-47D HELICOPTER; American Gear Manufacturers Association, Aerospace Gearing Committee Meeting, Lake Tahoe, Nevada; March 1979.

5. Lenski, Jr., J.W.; ADVANCED TRANSMISSION COMPONENTS INVESTIGATION PROGRAM - BEARING AND SEAL DEVELOPMENT; United States Army Aviation Research and Development Command, TR80-D-19; St. Louis, Missouri; August 1980.

6. Townsens, D., Baber, B., and Nagy, A.; EVALUATION OF HIGH CONTACT RATIO SPUR GEARS WITH PROFILE MODIFICATION; NASA Technical Paper 1458; Washington, DC, September 1979.

7. Keller, C.; ADVANCED TECHNOLOGY HELICOPTER TRANSMISSION LUBRICANT; SER 510113, (Navy Contract N00140-82-C-3723) Naval Air Propulsion Center, Trenton, New Jersey, March 1983.

8. Drago, R.; OPTIMUM LUBRICATING OIL STUDY; D210-11965-1; (Navy Contract N00140-82-C-3722) Naval Air Propulsion Center, Trenton, New Jersey, September 1982.

9. Lemanski, A.J., Lenski Jr., J.W., and Drago, R.J.; DESIGN, FABRICATION, TEST AND EVALUATION OF SPIRAL BEVEL SUPPORT BEARINGS (TAPERED ROLLER); Boeing Vertol Company, USAAMRDL TR73-16, Eustis Directorate, United States Army Air Mobility Research and Development Laboratory, Fort Eustis, Virginia; June 1983.

10. Lenski Jr., J.W.; TEST RESULTS REPORT AND DESIGN TECHNOLOGY DEVELOPMENT REPORT - HLH/ATC HIGH SPEED TAPERED ROLLER BEARING DEVELOPMENT PROGRAM; Boeing Vertol Company, USAAMRDL TR74-33, Eustis Directorate, United States Army Air Mobility Research and Development Laboratory, Fort Eustis, Virginia; June 1974.

11. FAFCOTE-TDC, THIN DENSE CHROME PLATED BEARINGS, Form No. 573, Fafnir Bearing Division of Textron Inc., New Britain, Connecticut 06050, 1984.

CONCLUSION

The developments described in this paper represent a few of the major accomplishments in advancing the technology of rotary-wing aircraft transmission components. The combined effect of these developments will provide a drive system with significant advantages, including lighter weight, less complexity and cost, fewer faying surfaces and, potentially, longer component life and increased reliability.

A few of these advances have already been incorporated into the modernized CH-47D helicopter. Although there has been no change in the basic arrangement and speed reduction of the CH-47C and CH-47D drive system, there have been significant improvements in weight, reliability, and life-cycle costs effected through the use of integral gears and bearings, high-temperature gear steel (VASCO-X2), tapered-roller bearings, an auxiliary lube system, and an integral oil-cooler system. The CH-47D transmissions have successfully completed extensive bench and flight testing and are now in production.

The next-generation transmission will incorporate many more advanced technological concepts to achieve the desired drive system goals mentioned earlier. Figure 14 illustrates how advances in technology can improve a transmission. The CH-47 engine transmission modifications over the years to increase its power capacity while keeping weight increases to a minimum are such an example. The original CH-47A helicopter was designed with the technology of the late 1950s and early 1960s. Over the years, changes were incorporated to increase the power capacity while maintaining the basic envelope. The CH-47C engine transmission was capable of a 50-percent increase in single-engine power with only a 17-percent increase in weight. The current production CH-47D engine transmission power capacity has increased an additional 23-percent with only a 2-percent increase in weight. Projections based on the advances discussed in this paper would result in an engine transmission that can transmit 85-percent more power than the original CH-47A and weigh less.

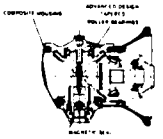
TRANSMISSION CONFIGURATION	CH-47A (1960)	CH-47C (LATE 1960'S)	CH-47D (MID 1970'S)	ADV. XMSN (1980'S)
				
DESIGN POWER				
S.E. T.E.	2,485 HP 4,970 HP	3,750 HP 6,000 HP	4,600 HP 7,500 HP	4,600 HP 7,500 HP
CONFIGURATION	STANDARD STEELS 52100 - BEARINGS 9310 - GEARS STANDARD BALL & ROLLER BEARINGS & SPACERS	MODIFIED STEELS CEVM M-50 - BEARINGS CEVM 9310 - GEARS OUT OF ROUND ROLLER BEARINGS WITH INTEGRAL SPACERS	MODIFIED STEELS CEVM M-50 - BEARINGS CEVM VASCO-X2 - GEARS OUT OF ROUND ROLLER BEARINGS WITH INTEGRAL SPACERS, HIGH-SPEED CLUTCH BEARINGS	MODIFIED STEELS CEVM CBS-600 BEARINGS VIM-VAR VASCO-X2 GEARS HIGH SPEED, CUP RIBBED TAPERED-ROLLER BEARINGS, COMPOSITE HOUSING
	SPLINED GEAR TO SHAFT	BOLTED GEAR TO SHAFT	ONE-PIECE INTEGRAL GEAR/SHAFT	ONE-PIECE INTEGRAL GEAR/BEARING/SHAFT
MAJOR COMPONENTS	27	24	20	15
FAYING SURFACES	45	38	31	18
NO. BEARINGS	8	8	7	5
TOTAL WEIGHT	105 LB	123 LB	125 LB	100.5 LB
S.E. HP / LB	23.67	30.49	36.80	45.77

Figure 14. Advancements in Transmission Design

In addition to reduced weight, many other significant advantages can also be achieved. Major parts count is reduced by 65-percent, and the number of bearings is reduced by 37-percent. Each of these items has a significant effect on initial cost and system reliability. Fewer bearings and faying surfaces will greatly reduce the major source of transmission removals and causes of component rejection. In approximately 20 years, the power transmitted per pound of transmission weight has doubled.

The marked advantages to a rotary-wing aircraft transmission system that can accrue from component development are evident. We believe that continuing research and development programs leading to integrated assembly and improved analysis and testing of advanced components will provide the technology to meet the goals of the 1980s and beyond. Results of programs to date indicate that continuation of these efforts will provide significant and fruitful results for future helicopter drive systems.

REFERENCES

1. Drago, R.J. and Lenski Jr., J.W.; DEVELOPMENTS IN THE DESIGN, ANALYSIS, AND FABRICATION OF ADVANCED TECHNOLOGY TRANSMISSION ELEMENTS; American Helicopter Society Paper RWP-12, Washington, DC, November 1982.

The composite rotor shaft was tested under combined bending and torsional fatigue loads. The bending loads applied are approximately double the design 8-degree flap angle load, and the torsional load is equivalent to the design torque rating of the shaft. The torsional loads are carried into and out of the composite tube through the radial pins connecting the upper and lower steel sections. The bending loads are taken by socket action between the inserted steel pieces and the tube inside diameter. Testing of the composite center section meets the design goals of the composite rotor shaft. These tests also demonstrate that composite structures can be used in this critical area of a helicopter drive system.

Composite Transmission Housings

Compared to the magnesium castings now used, potential advantages of a composite transmission housing include thermal stability, excellent specific stiffness and strength, and resistance to corrosion. In addition, with the use of a high-temperature polyimide matrix, the stiffness and strength of the assembly can be maintained to 450°F or even higher, depending upon the choice of matrix material.

A CH-47 engine-mounted nose gearbox designed and fabricated from graphite and polyimide composite material. This gearbox is a single-bevel-mesh unit with a reduction ratio of 1.23 to 1 and a power capability of 4,600 hp at an input speed of approximately 15,000 rpm. The production gearbox housing is a magnesium casting with a weight of 25 pounds.

The fabrication method for this housing was selected on the basis of potential minimum production cost; it eliminates hand layups, multiple cure cycles, and secondary bonds. Filament winding appears to best fulfill these requirements. A compatible graphite filament and polyimide resin system was selected from a number of candidates with temperature capability appropriate to current lubricating oils (around 300°F oil-out) with a suitable margin for emergency mode oil-off operation. This margin requirement eliminated epoxy systems from consideration. Therefore, Kerimid 711, a modified bismalyimide resin, and Hercules AS-4 graphite fiber were selected.

The properties of the composite housing made possible deflections at key points equal to or less than those of an equivalent magnesium housing and a weight saving of approximately 20 percent was effected.

The dynamic components of a CH-47D engine transmission were installed into the composite housing. The gear teeth and composite housing were strain-gaged in critical areas, and a series of static and dynamic tests was conducted with the test rig, Figure 13, which shows the composite housing installed in the test stand along with a standard magnesium-housing engine transmission. The composite housing successfully completed a series of static load tests at ambient and elevated temperatures. Data were recorded for loads up to 120 percent of single-engine power and compared with existing data for a magnesium housing.

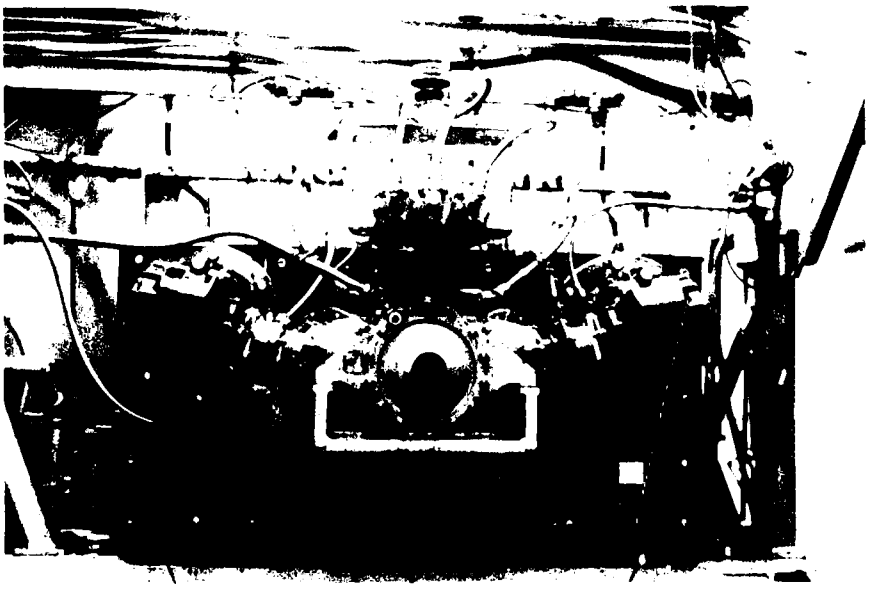


Figure 13. Gearbox Test Stand

Test results indicate that a composite material can be used in the fabrication of a transmission housing, and it will achieve design objectives.

The improvements in weight and especially stiffness achieved through the use of composite materials almost insures their application to future transmission designs.

References

1. Design of High Contact Ratio Gears, K.M. Rosen, H.K. Frint, American Helicopter Society, May 1981.

2. Report on Advanced Transmission System Integration Tests, J.H. Mancini, H.K. Frint, American Helicopter Society, November 1982.

3. Development of Helicopter Transmission Components for the 1980s, Roy A. Battles, American Helicopter Society, HPS-10, November 1979.

4. Geared Power Transmission Technology, J.J. Coy, NASA Conference Publication 2210, 1980.

5. Evaluation of High-Contact-Ratio Spur Gears With Profile Modification, D.P. Townsend, A. Nagy, B.B. Baber, NASA Technical Paper TP-1458.

6. The Lynx Transmission and Conformal Gearing, B.A. Shotter, Society of Automotive Engineers, No. 781041, November 1978.

7. Experiences With Conformal/W-N Gearing, B.A. Shotter, World Congress on Gearing, Paris 1977.

8. Some Work on the Selection of Materials Suitable for Gears Operating From Room Temperature to 600°F, J.B. Seabrook, General Electric Materials and Processes Laboratory Report No. R56TG837, October 1956.

9. Endurance and Failure Characteristics of Modified VASCO X-2, CBS600 and AISI 9310 Spur Gears, D.P Townsend, E.V. Zaretsky, NASA Technical Memorandum 814213 August 1980.

10. Status of Understanding, E.N. Bamberger, International Conference on Tribology, April 1980.

11. Effect of Shot Peening on Surface Fatigue Life of Carburized and Hardened AISI 9310 Spur Gears, D.P. Townsend, F.V. Zaretsky, NASA Technical Paper 2047, August 1982.

12. Developments in the Design, Analysis, and Fabrication of Advanced Technology Transmission Elements, R.J. Drago, J.W. Lanski Jr. , American Helicopter Society, November 1982.

13. An Update on the Life Analysis of Spur Gears, J.J. Coy, D.P. Townsend, E.V. Zaretsky, NASA CP2210, 1982.

14. Life and Reliability Model for Helicopter Transmissions, J.J. Coy, R.J. Knorr, M. Savage, NASA TM82976, November 1982.

15. Evaluation of Dynamic Factors for Spur and Helical Gears, A. Seireg, D.R. Houser, Transactions of the ASME, May 1970.

16. Dynamic Tooth Loads and Stressing for High-Contact-Ratio Spur Gears, R.W. Cornell, W.W. Westervelt Journal of Mechanical Design, January 1978.

17. Analysis of the Vibratory Excitation of Gear Systems: Basic Theory, W.D. Mark, Acoustical Society of America, May 1978.

18. Gear Mesh Excitation Spectra for Arbitrary Spacing Errors, Load and Design Contact Ratio, E.P. Remmers, Journal of Mechanical Design, October 1978.

19. Compliance and Stress Sensitivity of Spur Gear Teeth, R.W. Cornell, ASME 80-C2/DET-24, August 1980.

20. A Computer Program for Vibration Analysis of Torsional Systems, A.W. Brunot, General Electric T.I.S., DF65MSD308, March 1965.

21. Gear-Excited Torsional Vibrations of Machine Drive Systems, N.F. Rieger, AGMA, October 1968.

22. Thermal Elastohydrodynamic Lubrication of Spur Gears, K.L. Wang, H.S. Cheng, NASA CR-3241, February 1980.

23. Full-Flow Debris Monitoring and Fine Filtration for Helicopter Propulsion Systems, T. Tauber, W.A. Hudgins, R.S. Lee, American Helicopter Society, November 1982.

24. Advanced Technology Helicopter Transmission Lubricant, C.H. Keller Jr., Sikorsky Aircraft, NAPC Contract No. N00140-82-C-3723.

25. Lubricant Effects on Efficiency of a Helicopter Transmission, A.M. Mitchell, J.J. Coy, AVRADCOM Technical Report 82-C-9.

26. A Preliminary Study of Lubricants for Advanced Turboprop Transmissions, D.B. Hester, General Electric Technical Memorandum No. 82-507, November 1982.

27. Rolling Contact Fatigue Life of AISI M-50 as a Function of Specific Film Thickness Ratio Using a High Speed R.C. Rig, A.H. Nahm, E.N. Bamberger, Journal of Lubrication Technology, Vol. 102, October 1980.

28. Specific Film Thickness - A Closer Examination of the Effects of EHL Film Thickness and Surface Roughness on Bearing Fatigue, C.N. Rowe, ASLE Transactions, Vol. 124, 4, 423-430.

29. Study of Lubricant Jet Flow Phenomena in Spur Gears - Out of Mesh Condition, D.P. Townsend, L.S. Akin, Journal of Mechanical Design, January 1978.

30. Into Mesh Lubrication of Spur Gears With Arbitrary Offset Oil Jet I - For Jet Velocities Less Than or Equal to Gear Velocity, L.S. Akin, D.P. Townsend, NASA Technical Memorandum 83040, November 1982.

31. Into Mesh Lubrication of Spur Gears With Arbitrary Offset Oil Jet II - For Jet Velocities Equal to or Greater Than Gear Velocity, L.S. Akin, D.P. Townsend, NASA Technical Memorandum 83041, November 1982.

32. Lightest-Weight Gears, R.J. Willis Jr., Product Engineering, January 21, 1963.

33. Design of a Synthesized Helical Gear Set, G.W. Eggeman, ASME 82-DET-73, September 1982

34. Application of Finite Elements to the Analysis of Gear Tooth Stresses, L. Wilcox, W. Coleman, ASME 72-PTG-30, October 1972.

DISCUSSION

Ph.Ramette, Fr

Could you state precisely the nature of the composition of the improved high temperature lubricant which you have tested?

Author's Reply

The lubricants used in the T64 are either MIL-L-7808 or MIL-L-23699. The correlation between the programme "Thermal Elastohydrodynamic Lubrication of Spur Gears" and the T64 planetary gear was done with field service experience and comparison with the results of other calculation methods.

H.Loustalet, Fr

You have shown a picture of a future turboprop using one stage of reduction. Do you think that such a high reduction ratio is achievable in one stage of reduction? What is the limit for this ratio?

Author's Reply

1. Yes. The gear set shown is of the "conformal" tooth form and is presented as a double-helical type. The face-to-diameter ratio of the pinion is 0.7 for each pinion helix. The "conformal" design allows for a pinion with an extremely low number of teeth.

2. This has not been explored.

J.Godston, US

Propeller or prop-fan pitch control studies under NASA contract are identifying concepts which will not require integration of the pitch control with the gearbox. Are you aware of these studies and programme?

You mentioned simple gearboxes like CT7, PW100 and Westland conformal simple gear for a single rotation propeller. What about counter-rotation?

Author's Reply

CT7 experience was inferred. Major control system suppliers are Woodward, Bendix and Hamilton Standard, and either may be specified by the customer. The result was a horror because each had a preferred geometry for specific pads difference preferred speeds, etc. The trend of packaging everthing in the propeller hub, with a simple drive shaft coming through the propeller shaft to provide power, simplifies the design of the power transmission gearing by not affecting gear arrangement selection. I know that studies are going on, but am not aware of publication.

To the best of my knowledge, the simplest gear arrangement for a counter-rotating turboprop fan drive is a free floating simple epicyclic differential gear.

ADVANCED GEARBOX TECHNOLOGY IN SMALL TURBOPROPELLER ENGINES

by

Cliff Browaridge and Derek Hollingworth
Pratt and Whitney Aircraft Canada
90 Dundas Street
Mississauga, Ontario L5A 3Z4
Canada

1 INTRODUCTION

Gearbox component analysis traditionally deals with the calculation of hertzian stresses at gear contacting surfaces and the fillet stresses at the tooth bases caused by the meshing loads. Major assumptions are often made regarding the dynamic loads and the variation of loads across teeth due to misalignment. Little attention is paid to gear weight optimization, or stresses generated at complex interactions such as splines or fretting surfaces between flanges.

This paper outlines current methods using 3D FE analysis that examines some of the more complex surface to surface interactions, as well as addressing the loading experienced between dynamically active teeth meshing at high speed.

To successfully design a light weight and durable gearbox for aircraft applications complex computer modelling is necessary and new theories of failure are needed to deal with such aspects as fretting fatigue.

2 PW100 GEARBOX AND INTAKE ARRANGEMENT

The PW100 engine uses a conventional gearbox/engine arrangement with an offset propeller and a ram air intake. The basic reasons for this arrangement have been discussed in detail in ref. 1 and are summarized below.

The offset arrangement gives excellent installation flexibility in that the propeller can be mounted above the engine centreline. This in turn allows for an easy attachment of accessories on the rear of the gearbox and above the engine where they are accessible for servicing. If a propeller brake is needed this can easily be attached to one of the layshafts, with a minimum rearrangement of shafting and bearings in the gearbox.

The offset inlet duct though unsymmetrical has a good cross section with a better hydraulic diameter than a narrow annular duct around the propeller spinner which would have a thick boundary layer and adversely affect the LP compressor performance.

The offset duct is inherently easier to design to limit foreign object damage because ice and bird ingestion can be easily exited and prevented from entering the engine by using inertial separation (see fig.1).

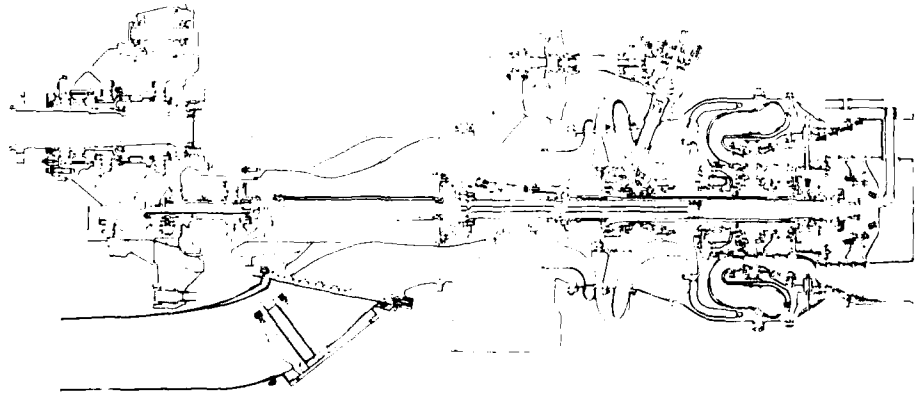


FIG. 1 PW100 CROSS-SECTION (TYPICAL)

The PW115 gearbox transmits 1500 HP with a gear ratio of 15.4:1 (see Fig.2). The gearbox consists of a two stage offset with a double layshaft connecting the two stages. The first stage helical pinion rotates at 20000 rpm and has a pitch line velocity of 10000 ft/min. The double helical pinion is electron beam welded to minimize length. The second stage transmits power via two layshaft pinions to a single bull gear that rotates at 1500 rpm. To save weight the bull gear web has many lightening holes and the rim is carefully tapered to provide an optimum load distribution across the width of the gear tooth. In the higher powered PW120 engine the second stage gear teeth are designed with high contact ratio teeth. This reduces tooth loading, bearing loads and gear noise.

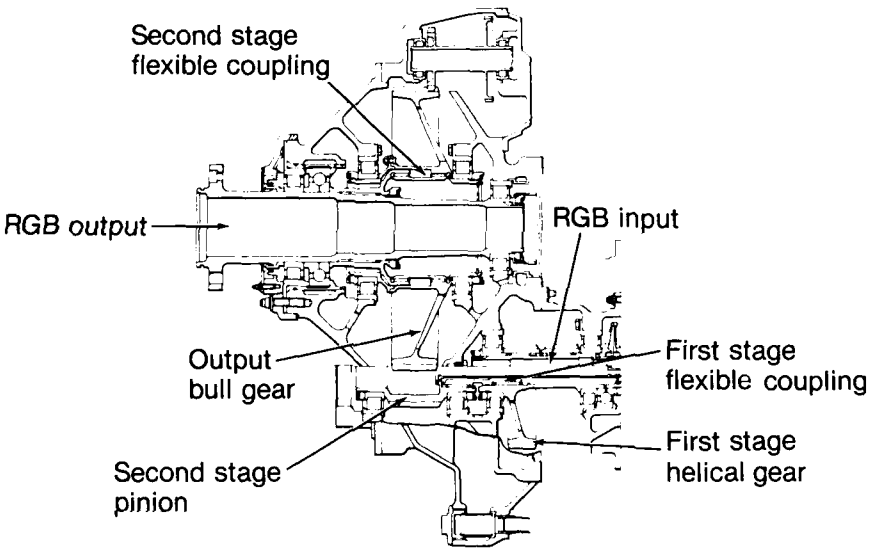


FIG. 2 PW115 GEARBOX ARRANGEMENT

In transmitting power from the bull gear to the propeller shaft a flexible coupling is used to isolate propeller shaft deflection from the final gear stage. This is because high aerodynamic propeller moments and gyroscopic moments cause significant shaft flexure. The propeller shaft is tapered carefully to match torque and bending loads for minimum weight. The propeller shaft and flange configuration is carefully sized to limit fretting damage at the front bearing and between the propeller hub and shaft flange faces.

Antifriction bearings are used throughout and bearings are sized to ensure an overall set life of greater than 5000 hours.

The torque shaft connecting the turbo machinery to the gearbox has high bending flexibility to absorb misalignment between the engine and gearbox. It incorporates diaphragms at each end and a torque meter to measure power transmitted. The power split is assured in the two layshafts by careful assembly procedures that ensure the maximum torque transmitted through one side is no more than 52.5% of total torque.

3 GEARBOX WEIGHT AND POWER TRANSMITTED

The gearbox arrangement was chosen after studies that compared first cost, reliability, efficiency and maintence cost. An extensive study of an advanced turbo prop gearbox design carried out at PWA (ref.2) also showed that the double layshaft split torque arrangement gave the highest reliability and lowest maintenance. This design however does not necessarily give the lightest weight configuration. Therefore great attention is paid to minimize weight.

Previous successful turbopropeller engines produced by PWC had used a two stage, inline, planetary gearbox. These had proved to have extremely low weight. The choice of the offset double layshaft arrangement with 11 bearings and 6 gears presented a major challenge in weight reduction whilst maximizing power and maintaining high reliability.

Optimization studies for minimum gear blank weights are carried out at PWC in accordance with methods outlined by R.J. Willis (ref.3). A method is presented here of comparing the torque/weight characteristics of all recent PWC gearboxes based on an early version of the PT6 engine. Comparative data is shown on Table 1.

Engine	Power	Prop. RPM	Gear Ratio	Torque lb.in.	Weight Index	Torque/wt. Index	Torque x GR/ wt. index
PT6A-27	680	2200	15	19,480	1,000	1.95	1.95
PT6A-41	850	2000	15	26,786	1,060	2.53	2.53
PT6A-45	1173	1700	17.6	43,187	1,725	2.52	2.96
PT6A-65	1250	1700	17.6	46,324	1,650	2.81	3.3
PT6A-50	1120	1210	22.8	58,337	3,020	1.93	2.94
PW-115	1500	1300	15.1	72,721	3,510	2.07	2.12
PW-120	2000	1200	16.7	105,040	4,120	2.40	2.65
PW-124	2400	1200	16.7	126,050	5,110	2.33	2.6

TABLE 1 : TORQUE/WEIGHT PARAMETERS

Gearbox power to weight effectiveness is best measured by contrasting torque transmitted to weight with some allowance for the gear ratio which in itself can be considered to cause an increase in weight. In the last two columns of Table 1 two parameters are shown that relate "Power to weight" effectiveness. They are a Torque/weight index and Torque times gear ratio/weight index. The latter is considered the more significant.

The results are shown graphically in Fig. 2. It can be seen that two slightly different impressions can be drawn. As the PT6 series was developed from 850 HP to 1250 HP there was an index increase from 1.95 for the A27 to 2.81 for the A65, a 44% increase. If the gear ratio is also considered the new index is 3.31, a 70% increase in load or torque carrying capacity per lb.

The A50 gearboxes seemingly poor rating can be explained by noting that the engine arrangement is significantly different than the PT6. It is a two mount plane engine, similar to the later PW100 series and as such the front mounts are integrated into the gearbox casing. It also has some accessories mounted on the gearbox requiring stiffening and additional pads. When the much higher gear ratio for this gearbox is included its index is then more comparable to the very efficient A65.

The PW100 series engines are also tabulated in Fig. 3. These are all independently designed gearboxes though the PW120 could be considered a growth version of the PW115. What is significant here is that the starting point for the PW115 is not dissimilar to the early PT6 A27. This seems to negate the idea that epicyclics are inherently lighter than split path. It is expected that during development the PW100 series will follow a similar improvement in torque/weight efficiency to that of the PT6 series engines.

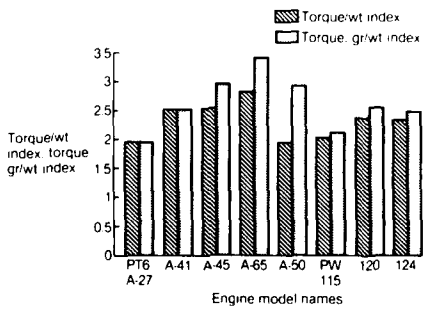


FIG. 3 TORQUE/WEIGHT PARAMETERS

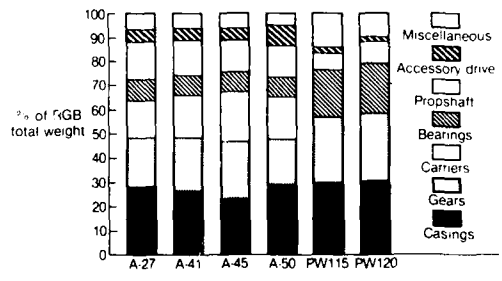


FIG. 4 RGB COMPONENTS WEIGHT BREAKDOWN

To ensure that effort in optimizing weight is applied to the most weight sensitive components a study was made of the individual component contributions. Fig. 4 shows these in graphical form. It shows the approximate contributions of each component group, gears, carriers, bearings, casing, accessory drives prop shaft and miscellaneous items.

It was found that the change from lightweight journal bearings which comprise only 10% of the weight of the PT6 gearbox increased to 20% for the PW100 which uses rolling element bearings. This is the penalty paid for higher durability roller bearings. Another finding was the increased percentage in casing weight in the PW100 which is partly due to mounts as explained earlier. These are two areas where greater effort will be made to limit weight increase.

4 GEAR COMPONENT STRESSES

In the design of advanced aircraft gearboxes conventional methods of tooth sizing have to be abandoned because as gear component weight is reduced, the rim thickness supporting that tooth is reduced and this can cause maximum stresses to appear at points different from the critical fillet stress location. It is important however to keep the highest critical stress at the fillet as broken teeth are less damaging than rim fracture.

In sizing gears, three basic tooth failure criteria have to be considered:

a) Tooth hertzian stresses
b) Maximum fillet(bending) stress
c) Tooth scoring

The objective in any gearbox design is to minimize each one of these stress indicators. Various ways can be found to limit them, although an approach to reduce the hertzian stress for example might not always necessarily reduce the bending stress or the scoring probability.

As the gear tooth contact takes place at high speed the dynamic effects of the impacting teeth, component windup, inertia and machining errors must be addressed. It is essential that before any final optimization of gear components is carried out the basic tooth to tooth dynamic loads are calculated. Because three stress parameters should be satisfied, very few gears can be said to be properly optimized.

5 GEAR DYNAMIC LOADS

Gear dynamic loads are a function of the overall system dynamics and certain assumptions have to be made regarding the effective moments of inertia of the interconnecting shaft and gear systems, the damping ratios in the teeth and the tooth spacing errors.

There are many other unknown factors but a computerized analysis has been developed by Hamilton Standard and this has been described in detail in many other published papers (ref.4,5). This method is proving to be extremely useful in enabling the designer to establish the basic dynamic characteristics of the gearbox and determine whether critical frequencies are generated in the running range of the gearbox.

If an analysis shows extremely high stresses due to resonance, steps are taken to change the stiffness characteristics of individual gears by using damping rings or changeing the gear geometry. Another option is to ensure that the gearbox is only run outside the critical speed ranges. Fig. 5 indicates that the PW115 first stage gears run outside the critical speed range, which are predicted in the range of 5000 and 7000 rpm. The pinion speed is 14,000 rpm at idle, 17,680 rpm at cruise and 19,987 rpm at take off.

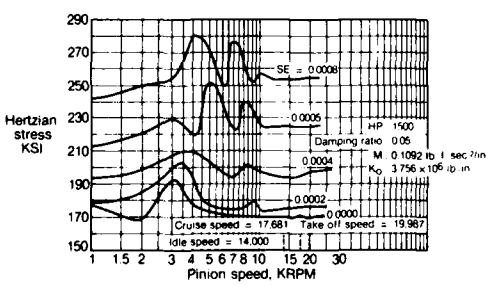


FIG. 5 EFFECT OF SPEED/SE ON HERTZIAN STRESS

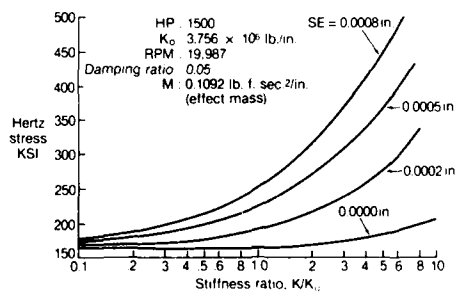


FIG. 6 EFFECT OF STIFFNESS/SE ON HERTZIAN STRESS

The data shown in Fig. 6 shows the influence of mesh stiffness/tooth spacing error. In general, an increase in spacing error results in a higher hertzian stress. As current gearbox quality standards assure tooth to tooth spacing errors of less than .0002 in. "the maximum" expected hertzian stress is approximately 230ksi.

An example showing the sensitivity of the stresses in the gears to stiffness ratio is shown in Fig.6. It indicates that as the stiffness ratio (above nominal gear tooth sizes) is doubled, the hertzian stress would increase from 180 to 230ks or, approximately 30%. This indicates a relative low sensitivity of stress as the components are either stiffened or made more flexible.

Another important feature of a dynamic analysis is that various gearbox parameters that are not too well understood can be examined and their influence on gear stresses assessed. If a particular parameter has only little effect on the calculated maximum stresses then knowledge of its nature or magnitude is unnecessary and there is little need to do any testing or further analytical work to determine its effect. A case in point is shown in Fig. 7. The choice of damping ratio is significant in the PW115 but not in the PW120. This is not surprising because the effective mass of the PW120 components is much greater compared to the critical mass, than is the PW115. It is therefore further removed from resonance conditions.

Another very useful feature of a dynamic analysis is the rate of change of fillet stress with spacing error. It is shown to be very dependent on the characteristics of the particular stage. Examination of the Fig. 8 shows that the second stage gear mesh of the PW115 gearbox is much more sensitive to spacing error than PW120. This is an unusual finding because the second stage of the PW120 uses high contact ratio teeth which are generally expected to be more sensitive due to the increased number of teeth in contact. In this case it is thought that the high moment of inertia of the larger propeller used in the PW120 is offsetting the higher sensitivity of the tooth contact geometry.

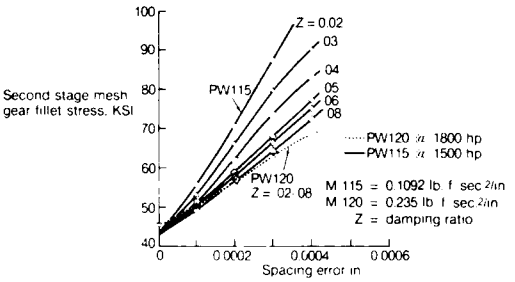


FIG. 7 EFFECT OF DAMPING RATIO ON FILLET STRESS

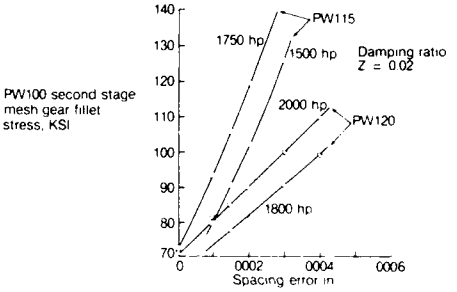


FIG. 8 EFFECT OF SPACING ERROR ON FILLET STRESS

Studies such as these combined with actual test data on gearboxes allow a much better understanding of the dynamic characteristics of the gears and enables the designer to quickly diagnose the causes of distress in development gearboxes.

6 HCR TEETH

The use of high contact ratio teeth has been mentioned in the preceding paragraphs and earlier papers from UTC representatives have reviewed the advantages of these teeth in some detail (Ref.1,5). Although the main advantage is that two to three teeth are always in contact, their use does impose some penalties. One mentioned earlier is their greater sensitivity to tooth errors than low contact ratio teeth. Another disadvantage is the higher sliding velocity resulting from their extended addendum, which results in an increased scoring probability.

Extensive analysis using finite element techniques backed up with photoelastic testing was carried out to assess very accurately the actual load sharing in HCR teeth and the effect of rim thickness on the final fillet stresses.

Fig. 9 shows a group of high contact ratio teeth being tested in a photoelastic rig. It clearly shows the position where three teeth are in contact. Fig. 10 shows how the tooth loading takes place as the gear rolls in and out of contact. On the left side of the figure the various zones along the tooth flank where 3 teeth and 2 teeth are in contact during the meshing cycle are shown.



FIG. 9 HCR TOOTH PHOTOELASTIC TEST

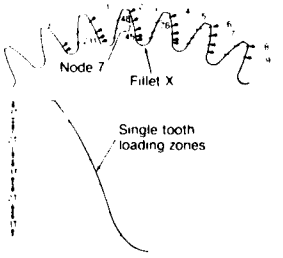


FIG. 10 LOADING PATTERN IN H.C.R. TEETH

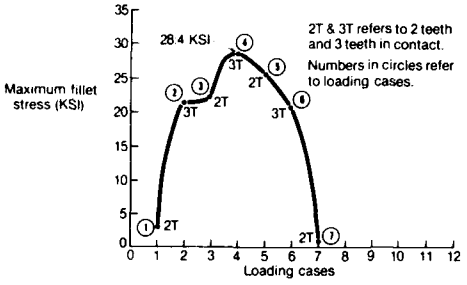


FIG. 11 FILLET STRESS AT 'X' DURING LOAD CYCLE

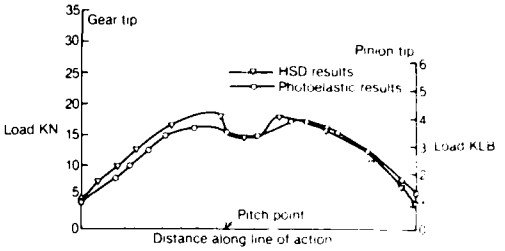


FIG. 12 TRANSMITTED LOAD ALONG LINE OF ACTION

Fig. 11 shows how the fillet stress on a particular tooth changes during the load cycle. The fillet stress builds up at the fillet as the tip of the gear is in contact then flattens as the tooth mesh goes through the two teeth contact phase. It then rises again as the tooth rolls through the pitch where three teeth are in contact. At this point it bears the largest percentage of load, and the adjacent teeth are loaded at their tip and root respectively.

The use of HCR gear results in a high cyclic change in torque as the load is passed between 2 teeth in contact to 3 teeth and back again before disconnecting. A notch occurs in the load versus contact ratio curve. This is shown in Fig. 12 which compares computer results with that of a photoelastic test.

The use of HCR teeth can give a tooth width reduction of as much as 20% over LCR teeth and results in a substantial saving of weight.

7 GEAR COMPONENT OPTIMIZATION

Previously mention was made of the need to carry out very extensive stress calculations on gear components to determine where the highest stresses are in tooth, rim, webs and shaft and to properly evaluate the range of stresses. Where low stresses are found material can be removed and weight savings effected.

Finite element methods are used extensively to ensure that there is:

(a) An understanding of the tooth load distribution across the tooth face width. This is a function of rim geometry and web stiffening. It is also a function of the misalignment between the parts. (b) The maximum cyclic stresses are calculated for webs that have been optimized for weight. The web is sized for LCF and HCF.

Fig. 13 shows the FE methodology that is used to properly evaluate the tooth load distribution across a face. Initially a 3DFF analysis is used to determine the stiffnesses of the teeth in slices across the face. These stiffnesses are then fed into a 2D FE analysis that uses a node tracking system to prevent tooth contours crossing each other. As two nodes record tensile forces they are released and the calculation repeated until an overall force balance is achieved.

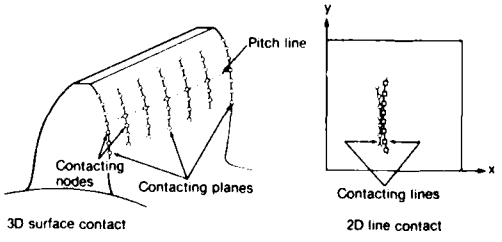


FIG. 13 FINITE ELEMENT METHOD FOR LOAD DISTRIBUTION

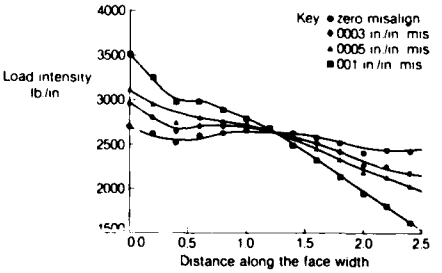


FIG. 14 LOAD DISTRIBUTION ACROSS FACE

Fig. 14 shows the results of a typical FE analysis using this technique for the bull gear, for aligned teeth, and teeth with various amounts of misalignment. The shape of contact follows a slight "W" shape which indicates the normal peaking of stress towards the centre of the gear due to web stiffness, as well as peaking of stress towards the ends due to edge effect.

Subsequent strain gauge testing will be conducted to calibrate whether this effect is "real" or an anomaly of the FE program.

Other FE computer programs are being used at PWC which utilize a similar method of node tracking on helical gear meshes and figure 15 shows results which indicate how a helical gear is loaded at an instant in time. Subsequent work will develop the method to predict bending stress fluctuations as the helical gears roll into and out of mesh.

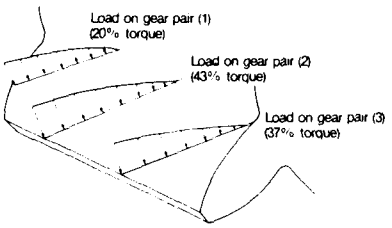


FIG. 15 HELICAL TOOTH LOAD DISTRIBUTION

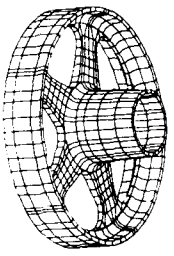


FIG. 16 FINITE ELEMENT MODEL FOR BULL GEAR

Other features of the gear components must be optimized for minimum weight and durability. Fig. 16 shows a FE grid used to optimize the webs in the bull gear. The two idler gear loads are applied as shown in Fig. 17 with a generated torque reacted at the hub. The tooth loading is distributed across the teeth according to the maximum calculated misalignment as indicated previously.

Specifically four FE elements are found to experience the maximum cyclic stresses. They are at points A, for nodes 5, 6, 15, and 16. The stresses are shown in Fig. 18.

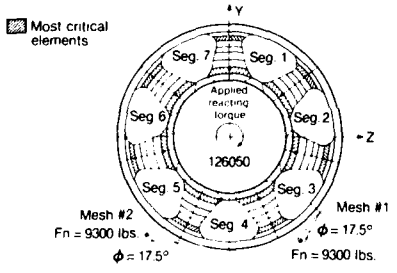


FIG. 17 BULL GEAR WEB OPTIMIZATION

Stresses at critical elements

Element	Max σ eff at A	Min σ eff at A	LCF σ mean	LCF σ alt	HCF σ mean	HCF σ alt
5	40.7	13	13.5	± 13.5	39.0	± 14.0
6	45.0	19	16.0	± 16.0	46.0	± 13.0
15	37.0	4	10.25	± 10.25	29.0	± 16.5
16	38.0	4	10.5	± 10.5	30.5	± 17.0

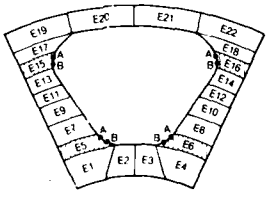


FIG. 18 STRESSES AT CRITICAL ELEMENTS

Examination of the table in Fig. 18 indicates that two fatigue calculations are carried out to account for both a low cycle fatigue and a high cycle fatigue condition at these critical locations. Fig. 19 indicates the stress cycle at the locations, as the bull gear rolls into and out of contact with the idler gear. A maximum stress of 45 ksi is experienced by E6, and 41 ksi by E5 when it is circumferentially in segment 4. Here it is at the bottom of the bull gear rotation (see Fig.17) and transferring high tangential loads from the teeth into the webs and into the hub.

The maxima for the other two elements E15 and E16 are experienced when they are in segments, 5 and 2 respectively. Obviously the stress cycle is complicated and the complete stress range is shown in Fig. 19. Because any particular element (e.g. E6) always experiences a significant steady stress component, as indicated by the variation in tensile stress (from 9 ksi to a 45 ksi) during every revolution, some means of assessing the combination of this low cycle fatigue with the tooth meshing high cycle fatigue stress must be considered.

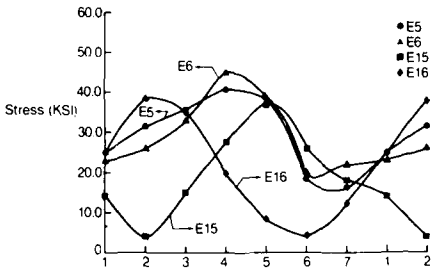


FIG. 19 STRESS CYCLE DURING BULL GEAR ROTATION

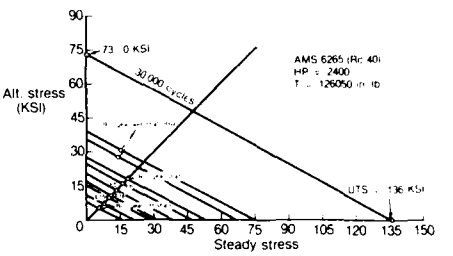


FIG. 20 EQUIVALENT HCF 'STEADY STRESS' VALUES

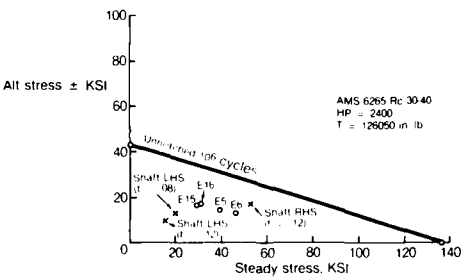


FIG. 21 BULL GEAR STRESSES - HCF GOODMAN DIAGRAM

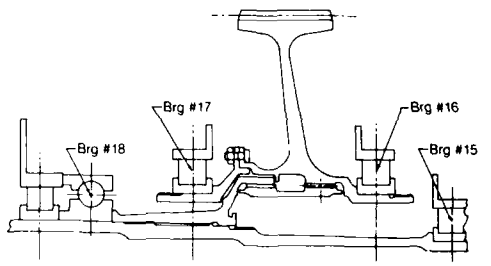


FIG. 22 BULL GEAR COUPLING

This equivalent steady stress used in combination with a high cycle stress is found by transposing the LCF cycle stress in Fig. 20 to the X axis (i.e. 46 ksi). It is then subsequently used in Fig. 21. This is essentially to take into account the extra damage that results when HCF is combined with LCF. Although this is an approximate method and is debated by many stress analysts, it does have a reasonable rationale behind it, in that it converts a 0-maximum fluctuating stress into an equivalent steady stress for further use in the HCF Goodman Diagram.

The results are summarized in the table shown in Fig. 18 and plotted in Fig. 21.

8 COUPLING AND SHAFT DESIGN

Other major items that require careful design in a gearbox are such items as couplings and flange design. Fig. 22 shows one of the arrangements considered in the second *stage bull gear design that allows the propeller shaft which carries large IP moment* from the propeller, to flex under these loads without affecting the bull gear.

The arrangement of a fixed spline on the propeller shaft which in turn carries the output torque through a floating flexible shaft, though complex and adding weight to the gearbox, nevertheless has the merit of allowing maximum flexibility between the bull gear and shaft.

This arrangement generates some additional moments due to misalignment between propeller shaft spline and the bull gear spline. The misalignment is made up of three components a) bearing internal clearance, b) thermal difference and c) basic machining misalignment. Calculations show the combined effect could be as high as .005 radians.

A simplified explanation of the capacity of a gear coupling to generate moments is shown in Fig. 23. From this it can be seen that the tilted spline which is loaded on opposite sides of its diameter as it transmits the torque can create two moments. The first is the tilting moment MT which is proportional to F x b where F is the localised force towards the ends of the teeth and b is the effective distance between them. This moment is a function of the torque transmitted and the lengtn of the teeth.

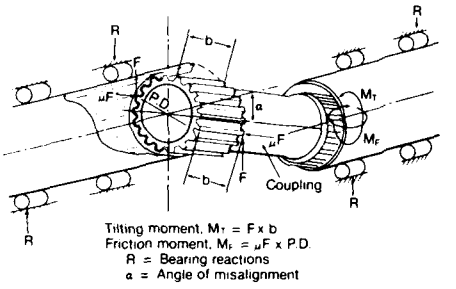


FIG. 23 FLEXIBLE COUPLING MOMENTS

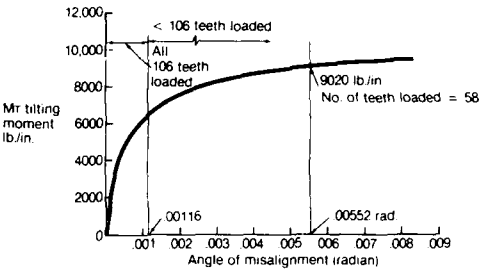


FIG. 24 COUPLING MOMENT VERSUS MISALIGNMENT ANGLE

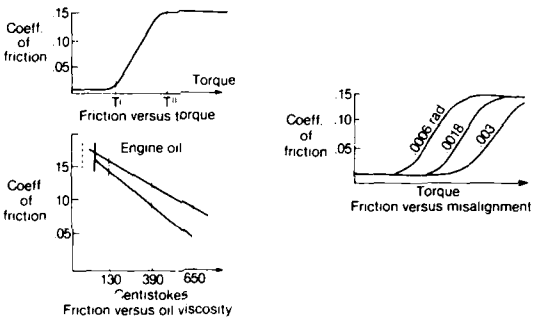


FIG. 25 COUPLING FRICTION - CALISTRAT DATA

Combined with this tilting moment is another which is defined as the friction moment, and this is proportional to friction force and the pitch circle diameter of the coupling.

These two moments are now combined and create a composite moment which in turn is resisted by the adjacent bearings. This increased loading on the bearings can cause a significant reduction in their B 10 lives.

Referring to the two moments and the simplified expressions used to show their effect it should be noted that the angle of misalignment is the significant parameter in determining the tilting moment, see Fig. 24. It can be reduced by minimizing misalignment or by reducing the effective length between contacting points along the teeth identified here as "b".

In the case of the friction moment only two parameters are significant, the friction coefficient and the pitch circle diameter. As the PCD is fixed for a given geometry the only controlling variable is the friction coefficient. Reference to literature on this subject indicates that the coefficient of friction can vary between .03 to .33.

Work by Calistrat (ref. 7) has shown that the friction coefficient can vary with oil viscosity (fig. 25) and is inversely proportional to viscosity. At 130 centistokes viscosity a coefficient of friction of .15 seems reasonable. He has also shown that for the particular couplings that he studied the coefficient of friction varied with both torque and angle of misalignment with the coefficient following a very interesting characteristic curve. A constant low coefficient is maintained initially with increasing torque which then rapidly increases to its maximum at a specific "threshold torque" where it then becomes constant again.

		No. of teeth	Max. tooth load	Misalignment moment lb.in.		
				M_t	M_r	M_c
Misalignment .0055 in./in.	Straight Splines	58	758	0.1	1076.1	1076.2
	Crowned Splines	88	589	.218	1149.7	1217.2
Aligned condition		146	276	--	---	---

TABLE 2 : MOMENTS IN SPLINE

If a value of 0.1 is assumed table 3 shows that the combined moment can vary the loads on the adjacent bearings from 1800 to 7600 and 3800 lb. respectively. This increase of 6? in load has the effect of reducing the No. 16 B10 life considerably from 50,500 hours to 10,700 hours. As the gearbox bearings are designed to a combined set life high induced moments such as these could give cause for a redesign of the bearings, greatly increasing the gearbox weight.

	Aligned		Misaligned		Crowned	
Bearing	load	B_{10} life	load	B_{10} life	load	B_{10} life
16	1800	50500	7600	10700	6600	17300
17	3800	10100	6500	20100	6100	22200

TABLE 3 : EFFECT ON BEARING LIVES

One way to obviate the effect of high misalignment loads is to crown the splines. This has the effect of reducing the effective *length* "b". Crowning in this case recovers the major life loss and restores the bearings lives to much more reasonable values of 17,400 hours and 22,200 hours respectively.

A further impact of the misalignment moment is to increase the stress level in the spline teeth themselves and this is shown in Fig. 26. Here it can be seen that under a .005 radians misalignment the tooth load for straight splines is 758 lbs. but this can be reduced significantly to 589 lbs. for crowned splines.

In gearbox design it is important to use gear couplings to give flexibility to the shafting system but account must be taken of the increased loads on the teeth and bearings from possible misalignment.

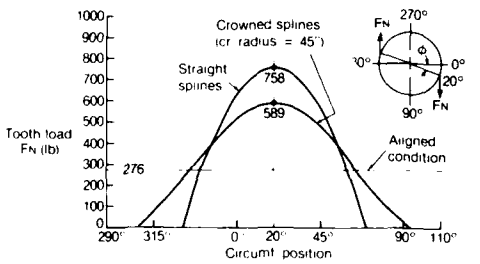


FIG. 26 COUPLING LOADS

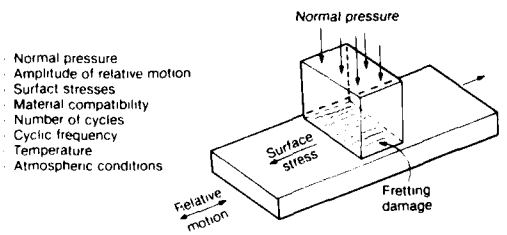


FIG. 27 FRETTING FATIGUE PARAMETERS

9. JOINT DESIGN AND FRETTING FATIGUE

Joints, snaps, spigots and flanges present a major challenge to the designer in preventing fretting damage and fretting fatigue. Bolts have to be properly torqued and sized to prevent joint loosening and bolt or flange failure.

Many joints are found in a gearbox and any one could be sited for detailed examination. The following example is chosen because it can be used to illustrate the complex factors that are interrelated in dealing with fretting fatigue.

Fretting fatigue has been shown to be related to many parameters. Here we enumerate the eight most significant. They are the load through the part (surface stress), clamping force, amount of slip between surfaces, number of cycles, frequency, material differences, atmospheric conditions and temperature (see Fig. 27).

Examining fretting fatigue as a purely stress related phenomenon and ignoring the frequency, atomospheric and temperature effects, the three major influences, surface stress, localised clamping force and relative slip can be modelled using 3D Finite Elements for the flange under consideration.

Research carried out by numerous researchers has shown that allowable fatigue stresses in high strength steels with ultimate tensile strengths as high as 180 ksi, can be as low as 10 ksi where fretting damage is excessive, Ref. 8, 9, 10.

Tests conducted at PWC on representative propeller shaft flanges have shown that fretting fatigue can indeed be experienced in high strength steels (AMS6415 Rc 40) with surface stress levels extremely low (10 ksi), where the localised clamping forces are as high as 20 ksi and the localised slip is in excess of .0002 in.

Fig. 28 shows a 3D model of the PW100 propeller hub/flange connection. The loading imposed on the interconnection is that caused by propeller aerodynamic (IP) moments. These cause a steady moment to be applied to the connection in flight due to the propeller centerline having a slight angle of attack to the incoming airflow. For a positive angle of attack this causes increased thrust on the starboard side of the propeller plane, and conversely reduced on the port side.

In effect the flange joint experiences a rotating moment that for the PW124 is estimated at take off powers to be as high as 50,000 lb.in.

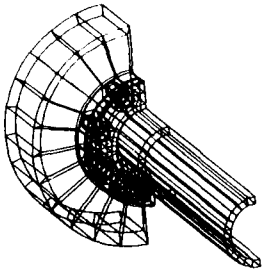


FIG. 28 HUB/FLANGE F.E. MODEL

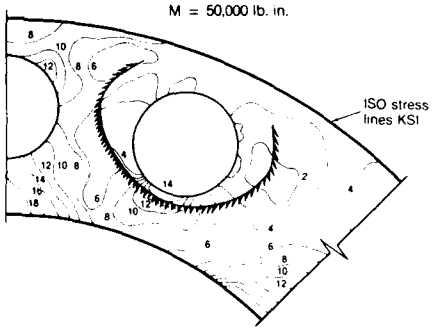


FIG. 29 FLANGE SEGMENT - SURFACE STRESSES

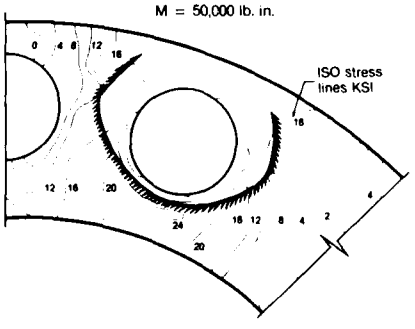


FIG. 30 FLANGE SEGMENT - CONTACT STRESSES

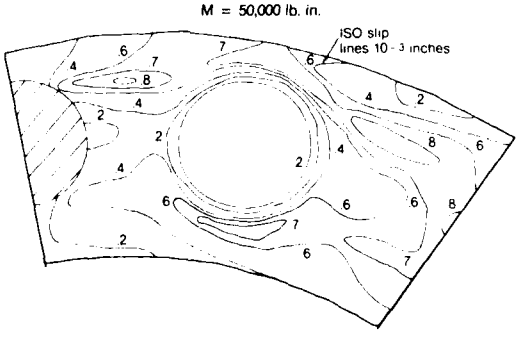


FIG. 31 FLANGE SEGMENT - CYCLIC SLIP

Figs. 29, 30 and 31 show the maximum cyclic surface stresses, maximum contact stresses and cyclic slips at a typical segment of the flange. The zone around the bolt hole is shown highlighted and can be seen as an undisturbed surface in actual tests. The machining marks are still visible after cyclic loading of greater than 30 x 10 cycles. The cyclic slip L. contours (Fig. 31) indicates relative slip to be less than .0001 in. confirming the test results that under the bolt the relative slip is virtually zero.

Areas where actual fretting fatigue cracks have been generated are coincident with the highest surface cyclic stress (12 ksi, Fig. 29), maximum contact stress (24 ksi, Fig. 30) and greatest relative slip (.000" in, Fig. 31). These zones are all inboard of the hole, and in a zone of extensive fretting damage.

From many tests on actual propeller shafts and hubs a composite diagram has been constructed which gives a possible approach to a set of fretting fatigue allowable curves. (see Fig. 32). However it must be remembered that these curves are not actual boundary curves drawn from dozens of statistically tabulated fatigue cracks. They are crack zone boundary lines drawn from FE iso-stress contours. They are only shown to describe the interaction of the three major components of fretting fatigue for these particular materials and this particular component configuration.

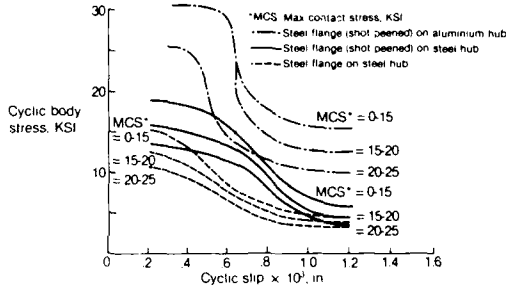


FIG. 32 FRETTING FATIGUE BOUNDARY LINES

The trend, established by other authors is shown, in that allowable cyclic stress reduces dramatically with increasing slip. It also shows that increasing contact stress also reduces the fatigue allowable stress. The combination of both increasing contact stress and slip is dramatic in reducing the allowable stress.

A third very important finding is that surface treatment such as shot peening, by generating high compressive residual stresses, allows much higher applied stresses to be carried by the components. Surprisingly when aluminium is the other contacting surface to steel perhaps due to the lower modulus of elasticity of the aluminium, the fretting fatigue allowable stress is increased dramatically. The lower modulus material may mean a lower transferred friction stress between the parts.

Much work has to be done to understand the correct combination of factors to limit fretting damage at jointed connections in gearboxes but this data (Fig. 32) does give some good guidelines for the elimination and control of fretting fatigue.

10 CONCLUSION

This paper has discussed some of the difficulties encountered in designing lightweight durable gearboxes. The increasing demand for higher power versus lightweight and high durability has shown the necessity for optimisation in all components.

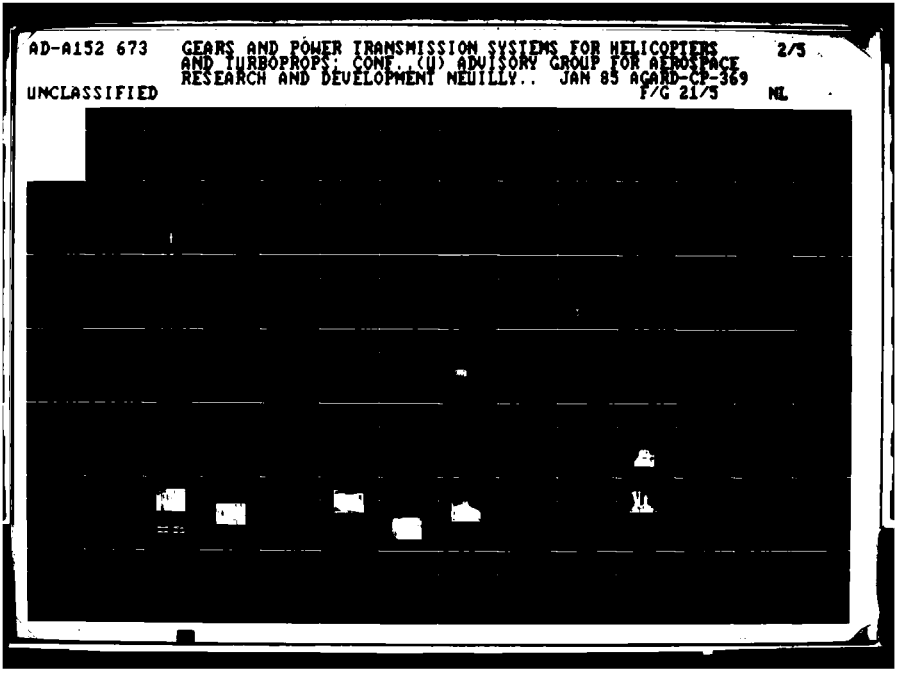
This could not be achieved without recourse to advanced finite element methods to correctly calculate contact loads between components and a proper understanding of the load paths through individual components. Also important is the need for very thorough calibration and subsequent testing of some of the complex empirical models needed to understand mechanisms that can cause fretting, bolt loads or creep between bearing races and shafts. Misalignments between shafts, particularly in casing moments through gear couplings must be accounted for not only in tooth sizing but also in assessing bearing lives.

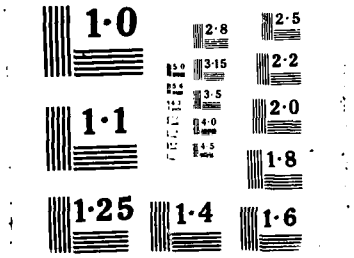
ACKNOWLEDGEMENTS

The authors are grateful to the following engineers whose reports formed the basis of the paper: A. Elkholy, S. Sundararaman, H.O. Lam, A. Probert, V. Smailes and S. Amin. Particular acknowledgement is also made to J. Strzesz, the research supervisor, under whose direction much of this work was conducted.

AD-A152 673 GEARS AND POWER TRANSMISSION SYSTEMS FOR HELICOPTERS AND TURBOPROPS: CONF. (U) ADVISORY GROUP FOR AEROSPACE RESEARCH AND DEVELOPMENT NEUILLY.. JAN 85 AGARD-CP-369 2/3

UNCLASSIFIED F/G 21/5 NL




1·0
1·1
1·25
2·8
3·15
3·5
4·0
4·5
2·5
2·2
2·0
1·8
1·4
1·6

REFERENCES

1) Morris, R.E., "The Pract & Whitney PW100, Evolution of the Design Concept", Canadian Aerospace Journal, Vol. 28, No. 3, Sept. 1982.

2) Godston, J., Kish, J., "Selecting the Best Reduction Gear Concept for Prop Fan Systems", AIAA/SAE/ASME 18th Joint Propulsion Conference, Cleveland, Ohio, June 1982.

3) Willis, R.J., "New Equations & Charts Pick off Lightweight Gears", Product Engineering January 1963.

4) Cornell, R.W., Westervelt, W.W., "Dynamic Tooth Loads and Stressing for High Contact Ratio Spur Gears", Journal of Mechanical Design, Vol. 100/69, Jan. 1978.

5) Rosen, K.M., Frint, H.K., "Advanced Transmission Component Development", AGARD Conference Proceedings No. 302.

6) Mancuso, J.R., "Moments and Forces imposed on power transmission systems due to misalignment of a crowned tooth coupling", Zulin Industries Inc. ER 71-E17.

7) Calestrat, M.M., "Friction between High Speed Gear Coupling Teeth", ASME, Vol. 103, Jan. 1981.

8) Milestone, W.D., "Fretting & Fretting Fatigue in Metal-to-Metal Contacts", ASME Design Engineering Conf. New York, April 1971.

9) Nishioka, K., Nishimura, S., Hirakawa, K., "Fundamental Investigations of Fretting Fatigue", JSME Vol. II, No. 45, 1968 (5 parts).

10) Wright, G.P., O'Connor, J.J., "The Influence of Fretting and Geometric Stress Concentration on the Fatigue Strength of Clamped Joints", Proc. Inst. Mech. Engineers, Vol. 18669/1972.

DISCUSSION

B.A.Shotter, UK

Do you make a different approach to the design process in the presence of fretting when using lubricated or unlubricated components?

Author's Reply

Yes. Lubricated couplings do not experience fretting. In a test rig with identical parts one dry and the other wet under the influence of a moment, the heavy fretting was completely diminished when lubricated.

The fretting fatigue damage I was referring to in my presentation was purely the case of flanges clamped together with bolts (under moment loading) with dry surfaces. Fretting damage is likely depending on the three parameters mentioned and if these factors are high, then fretting fatigue is likely.

D.Berthe, Fr

In the gear dynamic analysis, is the damping coefficient calculated from squeeze film, structure damping, or is it determined from experiments?

Author's Reply

The damping coefficient of 0.02 is structural damping. This seems to be a reasonable number that relates to experience.

H.W.Ferris, US

Service difficulties are currently a problem on the clamping of propellers to flanges and spiral bevel gears to gearshafts where the working stresses cause fretting on *flanging* surfaces and bolts resulting in fatigue failures of bolt heads and/or flanges. These are corrected usually by increased clamping via more bolts or a decrease in deflection by using thicker flanges.

Are these two common failure modes related — one wet and one dry?

Author's Reply

I am not familiar with the bevel gear problem. The propeller flange problem of fretting can be solved by increased clamping. The A45/A65 engine has experienced some bolt failures in the field. This may be due to inadequate bolt clamping. The 1P aerodynamic moments on these engines as calculated and measured are not sufficient to cause bolt failures. However, other vibration loading not too well understood could be a problem and should be investigated.

Fretting fatigue is not a problem with A45/A65 engines as the design of the flange is such that very small cycle slip takes place. Some fretting damage is inevitable on this type of design and is solved by shimming or surface regrinding or shot peening at overhaul.

THE HELICOPTER TRANSMISSION DESIGN PROCESS

Roy Battles

Chief Transmission Design
Bell Helicopter Textron
P. O. Box 482
Fort Worth, Texas 76101 USA

SUMMARY

The purpose of the helicopter transmission or drive system is to deliver power from the engine(s) to the rotors and also to accessories such as hydraulic pumps, generators, and air conditioner compressors. The design of a new helicopter drive system involves an extensive series of tasks that may take three or four years from predesign to qualification. Even after the new drive system is qualified, the transmission designer's work is not complete. The designer must keep himself aware of how the system is performing in the field to correct any service-related problems and to further his knowledge for the next design. The transmission design process can be divided into six major tasks: predesign, design, manufacturing coordination, bench testing, aircraft testing, and field service support. A flowchart summarizing the helicopter transmission design process is shown in Figure 1.

PREDESIGN

During the predesign phase, the general arrangement of the transmission system is determined and the parameters that affect the transmission system design are prescribed in a design specification. The interfaces of the transmission system with all other aircraft systems must be defined. This process is not a simple one-time effort, but one that is iterated several times to determine the best performing, most cost-efficient configuration.

The starting point for any design is the definition of the mission profile. The primary mission may be personnel or cargo transport, observation, or attack. Infrequent transient torque applications may be required for high maneuverability during nap-of-the-earth or combat flight. Or, consideration may be required for repeated-heavy-lift or ground-air-ground operation for a cargo mission. Once the mission is defined, the basic size and weight of the helicopter can be established. Then the number, size, and type of engines as well as the number, size, and type of rotors required to meet the performance goals of the mission can be determined. The type and number of accessories to be driven by the transmission must also be determined, and consideration must be given to the provision of redundant drive paths for essential multiple accessories such as flight control hydraulic pumps.

Often the transmission provides the mounting of the rotor to the airframe. A transmission that combines power from two engines may also be used as part of the mounting system for the engines. There are a variety of mounting systems in use for attaching transmissions to the airframe. These include rigid, elastomeric, nodalized beams, and mercury dampers. The mounting system is critical in minimizing the transfer of rotor vibration to the airframe and passengers. The type of mounting system used also determines to a large degree the type of drive shafts and couplings that can be used. The dynamic characteristics of some rotor systems require not only vertical oscillatory displacement, but also pitch oscillatory displacement of their mounting system. Thus, the couplings and drive shafts must be capable of accommodating changes in both angle and length. Additionally, the mean length of any engine-to-transmission external drive shaft must be considered so that coupling misalignment capability is not exceeded. A transmission may also interface with controls for the rotor. Often, rotor controls are mounted on the transmission housings or control tubes located inside the transmission output shafts.

When the interfaces with the engine(s), rotors, accessories, mounts, shafting, and controls are finalized, design criteria or a specification can be prepared that defines the requirements that the helicopter and the transmission system must meet.

The speeds and directions of rotation of the rotors and engine output shaft must be defined. The total transmission ratio can then be determined along with potential gear arrangements to obtain the required direction of rotor rotation and to drive the required accessories.

The engine(s) power ratings must be specified. The ratings may include takeoff, continuous, contingency, one engine inoperative, and transient. Normally an engine is significantly derated from its maximum capable sea-level, standard-day operating power to enhance an aircraft's high-altitude and high-temperature performance. Transient torque capabilities for the engine(s) must be defined and controlled by fuel flow restriction, torque-limiting devices, or the pilot.

The calculated flight and crash loads that the transmission mounting system and transmission housings must withstand must be defined. The environmental operating

temperatures must be defined so that transmission oil coolers can be sized and so that lubricating oils and greases can be selected. Normally a military helicopter is required to operate worldwide in temperatures from 219 K (-65°F or -54°C) to 325 K (125°F or 52°C).

The maintainability requirements for the drive system and helicopter should be defined. Typically, maintainability requirements for the total helicopter are approximately 1.0 man-hour of unscheduled maintenance and 0.5 man-hour of scheduled maintenance per flight-hour.

The reliability or component life for the transmission system must be defined. Additionally, it must be decided whether the system is to be maintained on-condition or whether a time-between-overhauls goal will be established. Current achievable time-between-overhauls are typically from 2500 to 5000 hours. Since gears and bearings are usually the critical life-limiting components in a transmission, the gear and bearing life in L_{10} terms should be defined. Bearing-life adjustment factors should also be defined. Life adjustment factors are typically used for lubrication, material, material processing, misalignment, and speed.

The survivability requirements for loss-of-lubricant operation and ballistic tolerance must be defined. Present designs must withstand a 7.62-mm HEI or 12.7-mm API ballistic hit and must operate a minimum of 30 minutes at a specified cruise power after loss of lubricant. These requirements place a premium on the use of tough, high-hot-hardness materials and redundant load paths.

There should also be both an internal and external noise limitation goal specified for the helicopter. The transmission system and accessories can be a major source of noise for the crew and passengers.

DESIGN

After the drive system general arrangement and design criteria are defined in predesign, the design of the transmission system can begin. The three primary tasks performed during the design phase are layout design, detail design, and design support testing. Layout design is accomplished by dividing the transmission system into major assemblies and assigning each to a senior designer. If the assembly is a complex one like a main rotor transmission or an engine combining transmission, an analysis specialist and lube system specialist may be assigned to assist the layout designer. The layout designer is guided by periodic design reviews by his peers and design supervision. The layout is a comprehensive definition of the critical dimensions of the transmission assembly. The layout drawing is supported by notebooks of dimensional tolerance stackups, stress calculations, computer analyses, and other design rationale.

The first task of the layout designer is to determine the transmission arrangement. The layout designer must give consideration to failsafe design by providing redundant load paths and clearances, to modular design so as to minimize secondary damage, to assembly and disassembly requirements with a minimum of special tools, and to repair of components during manufacture or overhaul. Additionally, the layout designer must make a risk assessment of each feature of his design and, if required, incorporate into his design an easily achievable alternate configuration. The layout designer may study several configurations to determine the safest, best performing, lightest weight, lowest cost design. A transmission mockup may be required at this time to finalize interfaces with other systems of the helicopter.

The layout design is normally started by sizing the gears and bearings of the transmission and then packaging them in a housing. For the foreseeable future, the type of gearing used in helicopter transmissions will be the same as today. The layout designer will use spiral bevel gears to change shaft direction. Parallel axis gearing such as spurs, high-contact ratio spurs, and helicals will be used in other stages. Epicyclic planetaries have been and will continue to be used for compact, lightweight, high-torque, final-drive applications. The gears are sized by high-speed computer programs that calculate bending stress, compressive stress, and flash temperatures for scoring. Gear rims and webs are sized by finite-element analysis to minimize stresses and place natural frequencies out of the operating range.

Once the gears are selected and sized, the size and type of bearings required to support the gears can be determined. The three primary types of bearings used in helicopter transmissions are cyclindrical roller, tapered roller, and ball bearings. Tapered roller bearings are normally used on slower speed shafting, since they cannot normally be successfully operated after loss of lubricant at rib velocities greater than approximately 20 meters per second (4000 feet per minute). High-speed computer programs are used to size the bearings, calculate internal geometry, and determine acceptable preloads for duplex and triplex ball bearings. Additional bearing design features that may be considered include locking of races to prevent creep, using bearing races integral with the gear shafts, and using special geometry to aid lubrication.

The location, size, and type of overrunning clutch(es) must be determined. Both sprag and roller ramp clutches are commonly used today. A significant difference between the two types of clutches is that the input torque must be applied to the inner shaft for the roller ramp and to the outer shaft for the sprag. Clutch location

is a compromise between torque and speed. It is desirable to have the clutch near the input, low-torque section of the transmission. However, clutches are speed limited. Depending on the size of the clutch, roller ramp clutches are generally limited to shaft speeds less than 8,000 rpm and sprag clutches to generally less than 12,000 rpm. Spring-type clutches with higher speed capability are being developed for future applications.

The lube system is sized by determining the combined flow required for critical gear, bearing, and clutch contacts. The scaverge pump(s), if required, and the pressure pump(s) can then be sized. Typical lube system capacity for a transmission is 7.1E-04 to 9.5E-04 cubic meters (0.75 to 1.0 quart) per 74.6 kilowatts (100 horsepower). High-pressure lube systems may be required to ensure jet stream penetration onto the gear tooth flanks of high-pitch-line velocity transmissions. Present transmission lubricant filtration systems employ combinations of 80-micron (0.003-inch) cleanable screens and 3-micron (0.0001-inch) disposable filters. Oil jet orifices should be protected against plugging by inlet screens. Splash lubrication may be used for simple, slow-speed transmissions such as tail rotor transmissions. Consideration should be given to backup lube systems for failsafe-designed transmissions.

Transmission diagnostic systems include oil temperature and pressure transducers, debris detectors, and torque-measuring devices. Debris detector technology has progressed from magnetic plugs to bayonet type electric chip detectors to burnoff chip detectors. New designs are using full oil flow debris monitors with fuzz-burning capability. Burnoff counters should be considered for incorporation into fuzz-burning debris-monitoring systems. With the torque splits within the transmission system, it may be desirable to incorporate a mast torquemeter into the transmission.

Present transmission housings are usually made from castings or forgings. Forged housings may be required to transfer rotor loads from the transmission to the airframe. Present commonly used housing materials include magnesium and aluminum alloys. Magnesium is used in less demanding structural applications. Composite housings and stainless steel weldments and investment castings are being developed for future designs. Finite-element analysis may be used to analyze complex shaped housings.

Present shaft seal technology uses a combination of elastomeric seals for slow-speed shafts and carbon mechanical seals for high-speed shafts.

The type of drive shaft couplings selected and designed is dependent on the misalignment and axial displacement that must be accommodated. Crown gear and flex-frame couplings can accommodate axial displacement and misalignment angles not exceeding approximately 4 degrees. Disc pack type couplings are used in applications with small misalignment angles, normally less than 0.75 degrees, and very small axial displacements.

When the layout design is complete, individual components are split off from the layout and assigned to detail designers. The detail designer prepares the engineering drawing that defines every feature of the component. Approximately 175 drawings are required to define small, single-engine helicopter transmission systems. More complex transmission systems may require approximately 300 detail drawings. The detail designer must be capable of defining the processes used to produce transmission components. Some of the items specified by the detail designer include the following:

- Tolerances within manufacturing machine and tooling capability.
- Gear manufacturing methods, including ground or unground roots, honing, allowable stock removal after heat treatment, involute modifications, and crown modifications.
- Type and size of starting material. The material may be bar, tubing, forging, investment casting, sand casting, or other.
- Heat treatment required, including case depth, case hardness, core hardness, and maximum percent carbon. Most power gears are either carburized or nitrided. Many other components are through-hardened.
- Shot-peening requirements, including size, intensity, and coverage of shot. A diagram showing locations of almen strips to measure intensity may be required.
- Dynamic balance requirements and provisions for balance material removal.
- Allowable weld repair limits on castings.
- Protective finishes on housings to prevent corrosion.
- Weld joint configurations.

The detail designer must also have a working knowledge of many inspection processes used for transmission components, including the following:

- Involute, lead, and tooth spacing inspection of spur and helical gears.
- Contact pattern inspection for spiral bevel gears.
- Radiographic inspection for castings and welded joints.

- Magnetic particle inspection for gears, shafts, and other critical magnetic components.

- Penetrant inspection for housings and other critical components.

The detailer should perform a failure mode and effects analysis on the component he is designing. The analysis should consider the likely primary and secondary static, fatigue, and wear failure modes and list the features incorporated in his design to prevent or mitigate those failures.

The detailer also designs the special assembly, disassembly, and alignment tools required for the transmission system.

The detail designer prepares design process specifications for spiral bevel gears that define the machine settings and tooling required to manufacture the gear as well as the contact pattern inspection requirements that the gear must meet.

Computer graphics are now used extensively by detail designers to produce drawings. When the transmission layout is also done by computer graphics, the detail drawing can be produced more efficiently. Computer graphics are more efficient in making dimensional stackups, performing weight trade-off studies, generating finite-element models, and determining interfaces with other system hardware.

Although the detail designer is primarily responsible for producing an accurate, well-designed component, his drawing is subject to a thorough check-and-balance system of reviews. A drawing normally must be reviewed and approved by the layout designer, checker, producibility specialist, stress analyst, weight analyst, materials specialist, group engineer, project engineer, and customer. Additionally, if the design is for a commercial helicopter, a Federal Aviation Administration designated engineering representative must approve the drawing.

Design support tests are required to provide data to support and improve the transmission design process. A major area of design support testing is material evaluation. A new material should be thoroughly investigated prior to committing it to production. Most of the design support tests are conducted using specimens rather than full-scale hardware to minimize cost.

Some initial screening tests for materials include mechanical property tests (tensile, yield, and elongation), heat treat response, impact strength evaluation at room temperature and subzero temperatures, fatigue strength evaluation (rotating beam and flexure), residual stress measurements, and corrosion evaluation. If the material shows promise, further tests are required. Additional tests for a new gear material include single-tooth bending fatigue, dynamic surface fatigue, scoring, hot hardness, and fracture toughness evaluations.

New transmission system lubricants must also be evaluated. Gear tooth scoring tests are conducted to evaluate a lubricating oil's load-carrying capacity. Crown gear coupling tooth wear and temperature tests may be used to evaluate a new grease.

MANUFACTURING COORDINATION

The transmission designer must participate in the manufacturing process of transmission components to fully understand how a component is made and to resolve any unforeseen problems. After a drawing is released to manufacturing, a planner prepares a sequential step-by-step definition of how the part is to be manufactured and records this on operation sheets. The transmission designer reviews the operation sheets with the planner to ensure that the procedure will produce a part meeting all drawing requirements. The planning review also gives the manufacturing planner an opportunity to identify potential manufacturing problems with the part and resolve them with the designer.

Some transmission components, such as bearings, oil pumps, oil coolers, clutches, oil filters, seals, debris detectors, transducers, and couplings. may be purchased from outside manufacturers. These purchased parts are defined on source-controlled drawings, meaning that only a manufacturer whose product has met all specified qualification requirements is allowed to produce the component. The transmission designer must coordinate with the vendor to ensure the part complies with the source-control drawing requirements. Normally a vendor will submit to the transmission designer a vendor drawing for approval. The drawing review process allows the vendor an opportunity to resolve any problems he may have in manufacturing or qualifying the part. Any vendor-conducted qualification tests and resulting test reports must be reviewed for compliance with drawing requirements.

The transmission designer works directly with manufacturing during development of acceptable spiral bevel gear tooth contact patterns. Machine setting deviations from the summary sheet are mutually reviewed and agreed to by manufacturing and the designer and are subsequently defined in the design process specification. Spiral bevel pattern development is a trial-and-error process, often requiring several grind and test iterations until an acceptable pattern is produced. A desirable contact pattern is one that at maximum load fills the tooth profile, just touching the top edge of the tooth, but being slightly in from the toe and heel. Additionally, the pinion tooth must be sufficiently modified to prevent any surface distress from tip interference.

The transmission designer must also prepare transmission acceptance specifications. Most major transmission assemblies are acceptance tested to gradually break in the contacts within the assembly and to provide assurance that the assembly will operate successfully in service. The acceptance specification defines the schedule of powers and speeds required in the test, post-test disassembly and inspection requirements, and the pass or fail criteria. The post acceptance test inspection typically evaluates gear tooth contact patterns, bearing race contact patterns, bearing ring creep, proper fastener torques, smoothness of shaft and bearing rotation, and oil seal leakage.

Occasionally components are manufactured that do not meet all engineering drawing requirements. These parts are submitted to a transmission design specialist who reviews the discrepant parts and determines if the part can be used as is, can be reworked, or should be scrapped. If the discrepant parts are reworked, the transmission design specialist must define the manufacturing and inspection operations necessary to salvage the parts. The layout and detail designers must anticipate rework requirements and incorporate rework capability into their designs wherever possible.

BENCH TESTING

A new transmission system must be extensively tested before it and the helicopter can be certified and delivered. The bench test may be conducted on the complete transmission system, an individual gearbox, or an individual component, depending on the type of test. The first tests conducted are development tests to identify any weakness or shortcomings in the design and to correct them by redesigning if necessary. Some of the development tests required for a transmission system include the following:

- Spiral bevel gear roll tests are conducted using an assembled gearbox to expedite tooth contact pattern development. Additional dynamic tests using the transmission assembly are required to further develop the desired tooth contact patterns for all gears in the drive system. Frequently, the gear sets must be redeveloped or modified and retested to obtain the desired contact pattern.

- Gear rims and webs are vibration tested to ensure the natural frequencies are outside of the operating range and to provide correlation for the earlier finite-element analysis.

- Critical gear members may be strain gaged and rolled through mesh under torque to determine actual operating tooth-bending stresses and to provide correlation to earlier tooth-bending stress calculations.

- Bearing operating temperatures are measured by locating thermocouples on the non-rotating bearing races during gearbox tests. Additional thermocouples may be located in the gearbox to determine hot spots to modify lubricating requirements and to identify likely loss-of-lubricant failure areas.

- Oil management tests are conducted on the transmission assembly to evaluate lube system performance, including proper cooling, flow, scavenging, jet targeting, and sump dwell time. Additionally, the pump(s) flow and pressure margins must be determined and any oil foaming must be eliminated.

- Debris detector capture efficiency tests are conducted on the transmission assembly by injecting debris into different areas of the gearbox and measuring the time until a warning light is activated.

Many transmission components require fatigue testing to provide confidence that oscillatory operating loads will not cause failures. In addition to normal operating oscillatory loads, ground-air-ground or start-stop cyclic loading may require fatigue testing. Depending on the number of specimens tested, a component may be overstressed from 125% to 200% to obtain a satisfactory level of confidence. Some transmission fatigue tests that are normally required are listed below:

- Dynamic gear tooth bending fatigue test in the gearbox assembly at 125% to 140% of the maximum normal operating stress. The test is continued until all gear teeth have accumulated a minimum of ten million cycles. The test may require using an improved oil and keeping the oil as cool as possible to prevent surface fatigue failures or tooth scoring.

- Rotor shafts or masts are normally fatigue tested as a component rather than with the drive system. Four to six masts may be tested simulating flight loading of thrust, shear, and moment to substantiate the mast.

- The transmission housing(s) that mounts the transmission and rotor to the airframe may be fatigue tested. It may also be required to fatigue test a housing that is subject to oscillatory control loads.

- Drive shaft coupling flexures are fatigue tested to substantiate them in bending fatigue.

- Sprag and roller ramp clutches are tested to demonstrate adequate surface fatigue life. If only one clutch specimen is tested, it may be tested at two times the maximum normal operating torque.

- Cooling fans may be required to be fatigue tested for start-stop cycles.

Static tests are often required for transmission housings and clutches. If a transmission housing has an analytical positive margin of safety less than 0.25, the housing requires static testing. Crash loads are usually the most severe static loads imposed on a housing. Contemporary military helicopters require a 16g crash load factor. Overrunning clutches may be static tested to a minimum of three times the maximum service torque the clutch must transmit without slipping or rolling over.

Failsafe tests may be required on drive shafts and gearbox assemblies. Contemporary military transmissions are required to operate a minimum of 30 minutes after loss of lubricant at the cruise power required for best range. To demonstrate the required 30-minute loss-of-lubricant capability, one gearbox assembly must operate for 1 hour minimum or two gearbox assemblies must operate for 30 minutes minimum during bench testing after the lubricant is drained. A bench test may be required to demonstrate that a drive shaft will transmit adequate torque after being ballistically damaged. Additional drive shaft bench testing may be required to show the shaft will operate safely after a flex frame or bolt failure.

After the development bench testing is completed, a preflight bench test of not less than 50 hours is conducted on the transmission system so that flight development of the helicopter can be performed concurrently with the remainder of the transmission bench tests. However, for safety the helicopter flight development operating time and power must not exceed the time or power of the transmission bench test program.

A prequalification bench test for 200 hours at powers up to 125% of maximum power is normally conducted on the complete transmission system to identify any weak areas remaining in the system after incorporation of the changes required by the development tests. The prequalification test is not a must-pass test, but should provide confidence that the qualification test can be successfully completed.

A 200-hour qualification bench test at powers up to 110% of maximum power is conducted to certify that the drive system is sufficiently developed for production. The qualification bench test must be completed without any failures or excessive wear. A failure during the test requires a penalty run to be conducted after changes are made to correct the problem.

AIRCRAFT TESTING

The transmission system must also be extensively tested on the aircraft, both tied down and in flight, so that it is subjected to the interactions of other helicopter systems. Prior to first flight, a limited tiedown test, normally of not less than 50 hours, is conducted to release the aircraft for flight. The first flights are used to evaluate handling qualities and performance and to expand the operational flight envelope. A load-level-survey is then conducted with an extensively instrumented aircraft to measure operating loads and drive shaft coupling axial displacement and misalignment angles. The loads and coupling data are used to verify component analytical substantiations and to correlate with previous calculated load data. The measured flight loads are also used for defining the test load spectrum used in the ground run qualification testing.

Vibration tests are conducted to determine drive shaft natural frequencies and ensure they are not within the operating range.

Cooling tests are conducted to demonstrate that the lube system has adequate cooling margins to operate in high ambient temperatures. Additionally, very low ambient temperature tests are often conducted to demonstrate proper transmission system operation.

Acoustical measurements may be made to identify sources of annoying noise and to determine acceptable attenuation methods.

The final qualification test is the ground run or tiedown test, which normally lasts from 200 to 250 hours, depending on the helicopter configuration. The ground run is primarily a drive system, rotors, and controls endurance test to demonstrate reasonably achievable operating intervals without failure. The drive system is typically cycled repeatedly through a 10-hour power spectrum consisting of 50% of the time at maximum takeoff power, 10% at 110% maximum takeoff power, and the remaining 40% at maximum continuous power. Additional tests, such as rotor brake engagements and clutch engagements, may be included in the ground run test. The ground run must be completed without failure or a penalty run may be required.

FIELD SERVICE SUPPORT

The designer must keep himself aware of how the transmission system is performing in service so he can correct any service-related problems. Lead-the-fleet inspections are an effective method used by the designer to gain knowledge of field-service performance. Lead-the-fleet inspections are complete drive system teardowns and inspections performed by a design team on selected high-time aircraft . The lead-the-fleet inspection provides data so that rational inspection and overhaul limits, component replacement or life limits, and reasonable transmission lubricant and filter change intervals can be established. The designer also helps prepare maintenance and overhaul manuals.

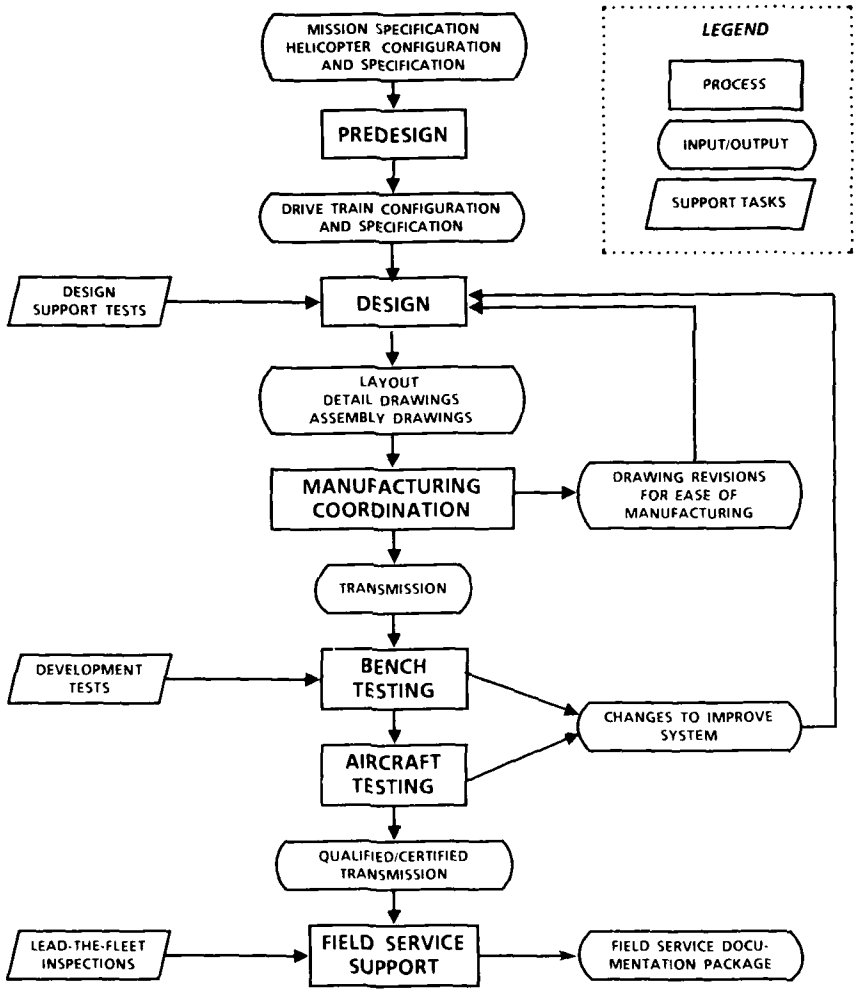


Figure 1. Flowchart summarizing the helicopter transmission design process.

DISCUSSION

D.G.Astridge, UK

I was interested in your comment on Bell's practice to introduce torquemeters in the main rotor drive-shaft. What type of torquemeters are used? Do they provide mean torque values only, or is the bandwidth sufficient to provide dynamic data (e.g. transients, blade passing frequency, or gear mesh frequency). Presumably on twin engine helicopters, the cockpit indication of separate input torques, or torque split is retained.

Author's Reply

The torquemeters used in the Bell Helicopter main rotor mast are of the shaft torsion type with the fixed end near the rotor hub and displacement measured near the bottom of the gearbox. The system is used to measure mean torque only. Bell practice is to strain gauge the main rotor mast and tail rotor output shafts during load-level-survey test to measure oscillatory torque during the complete flight operational spectrum. Both engine(s) torque and mast torque is displayed on the instrument panel. Since torque is split in several directions (main rotor, tail rotor, and accessories) in a helicopter drive system, the mast torquemeter is used to optimize helicopter flight performance by accurately measuring main rotor mast torque.

LOGICIEL DE CONCEPTION DES DENTURES D'ENGRENAGES POUR REDUCTEURS ET BOITES DE VITESSES

MM. L. FAURE et A. BORRIEN
CETIM
52, Avenue Félix Louat
60300 - SENLIS, FRANCE

L'objet de cet exposé est de présenter les possibilités offertes par le logiciel de Conception des Dentures d'Engrenages par Ordinateur (C.A.D.O.R) qui a été élaboré par le CETIM.

Dans la première partie de la conférence, il est présenté la structure du programme d'entrée du logiciel qui permet au concepteur d'obtenir très rapidement les caractéristiques géométriques optimales d'un engrenage qui doit répondre à un cahier des charges donné.

Dans la deuxième partie, il sera surtout mis l'accent sur les possibilités offertes par la combinaison des différents programmes composant le logiciel qui permettent à l'utilisateur :

- de s'assurer du bon dimensionnement de l'engrenage

- de fixer le tolérancement qui lui garantira la précision et le jeu qu'il désire.

PRESENTATION

La détermination d'engrenages fonctionannt dans des conditions de couple ou de vitesse élevée nécessite souvent une étude approfondie de la denture pour définir des caractéristiques qui prennent en compte le maximum de paramètres. Jusqu'à présent, dans la plupart des cas industriels, ces caractéristiques sont obtenues à partir d'abaques, de formulaires ou par extrapolation à partir d'anciennes fabrications. Des essais de fonctionnement permettent, après coup, de modifier les caractéristiques et de tendre ainsi vers une solution optimisée.

Grâce aux calculateurs, on peut maintenant envisager un grand nombre de calculs au stade de l'avant projet de façon à pouvoir prédire avec une grande précision les performances futures des engrenages. De cette façon, les essais ne constituent pas une étape de mise au point de la denture elle-même mais [illegible] de contrôle des performances globales du matériel testé.

Avec la généralisation des traitements de durcissement superficiel tels que cémentation-trempe ou nitruration, le concepteur est amené à prendre en compte les déformations des dentures sous charge de façon à réaliser des corrections géométriques pour éviter les surcharges localisées qui conduisent irrémédiablement à une rupture ou un écaillage prématuré des dents.

Pour répondre à ces besoins industriels, le CETIM a développé un logiciel de calcul des dentures d'engrenages sur ordinateur (CA.D.OR). Ce logiciel permet de réaliser des tâches multiples telles que des devis, des calculs de conception ou d'avant projet ainsi que des vérifications de dimensionnement selon différentes méthodes normalisées. L'évolution actuelle de ce logiciel doit permettre un couplage progressif de cet outil de travail avec les moyens modernes de "dessin assisté par ordinateur" et de "conception assistée par ordinateur". (cf figure 1).

CALCULS D'AVANT PROJET - DEVIS - CHIFFRAGE

Le but de ce programme est de déterminer rapidement les nombres de dents, le module, la largeur de denture, l'angle d'hélice et les coefficients de déport pour transmettre une puissance demandée à une vitesse donnée et dans un entraxe imposé.

Plusieurs cheminements sont possibles dans ce programme suivant que l'on s'oriente vers un acier de cémentation, de nitruration, de trempe superficielle par induction ou traité dans la masse.

Les données à introduire dans le programme sont :

- la puissance à transmettre

- l'entraxe du carter

- la vitesse de rotation

- le rapport de réduction

- les caractéristiques du matériau choisi

- Contrainte limite de fatigue en flexion

- Pression limite de fatigue de contact.

Par défaut, le programme travaille avec un outillage standard ISO mais il est possible de lui introduire des caractéristiques spécifiques et notamment celle des outils à protubérance. (cf figure 2).

Le programme fait le choix d'un module et fournit les premiers résultats géométriques :

. Les nombres de dents pour satisfaire au rapport de réduction.

. L'angle d'hélice pour passer dans l'entraxe sans surcharger axialement les roulements.

. La somme des coefficients de déport

. La répartition des déports entre le pignon et la roue pour minimiser les glissements spécifiques (cf figures 3 et 4)

. Les diamètres extérieurs des pièces pour réaliser les ébauches.

Dans la partie suivante, le programme calcule la largeur de denture minimale pour répondre au problème de tenue en pression superficielle. Si cette valeur est éxagérément grande ou petite en regard du module et des diamètres des pièces, il est possible de modifier la valeur de l'entraxe en retournant en début de programme.

A partir de la largeur de denture optimisée, le programme effectue un calcul de dimensionnement en rupture et donne le coefficient de sécurité correspondant. Si ce coefficient est trop faible, le module est augmenté et le calcul repris.

Le temps d'exécution d'un calcul d'avant projet pour un engrenage est d'environ 15 minutes. On remarquera que l'entraxe étant fixé, la somme des déports et l'angle d'hélice sont des paramètres interdépendants. L'angle d'hélice minimum doit permettre un rapport de recouvrement suffisant tandis que la somme des déports est choisie dans une fourchette en privilégiant soit la tenue en rupture, soit le rapport de conduite.

En amont des programmes de calcul de chaque train d'engrenage, il peut être nécessaire d'avoir recours à un programme de calcul cinématique, notamment pour les trains planétaires, dans le but de connaître avec exactitude les vitesses relatives de chaque pignon et la puissance transmise par chaque engrenage en tenant compte du rendement de la chaine cinématique envisagée.

DEFINITION DES CARACTERISTIQUES GEOMETRIQUES DE FABRICATION

A l'issue de l'étude d'avant projet, on connait l'encombrement radial et axial nécessaire, ainsi que le type d'acier et de traitement thermique à prévoir. Il est donc possible d'estimer le coût de la réalisation de l'engrenage. Pour accéder à la connaissance de toutes les cotations du plan d'exécution, il faut franchir une deuxième étape.

C'est le second module du programme CA.O.GR. qui permet de réaliser ce passage. Il est nécessaire pour cela, de communiquer au programme les données précises de l'outillage qui sera utilisé pour la réalisation (saillie d'outil, arrondi de sommet d'outil, protubérance, surépaisseur d'ébauche) et dans le cas d'un outil-pignon (nombre de dents de l'outil et état d'affûtage). On peut également introduire un chanfrein en bout de dent en indiquant l'angle d'inclinaison du chanfrein et le creux actif d'outil (cf figure).

Ces informations permettent au programme de vérifier les caractéristiques géométriques obtenues précédemment, d'effectuer un tracé à grande échelle d'une dent complète pour visualiser le profil obtenu lors du taillage et mettre en évidence une éventuelle erreur de conception due à un mauvais choix d'outillage ou à un coefficient de déport inadapté. En outre, le tracé des dentures après ébauche permet de mettre en évidence la position de descente limite de la meule de rectification pour éviter un contact indésirable avec le profil de raccordement.

Le programme étudie ensuite l'engrènement des deux dentures et donne les principaux paramètres de l'épure d'engrènement : longueurs d'approche et de retraite, rapport de conduite, rayons actifs de pied, rayon de plus haut contact unique, glissements spécifiques. (cf figure 5)

Les interférences de fonctionnement sont également signalées : interférence primaire pour les engrenages extérieurs, interférence primaire, secondaire et avec les profils de raccordement pour les engrenages intérieurs.

L'utilisateur introduit ensuite les tolérances d'usinage des portées de roulements, tolérance d'entraxe et le jeu de fonctionnement désiré maximum et minimum. Le programme donne les tolérances de fabrication des engrenages et cotes sur k dents et en cotes au pied. Ces tolérances peuvent être directement mentionnées sur le plan de fabrication ou transformées en classe de tolérance à partir de la norme ISO 1328. (cf figure 6).

FINE FILTRATION - AN ATTRACTIVE ROUTE TOWARDS LOWER HELICOPTER OPERATING COSTS

by

Dr P B Macpherson

Head of Tribology Research,
Westland Helicopters Limited,
Yeovil, Somerset, England.

SUMMARY

Helicopter transmission Times Between Overhaul (T.B.O's) appear to be surprisingly low but, even so, Mean Times Between Removal (M.T.B.R's) tend to be much lower. Causes of early removal are varied and do not all, by any means, relate to Tribological problems, although cost analyses suggest strongly that if the bulk of such problems could be eliminated, reductions in annual helicopter ownership costs would be very substantial indeed. In short the main key to lower costs lies in improved mechanical reliability. Research, supported by trials experience, suggests that, provided a gearbox is free from design deficiencies, the replacement of a gas turbine oil by a suitable gear oil combined with 3 μm absolute filtration would result in appreciably higher TBO's and enhanced reliability. To treble existing TBO's would appear to be a realistic target. Fine filtration on its own can impart well worthwhile improvements and can readily be introduced by retrofit action.

This paper briefly describes the background research and trials experience that led to the adoption of fine filtration. However, the fitting of such a unit in itself is insufficient. To be fully effective it is imperative that the gearbox starts off life in the cleanest possible condition. To achieve this does mean revising standard production methods.

Helicopter transmission work has reached an interesting stage in its evolution in that research completed during the last 15 years is now being applied. TBO's could be phased out within the forseable future and gearboxes fall into the "Fit and Forget" category where they belong.

INTRODUCTION

It is not always appreciated just how much more important are airworthiness considerations of a helicopter transmission, compared with those of an engine. An engine failure is rarely more than an embarrassment, even in single engine aircraft, whereas a helicopter gearbox failure is serious because it can, so readily, result in a fatality. Vinall, Ref 1, includes a series of airworthiness statistics relating to helicopter transmission. The picture he paints is gloomy. His study reveals that "Transmission and Rotor systems make a major contribution to rotor craft accident rate and that improvement by at least one order would be required for rotor craft to achieve the same levels as fixed wing aircraft."

During recent years attention has been focused on the high costs of operating helicopters. Again, compared with fixed wing aircraft the price that has to be paid for the convenience of vertical flight and hover is so high that the civil market is no where near approaching its potential and is unlikely to do so until overall costs can be substantially reduced. Transmission and Rotor systems account for much of the apparently high costs of operating a helicopter. It seems obvious that were it practicable to increase TBO's of transmission assemblies, to bring them more closely into line with engine practice, very worthwhile savings could be introduced.

Although TBO's are relatively low, a surprising high proportion of transmission assemblies suffer early failures and have to be removed prematurely if MTBR's are low in relation to TBO's. Unscheduled failures are invariably disruptive and expensive.

Improved reliability of transmission leading to larger TBO's and MTBR's along with, most importantly, enhanced airworthiness would appear to be an essential target. It is not the intent of this paper to present detailed cost analyses, even were full facts available to

DISCUSSION

A.Watteeuw, Be

(1) What is the experience with the results from different methods: ISO, DIN, AGMA (For Hertzian contact pressure and tooth root (bending) strength)?

(2) Are your programmes still valid when the value of the factor E_1 exceeds 2?

(3) Do you take account of the surface roughness on the flanks and roots of the teeth in your programmes for calculating Hertzian contact resistance and tooth root (bending) strength.

Author's Reply

(1) The results obtained by the different methods show some differences, notably in the manner in which the different materials and (heat) treatments are handled. For example, the nitriding treatments are handled differently following the specifications used. Determination of life is also handled differently, notably for surface pressure. As concerns the factors related to geometry of the mesh some differences can also show up. Generally these differences are small.

(2) When E_1 exceeds the value 2, the programme follows the indications of the normal criteria. Discussions should rather bear on the validity of the normal criteria for this case. For the dynamic factor k, of the ISO method the effect of values of the factor E_1 is > 2 is taken into account.

(3) The values of surface roughness on the flanks and roots of the teeth are taken into account by the programme. On the other hand, no indication is furnished in the specifications on the method for measuring the surface roughness. Interpretation is therefore subjective and no limits on surface roughness, as a function of the method of finishing and of the dimensions of the components, is provided.

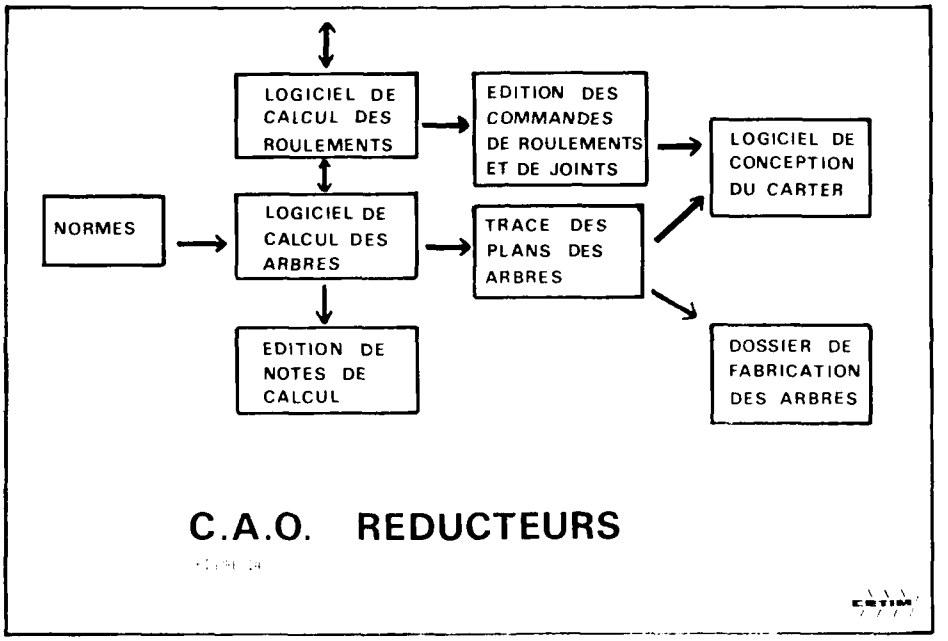
B.R.Reason, UK

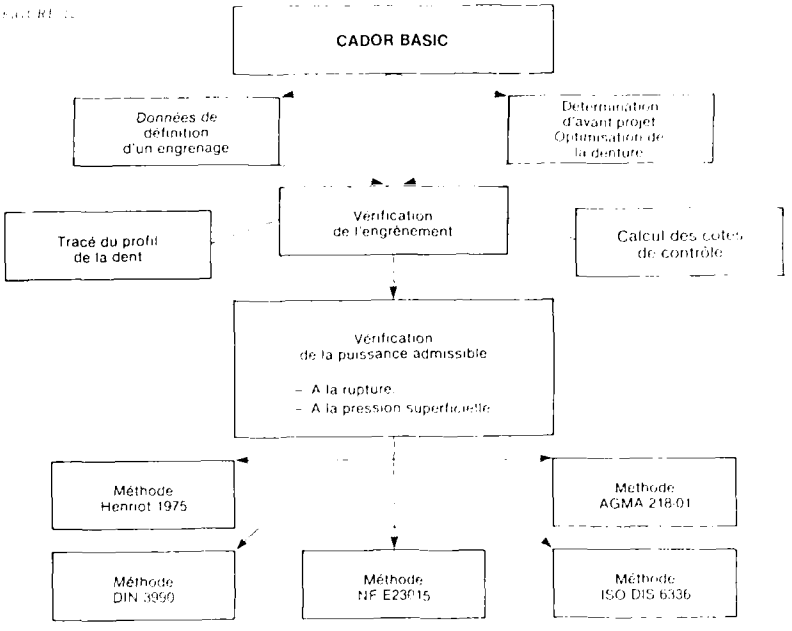
Does your programme predict the localised temperatures in the contact zone on the basis of the flash temperature of the lubricant and the likely surface finish after running-in?

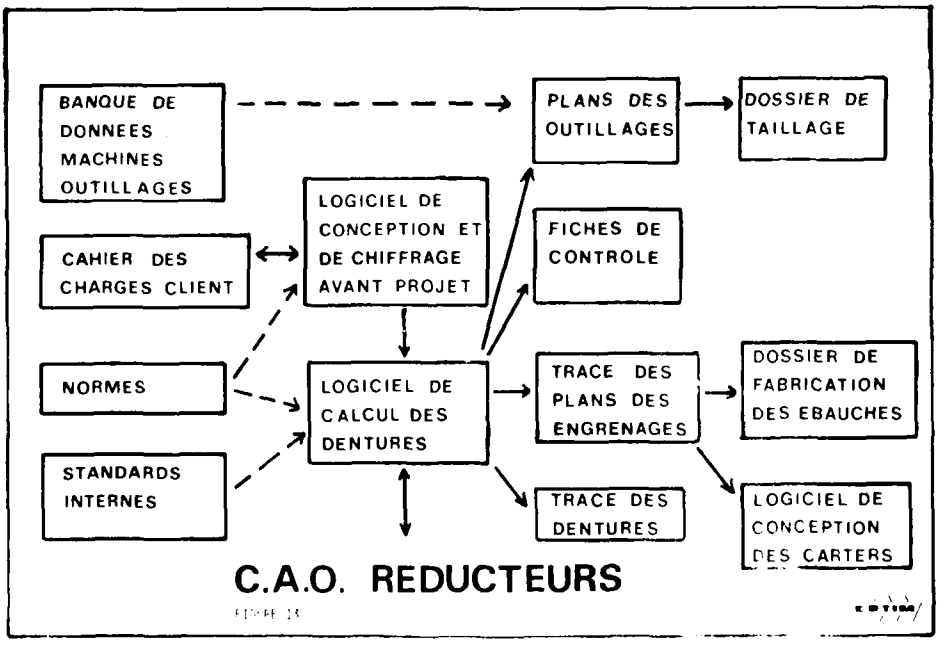
If so, what scuffing criterion do you employ and what experimental verification have you made on the basis of testing work and field experience?

Author's Reply

We have put into our programme both the integral temperature method and the method of flash temperature. The correlations between the results of these calculations and the examples of scoring in industrial applications are difficult to establish at present. The experts of TC60 at ISO are discussing formulation of a future of method of calculation that could be used internationally. Also the programmes which we have developed in this area are utilised at CETIM, but they have not been commercialised for outside use at this time. That would be dangerous!


LOGICIEL DE CALCUL DES ROULEMENTS
EDITION DES COMMANDES DE ROULEMENTS ET DE JOINTS
LOGICIEL DE CONCEPTION DU CARTER
NORMES
LOGICIEL DE CALCUL DES ARBRES
TRACE DES PLANS DES ARBRES
EDITION DE NOTES DE CALCUL
DOSSIER DE FABRICATION DES ARBRES
C.A.O. REDUCTEURS


CADOR BASIC
Données de définition d'un engrenage
Détermination d'avant projet Optimisation de la denture
Vérification de l'engrènement
Tracé du profil de la dent
Calcul des cotes de contrôle
Vérification de la puissance admissible
- A la rupture
- A la pression superficielle
Méthode Henriot 1975
Méthode AGMA 218.01
Méthode DIN 3990
Méthode NF E23015
Méthode ISO DIS 6336


BANQUE DE DONNEES MACHINES OUTILLAGES
PLANS DES OUTILLAGES
DOSSIER DE TAILLAGE
LOGICIEL DE CONCEPTION ET DE CHIFFRAGE AVANT PROJET
CAHIER DES CHARGES CLIENT
FICHES DE CONTROLE
NORMES
LOGICIEL DE CALCUL DES DENTURES
TRACE DES PLANS DES ENGRENAGES
DOSSIER DE FABRICATION DES EBAUCHES
STANDARDS INTERNES
TRACE DES DENTURES
LOGICIEL DE CONCEPTION DES CARTERS
C.A.O. REDUCTEURS



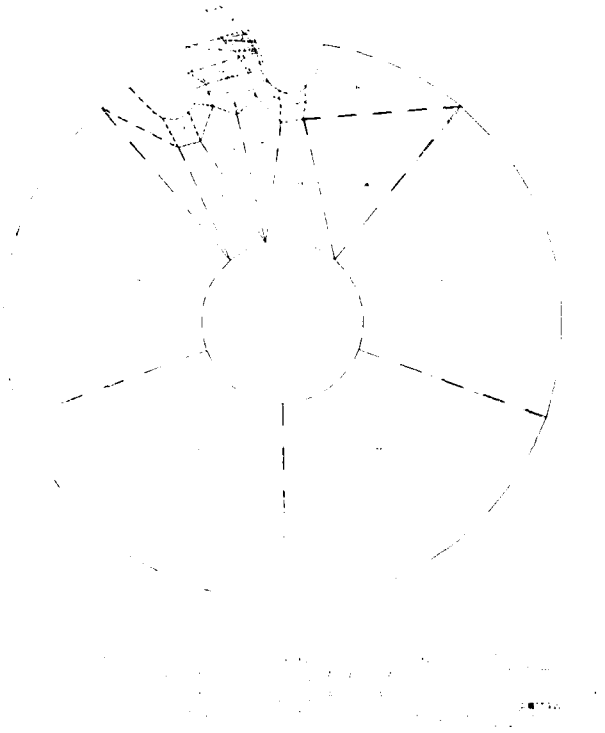


FIGURE 10

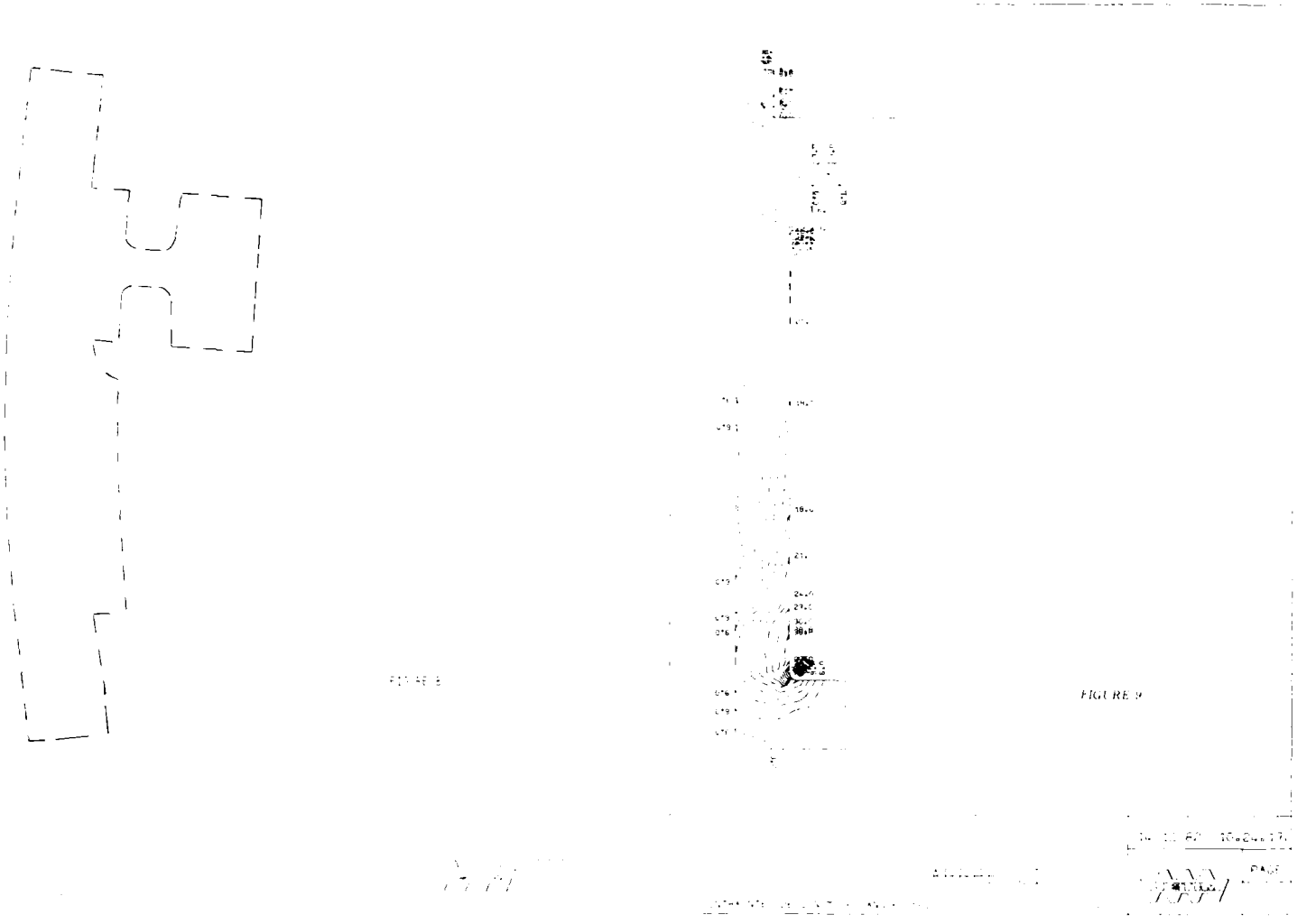


FIGURE 9

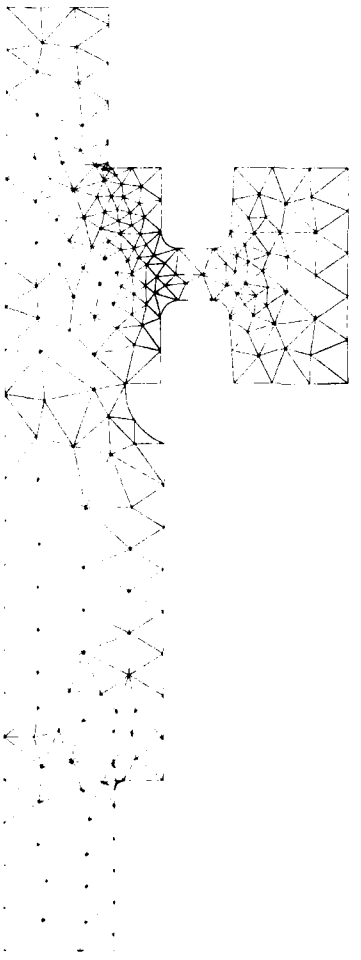
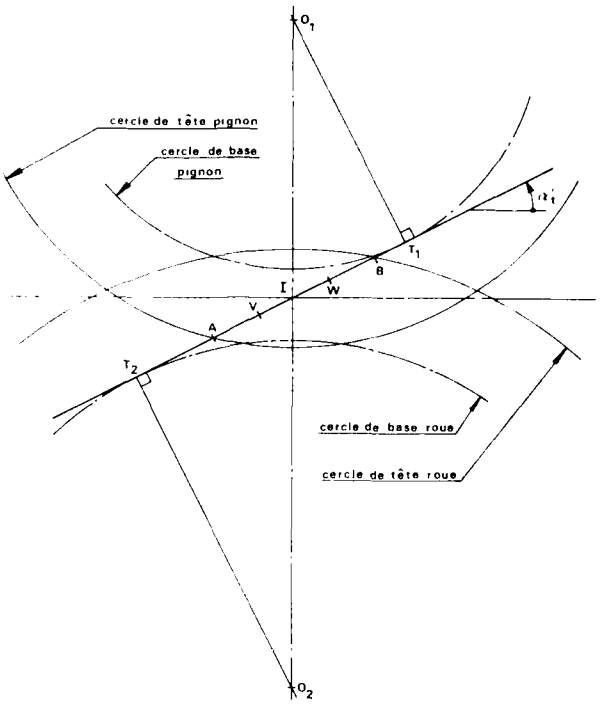


FIGURE 7


O_1
cercle de tête pignon
cercle de base pignon
α_t
T_1
B
I
W
V
A
T_2
cercle de base roue
cercle de tête roue
O_2

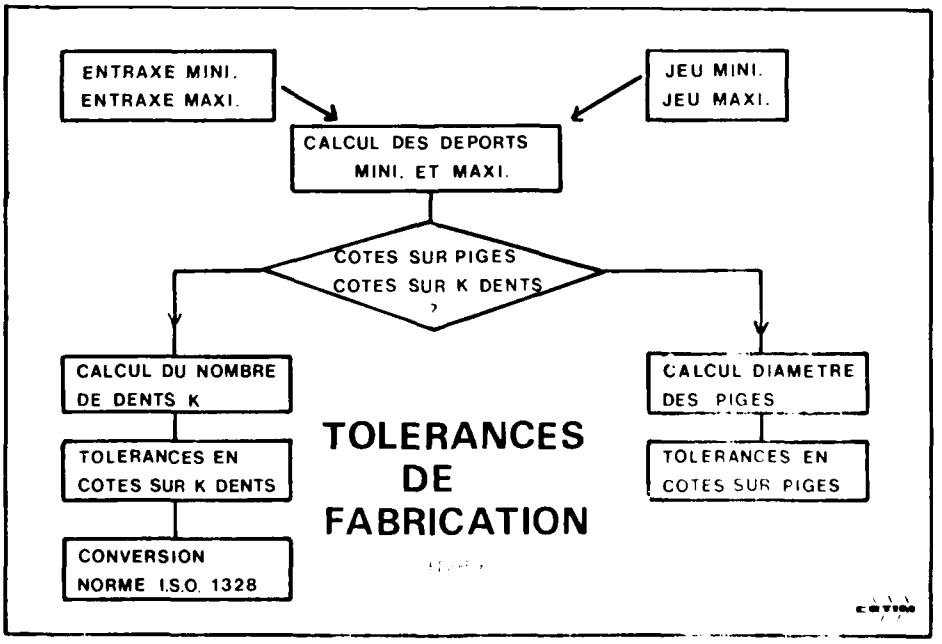
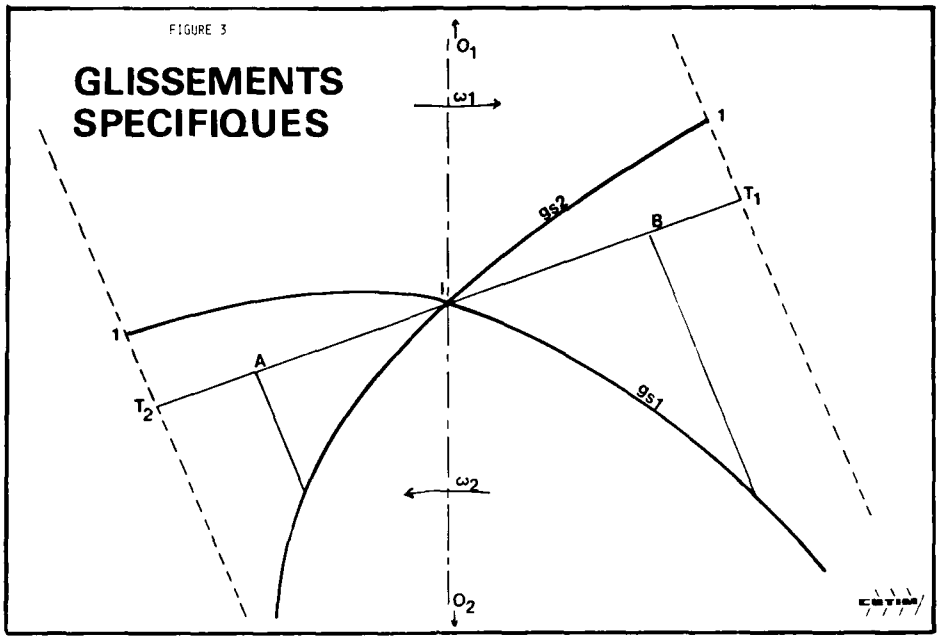

ENTRAXE MINI.
ENTRAXE MAXI.
JEU MINI.
JEU MAXI.
CALCUL DES DEPORTS MINI. ET MAXI.
COTES SUR PIGES
COTES SUR K DENTS
?
CALCUL DU NOMBRE DE DENTS K
TOLERANCES EN COTES SUR K DENTS
CONVERSION NORME I.S.O. 1328
TOLERANCES DE FABRICATION
CALCUL DIAMETRE DES PIGES
TOLERANCES EN COTES SUR PIGES

FIGURE 3



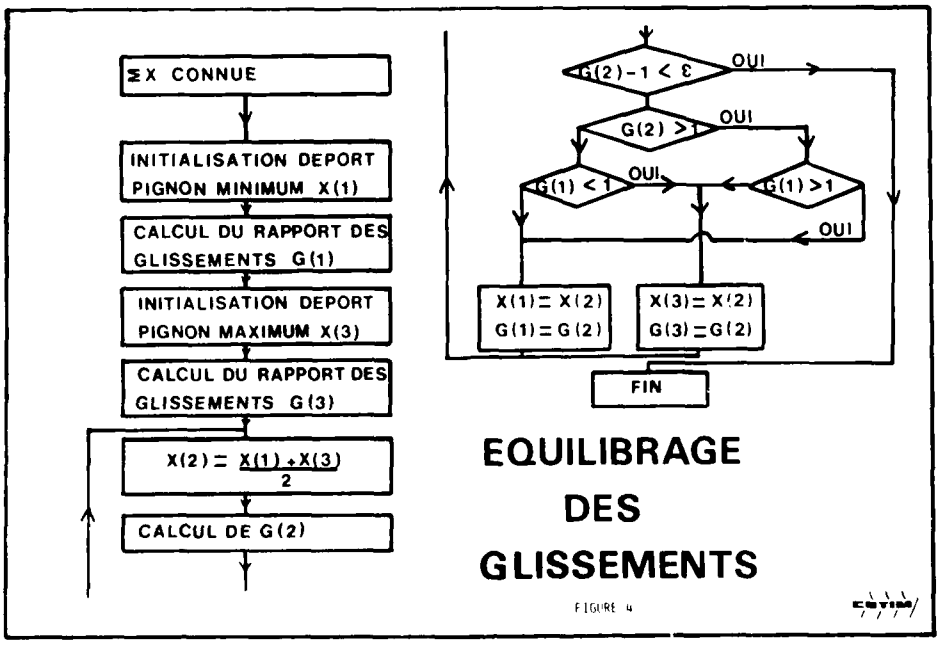


FIGURE 4

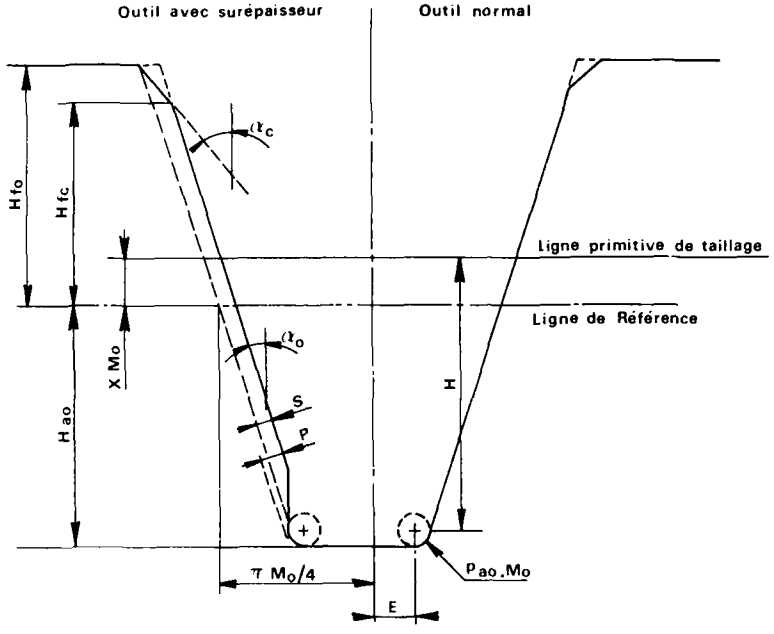
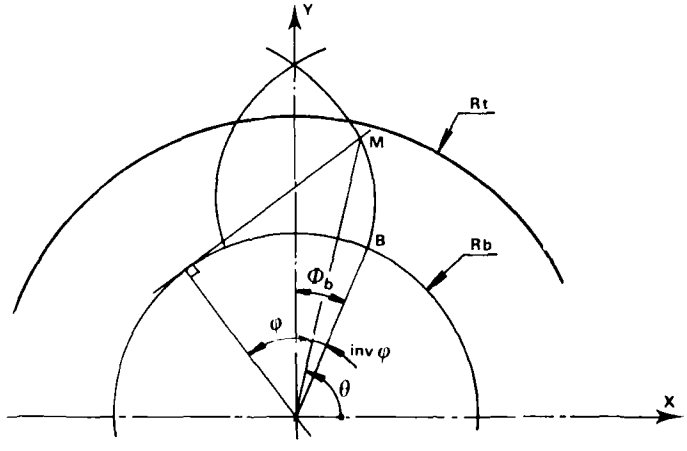

Outil avec surépaisseur
Outil normal
Hfo
Hfc
αc
Ligne primitive de taillage
Ligne de Référence
X Mo
αo
Hao
S
P
H
π Mo/4
E
Pao.Mo

FIGURE 2


Y
Rt
M
B
Rb
Φb
φ
inv φ
θ
X

CONCLUSION

Les développements rapides des moyens de CAO et DAO et leur utilisation dans les bureaux d'études de mécanique permettent un gain de temps, de performances, et de fiabilité. Dans un avenir proche, les liaisons entre banques de données, outils de conception et outils de production rendues accessibles à tous, permettront de s'affranchir des tâches de calcul proprement dit pour donner à l'esprit de création sa véritable dimension.

Le logiciel CA.D.OR. n'a pas la prétention de fournir actuellement tous les éléments utiles à un ingénieur de bureau d'études. Il marque cependant une première étape de l'évolution des techniques actuelles de conception dans le domaine des engrenages.

Qui peut utiliser CADOR BASIC ?

CADOR BASIC a été conçu pour aider les ingénieurs et techniciens de bureau d'études à calculer les engrenages.

Son emploi ne nécessite pas de connaissance particulière en informatique. Il libère le projeteur des calculs fastidieux et lui permet d'exercer pleinement sa créativité et son savoir-faire.

Les résultats qui lui sont fournis lui permettront :

- de donner des indications précises à l'atelier,
- de fournir au commercial certaines données très utiles,
- de rédiger plus facilement les notes de calcul qui sont de plus en plus souvent demandées.

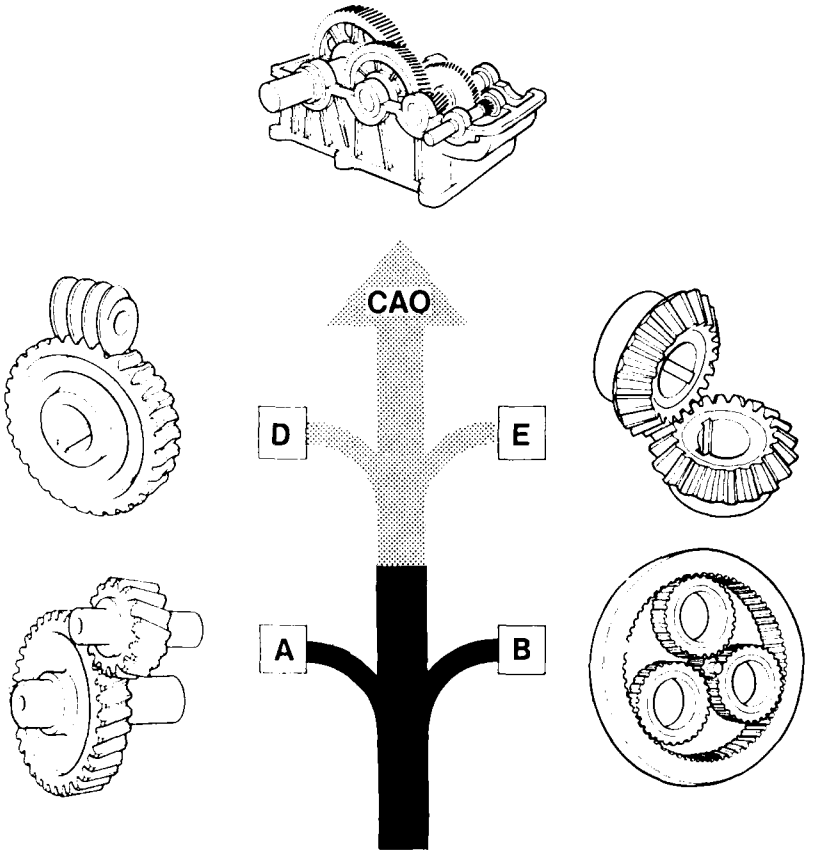


FIGURE 1

L'emploi de matériaux avec traitement de durcissement superficiel peut donner lieu également à des vérifications concernant l'épaisseur de la couche traitée et les valeurs de dureté au sein de cette couche.

Les principales méthodes normalisées et d'emploi international sont :

- Les normes AGMA

- Les normes ISO

- Les normes DIN

Bien souvent, le choix de la méthode est dictée par le client dont l'expérience avec utilisation de l'une d'entre elles, lui facilite les comparaisons entre résultats. En effet, certaines différences peuvent apparaitre au niveau des résultats entre les différentes méthodes. Elles sont dues généralement à des divergences dans la prise en compte des paramètres d'influence et notamment le comportement en fatigue des matériaux.

Le concepteur a besoin d'avoir un éventail de programmes pour utiliser les méthodes les plus adaptées au cas traité et effectuer des comparaisons avec des appareils existants.

Dans les normes AGMA, la méthode générale 218.01 est une révision récente des anciennes normes 210.02, 211.02, 220.02, 221.02. Dans cette norme, les fascicules d'application correspondants à des utilisations bien spécifiques des engrenages sont utilisés de préférence à la norme générale.

Le projet de norme générale ISO (DIS 6336) comprend 3 méthodes de base dont la complexité est fonction de la précision désirée sur le résultat. Des fascicules d'applications spécifiques existent également (automobile, marine, ...) mais seule la norme générale fait foi en cas de litige. Les normes d'applications spécifiques s'écartent assez largement de la norme générale.

La norme DIN 3990 est assez proche de la norme ISO dans sa conception mais présente quelques différences:

. Facteur de forme Y_F pour les dentures hélicoïdales

. Facteur de correction de la pression Z_B entre le point primitif et le point de plus bas contact unique W. (pour les pignons de moins de 20 dents).

La norme DIN possède également plusieurs degrés de complexité suivant la précision recherchée.

En France, la norme AFNOR E23015 correspond à la restriction de la norme ISO pour les engrenages de mécanique générale. La vitesse linéaire doit être inférieure à 50 m/s et la largeur de denture ne peut excéder deux fois le diamètre primitif.

L'application de ces différentes méthodes de calcul à un exemple concret est extrêmement difficile si on ne dispose pas d'un moyen informatique sur lequel ces programmes sont mémorisés. Il suffit de quelques minutes au logiciel CA.D.OR. pour déterminer la puissance transmissible par un engrenage selon l'une quelconque de ces méthodes. Grâce à cette aide il est possible de répondre rapidement à des appels d'offres (cf figure 12).

CONCEPTION ASSISTEE PAR ORDINATEUR (C.A.O Réducteurs)

Si le calcul automatique de la géométrie et du dimensionnement des engrenages est un élement important de la conception des réducteurs, les autres organes mécaniques contenus dans ces matériels doivent également être déterminés par calcul. C'est le cas pour les roulements, les arbres, les corps de roue, les carters. Les différents types de liaison entre organes nécessitent aussi des calculs : frettage, cannelures, clavettes, collage.

L'évolution rapide des logiciels de dessin sur écran et sur table traçante, ainsi que l'accès à des banques de données, donne au concepteur des outils très performants qui permettent de faire la synthèse simultanée de nombreuses informations et de tendre ainsi vers une réalisation optimisée.

Les travaux actuels sur le logiciel CA.D.OR. portent sur le couplage avec des programmes de conception assitée par ordinateur et de dessin assisté par ordinateur, appliqués aux ensembles réducteurs. Par exemple, une série de dessins de carters de base sont stockés sur un fichier; le programme rappelle l'un d'eux à l'écran pour que le concepteur puisse y apporter les modifications tenant compte du cahier des charges (fixation, encombrement, position par rapport à l'environnement). Le dessin du nouveau carter peut alors être obtenu sur table traçante immédiatement.

Nous avons reproduit sous forme d'organigramme, la structure d'un ensemble de "Conception Assistée par Ordinateur" telle que nous la concevons pour la réalisation d'ensembles réducteurs ou multiplicateurs de vitesse ayant de la puissance à transmettre (cf figures 13 et 14).

ETUDE DE LA FINITION DE L'ENGRENAGE

De plus en plus de réalisations industrielles de grande performance nécessitent la correction des dentures des engrenages, en fonction de la vitesse de rotation, du niveau de charge, et des déformations des pièces en fonctionnement.

Ces corrections peuvent être :

Transversales : - dépouille de tête
- dépouille de pied

Longitudinales: - bombé de denture
- dépouilles d'extrêmité
- correction d'hélice

a/ Corrections longitudinales

Chaque ligne d'arbre de la chaine cinématique étudiée peut être mise en équilibre statique, sous l'action des efforts provenant des organes moteur et résistant, et la réaction sur ses appuis.

La structure est discrétisée par la méthode des éléments finis par le programme CA.ST.OR. (Calcul des Structures par Ordinateur) mis au point au CETIM. Les paliers seront modèlisés par des conditions de blocage appropriées et les efforts aux engrènements sont appliqués dans les trois directions de l'espace (cf figure 7)

Les efforts sont décomposés par le programme en série de Fourier et la solution pour la déformée de l'arbre dans n'importe quel plan est obtenue par recombinaison des résultats correspondants à chaque harmonique.

La connaissance de la déformée statique de chaque arbre permet de localiser les points ou la portée des dents est prépondérante. Par différence algébrique des déplacements à chaque extrêmité de la denture, dans le plan radial et tangentiel, on met en évidence les surplus de matière et la correction à effectuer pour obtenir une répartition optimale de la charge. (cf figure 8 et 9)

Généralement, on reporte toutes les déformations sur le pignon et seul celui-ci est corrigé à la rectification en donnant une forme bombée à la denture à l'aide d'une came ou en modifiant légèrement l'angle d'hélice. Cette opération présente en outre l'avantage de reprendre les déformations dues au traitement thermique.

Le programme CA.D.OR. tient compte de cette correction pour le calcul du facteur de portée longitudinale.

b/ Corrections transversales

Un engrenage avec des dents à profil en développante est une transmission homocinétique, l'engrènement des profils conjugués se faisant théoriquement sans chocs. Pratiquement, à cause des erreurs de pas et de profil et à cause de la flexion des dents sous charge, il y a choc à la prise d'engrènement, choc qui est à l'origine de bruit et de variation dynamique de la charge.

Le but est de minimiser ce choc en adoucissant la prise d'engrènement. Le module de géométrie de CA.D.OR. a permis de connaitre la position des points correspondants à la limite du contact unique. Ces points repérés sur la denture par les lettres V et W permettent de définir la partie du profil concernée par la dépouille. La dépouille de tête est comprise entre le point V et le rayon actif de tête du pignon. La valeur de la dépouille normale au profil est obtenue à partir du calcul de la rigidité d'une paire de dents conjuguées, de la charge appliquée et des erreurs de pas (cf figures 10 et 11).

Le pignon étant seul dépouillé, on reporte la valeur théorique de la dépouille de tête obtenue sur le profil de la roue conjuguée, sur le pied de la denture du pignon. La dépouille de pied sur le pignon est comprise entre le point W et le rayon actif de pied.

Les corrections en dépouille sont prises en compte par le programme CA.D.OR. pour le calcul du facteur dynamique K_v à condition que la qualité de l'engrenage soit au moins 5 ISO 1328 .

DIMENSIONNEMENT

Les méthodes de dimensionnement des engrenages sont basées sur la vérification de 3 critères de résistance :

- La résistance à la fatigue de flexion en pied de dent

- La résistance à la fatigue de pression sur les flancs de dent

- La résistance au grippage

Pour certains types d'engrenage, des critères de résistance statique peuvent également être vérifiés.

the author. Improved airworthiness would tend to follow from better reliability, so attention is focused on cost effectiveness of increasing TBO's and MTBR's. Possible savings are considered on a broad basis to provide an indication only in order to ensure that what appears obvious can, in fact, be realised.

CURRENT POSITION

Gearbox TBO's tend to be about 1000 hours for military and 2000 hours for civil operation. This difference results, in part, from the less exacting roles involved in civil aviation, coupled with the fact that pilots are more mature. In many cases civil maintenance is superior to military. TBO's are increased, mainly, on the strength of operating experience and this is acquired at a considerably higher rate in the civil field. (1500 against 300 flying hours per annum). Because of the many differences between civil and military performance, for convenience, only the latter will be considered. It must, however, be borne in mind that, today, both initial and maintenance costs of a military helicopter are only a fraction of the total fully equipped cost.

Following the introduction of a new model, a failure pattern is established at an early stage of operation and, always, there is one component part that holds back a TBO uplift. Frequently this is a bearing and the question arises as why not introduce a modification to increase the life of that bearing? In the past the incentive to fund such modification action has not been particularly strong. The manufacturer cannot guarantee the success of any alteration and this particularly applies to bearings. The Services tend to provision for spares early on in the life of a new helicopter when actual or predicted TBO's are relatively low. The result is that once having purchased an adequate supply of spare gearboxes, fewer of these would be required following an increase in TBO. Hence the lack of incentive to support modification action aimed purely at increasing TBO's. Cynics will claim that, equally, it pays the manufacturer to keep TBO's low. Certainly in the cost conscious and competitive climate ruling today such a claim would be difficult to substantiate.

In recent years the position has been some what different in that the Services are keen to see the introduction of longer TBO's. What then should the target TBO be for a military helicopter? If a realistic level be reached then TBO's would be phased out as, indeed, is likely to be the case as more reliance can be placed on effective monitoring. 300 hours flying per annum appears to be a general mean figure. Prudence suggests that a gearbox should be opened up on a calendar basis for internal inspection. The period would vary with environment but, possibly, one of 6 years duration would be reasonable, say, the equivalent of 5 years flying ie 1500 hours. It would be convenient for the period to coincide with a complete overhaul. There are occasions when an extended TBO would prove useful and, hence, one set at 2500 hours should be more than adequate.

FUTURE REQUIREMENTS

On accepting a requirement for a 2500 TBO the aim must be that all gearboxes attain at least 1500 without failure. Removal on the proposed calendar basis would, in practice, place transmission in the 'Fit and Forget' category, apart from a minimum of routine maintenance. It would appear to be wholly realistic to bring about an increase in gearbox TBO's from 1000 to 2500 hours, with no relaxation in reliability, to give a MTBR of at least 1500 hours. Note that in the present context TBO times are genuine and exclude the need to change a part during a TBO period if this involves gearbox removal.

Before considering how best to tackle the problems associated with increasing TBO's, attention should be given to the cost effectiveness of such action.

COST EFFECTIVENESS

A few years ago an independent cost study was made to ascertain whether worthwhile savings would result from an uplift of 50% in transmission TBO's. Conclusions reached were that estimated savings were so large that any expenditure necessary to achieve the uplift would be of insignificant proportion. Details of the study are not available for publication. We can, however, obtain an idea of the dimension of costs involved from published literature. From Refs 2 and 3, income derived from the sale of spares amounts to between 40 and 50% of total sales in the helicopter division ie approximately £100,000,000, correcting for inflation. If the spares service, say, 1000 helicopters then the annual cost per helicopter will be some £100,000. The size of vehicle ranges from large to small so this figure is probably representative of the medium size military helicopter because civil spares requirements would have been low during the years considered. We can now quantify costs very approximately as being £300 per flying hour for spares alone. Transmission spares would account for a fair proportion of this hourly total. For present purposes it will suffice to note that whatever the actual figure may be, it will be sufficiently large to offer ample scope for a reduction to be worthwhile. Obviously labour costs and capital investment would also be reduced by enhanced reliability and extended TBO's. The value to be attached to improved airworthiness is a matter of conjecture but can be regarded as an additional bonus.

WAYS OF INCREASING TRANSMISSION TBO'S

A gearbox that is free of design and production deficiencies will eventually fail from fatigue and wear. To obtain a respectable TBO it is necessary to minimise both of these damaging mechanisms. Bending and torsional fatigue lives must, of course, be in excess of the target TBO and then the problem falls within the realms of Tribology. In the past, rolling fatigue has been the main concern with respect to long lives but more recently wear, initiated by micro cracking and micro pitting, is causing problems, especially as wear rates can be extremely high. The trend towards the use of lighter oils is responsible for such wear. Fretting, as a form of wear, can be designed out in most locations excepting lubricated splines.

The requirement to operate on a gas turbine oil, understandable as it may be from a logistics viewpoint, does constitute a handicap. Such oils are unsuitable for gearbox operation and, although they are extensively used, the price paid is high. TBO's and MTBR's are lower than need be and the cost of overhaul higher. Scuffing can readily arise and it is the norm to find micro- pitting and spline wear at overhaul. Refs 4 and 5 show that when operating with a suitable gear oil neither spline or scuffing is likely to arise. This claim has been fully substantiated by running fatigue tests in main and tail gearboxes.

To achieve longer TBO's and cheaper overhauls demands, as a first step

a) modification action to design-out known weaknesses and
b) the use of a suitable transmission oil.

The question now arises as to whether this alone is sufficient. It is difficult to answer such a question but an indication can be obtained from basic reliability concepts. Consider a gearbox with a total of 25 major gears and bearings. For an assembly life of 2,500 hours, each item must have a B_{10} life of 25 x 2,500 = 62,500 hours. Individual lives are more likely to be in the 5/10,000 hours, even if the gears are cleared for infinite life, and so it is necessary to look for an order of magnitude increase in lives. Being realistic, it has long been realised that such basic statistics are not necessarily borne out in practice. It has been demonstrated, for example, that a bearing failure could be expected in a main gearbox every flight. Fortunately this does not happen. Nevertheless it can be concluded that substantial increase in individual component life is a firm requirement. A conventional approach of added weight and use of more sophisticated materials can generally be ruled out. Hence an alternative approach has to be sought.

High wear rates, even under conditions of nominally pure rolling, can be induced to order in the laboratory, at stresses below design maximum, when using a 5 c.St oil. Oils that conform to Eng.R.D. 2497 display a pronounced surface temperature distress gap because, essentially, they rely upon e.p. reaction to provide protection. Ref 6. The combination of low oil film thickness, and hence low λ value, and only modest e.p. reaction at medium temperatures, leads to tensile residual stresses in asperities following plastic deformation, microcracking, detachment of particles from the extreme surface layer and, hence, rapid wear. Friction between colliding asperities is a dominant feature through the generation of large traction forces at discrete points in the surface. Excessive wear in gear flank profiles is sometimes experienced in helicopter gearing applications, Fig 1 from Ref 6. Anti-wear additives in the oil can alleviate this problem. Likewise fretting in lubricated surfaces can be eliminated by the choice of appropriate anti- oxidant additives. Scuffing need never arise if gears and bearings are suitably lubricated. A gear oil complete with an efficient additive package will give longer rolling fatigue lives, again, through a reduction in traction.

Extensive accelerated testing is a helicopter gearbox suggests that the adoption of an appropriate oil would enable suitably designed and manufactured gearboxes to reach a 2,500 hour TBO. Why then not simply change to a more effective oil to reap the benefits of substantially reduced operation costs? Maybe, in practice, there is no need to consider any further action - we simply do not know. What we do know is that there is a limit to conditions that any oil will tolerate and that these conditions can be exceeded locally in helicopter gearboxes. This especially applies at the upper limit of ambient temperature when deflections are large and differential expansion between materials is at a minimum.

Consider a typical semi-log S/N curve. At operating stresses the slope of the curve is very low and, accordingly, only the equivalent of a small reduction in stress is required to increase life by an order of magnitude. A change in oil could well bring about a 6-fold increase or more, but it will require only the equivalent of a small increase in stress to lose this gain. To achieve an increased life with ample margin means re-locating the curve at a higher stress level. The oil can, in fact, do this by minimising surface damage through the formation of chemical films, but the degree of improvement is temperature sensitive.

In all forms of fatigue testing the condition of the specimen surface is critical. A well finished specimen will require relatively high stresses to cause failures but the presence of a minor scratch will lower a S/N curve appreciably. In the case of rolling fatigue surface topography will change with time and, following the running-in period, the surface will tend to deteriorate with time, in anything other than full film conditions. Helicopter transmission steels will exhibit an endurance limit, the level of which will depend upon the state of the surfaces, and so the endurance stress level will tend to become less with time. It is frequently claimed that endurance limits do not apply in

rolling fatigue. This is not so - it is its value that is varying with time. This can be seen by applying strain energy concepts to combine reverse bending and reverse torsion fatigue results to provide a theoretical rolling fatigue S/N curve. In all cases pronounced knuckles will be apparent in a log/log S/N curve. Experimental confirmation is available where it can be demonstrated that, with a full film and freedom from debris penetration within the contact, pitting can be prevented completely within practical testing times. The message is clear that to raise, or to prevent the lowering of, the S/N curve it is necessary to protect the surfaces and prevent as much damage as possible. The rolling-in of debris, and consequent plasticly formed dents, is a prime cause of surface deterioration. Accordingly, it can reasonably be predicted that the introduction of fine filtration will result in much increased lives, brought about by the S/N curve being located at a higher stress level.

EFFECTS OF FINE FILTRATION

The influence of filtration level on rolling element bearing life was studied in some detail a few year ago, Ref 7. Prior theoretical studies suggested that debris shape was important as this will determine whether deformations between trapped debris and the bearing tracks will be elastic or plastic. Only the latter will be damaging. For this reason the use of artificial contaminants, such as fine dust, was ruled out on the grounds of completely different shape and modulus of elasticity. Debris was generated in a gear machine and confirmed as being representative of that found in a helicopter gearbox. Overall results are shown in Fig 2, the curves being based on Weibull lines obtained from sample sizes of 10 minimum.

It will be noted from Fig 2 that lives are related to absolute filter rating in the 3 to 40μm range, the approximate power being ~ 2/3. Under conditions of the test that rate of improvement fell off as filtration level was reduced below 3μm. As these conditions were reasonably representative of helicopter gear and bearing contacts it was concluded that there was little need to fit filters finer than 3μm to the gearbox. The increase in B_{50} live was broadly as predicted from rather basic theoretical considerations.

A result of interest is that initial running for 30 mins with a 40μm filter before changing to a 3μm unit resulted in a life only little better than obtained with a 40μm filter throughout. In other words, irreversible damage was incurred during the initial running. This observation suggests that, in practice, much of the advantage to be obtained from fine filtration will be lost unless the gearbox is built to a high standard of cleanliness. Results from the Fort Rucker trials, Ref 4, could be interpreted as providing evidence to contradict the above observation. It is reported that the fitting of 3μm filters to transmissions that had previously been running under 40μm filtration produced satisfactory results. These results relate to qualitative assessments of component condition at strip, rather than ultimate lives. The advantages to be derived from 3μm filtration were not being realised in full and this makes the conclusions so very encouraging. It must, of course, be accepted that laboratory evaluations of the type undertaken should not be interpreted literally. A reasonable conclusion to that work is that substantial increases in TBO could be anticipated and the Fort Rucker experience certainly supports the claim.

Analysis of the laboratory results provide an insight into the damaging influence of debris. Fig 3 suggests that below a certain size, particles will simply pass through the contact without causing damage, where as larger particles reduce lives. The similarity between the influences of surface roughness and filter rating can be seen by comparing Figs 2 and 4. This would suggest that the damaging mechanism is similar, but not necessarily the same, in both cases. From Figs 5 and 6 it would appear that the Weibull slope variation with both roughness and filter rating is also similar and this tends to support the foregoing suggestion.

From an S/N obtained prior to the filter rating evaluations the expected life for a given stress is predicted. The life subsequently obtained with 40μm filtration can be related to a stress level. The same duration life will require a much increased stress for failure with 3μm filtration. By presenting results in terms of 'Equivalent Load', which is analogous to a weight handicap in racing terms, it can be seen from Fig 7 that the load would have to be increased some 6-fold with 3μm filtration to give the same life as for 40μm filtration. Thus, as originally predicted, the effect of finer filtration is to reduce the rate of degradation of the S/N curves. By protecting the surfaces from debris induced damage, rolling fatigues lives can be increased with an ample margin in stress and this points the way to increase TBO's reliability.

The smaller helicopter gearboxes such as those associated with the tail rotor drive are usually splash lubricated. Often the TBO's of these gearboxes exceeds that of the corresponding main gearboxes. Is there then any real need for filtration? At overhaul the bearing tracks in the these small gearboxes are usually covered with debris dents yet the lives appear to be unaffected. The reason for this is that, in flight, transmitted torque through the tail system is, mostly, only a fraction of design maximum. Thus, other than for short periods the bearings are over-designed, and tend to suffer accordingly from skidding, but can accommodate surface deterioration because of the low mean stresses.

It is often the case that one or more bearings are responsible for holding down TBO's. Although this factor influenced the choice of bearings for studying the influence of filtration, the results are equally applicable to gears and also, for different reasons, to seals. Seal failures arise too frequently and are, on occasions, responsible for the low MTBR's recorded. The ingress of debris into a seal is a major cause for failure. With lip seals debris beds into the 'Rubber' which then acts as a lap, heats up, hardens and cracks. With face seals perfectly made and running true, theoretically a separating oil film cannot be generated. Minor imperfections, such as surface waviness and misalignment ensure the presence of an adequate oil film of sufficient dimension to allow the ingress of debris, the presence of which can cause quite rapid surface deterioration and seal failure.

In the U.K. it is not the practice to change gearbox oil between overhauls. The condition of the oil often leaves much to be desired, especially as a result of water contamination, Ref 9. One conclusion reached from the Fort Rucker trials was that 3μm filtration would enable oil life to be extended from 300 to 1000 hours. It can be expected that fine filtration will generally prove beneficial in maintaining the quality of the oil.

FUTURE DEVELOPMENTS

Looking further ahead no externally located filtration systems can help with respect to the first pass of internally generated debris. The damaging size range, for any contact conditions, is relatively narrow - too small and it passes through and too large it is diverted to one side. Work is proceeding to relate this size range to operating conditions and to develop finishing processes that will minimize the generation of damaging size debris.

Although in the laboratory evaluations the rate of life improvement fell off at filtration levels below 3μm some benefit was still being derived right down into the sub micronic regions. This is understandable when a representative thickness of oil film separating asperities is only 0.0125μm (0.5 μins) and, indeed, it may logically be argued that filtration should be aimed at such very small dimensions. However, in practice, it would seem probable that chemical films provide more protection than do the micro E.H.D. oil films at that level. A case can nevertheless, be made for polishing the oil and sub micronic particle extraction may well be sought in the future. For the present, and immediate future, 3μm filtration is a practical level for which filter units are readily available. Experience could show routine oil polishing at predetermined intervals throughout a TBO to be desirable. This would complement 3μm filtration and its introduction would present few problems. Similar processing is already applied to Hydraulic fluids. What is by no means clear is whether the removal of submicronic particles can be achieved without degradation of lubricating performance. A perfectly clean oil that will not lubricate until is has become re-contaminated offers little attraction. Impuries play a role in the action of certain additives. Little is known about the mechanisms involved but studies are now in hand.

The need for better "House Keeping" practice in the manufacture of transmission has been acknowledged by the author's company. Steps are being taken to ensure that completed gearboxes are reasonably free from debris contamination and that the generation of debris during the running-in period will be minimised. Only experience will determine how far it is necessary to go to prevent an ingress of dirt. Present thinking is that full clean room conditions, as applied by hydraulics, will be unnecessary. Studies into optimising finishing operations after machining are underway and these relate, also, to bought-in items such as bearings. Much work remains to be done but progress to date is encouraging. It is interesting to note that this particular operation, costly as it is to introduce, could well result in lower costs for a superior product.

CONCLUSIONS

It seems to be agreed generally that steps should be taken to reduce costs of ownership of helicopters and, at the same time, improve reliability and airworthines. Maintenance of transmission accounts for a fair proportion of overall costs and results, to a degree, from low TBO's and even lower MTBR's. Action is required to increase TBO's and bring MTBR's up to the same level, or that of removal based on calendar conditions ie no unscheduled removals. TBO's of 2500 and 5000 hours for military and civil helicopters respectively would be realistic targets, with scope for advancing civil ones to 7500 hours. Eventually TBO's are likely to be phased out as more confidence is placed on monitoring techniques.

If a gearbox be brought up to a standard whereby TBO's are limited by Tribological consideration only, such as pitting, scuffing and wear, to include fretting, then evidence exists to suggest that these problems can be overcome by substitution of a suitable oil. The position will, however, remain marginal unless means are introduced for more effectively maintaining a good surface finish on contacting surfaces and this can best be achieved by fine filtration, following a clean build standard. Fine filtration on its own will effect a worth while improvement but have little influence on scuffing and fretting of lubricated surfaces. Micropitting will remain a problem. Even if such problems do not already arise within a 1000 hour TBO's, will the same be true at 2500?

Cost savings cannot be quantified in this paper and it can only be claimed that they could be very substantial indeed. The introduction of fine filtration could, it is confidiently predicted, pave the way for helicopter transmissions to be placed in the 'Fit and Forget' category to which they rightly below.

ACKNOWLEDGEMENTS

The author wishes to thank Westland Helicopters Limited for permission to publish this paper.

REFERENCES

1. Vinall, P D, "Airworthiness of Helicopter Transmissions". Symp on Helicopter Transmission. Roy. Aer. Soc. London, Feb 1980.

2. Westland P.C. Annual Reports, 1980-83.

3. Westland P.C. Annual Reviews, 1981-83.

4. Tauber, T, Hudgins, W A and Lee, R S "Oil Debris Assessment and Fine Filtration in Helicopter Propulsion Systems", Oil Analysis Workshop/symp. Pensacola. May 1983.

5. Spikes, H A, and Macpherson, P B, "The Design, Formulation and Testing of a New Type of Lubricant for Helicopter Gearboxes". Trans. Inst. Pet. Conf. on Performance and Testing of Gear Oils and Transmission Fluids. London 1980.

6. Newley, R A, Spikes, H A and Macpherson, P B, "Oxidative Wear in Lubricated Contacts". Journ of Lub. Tech. October 1980, Vol 102/539.

7. Macpherson, P B "Future Requirements for a Helicopter Transmission Lubricant" ASLE-ASME Seminar on Lubricants for Extreme Environments, Washington, Sept 1982.

8. Bhachu, R, Sayles, R and Macpherson P B, "The Influence of Filtration on Rolling Element Bearing Life" Proc. 33rd MFPG on Innovaton for Maintenance Technology Improvements Nat. Bur. Standards Special Pub. 640, Washington, April 1981.

9. Spikes, H A and Macpherson, P B, "Water Content of Helicopter Gear Oils". ASME Internation Power Transmissions and Gearing Conf. San Francisco, Aug. 1980. No. 80-C2/DET-12.

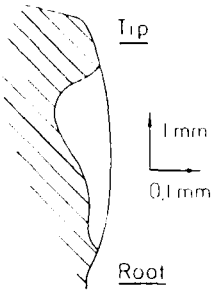


FIG. 1 WEAR IN HARDENED AND GROUND SPUR GEAR (REF. 7)

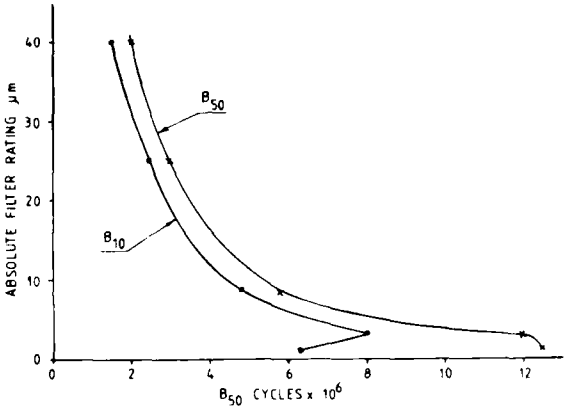


FIG. 2 FILTER RATING V LIFE CYCLES

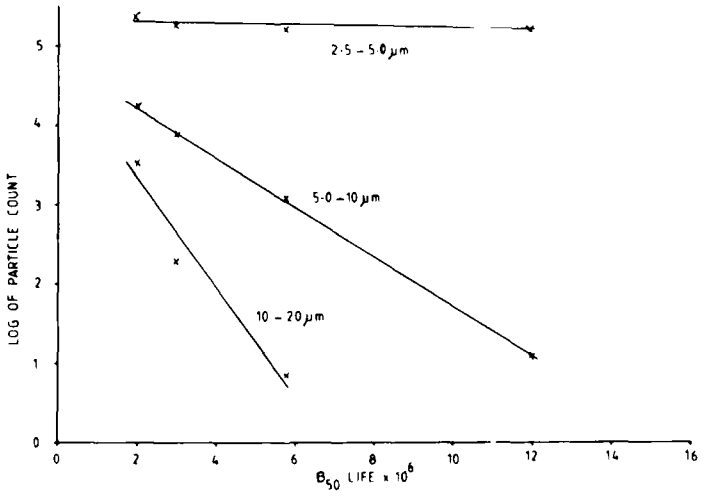


FIG. 3 PARTICLE COUNT V LIFE CYCLES

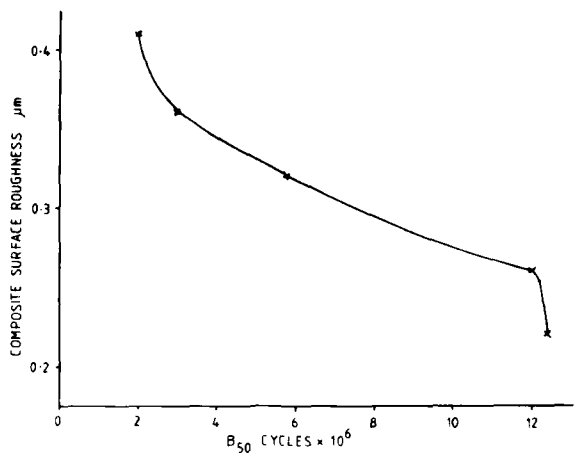


FIG. 4 SURFACE ROUGHNESS V LIFE CYCLES

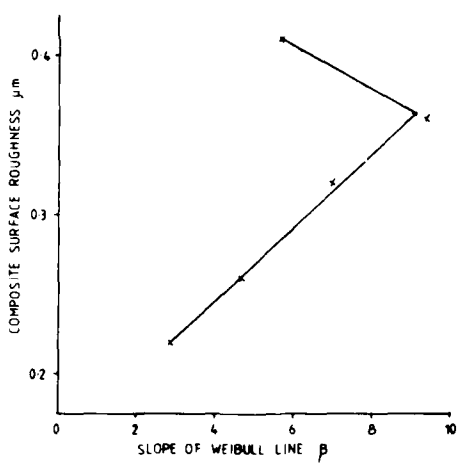


FIG. 5 SURFACE ROUGHNESS V WEIBULL SHAPE PARAMETER

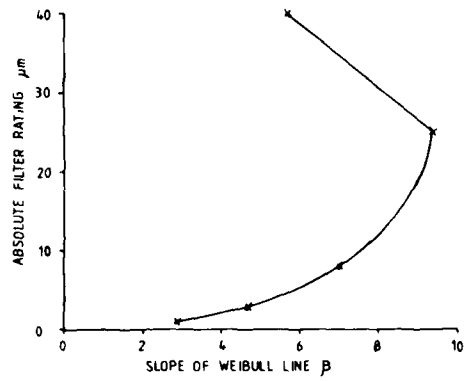


FIG. 6 FILTER RATING V WEIBULL SHAPE PARAMETER

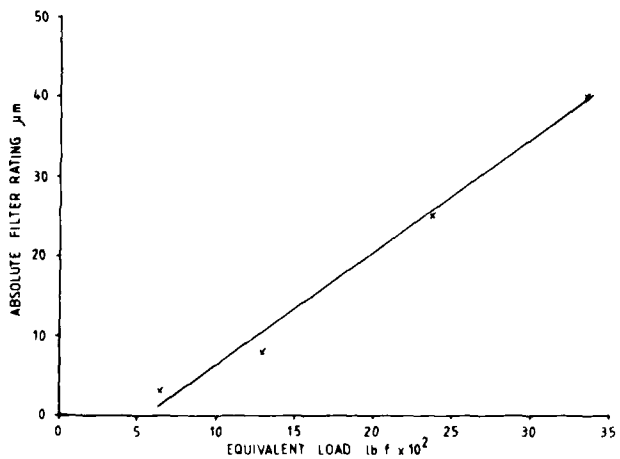


FIG. 7 FILTER RATING V EQUIVALENT LOAD

DISCUSSION

R.J.Drago, US

Fine filtration is more complex in a system point of view. Why not simply use a higher viscosity oil to prevent damage to surfaces while making *no* other changes to the system?

Comment: R.Battles, US

Commercial helicopter operators use better lubricating oils than the military to achieve time between overhauls twice or greater than military TBO's.

Load Capacity of Cages of Roller Bearings for Planet Wheels

Prof. Dr.-Ing. F. Jarchow and Dr.-Ing. P. G. Hoch
Ruhr-University Bochum, Germany

Summary

In planetary gears the rotation of the planet-carrier generates forces of inertia, which can cause fatigue failures of the cages in roller bearings of planet wheels. By means of computer routines forces of inertia and counter forces as well as stress resultants, nominal stresses, stress concentration factors and stress gradients are calculated for bearing cages of various design. Yield strength and fatigue strength of samples of cage material are determined experimentally, and fatigue stress diagrams for cages of different shape and material are worked out. The thus calculated safety factors against fatigue failure are confirmed by test runs of bearings on a test bench. The results of the investigations are summed up in easily applicable charts.

1. Introduction

In addition to tooth forces and forces of inertia caused by the rotation relative to the planet-carrier, planet gear bearings are subject to other forces of inertia, which are generated by the rotation of the carrier. These additional forces of inertia strain the rollers, the raceways and to a great extent the cages of the rollers. Thus it is possible that the life time of the bearings is not limited by fatigue of rollers or races but by fatigue fractures of the cages. In this treatment there will be presented a method for calculating the load capacity of cages.

2. Types of bearings and cages

The cages of cylindrical and spherical roller bearings usually have two rings connected by beams. The rollers are placed in the pockets between rings and beams and guide the cages axially and tangentially. In radial direction the cages are guided either by some of the rollers or otherwise by the outer or the inner rings of the bearings. The former kind of radial guidance is called roller guidance and the latter is called ring guidance.

Different cage designs are:

- sheet metal cage
- massive cage
- riveted cage

Usual materials are:

- steel
- brass
- aluminium
- plastics (synthetic material)

A sheet metal cage is shown in figure 1 and characteristic details of usual massive cages are shown in figure 2 and 3 and of riveted cages in figure 4 and 5 as examples.

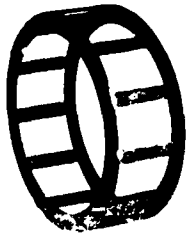


Figure 1: Sheet metal cage

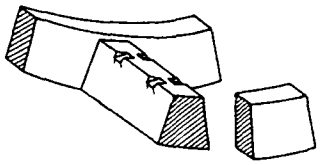


Figure 2:
Broached solid brass cage

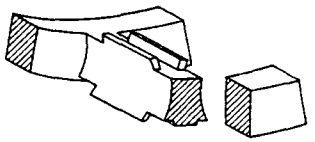


Figure 3:
Injection molded plastic cage

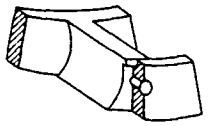


Figure 4:
Cage with riveted pins

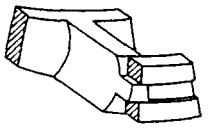


Figure 5:
Cage with riveted spigots

All bearings that are treated in this report are specified in table 1 with their dimension series number, material, type of design, and type of radial guidance.

Table 1: Bearings treated in this report

No.	type of bearing	dimension series No.	sign of	material	cage design	guidance
1	cylindrical roller bearing	23 E MPA	FAG	brass	broached	outer ring
2		23 MA	FAG	brass	riveted steel pins	
3		23 E MA6	SKF	brass	riveted	
4		3 E MA6	SKF	brass	spigots	
5		23 E CP	SKF	plastics	injection molded	roller
6		3 E CP	SKF	plastics		
7		23 E CPA	SKF	plastics		outer ring
8		23 E JP1	FAG	steel	pressed	roller
9	spherical roller bearing	223 ES TVPB	FAG	plastics	injection molded	inner ring

3. Forces of inertia

Figure 6 shows a segment of planet-gear bearing with forces of inertia acting on it. The following symbols and indices are used:

0	gearbox	a	acceleration
1	planet-gear carrier	c	coriolis
2	bearing inner ring	m	mass
3	bearing outer ring	n	normal
4	cage	r	cage ring
F	force	s	cage beam
P	rotation pole	w	roller
S	center of gravity	ω	angular velocity

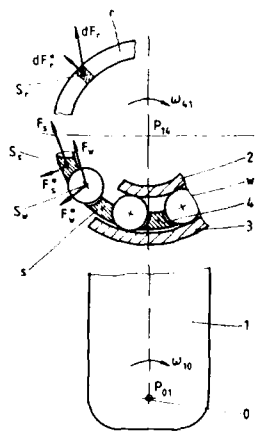


Figure 6: Forces of inertia at the planet-gear bearing

Constant angular velocities assumed, the accelerations a 41n and a 41c cause the constant radial forces

$$F_s^* = m_s \overline{S_s P}_{14} (\omega_{41}^2 + 2 \omega_{41} \omega_{10}) \quad (1)$$

$$dF_r^* = dm_r \overline{S_r P}_{14} (\omega_{41}^2 + 2 \omega_{41} \omega_{10}) \quad (2)$$

$$F_w^* = m_w \overline{S_w P}_{14} (\omega_{41}^2 + 2 \omega_{41} \omega_{10}) \quad (3)$$

and the acceleration a 10n cause the forces of variable magnitude and direction

$$F_s = m_s \overline{S_s P}_{01} \omega_{10}^2 \quad (4)$$

$$dF_r = dm_r \overline{S_r P}_{01} \omega_{10}^2 \quad (5)$$

$$F_w = m_w \overline{S_w P}_{01} \omega_{10}^2 \quad (6)$$

The forces are applied at the centers of gravity S_s of cage beam, S_r of cage ring element and S_w of roller.

Figure 7 shows a segment of the cage k and the roller w with the force of inertia F w caused by the acceleration a 10n. An x-y coordinate system is applied which is fixed to the planet carrier with its origin in the center of the bearing.

The force F w is resolved into the components F ws directed on the beam and F wr on P 14. F wr like F* w acts on the outer bearing ring and has no influence on the load of the cage. F ws is resolved into the components F wsy and F wsx. The sum of all components F wsx is either negligible or zero. With the mass m k of the cage and with the centre distance a of the planetary gear follows the sum of all components in y-direction

$$\Sigma F_{iy} = \omega_{10}^2 \, a \, m_K + \Sigma F_{wsy} \quad (7)$$

ΣF iy acts either on the bearing rings or on the supporting rollers, depending on the type of cage guidance.

ΣF iy can be calculated approximately and is then called F q. With the number of rollers z w follows

$$F_g = \omega_{10}^2 \, a \, (m_K + \frac{z_w}{2} m_w) = \omega_{10}^2 \, a \, m_g \qquad (8)$$

m g means a mass that is relevant for the load on the cage.

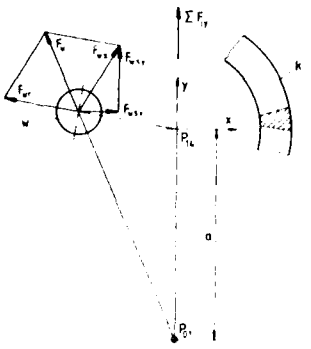


Figure 7: Forces of inertia acting on the cage

It is advantageous to use a relative sum of forces of inertia of cage and rollers to obtain a nondimensional representation. Dividing F g from eq. (8) by the modulus of elasticity E and the cross sectional area A r1 of a cage ring r 1 gives the nondimensional acceleration

$$a_{10n} = \frac{F_g}{E \, A_{r1}} = \frac{\omega_{10}^2 \, a \, m_g}{E \, A_{r1}} \qquad (9)$$

4. Supporting forces

The force F g as a function of a 10n causes supporting forces, which depend on the type of cage guidance.

If the cage is guided by rollers, the supporting forces act between the supporting rollers and the beams. The number of supporting rollers and the magnitude of the supporting forces depend on the cage clearance and elasticity.

If the cage is guided by the bearing ring, there is a supporting pressure between the cage rings and the guiding ring of the bearing. The pressure distribution is influenced by the cage clearance and the cage elasticity as well. Solid state contact and hydrodynamic contact are discerned.

4.1 Ring-guidance

There is a solid state contact between the cage rings and bearing ring, if the angular velocity . 41 is too small to generate a hydronamic pressure. For calculating the supporting pressure of solid state contact an equivalent ring as shown in figure 8 is used. This is the model of a cage guided by the outer ring; cages guided by the inner ring are treated in a similar way.

The equivalent ring of the cage is represented by the centre O r and the radius r r. It is displaced from the centre of the bearing O L about . r, which is half of the radial cage clearance S r. The cage thus contacts the ring of the bearing at point II. The equivalent ring has the cross sectional area A r and furthermore, mass and elasticity. The acceleration of a mass-element . mr causes the distributed loads q rt (φ) and q rr (φ). These loads effect the tangential deflections v (φ), the radial deflections w (φ) and the rotations ϑ (φ). Because of the properties of symmetry only half of the ring is taken into account with a guiding at point I and a fixed end : point II. Within the angle . max the radial deflections of the equivalent ring w (φ) are limited by the circular outline of the bearing ring with its radius r 1. At the point φ i for example the possible deflection is h j (φ). The curvatures of the equivalent ring and the outer bearing ring are identical within the angle of contact . max.

Finite beam elements are used to calculate the angle of contact . max and the pressure distribution between the rings. The calculated pressure distributions within the angle . max in a cylindrical roller bearing 2309 E MPA subjected to 300 and 600 times the acceleration due to gravity g are plotted in the figures 9 and 10.

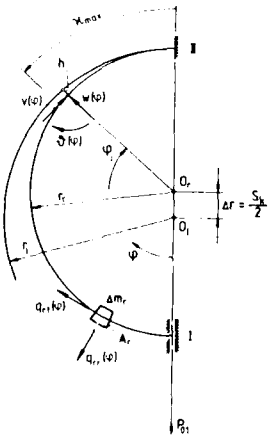


Figure 8: Equivalent ring of a cage guided by the outer ring of a bearing with solid state contact

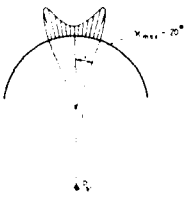


Figure 9: a_{10n} = 300 g



Figure 10: a_{10n} = 600 g

Figures 9 and 10: Supporting pressures of solid state contact under various accelerations a_{10n}

Hydrodynamic pressure needs high relative speed of the planet gear. The cage then might be supported by an oilfilm between the rings of cage and bearing. However, traces of wear on the rings indicate mixed friction, when there are high accelerations a 10n . Therefore the supporting pressure distribution of solid state contact is used to calculate the cage loads.

With usual relative speeds of planet gears a supporting hydrodynamic pressure is generated only at slow speeds of the planet carrier. In these cases the acceleration a 10n is insignificant for fatigue failure of the cage. If wear must be avoided [1] describes a method to calculate a safe acceleration a 10n for a given minimal oilfilm thickness.

4.2 Roller-guidance

A roller guided cage with the beams S and some rollers w is represented in figure 11.

The rollers run on the raceways, which are not shown in the figure 11, in a distance r w from the centre of the bearing O L. The forces of inertia caused by the acceleration a 10n make the rollers and the cage move away from P O1. The centre of the cage O K is displaced about e a in y-direction so that the beams S 1, S 2 and S n contact the rollers w 1 and w n.

The single supporting forces F we1 and F wen raise at the edges of the beams. They counter-balance the forces of inertia of the cage and the rollers. The total forces of the rollers F wq1 and F wqn are the geometric sum of the single supporting forces F we and are taken by the inner ring of the bearing.

The forces of inertia and the supporting forces that act on the cage cause elastic deformations of the cage rings. A radial deflection of the beams makes the rollers turn aside in tangential direction. If the clearance S wa2 or S wij between the roller w 2 or w j and the outer or inner edge of the beam is used up, this roller supports the

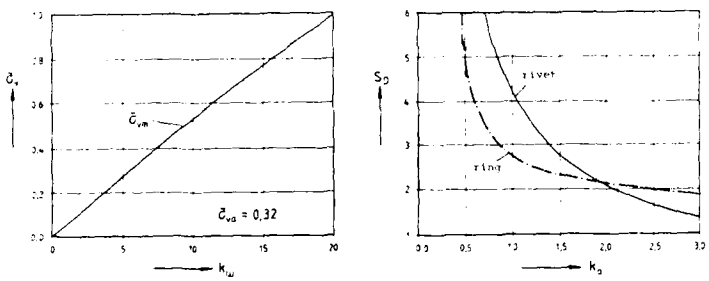


Diagram A: Nondimensional equivalent stress

Diagram B: Safety factor against fatigue failure

Table 1: Characteristic factors

Bore diameter No.	04	05	06	07	08	09	10	11	12	13	14	15	16
$K_\omega \cdot 10^{-3}$	2,44	2,94	3,47	3,20	3,23	3,42	3,43	3,79	3,89	3,4	3,73	2,35	2,42
$k \cdot 10^{-3}$	5,7	7,4	7,9	10,3	10,5	11,3	11,2	24,4	23,7	24,1	24,7	8,6	8,8

Chart 3: Cylindrical roller bearings 23 E MA6, cage with riveted spigots and guided by the outer ring

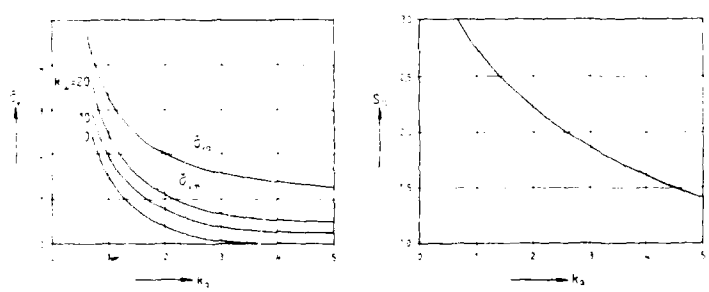


Diagram A: Nondimensional equivalent stress

Diagram B: Safety factor against fatigue failure

Table 2: Characteristic factors

Bore diameter No.	04	05	06	07	08	09	10	11	12	13	14	15	16
$K_\omega \cdot 10^{-3}$	2,44	2,94	3,47	3,20	3,23	3,42	3,43	3,79	3,89	3,4	3,73	2,35	2,42
$k \cdot 10^{-3}$	5,7	7,4	7,9	10,3	10,5	11,3	11,2	24,4	23,7	24,1	24,7	8,6	8,8

Chart 4: Cylindrical roller bearings 3 E MA6, cage with riveted spigots and guided by the outer ring

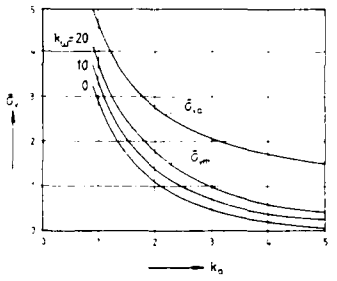


Diagram A: Nondimensional equivalent stress

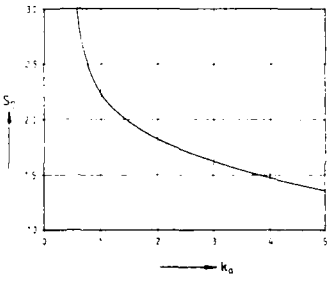


Diagram B: Safety factor against fatigue failure

Table C: Characteristic factors

Bore diameter No.	04	05	06	07	08	09	10	11	12	13	14	15	16
k_a 10^{-3}	0,61	0,81	1,14	1,15	1,19	1,22	1,35	1,7	1,79	1,82	2,04	2	2,23
k_M 10^{-3}	11,7	14,6	25,5	23,7	25,5	28,7	31,4	31,7	32,3	32,8	36,8	40,3	41,8

Chart 1: Cylindrical roller bearings 23 E MPA cage guided by the outer ring and broached from solid brass

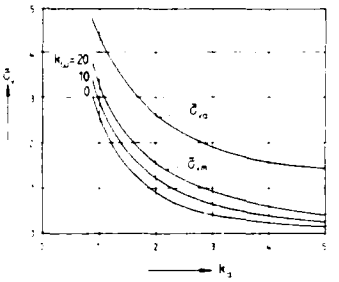


Diagram A: Nondimensional equivalent stress

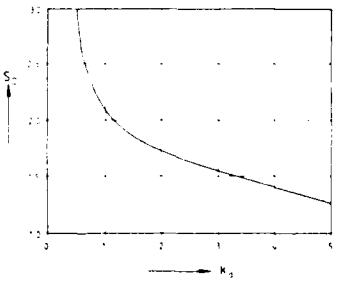


Diagram B: Safety factor against fatigue failure

Table C: Characteristic factors

Bore diameter No.	04	05	06	07	08	09	10	11	12	13	14	15	16
k_a 10^{-3}	1,14	1,37	1,92	1,94	1,99	2,07	2,19	2,4	2,5	2,8	3,4	3,27	3,42
k_M 10^{-3}	23,6	27,1	38,1	38,4	44,2	45,4	47,2	57,3	59,2	67,2	68,3	74,2	77,6

Chart 2: Cylindrical roller bearings 23 MA cage riveted with steel pins and guided by the outer ring

the safety factor against yield failure is

$$S_F = \frac{\sigma_{0,2} - \sigma_{0,2} \cdot \sigma_m}{\sigma_{vm} + \sigma_{va}} \geq 1,5 \qquad (33)$$

and alternatively to the diagrams B in the charts the safety factor against fatigue failure is

$$S_D = \frac{\sigma_W \cdot \sigma_{zW} \cdot \sigma_{vm}}{\sigma_{va} \cdot \left(\frac{\sigma_{0,2} \cdot \sigma_B}{\sigma_W \cdot \sigma_{zW}} - 1 \right)} \geq 2 \qquad (34)$$

Table 2 is an index of all charts and contains all necessary data to calculate S B, S F and S D according to the eq. (32), (33), (34) for given bearings. The material strengths of plastics are valid for a temperature of ϑ = 23°C and a relative moisture of 0,2 %. f can be taken from figure 28.

Table 2: Strengths of cage materials and factors to calculate safety-factors

Dimension series No.	cage material	Chart No.	$\sigma_{0,2}$	σ_W		
23 E MPA	brass	1	2,85	1,2	0,8	1,0
23 MA	brass	2	3,1	1,2	0,8	1,0
23 E MA6	brass	3	3,0	1,2	0,8	1,0
3 E MA6	brass	4	3,2	1,2	0,8	1,0
23 E CP	plastics	5	3,2	1,4	1,0	f(ϑ,)
3 E CP	plastics	6	3,2	1,4	1,0	f(ϑ,)
23 E CPA	plastics	7	3,3	1,4	1,0	f(ϑ,)
23 E JP1	steel	8	2,4	1,3	0,9	0,56
23 ES TVPB	plastics	9	3,3	1,4	1,0	f(ϑ,)

cage material	material strengths in N/mm^2		
	σ_B	$\sigma_{0,2}$	σ_{zW}
brass	465	260	190
steel	340	230	175
plastics	160	105	46

The safety factor against fatigue failure in diagram B of chart 1 and 2 for the cylindrical roller bearings 23 E MPA and 23 MA - see table 1 No. 1 and No. 2 - decreases only slightly with increasing acceleration factors. Therefore, deviating from eq. (35) a safety factor S D $\geq$ 1,5 is permissible.

The stresses and safety factors in chart 3 for the cylindrical roller bearings 23 E MA6 - see table 1 No. 3 - with a riveted cage are valid for critical cross sections of the spigots. The graph of the safety factor of the ring is plotted in diagram B too. Below K a = 1,9 the safety factor of the ring is less than the safety factor of the rivet.

The experiments with roller bearings 23 E MA6 according to [2] led to fatigue failures of spigots. Further experiments showed that loosening of the riveted rings can occur, even if the acceleration a 10n is relative small. To prevent the loosening of a riveted ring the condition S D $\geq$ 2,5 for the riveted spigots should be observed.

$$K_{FE} = \frac{F}{E+F} \quad 0,4 \tag{30}$$

and in case of rotating outer ring

$$K_{FE} = \frac{E}{E+F} \quad 0,6 \tag{31}$$

In eq. (29) ω_{p1} means the angular velocity of a planet wheel relative to the planet carrier.

Often the ring gear of a planetary gear set is fixed at the housing. In such cases is $K_\omega = 0$. With $K_\omega = 0$ the safety factor against fatigue fracture of the critical section can be taken from diagram B depending on the acceleration factor K a. K_ω affects only the mean stress, which has only a little influence on the permissible alternating stress. Therefore the diagramm B can be used, even if $K_\omega \neq 0$. The error is less than 5 %, if $\sigma_{vm}/\sigma_{va} < 0,5$ and $S_D = 2$.

The safety factor on the ordinate of diagram B in the charts 5, 6 and 8 for roller guided cages of bearings with the dimension numbers 23 ECP, 3 ECP and 23 E JP1 - No. 5,6 and 8 in table 1 - is divided by a correcting factor K S. This correcting factor depends on the bore diameter and can be taken from table C.

The material strength of plastics is influenced by temperature and moisture. In the charts 5,6,7 and 9 for bearings with the dimension numbers 23 ECP, 3 ECP, 23 ECPA and 223 ESTVPB - No. 5,6,7 and 9 in table 1 - this influence is considered by the condition factor β. This factor can be taken from figure 28 as a function of the temperature ϑ and the relative moisture φ. In normal air of 23°C and 50 % relative moisture the plastic material used for cages is able to absorb up to 1,9 % moisture. This however may take some 100 days since molding.

The material strength and the modulus of elasticity as well decrease with raising temperature and moisture. In the charts an approximately constant ratio of material strength and modulus of elasticity is assumed.

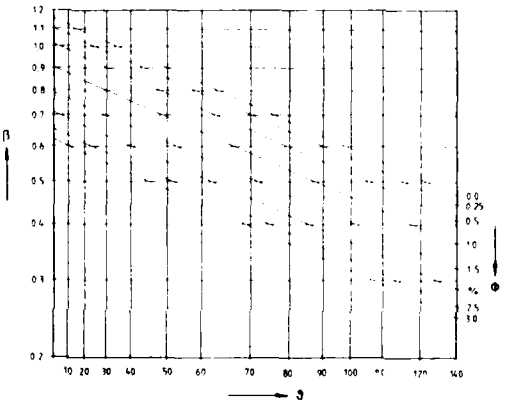


Figure 28: Condition factor β of plastics depending on the relative moisture φ and the temperatur ϑ

In the chart 8 for cylindrical roller bearings 23 EJP1 with sheet metal cages - No. 8 in table 1 - the condition factor β is set to 0,56. The factor β here takes into account the decrease of material strength caused by the plasticly deformed beads that hold the rollers.

With the nondimensional stresses σ^*_{vm} and σ^*_{va} from the diagrams A in the charts the stresses σ_{vm} and σ_{va} are calculated according to eq. (22), (23). With σ_{vm} and σ_{va} the safety factor against forced rupture is

$$S_B = \frac{\sigma_{0,2} \cdot \beta}{\sigma_{vm} + \sigma_{va}} \geq 2,5 \tag{32}$$

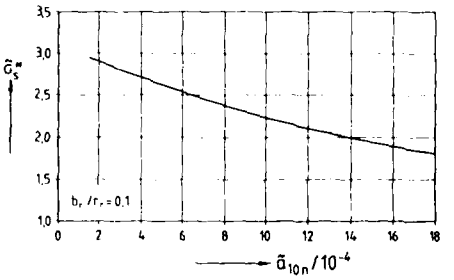


Figure 27: Modified stress of cage plotted against the nondimensional acceleration ã 10n

In the charts diagram A represents the nondimensional equivalent mean stress vm and alternating stress va as a function of the acceleration factor K a and the angular velocity factor K . The real maximum mean stress vm and the real maximum alternating stress va of the endangered point in the critical section are obtained by multiplying the nondimensional stress with the stress factor K - taken from table C - and the acceleration a 10n = 10 a, so that

$$\frac{\sigma_{vm}}{Nmm^{-2}} = \frac{\omega_{10}^2\, a}{m\, s^{-2}}\, K \cdot \sigma_{vm} \tag{22}$$

$$\frac{\sigma_{va}}{Nmm^{-2}} = \frac{\omega_{10}^2\, a}{m\, s^{-2}}\, K \cdot \sigma_{va} \tag{23}$$

The acceleration factor K a is calculated with the bearing factor K L from table C:

$$K_a = \frac{\omega_{10}^2\, a}{m\, s^{-2}}\, K_L \tag{24}$$

The angular velocity factor K is given by:

$$K_\omega = \frac{r_r}{a}\,(1 + \frac{\omega_{41}}{\omega_{10}})^2 \tag{25}$$

in case of rotating inner ring with

$$\omega_{41} = \omega_{21}\,\frac{F}{E+F} \tag{26}$$

and in case of rotating outer ring with

$$\omega_{41} = \omega_{31}\,\frac{E}{E+F} \tag{27}$$

In the eq. (26), (27) E is the diameter of the raceway of the outer ring and F is the diameter of the raceway of the inner ring. Simplifications leads to

$$r_r\quad \frac{D_L + d_L}{4} = \frac{d_{mL}}{2} \tag{28}$$

with the outside diameter D L and the bore diameter d L of the bearing and further

$$K_\omega = \frac{d_{m1}}{2a}\,(1 + K_{FF}\,\frac{\omega_{p1}}{\omega_{10}})^2 \tag{29}$$

Using standard dimensions in case of rotating inner ring gives

The maximum stress in ring guided cages usually occurs at point 3 of the critical section of the ring - see figure 18 -. It was found that the influence of l sg/r r and b r/r r can be neglected, as far as the dimensions are practically useful.

On the countrary the nondimensional acceleration $\hat{a}$ 10n and the relative cage clearance $\psi = \Delta r/r\ r$ have a great effect on the nondimensional alternating stresses at the endangered point 3. The results of the calculations with various $\hat{a}$ 10n and ψ indicate a correlation of these two parameters. In figure 26 the nondimensional alternating stresses $\hat{\sigma}$ ar3 are plotted against the quotient of nondimensional acceleration $\hat{a}$ 10n and the cage clearance ψ for various relative heights of the ring h r/r r. The relative height of the ring has only a little effect on the nondimensional alternating stress.

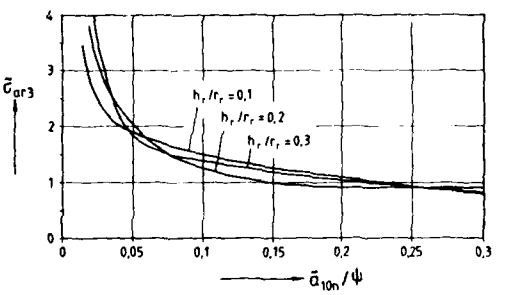


Figure 26: Nondimensional alternating stress $\hat{\sigma}$ ar3 at the endangered point 3 in a ring section of a ring guided cage plotted against the quotient of nondimensional acceleration $\hat{a}$ 10n and the relative cage clearance ψ for various relative heights of the ring h r/ r r

A cage of plastics was used as base of the studies of roller guided cages. Such cage are used increasingly in all types of cylindrical roller bearings because of low costs, easy installation, and safe guiding of the rollers.

The influences of

- relative heights of the beam h_s/b_s
- relative length of the beam l_{sg}/r_r
- relative width of the ring b_r/r_r

on the maximum equivalent alternating stress that occurs at point 2 of the cross section of the beam - see figure 17 - were investigated.

The result of the studies of roller guided plastic cages is a modified stress $\hat{\sigma}^*S$ that is plotted against the nondimensional acceleration $\hat{a}$ 10n in figure 27 for a relative ring width b r/r r = 0,1.

The nondimensional equivalent alternating stress at point 2 of the critical cross section of the beam - see figure 17 - is approximately by given

$$\hat{\sigma}_{vaS2} = \hat{\sigma}^*_S \sqrt[3]{\frac{l_{sg}}{r_r}} \frac{h_s}{b_s} K_{rb} \qquad (21)$$

K rb means the factor of ring width.

For the roller guided plastic cages of the cylindrical roller bearings 23 ECP and 3 ECP - see table 1, No. 5 and 6 - K rb 1 can be assumed.

11.2 Charts to determine the load capacity of bearings

The results of the studies of ring and roller guided cages are summed up in easily applicable charts. The approximate geometric similarity permits a nondimensional representation.

The functions plotted in the charts that are used to determine stresses and safety factors of the endangered points are based on nondimensional shape and load factors. The nondimensional shape factors are mean values within the bearing dimension series. Effects on stresses and safety factors caused by the deviations from the mean values are considered by factors that depend on the bore diameter No.. Nine charts help to select roller bearings from table 1 considering their load limits.

determination of the critical operating condition that causes fatigue failure the load was reduced step by step until no failure occured.

11. Results

The results of the tests are shown in figure 24. The limits of acceleration a 10n of bearings with the bore diameter No. 09 are plotted as multiples of the acceleration due to gravity g.

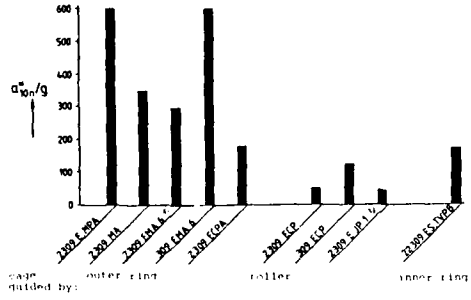


Figure 24: Limits of centrifugal acceleration
1) taken from [2]
2) taken from [4]

The sufficient conformity of theorie and experiments is shown in [1]. Figure 25 for example presents a test bearing 2309 MA with a broken comb-ring. The fracture adjacent to the beam was predicted by the calculation.



Figure 25: Cylindrical roller bearing 2309 MA with fatigue fracture of the comb-ring

11.1 Influence of different parameters on nominal stresses

The influence of load and of cage design on nominal stresses was studied by variating the input data of the computer program. Just the characteristic factors that have an influence on the endangered point of the cage were variated. In ring guided cages the cross section of the ring - see figure 18 - is usually the critical one, whereas in roller guided cages the cross section of the beam - see figure 17 - is relevant.

The following characteristic geometric factors of ring guided cages were variated to study their influence on the relevant stresses under various nondimensional accelerations $\hat{a}$ 10n from eq. (9):

- relative length of a beam l_{sg}/r_r
- relative width of a ring b_r/r_r
- relative height of a ring h_r/r_r
- relative radial cage clearance $\psi = \Delta r/r_r$

These factors influence the distribution of the supporting pressure - see figures 9 and 10 - and therefore the relevant stresses of the ring.

factor 8, which will be explained in chapter 11.2

9. Safety factors

The safety factors are calculated as follows: The safety against force rupture

$$S_B = \frac{\tilde{\sigma}_B}{\tilde{\sigma}_{vm} + \tilde{\sigma}_{va}} \geq 2,5 \qquad (18)$$

the safety against yield failure

$$S_F = \frac{\tilde{\sigma}_{0,2}}{\tilde{\sigma}_{vm} + \tilde{\sigma}_{va}} \geq 1,5 \qquad (19)$$

the safety against fatigue

$$S_D = \frac{\tilde{\sigma}_A}{\tilde{\sigma}_{va}} \geq 2 \qquad (20)$$

10. Test bench and experimental research

The calculated relevant stresses are verified by experimental research on a test bench by simulating working conditions and loads of bearings in planet gears. Load limits which prevent fatigue are the results of these tests. The calculation is verified, if its result is S D = 1, with the experimentally determined load limits used as input data.

A scheme of the test bench is schown in figure 23.

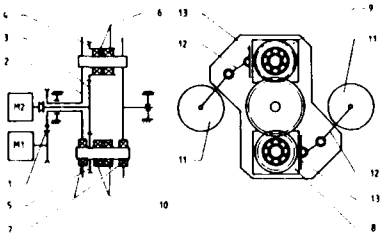


Figure 23: Scheme of the test bench

M1, M2,	D.C.motors	7	Test bearing with rotating inner ring
1	V-belt drive	8,9	Planet gear masses
2	Planet carrier	10	Support bearings
3	Sun gear	11	Centrifugal masses
4,5	Planet gears	12	Levers
6	Test bearing with rotating outer ring	13	Plates

The planet carrier 2 is driven with a V-belt 1 by the speed variable direct current motor M1. The sun gear 3, meshing with the planet gears 4 and 5 is driven by the speed variable direct current motor M2. The planet gear 4 is beared by the test bearings 6 with rotating outer rings. Planet gear 5 is beared by the test bearings 7 with rotating inner rings. The centrifugal forces that act on the planet bearings are caused by the masses 8 and 9. Support bearings 10 are placed in mass 8. The test bearings 6 are loaded by the mass 9 and an intermediate slide bearing. Centrifugal masses 11 simulate the tooth forces. They act upon the masses 8 and 9 by means of levers 12 and plates 13. The masses 11 can be exchanged to simulate realistic combinations of centrifugal and tooth forces.

To determine the load limits of cages endurance tests were made until fatigue failure occured. In high speed planetary gears scuffing or undue wear of the cages in the planet bearings are possible as well. This wear is caused by mixed friction of the cage rings and the bearing ring, if the cage is ring guided. Exessive loads prevent the generation of a hydrodynamic oilfilm and cause solid contact of the rings. For an exact

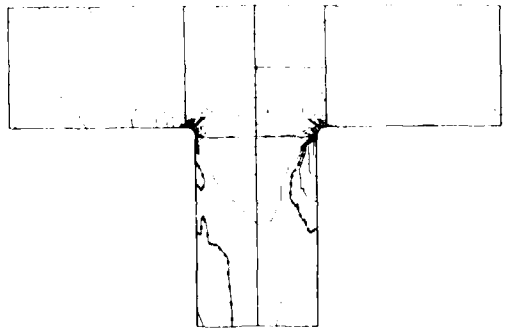


Figure 21: Plane model of a cage broached from solid material with lines of equal stress

8. Strength

Figure 22 shows a Smith-diagram, which contains limiting values of the alternating stresses as a function of the mean stresses taking into account material and shape. This diagram is based on material strength of samples of cage material represented by the yield strength σ B, the 0,2 % proof stress σ 0,2, and the fatigue strength σ ZW. If there is a definite begin of the plastic deformation, the yield strength σ F is used instead of σ 0,2. The factor δ 0,2 respects the unequal magnitude of stresses and the factor δ W the stress gradients in a cross section and both are dependent on σ 0,2 or σ F, respectively. σ ZW is determind with a polished sample. Deviating values of σ ZW caused by a rougher surface are considered by the factor κ. For a detailed explanation of δ 0,2, δ W, and κ see [1] and [3].

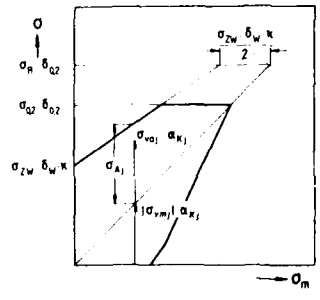


Figure 22: Limiting values of alternating stresses as a function of the mean stresses

The limiting value of alternating stress σ Aj is a function of σ m = σ vmj = σ vmj α K. j indicates the endangered point of ring, beam, or rivet.

A nondimensional Smith diagram is prefered. The nondimensional strengths are defined similar to the nondimensional stresses, using the fictive stresses σ S, r, n, q according to eq. (10) and furthermore considering the stress concentration factor α K. The nondimensional Smith-diagram can be obtained with

$$\sigma_B = \frac{\sigma_{0,2}\ \sigma_B\ \beta}{\sigma_{S,r,n,q}\ \alpha_K} \tag{15}$$

$$\sigma_{0,2} = \frac{\sigma_{0,2}\ \sigma_{0,2}\ \beta}{\sigma_{S,r,n,q}\ \alpha_K} \tag{16}$$

$$\sigma_{ZW} = \frac{\kappa\ \sigma_W\ \sigma_{ZW}\ \beta}{\sigma_{S,r,n,q}\ \alpha_K} \tag{17}$$

The material strenghts of cage and samples may differ because of the manufactouring method or the working condition of the bearing. This is considered by the condition

ses $\tilde{\sigma}_{uj}$, $\tilde{\tau}_{uj}$

$$\tilde{\sigma}_{mj} = \frac{\tilde{\sigma}_{oj} + \tilde{\sigma}_{uj}}{2} \quad ; \quad \tilde{\tau}_{mj} = \frac{\tilde{\tau}_{oj} + \tilde{\tau}_{uj}}{2} \tag{11}$$

and the nondimensional alternating stresses are

$$\tilde{\sigma}_{aj} = \tilde{\sigma}_{oj} - \tilde{\sigma}_{mj} \quad ; \quad \tilde{\tau}_{aj} = \tilde{\tau}_{oj} - \tilde{\tau}_{mj} \tag{12}$$

The nondimensional equivalent stresses are calculated according to the following equations

$$\tilde{\sigma}_{vmj} = \sqrt{\tilde{\sigma}_{mj}^2 + 3\,\tilde{\tau}_{mj}^2} \quad ; \quad \tilde{\sigma}_{vaj} = \sqrt{\tilde{\sigma}_{aj}^2 + 3\,\tilde{\tau}_{aj}^2} \tag{13}$$

[1] developed a computer program to calculate the stress resultants and the nominal stresses of the critical sections of cages of roller bearings used in planet gears. Some results for various cages are presented in [1].

7. Maximum stresses and stress concentration factors

The deflection of the lines of force at the junction of ring and beam or beam and rivet causes higher stresses. The maximum stresses are given by multiplying the nominal stresses with the stress concentration factor α_{Kj}:

$$\hat{\sigma}_j = \alpha_{Kj}\,\sigma_j \quad ; \quad \hat{\tau}_j = \alpha_{Kj}\,\tau_j \tag{14}$$

The stress concentration factors α_{Kj} of the endangered points j of the critical sections of beam, ring, and rivet are not easily obtainable. However the stress concentration of the critical sections is calculable using the finite element method. The stress concentration factors are derived from the comparison with the nominal stresses.

The exact calculation of the stress concentration factors requires a three-dimensional idealisation of the cage. However the numerical expenditure for such a finit element model would be far too great. Therefore an idealisation with plane elements is used. A cage segment with a part of the ring and a part of the beam, as shown in figure 20, is analysed. The forces F r and F s acting on the cage segment are derived from the calculation of the entire beam model of the cage - see figure 16 -

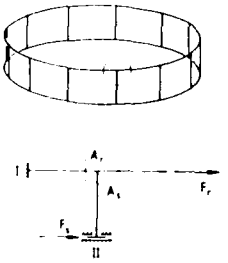


Figure 20: Beam model to determine stress concentration factors

The nominal stresses in the cross section A r of the ring and the cross section A s of the beam are calculated applying the boundary conditions that are shown in figure 20.

The externel loads calculated from the beam model are transfered to the plane model. Figure 21 shows as an example the plane model of a cage broached from solid material. Expecially the radii at the joint of ring and beam are considered Dimensions, loads and boundary conditions of the plane model and the beam model are identical.

Lines of equal stress are plotted in figure 21. At the joint of ring and beam there is a stress concentration. The maximum stresses occur in the ring just beside the radii. The quotient of the maximum equivalent stress and the nominal equivalent stress $\hat{\sigma}_v/\sigma_v$ is the stress concentration factor α_K. In this example it is $\alpha_K = 2{,}1$.

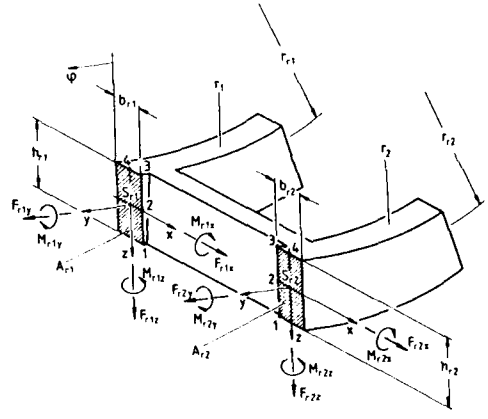


Figure 18: Segment of a cage and stress resultants in the critical sections of the rings

A beam of a cage with riveted spigots is shown in figure 19. The critical section is its joint with the beam with the height h n, the width b n and the area A n. The origin of the x,y,z-coordinate system lies in the centre of gravity S n. The normal force and the traverse forces F ny and F nz act on the rivet. The traverse loads in y- and z-direction are assumed as triangular distributed loads q ny and q nz on the length l n. This assumption bases on experiences of [2], who found that rivets loosen before breaking. In this case the beams are joined with the comb ring at one end only. Beyond that the riveting causes a better contact at the outer edges of the spigots.

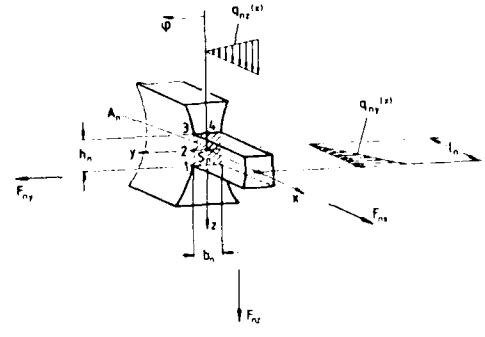


Figure 19: Loads on a spigot with rectangular cross section

The stresses in riveted pins - see figure 4 - are determined using the same assumptions.

In the endangered points j = 1,2,3,4 of the beam s, the rivet n and the rings r1, r2, the sum of all the nondimensional normal stresses is named $\hat{\sigma}$ j, and the sum of the nondimensional shear stresses is named $\hat{\tau}$ j.

To obtain the real stresses, the nondimensional stresses are multiplied with

$$\sigma_{S,r,n,g} = \frac{\omega_{10}^2 \; a \; m_g}{A_{S,r,n}} = \frac{F_g}{A_{S,r,n}} \qquad (10)$$

the quotient of the total support force F g from eq. (8) and the cross sectional area of a beam A s, of a ring A r, or of a rivet A n.

The stresses $\hat{\sigma}$ j and $\hat{\tau}$ j of beams, rings and rivets change with the cage rotation relative to the planet carrier. This rotation is discribed by the angle Ψ . The nondimensional mean stresses are calculated from the maximum stresses $\hat{\sigma}$ oj, $\hat{\tau}$ oj and the minimum stres-

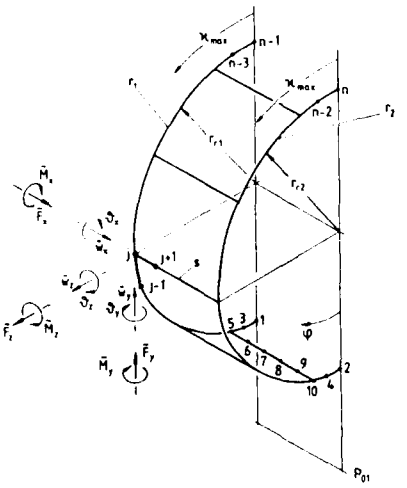


Figure 16: Cage idealised as a structure of finite beam elements

known from the calculations with the equivalent ring - see figure 8 - are used as boundary conditions.

When calculating the stress resultants it is sufficient to consider only half of the cage, because loads and deformations are symmetrical.

When analysing riveted cages - see figures 4 and 5 - the nodes representing the riveted joints of ring and beams are assumed to transmit only forces and no moments.

6. Nominal stresses

The nominal stresses of the critical sections are calculated from the stress resultants.

The critical section of the beam is at its joint with the ring. It has the cross section area A S and is shown in figure 17. The origin of the x,y,z-coordinate system lies in the centroid S S. The stress resultants F and M counterbalance the external loads.

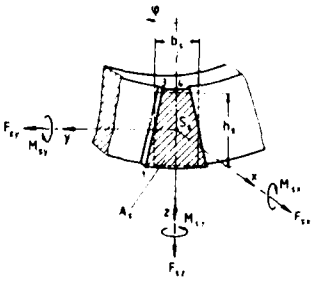


Figure 17: Segment of a cage and stress resultants in the critical section of the beam

A rectangle of the same area with the height h s and the width b s is used to calculate the shearing stresses due to the forces F sy, F sz and the torsional moment M Sx. 1, 2, 3 and 4 indicate the most endangered points of the section.

The critical sections of the rings r 1 and r 2 with the heights h r1, h r2, the width b r1, b r2 and the areas A r1, A r2 are situated just beside the beam as shown in figure 18. The origins of the x,y,z-coordinate systems lie in the centroids S r1, S r2. The endangered corners 1 and 3 have no shear stresses.

The cross sectional areas of rivets may be circular or rectangular as well.

The total support forces of the rollers F wgj are calculated with the boundary conditions w (φ_A) = w (φ_m) = 0 for the supports A 1 and A n in the same way as the supporting pressure of the solid state contact was calculated. (see 4.1)

In figures 13 and 14 results are shown of a cylindrical roller bearing 2309 E CP - see table 1, No. 5 - with the cage supported at the inner edges of the beams. The total supporting forces F wg and the deformed ring of the cage subjected to accelerations a 10n of 50 and 100 times the acceleration due to gravity g are presented. The limits of radial deflections are set by the circles with the radii r I an r II.

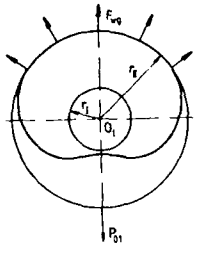


Figure 13: a 10n = 50 g

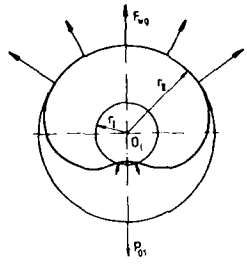


Figure 14: a 10n = 100 g

Figures 13 and 14: Deformed equivalent ring and total supporting forces of the rollers under various accelerations a 10n

5. Stress resultants calculated using finite beam elements

Figure 15 shows the segment of a cage with the rings r 1 and r 2 and with the beam S. x,y,z-coordinate systems are used with their origins fixed the centroids of the cross sections of the two rings S r1 and S r2, and of the beam S S. The x-axis is directed axially, the y-axis tangentially and the z-axis radially.

There are 6 stress resultants in every cross section, namely the forces F x, F y, F z and the moments M x, M y, M z. They are caused by forces of inertia that act on the rings, beams and rollers (see chapter 3) and supporting forces from the cage guiding (see chapter 4).

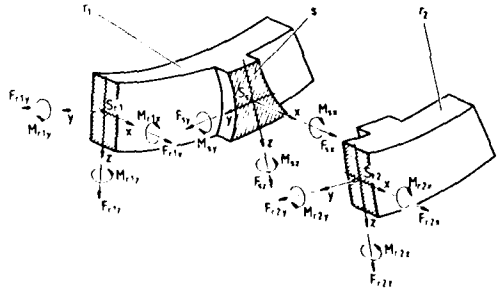


Figure 15: Stress resultants of a cage

The stress resultants are calculated using finite beam elements. These elements have 6 degrees of freedom, which are the displacements w x, w y, w z and the rotations ϑx, ϑy, ϑ z; their positive directions are indicated by the arrows in figure 15.

For an easier comparison of various cage dimensions and designs the nondimensional forces $\hat{F}$ = F/(E A r1), moments $\hat{M}$ = M/(E AR1 r r1), and displacements $\hat{W}$ = W/r r1 are used. r r1 means the radius of the cenroidal circle of the ring r 1.

The cage is idealized as a structure of straight and bended beam elements as shown in figure 16.

The external loads $\tilde{M}$ and $\tilde{F}$ are caused by forces of inertia. If the cage is guided by rollers, additional supporting forces act on the beams. If the cage is guided by rings, the cage rings and the bearing ring contact within $\cdot$ max. The radial deflections that are

cage too.

The supporting forces in figure 11 act on the outer edges of the beams; the cage excentricity is then named e a. There are analogous cages with supporting forces acting on the inner edges; in this case the excentricity is named e i.

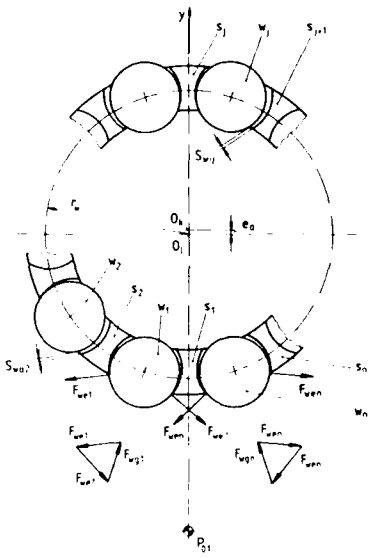


Figure 11: Roller bearing with a roller guided cage

Depended on the acceleration a 10n the supporting forces may act on the outer as well as on the inner edges of the beams.

Similar to the calculation of the supporting pressure of ring guided cages, an equivalent ring is used to calculate the supporting forces F wg of the rollers.

The equivalent ring with supporting forces acting on the outer edges of the beams is shown in figure 12. The mass having equivalent ring with it's radius r r and centre O r is displaced from the centre of the bearing O L about e a. The distributed loads q rt (φ) in tangential and q rr (φ) in radial direction are caused by the acceleration a 10n of the mass-segment Δ mr. These loads effect deflections v (φ) in tangential and w (φ) in radial direction and rotations ϑ (φ). The possible deflections in radial direction h Ij and h IIj are limited by circles with the radii r I = r r - e a and r II = r r + e i at those points where rollers lie momentarily. The rollers w 1 and w n that support the cage in figure 11 are idealised as supports A 1 and A n in figure 12.

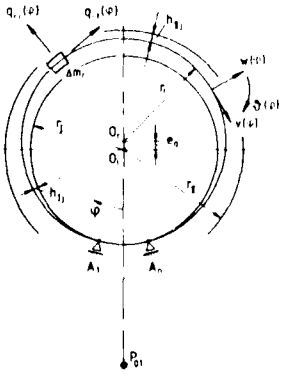


Figure 12: Equivalent ring of a cage that is supported at the outer edges of the beams

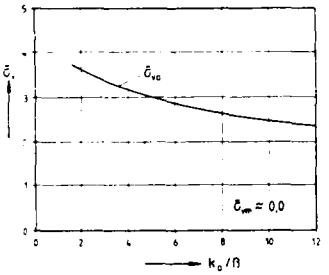


Diagram A: Nondimensional equivalent stress

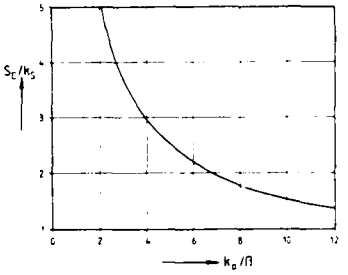


Diagram B: Safety factor against fatigue failure

Table C: Characteristic factors

Bore diameter No.	04	06	08	09	10	12	14	16
$k_L \cdot 10^{-3}$	5,76	6,73	10,8	15,2	16,7	20,3	21,8	26,4
$k_\sigma \cdot 10^{-3}$	8,05	15,3	21,3	36,3	25,0	34,8	33,8	41,7
k_S	1,25	0,76	0,88	0,73	1,12	1,02	1,12	1,08

Chart 5: Cylindrical roller bearings 23 ECP, cage injection molded of plastics and guided by rollers

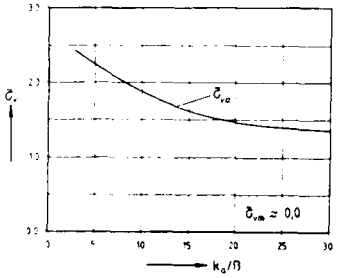


Diagram A: Nondimensional equivalent stress

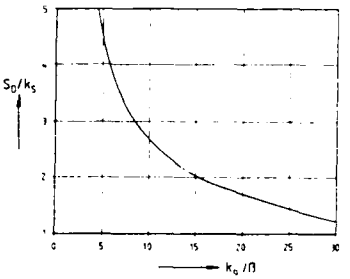


Diagram B: Safety factor against fatigue failure

Table C: Characteristic factors

Bore diameter No.	04	06	08	09	10	12	14	16
$k_L \cdot 10^{-3}$	6,46	6,69	[illegible]	12,3	12,2	14,8	18,2	[illegible]
$k_\sigma \cdot 10^{-3}$	6,73	[illegible]	[illegible]	25,4	[illegible]	[illegible]	27,3	[illegible]
k_S	1,24	1,79	0,99	0,62	0,3	0,89	0,86	0,86

Chart 6: Cylindrical roller bearings 3 ECP, cage injection molded of plastics and guided by rollers

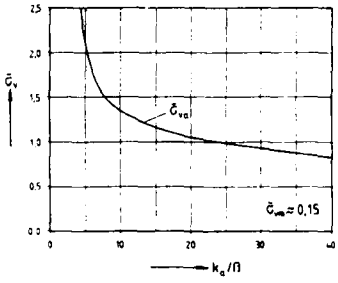


Diagram A: Nondimensional equivalent stress

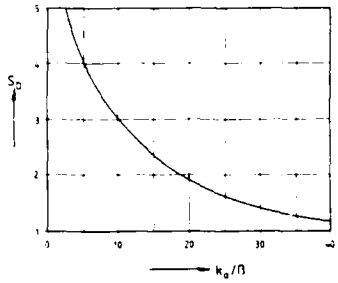


Diagram B: Safety factor against fatigue failure

Table C: Characteristic factors

Bore diameter No.	04	06	08	09	10	12	14	16
$K_L \cdot 10^{-3}$	5,78	6,73	10,8	15,2	16,1	20,3	21,8	26,4
$K_a \cdot 10^{-2}$	9,24	10,8	17,2	24,3	25,3	25,7	32,5	42,4

Chart 7: Cylindrical roller bearings 23 ECPA, cage injection molded of plastics and guided by the outer ring

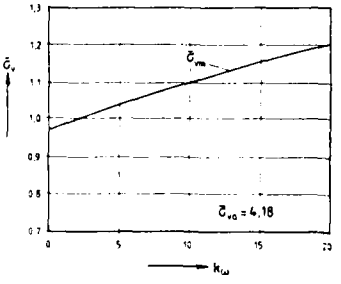


Diagram A: Nondimensional equivalent stress

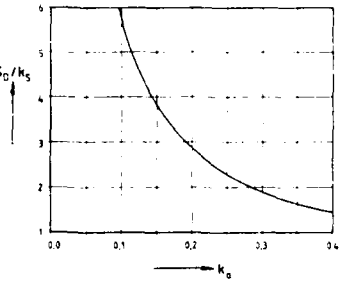


Diagram B: Safety factor against fatigue failure

Table C: Characteristic factors

Bore diameter No.	05	06	07	08	09	11	13
$K_L \cdot 10^{-3}$	0,64	0,92	0,96	1,13	1,15	1,76	1,78
$K_a \cdot 10^{-2}$	27,3	41,6	42,3	51,8	60,9	89,9	98,3
k_S	1,13	1,06	1,09	0,92	0,9	0,94	0,80

Chart 8: Cylindrical roller bearings 23 E JP1, cage pressed from steel plate and guided by rollers

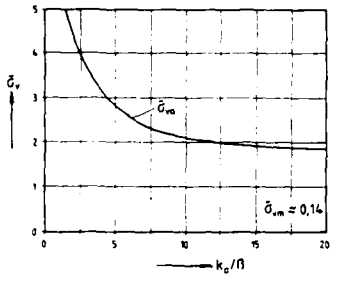


Diagram A: Nondimensional equivalent stress

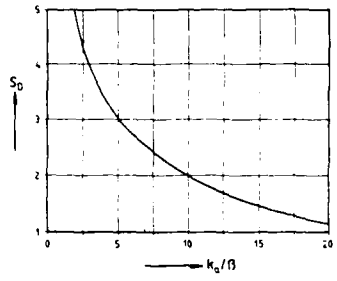


Diagram B: Safety factor against fatigue failure

Table C: Characteristic factors

Bore diameter No.	06	07	08	09	10	11	12	13	14	15	16
$k_t/10^{-3}$	7,5	7,75	8,25	9,24	10,6	12,5	14,1	15,6	17,5	19,4	21,9
$k_\gamma/10^{-3}$	11,4	11,8	12,5	14,0	16,2	19,0	21,5	23,8	26,6	29,5	33,3

Chart 9: Spherical roller bearings 223 ES TVPB; cage injection molded of plastics and guided by the inner ring

12. Literature

[1] Hoch P. G.: Tragfähigkeit von Käfigen in Rollenlagern für Planetenräder. Schriftenreihe: Heft 83.13, Ruhr-Universität Bochum, Institut für Konstruktionstechnik, 1983

[2] Hoffmann N.: Einfluß von Massenkräften auf die Gebrauchsdauer gleichförmig umlaufender Planetenrad-Wälzlager. Forschungsheft 57, Vorhaben 22/I, Forschungsvereinigung Antriebstechnik e.V., Frankfurt, 1978

[3] VDI-Richtlinie 2226: Empfehlungen für die Festigkeitsberechnung metallischer Bauteile, Beuth Vertrieb GmbH, Berlin und Köln

[4] Düser E.: Tragfähigkeit von Blech- und Massivkäfigen in Zylinderrollenlagern für Planetenräder. Schriftenreihe: Heft 82.10, Ruhr-Universität Bochum, Institut für Konstruktionstechnik, 1982

LOAD CARRYING CAPACITY OF DOUBLE CIRCULAR ARC GEARS

M.A.K. FAHMY
Dr. Eng.
Inspectorate International S.A.
Rue des Moulins 51
2004 Neuchatel / Switzerland

R.E. JONCKHEERE
Professor
University of Brussels (V.U.B.)
Pleinlaan 2
1050 Brussels / Belgium

Summary

This paper embodies an overview of some experimental and numerical investigations into several aspects of the load-carrying capacity of double circular arc (D.C.A.) gear teeth. Tooth deflection and bending moment distribution were studied using three dimensional holographic interferometry, whereas rootstresses were determined by means of miniature straingages. The finite element method and finite difference method were used to determine deflections numerically.

Introduction

One of the tooth profiles which provides a much larger contact area than the commonly used involute and hence has a larger load carrying capacity and still satisfies the basic law of gearing is the Wildhaber-Novikov circular arc tooth.
Double circular arc (D.C.A.) tooth profiles, fig. 1, are relatively new and derive from single circular arc profiles (1,2,3,4,5).
D.C.A. gears provide face contact and no progressive contact on the profile. The contact between mating teeth occurs in two points, fig. 2, one on the addendum, the other on the dedendum, the distance between these points depending on helix angle and pressure angle. Under load, the contact points change into elliptical areas.
These large contact areas between the mating convex and concave profiles move axially, at constant sliding speed, from one end of the tooth to the other, resulting in face contact. This contrasts with the involute, where the contact area moves from the tooth root to the tip.
In D.C.A. gears the problem of determing tooth deflection, bending moment distribution root stresses, contact stresses is exceptionally difficult as the load is concentrated in two elliptical areas, depending on tooth curvature, applied load, helix angle, gear material, etc. In order to simplify the investigation the two loads on addendum and dedendum were considered to be equal, which is an adequate first approximation of the problem.

D.C.A. Tooth Deflection and Bending Moment Distribution

Static Deflection was determined experimentally on a D.C.A. gear tooth model enlarged ten times and molded from a urethane elastomer. Tooth dimensions are given in fig. 3 and table I. The loading rig applies the two loads on addendum and dedendum - through two screw devices with built-in calibrated force transducers. Load positions can be adjusted along the entire profile, see fig. 4.
Deflection was measured under loads of 0,5 1 1,5 and 2 newtons, which is equivalent to loads 10.000 times as great on the same gears made out of steel. The loads were applied at 12 different positions on the addendum and dedendum lines of contact.
Deflection values were determined by holographic interferometry with double exposure holograms using an Argon ion laser at 488 nm wavelength, all fringe readings being made from image reconstruction in laser light.(7).
The elastic properties of the urethane elastomer used in this investigation and its suitability for simulating the behaviour of steel were obtained from various tensile tests. Stress-strain characteristics show good proportionality and the test loads correspond to the extent of linear portion, inferring that results obtained on the elastomer model are to a reasonable degree applicable to a steel gear tooth. The Poisson ratio was found to be 0.4 for the urethane elastomer. Tooth deflection along the path of contact under a load of 0,5 N (5.000 N on steel tooth) divided equally over addendum and dedendum points of contact is shown in fig.5
for a tooth with 4 mm normal module and 30 degree helix angle, the load positions being chosen 0,25 B apart. The effect of load variations is shown in fig. 6
indicating the slope is markedly higher at the start of tooth contact than in the centre zone due to the relatively low tooth stiffness at its extremities.
Deflection could be considered proportional to the applied load and inversely proportional to the normal module, all other parameters remaining constant, as resulted from 27.000 measurements. The following relationship was derived for the deflection of the mean path of contact

$$w = \frac{S_n \cdot \eta}{(Pa + Pd)} \left(\frac{M_N}{}\right)^{-1}$$

where S = materials factor (1,0104 for urethane, 1,0 for steel)

η = deflection coefficient, see fig.7

M_n = normal module (mm)

Pa, Pd = combined loads on addendum and dedendum

The maximum value of the deflection coefficient for various helix angles is given in table II
Bending moment distribution along the built-in edge of the tooth is a very important data especially for high-power transmissions. The method of finite difference equations has been applied to a thin cantilever plate model to determine bending moments from deflections, at various points along and across the D.C.A. tooth.
As a result of this investigation bending moment distribution can be written in the following form:

$$M_y = f.\gamma\ (Pa + Pd)\ Nm$$

where f - materials factor

$(1.0X10^{-1}$ for steel, $1.0x10^{3}$ for urethane)

γ = coefficient of bending moment distribution, shown in fig. 8 and table III

Measurement of D.C.A. Tooth Root Stresses with Electric Strain Gages

In this investigation three pairs of D.C.A. teeth with different helix angles of 20°, 30°, 40° were cut from: steel according to dimensions in the normal plane shown in fig. 3 and table I.
The stresses were measured by miniature electric resistance strain gages (1 mm gage length) using static strain meter and switch box, at circumferential loads of 2.500-5.000-7.500-10.000-12.500-Newtons.
Strain gages were pasted at 5 points of the critical section, see fig.9 , determined by applying Hofer's method and isotropic wedge theory at the root fillet. Compressive stresses were measured with thirty strain gages in total which were pasted on 3 teeth for each of the two meshing gear.
In the static loading test rig used in this experiment a test gear can be loaded at arbitrary meshing positions with a power screw of maximum loading capacity of 2.000 Newton, and a loading bar by fixing a supporting gear. The applied load value is detected from the readings of the loading cell strain gages. The meshing positions are determined by measuring the distance between two specific gear teeth in one pair of gears with a measuring microscope and a graduated scale.
Fig.10 shows the meshing positions selected for measurement and calculation of root stresses.
Fig.11 shows an example of the measured root stress distribution in longitudinal direction under load 12.500 Newton and helix angle of 30°. It is found that maximum root stresses occur at the meshing position (17), which coincides almost with the outer point of single tooth pair contact, in the central transverse plane. The absolute value of the ratio of the maximum root stress at the compressive side to that at the tensile side is about 1.5. This may be attributed to the effect of the radial component of the tooth load applied on two loading points, one on the addendum and the other on dedendum at the same time.
The position of critical section is determined by applying isotropic wedge theory on the normal section.
The length (H) from critical section to the tip of tooth and the chordal thickness at the critical section are measured to be used for stress calculation.
According to the calculated results in fig.12 , the stresses in double circular arc tooth profile gear teeth are nearly equal at all the positions along the tooth traces; however, it will be obvious from the experimental results in fig.11 , that the stress at the end parts of the tooth traces are a little smaller than those at the centre part. This difference between calculation and experiment is explained by the fact that decrease of the tooth stiffness at the end part of the tooth trace has not been accounted for in the calculations.

Tooth Deflection By Finite Element Method

Because of the complexity of the bending stress distribution in D.C.A. gears, the effect of shear deformation, the large face width, the part convex, part concave tooth or file, the semi-ellipsoidal contact pressure distribution and the effect of helix angle on tooth stiffness an analytical solution of the elastic problem seems out of the question and a three-dimensional F.E. analysis seemed appropriate (8) using the SAP-5 program.
This analysis like all the others in this overview is carried out in static conditions, and the effect of tangential forces due to Coulomb friction at the contact surfaces of mating gears is being neglected. One may assume that these friction forces are small indeed, as in the case of D. C.A. gears the points of contact slide with constant speed along the tooth surface, assuring adequate lubrication.
A three dimensional solid element of the type PR 20 is chosen. The gear tooth was discretized into 480 elements of this type so as to have an adequate presentation of the varying elliptical loads on the tooth surface.
The results obtained are reasonably close to those obtained by 3 D-holographic interferometry.
Fig. 13, shows the deflection distribution along the path of contact as the load moves from start to end of contact, whereas fig. 14,15,16 show the FE model unloaded, respectively loaded at the start and in the middle of the tooth contact.

Bend Strength of Double Circular Arc Tooth Profile Gears

In this research work the given moment relationships were obtained from the strain readings e_x for tested gears, in each case the load was compared to the corresponding e_x due to a full load applied at the addendum point of contact in the model.
In converting the strain readings taken on steel gears into moments for all the reported conditions, it was assumed that $M_y = \mu M_x$ at all points from which:

$$\sigma_y = \mu \sigma_x$$

and

$$e_x = \frac{(1 - \mu^2)\sigma_x}{E}$$

Where M_x, M_y = moment per unit length in the X- and Y-directions

σ_x, σ_y = stresses in the X- and Y-direction

e_x = strain in the X-directions

μ = Poissons ration

E = modulus of elasticity

t = tooth thickness at the considered section.

The principal stresses and their inclination to the fixed edge were calculated from the strain measurements. It was found that the magnitude of the principal stress at all critical points is 10 to 20 % (percent) higher than the value of $(E.e_x)$ or, in other words, it is from 0 to 10 % higher than in the value of σ_x defined by:

$$\sigma_x = \frac{6 M_x}{t^2} = \frac{E e_x}{(1 - \mu^2)} \qquad (1)$$

$$M_x = \frac{1}{6} \cdot \frac{E. e_x . t^2}{(1 - \mu^2)} \qquad (2)$$

Bending stress S_b can be calculated as follows:

$$S_b = \frac{M}{Z_e} \qquad (3)$$

Where Z_e = an equivalent modulus in bending for the critical tooth section per unit length. And the maximum bending stress

$$S_{b_{max.}} = \frac{M_{max.}}{Z_e} \qquad (4)$$

$M_{max.}$ = the maximum bending moment per unit length along the root may be written:

$$M_{max.} = C \cdot q_n \cdot h \qquad (5)$$

Where h = tooth heigth
C = reduction factor due to the inclination of the load line.
(C = 0.65 for circular arc gears)

q_n = maximum load intensity during one meshing cycle W_n / L_m.

and W_n = total transmitted load = normal load = $W_{a_n} + W_{d_n}$.

Where :

W_{a_n} = Addendum normal load

W_{d_n} = Dedendum normal load

L_m = minimum length of contact during the mesh cycle $F.m_n$

F = Face width

m_N = Load sharing factor = $0.95\ Z/p_n$

p_n = Normal base pitch = $\pi \cdot M_N \cdot \cos\beta$

M_N = Normal module

β = Helix angle

Z = Length of line of action

= Tooth face width in case of double circular arc gears.

$$M_{max.} = 2.15\ \frac{W_n \cdot M_N \cdot h \cdot \cos\beta}{F^2} \qquad (6)$$

$$S_{b_{max.}} = C \cdot \frac{W_t}{F \cdot m_N} \cdot \frac{P_d}{Y \cdot \cos^2\beta} \qquad (7)$$

where W_t = total tangential load

P_d = diametral pitch = $\frac{N}{D}$, N = No. of teeth

D_p = pitch diam. of gear

P_d = π / P_c , P_c = circular pitch

P_c = D_p / N , P_N = normal circular pitch

P_N = $P_c \cdot \cos$ = $\pi \cdot M_N$

The value of the total tangential load can be found as follows:

W_t = $W_n \cdot \cos \phi_n \cdot \cos\beta$

ϕ_n = normal pressure angle

$$Z_e = \frac{Y \cdot h \cdot \cos\beta}{P_{d_n} \cdot \cos \phi_n}$$

P_{d_n} = normal diametral pitch

$$Z_e = Y \cdot h \cdot \frac{D_p \cdot \cos^2\beta}{N \cdot \cos \phi_n} \qquad (8)$$

Where the factor Y = geometry factor obtained in the normal plane and from equations (2) and (4) , (6) and (8), we found that:

$$S_{b_{max.}} \quad \frac{1}{\quad} \cdot \frac{E}{(1 - \mu^2)} \cdot \frac{t^2 \cdot N \cdot \cos \phi_n}{h \cdot D_p \cdot \cos^2\beta} \cdot \frac{\sigma_{x.\,ax.}}{\quad} \qquad (9)$$

and from equations (2) and (6), the maximum tangential load can be calculated.

From equations (6) and (8) into (4):

$$S_{b_{max.}} = 2.15\ \frac{W_{t_{max.}} \cdot M_N \cdot N}{Y.F^2 \cdot D_p \cdot \cos^2\beta} \qquad (10)$$

From the measurements taken in this research the value of the stress $S_{b_{max.}}$ was found and applied in equation (10) to find the value of $W_{t_{max.}}$ which was checked again with the actual values of load on the gear teeth.

The value of the maximum bending stress of material $S_{b_{max.}}$ can be found from the gear material. The value of the real actual tangential load $W_{t_{max.}}$ can be calculated from measurements. Then the value of the geometry factor "Y" can be calculated from Equation (10).

For all measurements done in this research for tested steel gears (5,000 readings) the average value of Y factor was calculated and compared to the values obtained from experimental work done in this research and found to be (Y = 0.752).
The maximum load carrying capacity formula of double circular arc tooth gears that can be used to design this type was derived from the experimental and theoretical study and found to be as follows:

$$W_{t_{max.}} = 0.465 \cdot S_{b_{max.}} \cdot Y \cdot \frac{F^2}{N} \cdot \frac{D_p}{M_N} \cdot \cos^2\beta$$

Where $S_{b_{max.}}$ = maximum bending stress of material of test gears used.

Bending and Contact Stresses of Double Circular Arc Tooth Profile Gears

Fig. shows the results of the stress calculation on gear teeth of double circular arc tooth, where line (B) shows the bending stress at the root in the case that contact is located at the center of face width, and line (1) are the results of simplified calculations corresponding to the line (B) and are obtained by assuming that the force is concentrated at the center of addendum and dedendum area of contact.

Line B_{WE} is obtained from Wellauer's method mentioned in (10).

Curve (B_m) which is calculated on assumption that the load is applied along the width of addendum elliptical contact shows a better result than Wellauer's method.

From this it follows that when helix angle is small, it is obvious that the bending moment at root must be calculated considering the area where the tooth load on addendum and dedendum is applied.

Curve (C) shows the results of the contact stress calculated for double circular arc gears, Fig. 18 shows the bending and contact stresses of single and double circular arc and involute profile gears (in case of large helix angle).

Fig.19 shows the bending and contact stresses of single and double circular arc and involute profile gears (in case of smaller helix angle).

There are many methods of stress calculations for involute helical gears, but in this research work, comparison was be made using the stresses calculated with the formulas used in practical gear design.
In the involute gears used for comparison, helix angle and normal module are chosen to be equal to the corresponding values of the single and double circular arc tooth profile gears, and to be of standard tooth and 20° normal pressure angle.

The contact stress of single and double circular arc gears is larger than that of the involute gears when the helix angle is larger, but in case of a smaller helix angle, the contact stress becomes smaller than that of the involute gears. also the curves show that the double circular arc gears tends to carry 1.5-2 times the load carried by the single arc gears of the same size and material.

Comparison Between The Different Methods Used

During this research work a complete study of root stresses was executed using experimental and numerical methods applied to the double circular arc tooth profile gears, all the results given by this method were compared to each other and at the same time to the previous research work on single circular arc gears and conventional helical involute gears.
Results obtained by the 3-D finite element method show a difference of 10 % from those obtained by 3-D holographic interferometry (7), and the results of both methods compared to the electric resistance strain gage measurements gives a greater difference than the last method represents the real loading conditions on real loaded test gears.
But both numerical and experimental methods show that the double circular arc gears are able to carry higher loads than the involute gears.

Fig. 20 shows root stresses measured and calculated by the different methods for double circular arc gears, when load is applied at the middle zone of contact.
Values of root stresses measured using electric resistance strain gages are greater than those calculated through numerical methods, the difference of the order of 20 - 25 % and this difference due to the variable factors, mounting conditions, loading conditions, tilting effect and the combined stiffness of teeth and material and teeth surface conditions.

Conclusions

Various modern scientific investigation methods were used to study the elastic behaviour of double circular arc tooth profile gears, such as 3-D Holography, 3-D finite elements, resistance strain gauges and the isotropic wedge theory.

The results of this research work are summarized as follows:

1. A deflection coefficient is experimentally derived and introduced in the deflection load relationship for different positionsof loading.

2. A bending moment distribution coefficient is numerically derived from deflection measurements and introduced in the bending moment distribution-load relationship for different positions of loading.

3. Under the same conditions of pressure angle, load applied, helix angle, normal module and tooth material, maximum deflection and maximum bending moment at built-in edge is less for double circular arc than that for single circular arc tooth profile gears which indicates that the first is stiffer than the second one.

4. The value of bending stress calculated from E.J. Welleuers' method is always greater than from values found in this research, especially when two methods becomes very large.

5. Calculated bending stress of single and double circular arc tooth profile is always greater than that of the involute gears in the range of helix angles 13°45' to 42°10'.

6. Contact stresses becomes smaller than that of the involute gears when the helix angle becomes smaller than 27°10'.

7. For double circular arc gears when increasing the load angle it tends to give better load carrying capacity and low accuracy of transmission but for smaller helix angles it shows better load carrying capacity and better transmission accuracy.

8. When decreasing the helix angle the tilting effect is reduced leading to better contact accuracy.

9. Results obtained by the 3-D finite element method show a difference of 10 % from that obtained by 3-D holographic interferometry.

10. By applying the apex of the isotropic wedge at 0.25 x the distance from tooth surface to the centerline of tooth profile, the values of root stresses calculated show a reasonable result as compared to those values, calculated by 3-D finite element method.

11. The maximum load which can be carried by the double circular arc gear tooth profile was experimentally and theoretically derived and found to be:

$$W_{t_{max}} = 0.466 \cdot S_{b_{max}} \cdot Y \cdot \frac{F^2}{N} \cdot \frac{D_P}{M_N} \cdot \cos^2 \beta$$

Where the geometry factor Y found to be 0.750 as experimentally calculated from the strain gauge measurements.

12. Comparative study between the conventional involute gears and single - double circular arc gears show that the double circular arc gears tends to carry 1.5 - 2.0 times the load which single circular arc gears of the same size and material can carry.

Bibliography

1. AGTI, S.P. and SHEVERS, R.A.

"An Investigation of Spiral Gearing"

A.S.L. Engineering, 1962

2. W. [illegible] DAVIES

"Spiral Gearing"

Machinery, January 13, 1960 - Volume 96

3. [illegible]

"The Load Capacities of Novikov Gears"

Machine Design, Sept. 17, 1964

4. ARIKA, I. and OHIRO, K.

"On the Load Capacities of Novikov Gears"

Bulletin of JSME, Vol.12, N° 51, 1969

5. ATTIA, A. Y.

"Bending Moment distribution on gear teeth for circular arc profile"

Trans. ASME, Oct. 12, 1972

6. ATTIA, A. Y. and FAHMY, M. A. K.

"Wear of Gears of Double circular Rac Tooth profile"

ASME - Design Engineering Technical Conference, Chicago, Illinois, Sept. 28 - 30, 1977

7. FAHMY, M.A.K. and JONCKHEERE, R.

"Deflection and Bending Moment Distribution of Gear Teeth of double circular Arc Profile using three-dimensional holographic Interferometry"

ASME - International Power Transmissions and Gearing Conference, San Francisco, Calif. August 18 - 21, 1980

8. FAHMY, M.A.K. and OVERMEIRE, M. V.

"Finite element analysis of double circular arc tooth-profile gears"

Proceedings of the eighth Canadian Congress of Applied Mechanics, Moncton, June 7 - 12, 1981.

9. FAHMY, M.A.K.

"Three dimensional finite Element Analysis of Deflection and Bending Moment Distribution in a double Circular Arc Gear Tooth"

Eleventh South Eastern Conference on Theoretical and Applied Mechanics (SECTAN XI), Huntsville, Alabama, April 8 - 9, 1982

10. WELLAUER, E. J. and SEIREG, A.

"Bending Strength of Gear Teeth by Cantilever Plate theory"

Trans. ASME, Series B, Vol. N° 82, N° 3, 1960.

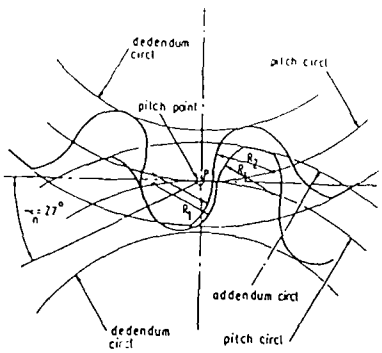


Fig. 1, Profile details of addendum-dedendum type of Wildhaber-Novikov gear

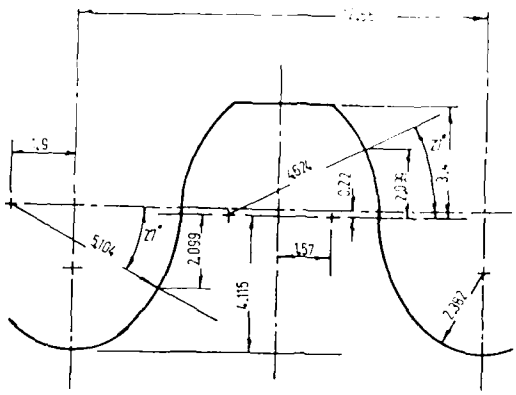


Fig. 3. Dimensions of double circular-arc tooth-profile test gear tooth in normal plane.

D = Distance between points of contact along the tooth.
d = Width of no-contact band.
S = Distance between points of contact across the tooth height.
H = Tooth height.

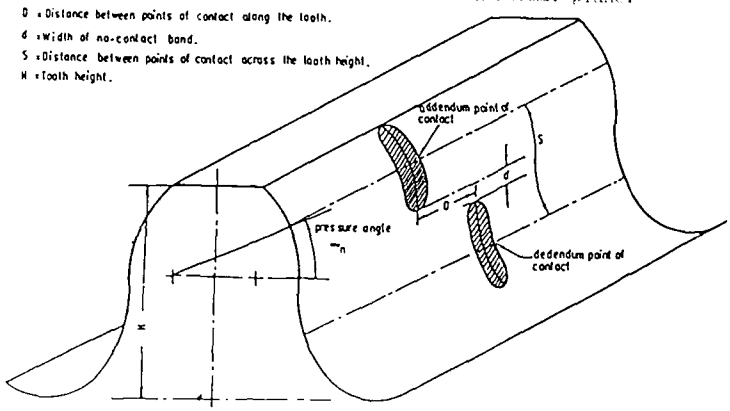


Fig. 2, shows the two points of contact on the tooth face.

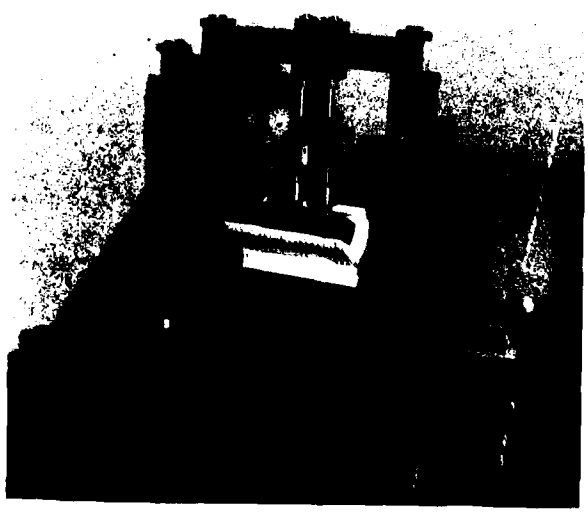


Fig. 4, View of testing test gear.

Table I. Dimensions of [illegible] test gears.

Dimensions	Drive	Driven
Normal module	4 mm	
Pressure angle	20°	
Number of teeth	22	
Face width	30 mm	
Profile shift	0	
Centre distance	100 mm	
Contact ratio	1.63	
Helix angle	28.37°	
Normal circular pitch	12.5715 mm	
Gear ratio	1	

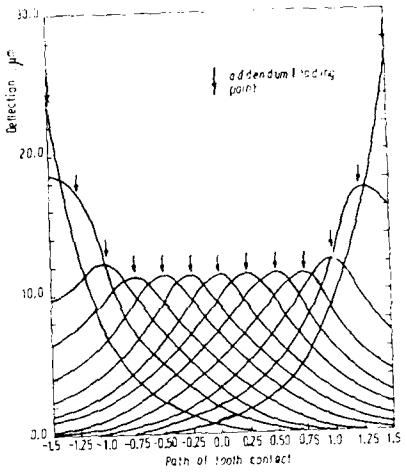


Fig. 5. Deflection of the path of contact under load of 0.5 N divided equally over add. - ded. points of contact for M_n 4 mm and 20° helix angle.

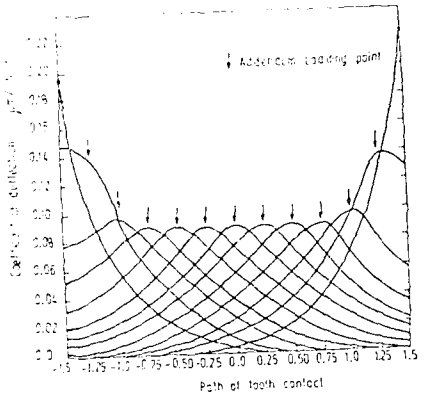


Fig. 6. Coefficient of deflection with [illegible] and position for 20° helix angle.

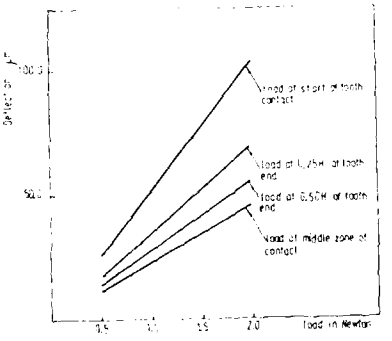


Fig. 7. Curves of deflection with [illegible] - ded. points of contact for different positions of load.

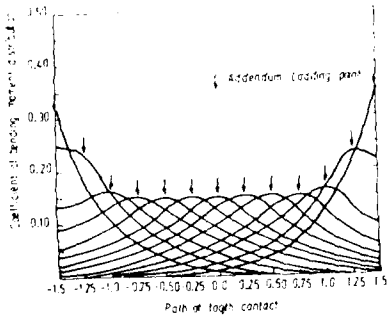


Fig. 8. Coefficient of bending moment distribution for 20° helix angle.

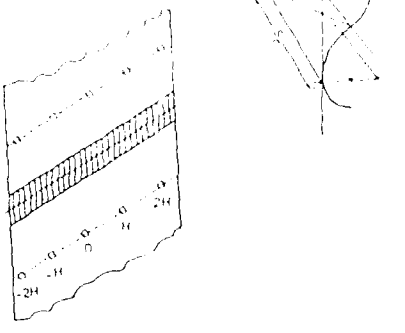
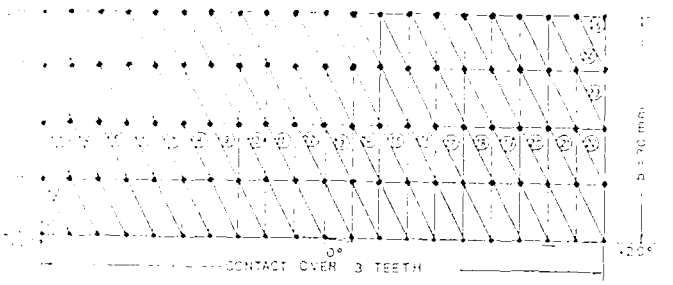
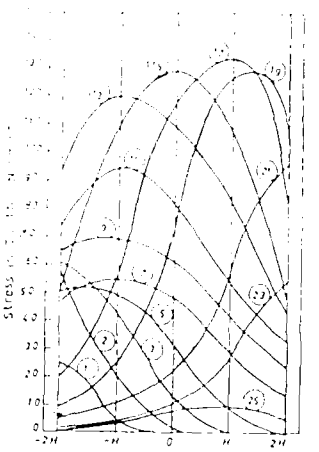


Fig. 9. [illegible] test gears.





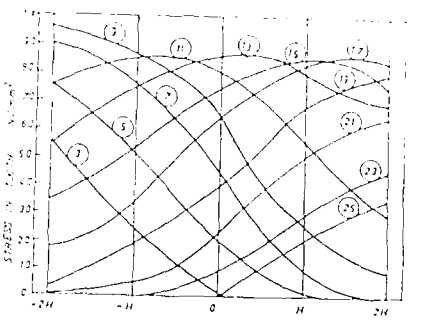


FIG. 12., Calculated root stress distribution in longitudinal direction.

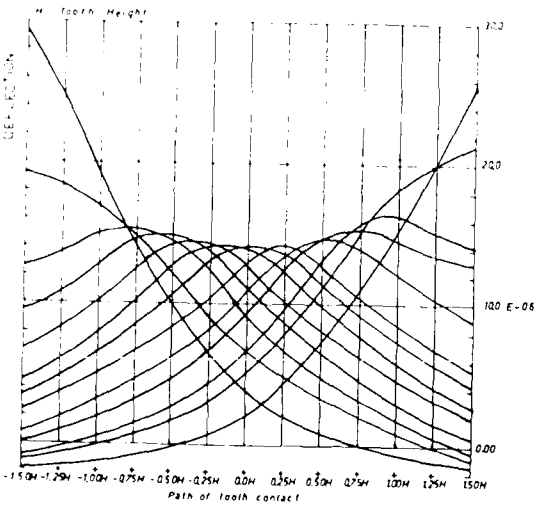


FIG. 13, Distribution of deflection along the path of contact.

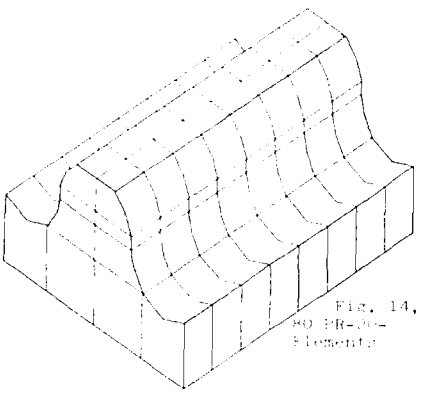


Fig. 14, 80 PR-20-Element

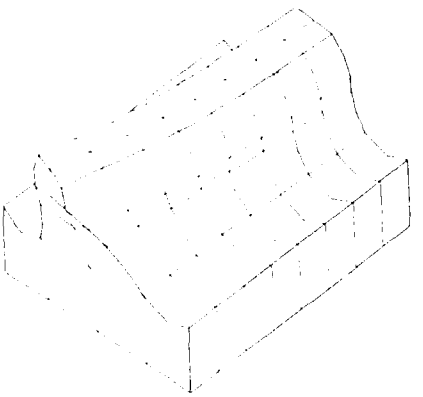


Fig. 15, Three-dimensional finite element mesh for one-half model at load applied at middle node of contact.

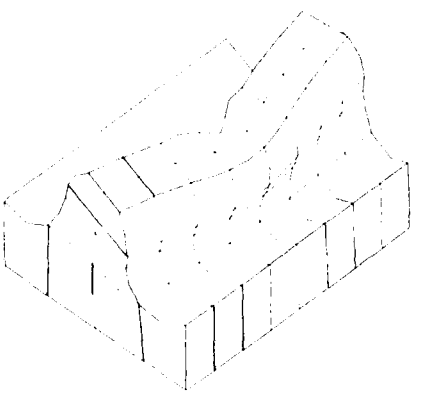


Fig. 16, Three-dimensional finite element mesh for one-half model at load applied at middle node of contact.

Table II, Give Maximum Values of the Tensile Stress Distribution Curves for Various Helix Angles

Form of Groove	Helix Angle			
	60°	70°	80°	90°
1.50 H	0.2545	0.2451	0.2315	0.2152
1.25 H	0.2365	0.2289	0.2181	0.2045
1.00 H	0.2195	0.2135	0.2046	0.1935
0.75 H	0.2040	0.1990	0.1917	0.1826
0.50 H	0.1910	0.1871	0.1809	0.1735
0.25 H	0.1810	0.1781	0.1730	0.1665
0.00 H	0.1750	0.1730	0.1700	0.1650
-0.25 H	0.1810	0.1781	0.1730	0.1665
-0.50 H	0.1910	0.1871	0.1809	0.1735
-0.75 H	0.2040	0.1990	0.1917	0.1826
-1.00 H	0.2195	0.2135	0.2046	0.1935
-1.25 H	0.2365	0.2289	0.2181	0.2045
-1.50 H	0.2545	0.2451	0.2315	0.2152

H = Unit Height

Table III Give Maximum Values of the Tensile Stress Distribution Curves for Various Helix Angles.

Form of Groove	Helix Angle			
	60°	70°	80°	90°
1.5 H	0.3750	0.3600	0.3350	0.3000
1.25 H	0.3552	0.3325	0.3045	0.2740
1.00 H	0.3400	0.3165	0.2870	0.2575
0.75 H	0.3300	0.3024	0.2675	0.2410
0.50 H	0.3200	0.3024	0.2675	0.2410
0.25 H	0.3022	0.3024	0.2675	0.2410
0.00 H	0.2922	0.3024	0.2675	0.2410
-0.25 H	0.3022	0.3024	0.2675	0.2410
-0.50 H	0.3200	0.3024	0.2675	0.2410
-0.75 H	0.3300	0.3024	0.2675	0.2410
-1.00 H	0.3400	0.3165	0.2870	0.2575
-1.25 H	0.3552	0.3325	0.3045	0.2740
-1.50 H	0.3750	0.3600	0.3350	0.3000

H = Unit Height

Demonstration of G-Met Corrective Machine Settings

In order to evaluate the effectiveness of the conversion of UMM-500 measurements into delta machine settings for the spiral bevel gear grinding machine, a sensitivity study was conducted in which bevel gears were ground and reground with machine settings that purposely deviated from the Gleason grinding machine summary settings in accordance with a specific matrix. This matrix involved 10 first order changes for the spiral bevel pinion and gear (Figure 15) and 8 second and third order changes for the spiral bevel pinion (Figure 16). Each setting change consisted of 5 variations including 1 baseline, for a total of 142 grinds (91 for the pinion and 51 grinds for the gear).

Gleason grinder first order changes

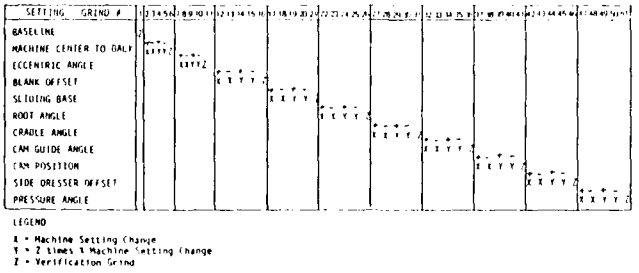


FIGURE 15 GEAR GRINDING MATRIX

Gleason grinder second and third order changes

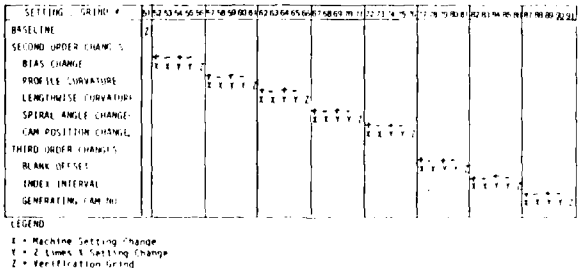


FIGURE 16 GEAR GRINDING MATRIX

To date, four specific grinding machine settings were used for evaluation.

- An eccentric angle change of zero degrees and five minutes (0°5')
- Machine center to back withdrawal of .020 inches
- A pressure angle change of zero degrees and thirty minutes (0°30')
- A root angle change of zero degrees and twenty minutes (0°20')

The eccentric angle change 0°5' resulted in a maximum deviation of -.0049 inches in the bevel pinion profile geometry as shown in Figure 17. When the pinion was reground to the corrective delta setting calculated by G-Met, this deviation was reduced to -0014 inches (Figure 18). A second regrind resulted in a maximum deviation of +.0003 inches as shown in Figure 19.

It has been shown that there is good correlation between the Gleason test machine patterns and the UMM-500 measurements. Figure 13 shows a plot of derived test machine values compared to UMM-500 values. The test machine values plotted are the observed distance from the end of the test machine pattern to the toe end of the tooth. These values are the measured surface deviation at the same point. The correlation between this data and the Gleason pattern is as expected.

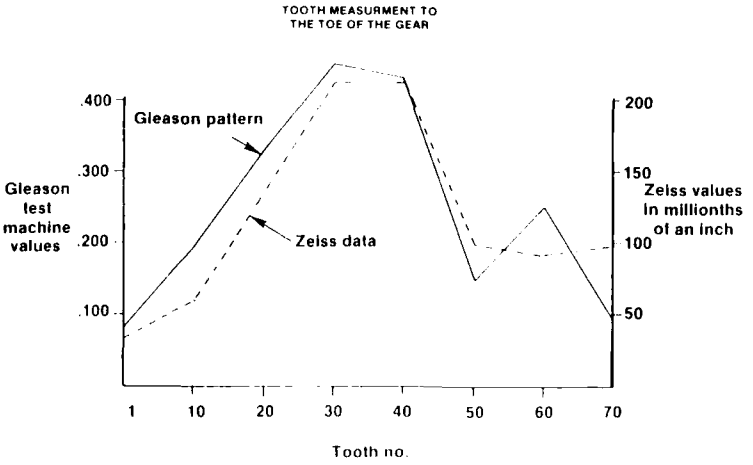


FIGURE 13 COMPARISON OF MEASUREMENT SYSTEMS

This tooth measurement system has proven to be useful in the analysis of variations which exist in master control gears and in production gears manufactured by different manufacturers even though test machine pattern comparisons showed no reason for rejection.

If the deviations from the nominal values, as measured on the UMM-500, are not acceptable, G-Met will permit calculation of corrective machine settings based on the magnitude of the measured differences and their location.

For the first time a spiral bevel gear tooth can be measured and compared quantitatively to its theoretical form. The primary advantages of this system are the degree of accuracy attainable, the capability to evaluate tooth geometry over the entire surface, the ability to calculate grinding machine setting changes, and the reduced time needed to accomplish the inspection process. A flow chart showing the manufacturing and inspection of a production spiral bevel gear set using this system, is shown in Figure 14.

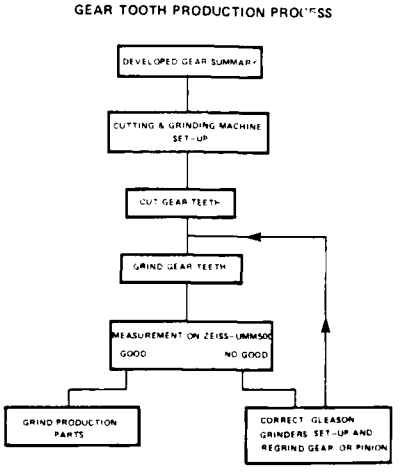


FIGURE 14 BEVEL GEAR PROCESSING FLOW CHART

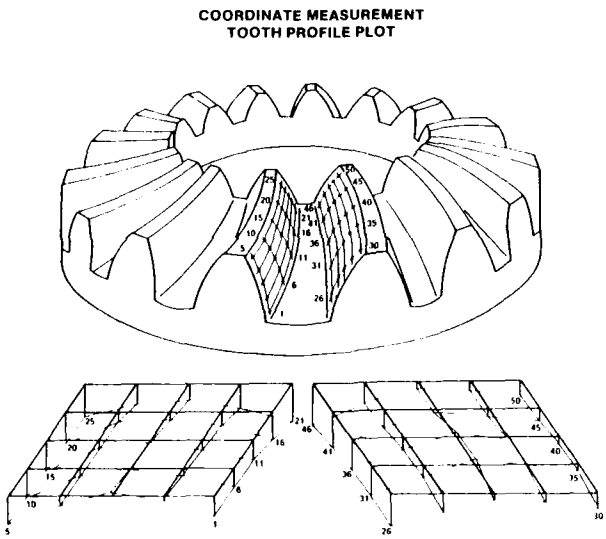


FIGURE 12 DISTRIBUTION OF MAPPING POINTS

Presentation of the results of the measurements are graphical plots, as shown in Figure 9, and a digital printout (Table I). The digital printout locates each grid point by column and row number. For each grid point, the X, Y, and Z coordinate values are listed as well as the x, y, and z deviations from the stored nominal values. The last column in the printout is the deviation in the surface normal dimension and is the value plotted in Figure 10.

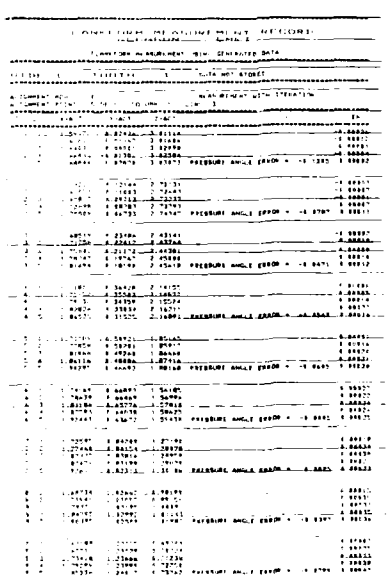


TABLE 1. DIGITAL PRINTOUT OF MEASURED POINTS

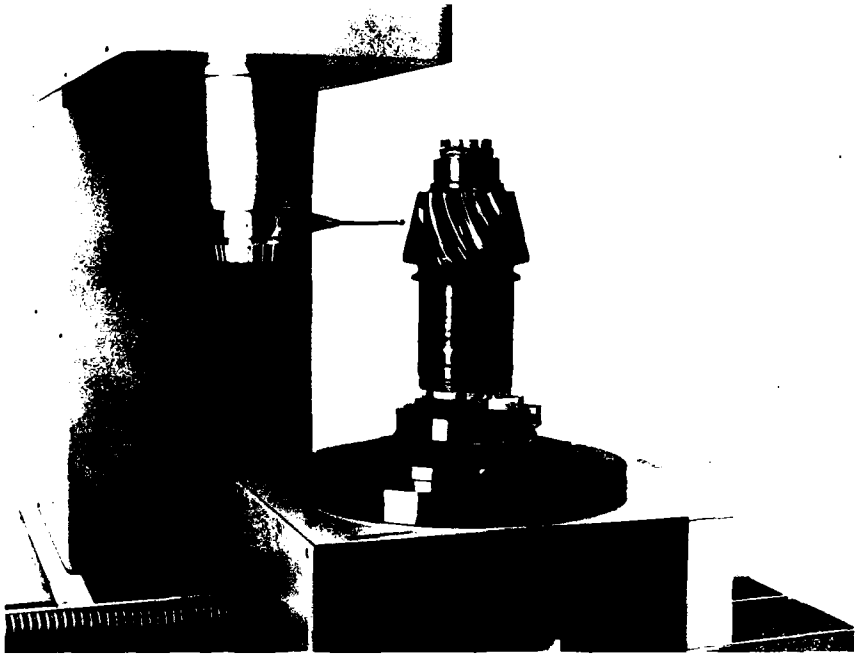


FIGURE 11 PINION SET UP IN THE UMM 500

When measuring the compound curved surfaces of spiral bevel gears, the "continuous probing" mode of the UMM-500 system is particularly beneficial. The machine can follow the contour of the part in a predetermined direction in the same manner as the follower head on a 3-D copy mill. The automatic positioning control that is actuated at probe contact scans the free axis of the machine until the inductive measuring system in the probe head is brought to its null point. The moment this condition is achieved all three machine coordinates are automatically transmitted to the computer; therefore, the probe may be locked in the X axis and be made to traverse to predetermined locations in the Y axis, while automatically following contour changes of the part in the Z axis, and the machine will remain at a preselected X-Y location until the probe has been nulled in the Z direction and the position information transmitted to the computer. It will then proceed to the next X-Y location.

Tooth flanks are measured in CNC mode. Nominal points on the network are loaded from the magnetic tape cassette into core memory and transformed into machine coordinates. The computer keeps track of the momentary position of the probe and determines the path to the next point. The measured deviations from the nominal surface are determined along the projected surface normals.

After measurement of a complete tooth flank, requiring approximately 3 minutes for 45 measuring points (see Figure 12), the probe automatically returns to its starting position and awaits further commands.

This improved method of tooth measurement and numerical representation of tooth errors at each specified probe point will provide a means for quantitative evaluation of the spiral bevel gear tooth profile in physical and measurable geometric terms without resorting to subjective visual comparisons of tooth contact patterns. This method will not only eliminate the need for a Gleason running test machine but will replace the Gleason gear blank checker, tooth spacing checker, tooth index machine, master control gears and associated set-up gages.

U.S. Army AVSCOM MANTECH Program

The overall objective of this program is to develop a manufacturing method and the technology required for an in-progress and final inspection of spiral bevel gears using a prototype, automated, mechanical contact coordinate measuring machine. The program comprises four phases. Phases I and II have been completed and Phase III is currently funded under Contract NAS 3 23465.

Phase I involved the definition and development of a final inspection technique for spiral bevel gears utilizing a three-coordinate measuring machine. The UH-60A BLACK HAWK main module bevel gear set was selected for evaluation and study. In this initial phase, a Zeiss UMM-500 universal measuring machine was procured, installed in the Sikorsky gear inspection department and converted for spiral bevel gear measurement by the addition of a rotary table and a Hewlett Packard (HP) computer package. Tooth profile measurements were taken on the master gears for the selected gear set, and on a number of production gear sets, using both the UMM-500 and a standard Gleason test machine. In Phase I, a final inspection process for spiral bevel gears, utilizing a computer controlled three-coordinate measuring machine, was demonstrated with positive economic and technical results.

Phase II involved the development of an in-process inspection technique for spiral bevel gears where the measured deviation from the nominal profile are converted into corrective grinding machine settings during the production cycle. A sensitivity study was made in which gear test specimens, ground with machine settings which purposely deviate from the normal settings, were measured on the UMM-500 and the corrective settings determined by the Gleason G-Met software package. A comparison of the calculated setting changes with the actual settings used to grind the gear specimens will validate the computer program. An alternate empirical approach, using the matrix of deviations caused by each independent setting change, will also be evaluated.

Phase III is a pilot production monitoring program on a production gear set and a qualification test on the experimental design.

Phase IV is concerned with the documentation of a new manufacturing and inspection specification for spiral bevel gears.

Advanced Bevel Gear Measuring Technique

The initial task was to demonstrate that the topology of a spiral bevel gear can be quantitatively measured and compared with the desired nominal values stored in the computer.

The simplist method for determining the nominal points on a gear tooth flank is by digitization of a master gear. The master gear is a carefully manufactured comparison gear with a developed profile that has been proven under load in the actual gearbox installation. The measuring machine is programmed to probe points on the flank of a master gear tooth for storage on a magnetic cassette tape. Specialized software permits rapid generation of an evenly distributed point network along either radial or axial sections after manual probing of the corner points (see Figure 10). The vector of the surface normal is determined mathematically from several automatically probed points in the vicinity of the specified network point. When making measurements, actual points on the test gear flank are numerically compared with stored point locations on the master gear flank. The master gear, since it is produced on the same equipment as the test gear, will generally contain some random form deviations that vary in magnitude from tooth to tooth on a given master gear and from one master gear to another. In general, it may become necessary, in this method, to create an average nominal master gear profile by integration over a large number of actual master gear flanks.

COORDINATE MEASURING SET-UP TECHNIQUE

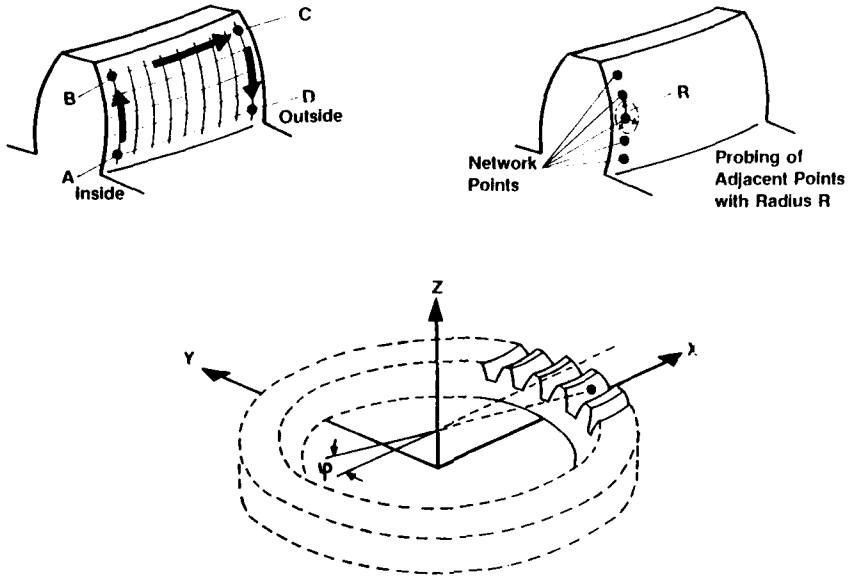


FIGURE 10 GENERATION OF NETWORK POINTS

Even though spiral bevel gears have a high degree of geometric complexity, it is reasonable to expect that the theoretical surface can be generated numerically by computer simulation of the manufacturing process. This, in fact, has been accomplished by the Gleason G-Met software package. G-Met is designed to provide the computer on the UMM-500 with the ability to:

1. Download theoretical tooth surface coordinate data and corrective matrix from the Gleason main frame computer.
2. Direct the machine to measure the tooth surface.
3. Compare measured data to theoretical or master gear data and calculate differences between the two surfaces.
4. Calculate corrective cutting/grinding machine settings based on the measured differences.
5. Make tooth spacing checks.

G-Met permits more freedom in the choice of the form and density of the point network and provides a more theoretical baseline than the measured master gear values, which themselves are subject to manufacturing errors. An evaluation of both methods will be made in this program.

The inspection process for a production gear will consist of setting up the gear in the UMM-500 and automatically probing the surface at the specified network point locations. To accomplish this, the gear is mounted on the coordinate measuring machine table or on the indexing table with its axis parallel to the Z axis of the machine (see Figure 11) with care being taken not to deform it while clamping. Part alignment is achieved by bringing the probe into contact at a series of points on a reference diameter to establish the location of the Z axis of the gear in relation to the machine axis. The reference coordinate system for the nominal data for the bevel gear is then located along the gear axis. Any desired zero point can be selected along this axis. In order to determine the angle of rotation of the gears polar coordinate system relative to the machine's coordinate system, a known point on the tooth flank is contacted and the deviation of this point from nominal is set to zero.

limited spatial probing in any of the three orthogonal directions. This machine, in conjunction with a sophisticated 3D software package, provides a distinct and quantitative means of measuring and mapping three dimensional surface contours. In order to accommodate the complex surface of the spiral bevel gear tooth, the Zeiss system also uses a precision indexing table, shown in Figure 8, which is integrated as the 4th axis in gear measuring programs. The computer program packet for gear measurement permits the determination of the face profile coordinates of spiral bevel gears at an unlimited number of probe points on the tooth surface and a point by point comparison with stored nominal reference values representing the master gear tooth profile. This reference data can be obtained either by measuring a master gear with the developed profile on the UMM or by computing the theoretical coordinate values at specific probe locations using the final grinding machine settings. By considering the deviations from the nominal values in the three axes and the normal vector, the computer determines the deviation of the surface normal at each probe point and prints it out. These values can be drawn by the HP plotter at a preselected scale, and interconnected to make up a three dimensional error diagram (see Figure 9).



FIGURE 8 ZEISS UMM 500 ROTARY INDEXING TABLE

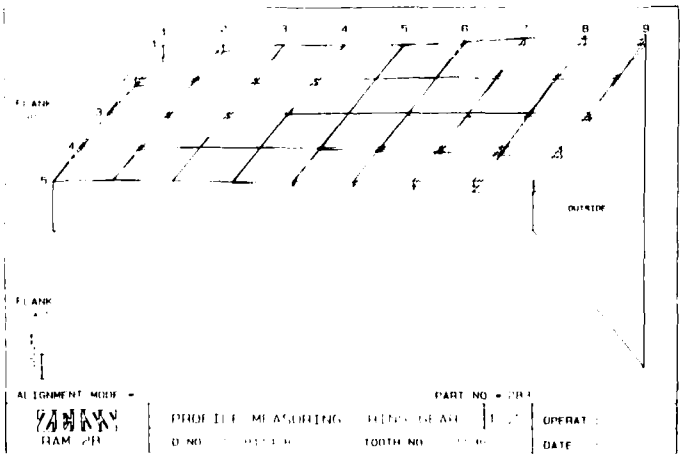


FIGURE 9 TOPOGRAPHICAL MAP OF GEAR TOOTH PROFILE

Once the development is complete, several sets of master control gears are made that duplicate the newly developed pair as precisely as possible. These control gears are used to inspect the production gears. They are run in the Gleason test machine against each mating gear subsequently produced by the final machine settings to visually inspect the contact patterns against those obtained from the developed master gear pair in order to maintain uniform quality.

The production process control for spiral bevel gears is, in effect, a miniature development process except that the changes required to keep a drifting pattern situation under control are more subtle and involve the visual comparison of a production gear pattern with the established master gear pattern and the necessary corrective changes to keep the two in agreement.

Improved Gear Manufacturing and Inspection Process

The quality control process described above has certain inherent disadvantages. First, the acceptance or rejection of a production gear is based upon a visual comparison of tooth contact patterns. Not only the size of the pattern, but its shape and location, are significant. Acceptance limits for these features are difficult to define qualitatively; therefore, the accept/reject decision becomes a subjective one and is subject to the human frailties of the operator. Second, the size, shape and location requirements of the tooth bearing pattern are peculiar to each gear mesh and gearbox mounting and no particular area, shape, or position can be considered universally ideal. Third, since the tooth contact is localized and tested under a very light load, the edges and corners of the tooth cannot be measured directly. It is necessary to determine, not only that satisfactory bearing patterns are obtained when the gears are mounted in their equivalent running position in the gear tester, but to what extent this pattern can be changed by axial and radial movements of the pinion axis, with respect to the gear axis, that would move the pattern to the limits of the tooth contact zone. This is known throughout the industry as the V and H check. By comparing patterns at these extreme V and H settings, a cursory check on lengthwise and profile curvatures is maintained.

It is apparent from the above discussion that a need exists for a more definitive and quantitative means of diagnosing whether specific in-process changes are necessary in the grinding machine settings to control the tooth profile geometry within rather narrow limits. This control is important for highly loaded gearing to prevent concentrations of load that could cause scoring, pitting or tooth breakage.

A Universal Coordinate Measuring Machine such as the Zeiss Model UMM500 shown in Figure 7 offers an effective alternative solution to the problem of spiral bevel gear tooth measurement and control. The UMM500 is a highly accurate three-coordinate measuring machine with an integrated Hewlett Packard (HP) 9836 computer system that permits un-



FIGURE 7 PROTOTYPE GEAR MEASUREMENT SYSTEM

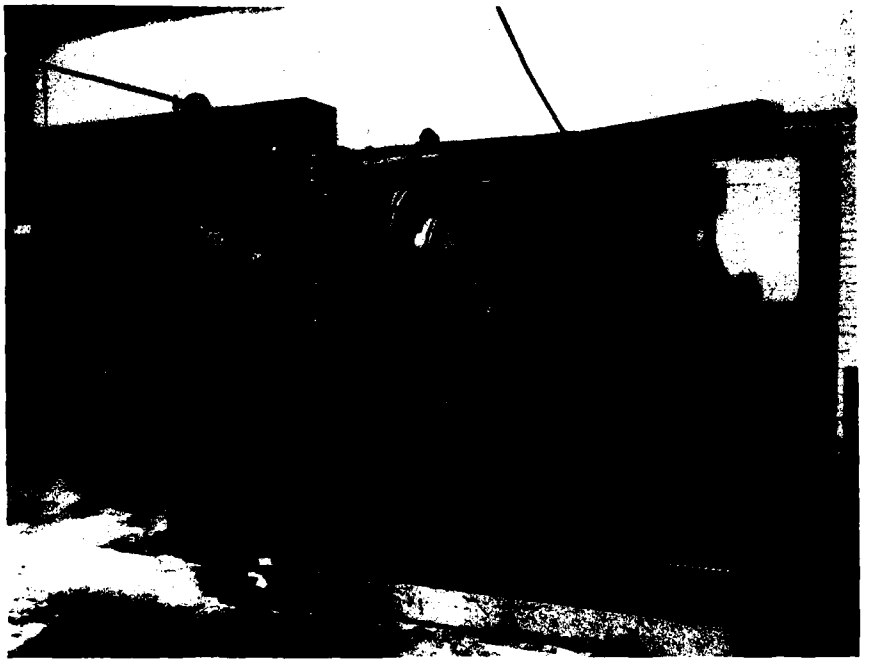


FIGURE 6 GLEASON HYPOID GEAR GENERATOR

After the gears are ground, they are installed in a Gleason universal test machine (Figure 1) that is set up using precision gage blocks or set up gages to the theoretical gear mounting distance. Using precision work holding equipment, the gear and pinion are mounted in the same relative position to each other as they will be when run in the actual transmission gearbox. The test machine also allows calibrated adjustments along the gear cone axis, along the pinion cone axis, and in the vertical offset direction.

The gear and pinion are rolled together in the test machine at a predetermined light brake load (approximately 100 in-lbs of torque) applied through the pinion spindle. Prior to running, the gear and pinion teeth are painted with a gear marking compound (similar to jeweler's rouge) that produces a rolling contact pattern on the gear and pinion flanks due to the surface contact between the mating teeth and wearing away of the marking compound (see Figure 2).

The gears ground to the undeveloped summary settings are then installed in a test gearbox and run under load. The observed composite gear contact patterns are a final indication of the acceptability of the manufactured tooth profile shape.

If the tooth profile contact does not meet the desired shape location and percentage of contact required by the application, the gears are disassembled for regrinding. The usual practice is to regrind, or develop, only the pinion member because it takes less machining time (due to fewer teeth), and because of the Gleason system convention for single side grinding of the pinion. At this point a gear engineer conducts an analyses of the dynamic load pattern, evaluates the Gleason test machine no-load pattern, and makes a judgment as to what changes are required on the pinion tooth to improve the dynamic load pattern. To assist the gear engineer in determining what move or correction to the Gleason grinding machine set up is most appropriate, the pinion cone axis and the vertical offset in the test machine can be adjusted to change the pattern size and location. These adjustments provide an indication to the gear engineer as to what grinding machine setting will be most effective. In most cases it takes a combination of two or more moves to correct a pattern and more than one combination can produce similar results; however, only one combination is optimum.

The pinion is reground to the new adjusted setting and the testing process repeated. The number of iterations necessry to obtain a satisfactory gear profile depends upon the skill and experience of the test machine operator and/or the gear engineers. This judgment process is probably the weakest link in gear tooth pattern development even with experienced machine operators.

The geometry and nomenclature of a spiral bevel gear set is shown in Figure 5.

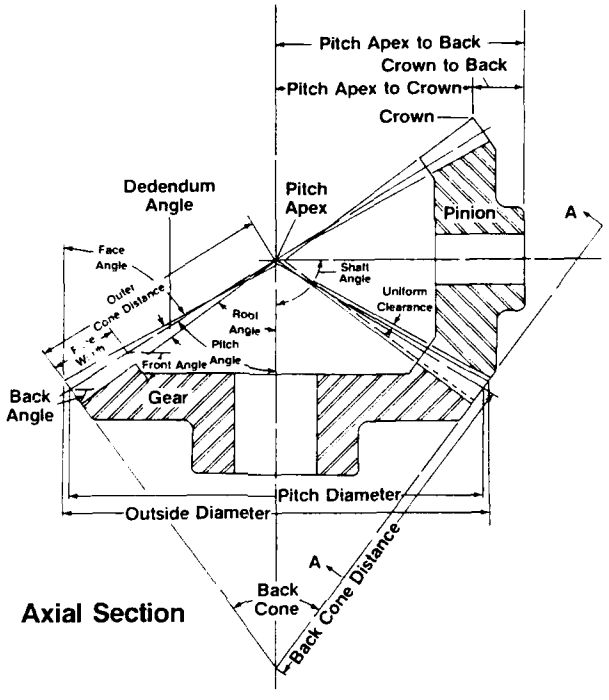


FIGURE 5 BEVEL GEAR NOMENCLATURE

Gleason gear grinding machine setting changes involve first, second, and third order changes. First order changes affect heel and toe pattern position as well as top and flank position. These changes are used in the final positioning of the tooth pattern. Second order changes include bias (diagonal movement) changes, profile change and wheel diameter changes. Third order changes include wheel dresser changes and heel and toe length changes. There are approximately fourteen machine settings that are used by the machine operator in first order changes that affect the shape and position of the gear tooth pattern. Second and third order changes require a calculation of values, using formulas provided by the Geason Works, by a gear engineer who is consulted prior to making second or third order changes.

When a new bevel gear set is to be produced in quantity, it is first necessary to "develop" the pair - that is, to determine the desired location and shape of the tooth bearing in the Gleason test machine that will provide a satisfactory full and uniform load bearing pattern when run in the production gearbox. This is currently accomplished by a trial and error process. The gear teeth are first semi-finish cut to size on a Gleason bevel gear generator (see Figure 6). The gear member of the pair is then set up in a Gleason bevel gear grinder (Figure 3) to the calculated but unconfirmed machine settings provided by a Gleason gear summary. This summary consists of approximately thirty machine settings for each side of the tooth. The gear member is ground "spread blade" (both concave and convex sides ground at the same time). The pinion member is set up and ground in the grinding machine to the unconfirmed pinion settings indicated on the summary. The pinion is ground "single side" requiring a separate set up for both the concave and the convex side.

This current method of manufacturing primary drive spiral bevel gears requires an experienced and qualified organization. It is often expressed that the development of a spiral bevel gear is more of an art than a science. This expression is based on the requirement for skilled bevel gear machine operators who must use their background experience to evaluate the position, shape and contour of the gear tooth pattern produced by the rolling test in the test machine. The machine operator's judgment is relied upon to determine what machine setting or combination of settings is best used to correct an undesirable featured in the test pattern.

The Gleason gear grinding process is a culmination of motions and tool paths that generate the bevel gear tooth form into a continually varying non-involute curve. Basically, the Gleason gear grinder, shown in Figure 3, has a cradle that supports the formed grinding wheel shown and has a radial oscillating motion while the wheel moves in and out of the gear tooth space. This cradle motion is controlled by a generating cam that can be adjusted through the cradle angle setting to modify the ratio of motion at one end of the oscillating arc in relation to the other end. The gear to be ground is mounted on a work holding fixture precisely centered to the work spindle that is in constant rotational motion in a controlled ratio to the cradle. The grinding wheel is mounted concentric to the cradle axis (see Figure 4) in a fixed relative position to the cradle center dependent upon the wheel radius, the spiral angle, and hand of spiral. The grinding wheel, in effect, acts as a single tooth of an imaginary generating gear. The wheel is dressed automatically at prescribed stages in the grinding sequence to maintain surface finish and profile accuracy.



FIGURE 3 GLEASON HYPOID GEAR GRINDER

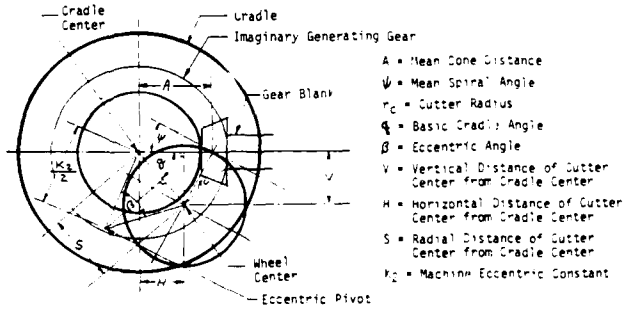


FIGURE 4 GRINDING MACHINE GEOMETRY

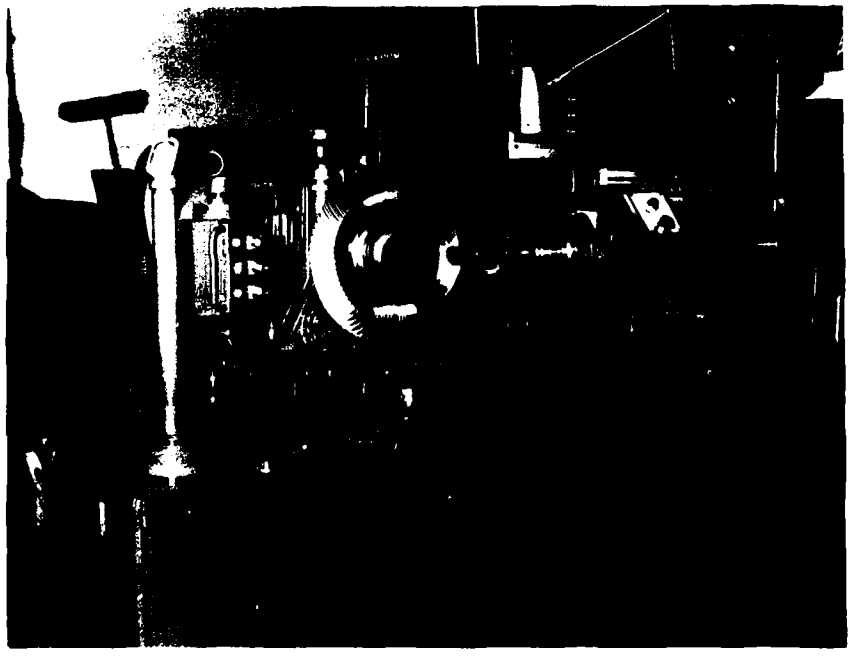


FIGURE 1 GLEASON ROLLING TEST MACHINE

control master gear simulating no-load operation under actual gearbox mounting conditions. Tooth contact patterns under these rotating conditions are observed by painting the teeth with a marking compound and running the gears with their mating master control gears for a few seconds in the gear tester under a light brake load. Because of the compound curvatures inherent in the spiral bevel gear tooth form and the profile modifications designed into the tooth geometry, these gears typically exhibit a localized composite tooth bearing pattern (Figure 2) which; ideally, should spread out under full load, filling the working area of the tooth with some easing off at the end areas of contact. The size, shape, and position of this tooth bearing pattern is a gross indication of the tooth topology both up and down the tooth profile and lengthwise along the tooth face.

PATTERN TAPE RECORD

MASTER GEAR #	PINION
CENTRAL BEARING - DRIVE	
CENTRAL BEARING - COAST	

FIGURE 2 SPIRAL BEVEL GEAR TOOTH CONTACT PATTERN

The goal of the design and profile development phase of spiral bevel gear manufacture is to obtain a localized test machine pattern of a size, shape, and location that will produce the desired full load pattern in the gearbox. The goal of the gear production phase consists of duplicating the desired tooth shape during a production run and from one production run to another.

MANUFACTURING PERSPECTIVE IN THE DESIGN OF BEVEL GEARING

by

A.J.Lemanski
Harold K.Frint and
Warren D.Glasow
Sikorsky Aircraft Division
United Technology Corporation
North Main Street
Stratford, Connecticut 06602
USA

Abstract

A manufacturing perspective of an advanced technique for the design and in-process inspection of spiral bevel gearing utilizing a computer controlled multi-axis coordinate measuring machine, is being developed at Sikorsky Aircraft under sponsorship of the U.S. Army AVSCOM Propulsion Laboratory, Cleveland, Ohio.

Both the designer and the gear manufacturing engineer will have more options in the analysis and manufacture of bevel gearing due to the positive control of the tooth profile geometry and related gear dimensions as permitted by the advanced technique.

The Zeiss Model UMM 500 universal coordinate measuring machine in conjunction with an advanced Gleason G-Met software package provides for a unique interaction between the designer and the gear manufacturer that permits rapid optimization of spiral bevel tooth geometry during initial tooth form development.

This paper describes an advanced design/production technique for the in-process inspection and manufacture of aircraft quality spiral bevel gearing. The technique involves mapping of spiral teeth over their entire working surfaces using the UMM 500 and quantitatively comparing surface normals with the nominal master gear values at some 45 grid points. In addition, this technique features a means for rapidly calculating corrective grinding machine setting changes for controlling the tooth profile geometry within specified tolerance requirements.

Introduction

The inspection of tooth profiles that is commonly performed on spur and helical gears is not feasible for spiral bevel gears because the tooth shape and thickness varies over its face width instead of being constant as in the case of spur and helical gears. Spiral Bevel Gears are currently inspected on Gleason test machines which provide a rotating check simulating no-load operation under actual gearbox mounting conditions. Tooth contact patterns under these conditions can be observed by painting the teeth with a marking compound and running the gear with its mating master control gear for a few seconds in the Gleason tester with a light brake load. The gears typically exhibit a localized composite tooth bearing contact pattern which, ideally, should spread out under the operating load, filling the working area of the tooth. The inspection task is a subjective one to ascertain an acceptable full load pattern from a localized composite pattern. The machine operators task is even more difficult because he must make a judgment to change the machine settings in order to correct an undesirable feature in the test pattern.

Therefore, this manufacturing process for spiral bevel gears is more time consuming and costly when compared to the spur and helical process of control.

Experience has also shown that highly loaded aircraft spiral bevel gears can develop a tooth scoring failure during initial transmission test stand running even though the tooth contact pattern is within specification limits as determined by the present method of control.

The current bevel gear method requires the use of master control gears which are manufactured by the same process used for the production gears. Also, duplicate masters are required for second and third source production and additional levels of master gear control. From a metrology point of view, it is most desirable to manufacture the control master gears to a higher level of accuracy which is currently not possible by the present method.

State Of The Art Of Spiral Bevel Gear Manufacture

The elemental inspection of tooth profiles that is commonly performed on spur and helical gears is not practical for spiral bevel gears because the shape and size of a bevel gear tooth varies over its face width instead of being constant as in the case of a spur gear. Spiral bevel gears are currently inspected on a specially-designed Gleason test machine, shown in Figure 1, which provides a rotating test of the gear with its

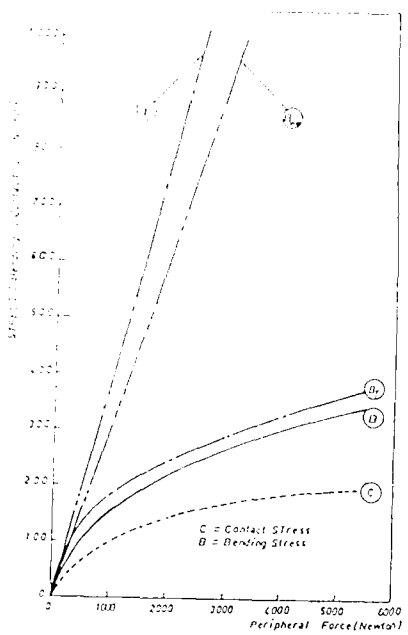


Fig. 17., Results of stress calculations on a double circular-arc tooth-profile steel gears.

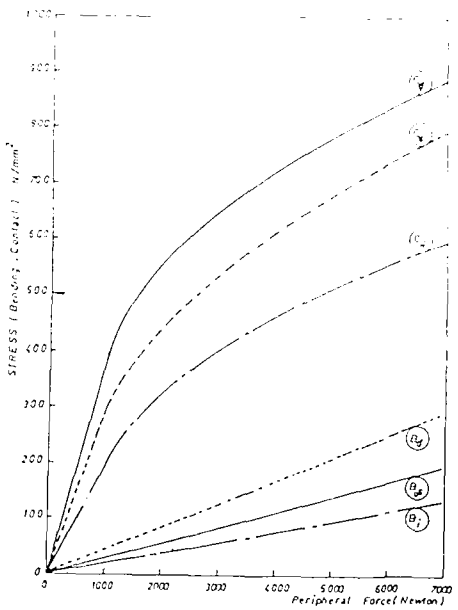


Fig. 18., Bending and contact stresses of both single-double circular-arc and involute profile gears in case of large helix angle.

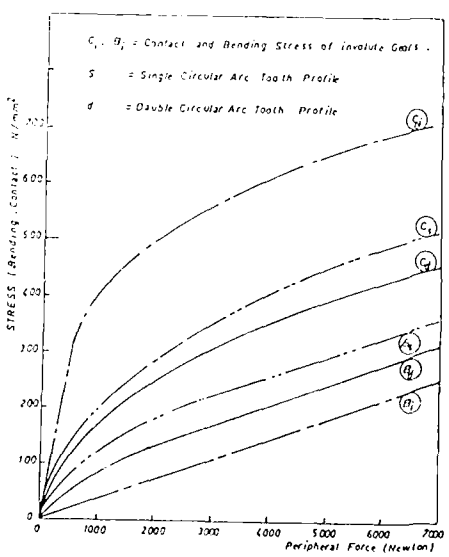


Fig. 19., Bending and contact stresses of both single-double circular-arc and involute profile gears in case of smaller helix angle.

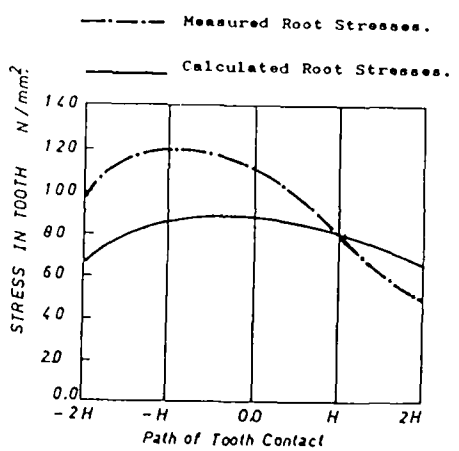
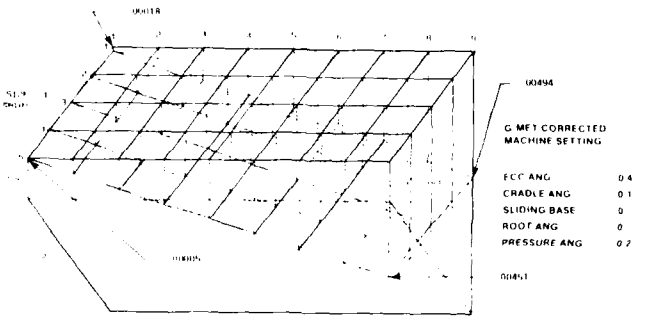
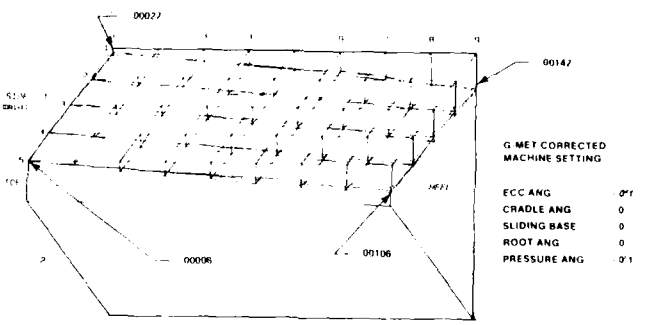


Fig. 20., Root stresses measured and calculated using different methods for double circular arc gears when load is applied at the middle zone of contact.
(Load = 1000 Newton and 30° helix angle.)



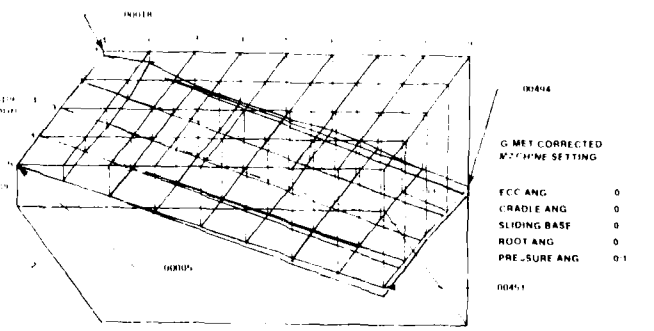
DEVIATIONS CONVERTED INTO CORRECTIVE MACHINE SETTINGS

FIGURE 17 INITIAL GRIND WITH A ECCENTRIC ANGLE CHANGE OF 0°5'



DEVIATIONS CONVERTED INTO CORRECTIVE MACHINE SETTINGS

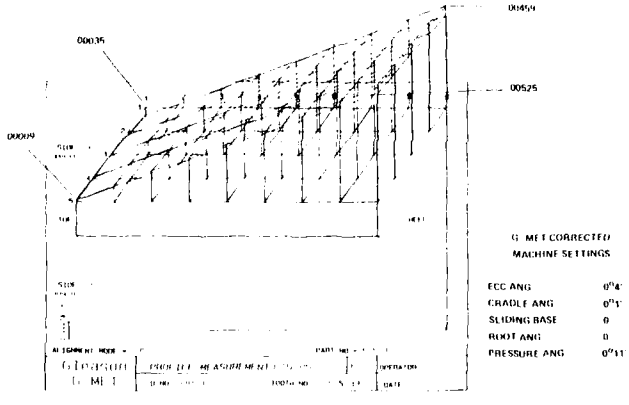
FIGURE 18 RESULTS OF 1ST CORRECTIVE GRIND



DEVIATIONS CONVERTED INTO CORRECTIVE MACHINE SETTINGS

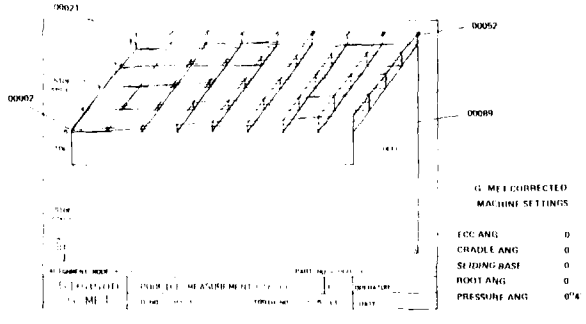
FIGURE 19 RESULTS OF 2ND CORRECTIVE GRIND

The machine center to back change of .020 inches withdrawal resulted in a maximum deviation of +.0053 inches in the bevel pinion profile geometry as shown in Figure 20. When the pinion was reground to the corrective delta setting calculated by G-Met, the deviation was reduced to +.0009 inches (Figure 21). A second regrind resulted in a maximum deviation of +.0004 inches as shown in Figure 22.



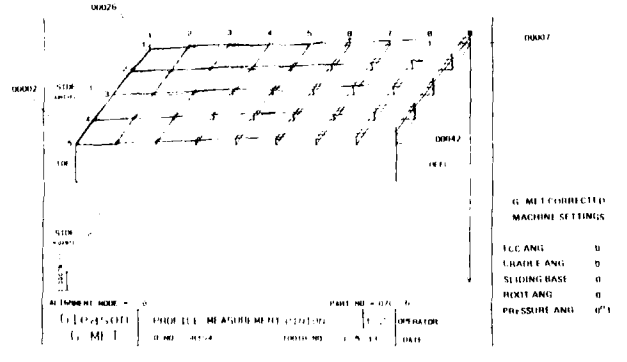
DEVIATIONS CONVERTED INTO CORRECTIVE MACHINE SETTINGS

FIGURE 20 INITIAL GRIND WITH A MACHINE CENTER TO BACK CHANGE OF M.C.B. W .020



DEVIATIONS CONVERTED INTO CORRECTIVE MACHINE SETTINGS

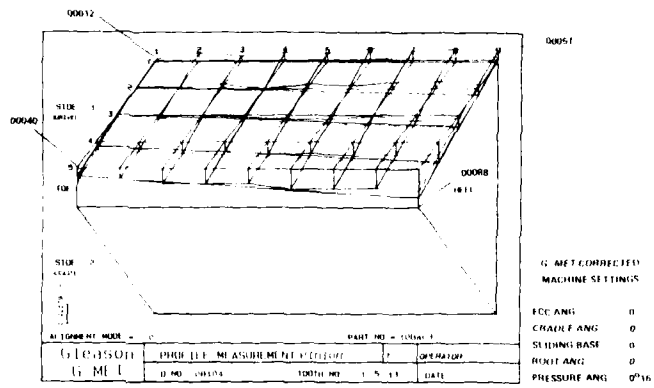
FIGURE 21 RESULTS OF 1ST CORRECTIVE GRIND



DEVIATIONS CONVERTED INTO CORRECTIVE MACHINE SETTINGS

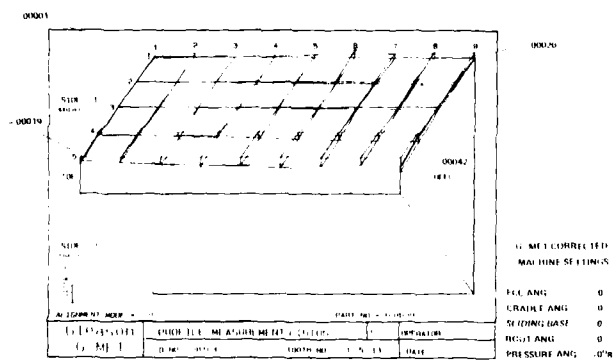
FIGURE 22 RESULTS OF 2ND CORRECTIVE GRIND

A pressure angle change of 0°30' resulted in a maximum deviation of -.0009 inches in the bevel pinion profile geometry as shown in Figure 23. When the pinion was reground to the corrective delta setting calculated by G-Met, this deviation was reduced to -.0004 inches (Figure 24). A second regrind resulted in a maximum deviation of - 0002 inches as shown in Figure 25.



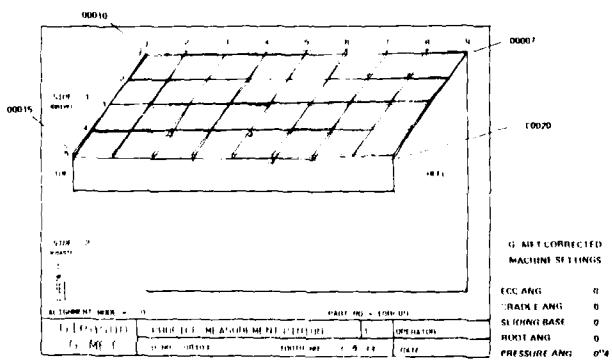
DEVIATIONS CONVERTED INTO CORRECTIVE MACHINE SETTINGS

FIGURE 23 INITIAL GRIND WITH A PRESSURE ANGLE CHANGE OF 0° 30'



DEVIATIONS CONVERTED INTO CORRECTED MACHINE SETTINGS

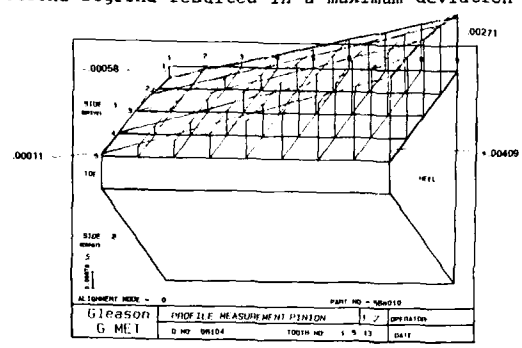
FIGURE 24 RESULTS OF 1ST CORRECTIVE GRIND



DEVIATIONS CONVERTED INTO CORRECTED MACHINE SETTINGS

FIGURE 25 RESULTS OF 2ND CORRECTIVE GRIND

A root angle change of 0°20' resulted in a maximum deviation of -.0041 inches in the bevel pinion profile geometry as shown in Figure 26. When the pinion was reground to the corrective delta setting calculated by G-Met, this deviation was reduced to -.0004 inches (Figure 27). A second regrind resulted in a maximum deviation of -.0002 inches as shown in Figure 28.

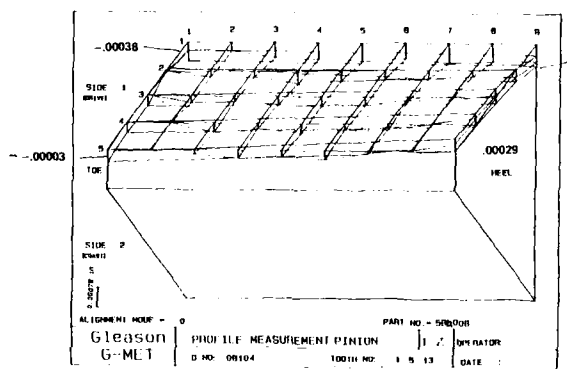


G MET CORRECTED MACHINE SETTINGS

ECC ANG	0° 3'
CRADLE ANG	0° 1'
SLIDING BASE	0
ROOT ANG	0
PRESSURE ANG	-0° 17'

DEVIATIONS CONVERTED INTO CORRECTIVE MACHINE SETTINGS

FIGURE 26 INITIAL GRIND WITH A ROOT ANGLE CHANGE OF 0° 20'

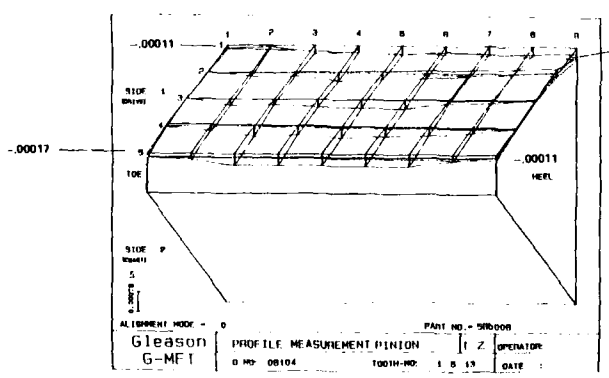


G MET CORRECTED MACHINE SETTINGS

ECC ANG	0
CRADLE ANG	0
SLIDING BASE	0
ROOT ANG	0
PRESSURE ANG	0° 8'

DEVIATIONS CONVERTED INTO CORRECTIVE MACHINE SETTINGS

FIGURE 27 RESULTS OF 1ST CORRECTIVE GRIND



G MET CORRECTED MACHINE SETTINGS

ECC ANG	0
CRADLE ANG	0
SLIDING BASE	0
ROOT ANG	0
PRESSURE ANG	0° 2'

DEVIATIONS CONVERTED INTO CORRECTIVE MACHINE SETTINGS

FIGURE 28 RESULTS OF 2ND CORRECTIVE GRIND

In all four of the above cases, the bevel pinion tooth profile geometry was restored to within acceptable limits in two regrinds using only first order changes. This demonstrates that the G-Met corrective procedure can be effective in correcting an out-of-tolerance tooth profile during the production process. This technique can eliminate the need for a final inspection.

Conclusions

Application of the improved inspection method for spiral bevel gears, described herein, can provide the following benefits:

1. Eliminates subjective tooth pattern interpretations and permits quantitative evaluation of tooth profiles.
2. A substantial reduction in Manufacturing and inspection manhours and associated cost.
3. In one set up all blank dimensions and tooth elements, including tooth spacing and index variation; can be measured.
4. Provides capability of measuring entire tooth surface rather than the localized contact area measured by the current technique.
5. Eliminates the need for, and costs associated with, metallic master control gears and working master gears used for production quality control. Also eliminates the inherent variability of master gears.
6. Produces both digital and graphical records of the tooth geometry.
7. Automatically calculates the most optimum grinding machine settings necessary to correct profiles with deviations outside the established tolerance range.

References

1. Lemanski, A.J., and Frint, H.K., Automatic Inspection and Precision Grinding of Spiral Bevel Gears, *AHS Paper No. A-84-40-34-5000, presented* at the 40th Annual Forum of the American Helicopter Society, Arlington, Virginia, May 16-18, 1984.

MANUFACTURING CONSIDERATIONS RELATED TO AIRCRAFT GEARBOXES

J.N. McDade, Director, Manufacturing and G.B. Collin, Manager Manufacturing Engineering
SPAR AEROSPACE LIMITED, 825 Caledonia Road, Toronto, Ontario, Canada M6B 3X8

SUMMARY

The manufacuture of state of the art aircraft gearboxes is at the upper end of the spectrum of mechanical technology. The considerations discussed here, primarily relate to the high costs involved in the application of this technology. The technology used in aircraft gearbox manufacturing, covers a whole gamut of methods, types of machining and chemical processing. While an aircraft gearbox manufacturer must aggressively ensure efficient productivity, his efforts are frequently negated by the requirements of the designer. As aircraft gear systems are required to transmit more power at greater speeds, the trend is to provide this performance with a minimum of increase in size and weight. This necessitates better dynamic capability, resulting from improvements in metallurgy, manufacturing equipment, techniques, and metrology. These improvements can be costly, it is therefore, encumbent on the designer to carefully consider his designs, in terms of producibility. This can best be done in close liaison with the manufacturing engineer.

An aircraft gearbox manufacturer's view point:

The business of manufacturing aircraft gearboxes and transmissions is very competitive, risky and costly. It is said that an aircraft hangs by its wings, but it is also true that the modern flying machine stays up, due to the reliability of its gearing. A gear failure, particularly in a helicopter power train, can be almost instantly catastrophic. The risk is obviated largely by the production of highly reliable components. This reliability is the prime reason for the high cost of power train transmissions. Of necessity, aircraft transmissions are designed to be as light and compact as possible, within the constraints of the applied loads. This design of minimum sized parts leads into minimal dimensional tolerances in all critical areas. The scope of aircraft gear manufacturing and related design is so large that it is possible only to touch on a few of the aspects here. This discussion is centered, primarily, around some of the considerations related to cost and reliability.

Combined configuration and tolerance criteria are the cause of costs being relatively high. Occasionally a designer delves into the unknown and develops a gearbox utilizing gears of either a non involute tooth form or unusual material. Our experience appears to tell us that deviations of this nature can be troublesome and expensive. The complete modern aircraft gearbox manufacturer must, in order to have good control of the manufacture and scheduling of his product, have a facility which incorporates all the expertise and controls needed for a cost effective, on time operation. The areas of expertise involved are in: Marketing - Proposals - Program Management - Manufacturing Engineering - Manufacturing and Quality.

In one sense, an independent gear house, such as our own, is at a disadvantage, due to the necessity of having systems which cater for the large variety of customer's requirements. In another sense, the independent gear house has advantages, resulting from the necessity of being more competitive, and also from contact with a variety of aircraft primes, their designers and manufacturing teams. We deal with many customers, from a number of different countries. Some customers use the various European specifications, some use American specifications and in addition, each customer has his own. Every customer also has different requirements related to program scheduling, monitoring engineering drawings and specifications. The cost of maintaining up-to-date specification libraries, along with the physical application of changes, is costly. Technical skills need to be high, and in some areas, very specialized. Those skills, as applied to aircraft gearing are relatively rare, this creates a situation where, regardless of the availability of work, we must maintain a core of these specialized people, in order that continuity be maintained from project to project. This again, is an area of additional cost that the nature of the business entails. Due to the continuous tightening of requirements and the necessity of maintaining reliability, a high quality gear manufacturer, has high yearly maintenance and capital budgets. A complete gearbox manufacturer must, due to the variable nature of the aircraft industry, be flexible in his ability to produce a wide variety of units differing considerably in size, complexity and precision. Gearboxes range in size and type, from small high speed engine accessory and power take-off units, up to the large low speed helicopter rotor drive transmissions. This again, is a cost factor related to the variety of equipment needed and to the amount of machine down-time.

As an interesting aside, our experience and expertise in the business led us, in the last few years, to the design and manufacture of the remote manipulator system, or mechanical arm , used in the American Space Shuttle Program, which is primarily for the retrieval and release of Satellites in earth orbit. Each joint, in the arm, comprises one or more very precise planetary type gearboxes. The arm has functioned very well, since its first flight in the Columbia.

Reverting to the subject discussion, it can be seen from the foregoing that our business is a very costly one, this along with the 'state-of-the-art' readiness, means that a continuing effort must be put into both minimizing cost and improving quality. This effort can be performed on both an informal and formal basis. Informal activity is normally going on continuously within a company and is such, that there is no formal record of either the cost of the change or the value of the improvement created. We prefer the more formal improvement programs, which include those used by some of our customers, examples of which are: Should Cost, Cost Superiority, and Target Zero. These programs are usually joint activities between the customer and the manufacturer, and generally involve design and quality improvements. Our own in-house program, which we call Q.C.R. - 'Quality Cost Reliability' - is of necessity, oriented more in the direction of improvements in methods and equipment, which includes a requirement of monitoring cost vs gain. The end result is the same ie: lower cost and better quality. Any program of this nature is beneficial to all parties. However, the best way to design a cost effective gearbox is for the designer to work hand-in-hand, with the manufacturer. We have been involved in a number of programs from the initial phase, which have resulted in simpler, more producible gearboxes. On the other hand, we have built expensive and troublesome gearboxes, where it was obvious that the potential manufacturer was not involved.

The constant quest for better productivity and quality, continually leads into acquisition of more sophisticated machinery. While in some areas machine builders have made great strides in the manufacture of equipment with flexibility, precision and speed of production, the makers of gear grinding machinery seem to have made few inovations in this area of considerable importance to our industry. This is probably due to the comparatively small market for machines, of this type. Methods of producing gear teeth are many and various FIG. I. Of these, the most commonly used for aircraft spur, helical and spiral bevel gears are: hobbing, shaping, form grinding, worm type generated grinding and Gleason System generating and grinding.

With possibly two exceptions, the modern gear grinding machines are basically very little different from the first grinders built. A similar statement may be made regarding gear metrology. In general, where precision aircraft gears are concerned, the inspection process is slow, tedious and very costly.

The manufacturing sequence involved can be very complex and at times, require as many as hundreds of individual machining or process operations in order to complete a part FIG II. The operations, which probably cause most concern, are carburizing and hardening. Distortions resulting from these operations, often make necessary, a number of additional machining operations and freqently necessitate extreme care at gear grinding. Carburized areas are usually local, which further increases the distortion, as a result of uneven stresses. Dealing with the results of this type of heat treatment, constitutes a large portion of the part cost.

A consideration which significantly effects the cost of aircraft gearing is the requirement to control stock removal, from a carburized surface. The designer should give very carefull consideration to the potential for heat treat distortion, when arriving at case depth, and hardness gradient requirements. An allowable stock removal, which is small, relative to the amount of distortion resulting from carburizing and hardening, can be very expensive to maintain.

Product reliability requirements force us into a great deal of repetitive and detailed inspection FIG. III. There are many special inspection methods, processes and equipment needed. In addition to the large amount of time involved, such items as gear tooth checking machines, costing in the order of $600,000. each, are used. All in all, a very costly part of the business and which in reality produces nothing, except the guarantee of reliability. One of the most important quality requirements, is traceability. This costly necessity involves the generation and retention of a lot of paperwork, and considerable time spent in the marking of parts and assemblies. An important design consideration should be the reduction of inspection requirements and most certainly a reduced amount of part marking FIG. IV.

While most of the previous concerns have been connected with gear teeth, a component of the gearbox which must not be forgotten, is the housing. Many aircraft gearbox housings are large and/or very complex. These housings are usually cast from light materials eg. magnesium or aluminum, and often require a great many machining operations, some of which are of high precision. Special care must be taken to minimize the effects of temperature and distortion. The manufacturer of the finished housing can, with his expertise, have a valuable input into the design of the basic casting.

From the previous discussion, it can be seen that there are many areas of concern, when thinking about cost. From an aircraft gearbox manufacturer's point of view, further examples of cost, which can be avoided by designers, are as follows:

a) The designer should dimension the part functionally, and for maximum tolerance.

b) Standardize internal, corner radii in increments of 1/16" or metric equivalent. This relates to standard cutting inserts FIG. V.

c) Use practical datums FIG. VI.

d) When possible, show allowable salvage or repair schemes on the part drawing. An example of which is the chrome repair of bearing journals.

e) On rotating parts, avoid bottle bore conditions where a boring bar length to diameter ratio would exceed 8:1. Preferably a ratio of not more than 5:1 should be used, for economic boring FIG. VII.

f) If the angular relationship of features is not important, this should be clearly stated on the drawing.

g) Show alternate designs, sources, material and hardware, were possible.

h) Avoid radial surfaces (or square shoulders), when possible, particularly on carburized rotating parts FIG. VIII.

i) Avoid corner undercuts, when possible, on carburized parts FIG. V.

j) Avoid blind splines. Through splines can be broached, in a lot of cases, with less time and generally exhibit less taper distortion thru heat treatment FIG. V.

k) Avoid hardened splines, if possible.

l) Where possible, match the case depth requirements for different areas of the part, to allow a single carburizing cycle FIG. IX.

m) Always provide a separate casting drawing. This avoids confussion.

n) Tapping blind holes - minimum of 4 pitch clearance between maximum full thread and minimum hole depth, is desirable.

o) Do not, for simplicity or as a disciplinary measure, automatically reject non conforming parts.

The world of the designer sometimes seems to be in the realm of the nebulous, guess and by god, and toss of the coin, to we, who are the blacksmiths of the industry. It is hard for us, at times, to see a reason why a designer should turn down a request to allow the use of a gearbox component, which is a very small amount outside the drawing requirement. We know from experience that quite often the designer rejects a deviation request, because it is the easy way out and sometimes, because he feels that his rejection will discipline the manufacturer. A designer should definitely think twice before doing something like this, as by doing so, he often very significantly raises the cost of parts to be manufactured, in the future.

A considerable amount of money could be saved if the aircraft industry, as a whole, got together and produced common metallurgical, quality and process specifications.

It is our experience that friendly man-on-man contact, between the prime and subcontractor, in conjunction with a free flow of all types of information, can greatly speed up the resolution of both design and manufacturing problems, along with the consequent reduction in costs. This can produce large benefits to all parties.

SPAR

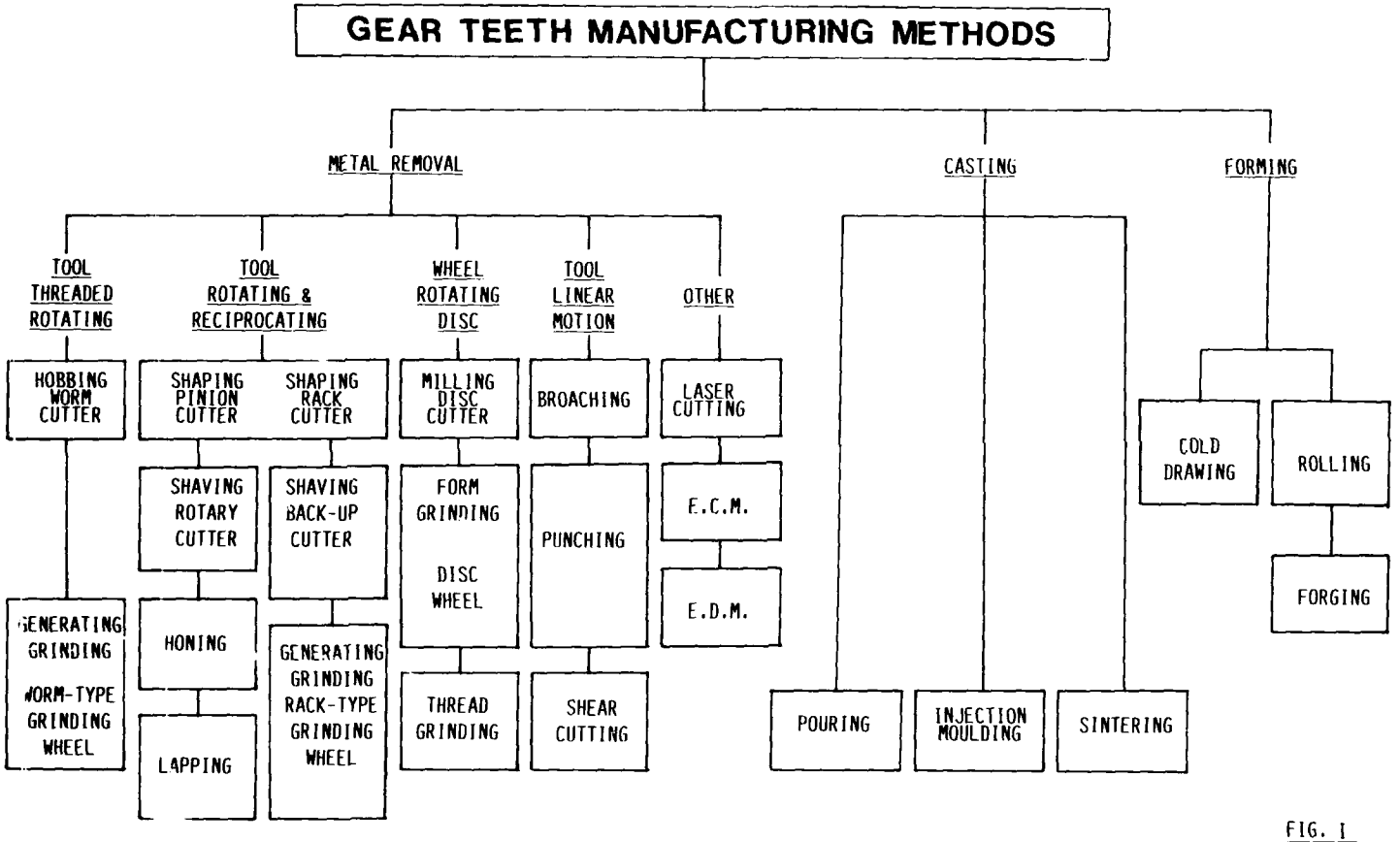

GEAR TEETH MANUFACTURING METHODS
METAL REMOVAL
CASTING
FORMING
TOOL THREADED ROTATING
TOOL ROTATING & RECIPROCATING
WHEEL ROTATING DISC
TOOL LINEAR MOTION
OTHER
HOBBING WORM CUTTER
SHAPING PINION CUTTER
SHAPING RACK CUTTER
MILLING DISC CUTTER
BROACHING
LASER CUTTING
SHAVING ROTARY CUTTER
SHAVING BACK-UP CUTTER
FORM GRINDING
DISC WHEEL
PUNCHING
E.C.M.
E.D.M.
GENERATING GRINDING WORM-TYPE GRINDING WHEEL
HONING
GENERATING GRINDING RACK-TYPE GRINDING WHEEL
THREAD GRINDING
SHEAR CUTTING
LAPPING
POURING
INJECTION MOULDING
SINTERING
COLD DRAWING
ROLLING
FORGING

FIG. 1

TYPICAL BEVEL PINION GEAR MANUFACTURING OPERATIONS

SPAR

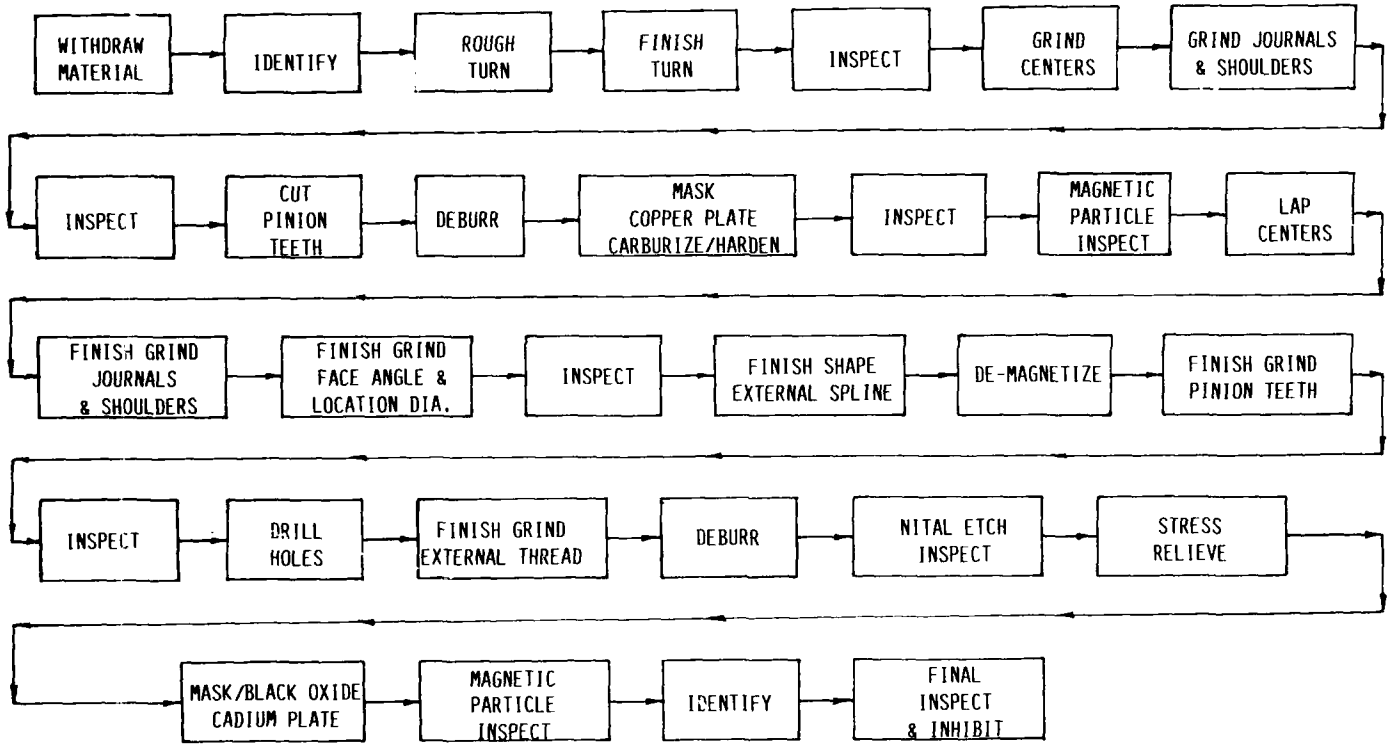


FIG. 11

INSPECTION FLOW CHART
FABRICATION TEST AND QUALITY VERIFICATION OPERATIONS

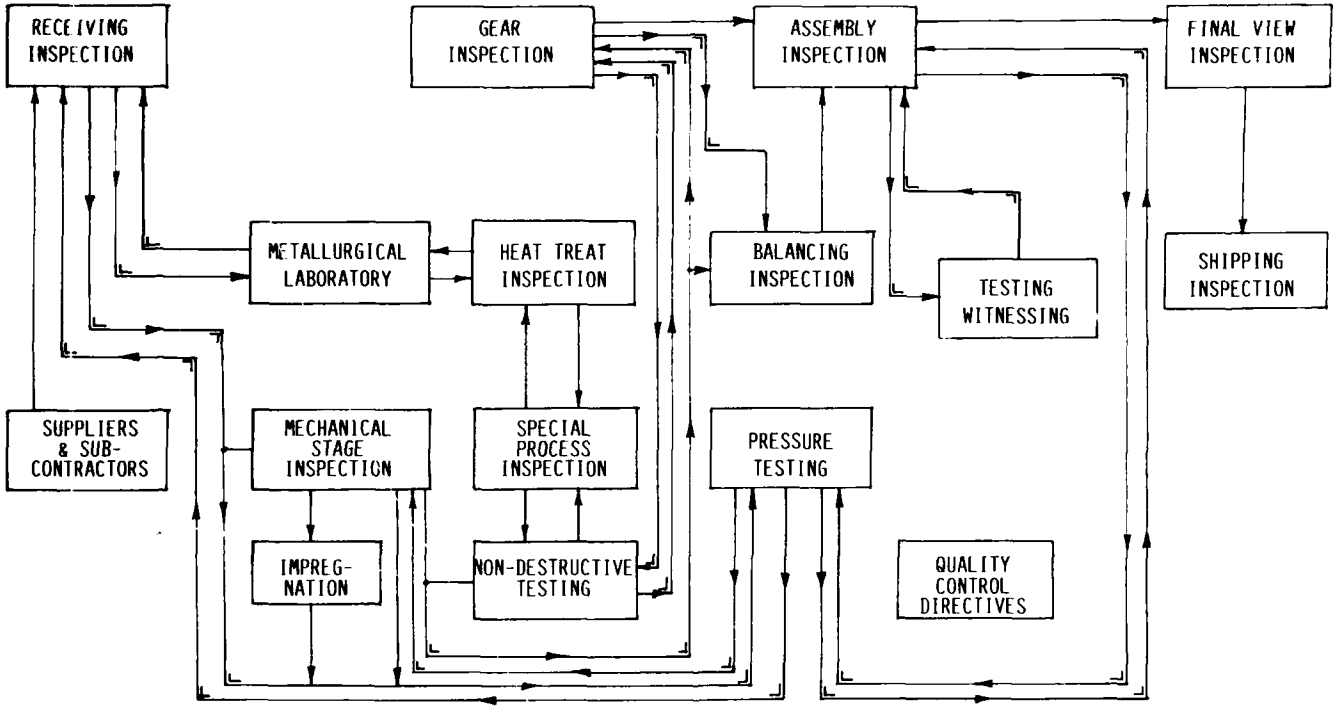
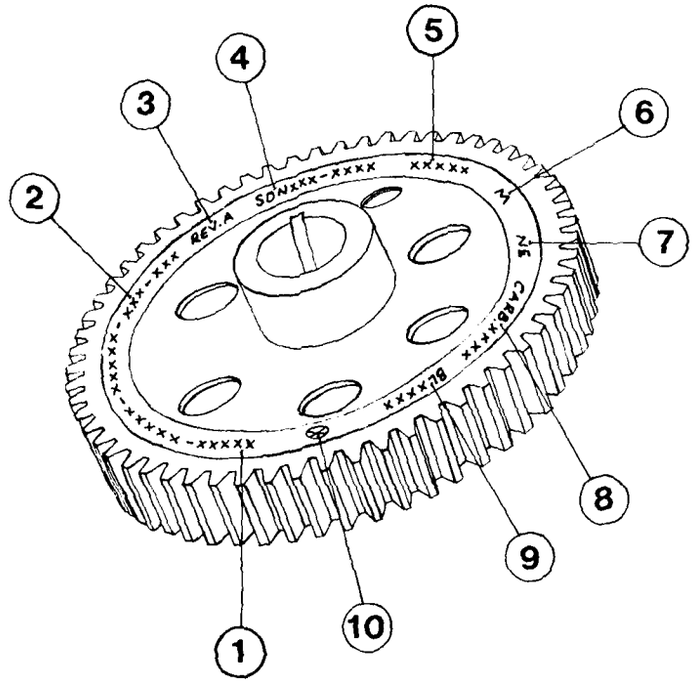


FIG. III

TYPICAL AIRCRAFT GEAR PART MARKING

FIG. IV



1. Part Number
2. Forging Number
3. Revision Letter
4. Serial Number
5. Material Heat Number
6. Magnetic Particle Inspection
7. Nital Etch
8. Carburize Heat Treat Lot Number
9. Back Lash (bevel gears only)
10. Supplier Final Acceptance Stamp

FIG. V

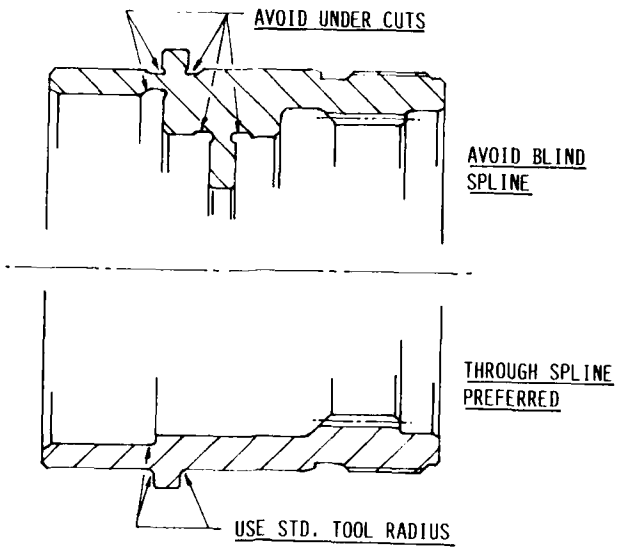

AVOID UNDER CUTS
AVOID BLIND SPLINE
THROUGH SPLINE PREFERRED
USE STD. TOOL RADIUS

FIG. VI

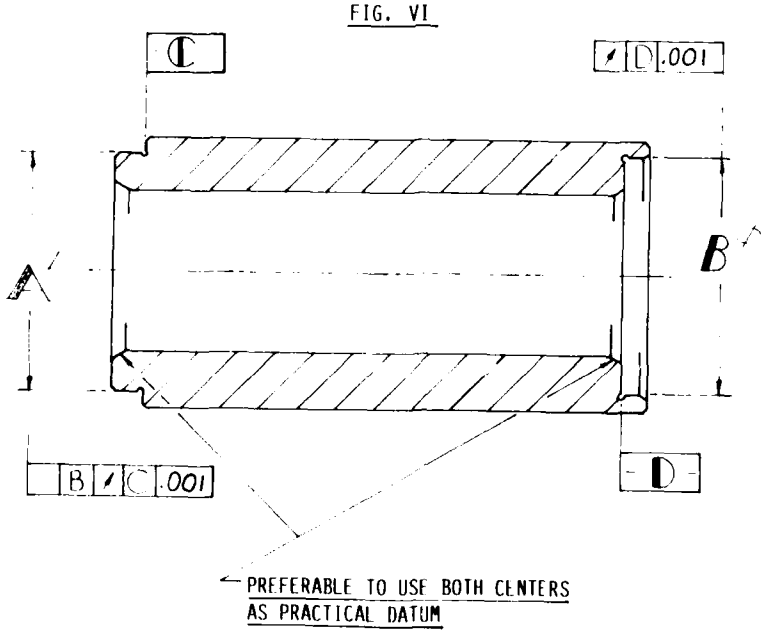
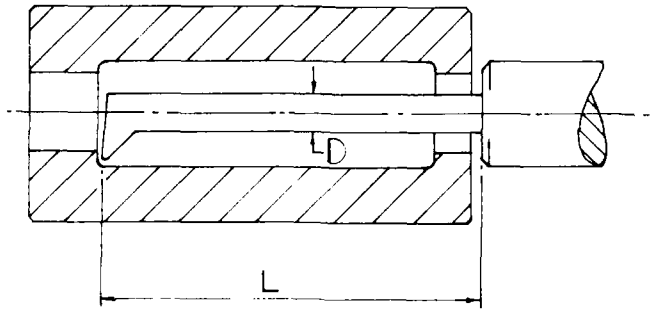

C
D .001
A
B
B C .001
D
PREFERABLE TO USE BOTH CENTERS AS PRACTICAL DATUM

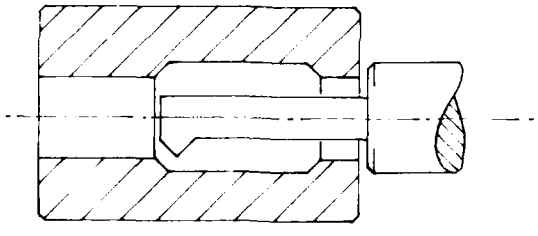
FIG. VII



L:D = ≥ 8:1

PREFERABLE L:D = ≥ 5:1

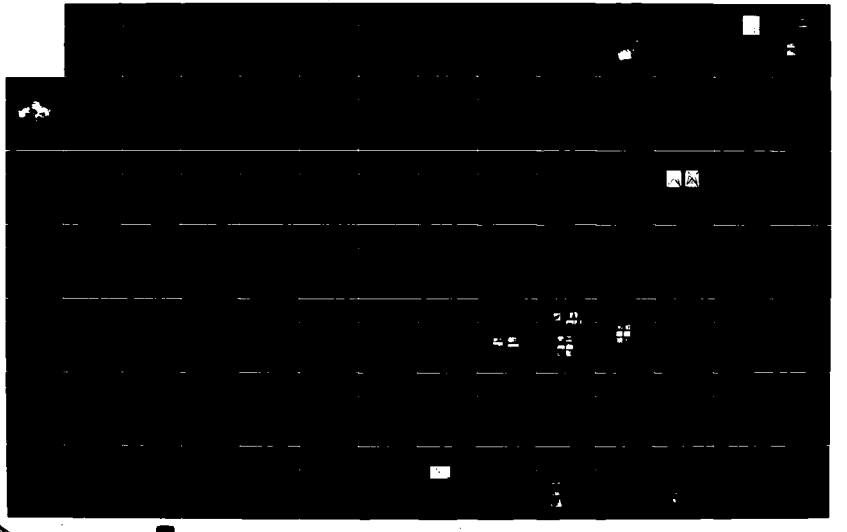
FIG. VIII



AVOID SQUARE SHOULDERS

AD-A152 673 GEARS AND POWER TRANSMISSION SYSTEMS FOR HELICOPTERS AND TURBOPROPS: CONF..(U) ADVISORY GROUP FOR AEROSPACE RESEARCH AND DEVELOPMENT NEUILLY.. JAN 85 AGARD-CP-369 3/3

UNCLASSIFIED F/G 21/5 NL



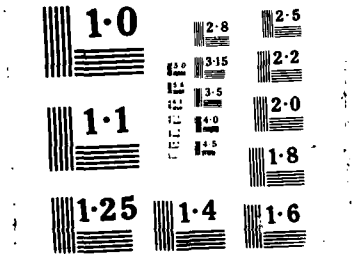
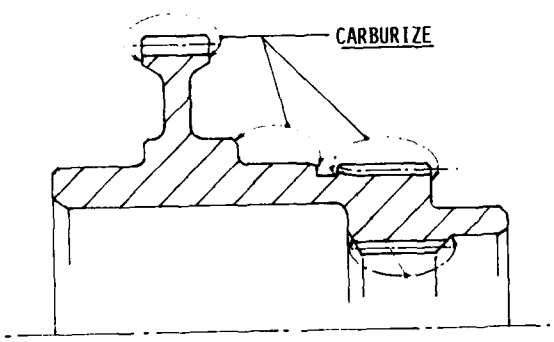

1·0
2·8
2·5
3·15
2·2
3·5
2·0
1·1
4·0
4·5
1·8
1·25
1·4
1·6

FIG. IX



CASE DEPTH IN 4 LOCATIONS SHOULD
FALL WITHIN SAME TOLERANCE BAND

POSSIBLE TECHNOLOGICAL ANSWERS TO NEW DESIGN REQUIREMENTS FOR POWER TRANSMISSION SYSTEMS

by
L. Battezzato and S. Turra
Transmission Engineering Dept.
Direzione Progettazione
FIAT AVIAZIONE
Corso Ferrucci, 122 - 10100 Torino
Italy

SUMMARY

In the new projects of gearboxes for aeronautical application, performed by FIAT AVIAZIONE, the specified requirements have become more and more severe asking for continuous technology advance.

This paper deals with the most important points put out by these specs, such as fail safety, reliability, low vibration and low noise, high working temperature, invulnerability and maintainability, of course combined with a low weight characteristic.

A detailed analysis is carried out to identify the guidelines for obtaining the best compromise among the above listed requirements, by applying a proven philosophy. The advantage of a reliable system capable of detecting failures in progress within the gearbox is also underlined as it can be a key point in defining the final design resulting from the optimization procedure.

FOREWORD

FIAT AVIAZIONE participated in the last thirty years with a number of partners to many programs, with the task of studying, designing, developing and manufacturing transmissions, especially conceived for aeronautical applications or requiring similar technologies.

To be short, among the most important programs we remind :

- The main transmissions for SUPERFRELON, PUMA and DAUPHIN helicopters with AEROSPATIALE.
- The transmissions for propellers and lift fans applied on French Hovercraft N 500 with SEDAM.
- The transmissions to accessories for the new PRATT & WHITNEY PW 2037.
- The transmissions to the main drive and to the accessories for PRATT & WHITNEY OF CANADA PT6B-36.

Finally we just started now the work on transmissions for the engine IAE V 2500. We don't mention here the programs for which we just produced the transmissions or under licence (as for the Italian Aviation Ministry), or subcontracted directly by the leader Firms.

The wide experience obtained in such a long period of working in the field of transmissions for aeronautical applications gave us the opportunity to live the evolution and the refinement of the specifications imposed during the years on the transmission designer.

It is interesting to note that the specifications dating back 20 or more years just asked for a transmission capable of running under the imposed loads, while the modern specifications establish a number of conditions detailing how the transmission shall run.

We can try to list the most important characteristics that should be offered by the new designs of transmissions :

- fail safety
- reliability
- low vibration level
- low noise generation
- high working temperature
- running capability in no oil condition
- invulnerability
- maintainability

together, of course, with an

- extreme lightness

of the assembly, as usual for aeronautical applications.

So the designer of new transmissions becomes more and more constrained within a number of different ties; he needs a clear understanding and knowledge of the state of the art in order to achieve the best compromise among the specified characteristics.

FAIL SAFETY

Every time and item is introduced into the general design of a system the designer must ask himself: "Which consequence derives for the system from a failure of this item?".

The best answer should be that the failure can be detected and shown to the operator, that the effect on the performance of the system is minor and that eventually the situation would not deteriorate to secondary

major failures causing the unserviceability of the system before the operator can take precautions. This ideal condition, of course, is very often unpractical for mechanical devices; the designer shall try anyway to do his best for approaching it as much as possible.

A good exercise we did in the past has been to cover the failure of a transmission lube pump and of relevant external piping and cooler. In fig. 1 we give a photograph and a schematic diagram of the solution: the pump n° 1 sucks oil from the tank, sends it to the cooler and back to the filter and to the lubrication circuit.

The pump n° 2 sucks oil at a lower level than the previous one and normally sends it back to the tank through the bypass valve. In case of failure of the external cooler circuit causing loss of oil, the oil level in the tank would decrease to the point that no oil will be sucked by the relevant pump; the reduction of pressure in the circuit will cause the pressure sensing valve to open and let oil from pump n° 2 be sent to filter and main lubrication circuit that will thus be fed at a pressure lower than normal. The fact that the transmission runs in emergency condition can easily by shown to the operator by pressure detectors located on the lubrication circuit.

Not always, of course, the fail safety requirements are answered in such an ideal way. The transmission has a lot of parts that cannot be doubled without an unacceptable impact on weight; their failure will certainly cause a reduction in the capabilities specified for the system. To be more clear on how to proceed, we can say that practically all the elements in the transmission shall be catalogued under two headings :

- vital elements, whose rupture doesn't allow the continuation of the mission or its interruption in safe condition for the crew and/or for the aircraft.
- secondary elements, that are not included within vital ones.

For the vital elements, the designer will put his best skill for covering the first failure by a doubling element or, if this procedure is unpractical, by assuring that the element will not fail during its service life.

Calculation or rig test and accurate manufacturing procedure will assure this capability (safe life capability).

In any case, each element (vital or secondary) must be carefully studied in its service ambient, and the best devices must be adopted in order to restrict possible immediate generation of secondary failures on other surrounding vital elements. The operator shall be left the time to be warned about what is going on and to conclude the mission in the least risky way.

As an example, we show the result of a study carried out on epicyclic stages applied on helicopter gear boxes, for increasing the fail safety of their design. Of course, in this case, there is no practical way of transferring the function of the system to other parallel elements.

The designer must then conceive the parts for a safe life capability and possibly introduce those features that increase the fail safety of the group by stopping or slowing the progress to secondary failures and that warn the operator about any inconvenient being generated, giving him the time for taking precautions before the failure can proceed to a catastrophic event.

We summarize in the following table the characteristics or the features we suggest to introduce in the design : the reader can see from fig. 2 how the newly conceived design is better than a 15 year old design, performed when the fail safety requirements were not given the right priority by the designer.

Features suggested for improving the fail safety characteristics of an epicyclic stage applicable on an helicopter main transmission

	Remarks
1. The planets shall be fitted on trunnions protruding from upper plate of planet carrier. The lower side of planet row shall be completely open.	Any particle detached from gears or bearings can be easily evacuated, thus reducing the risk of bigger damages for the other parts if they were captured within rotating gears.
2. A large volume shall be left under the stage, limited in its lower side by a flat separator.	Any detached particle can't contaminate the other stages underneath. Separation of big chips will not cause anchor on any obstacle with risk of higher damages. This feature is estimated as being a big improvement. In the old design the planets are jammed in a tight volume, thus rendering the evacuation of chips quite difficult and secondary effects highly probable.
3. The ring gear shall be centered in the lower and upper casings.	A crack in the structure of the ring causing its opening can be contained by casings.
4. The planet trunnions will have an internal back up system capable of supporting the planet in case of trunnion failure.	

	Remarks
5. All lubrication oil falling from epicyclic stage shall collect and pass by a chip detector equipped with remote indication to cockpit.	Any failure causing detachment of particles can be detected in its early stages and the consequent precautions taken by the operator.
6. One or more vibration pick-up shall be placed in proximity of ring gear attachment. Their signals shall be analized and the amplitudes found for given meshing frequencies supplied to the operator.	It will be possible to detect any failure causing anomalies in the meshing regularity (failure of any severity going from contact surface damage to total detachment of some teeth).
7. A shear section shall be located on main rotor drive shaft and on drive/s from engine/s.	In the case of a sudden blockage in any part of the main transmission, the failure of shear sections allows the main rotor and some vital accessories to be kept running for a safe landing of the a/c in autorotation.

RELIABILITY

Reliability can be defined as the capability of the transmission to perform according to the specification for the given TBO (Time Between Overhauls); the more the MTBR (Mean Time Between Removals) approaches the TBO, the more the transmission is realiable.

A definition like this is very simple; the actions to be taken and the rules to be followed for obtaining the aim are numerous and much less simple to be written.

The way to proceed is dictated to the designer by his past successes or unsuccesses, and as such will reflect his experience, knowledge and personality; as such, the answer that can be given to a problem will change with the time to reflect the sum of experiences the designer accumulated.

It is out of any doubt, then, that the more experienced is the designer, the more proven and sound and successful his answer will be.

According to our past experience, certain areas must be accurately checked when designing and when manufacturing a transmission, because anything forgotten in that field can cause dramatic reductions of MTBR in service or tedious debugging procedures in development.

Just for example, and not with the hope of being exhaustive, we list here few areas that require accurate thinking :

a) gear teeth
- possible stress concentrations on teeth as a consequence of
  - . deformation of gearshaft support, under normal running or test loads
  - . thermal expansion characteristics of gear and of support structure
  - . tolerance of features defining the relative position of mating gears
- lubrication effectiveness at the different load and speed ratings.

  In particular the high speed ratings, giving high sliding velocity, and the low speed ratings that possibly impose a load on the teeth before the lubrication can become effective, must be regarded as capable of damaging the tooth contact surfaces.

- quality of lube oil :
  Its specification and brand should be considered in order to assure it is adequate for the application. Its cleanness, or its freedom from foreign particles capable of damaging mating tooth surfaces, must also be regarded as an important factor.

- capability of the manufacturer to take control and corrective actions on the production, in order not to allow the introduction of unknown factors leading to premature and random failures.
  For this reason, it is common practice, in manufacturing of parts for aeronautical application, to freeze the procedures judged capable of affecting their final characteristics (mainly heat treatment and finish machining operations).

b) Bearings
- choice of the most adequate type and geometry;
- correct interference with external and internal seats;
- internal clearance;
- correct position of contact patterns between races and balls or rollers;

c) Splines
- correct tooth geometry and adequate lubrication for splines that are movable under loads;
- adequate male/female interference for avoiding relative movement on splines specifically designed for being fixed.

d) Freewheels
- aligment on outer and inner rings;
- no external load to be applied on freewheel;
- aboundant lubrication to be assured with oil having the adequate viscosity level.

e) General

- Very strict rules must be applied in the allowance for design evolution. As a principle, no design or manufacturing procedure change shall be adopted, without first conducting a complete test program as an assurance that no risk of performance decay will be generated.
- The oil flow sent to the parts to be lubricated shall be adequate; an excess in oilflow will cause frothing and high power dissipation; an insufficient lubrication will cause an increase of the local temperature of sliding surfaces to values possibily unacceptable for the material.
- Attention must be paid to oil also for another reason; after doing the functions it must perform (lubricating and cooling) it has to be ducted as fast as possible out of contact with rotating parts, otherwise in most cases it will remain trapped within rotational elements that will act as real power absorbing hydraulic brakes.
- The bearing support elements and the gearshaft structure must be so stiff that their deformation will not significantly change the geometry and the behavior of mating teeth under all the excursion of applied loads.
- The most risky natural frequencies of the transmission and of relevant supports must be sufficiently far away from possible excitations.

LOW VIBRATION LEVEL AND LOW NOISE GENERATION

Vibration and noise are generated by the transmission housing structure, mainly excited by load variations in the gear meshing.

It is certainly important to act on the way these loads are transmitted to the structure in order to reduce their effect by :

- choosing a convenient shape and dimension of the structure in order to avoid any natural frequency to be excited by meshing frequency.
  A very effective method we use in FIAT for detecting the natural frequencies of a given structure, other than the calculation when the structure is sufficiently simple, is the holography method using laser light. In fig. 3 we give an example of the procedure : first a scan of the vibration amplitudes for a constant exciting power gives the natural frequencies; then the hologram taken for each of those frequencies offers the shape of the relevant modes. The actions for displacing the value of natural frequencies, if required, can then be taken with a better knowledge of the real situation.
- introducing dampers that would absorb part of the total energy introduced by the vibration source.
- applying extra-masses in convenient points as a last chance possibility for dropping the natural frequency of the structure out of the exciting load frequency.

Clearly the first action, although difficult to be performed, gives the best results because it allows at least a partial solution of the problem with a minor impact on weight.

We must recognize anyway the most logical way to proceed is to face the problem directly in its origin, the gear meshing. Here a lot of work can be done, that can save more costly interventions on external structures. The action to be taken shall be in the sense of reducing possible changes in the actual transmission ratio of meshing gears or along the contact on the same tooth pair or in the passage to subsequent pairs.

Many authors have identified which actions must be undertaken :

- to increase the total contact ratio by
  . increasing the addenda of spur gears (HCR or high contact ratio gears, having the profile contact ratio higher than 2, are defined with this aim).
  . increasing the helix or spiral angle and, particularly for bevel gears, assuring the largest possible dynamic contact pattern between meshing teeth.
  . reducing the pressure angle.
  . increasing the number of teeth (by using a finer pitch)
- to improve the accuracy by reducing
  . relative position of tooth profiles,
  . position of teeth relative to gearshaft supports
- to modify the involute profile for avoiding that position errors and deformations of teeth under load cause sudden engagement of teeth, thus generating heavy shocks on the gearshaft supports.
- to reduce the pitch line velocity by reducing the diameter of gears.
  Attention must be paid to the fact that any decrease in diameter will ask for an increase of gear face width : this will require closer tolerances on aligment of the pair for avoiding unequal load distribution along teeth.

Very good results in this field were obtained by FIAT with the optimization of bevel gears contact patterns and by adoption of HCR spur gears. In bevel gears, for example, the increase of the contact pattern area demonstrated to be a powerful way to reduce noise and vibration on transmissions. Of course the manufacturing of a bevel pair becomes more difficult than traditionally because :

- the setting of the grinding machine must be much more accurate

- the control of the active surface shall be based on sophisticated procedures.
  We remind here some possibility offered by numerical control machines capable of supplying a grid of profile positions relative to a given correct master gear or by newly developped machines that visualize transmission ratio irregularities of a given pair or train of gears.
  The use of traditional contact pattern check with Tester Machines can only be a side control mainly adopted for checking the manufacturing constancy. Modern computer programs help the Manufacturer by supplying him the information on how to modify the machine setting in order to obtain the wanted modification on the grid of profile positions.
  Just as an example of application of this technique, in fig. 4 we give the results obtained in one application.

- when lengthening and widening the contact pattern, it is necessary to take care of the effect this modification can induce, consisting mainly in the frequent displacement of the contact pattern over the borders of the tooth flank as this effect can cause load concentrations with scoring leading rapidly to the deterioration of the surface.
  For this reason, manufacturing tolerances and mounting procedures must be kept under rigid control.

In fig. 5 we give . example of the contact pattern shapes adopted in a helicopter gearbox produced in FIAT AVIAZIONE, before and after a noise reduction campaign. The obtained noise reduction of the stage is of the order of 10 dB over 100 dB.

Fig. 6, instead, gives an idea of the modification introduced in the epicyclic stage of the same gearbox by adopting HCR gears.

The contact ratio went up from 1,47 to 2,04 with a noise abatement in the stage of 8 dB over the original 98 dB.

We underline the care to be taken in manufacturing these gears. The position error of teeth must be reduced to the minimum obtainable with existing machine tools and the profile must have a correction capable of assuring an adequate load distribution on teeth along the contact line.

The literature gives some other features that, we recognize, can be useful in reducing the transmission of vibration such as, for example :

- damping materials bonded to vibrating surfaces or filling hollow shafts

- vibration absorber masses that can counteract the vibration of the main structure, thus attenuating the effects on the aircraft body

- enclosures containing the noisy structure that avoid most of the noise to reach the surrounding ambient.

As a principle these features have never been applied by us, mainly because they heavily impact on weight. Our suggestion is to utilize them possibly for small corrections to be obtained lastly on a fully defined design, when all the previous possibilities have been evaluated and adopted whenever convenient.

HIGH WORKING TEMPERATURE

In recent years, the working temperature in transmission gearboxes showed a continuous trend to increase for many different reasons that we can refer, mainly, to the need of weight minimization. In fact, with this aim :

- gears are operated at the highest possible stresses, thus increasing the heat to be dissipated;

- the temperature of oil is increased to the highest possible level with the consequent possibility of reducing the dimensions of the heat exchangers and the quantity of oil to be kept in oil tanks.

The effects of both actions, of course, are beneficial on the weight of the system. Furthermore, in aeronautical applications the transmission is required to show its capability to run, for periods going up to 30 or 60 minutes, after leaking out the lube oil.

The high working temperature affects characteristics of metal structure, thus weakening the transmission elements, and reduces the effectiveness of lubricating oil, thus increasing the probability of serious damages of the parts : with gears for example quite often, as a consequence of the above conditions, problems of scuffing, spalling and scoring will arise.

The designer must therefore seek those design choices that allow for a reduction of the risks due to high running temperature :

- to use small gear modules for reducing the sliding velocity and to study suitable profile modifications, in order to reduce the combined effect of sliding velocity and high contact stresses.

- to adopt the most convenient type and geometry of bearings, considering the possible sliding effects of rolling elements on races and internal preloads, as these are major effects of power loss.
  The dimensions and shape of cage pockets are also important for minimizing the loads transmitted between rolling elements and cage. The lube oil must be fed in a convenient way for assuring that the critical points are reached.

- to define a suitable lubricating system, capable of keeping the temperature of sliding surfaces in gears and bearings within acceptable limits and of generating an adequate oil film thickness between the mating surfaces with the aim of preventing metal to metal contact.

- to adopt the adequate oil seals and possibly to assure their lubrication and cooling for avoiding the ra

pid deterioration of the sliding surfaces.

All the above points fix some rules to be followed for obtaining a sound design, but don't give any possibility to go to a temperature level much higher than traditionally experienced. The materials normally used for gears, the well known AISI 9310 or similar case hardening steels, don't allow to run the transmission at temperatures higher than 180°C for long time without causing an unacceptable reduction in the surface hardness.

This phenomenon becomes even more important in the case of running in no oil condition, when the hardened surface can soften and get destroyed in few minutes.

We have two answers for these problems :

- to use a nitriding steel, that can run at a temperature of 450°C (against 180°C max acceptable for case hardened steels).
  The no oil condition can then be suffered much better.
  This solution has anyway some disadvantages caused by the thinner hardened skin that, especially for large and thin web gears, possibily doesn't give allowance for grinding after heat treatment, if a final grinding operation is required by the needed tooth precision.

- to use newly developped carburizing steels capable of displacing the critical temperature from 180°C up to 300°C.
  Among these steels, proposed by different Vendors, we have examined and tested the following types :

  . VASCO X 2M CM
  . Carpenter EX 00053
  . CBS 600.

  All of them offer a big advantage, even if lesser than nitriding steels, over the AISI 9310 when running without oil; for example the surface hardness remains higher than 60 HRC after long soaking at temperatures of 300°C.
  The manufacture can take advantage of the higher grinding allowance offered by their thicker hardened skin.
  Some relative data sufficient for putting the three steels in a value scale have been worked out; we just prefer not to give them here officially because this can be a delicate matter, influenced by the heat treatments carried out by us.

At this point of the evaluation of material for gears, the next necessary step to be made is evidently on lubricants. In fact, present lube oils cannot be effective at temperatures higher than the mentioned 180°C. Now, as the new gear materials give the possibility to increase consistently the normal running temperature, a new lubricant capable of the required characteristics of stability, cooling and lubricating effectiveness at higher temperatures, would represent a great progress.

INVULNERABILITY

Military requirements ask for transmissions capable of surviving and working satisfactorily for a certain period of time in the case some vital parts are damaged by impact of bullets or foreign objects.

Possible ways that can be followed in order to assure an acceptable level of invulnerability are :

- to put external protections on the most delicate areas, using shock absorbing walls capable of deviating the bullets or absorbing their energy. This solution causes a weight growth, generally not acceptable.

- to locate the transmission in the safest position, by sorrounding it with a number of accessories, fire walls and similar devices whose damage will not interrupt the vital functions of transmission.

- to properly shape the casings, in order to avoid frontal impact of bullets.

- to use special materials for the casings (for example composite materials) that can suffer, without major side effects, damages and perforation due to bullets.

- to oversize some parts, like shafts, bearings and flexible couplings or to shield them with steel liners if they cannot be protected in other way.

- to double some functions, with parallel elements in order that the loss of one device doesn't affect the capability of the other to satisfy the needs of the mission.
  This philosophy has been largely used by us in the definition of the lube and heat exchange systems. In multiple engine helicopters, the solution of collecting the power at the last reduction stage is the less vulnerable solution because damages caused on one transmission chain are less likely to affect the other parallel power paths.
  The suggested precaution in this case is to accurately study some shields and baffles capable to stop the detached particles from moving free inside the gearbox and damage the surrounding unaffected parts.
  The same philosophy has been often used in defining the suspension system of the powerplant (engine + transmission) on the A/C.

MAINTAINABILITY

It can be defined as the minimization of the "task of maintenance in service". As such two possible ways are offered for achieving this goal :

. to increase the T.B.O. or, following the modern tendency of adopting the procedure of "maintenance on

condition", the MTBR.
With such a procedure the transmission is allowed to run as long as the rising of a trouble is detected. Of course this procedure will be fully and satisfactorily adopted only if a monitoring system is defined, capable of detecting the rising of any inconvenience and of warning the operator about it.
At the moment, unfortunately, this technology is not completely developed.

to reduce the task necessary to perform inspections and revisions such as for example :

a) to put the monitoring instruments in accessible and visible location for easy reading and monitoring;

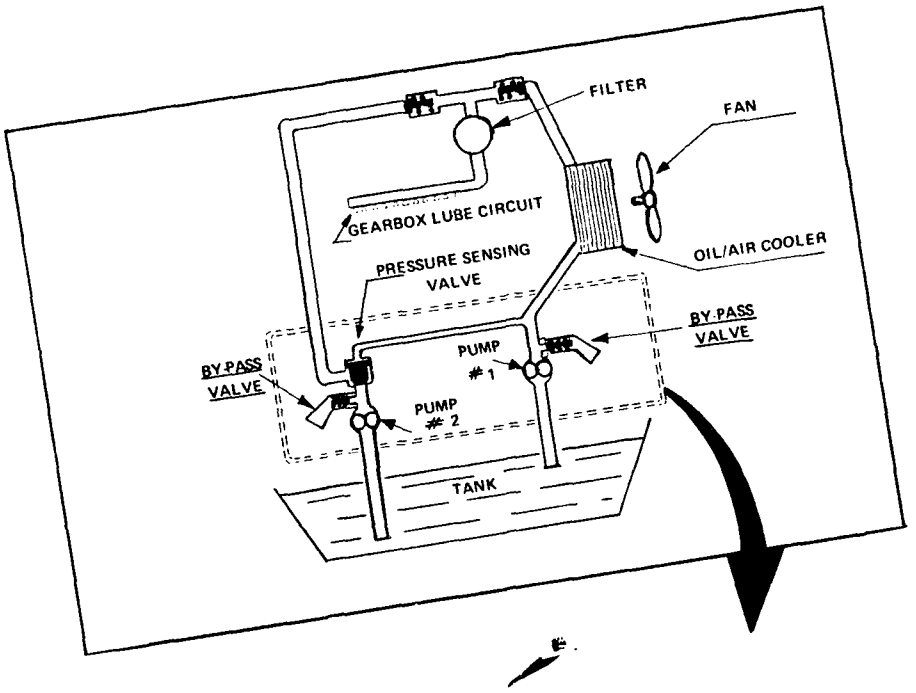
b) to design the whole assembly so that it can be split in detachable subassemblies or modules separately maintainable.
The designer shall care for making easily removable from on board of the vehicle those elements or groups, which are more likely to be damaged or deteriorated, such as, for example, high speed stages, *free-wheels, oil pumps, filters, lube nozzles,* heat exchangers, etc. Ideally the intervention for maintenance of these elements should be carried out in the simplest manner, i.e. without requiring the removal of adjacent parts, without leaving detached loose parts, without asking for the use of special tooling.
Of course the maximum advantage of modular maintenance will be obtained when the monitoring devices said in a) above will allow the identification of the trouble point, so that the intervention will be local; our feeling anyway is that a lot of development is still to be done in this field.
We note here finally, while speaking about modularity, that this characteristic is highly advantageous also for an easier overhaul on ground on the whole transmission, because it renders the strip and rebuild activity much shorter.
As an example of application of these concepts, we show an exploded view of a gearbox designed by FIAT AVIAZIONE, where the extreme modularity of the whole design (see fig. 7) can be easily noted.

CONCLUSION

The analysis of the requirements to be satisfied in the design of a modern transmission shows that the choice of the best compromise is really a difficult task to be performed. Luckily, new technologies supply us the possibility to improve the speed and the reliability of analysis and to reduce the drafting time.

For a given problem, then, more resources can be used for increasing the number of studied solutions, for deepening the relevant analysis and for comparing the results in view of a more conscious and dependable final choice.

Let's not forget anyway that the improvement of technology will never eliminate the need of the experienced Designer; only he,using technology as a tool, will eventually be able to impress the personality of his experience on the design.



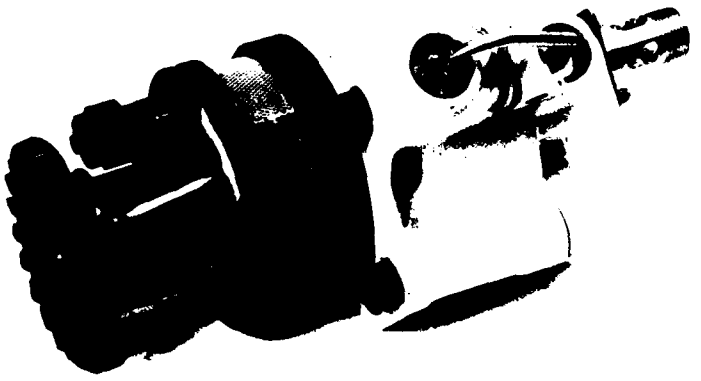


Fig. 1 - Schematic diagram and picture of a fail safe pump applied on a transmission designed by FIAT AVIAZIONE.

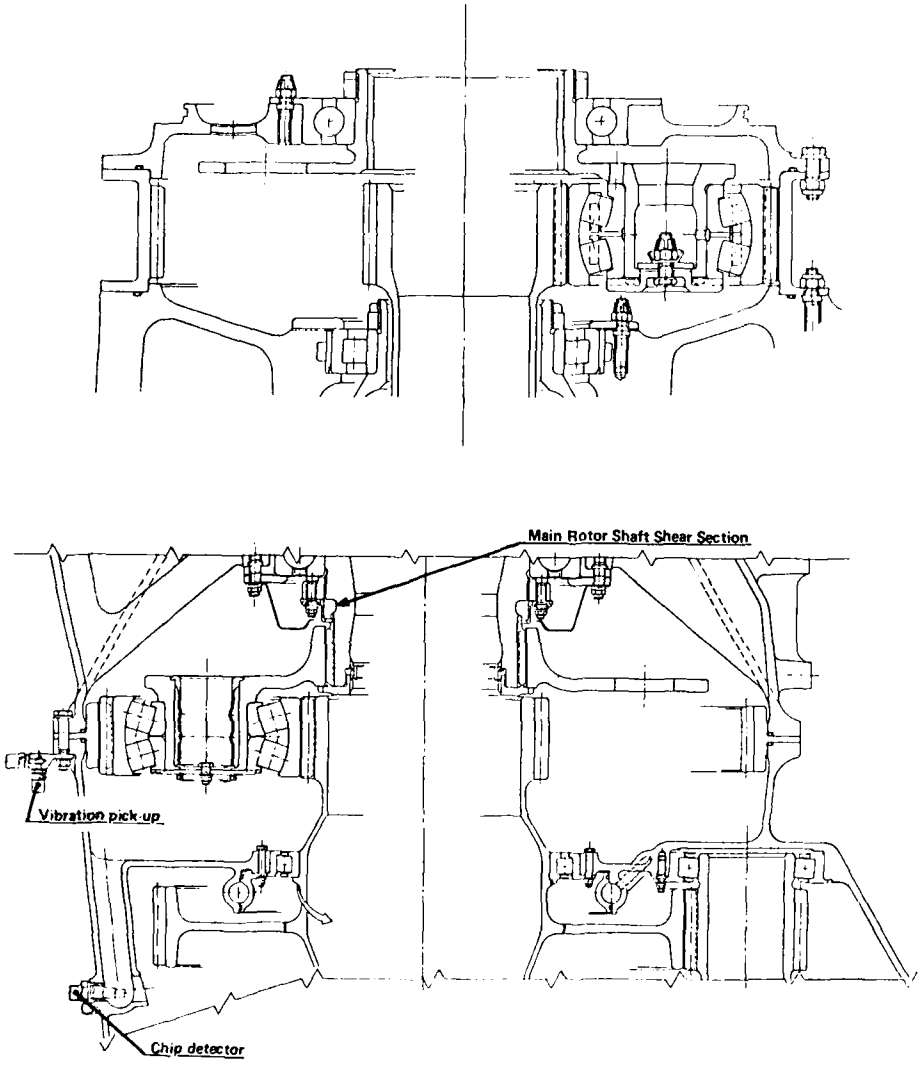


FIG. 2 - Longitudinal sections of two helicopter gearboxes. The second is the result of an optimized fail safety design.

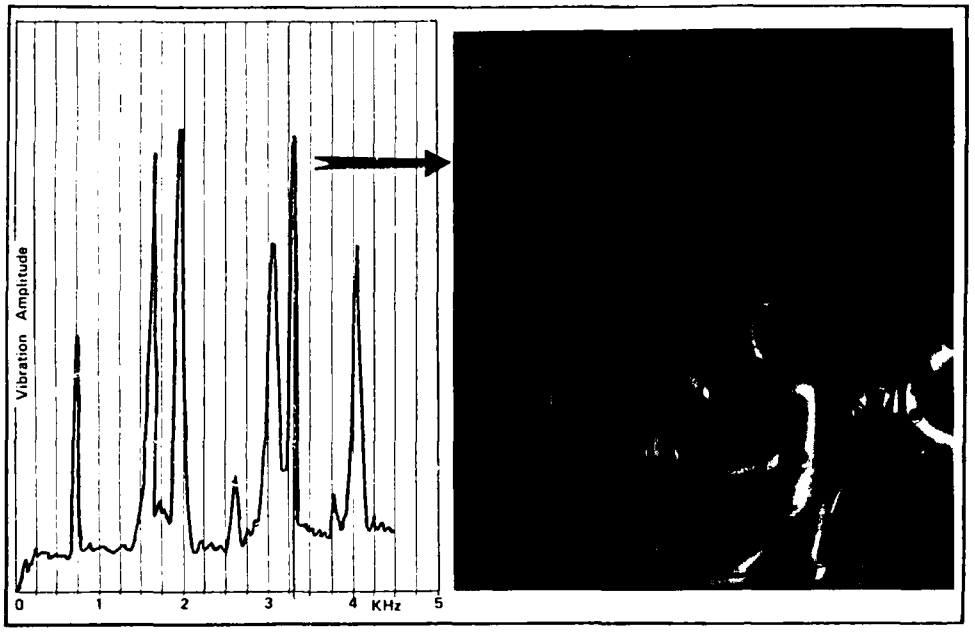


FIG. 3 - Example of natural frequency search diagram and of single mode hologram of a helicopter main gearbox casing

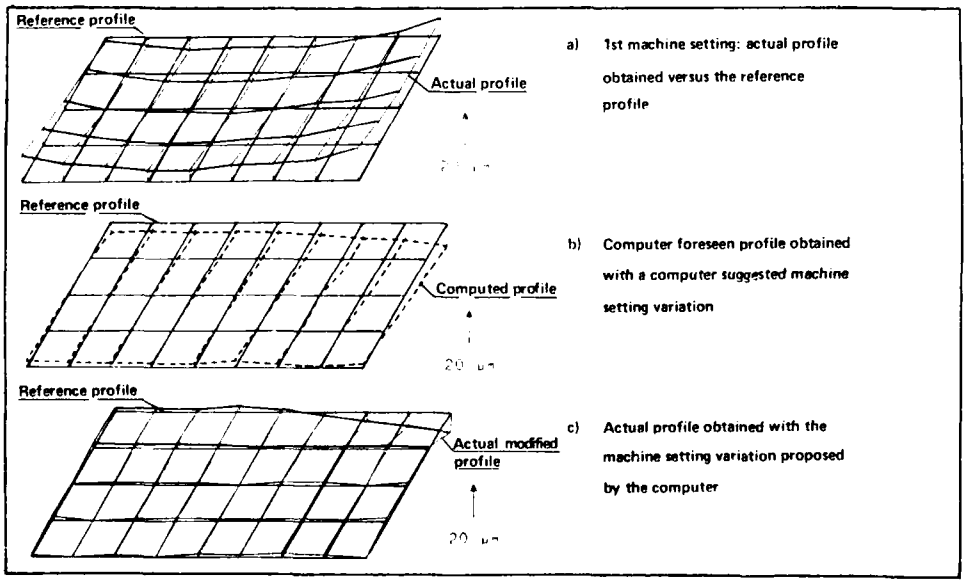
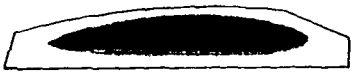
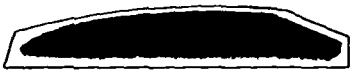


FIG. 4 - Example of application of the profile position grid technique



a) Traditional Contact Pattern



b) Increased Contact Pattern

FIG. 5 - Example of dynamic contact patterns obtained on a bevel pair of a helicopter gearbox. The noise abatement obtained going from a) to b) is 10 dB over 100 dB

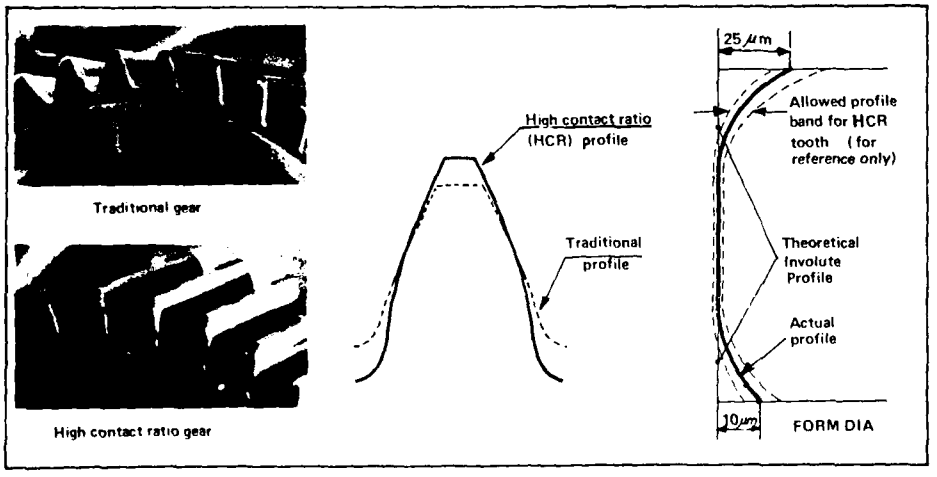


FIG. 6 - Application of HCR profile on the bevel pinion of a helicopter gearbox

DISCUSSION

A.Borrien, Fr

The definition of case depth that you have given corresponds to the depth at which the hardness is 520HV. Does this value come from the normal specifications or from particular standards?

Author's Reply

The hardness of 520HV comes from the specifications of the client, the builder. Personally, I prefer for high quality case hardened materials (1% chrome, 4.4% nickel) a limit of 550HV for the effective case depth.

B.A.Shotter, UK

The analysis of this problem is even more complex than the author has suggested. The root stress fluctuations which are experienced by planet or idler gears are significantly different to those of unidirectionally loaded teeth. In the case of contact stresses one has to be careful as to the surface fatigue initiation mode: many examples of surface breakdown start as micropitting. In this case, the origin of the failure is much smaller than the Hertzian contact width. The propagation of this damage is highly dependent upon the stress state of the surface layers. Thus, whilst the authors' approach is considered to be an excellent starting point, even more factors have to be considered to make full appraisal of the required case definition.

Author's Reply

I agree with the point of view of Mr Shotter

But, nevertheless, it cannot be contested that the effective case depth on the flanks and in the root radius have a different optimum value for endurance limit for contact stress and bending stress.

The actual information on the drawings and in the specification is often inadequate.

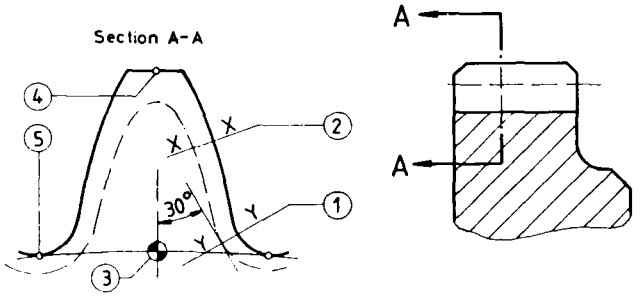
Namely : 1. On the flanks a minimum effective case depth larger than the "depth of maximum shear stress" is asked but no maximum because this maximum does not decrease the strength against Hertzian pressure.
As you can see in figure 4.1.1. we reach an optimum at 0.3 modul.

2. On the 30 tangent in the root-radius - a minimum effective case depth of 0.1 modul and a maximum of 0.3 modul is asked because both a bigger and a smaller layer decrease the strength against bending stress (figure 4.1.2.).

So, for example - taken in 1.1. - we can recommend the following specification.

INSPECTION METHOD CONTROL

HARDNESS DETERMINATION



1	EFFECTIVE CASE DEPTH X-X	MIN. 0,55 mm	MAX —
2	EFFECTIVE CASE DEPTH Y-Y	MIN. 0,27 mm	MAX. 0,45 mm
3	TOOTH CORE HARDNESS	MIN. 420 HV	MAX. 480 HV
4	SURFACE HARDNESS	MIN 670 HV	MAX. 775 HV
5	SURFACE HARDNESS	MIN 670 HV	MAX. 775 HV

NOTES.

1 EFFECTIVE CASE DEPTH IS THE LENGHT OF LINE X - X OR LINE Y-Y MEASURED FROM THE SURFACE TO THE LAST POINT TOWARD THE CORE HAVING THE REQUIRED MINIMUM HARDNESS VICKERS 520 HV
2 LINE X-X IS LOCATED ON THE WORKING PITCH CIRCLE, SQUARE TO THE TOOTH FLANK
3 LINE Y-Y IS LOCATED AT SQUARE ON THE 30° TANGENT TO TOOTH ROOT RADIUS.
4 THE TOOTH CORE HARDNESS IS TO MAKE IN THE CENTER OF THE TOOTH TO THE ROOT CIRCLE. (±1mm)

REFERENCES : 1. Beanspruchungsgerechte Wärmebehandlung von einsatzgehärteten Zylinderrädern
K. Börnicke 1976

2. Carburizing and carbonitriding.
A.S.M. 1977

3. Maschinen-elemente band II
G. Niemann H. Winter 2e Edition

4. Tandwielen
Prof. R. Snoeys Ir. R. Gobin 1979

5. Traité theorique et pratique des engrenages 1
G. Henriot 6e edition

6. I.S.O. DP 6336
The calculation of load capacity of spur and helical gears.

ACKNOWLEDGMENTS : The author is gratefully indebted to the following people for valuable suggestions and help during the project : 1. Dr. J. Van Beghem
CRIF/WTCM Gent - Foundry research centre

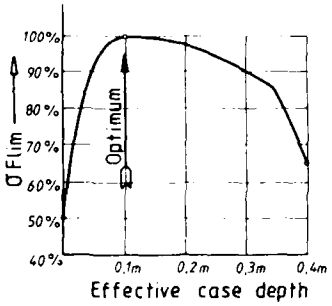
2. Mr. Philippe Queille
L'Air Liquide France - Claude Delorme research centre

3. Mrs. Hilde Watteeuw
M.C. Watteeuw - N.V. - Brugge - Quality Control Laboratory

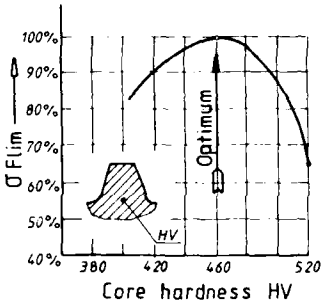
I.S.O. only mentions that the endurance limit for case hardened alloy steel is applicable to an effective case depth of at least 0,15 module on a finished part. This means, for aircraft quality, after grinding the flanks and the root-radius. According to K. Bornicke - the resistance against breakage in the tooth-root with case hardened steel depends on the effective case depth in the root-radius - at 30° tangent (figure 3.1.2.).

3.4. ADEQUATE CASE DEPTH FOR TOOTH BREAKAGE.

The figure below 3.3.1. shows very clearly the endurance limit value in function to the case depth. The optimum limit for bending endurance occurs when we have a case hardened layer 0,1 modul. A smaller layer decreases the limit quickly. A bigger layer decreases the limit slowly till 0,3 modul and from then on, the limit decreases more quickly. The core hardness at the rooth-cylinder, measured at the tooth-center, is also very important for the bending stress limit value.
Bornicke and also G. Niemann-H. Winter both agree on the case depth and the core hardness to obtain a maximum resistance. Values of these are printed in figure 3.3.2.



Effective case depth
Fig 3.3.1



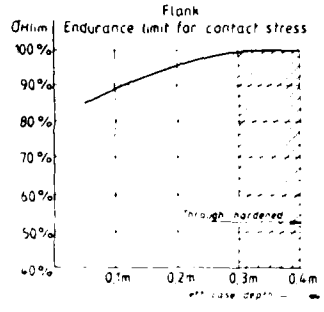
Core hardness HV
Fig 3.3.2

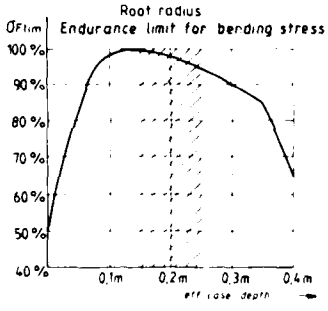
Again, three important conclusions are to be made :

1. A surface hardness of 670-755H_{V1} guarantees a maximum resistance against tooth breakage.
2. The core hardness is an important parameter for the strength resistance of gear-teeth. For high quality alloy steel a core hardness of 400-460 H_{V10} must be obtained.
3. The effective case depth - measured in the root radius at 30° tangent - is optimum 0,1 modul - but may not exceed 0,3 m. A tolerance of 0,15 - 0,25 modul is usually applicable.

4. PROPOSAL for SPECIFICATION of CASE DEPTH - SURFACE and CORE HARDNESS on CASE HARDENED STEEL GEARS.

When we put the conlclusions about the endurance limit for Hertzian stress and tooth-root-stress together - we see that a different adequate case depth is asked.





3.3. ENDURANCE LIMITS FOR BENDING STRESS.

The nominal bending endurance limit takes into account the influence of the material on the tooth root stress witch can be permanently endured. A running time of 3.10^6 cycles is regarded as the beginning of endurance limits.
The limit can be found by pulsating tests or gear running tests for any material and any state of that material. Limiting values, obtained by field of experience, can also be used.
If such data are not available, guide values can be determined with the help of the fields in figure 3.2.. The here indicated values for nominal bending endurance limits apply to the following gear dimensions at service conditions :

- Module m = 3 up to 5 mm Helix angle = 0° - Stress correction factor Y_{ST} = 2.1
- Roughness in the tooth root R_{tm} 10µm - Linear speed v = 10 m/s
- Basic rack according to I.S.O. 53-1974 - Facewidth b = 10 up to 50 mm.

The values included in the diagrams correspond to a failure probability of 1 %.

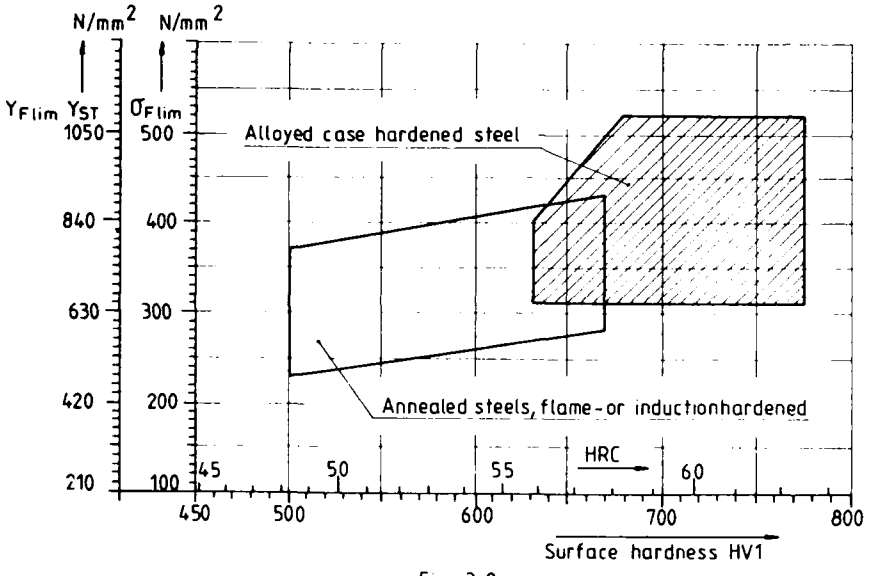


Fig 3.2

The bending endurance limit for case hardened alloy steel, shown in figure 3.2. has a very wide range. Values for $\sigma_{F\ lim.} \cdot Y_{ST}$ go from 650 N/mm2 to 1.300 N/mm2. You can find more specific values in some gear literature, such as in the German book "Machinen-elemente G. Niemann H. Winter", from which we take the following values for "bending endurance for case hardened steel (according to D.I.N. 1 7210).

DIN 1 7210 Quality	Core hardness HV_{10}	Surface hardness HV_1	Bending endurance limit Flim. . Y_{ST}	static
16 MnCr5	270	720	860 N/mm2	2150 N/mm2
15 CrNi6	310	730	920	2300
17 CrNiMo6	400	740	1000	2800

Gears as used for aircraft are of high quality steel, for example 17CrNiMo6 and even the higher classed 14CrNi18.
For the bending stress limit we have the same main influencing factors to aim at the optimum as for the contact stress limit (see text 2.3.).

3.2. METHOD-B of the I.S.O. APPROACH of TOOTH BREAKAGE.

Hereby it is assumed that the highest tooth root stress arises by applying a force at the outer point of single tooth pair contact.

3.2.1. Tooth root stress.

$$- \sigma_F = \sigma_{FO} \cdot K_A \cdot K_V \cdot K_{F\beta} \cdot K_{F\alpha} \leq \sigma_{FP} \qquad \text{Wherein :} \quad (11)$$

σ_{FO} : the local tooth root stress defined as the maximum stress at the tooth-root when loading a flawless gear by the static nominal moment.

K_A : application factor

K_V : dynamic factor

$K_{F\beta}$: longitudinal load distribution factor for tooth-root-stress

$K_{F\alpha}$: transverse load distribution factor for tooth-root-stress.

$$- \sigma_{FO - B} = \frac{F_t}{b \cdot m_n} \cdot Y_F \cdot Y_S \cdot Y_\beta \qquad \text{Wherein :} \quad (12)$$

F_t : Nominal tangential load.

b : Facewidth.

m_n : Module, normal section

Y_F : Tooth form. factor.

Y_S : Stress correction factor.

Y_β : Helix angle factor.

3.2.2. Permissible tooth root stress.

$$- \sigma_{FP} = \frac{\sigma_{F\ lim.} \cdot Y_{ST} \cdot Y_{NT}}{S_{F\ min.}} \cdot Y_{\sigma rel T} \cdot Y_{R\ rel\ T} \cdot Y_X \qquad \text{Wherein :} \quad (13)$$

$\sigma_{F\ lim.}$: Nominal bending endurance limit.

Y_{ST} : Stress correction factor, for testgear dimensions.

Y_{NT} : Life factor for tooth-root-stress related to test gear dimension.

$S_{F\ lim.}$: Minimum safety factor.

$Y_{\sigma rel\ T}$: Relative sensitivity factor, related to the test gear dimension (takes into account the notch sensitivity).

$Y_{R\ rel\ T}$: Relative surface condition factor.

Y_X : Size factor for tooth root strength.

3.2.3. Arithmetic safety factor for tooth root stress.

On the basis of the strength determined at a test gear. The factors were named above.

$$- S_F = \frac{\sigma_{F\ lim.} \cdot Y_{ST} \cdot Y_{NT}}{\sigma_{FO - B}} \cdot \frac{Y_{\sigma rel\ T} \cdot Y_{R\ rel\ T} \cdot Y_X}{K_A \cdot K_V \cdot K_{F\beta} \cdot K_{F\alpha}} \qquad (14)$$

So, the hardness gradient can be seen as the limit of allowable shear stress. When we study this line, we see that "b" is the zone where pitting appears for case hardened alloy steel. (see figure 2.5.b.). There are three conclusions to be made when we study figure 2.5.2. :

1e : The surface hardness is less important with respect to pitting. This is the reason why we can take a bigger tolerance, namely (zone "c") 670-775 HV1.

2e : The effective case depth must be larger than the "depth of maximum shear stress". A bigger hardened layer on the flanks can never be harmful or decrease the strength against Hertzian pressure.

3e : A higher core-hardness can also improve the strength against Hertzian pressure. This because the hardness gradient becomes flatter. As you can see in figure 2.5.b., the curve "2" is flatter than curve "1" and has a higher limitvalue against shear stress.

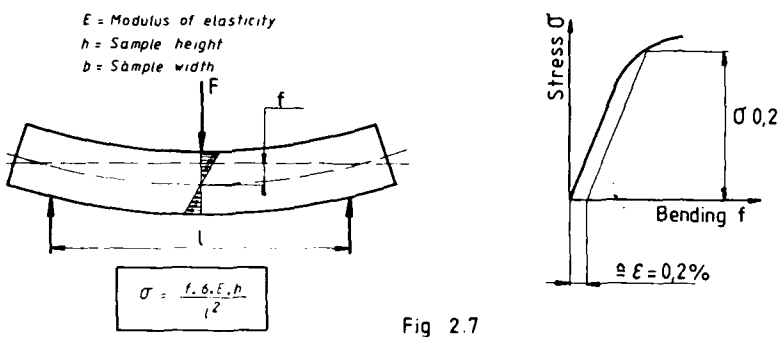


Fig 2.7

3. CALCULATION OF TOOTH STREGTH

3.1. TOOTH BREAKAGE and TENSILE STRESS at the TOOTH ROOT.

In the first place, gear-teeth must be resistant against tooth breakage. This means that there must be enough resistance, in the root radius against the occurring tensile stress.
The calculation of this resistance is based on those used for a steel beam, loaded on its free end with a force F.
In the clamped area, a tensile stress σ_F arises (figure 3.1.1.).
A gear tooth is different from a square beam in form and function.
The tooth load in case of single engagement, this means that only one flank pair is in contact, is shown in figure 3.1.2.
The tooth form factor Y_F is the most important parameter in the calculation of tooth strength. This factor depends on the involute form, the value of the root radius, the pressure angle and the pressure angle of the highest point for single contact.
As for Hertzian pressure - the tooth breakage has been studied by I.S.O. (*) We have accepted method-B and a copy of the formula is given as information. Further, we will concentrate on the case depth in the tooth root radius and its relation to the bending-endurance limit σ_{Flim}.

(I.S.O. / DP 6336)

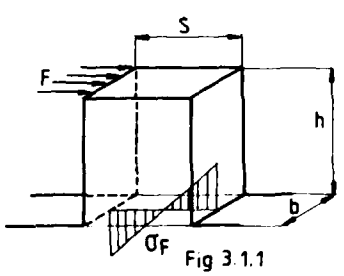


Fig 3.1.1

$$Y_F = \frac{6(h_F/m_n)\cos\alpha_{en}}{(S_{Fn}/m_n)^2\cos\alpha_n}$$

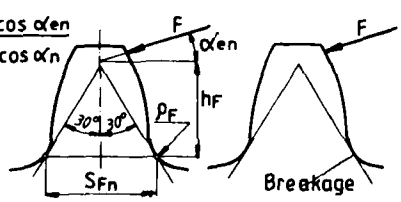


Fig 3.1.2

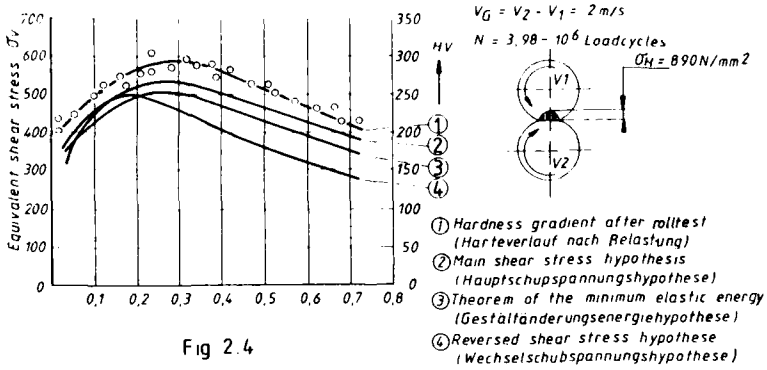


Fig 2.4

Further experiments have shown that theorem of the minimum elastic energy σvg is the most real approach for the shear stress.
As already said before, the yield point defines the limit stress of alloy steel gear. The figure 2.5.1., illustrates the evolution of shear stress and the depth of maximum shear stress when the Hertzian pressure increases. As you can see, they both enlarge respectively from σvg1 to σvg2 and from T1 to T2. This means that the depth of maximum shear stress lies deeper under the surface. Flank damage or pitting occurs in the lined part "a" of the curve.

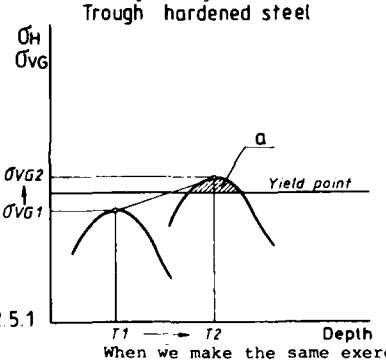


Fig 2.5.1

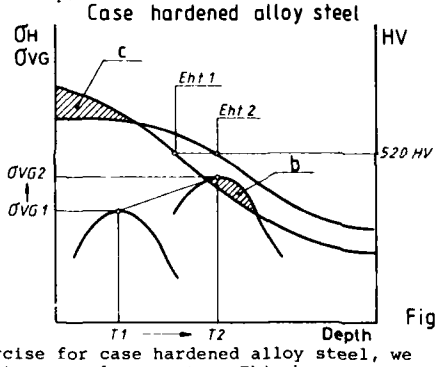


Fig 2.5.2

When we make the same exercise for case hardened alloy steel, we have to take the σ0,2 limit as equal parameter. This because, as said before, the determination of the yield point in a hardened layer of case hardened alloy steel is practically impossible. σ0,2 is the limit where an irreversible deformation of 0,2 % appears in the bending test. (see figure 2.7.)
It has already been proved that the curve of σ0,2 limit and the hardness gradient have a parallel trend. For each quality of case hardened alloy steel, there is a correlation between the σ0,2 limit and the hardness gradient. (see figure 2.6.1. and 2.6.2. an example for 16 MnCr5 - K. Bornitze).

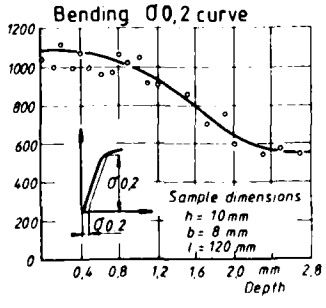


Fig 2.6.1

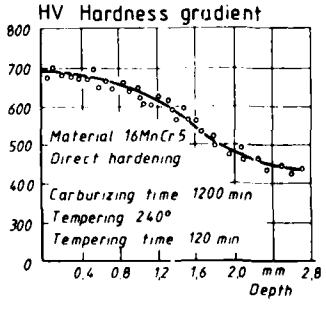


Fig 2.6.2

Two cylinders represent two meshing gear teeth with respective curvilined radius of ρ_1 and ρ_2. When they are pressed together with a load F_n, then Hertzian pressure and a flat surface occurs in the contact area. This surface has a value of "2a" (see fig. 2.1.

Furter, we refer to G. Henriot #1 and the most current theory about the origin of pitting. The total flattening, the amount of the flattenings of both gear teeth, on the radius is : u = 0,0005 Fnu with : (5) Fnu = Nominal tangential force (in Newton) on the reference cylinder, in a transversed section on the facewidth of 1mm.
The length of the flat surface 2a is :

$$2a = 0{,}063\sqrt{Fnu \cdot \rho r} \qquad \text{wherein : (6)}$$

ρr = relative profile radius and :

$$\frac{1}{\rho} = \frac{1}{\rho_1} \cdot \frac{1}{\rho_2} \qquad (7)$$

The figure alongside illustrates the different pressures in the subsurface, down to the core for cylinder ρ_2, following stresses can be distinguished :

σ_z = with a direction axis O-Z

σ_y = with a direction axis O-Y

σ_x = with a direction axis O-X

σ_y and $\sigma_z = \sigma_H$ on the surface

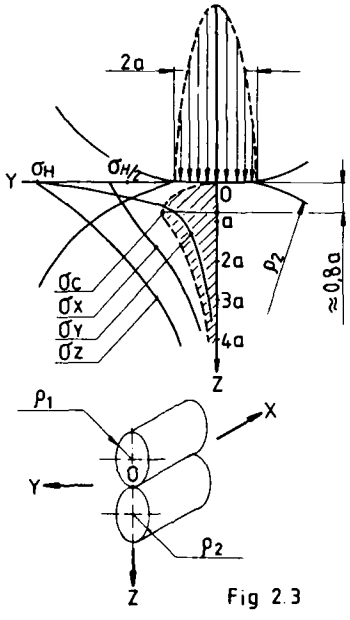


Fig 2.3

σc, the shear stress, is the result of two squared stresses. This shear stress is at its maximum under an angle of 45°, with value which is half the difference from the normal stresses.
The shear stress is zero at the surface and comes to its maximum on the "depth of maximum shear stress" ≈ 0,8 a (8)

$$\sigma c \approx 0{,}3\,\sigma_H \qquad (9)$$

$$\approx 59\sqrt{Fnu \cdot \frac{1}{Pr}} \qquad (10)$$

This shear stress is very important because it is the most important cause of pitting. For case hardened alloy steel, we must obtain a hardened layer (eff. case depth) of at least twice the depth of maximum shear stress.
Most publication stipulate that σc may not exceed the Yield point of the used steel. But, the determinationsof the Yield point in a hardened layer of case hardened alloy steel is practically impossible !

Klaus Bornecke #2 has made a study about the heat treatment of case hardened cylindrical gears and their load capacity. We have made a summary with the most important particulars.
In this exposition, the shear stress is a standard stress, which can be diffined by three hypothesises :

1. Main shear stress Vsub
2. Theorem of the minimum elastic energy VG
3. Reversed shear stress VW

The comparison of these three stresses is represented in fig. 2.4.

#1 : Georges Henriot : Traite theorique et pratique des engrenages 1. Chapitre VII

#2 : Klaus Bornecke : Beanspruchungsgerechte Wärmebehandlung von einsatzgehärten Zylinderrädern.

2.2.2. Allowable contact stress (Permissible Hertzian pressure)

$$\sigma_{HP} = \frac{\sigma_{Hlim} \cdot Z_N}{S_{Hmin}} \cdot Z_L \cdot Z_R \cdot Z_V \cdot Z_W \cdot Z_X \qquad \text{Wherein :} \qquad (3)$$

σ_{Hlim} - Endurance limit for contact stress
S_{Hmin} - Minimum demanded safety factor for contact stress.
Z_L - Lubricant factor
Z_W - Work hardening factor
Z_X - Size factor for contact stress.
Z_R - Roughness factor
Z_V - Speed factor
Z_N - life factor for contact stress.

2.2.3. Safety factor for contact stress (against pitting)

$$S_H = \frac{\sigma_{Hlim} \cdot Z_N}{\sigma_{HD}} \cdot \frac{Z_L \cdot Z_R \cdot Z_V \cdot Z_W \cdot Z_X}{K_A \cdot K_V \cdot K_{H\alpha} \cdot K_{H\beta}} \qquad (4)$$

The factors were named above

2.3. ENDURANCE LIMIT FOR CONTACT STRESS.

The endurance limit for contact stress can be regarded as the level of Hertzian stress wich a material will endue without damage for at least 50.10^6 loadcycles. Testing discs in disc machines gives an indication of trends of relative values of endurance limit for contact stress. These values can also be established on the basis of data from gears in service.
The fig, alongside can be used as a guidance for surface hardened steels - when the requisite data are not available.
The values correspond to a failure probability of 1%. The endurance limits for Hertzian pressure shown in this diagram are valid for a mean surface roughness Rtm = 3µm (Z_R = 1) a tangential speed V = 10m/s (Z_V = 1) and an oil viscosity ν = 100 mm^2/S (Z_L = 1).
When we look at the graphics zone concerning case hardened alloy steel, principally used for aircraft gears, this zone contains a very wide range for Hertzian pressure endurance values, namely from 1300 to 1650 N/mm^2.
For high quality gears used in aircraft, we must aim at the optimum. This optimum is mainly influenced by :

1. Material composition
2. Mechanical properties.
3. Hardening process, depth of hardened zone, hardness gradient.
4. Structure (forging-rolled bar-cast).
5. Residual stresses.
6. Material cleanline and defect.
   We will concentrate on point 3.
   According to the I.S.O.-diagram, it is necessary to have a surface hardness of 670-775 H_{V1}, in order to reach a maximum endurance limit for contact stress (1650 N/mm). Nearly the whole gearliterature agrees on these values. But what about the case depth with regard to the limit for Hertzian pressure ? Only an "adequate case depth" is stipulated by I.S.O. We have examined this element more closely.

(* by I.S.O. / DP 6336 III).

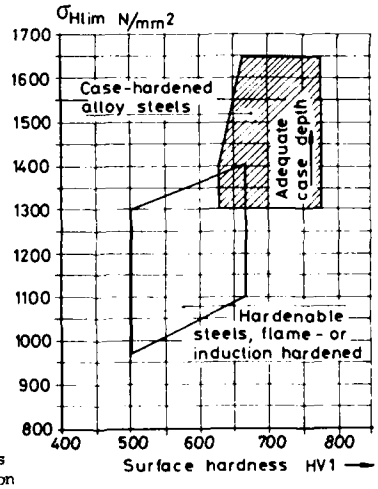


Fig 2.2

2.4. ADEQUATE CASE DEPTH FOR CASE HARDENED ALLOY STEEL.

2.4.1. Shear stress in the subsurface layer.

Not only the Hertzian pressure, but also an appearing micro-stress in the subsurface layer is the cause of pitting. Hertz already knew this - but up to now there is still no agreement about this shear stress.

2. CALCULATION OF SURFACE DURABILITY (PITTING).

2.1. HERTZIAN PRESSURE

Pitting is small material particles breaking out of a tooth flank, leaving pits. This flank damage can be caused by the reversed stress fatigue in the contact area of underload meshing gear-teeth. It arises when the occurring contact stress exceeds the allowable contact stress and depends on the number of load cycles.
Pitting principally appears in the dedendum flank where a negative sliding speed occurs. The small pits, near the root fillet of a case hardened tooth can become the origin of a crack -possibly leading to tooth-breakage. It can also cause unacceptable vibrations and excessive dynamic overloads.
For these reasons Pitting is intolerable for aircraft gears.

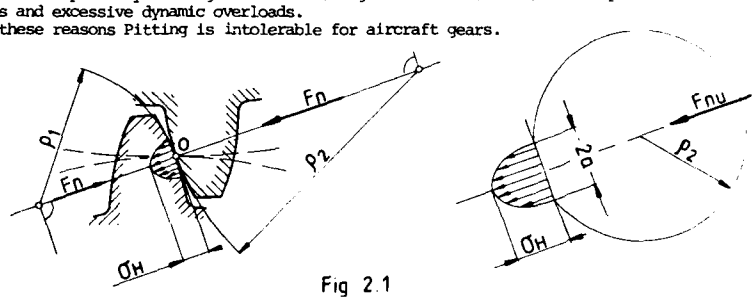


Fig 2.1

The load capacity of tooth flanks is determined according to the principle and formula of HERTZ. Therefore contact stress is sometimes called "HERTZIAN PRESSURE".
By ISO ✱ the basic Hertzian formula is elaborated and completed with all possible factors which can effect the load capacity and surface durability. Therefore, we take this approach as startingpoint in our further explanation.
Further we only examine the endurance limit for contact stress (σ_{Hlim}) - for its involvement with the "case depth".

2.2. ISO APPROACH OF SURFACE DURABILITY (PITTING)

2.2.1. Contact stress (Hertzian pressure) at the operating pitch circle .

$$\sigma_H = \sigma_{HO} \sqrt{K_A \cdot K_V \cdot K_{H\alpha} \cdot K_{H\beta}} \leq \sigma_{HP} \qquad \text{Wherein :} \qquad (1)$$

σ_H - Basic value of contact stress
K_A - Application factor
$K_{H\beta}$ - Longitudinal load distribution factor for contact stress.
$K_{H\alpha}$ - Transverse load distribution factor for contact stress.
σ_{HO} - Allowable contact stress (permissible Hertzian pressure).
K_V - Dynamic factor.

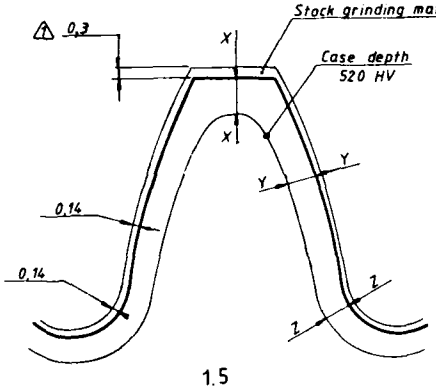
$$\sigma_{HO} = Z_H \cdot Z_E \cdot Z_\varepsilon \cdot Z_\beta \sqrt{\frac{F_t}{d_1 \cdot b} \cdot \frac{u+1}{u}} \qquad \text{Wherein} \qquad (2)$$

Z_H - Zone factor
Z_β - Helix angle factor
d_1 - Reference diameter of pinion
Z_E - Elasticity factor
F_t - Nominal tangential load
Z_ε - Contact ratio factor
b - Facewidth
u - Gear ratio z_2 / z_1

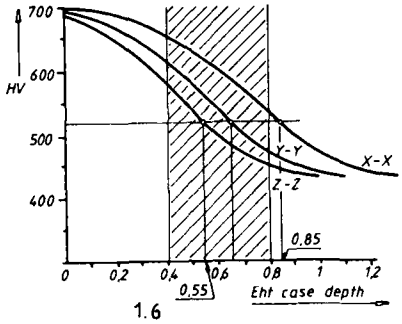
✱ The calculation of load capacity of spur and helical gears.
(I.S.O. / DP6336)

1.2. Corrective actions.

The following manufacture-lot will now be carried out with more surplus material at the tip. In the premachining we enlarge the outside diameter so that there is a surplus grinding material of 0.3 mm at the tip. On the flank and in the root we keep the surplus grinding material of 0.14.
After the heat treatment, with the same cyclus as above, we obtain on the finished gear an effective case depth of 0.85 mm at the tip, 0.7 mm on the flank and 0.55 mm in the root (see figure 1.5. and 1.6.). We can already see an improvement here of the depth at the tip. But we still remain 0.05 above the maximum limit.
A larger surplus material at the tip during premachining could result in a far too low surface hardness at the tip of the finished part.



1.5

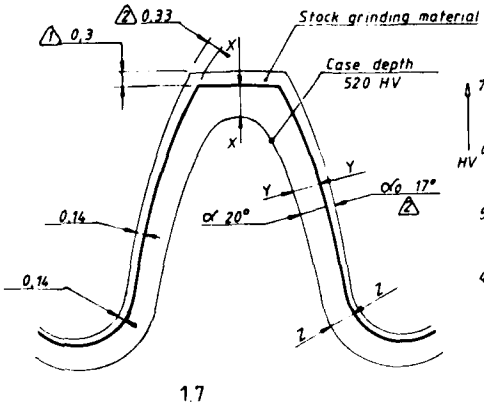


1.6

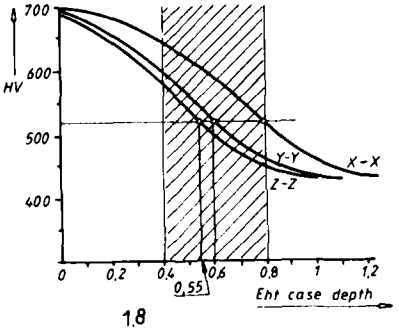
A second corrective action is applied to the following fabrication lot. Besides enlarging the outside diameter we also modify the tooth thickness at the tip. We realize this by using a hob with a special basic profile.
Namely :

- with a pressure angle of 17° (instead of 20)
- a tooth thickness in the root of the gear unmodified.
- the tooth thickness on the tip enlarged per flank to a grinding surplus value of 0.33 mm (see fig. 1.7.)

After the heat treatment and finish-grinding we obtain new results, namely
Eht tip = 0.8 flank = 0.65 root = 0.55 mm.
Now we are all over within the required toelerances. (see figure 1.7 and 1.8)
But did we manufacture a better gear now ?
Certainly not. In order to prove this we have to study more thoroughly the theory concerning the load capacity of gears.
After this (chapter 4) we will try to stipulate a better or more explicit specification about case depth and hardness.



1.7



1.8

CASE DEPTH ON FLANKS OF GEARS FOR HELICOPTER GEARBOXES.

Mr. André Watteeuw - Technical Director
M.C. WATTEEUW N.V.
't Kloosterhof, 92

8200 BRUGGE - BELGIE

One of the most difficult and delicate operations during the manufacturing process of gears for helicopter gearboxes and aircraft gears is the heat treatment. Case hardened alloy steel of high quality are mainly used for aircraft gears.
Not only a good structure in the case hardened tooth but also the surface hardness, the core hardness and case depth are very important for the load capacity of these gears.
On the drawing and in the specifications belonging to it, values and tolerances have been provided for the above-mentioned hardnesses. These, however, are not always adequate to guarantee a good manufacture.

1. OBTAINED RESULTS AND POSSIBLE CORRECTIVE ACTIONS.

1.1. OBTAINED RESULTS.

In order to make our exposition more clear, we will illustrate it with a practical example.
Gear 33 teeth - modul 1.81(D.P.14) - 20° pressure angle - 0° helix angle.
Material chemical composition C:0.16 - Si = 0.26 - Mn = 0.56 - Cr = 1.04 - Ni = 4.39
Tolerances on the drawing concerning hardness and case depth :
effective case depth minimum 0.4 mm maximum 0.8 mm (Eht).
Surface hardness minimum 650 HV Core hardness minimum 390 HV .
At first sight these are wide tolerances which can easily be realized. But experience shows us that expecially the case depth is very often the cause of problems. Certainly to keep up the required tolerance limits along the whole toothform, tip, flank and root.
Most specifications forget to determine where the Eht has to be measured. In this case, manufacturing has to stick to the limits of the case depth, both at the tip, flank and root.

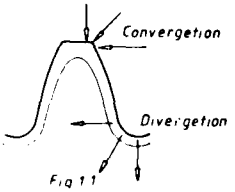


Fig 1.1

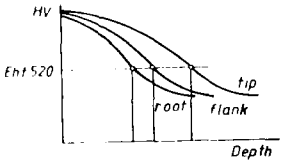
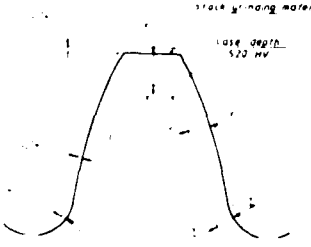
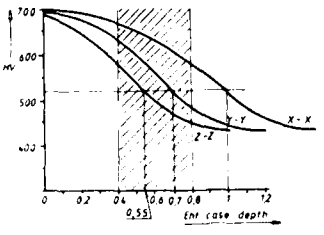


Fig 1.2

It is a well-known phenomenon that during the carburizing process the teeth of a gear take up more, but also deeper, carbon at the tip than in the root. The reason for this is the converging at the tip and the diverging in the root fillet during the penetration of gas in the carburizing process. As a result of this a carburized area at the edge arises which does not run parallel with the outer edge of the tooth form. The area is deeper at th tip and smaller in the root (see figure 1.1.)
By means of several microhardness measurements, every 0,2 mm from the edge to the core, a hardness gradient can be drawn up.
When we take the value of 520 HV as the limit hardness for the effective case depth Eht), we obtain three different curves.
The Eht values for the measurements at the tip, flank and root radius are different. (see figure 1.2.).
We return to our practical example. The aircraft gear is ground after the heat treatment because of precision reasons.
Therefor it is necessary to foresee surplus material for grinding during pre-machining, as well at the tip and on the flank as in the foot.





DISCUSSION

R.Battles, US

1. Are the teeth tip radiuses or edge breaks accounted for in the 2.04 calculated contact ratio?
2. With the involute tip or flank modifications is a contact ratio greater than 2.00 maintained when operated at reduced loads?

Author's Reply

1. The profile contact ratio value of 2.04 is the minimum calculated taking into account the minimum outside diameters of mating gears and their maximum tooth tip chamfers or radii.
2. Profile modifications are necessary to assure a smooth engagement between mating tooth pairs.

   Their values (and tolerances) must be chosen assuring that at whatever power level the stresses are within the limits.

   It is true that at a certain point, when reducing the power, the contact ratio falls below 2.00. That condition must be looked at, as it is normally the most stressing one.

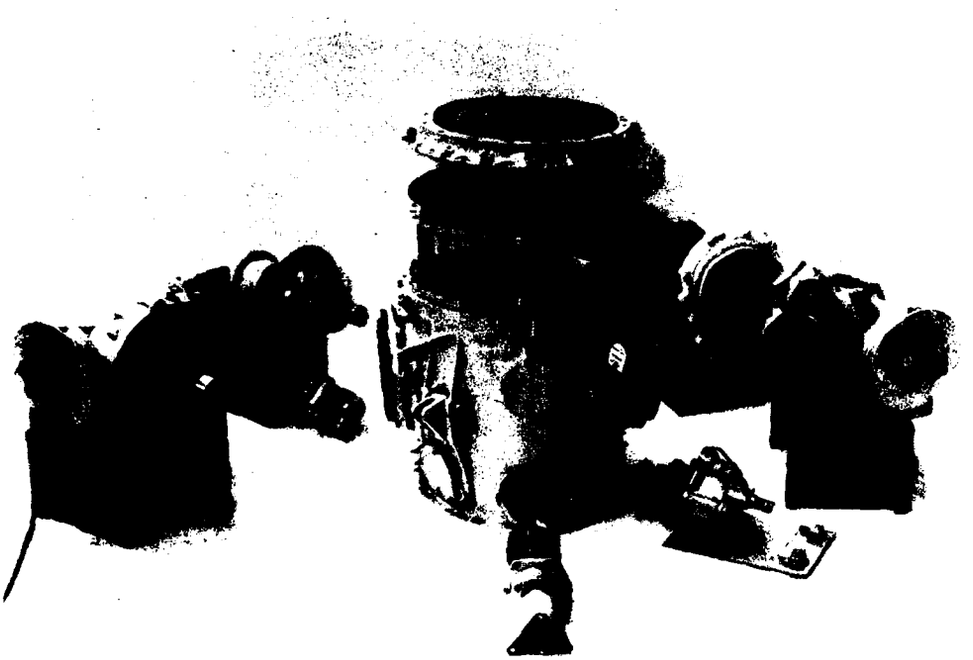


FIG. 7 - Exploded view of a helicopter gearbox designed and manufactured by FIAT AVIAZIONE. The extreme modularity of the design can be noted.

TRANSMISSION EFFICIENCY MEASUREMENTS AND CORRELATIONS WITH PHYSICAL CHARACTERISTICS OF THE LUBRICANT

John J. Coy
Propulsion Laboratory
AVSCOM Research and Technology Laboratories
Lewis Research Center
Cleveland, Ohio 44135

Andrew M. Mitchell and Bernard J. Hamrock
National Aeronautics and Space Administration
Lewis Research Center
Cleveland, Ohio 44135

SUMMARY

Data from helicopter transmission efficiency tests have been compared to physical properties of the eleven lubricants used in those tests. The tests were conducted with the OH-58 helicopter main rotor transmission. Efficiencies ranged from 98.3 to 98.8 percent. The data was examined for correlation of physical properties with efficiency. There was a reasonable correlation of efficiency with absolute viscosity if the viscosity was first corrected for temperature and pressure in the lubricated contact. Between lubricants, efficiency did not correlate well with viscosity at atmospheric pressure. Between lubricants, efficiency did not correlate well with calculated lubricant film forming capacity. Bench type sliding friction and wear measurements could not be correlated to transmission efficiency and component wear.

INTRODUCTION

In refs. 1 and 2 results were presented from efficiency testing of eleven different lubricants in an OH-58 main rotor transmission. The tests showed that the efficiency ranged from 98.3 to 98.8 percent, depending on the lubricant used. Furthermore, the efficiency for a given lubricant showed an increase with increasing inlet temperature with two exceptions, where the efficiency decreased with increased temperature. Since temperature affects viscosity, there was an increase in efficiency with a decrease in viscosity for a given lubricant, but no correlation among all the lubricants as a group was found.

The generally high efficiency was no surprise since it has long been recognized that the mechanical efficiency of helicopter power trains is quite high. Usually a planetary reduction has 3/4 percent loss, and a single bevel or spur gear mesh has 1/2 percent loss (ref. 3). Compared with the large amounts of power available from the engines of a helicopter, it may seem that fractions of a percent of the power lost in the power train path are inconsequential. However, the impact of higher losses is to require larger and heavier oil cooling systems. This effect adds to reduce helicopter payload and reduce survivability in a hostile area. Moreover, when the results from the work presented in refs. 1 and 2 are considered where there was as much as 50 percent variation in power losses among the lubricants tested, the impact on oil cooler weight, size, and vulnerability become very significant. By proper selection of lubricant, the operating envelope and payload capacity of the helicopter can be improved.

There are many factors which act together in causing the power loss in a helicopter transmission which is a rather complicated assembly of gears, shafts, seals, and bearings. In a typical application it is expected that sliding, windage, churning and pumping losses all play a role, as do a variety of physical parameters of the lubricant which are important in the particular mechanism of lubrication.

There have been significant contributions to the theory of power losses in transmission components. Martin (refs. 4 and 5) considered power loss between gear teeth. Townsend, Allen and Zaretsky (ref. 6) considered bearing power loss. Anderson and Loewenthal (ref. 7) gave a comprehensive analytical treatment of power loss in gear sets, including gear losses and bearing losses. Townsend and Akin (refs. 8 to 10) have concluded that efficiency and cooling in gear sets is optimum with radially directed lubricant jets on the exit side of the gear mesh. Murphy et al., (ref. 11) in their study of low-speed worm drives have concluded that synthetic oils with the lowest traction coefficients give the highest efficiencies.

The effort described in refs. 1 and 2 has been continued by investigating the physical properties of the lubricants. Results of the properties and characterization of the lubricants, including pressure-viscosity and friction effects, are reported in ref. 12.

In view of the aforementioned progress, the objective of the work presented herein was to summarize and compare the previously measured helicopter transmission efficiencies with the newly available physical characteristics of the lubricants.

Specifically, the pressure-viscosity effects and the friction effects were examined for possible correlation with measured transmission efficiency. The results of that investigation are reported herein.

APPARATUS, SPECIMENS, AND PROCEDURE

Transmission Test Stand

Figure 1 shows the NASA 500 hp helicopter transmission test stand, which was used to run the efficiency tests. The test stand operates on the "four-square" or torque regenerative principle, where mechanical power is recirculated around the closed loop of gears and shafting, passing through the test transmission. A 149 kW (200 hp) SCR controlled dc motor is used to power the test stand and control the speed. Since the torque and power are recirculated around the loop, only the losses due to friction have to be replenished.

An 11 kW (15 hp) SCR controlled dc motor driving against a magnetic particle clutch is used to set the torque in the test stand. The output of the clutch does not turn continuously, but only exerts a torque through the speed reducer gearbox and chain drive to the large sprocket on the differential gear unit. The large sprocket is the first input to the differential. The second input is from the upper shaft which passes concentrically through the hollow upper gear shaft in the closing end gearbox. The output shaft from the differential gear unit is the previously mentioned hollow upper gear shaft of the closing end gearbox. The torque in the loop is adjusted by changing the electrical field strength at the magnetic particle clutch. The 11 kW (15 hp) motor was set to turn continuously at 70 rpm.

The input and output shafts to the test transmission are equipped with speed sensors, torque meters, and slip rings.

Figure 2 is a schematic of the efficiency measurement system. The system allows the helicopter transmission to be operated in a thermally insulated environment with provisions to collect and measure that heat generation due to mechanical power losses in the transmission. In this schematic, the instrumentation used to measure torque and speed, and hence power input to the test transmission is not shown. The original oil-to-air heat exchanger which is standard flight hardware was replaced with an oil-to-water heat exchanger so as to allow more precise measurements of the heat rejection during an efficiency test run. By using the water to remove heat, any uncertainty of the correct value for specific heat of the oil was removed.

Figure 3 shows the test transmission mounted in the test stand. Figure 4 shows the test stand with the insulated housing around the test transmission. Thermocouples were placed at various locations inside the insulated housing to verify the adequacy of the insulation.

Test Lubricants

All the lubricants were near to the 5 to 7 centistoke range in viscosity and were qualified for use or considered likely candidates for use in helicopter transmissions. All the lubricants were tested (ref. 12) using new and used samples after completion of all efficiency test runs. Tables I to X, list the test lubricants, their specification, basestock characterization, physical properties, and chemical analysis performed. The methodology used is available in ref. 12.

Test Transmission

The test transmission was the main rotor transmission from the U.S. Army's OH-58 light observation helicopter as described in ref. 13 and shown in Fig. 5. The transmission is rated for 210 kW (270 hp) continuous duty and 236 kW (317 horsepower) at takeoff for 5 min. The 100-percent input speed is 6060 rpm. The input shaft drives a 19 tooth spiral bevel pinion. The pinion meshes with a 71 tooth gear. The input pinion shaft is mounted on triplex ball bearings and one roller bearing. The 71 tooth bevel gear is carried on a shaft mounted in duplex ball bearings and one roller bearing. The bevel gear shaft drives a floating sun-gear which has 27 teeth. The power is taken out through the planet carrier. There are three planet gears of 35 teeth which are mounted on spherical roller bearings. The ring gear (99 teeth) is splined to the top case and therefore is stationary. The overall gear ratio is 17.44:1 reduction.

The planet bearing inner races and rollers are made of AISI M-50 steel. The outer races and planet gears, which are integral, are made of AISI 9310. The cage material is 2024-T4 aluminum. The gear shaft duplex bearing material is CVM 52CB. All other bearings are made of AISI 52100 with bronze cages. The sun gear and ring gear material is Nitralloy N (AMS6475). The input spiral bevel gear-set material is AISI 9310. Lubrication is supplied through jets located in the top case, with circulation provided by an integral pump.

Test Procedure

Before the start of each efficiency test, the transmission and heat exchanger were cleaned out with solvent and the transmission components were visually inspected. Gear tooth surfaces were photographed. The transmission was then assembled and mounted in the test stand and filled with oil. The rig was run briefly to check for oil leaks. Then the loose fill insulation was added, filling the plexigiass box to completely surround and thermally insulate the test apparatus and transmission.

Efficiency test runs were made with the oil inlet temperature controlled to within less than one degree kelvin. Tests were run at oil inlet temperatures of approximately 355 K (180° F) and 372 K (210° F). The torque on the input shaft was 352 N-m (3118 lb-in) for each run. The input speed was 6060 rpm. This corresponds to the full power condition on the test transmission. The oil inlet and oil outlet temperatures were monitored until equilibrium conditions were established, which generally took about 20 to 30 min. The efficiency tests were then started. Water was collected in the weighing tank and data were recorded for total water weight, inlet and outlet temperatures for the water and oil, and flow rate for the water and oil. Vibration spectrum records were taken once each minute for a total test time of approximately 30 min for each test temperature.

After the tests were completed the transmission was disassembled, cleaned and visually inspected for changes in the gear and bearing surfaces. Photographic records were made. The lubricant was saved for later analysis. The efficiency was calculated from the heat balance on the water that flowed through the heat exchanger.

RESULTS AND DISCUSSION

The experimentally determined efficiencies are listed in Table XI and plotted against oil inlet temperature in Fig. 6. The range of efficiencies varied from 98.3 to 98.8 percent. This is an overall variation in losses of almost 50 percent, relative to the losses associated with the maximum efficiency measured.

In general, the higher test temperature for a given lubricant yielded a higher efficiency. The exceptions were with lubricants E and C, which were different types of synthetic lubricant. Lubricant G, being more viscous than the other lubricants could not be tested at the targeted oil inlet temperature. This was because the heat generated could not be removed with the existing water/oil heat exchanger. The test temperature increased to 378.5 K with the heat exchanger at full water flow capacity. At the higher temperature the efficiency for oil G was consistent with the efficiencies for the lower viscosity oils. The two automatic transmission fluids (A and B) and the Type I Synthetic Gear Lubricant (E) yielded significantly lower efficiencies as a group.

For meshing gear teeth, pure rolling exists at the pitch point, with increasing amounts of relative sliding as the contact point moves away from the pitch point. (Based on the research presented in ref. 7, the major power loss in the transmission has been determined to be due to sliding in the gears and bearings.) For higher amounts of sliding in an elastohydrodynamic contact, Couette flow predominates. Since the power loss for Couette flow with a Newtonian fluid is proportional to the absolute viscosity, a possible correlation of efficiency and viscosity was investigated. In Fig. 7 the efficiencies are plotted against the lubricant absolute viscosity at the inlet temperature. The correlation of efficiency with viscosity is rather limited. It is interesting to note that while the Mil-L-7808 lubricant (lubricant H) was the lowest viscosity oil, the efficiency was no better than the Mil-L-23699 lubricants (lubricants C, D, I, and K). By the plotted results, it is clear that viscosity variation is not the primary reason for the varying efficiencies between the different lubricants. But there is a general trend to higher efficiency for lower viscosity for all the lubricants except C and E. The slope of the aforementioned trend is identical for a large number of the lubricants.

While it is true that the elastohydrodynamic lubrication film thickness is determined by the fluid properties at the inlet, the traction and friction properties are determined by the properties within the contact area itself. Therefore, it may be more correct to use viscosity that is obtained from a viscosity equation that takes into account the pressure effects by using the Barus equation (ref. 14). A representative pressure of 0.6 GPa was used to correct the viscosity via the Barus relation. The corrected viscosity was investigated to determine if a correlation with efficiency existed. The results are shown in Fig. 8. The correlation is better than that in Fig. 7 in that lubricant H is now included in the major trend of decreasing efficiency with increasing viscosity at contact pressure conditions. Lubricants C and E continue to have reverse trends from the majority of other lubricants. The data for lubricants F and G which are the only synthetic hydrocarbon type lubricants are above the major trend line that was fitted to the lubricants.

In hydrodynamic lubrication, Couette flow predominates, but in elastohydrodynamic lubrication, (for pure rolling) Poiseuille flow is predominant. For Poiseuille flow, the power loss is proportional to the lubricant film thickness. Therefore, a possible correlation of efficiency with lubricant film thickness forming capacity at the inlet temperature was investigated. The film forming capacity is the product of absolute

viscosity (at inlet conditions) and pressure viscosity exponent, each raised to the 0.68 and 0.49 power, respectively (ref. 15). Results that are very similar to those of Fig. 7 were obtained when efficiency was plotted against the elastohydrodynamic film forming capacity. It can be concluded that the correlation of efficiency with film forming capacity is also rather limited.

In order to relate transmission efficiency to some readily measurable physical property of the lubricants, the friction coefficient of the lubricants was measured using the LFW-1 tester (ref. 12). There was much scatter in the friction data from this test (table X). The mean value for friction was examined for any correlation with calculated lubricant film thickness or viscosity at 373° C and 0.55 GPa which were the conditions of the LFW-1 test. There was a general linear regression trend of increasing friction with increasing viscosity which agrees with pure hydrodynamic fluid flow. In addition, there was a general linear regression trend of increasing friction with increasing film thickness which agrees with the previously mentioned postulate of Poiseuille flow in conjunction with elastohydrodynamic lubrication. When the efficiency was plotted against the mean friction coefficient for 373 K (212° F) it was found that a linear regression trend of decreasing efficiency with increasing friction coefficient existed. However, there was much scatter in the data. Additionally, for an individual lubricant, efficiency could not be determined based on the LFW-1 type measurement of friction coefficient. Furthermore, severe wear was observed on the LFW-1 test specimens. Visual inspection of the transmission components after each test run showed no indications of wear or degradation (ref. 1). In fact, the black oxide coating which was placed on the gear surfaces during manufacturing was hardly worn off. Hence, it must be concluded that bench type sliding friction and wear measurements cannot be correlated to transmission efficiency and component wear.

It is believed that the lower efficiencies for lubricants A, B, and E as well as the mentioned reverse trends of lubricants C and E are related to traction coefficient characteristics which are a function of the lubricants non-Newtonian constitutive relations as affected by lubricant base stock and additive package chemistry. The lubricant constitutive relations were studied by Höglund (ref. 16) and Kuss, et al. (ref. 17). The lubricant rheology study of Höglund was aimed at defining the dependence of lubricant traction behavior as a function of pressure and temperature. Höglund's measurements (ref. 16) were made for a broad sample of lubricants which included many of the types used in this study. The constitutive relations were characterized as follows. There was generally a limiting shear stress, beyond which the fluid was unable to support a stress that was calculated by the Newtonian expression where stress is proportional to strain rate. There was also a critical pressure or "solidification" pressure beyond which the lubricant limiting shear stress increased linearly with pressure. The solidification pressure increased with temperature. In Höglund's study, the ranking of lubricants with increasing solidification pressure at 373 K (212° F) was a synthetic traction fluid (1.07 GPa), a lithium soap grease (1.37 GPa), three paraffinic mineral oils (1.48, 1.66, 1.77 GPa), and finally the synthetic hydrocarbon and synthetic ester lubricants which did not solidify up to the limit of the test rig (2.2 GPa) at the 373 K (212° F) temperature. These synthetics did solidify at lower temperatures which in one case was as low as 313 K (104° F) for a polyalphaolefin/polyolic ester synthetic lubricant.

What is significant about Höglund's results in relation to the present study, is that he shows there can be a large difference in the manifested frictional losses among various lubricants at the same pressures and temperatures as a result of the solidification pressures being different. It is believed that the lower efficiency with lubricants A, B, and E are due to there being a lower solidification pressure for these lubricants.

In the study of Kuss, et al. (ref. 17) it was shown that the addition of 9.6 percent sulphur to a base stock caused a drastic change in the viscosity versus pressure characteristics. For the base stock, there was generally an exponential trend of increasing viscosity with pressure up to 200 MPa (which is as far as the data points were taken). The addition of sulphur produced a knee in the viscosity versus pressure relation beyond which the viscosity increased even more rapidly with pressure. For the range of temperatures 298 to 323 K (77° to 122° F) investigated, the knee in the curve ranged from 40 to 190 MPa (276 to 1310 psi). What is significant about this in relation to the efficiency measurements presented here is that the measured viscosities presented in Table III and used for the possible correlation in Fig. 7 are for atmospheric pressure only. The viscosity at high pressures such as exist in the gear and bearing contact regions would be different, from that calculated using the pressure-viscosity coefficient with the Barus equation. Hence, an improved correlation may be obtained if the lubricant rheological properties that affect traction measured under conditions of pressure and temperature representative of the efficiency test conditions reported herein.

The reason for the decrease in efficiency with increase in temperature for lubricants C and E is unknown, but may be related to increased activity of the particular additive packages at the higher temperatures which may cause rheological changes in the fluid in conjunction with formation of chemically absorbed surface films. Lubricant E (table IX) has large amounts of chlorine, zinc, sulphur and barium which are indicative of large amounts of antiwear and detergent additives being present.

Tables VI to X give the comparison between the lubricant analyses performed before and after the efficiency test runs. It is noticed that lubricants A and C showed significant increases in the iron content (table VI). Also, lubricant E showed a strong acid value before and after the test runs (table VII). These three lubricants were among the ones giving deviant performances for efficiency.

SUMMARY OF RESULTS

Data from helicopter transmission efficiency tests have been reviewed and compared with data characterizing the physical and chemical properties of the lubricants used in the transmission. The transmission efficiency tests were conducted using eleven different lubricants in the NASA Lewis Research Center's 500 hp torque regenerative helicopter transmission test stand. The test transmission was the OH-58A helicopter main transmission. The mechanical power input to the test transmission was 224 kW (300 hp) at 6060 rpm. Tests were run at oil-in temperatures of 355 K (180° F) and 372 K (210° F). The efficiency was calculated from a heat balance on the water running through an oil-to-water heat exchanger while the transmission was heavily insulated. The test lubricants were analyzed for their physical and chemical properties. Newly available data on pressure-viscosity characteristics as well as friction data from LFW-1 type testing were examined for possible correlation with the efficiency data.

The following results were obtained.

1. There was a reasonable correlation of efficiency with absolute viscosity (corrected for temperature and pressure in the contact).

2. Between lubricants, efficiency did not correlate well with absolute viscosity at atmospheric pressure.

3. Between lubricants, efficiency did not correlate well with calculated lubricant film forming capacity.

4. Bench type (LFW-1) sliding friction and wear measurements could not be correlated to transmission efficiency and component wear.

REFERENCES

1. Mitchell, Andrew M. and Coy, John J.: Lubricant effects on Efficiency of a Helicopter Transmission. NASA TM 82857, AVRADCOM TR 82-C-9, 1982.

2. Mitchell, Andrew M. and Coy, John J.: Lubricant Effects on Efficiency of a Helicopter Transmission. NASA TM 82857, AVRADCOM TR 82-C-9, 1982.

3. Shipley, E. E.: Loaded Gears in Action. Gear Handbook, D. W. Dudley, ed. McGraw-Hill, 1962, pp. 14-1 to 14-60.

4. Martin, K. F.: A Review of Friction Predictions in Gear Teeth. Wear, vol. 49, no. 2, Aug. 1978, pp. 201-238.

5. Martin, K. F.: The Efficiency of Involute Spur Gears. J. Mech. Des., vol. 103, no. 1, Jan. 81, pp. 160-169.

6. Townsend, D. P.; Allen, C. W.; and Zaretsky, E. V.: Study of Ball Bearing Torque Under Elastohydrodynamic Lubrication. J. Lubr. Tech., vol. 96, no. 4, Oct. 74, pp. 561-571.

7. Anderson, N. E.; and Loewenthal, S. H.: Effect of Geometry and Operating Conditions on Spur Gear System Power Loss. J. Mech. Des., vol. 103, no. 1, Jan. 81, pp. 151-159.

8. Townsend, D. P.; and Akin, L. S.: Analytical and Experimental Spur Gear Tooth Temperature as Affected by Operating Variables. J. Mech. Des., vol. 103, no. 1, Jan. 81, pp. 219-226.

9. Townsend, D. P.; and Akin, L. S.: Study of Lubricant Jet Flow Phenomena in Spur Gears - Out of Mesh Condition. J. Mech. Des., vol. 100, no. 1, Jan. 1978, pp. 61-68.

10. Akin, L. S.; and Townsend, D. P.: Cooling of Spur Gears with Oil Jet Directed into the Engaging Side of Mesh at Pitch Point. International Symposium on Gearing and Power Transmissions, vol. 1, Tokyo, 1981, pp. 261-274.

11. Murphy, W. R.; et al.: The Effect of Lubricant Traction on Wormgear Efficiency. AGMA Paper P254.33, Oct. 1981.

12. Present D. L., et al.: Advanced Chemical Characterization and Physical Properties of Eleven Lubricants. (SWR-6800-280/1 AFLRL-166, Army Fuels and Lubricants Research Lab; NASA Order C-67295-D.) NASA CR-168187, 1983.

13. Townsend, D. P.; Coy, J. J.; and Hatvani, B. R.: OH-58 Helicopter Transmission Failure Analysis. NASA TM X-71867, 1976.

14. Barus, C.: Isothermals, Isopiestics and Isometrics Relative to Viscosity. Am. J. Sci., vol. 45, 1893, pp. 87-96.

15. Hamrock, B. J., and Dowson, D.: Isothermal Elastohydrodynamic Lubrication of Point Contacts. Part III - Fully Flooded Results. J. Lub. Tech., vol. 99, no. 2, Apr. 1977, pp. 264-276.

16. Höglund, E.: Elastohydrodynamic Lubrication - Interferometric Measurements, Lubricant Rheology and Subsurface Stresses. Doctoral Thesis, LULEÅ University of Technology, Sweden, 1984:32D.

17. Kuss, Von. E.; Vogel, W.; and Deymann, H.: Viskositäts - Druckabhängigkeit Verschiedener Esteröle. Tribologie und Schmierungstechnik, 30 Jahrgang, 5, 1983, (in German). pp. 283-290.

18. Evaluation of a Calorimetric Iron Kit (CIK) as a Supplemental Oil Analysis Technique. AFWAL-TR-80-4022, U.S. Air Force Report, Feb. 1980.

19. Greenberg, M. K.; and Newmann, F. K.: Application of Energy Dispersive X-Ray Fluorescence Spectroscopy to the Analysis of Contaminants in Fuels and Lubricants. Report AFLRL No. 102, U.S. Army Fuels and Lubricants Research Laboratory, 1978, (AD-A062792).

TABLE I. - TEST LUBRICANT TYPES

Lubricant NASA code (AFLRL code)	Specification	Generic type/Basestock
A (11252)	DEXRON II GM 6137-M	Automatic transmission fluid/mineral oil
B (11268)	DEXRON II GM 6137-M	Automatic transmission fluid/mineral oil
C (11259)	MIL-L-23699	Turbine engine oil/ester (PE)
D (11254)	MIL-L-23699	Type II synthetic gas turbine engine oil/ester (PE)
E (11256)		Formulated gear lubricant/dibasic acid ester
F (11258)		NASA gear test lubricant - synthetic paraffinic with antiwear additives/synthetic hydrocarbon (PAO)
G (11260)	MIL-L-21040 MIL-L-46152	Synthetic fleet engine oil/mixture of 80 percent synthetic hydrocarbon (PAO) and 20 percent ester (TMP)
H (11262)	MIL-L-7808	Turbine engine oil/ester (TMP)
I (11264)	MIL-L-23699	Type II turbine engine oil/mixture of 50 percent TMP ester and 50 percent PE ester
J (11270)	MIL-L-23699	Type II turbine engine oil/ester (PE)
K (11266)		Turbine engine oil/mixture of 99 percent PE ester and 1 percent DPE ester

PE = pentaerythritol
TMP = trimethylolpropane
PAO = polyalphaolefin
DPE = dipentaerythritol

TABLE II. - SPECIFIC GRAVITY DATA ACCORDING TO ANSI/ASTM SPECIFICATION D-1481, API GRAVITY ACCORDING TO ANSI/ASTM [a]SPECIFICATION D-1298 (DATA FROM REF. 12)

Lubricant code	Specific gravity at listed temp			API gravity
	313 K	355 K	373 K	288 K
A	0.8620	0.8558	0.8514	29.8
B	.8626	.8548	.8546	29.9
C	.9973	.9862	.9843	8.2
D	.9868	.9768	.9746	9.7
E	.9322	.9211	.9201	17.7
F	.8262	.8108	.8088	36.0
G	.8629	.8536	.8527	29.6
H	.9442	.9320	.9313	15.7
I	.9659	.9568	.9546	12.8
J	.9856	.9759	.9747	10.1
K	.9829	.9721	.9725	10.3

[a]ANSI/ASTM, American National Standards Institute/American Society for Testing and Materials

TABLE III. - KINEMATIC VISCOSITY DATA ACCORDING TO ANSI/ASTM SPECIFICATION D-455 (DATA FROM REF. 12)

Lubricant code	Viscosity at listed temp. cSt		
	313 K	355 K	373 K
A	37.48	10.48	7.01
B	33.15	9.64	6.52
C	26.40	7.69	5.13
D	26.17	7.50	5.00
E	33.91	8.91	5.87
F	28.01	8.15	5.36
G	56.65	15.05	9.83
H	13.16	4.73	3.38
I	24.19	7.18	4.85
J	24.76	7.23	4.89
K	26.39	7.61	5.09

TABLE IV. - SPECIFIC HEAT DATA DETERMINED BY DIFFERENTIAL SCANNING CALORIMETRY (DATA FROM REF. 12)

Lubricant code	Specific heat at listed temperature					
	313 K		373 K		413 K	
	Cp	σ	Cp	σ	Cp	σ
A	0.42	0.091	0.42	0.12	0.44	0.14
B	.50	.048	.50	.051	.49	.07
C	.33	.097	.32	.097	.32	.091
D	.33	.071	.34	.072	.34	[a].084
E	.68	.11	.73	.13	.76	.20
F	.53	.12	.54	.13	.54	.14
G	.50	.091	.47	.058	.42	.059
H	.37	.036	.30	.037	.31	.094
I	.53	.060	.47	.039	.44	[a].075
J	.47	.031	.48	.030	.49	.030
K	.44	.073	.38	.076	.34	.075

[a]For calculation of Cp and and σ (std. deviation) one value, inordinately different from the others, was discarded. Thus, four values rather than five were used to determine these data.

TABLE V. - PRESSURE-VISCOSITY COEFFICIENTS FOR TEST LUBRICANTS EXPRESSED AS RECIPROCAL ASYMTOTIC ISOVISCOUS PRESSURE (DATA FROM REF. 12)

Lubricant code	Reciprocal asymtotic isoviscous pressure α^*, GPa^{-1} at listed temperature		
	313 K	373 K	423 K
A	15.37	11.72	10.22
B	14.96	11.85	10.34
C	11.63	10.03	8.81
D	12.43	9.94	8.71
E	15.53	11.51	9.88
F	13.44	11.14	9.53
G	13.80	11.34	10.36
H	11.53	9.14	7.95
I	12.08	9.24	8.34
J	11.96	9.23	8.30
K	11.40	9.50	8.32

TABLE VI. - TOTAL IRON ANALYSIS BY CALORIMETRIC METHOD (REF. 18) (DATA FROM REF. 12)

Lubricant code	Iron content, ppm	
	New	Used
A	1	4
B	<1	<1
C	1	6
D	<1	1
E	<1	1
F	<1	2
G	2	3
H	<1	1
I	<1	<1
J	<1	<1
K	<1	<1

TABLE VII. - LUBRICANT ACID ANALYSIS ACCORDING TO ANSI/ASTM SPECIFICATION D-664 (DATA FROM REF. 12)

Lubricant code	Total acid number Mg KOH/g	
	New	Used
A	0.54	0.54
B	.62	.62
C	.01	.02
D	.07	.07
E	[a]15.8	[a]15.7
F	.42	.51
G	3.2	3.5
H	.34	.34
I	.34	.38
J	.51	.38
K	.48	.43

[a]Strong acid value = 7.1 on samples

TABLE VIII. - PARTICULATE CONTAMINATION COUNT ACCORDING TO SAE AEROSPACE RECOMMENDED PRACTICE ARP 598A (DATA FROM REF. 12)

Lubricant code		Number of particles/100 ml					
		Particle sizes in micrometers					
		5-15	15-25	25-50	50-100	100	Fibers
A	New	17	2	2	4	10	12
	Used	4	1	6	7	11	10
B	New	6800	2980	200	40	44	112
	Used	49	51	27	23	16	18
C	New	72	36	18	12	10	7
	Used	4	1	2	1	5	9
D	New	685	275	35	22	15	20
	Used	200	65	38	24	21	39
E	New	120	60	23	25	22	33
	Used	44	7	10	13	12	19
F	New	60	16	30	13	7	22
	Used	475	8	2	5	[illegible]	52
G	New	49	39	45	38	34	78
	Used	4740	10	11	9	6	34
H	New	1780	72	45	40	25	32
	Used	1850	118	108	60	52	62
I	New	54	23	17	16	4	19
	Used	840	660	450	210	80	120
J	New	47	22	10	7	12	18
	Used	36	18	14	8	11	29
K	New	185	175	100	70	35	45
	Used	105	48	35	21	20	22

TABLE IX. - WEAR METALS TEST RESULTS USING X-RAY FLUORESCENCE FILTER METHOD (REF. 19) (DATA FROM REF. 12)

Lubricant Code		Elements (PPM)													Limit(3) of Detection (PPM)
		Mg	Al	Cl	Fe	Ni	Cu	Pb	Zn(1)	P(2)	S(2)	Ca(2)	Ba(2)	Si	Mn	
A	New	0.48	-----	2.47	----	----	----	0.21	----	0.18	4.71	----	0.23	----	----	0.11
	Used	----	5.91	1.12	0.51	0.10	0.14	----	0.11	.17	1.12	----	0.12	----	----	.09
B	New	0.86	-----	1.80	----	----	----	----	0.88	0.47	10.40	----	-----	0.33	----	0.21
	Used	.60	4.00	1.90	0.57	----	----	----	.74	.27	7.40	----	-----	.90	----	.23
C	New	0.28	-----	0.73	0.13	----	----	----	----	0.26	-----	----	-----	----	----	0.09
	Used	----	2.97	1.04	2.19	0.21	0.12	----	0.15	.19	0.20	----	-----	----	----	.09
D	New	0.27	-----	0.90	----	----	----	----	----	0.16	-----	----	-----	----	----	0.11
	Used	----	12.7	2.08	1.16	0.24	0.19	0.20	0.20	.71	0.51	----	-----	----	----	.15
E	New	0.16	0.19	2.57	0.10	----	----	1.28	2.27	2.15	13.01	0.29	10.16	----	----	0.09
	Used	.12	1.69	1.61	.26	---	0.11	----	3.71	.94	4.29	----	2.43	----	----	.09
F	New	0.31	-----	0.45	----	----	----	----	----	0.19	2.08	----	-----	----	----	0.10
	Used	5.36	-----	2.49	----	----	----	----	----	2.42	51.0	----	-----	----	----	.55
G	New	1.31	-----	4.91	----	----	----	----	1.51	0.70	5.29	8.64	-----	----	----	0.43
	Used	.39	0.67	1.49	0.22	----	----	----	0.39	----	.89	2.53	-----	----	----	.13
H	New	0.29	-----	3.81	0.11	----	----	0.16	----	0.47	0.21	----	-----	----	----	0.10
	Used	.67	4.68	16.68	.74	----	0.26	----	0.62	2.37	3.20	3.47	-----	----	----	.25
I	New	0.33	-----	0.56	----	----	----	0.11	----	0.58	-----	----	-----	----	----	0.10
	Used	.34	1.18	.85	0.58	----	----	.12	0.13	.46	0.16	----	-----	----	----	.11
J	New	0.23	-----	0.29	0.07	----	----	----	0.02	0.29	0.06	----	-----	----	0.10	0.07
	Used	.56	-----	.33	.11	----	0.21	----	.29	1.11	.31	----	-----	----	----	.08
K	New	0.60	-----	9.80	0.28	----	----	----	----	2.51	-----	----	-----	----	----	0.24
	Used	1.26	0.39	7.40	.56	----	----	0.65	----	1.86	-----	----	-----	----	----	.37

(1) Zn could be due to wear when present with copper, or as an additive when present alone.
(2) P, S, Ca, Ba probably present as additives.
(3) Limit of detection for sample, when - shown, element is less than this value.

TABLE X. - LFW-1 FRICTION AND WEAR TEST RESULTS (LUBRICANT TEMP. 373 K HERTZIAN PRESSURE 0.55 GPa) (DATA FROM REF. 12)

Lubricant code		Coefficient friction after cycle					Avg coeff of friction	Mean coeff of friction	Avg wear scar width, mm	Mean wear scar width, mm	Weight loss, mg			
		400	800	1200	5400	10 000					Block	Ring	Total	Mean
A	New	0.042	0.042	0.054	0.065	0.059	0.055	0.053	1.12		0.5	1.4	1.9	2.0
	Used	.042	.044	.053	.053	.053	.050		1.02		.4	1.7	2.1	
B	New	0.026	0.024	0.024	0.029	0.029	0.026	0.027	1.02	0.91	0.5	1.6	2.1	2.0
	Used	.026	.027	.026	.029	.029	.027		.79		.8	1.1	1.9	
C	New	0.042	0.026	0.026	0.021	0.021	0.025	0.024	1.14	1.12	0.7	1.7	2.4	3.1
	Used	.026	.021	.018	.029	.018	.022		1.09		2.3	1.4	4.1	
D	New	0.026	0.024	0.021	0.015	0.015	0.020	0.017	1.19	1.12	1.9	1.5	2.9	2.4
	Used	.018	.015	.015	.012	.012	.014		1.04		.2	1.7	1.9	
E	New	0.029	0.029	0.026	0.026	0.026	0.027	0.035	1.04	0.95	1.3	0.9	2.2	2.0
	Used	.044	.041	.041	.041	.041	.042		.86		.2	1.6	1.8	
F	New	0.044	0.044	0.041	0.059	0.059	0.049	0.034	1.02	1.02	1.4	1.7	3.1	2.9
	Used	.024	.021	.018	.015	.015	.019		1.02		.1	1.7	1.8	
G	New	0.042	0.042	0.033	0.021	0.021	0.032	0.033	1.22	1.10	1.1	1.3	2.4	2.0
	Used	.026	.024	.024	.042	.032	.028		.92		.2	1.4	1.6	
H	New	0.021	0.021	0.015	0.018	0.021	0.019	0.022	0.99	1.11	1.4	1.8	3.2	2.8
	Used	.029	.024	.024	.026	.021	.025		1.22		.2	2.1	2.3	
I	New	0.035	0.029	0.026	0.041	0.041	0.034	0.034	1.19	1.21	1.1	1.3	2.4	2.4
	Used	.038	.038	.038	.029	.029	.034		1.22		.3	2.5	2.8	
J	New	0.047	0.047	0.041	0.026	0.026	0.037	0.041	1.07	1.06	0.3	1.0	1.3	1.9
	Used	.029	.029	.029	.018	.018	.025		1.04		1.0	1.5	2.5	
K	New	0.025	0.021	0.018	0.015	0.015	0.019	0.022	1.12	1.21	0.4	1.0	1.4	1.5
	Used	.035	.029	.026	.018	.018	.025		1.30		.1	1.4	1.5	

TABLE XI. - MEASURED EFFICIENCIES

(DATA FROM REF. 1)

Lubricant code	Efficiency	Inlet temp., K
A	0.9840	361.5
	.9850	375.0
B	.9833	356.8
	.9843	375.0
C	.9876	366.4
	.9873	371.5
D	.9860	356.1
	.9874	370.1
I	.9835	361.0
	.9832	371.5
F	.9865	355.7
	.9877	372.0
G	.9873	378.7
H	.9870	355.6
	.9879	372.1
I	.9864	355.6
	.9882	372.2
J	.9864	355.6
	.9877	372.3
K	.9869	355.6
	.9882	372.3

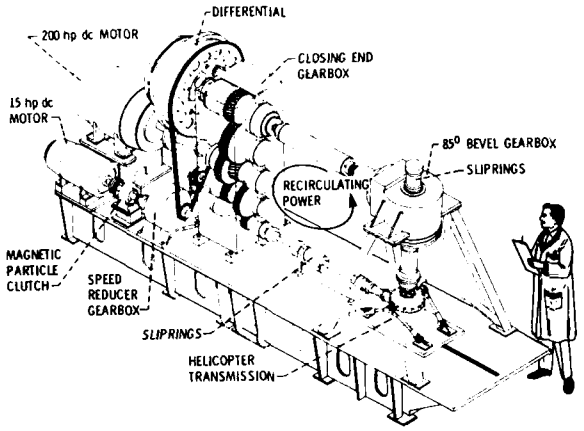


Figure 1. - NASA 500 hp helicopter transmission test stand.

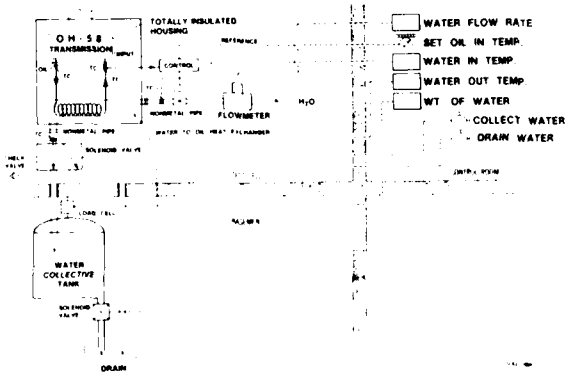


Figure 2. - Schematic of measurement system.

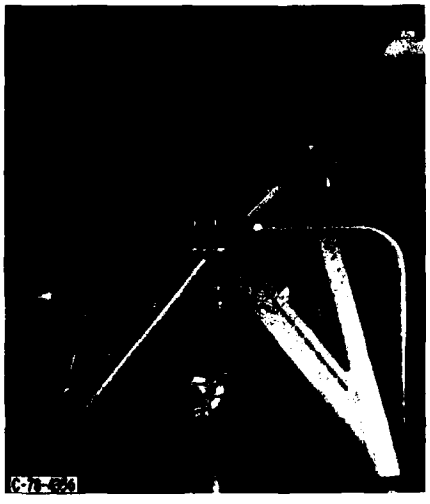


Figure 3. - View of test stand showing OH-58 transmission installed.

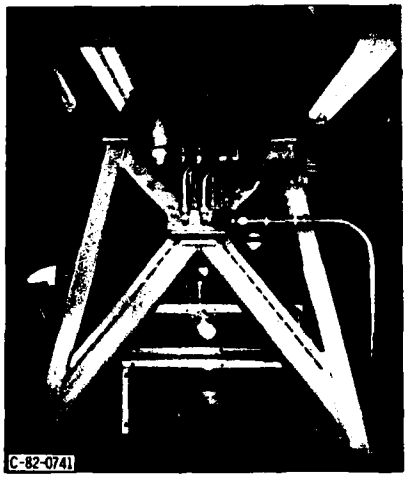


Figure 4. - View of test stand showing insulated transmission housing.

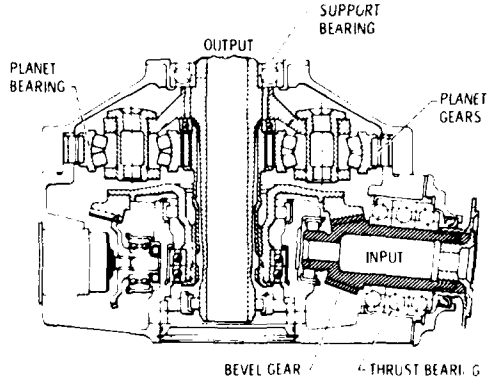


Figure 5. - Cross section of OH-58 helicopter transmission.

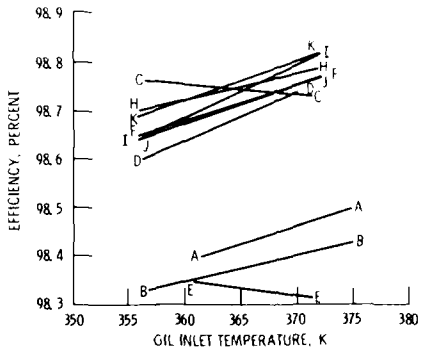


Figure 6. - Experimental efficiency correlated with inlet oil temperature.

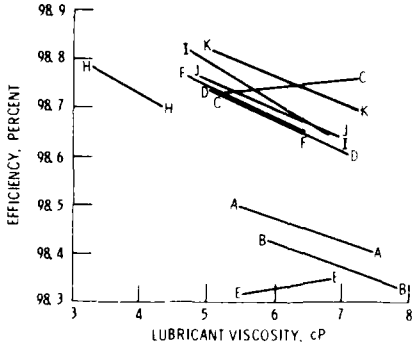


Figure 7. - Experimental efficiency correlated with lubricant viscosity.

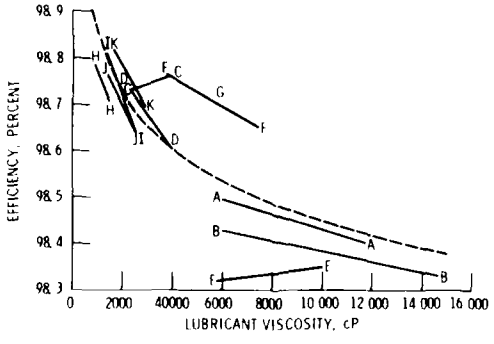


Figure 8. - Experimental efficiency correlated with lubricant viscosity at 0.6 GPa pressure and inlet temperature conditions.

DISCUSSION

R.W.Snidle, UK

1. From your tests, is it possible to estimate the relative contributions of tooth contact friction, bearing friction, etc. to the total power losses?

2. In your calculation of "corrected viscosity", what temperature have you assumed?

Author's Reply

1. References 4, 5, 6, 7 are detailed experimental and analytical studies of various components (such as bearings, gears, etc.) which generate power loss contributions. The details of individual contributions have been examined, but there is work to do yet. The test rig described in this paper has not been used to isolate contributions of individual components. However, we have studied the parametric effects of load, speed, and inlet temperature, as well as using four planet gears instead of three.

2. The temperature used was the inlet temperature. We tried average temperature between inlet and outlet, too. But the correlations thus obtained were much the same as those with inlet temperature. It was believed that the major power losses come from sliding in the EHL contact, and since the EHL film thickness is affected by inlet temperature that, therefore, the best temperature to use is the inlet temperature.

H.I.H.Saravanamuttoo, Ca

Would it not be more useful to show results as (1 − efficiency), because this is directly proportional to the heat rejection? A drop in efficiency from 99% to 98.5% may not appear large, but results in a 50% increase in heat rejection. The heat rejection problem is extremely important when considering the development of high power turboprops.

Author's Reply

We agree that the data on power loss could be plotted as total heat rejection. The resulting plots may then be more dramatic.

E.Saibel, US

Were the oils used in the test Newtonian? If not, viscosity alone is not sufficient to characterize the oil.

Author's Reply

The oils used are commonly believed to be Newtonian, however, they almost certainly are not. The evidence and associated commentary on this are brought out in the details of the paper, but were not discussed in the oral presentation because of time limitations. It is believed that further work that is ongoing to determine the rheological properties of these oils will help explain the power loss behaviour.

B.R.Reason, UK

I think the pressure viscosity effect is important in the present problem, however the pressure viscosity index is itself effected by temperature, and this variation is dependent on the particular lubricant used. If a temperature correction to the index was employed, it would seem advantageous to measure this temperature around the entrance to the conjunction zone of the meshing teeth. Was this in fact done?

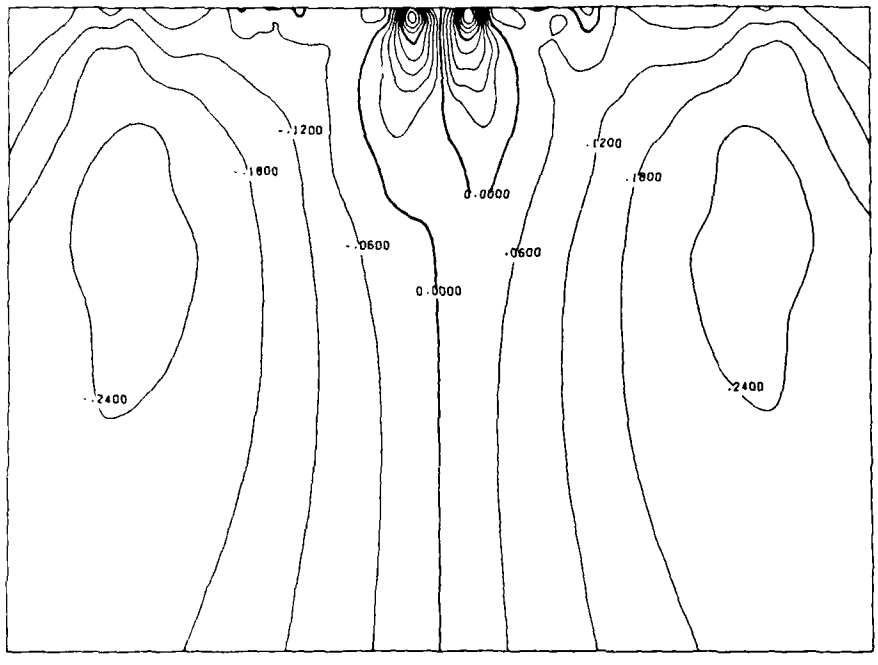
Author's Reply

It was assumed that the inlet temperature to the EHL contact was the same as the inlet temperature to the transmission. This assumption is good for some of the contacts, but almost certainly not for others. A component-by-component account of each contribution to the power loss has not been attempted yet. When this is attempted, we will place thermocouples throughout the gearbox in strategic places to try and get the best estimate of the inlet temperature to the conjunction at each component.

H.Blok, Ne

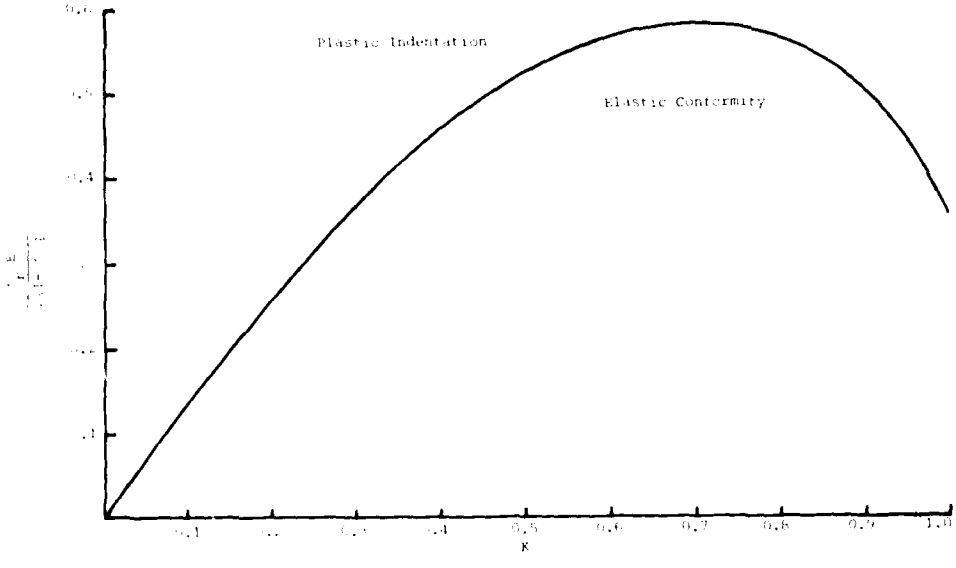
In their Figure 8 the authors showed that the introduction of two "corrected" viscosity yields an overall correlation for the helicopter transmission concerned. Presumably there is a variety of reasons why even this correlation is far from perfect, for instance in that it does not result in one single curve or in a well ordered family of curves.

A major reason is presumably to be sought in the fact that in the present paper only the total power losses have been determined and that these consist of various components that so far are unknown, such as losses due to tooth friction, churning, expulsion of the oil from the tooth spaces in mesh, and bearing friction, whilst each component is subject to its own individual model law. A more refined correlation might presumably be established once the authors should have succeeded in breaking down the total losses into the individual components. After all, already over 45 years ago the discussor applied this theory successfully as a basis to experimentation for a similar purpose in quite a variety of automobile transmission and rear axles.

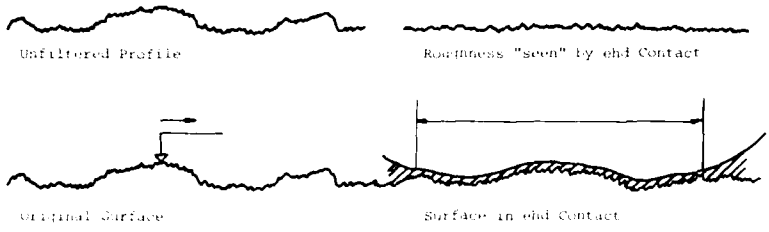


[illegible] of the [illegible] shear stress below a dental post similar to that of Figure 9. The [illegible] shown around the edges of the post are shown in the top portion of the figure.

Plot of $K = v = \frac{\sigma_r E}{\gamma(1-\nu^2)a}$



[illegible]



[illegible] The [illegible] profile [illegible] of the surface roughness, as it [illegible] the [illegible] "seen" by, i.e. [illegible] the [illegible] of a specimen, while the right, [illegible] and [illegible] of the [illegible] of surface [illegible] wear. Note that in this roughness [illegible] [illegible] original [illegible] "as left" profile would not represent the roughness "seen" [illegible] [illegible] "as left" [illegible].

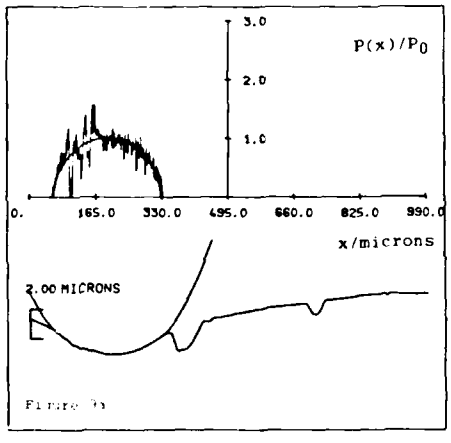


Figure 9a

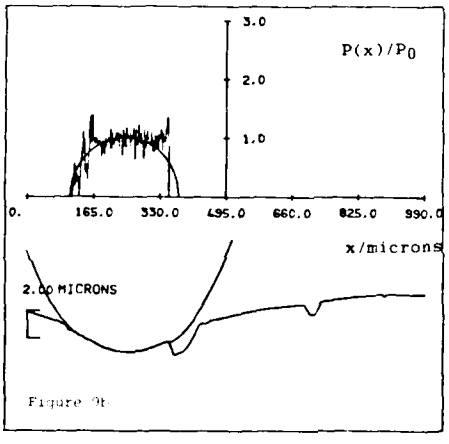


Figure 9b

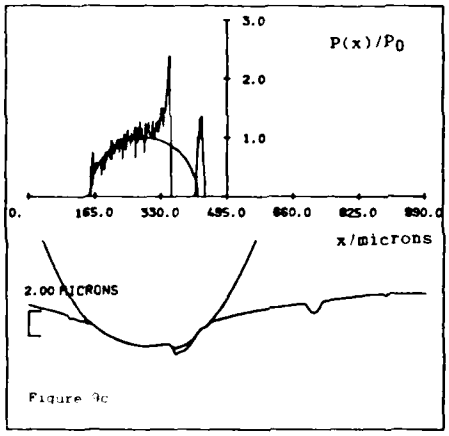


Figure 9c

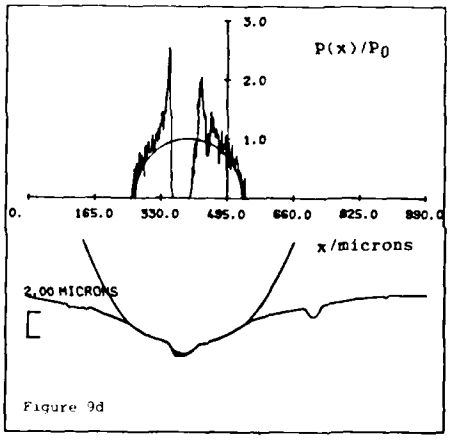


Figure 9d

Figures 9a-d Sections through the elastic contact geometry of a smooth roller loaded against the surface shown in Figure 4 as it moves across the debris created dents. The Figures also show the normal elastic stress distribution compared to the smooth surface Hertzian theoretical distribution. Note the variations in stress created by the surface roughness and particularly the very high concentrations of stress as the roller experiences the relatively sharp edges of the debris dent.

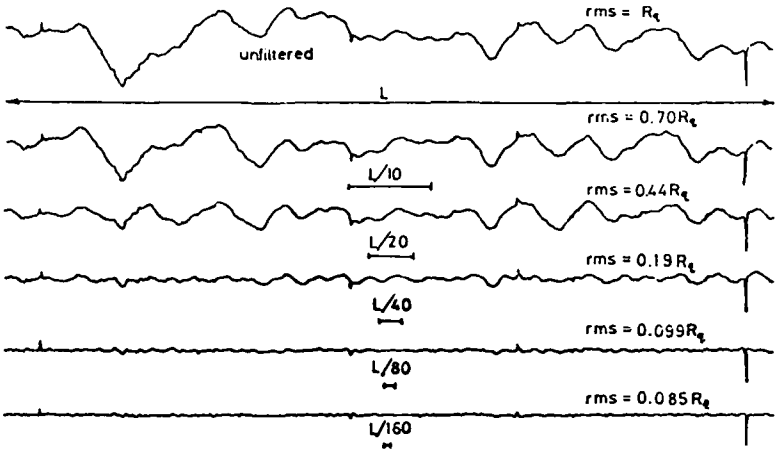
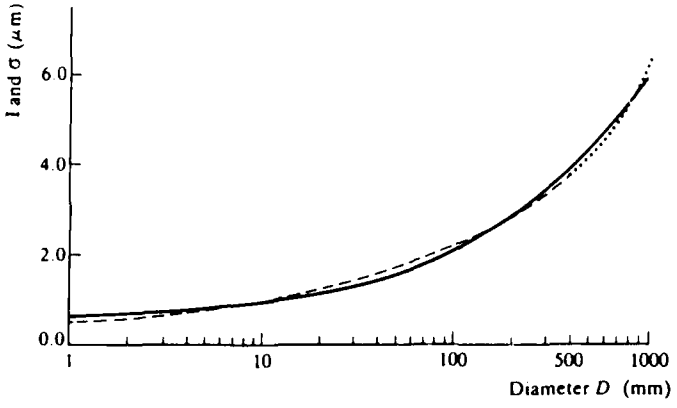


Figure 6 High-pass filtering of a raceway profile at the cut-off lengths shown using the cubic spline averaging filter incorporated in the surface analysis software.



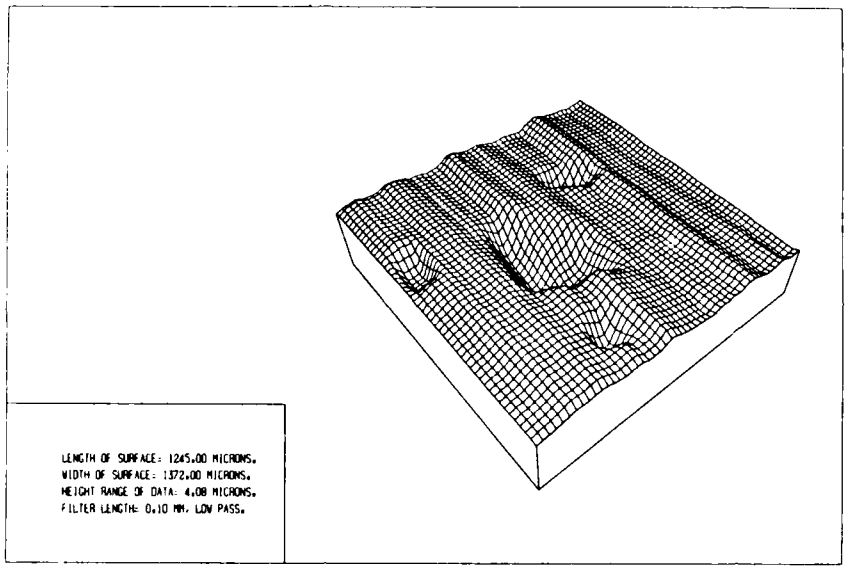


Figure 4. 3-D surface map showing debris indentation damage on a roller bearing surface.

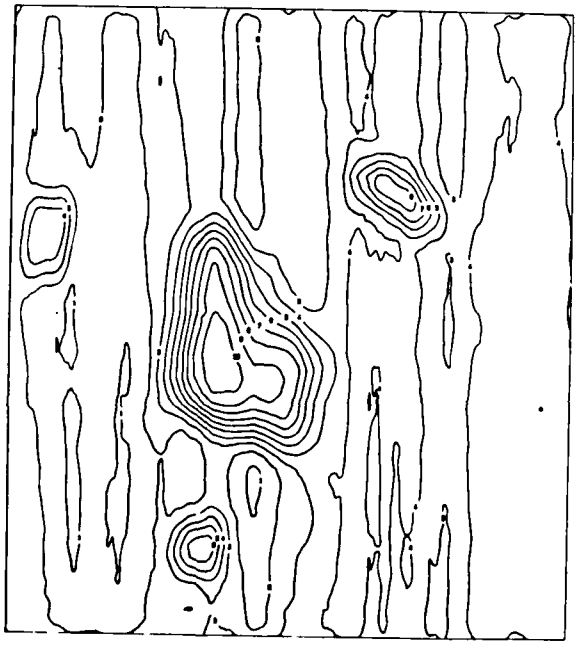


Figure 5. Contour map of damaged bearing surface shown in Figure 4. Contours at 0.4 microns intervals.

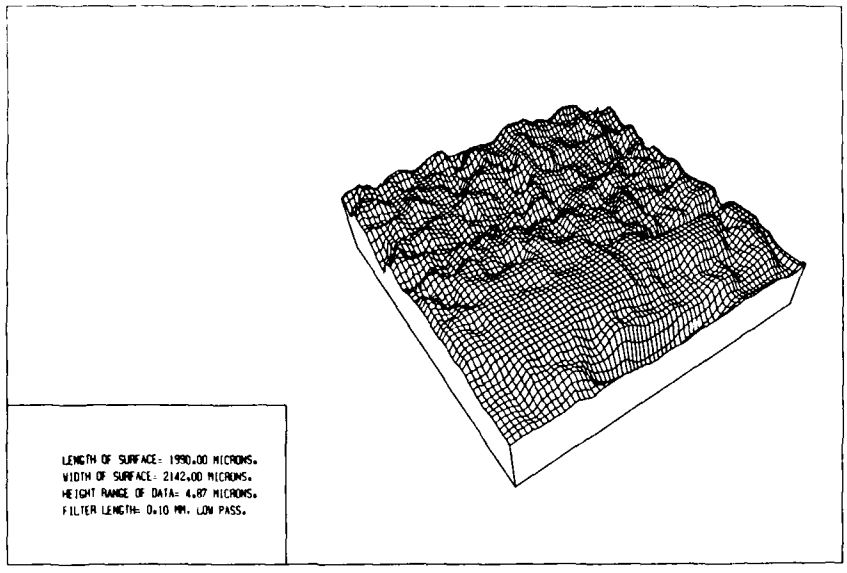


Figure 3 3-D surface map of a damaged roller bearing surface. Note the plotting technique has the ability to show perspective.

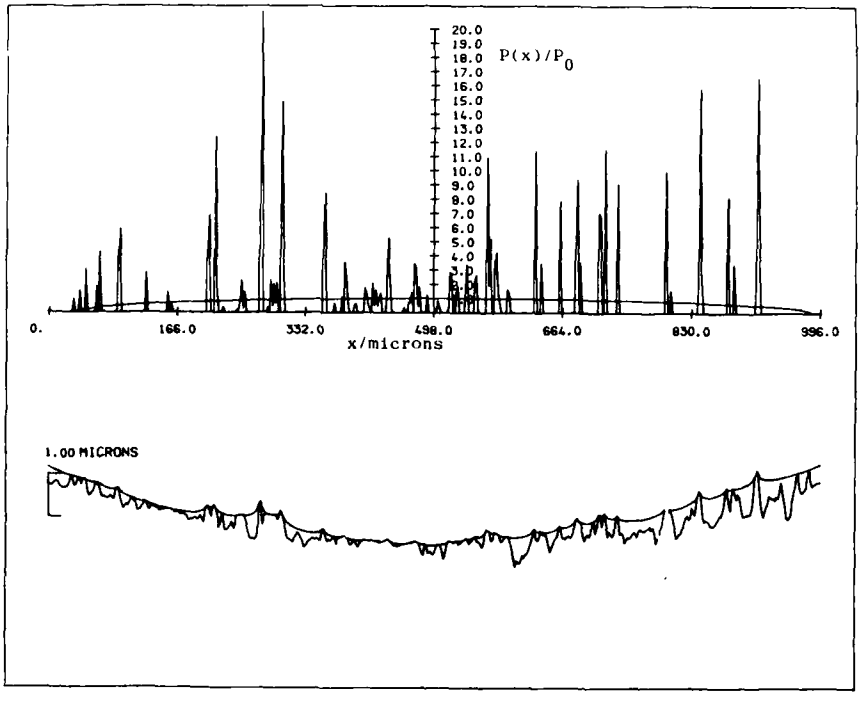


Figure 4 Pressure distribution for a rough surface loaded against a smooth cylinder of large radius. The individual contact spots can be seen. The local pressures are far in excess of the theoretical pressures which are plotted for comparison.

(14) Leaver, R.H., Sayles, R.S. and Thomas, T.R. "Mixed lubrication and surface topography in rolling contacts", Proc. I.Mech.E., 188, (1974).

(15) Thomas, T.R. "Rough Surfaces": Longman, (1982).

ACKNOWLEDGEMENTS

The authors would like to thank our colleagues, Martin West for the use of his 3-dimensional surface plotting programmes, Dr. P.B. Macpherson for his assistance in all the research work reported, and also to express their gratitude to the Ministry of Defence and the U.S. Navy's Office of Naval Research who are sponsoring parts of the work reported.

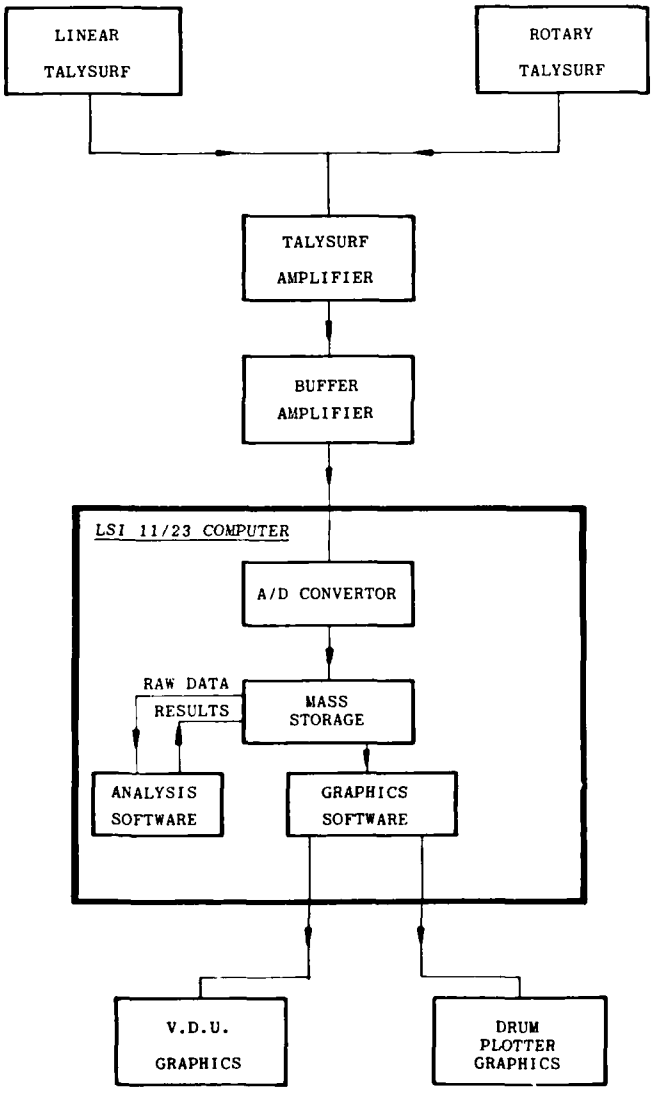


Figure 1 Schematic diagram showing the Talysurf 4 programme development and analysis system.

Asperity Conformity

As surface asperity wavelengths increase, their slopes reduce. Thus although an rms or cla roughness measurement will be strongly affected by the long-wavelength content of the roughness, the severity of such asperities is relatively low and it is important in contact problems not to allow this influence to dominate roughness data.

The problem is dipicted in Figure 8 where the output from a stylus measuring device is compared with the relative roughness seen by a Hertzian contact. Just as with the plasticity index applied to short wavelength features, where the asperities are sharp enough to plastically deform under almost any load, a similar long-wavelength conformity index will exist, where a contact can accommodate the long-wavelength height variations by elastic conformity, without any change in the applied load. Thus as Figure 8 depicts, the roughness a gear or roller bearing contact experiences, is that range of asperity wavelengths which are severe enough not to allow conformity to occur.

Figure 9 shows the contact of a roller against a roller bearing raceway surface (13). The scale is adjusted to show the effects of conformity, or non-conformity, as the roller encounters a plastically deformed surface dent, which was produced by a particle of rolled in debris during the filtration tests reported in (8). The Figures are produced by a numerical force-displacement technique of elastic contact. The results shown correspond to a dry contact situation and variations in pressure, shown as due to local asperity effects about a mean Hertzian distribution, would likely be modified when the surfaces are interspersed between a lubricant film. However with such a film under ehd conditions, and therfore in a glassy state, it is not clear to what extent the film will accommodate the roughness by similar local variations in pressure and the formation of micro ehd films, or, whether side-leakage of lubricant, on an asperity scale, would prevent micro ehd formation, and the roughness would therefore maintain its identity through the contact.

Investigating the contact in this way allows the use of wavelength and height restrictions to be imposed on measurements of roughness. Thus to define a representative Λ (film thickness/rms roughness) value for an ehd gear or roller bearing contact, the roughness needs to be defined as relative to the deformed surface. This can be achieved by high-pass filtering the profile signal prior to computing the rms roughness and calculating the Λ value. This philosophy is not new, Leaver, Sayles and Thomas (14) introduced the technique when analysing the performance of taper roller bearings operating under partial ehd. They showed that by filtering the roughness profiles at a wavelength equivalent to the Hertz contact width, much better agreement was ahcieved between electrical contact resistance measurements and surface contact theories based on the calculated Λ values. The same philosophy was later applied successfully to several surface contact related problems ( ), and the term "functional filtering" was adopted to described the technique. This functional filtering concept has been taken a step further in this paper, which should lead us to a better definition of the roughness and performance of gear and bearing contacts.

REFERENCES

(1) Whitehouse, D.J. "Improved type of wavefilter for use in surface-finish measurement", Proc. I.Mech.E, 182, pt3K (1968).

(2) Whitehouse, D.J. and Reason, R.E. "Equation of the mean line of surface texture found by an electric wave filter", Rank Organisation, (1965).

(3) Sayles, R.S. and Thomas, T.R. "Surface topography as a non-stationary random process", Nature, 271, (1978).

(4) Sayles, R.S. and Poon, S.Y. "Surface topography and rolling element vibration", Precision Engg., 3(3), (1981).

(5) Sayles, R.S. et al. "Elastic conformity in Hertzian contacts", Tribology Int., Dec., (1981).

(6) Hertz, H. "On the contact of rigid elastic solids and hardness", Miscellaneous papers; Macmillian, London, (1896).

(7) Popinceanu, N.G., Diaconescu, E. and Cretu, S. "Critical stresses in rolling contact fatigue", Wear, 71, (1981).

(8) Sayles, R.S. and Macpherson, P.B. "The influence of wear debris on rolling contact fatigue", Rolling Contact Fatigue Testing of Bearing Steels, ASTM STP771, J.J.C. Hoo, Ed., ASTM, (1982).

(9) Harries, C.J., Webster, M.N. and Sayles, R.S. "Bi-modal failure mechanisms in tribological components", Reliability Engineering, 4, (1983).

(10) Cheng, H.S. and Mrinal Ball "Stress distributions around the furrows and asperities in ehl line contacts", Solid Contact and Lubrication Seminar, ASME, Chicago, November, (1980), AMD-Vol. 39.

(11) Wedeven, L.D. "Influence of debris dent on ehd lubrication", Trans. ASLE, 21, (1977).

(12) Timoshenko, S. and Goodier, J.N. "Theory of Elasticity": McGraw-Hill, (1951).

(13) Sayles, R.S., Webster, M.N. and Macpherson, P.B. "The influence of some tribological problems on mechanical reliability", Published by I.Mech.E. Conf. on Mechanical Reliability, London, July, (1984).

where $k = \frac{a}{r}$, the non dimensional radius of the pressure distribution and,

$\delta_r = \frac{w_o - w_r}{r}$, the non dimensional normal displacement. Also

$$F(k) = \int_o^{\pi/2} (1-k^2\sin^2\theta)^{\frac{1}{2}}\, d\theta - (1-k^2) \int_o^{\pi/2} \frac{d\theta}{(1-k^2\sin^2\theta)^{\frac{1}{2}}} \qquad (6)$$

Expression 6 now relates the difference in elastic surface displacements, δ_r*, to the size of the pressure distribution, k. The integrals in equation 6 are elliptical integrals of the first and second type, hence their values, for a given value of k, may be looked up in tables. Figure 11 represents the values of the rhs of equation 5 for values of k up to 1, i.e. where the displacements at radius r are located at the edge of the uniform pressure. If the value of q used in the analysis is set at the indentation hardness of the material being considered Figure 11 represents the limiting values for elastic conformity around an idealised particle.

For a particular value of k, essentially the particle radius, we can find a limiting value of δ_r, a measure of the particle thickness to which the contact can elastically conform. For a particular case we can choose r to be the half width of the gear or bearing contact, thus our conformity criterion will be set to be within the contact zone, all the parameters being non-dimensionalised with respect to the half width. In real situations we would be concerned with values of k between 0 to 0.5, as at higher values the particle would be carrying a substantial amount of the load and it is unlikely that ehd support would be available.

For particles that have a size and shape that would be outside the elastic conformity region marked in the figure, we would expect local surface plastic flow to occur until the gear or bearing surfaces were close enough together to offer ehd support, hence leaving permanent surface damage.

This form of analysis suggests that particles of particular shape, or aspect ratio, are less damaging, and that the final form of any particle softer than the mating surfaces will assume this shape following rolling and plastic deformation. This could well help to explain the large amount of "platelet" debris found in gear and bearing lubricant systems. Interpretation of this latter effect in terms of the contacting surfaces, would suggest that debris dents would assume shapes similar to the deformed debris, and infact this is what is seen in practice (8) and debris dents appear to be relatively shallow compared to their extent in the plane of the surface. The analysis also helps to explain why dents appear which are much larger in mean diameter than the lubricant filtration system would seem to allow, were the particles to maintain their initial size and shape. Also if the form of plastic deformation we have described is accepted, the volume associated with a particular debris dent can be used to estimate the original mean particle diameter, which when compared to filter ratings, has allowed a more sensible explanation of our earlier results (8). Such analyses also give use a better idea of the maximum size of damaging particle.

DISCUSSION AND CONCLUSIONS

The influence of surface irregularities on component performance is considered as a bandwidth sensitive problem. The examples presented of this approach range from dimensional tolerance, where long-wavelength effects are important, down to very short-wavelength roughness which is shown to effect the performance of bearing and gear contacts.

This approach to roughness related problems is shown to depend on defining the wavelength of surface irregularities which are most influential, and several new methods of arrive at this information are presented.

Elastic Hertzian Contact

The first of these methods involves the use of an elastic contact computer program developed to investigate the effects of debris indentations on fatigue life. The prelimary results of this work are shown to offer considerable potential in understanding and solving problems of surface contact, not least of which, is the techniques ability to define which surface features produced on a surface are most damaging to the contacting surfaces.

3rd Body Effects

A second, and new approach to surface contact related problems, is a theoretical definition of the influence of 3rd bodies within Hertzian contacts. Third body contact mechanics is a much neglected area of tribology, and yet a great deal of evidence exists to show that effects such as debris initiated fatigue are becoming more and more important, particularly as steel qualities continue to improve. Our preliminary analysis shows that permanent damage to gear and bearing surfaces is very dependent on the shape as well as the size of debris the contacts must accommodate. Results from previous filtration and fatigue life studies seem to confirm the general message obtained from this analysis.

---

*The graph is drawn for one surface only, in the real case the elastic displacements due to both surfaces may be taken into account by looking up the δ_r for each surface and adding them, obviously for similar materials δ_r may simply be doubled.

The input of surface geometry to this program can take any form, but is ideally suited to accept digitised surface profile data. The choice of the roller dimensions, roller position, elastic constants and the total normal force are also input, thus allowing the pressure distribution to be calculated from the real profile data. The authors believe that this technique of loading real surface profiles in an elastic manner is unique.

Analysis of the pressure distribution around a real debris dent

The computer program described has been used to calculate the pressure distribution around a debris dent produced during the experimental tests described in (8). The values for the load, Young's modulus and roller dimensions reported in (8) were also used in order to reproduce, as nearly as possible, the true experimental conditions. Figures 9a,b,c and d show the calculated pressure distributions superimposed over the smooth case theoretical results. The diagrams represent a history of the normal pressures as the debris dent moves through the contact zone.

The results indicate that pressures in excess of 2.5 times the theoretical maximum pressure can exist on the contacting surfaces. The analysis of the state of stress beneath the surface subjected to such a pressure distribution is also being carried out by means of a finite element technique. Figure 10 shows a preliminary result, in the form of a contour map of shear stresses due to the presence of a dent in the contact. From results such as this, it seems clear that the assumption of a state of Hertzian stress being present in the contact zone is often inadequate if a true picture of the fatique mechanism is to be derived. Furthermore the sharp peaks seen in the pressure distribution can be seen to produce significantly high shear stresses close to the bearing surface. Such results would confirm the reported findings (8,9,11) that debris initiated fatigue is surface originated, and not sub-surface, as the classical analysis would suggest.

The effects of the presence of an ehd or partial ehd lubricant film, and the extent of local plastic deformation are the subjects of continuing research with this technique. Further research by the authors is also in hand on how dents are actually formed, and it is appropriate to explain some of our preliminary theoretical results in this paper.

The Formation of Indents

The particle indentation problem may be considered as an independent effect from the normal ehd contact, if we can assume that the load carried by the particle is small compared with the total load carried by the contact. To model the effect of particle indentation the authors have investigated the surface displacements due to a uniform pressure distribution which has a circular plan form, thus modelling idealised disc type debris. The analysis uses the well known half space solution found in (12). Although real debris will not be regular in shape a uniform pressure distribution would be a reasonable approximation if the loads are high enough to cause local yielding of the particle and bearing or gear surface. Clearly to cause damage within the contact region, there must be permanent plastic deformation, hence the authors feel that the uniform pressure distribution chosen is a good starting point.

In the analysis we require to find the size and shape of debris that can cause the permanent deformation that has been observed in practice, Figure 4. In the real case the contact loads will be supported by a mixture of the normal ehd load and the load transmitted throught the debris, the proportion of these loads being unknown. However we can assume that once the surface deformation, due to the debris, are such that the fluid film can offer support, then the rest of the load will be taken by ehd support. Thus the analysis is concerned with investigating the surface displacements, using elastic half space theory, to determine the size and shape of particles that will allow elastic conformity within the ehd contact region.

From Timoshenko [12] we have the expressions for the surface displacements due to a uniform circular load:

$$w_o = \frac{a(1-\nu^2)q}{E} \qquad (3)$$

$$w_r = \frac{q(1-\nu^2)}{\pi E}\left\{ r\left[\ln\left(\frac{a}{r}\right)+\left(\frac{a}{r}\right)^2\sin^2\theta\right)^{\frac{1}{2}}d\theta - \left(1-\left(\frac{a}{r}\right)^2\right)\int_0^{\pi/2}\frac{d\theta}{\left(1-\left(\frac{a}{r}\right)^2\sin^2\theta\right)^{\frac{1}{2}}}\right\} \qquad (4)$$

where:

- a = radius of uniform pressure distribution
- q = uniform pressure
- E = Young's modulus
- ν = Poisson's ratio
- r = radius at which displacement is calculated
- w_o = displacement at centre of pressure distribution
- w_r = displacement at radius r, outside the pressure circle

We may now formulate an expression for the difference in elastic displacements between the centre of applied pressure and a point radius r away from the centre.

$$\frac{\delta\pi E}{q(1-\nu^2)a} = \left[\kappa - \frac{2}{\pi}F(\kappa)\right] \qquad (5)$$

SURFACE TOPOGRAPHY AND CONTACT VIBRATION

The dynamic characteristics of rolling, and rolling and sliding vibration are complex, and although a large proportion of generated noise can be attributed to rotational and cyclic frequencies of the mechanisms involved, a good deal of noise is generated by relative motion of the interacting surface topographies of the contacting components. Such effects are also limited by bandwidths of surface irregularities which influence the frequencies of vibration.

Form and Waviness Effects

In the context of a rolling bearing or gear we can regard waviness as those features of the surface topography which are prominent over a scale greater than the Hertz elastic contact dimension (Figure 8). The significance of such features can be considered in the ideal case in which the condition of full elastohydrodynamic (ehd) lubrication exists (Figure 8). The velocity of vibration normal to the direction of motion is:

$$v = \frac{dz}{dt} = \frac{dz}{dx}\frac{dx}{dt} = u\frac{dz}{dx} \qquad (2)$$

where u is the relative velocity in the direction of rolling and $\frac{dz}{dx}$ the slope of the surface features the rolling element encounters. In general slopes are relatively small on long-wavelength features, and consequently waviness feature only becomes a serious problem when components possess relatively high amplitude features such as chatter marks.

Surface Texture Effects

In a previous paper Sayles and Poon (1981) defined surface texture as the range of topographic features which are prominent on a scale comparable to, or less than, the Hertz elastic contact dimension (Figure 8). They went on to show that an even shorter wavelength demarcation can exist as that at which surface feature may geometrically conform to each other by local elastic deformation. This demarcation was shown to be expressed approximately by a conformity parameter (5), which was used in conjunction with the structure function or correlation function to define the approximate spatial size of asperity to which conformity could be expected to occur.

When conformity does occur on a repeating basis, as new surface elastic contacts are formed and released, then noise will be generated. The reduction of this form of noise relies on knowing the asperity sizes which are responsible, and removing or reducing the magnitude of these features during the manufacturing and finishing processes.

The concept of conformity is taken further in later sections of this paper, where it is shown to be a more general surface contact concept, and applicable to mamy more tribological problem areas. The effects of the remaining non-conforming asperities, wear debris, and the surface damage resulting from such effects are also discussed more fully later in the paper as they represent topics of much more up to date research.

FATIGUE FAILURE

The analysis of rolling contact fatigue has historically centred around the assumption that the contact pressure distribution, can be approximated by the semi-elliptical distribution obtained by Hertz (6). There have been numerous fatigue models presented, Popinceanu et al (7) compare a number of these with experimental data. In practice it is found that under service conditions, bearings often exhibit several different failure modes, and failure times differ greatly from those predicted by classical analysis.

The presence of bi-modal effects seen in many of the published Weibull distributions for rolling contact fatigue, implies that there are at least two competing fatigue mechanisms. Sayles and Macpherson (8) and Harries et al (9) suggested that a bi-modal mechanism, can be accounted for by considering surface, and sub-surface, crack initiation. Sayles and Macpherson (8) correlated early life roller bearing fatigue with the level of contamination present in the lubricant and an important conclusion from their work was that it is not the continued presence of debris in the lubricant, but the initial damage to the bearing surface, that leads to failure.

Figure 4 shows a three dimensional surface plot of a bearing surface taken from one of the test specimens used in (8). The surface damage from the 'rolled in' debris is obvious. Evidence suggests that such defects are responsible for many of the failures in rolling contacts and a great deal of research is in hand to understand the mechanisms involved.

One of the essential aspects of this problem is understanding the influence of such defects on the pressure distribution and film thickness within a Hertzian contact. Cheng and Bali (10) have solved the governing coupled ehd equation, for line contact, with a mathematically idealised furrow or asperity, and Wedeven (11) has used an optical ehd test machine to measure departure from the classical EHD conditions, caused by a debris initiated dent, but to date, no complete solution of the problem has been put forward. The authors have devised a numerical technique, which allows calculation of the normal contact pressures for a roller loaded against any surface profile. The computer program involved solves the general 2-dimensional dry contact problem, but differs from previous work as it incorporates a specialised algorithm to cope with real rough surfaces, and therefore allow the apparent contact area to consist of many interelated contact spots.

little to do with the generation of end lubricant films. With this problem in mind, the window must concentrate attention on the short spatial features which can penetrate the end film and lead to problems such as excessive plastic deformation, noise, reduced fatigue lives and scuffing.

Filters

Having defined the "window" or spatial range of roughness involved in a particular problem both analogue and digital filters can be employed for pre-analysis processing, but in general digital filters are the most useful. Many digital filters exist, the majority being defined as analogues of real time filters and designed for harmonic analysis where a known frequency response is required. Filters like this often suffer from phase-distortion although this has been overcome in some cases when formulating the digital analogues (Whitehouse (1968)).

The earliest digital filters used for surface analysis were the moving average type (Whitehouse and Reason (1965)) where a chosen length, say the nominal conatact length, is moved across the surface profile averaging over the length to generate the low-pass output. The high pass output being simply the difference between that and the original profile. Such filters have an obvious advantage as they simulate quite closely the action of components in nominal contact and relative motion. A disadvantage of such filters is that their characteristics cannot be defined without knowledge of the input signal; however, filters of this type are simple and fast in operation. Typical examples of the output from a cubic spline averaging filter encorporated in the topography analysis software TPROFK are shown in Figure 6.

SOME EXAMPLES OF TOPOGRAPHY MEASUREMENT AND ANALYSIS

Through several examples we will show how surface metrology can offer a detailed insight into many aspects of gear and rolling element bearing quality and production. The examples are chosen firstly to make use of the techniques we have described, and secondly to show how disparate scales of size can be treated in similar ways.

DIMENSION AND TOLERANCE

It has been well known for many years that the tolerance of machined components must be increased with component size. The reasons for this are never clearly defined although in BS4500 (1969) it is stated that to some extent this can be explained by an increased difficulty in manufacture. Thermal expansion effects must also be considered as these increase with component size, but are generally small in relation to tolerance with components below 500mm diameter. BS4500 gives empirical laws which relate tolerance to diameter and it is quoted that these relationships are derived from "extensive practical investigations", but the fundamental reasons why this should be so are still somewhat obscure. As an example, a 3cm diameter shaft, produced on say a lathe, would be associated with tolerance under the IT10 grade of 40μm, whereas the same machine and tolerance grade allows a 25cm shaft, 84μm.

Section 1.6 of BS4500 suggests that geometry, form and surface texture must also be considered in some circumstances. We would suggest that this is the principal reason why tolerance is necesary. The increase in difficulties in manufacture with component size stated as a reason by BS4500 is simply another way of stating that all surfaces exhibit a broad bandwidth of surface features, and that as the size increases, the number of wavelengths of potential surface geometric errors also increase.

With random long-wavelength variations in topography, which are outside the bandwidth associated with the small scale machining marks, Sayles and Thomas (1978) have shown that many surfaces exhibit an increasing roughess with length which follows a common law of,

$$\sigma = K(L)^{\frac{1}{2}} \qquad (1)$$

where σ is the rms roughness, L is the length of the surface and K is called the "topothesy" and is a constant for a given surface (1). In Figure 7 this equation is added to the small scale machining roughness R_{qt} and plotted against the empirical equations governing tolerance grades IT5-16 of BS4500 up to 500mm. The Parameter Rqt and the topothesy are chosen so that the curves overlap, however the values used are typical of an average ground surface. The fact that the curves do overlap is unimportant other than it provides the best way of comparing the trends.

The agreement in trend is suprisingly good even to the extent of anticipating tolerances requirement above 500mm and given by a separate equation in BS4500 which is shown by the dashed line. The figure demonstrates that for a given tolerance grade, to maintain a constant grade of fit, we are increasing the tolerance in the same way as the surface topography is changing. In other words we are maintaining the same relative surface interface conditions.

From a production engineering point of view Equation 1 can be considered at two different levels. Firstly it gives us an insight into the way in which the increase in tolerance is linked to size; an empirical fact which has long been established and taken for granted. Secondly, and on a more practical level, it can provide the production engineer with a means of monitoring the condition of a machine. We know that machines producing the same components can generate differeing values of K, and therefore K is a good measure of machine condition and environment. Thus in demonstrating that the topothesy K can be related to a class of tolerance, it seems possible to classify a machine quality in terms of its ability to produce components within a given tolerance grade. Periodic checks on the value of K being produced, would also act as a good indication of the potential useful life of the machine.

bearing and gear systems. In achieving this we will consider all aspects of surface metrology, from at the large scale, the relation between geometric error, tolerance and component size, through a range of bandwidths of importance, to features on the surface existing over linear dimensions a millionth and less of the component size.

HOW TOPOGRAPHY CAN INFLUENCE THE COMPONENT'S FUNCTION

To gain insight through metrology we require, at least initially, a complete record of the boundary between the component and its surroundings. Using the frame of reference of each function of the component as a window, we must examine this record for differences between the real components and the intended geometric shape, and using our experience and knowledge assess the functional efficiency of that component.

As an example of this principle and why it should be necessary, consider the case of a journal bearing. Normally the diameter, tolerance, and surface finish are regarded as the essential quality requirements. Under the right conditions the journal generates a hydrodynamic oil film over a substantial portion of the bearing circumference and the oil film thickness can be affected by the detail surface form over the arc of contact sustaining the load. Therefore specification of the diameter and tolerance can only satisfy part of the geometrical requirement. In this respect we can quote the classic, but still valid example of three or five point lobing giving a constant diameter. Even if we could get such a shaft to run freely in a bearing, its ability to generate an adequate oil film would be in doubt and the ensuing problem of vibration would almost certainly lead to difficulties.

The measurement of surface finish can be criticised for completely the opposite reasons. All surface measuring instruments employ some form of meter cut-off (the necessity for this will be discussed later). BS 1134 would recommend a 0.8mm cut-off, i.e. variations in surface height occurring over distances, in the plane of the surface, greater than 0.8mm would be ignored in the roughness value. Except for very small shafts the width of the oil film would be many times greater than 0.8mm and as a consequence the roughness measured could be of only secondary importance to the function. The cut-off we apply should ideally be of similar dimensions to the width of the oil film, thus expressing the roughness over the full range to highlight where intimate surface contact, and as a consequence, wear, fatigue and other surface problems are likely to occur.

MEASUREMENT AND ANALYSIS

Measurement

To achieve this form of analysis through measurement we must consider size, geometry and surface finish as the same problem, they can never be divorced in metrology, their terminology simply changes the scale of emphasis to different aspects of the surface topography. To gain insight through detailed surface examinations we must first collect a record of the surface. The computer based system developed at Imperial College is outlined in Figure 1, and consists of tactile surface measuring equipment, which in operation is not unlike conventional hi-fi reproduction systems, and connected to a PDP11/23 computer. The computer converts the analogue signal from the instrument being used into a digitial record of the surface. The speed of surface traversing is set to ensure that within the resolution we require (from the sampling interval we need between adjacent digitised ordinates up to the total traverse length) the signal reaching the computer is a true unfiltered record of the surface we are examining.

The computer converts the analogue signal into a series of integer numbers between -2048 and +2048, which represent +5.1V of the signal, and holds these in memory until traversing is complete. These numbers (1024 is usually found to be sufficient) can then be stored on disc files as a permanent record for future analysis, and also plotted on the VDU screen in various forms to construct the amplified surface profile or even in the form of many profiles to reconstruct the whole surface (Figure 2).

Analysis

The modern computer offers a multitude of ways in which data of the form representing a continuous, often random function, can be analysed very quickly. Table 1 shows the major options available through the general analysis program (TPR-FFT) used for our surface metrology research. With limited computer storage it is convenient to write analysed data to disc before examination. The data can then be read and listed on the VDU or printer, or by use of further software, any of the required functions generated can be picked from the file and plotted on the VDU or drum plotter as a permanent record.

The authors have also developed more advanced software for special applications. One example is the simulation of elastic contact between two or more machined surfaces. Measured or analysed surface information can be combined within the computer to investigate the effect of finishing and production processes on the interface conditions likely to occur in practice (Figure 3). A further example involves the representation of 3-dimensional surface information. Figures 4 and 5 show some results from software we have developed to represent isometric views and produce contour maps of surfaces.

The Need for Filtering

Throughout this paper we will consider roughness as a wavelength, as well as a height dependent problem. Each problem considered must be viewed through a "window" which defines the spatial size of surface asperities influencing the problem. For example the very short wavelength roughness features on a roller bearing have little influence on the bearings tolerance, this is mainly sensitive to long wavelength variations in form and out of roundness. Conversely such long wavelength features have

THE CHARACTERISTICS OF SURFACE ROUGHNESS IMPORTANT TO GEAR AND ROLLING BEARING PROBLEMS

by
R.S. Sayles and M.N. Webster
Tribology Section,
Department of Mechanical Engineering,
Imperial College,
Exhibition Road,
London, SW7 2BX.

SUMMARY

The role of surface roughness in rolling and rolling and sliding contacts is examined in the light of present concepts and ideas. Examples of the influence of roughness, and the important characteristics of this roughness, are drawn from helicopter transmission and rolling bearing research at Imperial College, London.

The important influence of geometry and roughness in tribological problems has been accepted for many years but only limited progress has been made in understanding the exact mechanisms involved and incorporating this knowledge into surface finishing processes designed to improve performance. This paper presents an approach to surface topography measurement and analysis which allows many of these problems to be examined in great detail. Examples of the approach are presented for several tribological problems including dimensional tolerance, rolling contact noise, and fatigue life, and in each case the character of the important range and size of surface roughness features is identified in terms of its influence on the specific problem under examination.

INTRODUCTION

The Need for Surface Metrology

The functional relationship of engineering components in an assembly is defined ultimately by the closeness to which the intended geometry is realised. Any concept embodied in an engineering drawing can only be approached in practice through controlling the accuracy of production and the means by which it is measured.

The ability to create and measure to required degrees of accuracy is a corner stone of mechanical engineering which Joseph Whitworth, in his Presidential address to the Institute of Mechanical Engineers in 1856 recognised in the following way;

> "I would next call your special attention to the vast importance of attending to the two great elements in constructive mechanics, namely, the true plane and the power of measurement."

Having recognised the power of measurement, Whitworth went on to say:

> "I hope the members of this Institution will join me in doing what we can with reference to these two important subjects - correct measurement, and its corollary proper graduation of size. The want of more correct measurement seems to pervade everything."

The reasonings underlining Whitworth's statements on geometry and dimension are as valid today as they were in his time. The sound basis which Whitworth and others like him set down has enabled the mechanical engineer to achieve a continuous increase in the accuracy and precision of manufacture and measurement.

Because of this, todays engineer is able to impose limits on geometry and dimension in a mass production environment which would have been unobtainable in Whitworths time. With modern transmissions and engine systems rolling element bearings are commonplace, millions of such bearings are produced every month in the UK alone, and yet the unit talked about for general bearing tolerances is tenths of thousandths of an inch (2.5μm with younger engineers); rolling element tolerance and geometry go down a further decade to variations in the order of 0.25μm, and surface finishes take us even further down the scale; roughness measurements specified to less than 0.025μm (less than 1 microinch) are commonplace. The difficulty and uncertainty in making measurements of this order is to be appreciated by the fact that the coefficient of thermal expansion of steel is about 0.012μm/mm/^{o}C.

In the sense that metrology is concerned with precision measurement it implies an attempt to assess the "true value" of the magnitude. It is, or at least it should be intimately bound up with both the source of the problem - to decide what is to be measured, to know and to discipline the inevitable uncertainties of measurement - and the use that is to be made of the answer; it is not a subject to be taken in total isolation. A corollary of the above thesis is that, put in proper prospective, surface metrology is designed to generate insight from measurement: it is to bring into prominence and describe the features that are most significant in relation to the applications in question.

With this aim in mind this paper will show how computer controlled surface metrology techniques can be used not only to offer solutions to metrological problems, but to gain insight into many aspects of

Author's Reply

Dr Blok is exactly right in his suggestion that a detailed accounting of all theoretical estimations of power loss should be carried out. The basis of this accounting is already in the literature (Refs 3—7) and in the references list below. There are some unanswered questions about friction (traction) effects and also more theoretical work on power loss of spiral bevel gears needs to be worked out. Dr Blok has given us the last two references which will be very helpful.

- Anderson, N. and Loewenthal, S.H.: "Efficiency of Non-Standard and High Contact Ratio Involute Spur Gears" ASME paper 84-DET-172.
- Anderson, N.; Lowenthal, S.H. and Black, J.D.: "An Analytical Method to Predict Efficiency of Aircraft Gearboxes" NASA TM 83716, (USAAVSCOM TR 84-C-8).
- Parker, R.J.: "Comparison of Predicted and Experimental Thermal Performance of Angular Contact Ball Bearings" NASA TP 2275, Feb 1984.
- Blok, H.: "Hydrodynamic Effects on Friction in Rolling with Slippage": Proc. Symp. on "Rolling Contact Phenomena", organized by General Motors Corp. in 1961, and edited by J.B.Bidwell: Elsevier Publ. Co., Amsterdam, Holland, 1962; pages 186—243; disc., pages 243—251.
- Blok, H.: "The Thermal Network Method for Predicting Bulk Temperatures in Gear Transmissions": Proc. 7th Round Table Discussion on Marine Reduction Gears, issued by STAL-LAVAL AB, Finspang, Sweden. For a French translation see, Bulletin No.59, pages 3—13, of Societe d'Etudes de l'Industrie de l'Engrenage, 15 rue Beaujon, Paris — 8e, France.

DISCUSSION

B.A.Shotter, UK

With fine ground surface finishes, the maximum surface slope can be significantly higher than the measuring stylus tip slopes. Thus, the recorded information does not truly represent the small scale features. Could the author comment on the significance of this?

Author's Reply

The small scale features on abraded surfaces can indeed possess very high slopes and SEM pictures will confirm this. The Talysurf cannot accurately record such features, particularly if the scale of the feature or asperity is in the order of the stylus radius (usually about 2 mm with standard styli) or the slope of the feature exceeds the stylus angle (usually 45°).

My first, and probably most useful comment is that such features are usually too small to be of significance in most engineering applications. I say this with some reservations, as I know of some applications where the small scale features are important. However, in many engineering applications, it is fair to say that if a small sharp stylus can plasticly remove such features under a very small applied load (usually about 100 mg), and bearing in mind that such asperities are often much lower in height than typical calculated lubricant film thicknesses, then it is difficult to foresee their their significance in a real engineering environment.

J.Godston, US

The 500 point pressure distribution discussed in the paper was analytical. How did you measure the local pressures — deformities? What size bearings, gears were used in your experiments and analysis?

Author's Reply

The local asperity deformations were calculated via the elasticity relations based on each 2 mm element being subjected to the appropriate level of uniform pressure. The experimental measurements of the undeformed surfaces were taken from ground surfaces, and with the debris indentation work, from small roller bearing raceways (about 1" I.D) which had undergone some running with oil contaminated with gearbox wear debris. This latter test allowed us to obtain surface profiles with real debris plastic indentations present.

PARAMETRES SIGNIFICATIFS DU COMPORTEMENT ET DES AVARIES DE SURFACE DU CONTACT HERTZIEN LUBRIFIE. APPLICATION AUX ENGRENAGES

D. BERTHE , Professeur
L. FLAMAND, Maître-Assistant

Institut National des Sciences Appliquées de Lyon
Laboratoire de Mécanique des Contacts
E.R.A. C.N.R.S. n° 070665
Bâtiment : 113
20, avenue Albert Einstein
69621 Villeurbanne Cédex - France

I - INTRODUCTION

La vie d'un mécanisme est souvent limitée par des avaries de surface. L'objectif de ce papier est de définir certains critères qui permettent d'apprécier la sévérité du fonctionnement du contact hertzien lubrifié et le risque d'avaries de surface.

En premier lieu, les familles fondamentales d'avaries de surface dans les contacts lubrifiés très chargés seront précisées. Ensuite, les modèles théoriques utilisés pour analyser le comportement mécanique et les paramètres de fonctionnement du contact seront définis. L'importance du facteur d'échelle sera notée.

Enfin, l'application de cette analyse aux problèmes d'endommagements des surfaces de dentures d'engrenages sera discutée.

II - AVARIES DU CONTACT HERTZIEN LUBRIFIE

II.1. - Position du problème

Schématiquement un contact est constitué de trois corps : les solides 1 et 2 et un milieu intercalaire dans lequel se réalisent la transmission de la charge et l'adaptation des vitesses relatives entre 1 et 2, (Fig.1). Lorsque ce milieu intercalaire est un écoulement fluide visqueux et que les massifs se déforment élastiquement sous l'effet des pressions dans l'interface le contact est dit hertzien lubrifié et le régime élastohydrodynamique. C'est le cas notamment pour les engrenages et les roulements.

Si la hauteur moyenne des aspérités des massifs est suffisante pour que des contacts directs existent, le régime est mixte. Une analyse mécanique à l'échelle de ces micro-contacts est alors nécessaire.

Des champs de contraintes, de déformations et de températures se développent dans chacun des milieux de ce contact. Ils sont dus au fonctionnement. La réponse de ces milieux et en particulier des solides 1 et 2 conditionne le bon fonctionnement du mécanisme ou les avaries de surface.

II.2. - Avaries de surface

Les avaries de surface dans les contacts hertziens en régime élastohydrodynamique ont fait l'objet d'une abondante littérature [1,2]. A titre d'exemple, l'A.G.M.A. défini 21 modes de détérioration des structures d'engrenage [3]. Toutefois, les mécanismes qui gouvernent ces dégradations ne sont pas encore entièrement explicités et la terminologie est imprécise. On distingue trois familles fondamentales :

- les fatigues superficielles associées aux effets normaux dans le contact,
- les usures corrélées aux effets normaux et tangentiels,
- les grippages reliés aux effets tangentiels et thermiques.

II.2.1. - Les fatigues superficielles

Elles apparaissent dans la zone de faible glissement. Elles sont de deux types :

- les avaries "profondes", appelées écailles, (spalls), sont des enlèvements de matière de quelques millimètres carrés de surface et de quelques dizièmes de millimètres de profondeur,(Fig.2). Les dimensions sont à l'échelle du contact global, c'est-à-dire du domaine hertzien classique. Elles apparaissent brutalement après une incubation. Un examen attentif montre qu'elles sont précédées par la création d'un réseau de fissures. Elles surviennent dans des contacts très chargés. Sur la figure 2, on observe une écaille survenue sur des surfaces en roulement presque pur. On remarque autour de cette écaille d'autres avaries de dimensions beaucoup plus faibles.

- les avaries "superficielles", appelées micro-écailles, (micropits), sont des enlèvements de matière de quelques centièmes de millimètres de diamètre et de profondeur, Fig.3. Ces dimensions sont à l'échelle de l'aspérité. L'incubation est plus courte que pour les écailles. Elles surviennent dans des contacts même peu chargés.

En tant que telles, ces micro-écailles n'empêchent pas le fonctionnement de l'engrenage. Par contre, elles accélèrent la formation des écailles, |4,5|. Elles sont donc dangereuses.

II.2.2. - Les usures

Elles apparaissent quelle que soit la valeur du glissement. Il s'agit d'enlèvement progressif de matière à l'échelle des aspérités issu de différents mécanismes : déformation plastique, abrasion, adhésion, usure chimique, figures 4 et 5, |6,7|.

II.2.3. - Les grippages

Ils apparaissent dans des zones de fort glissement. Ils se manifestent par la fusion des couches superficielles des massifs. Ils sont accompagnés d'émission de fumée et de bruit et d'augmentation de la force de frottement, |8|. Ils détruisent la micro-géométrie des surfaces, voire la géométrie par des arrachements et des transferts métalliques d'un massif à l'autre, (Fig.6 et 7). L'augmentation relative de la hauteur des aspérités est de l'ordre de 1 à 5. Les grippages surviennent toujours brutalement. Ils sont reliés à la température dans le contact et à la physicochimie du lubrifiant.

III - MODELISATION MECANIQUE DU FONCTIONNEMENT D'UN CONTACT HERTZIEN

III.1. - Position du problème

Dans cette analyse seul l'aspect mécanique est abordé. Cependant, les aspects métallurgiques et physicochimiques ne sont pas écartés, mais l'état physicochimique du contact au sens large est considéré comme une *condition aux limites du problème mécanique*. Le fonctionnement du contact lubrifié est analysé en considérant les trois éléments suivants :

- la séparation ou épaisseur *moyenne* du film visqueux lubrifiant, due aux caractéristiques de l'engrenement,
- le champ de contraintes induit en particulier par la déformation imposée par la séparation,
- le champ de température résultant de la dissipation dans le film séparateur.

III.2. - La séparation

Dans un contact hertzien lubrifié, les pressions sont suffisantes pour augmenter la viscosité du lubrifiant et pour déformer les surfaces. Au cours des vingt dernières années, de nombreuses études expérimentales et théoriques ont montré que :
- un film d'huile d'épaisseur comprise entre 0,01 et 1 µm peut se former dans un contact hertzien pour des gammes de charge et de vitesse très étendues,
- des théories analytiques ou numériques permettent de calculer ces films,
- la concordance entre les résultats expérimentaux et théoriques est excellente.

Formellement, le contact est décrit par :
- sa géométrie, sa cinématique et la charge transmise,
- le comportement du lubrifiant, (thermo et piézoviscosité),
- l'équation de l'écoulement ou équation de Reynolds pour le film,
- l'équation de l'élasticité pour la déformation des surfaces,
- l'équation de l'énergie dans les différents milieux pour le champ de température.

III.2.1. - Valeur de la séparation

Hypothèses : écoulement isotherme, surfaces lisses, lubrifiant surabondant.

Pour un contact cylindre infiniment long, Fig.8a, l'épaisseur du film ou séparation au centre du contact est donnée par la relation de Dowson et Higginson, |9| :

$$H_o = 0.98\, U^{0.7}\, G^{0.6}\, W^{-0.13} \qquad (1)$$

Pour un contact elliptique, Fig.8b, l'épaisseur du film au centre du contact est donnée par la relation de Hamrock et Dowson, |10| :

$$H_o = 1.691\, U^{0.67}\, G^{0.53}\, W^{-0.067}\, |1 - 0.61 \exp(-0.73\, K)| \qquad (2)$$

Dans ces expressions, les variables non dimensionnées sont :

$$U = \mu_o (U_1+U_2)/E\,R_x \qquad G = \alpha E$$

$$W = w/E\,R_{x_2}\,L \qquad H = h_o/R_x$$

$$W_* = w/E\,R_x \qquad K = 1.03\,(R_z/R_x)^{0.64}$$

$$E = \left[1/2\left((1-\nu_1^2)/E_1 + (1-\nu_2^2)/E_2\right)\right]^{-1}$$

$$R_x = \left(1/R_{x_1} + 1/R_{x_2}\right)^{-1}$$

$$R_z = \left(1/R_{z_1} + R_{z_2}\right)^{-1}$$

Les paramètres sont définis de la façon suivante :

* μ_o est la viscosité dynamique dans l'entrée du contact,
* U_1, U_2 sont les vitesses de roulement dans la direction x,
* R_{x1} et R_{x2}, R_{z1} et R_{z2} sont respectivement les rayons de courbure des surfaces 1 et 2 dans les directions x et z,
* W est la charge normale dans le contact,
* α est le coefficient de piézoviscosité du lubrifiant,

$$\mu(p) = \mu(p_o)\,\exp\left[+\alpha(p-p_o)\right]$$

* E_1 et E_2, ν_1 et ν_2 sont respectivement les modules de Young et les coefficients de Poisson des massifs 1 et 2,
* h_o est l'épaisseur réelle au centre du contact,
* L est la longueur des cylindres, (selon z).

Les expressions (1) et (2) ont été vérifiées expérimentalement de nombreuses fois, [11-13]. L'erreur commise est inférieure à 10 %.

III.2.2. - *Eléments pondérateurs de cette séparation.*

Depuis les approches ci-dessus, les effets de trois phénomènes ont été précisées.

A - l'effet de l'échauffement caractérisé par le coefficient de correction thermique qui provoque une diminution de la séparation :

$$H_T = \phi_T\,H_o$$

Ce coefficient dépend de la somme des vitesses dans le contact, de la conductivité thermique du lubrifiant, de la viscosité et de la température absolue à l'entrée du contact, [14]. Sa variation entre 1 et 0.27 a été confirmée expérimentalement avec une précision de 20 %, [15].

B - l'effet des rugosités dépend de la valeur de leur hauteur et de leur orientation par rapport aux vitesses de roulement. Il est caractérisé par le facteur ϕ_R, tel que :

$$H_R = \phi_R\,H_o$$

qui peut varier entre 0.42 et 1.29, [16-17].

C - l'effet de l'alimentation en lubrifiant dépend de la longueur du domaine rempli d'huile, c'est-à-dire de l'abscisse d'entrée. Il est caractérisé par le facteur ϕ_A, tel que :

$$H_A = \phi_A\,H_o$$

qui peut varier de 0.6 à 1.0, [18].

En résumé : pour un contact rugueux l'épaisseur dimensionnée de la séparation au centre du contact est donnée par l'expression :

$$h_o = R_X\,\phi_T\,\phi_R\,\phi_A\,H_o$$

Typiquement elle varie de 0.1 à 2 µm.

III.3. - **Les contraintes**

Il faut introduire deux échelles d'analyse à l'image des longueurs caractéristiques D_1 et D_2, (Fig.9).

La première dimension D_1 est analogue à la longueur totale du contact hertzien 2a. Elle découle de la géométrie globale du contact et de la charge normale qu'il transmet. Dans le cas lubrifié, la théorie de Hertz demeure applicable pour le calcul des contraintes, [19].

La seconde dimension D_2 est analogue à la longueur moyenne du contact au niveau des aspérités déformées dans le contact réel. Elle découle de la géométrie locale moyenne de ces aspérités et de leur déflexion moyenne, elle-même liée au rapport de rugosité σ_c/h_m.

Ces deux échelles sont analysables séparemment, |19,20|.

a) - Analyse globale, échelle D_1

L'approche globale à l'échelle D_1 est bien connue, il s'agit de l'approche hertzienne. Elle permet de calculer la dimension de l'siré de contact, la pression maximale hertzienne et les contraintes dans le massif.

Dans le cas d'un contact cylindrique de grande longueur L, suivant Oz, si b représente la demi-largeur de la zone de contact suivant Ox, il vient :

$$b = (8WR_x/\pi EL)^{1/2} \quad \text{et pour} \quad x = 0 \quad \begin{cases} p_o = 2W/\pi bL \\ \tau_{max} = 0.3\, p_{max} \end{cases}$$

b) - Analyse locale, échelle D_2

Lorsque la séparation moyenne h_m est plus petite que la hauteur des aspérités, des contacts locaux se produisent. La déformation des aspérités qui en résulte est imposée par les caractéristiques du film séparateur, notamment sa raideur, |21|. Sur les aspérités déformées apparaissent des pressions supérieures à la pression globale hertzienne ainsi que des maxima secondaires de contraintes, notamment des contraintes de cisaillement à une profondeur sensiblement D_2, (Fig.10). Ces sur-contraintes sont fonction du rapport de la hauteur des aspérités σ_c à la séparation h_m et du rayon de courbure moyen des aspérités β_c.
σ_c est la hauteur quadratique composite et a pour valeur :

$$\sigma_c = (\sigma_1^2 + \sigma_2^2)^{1/2}$$

σ_1 et σ_2 étant les hauteurs quadratiques des rugosités de chacune des surfaces 1 et 2.

c) - Analyse simultanée.

Dans les cas de fonctionnement très sévère, c'est-à-dire lorsque le rapport de rugosité σ_c/h_m est très supérieur à 1, les longueurs caractéristiques D_1 et D_2 peuvent être du même ordre de grandeur. Le rapport d'échelles D_2/D_1 est lié à la valeur moyenne de l'aire réelle de contact rapportée à l'aire totale ou apparente, |22,23|.

III.4. - Les températures

La dissipation due au cisaillement de l'écoulement du lubrifiant dans le contact provoque une augmentation de température dans le film et dans la peau des massifs.

Différentes études, |22,23|, ont montré que la température maximale des surfaces des massifs est donné avec une précision suffisante (20 %), par le concept de "flash temperature", |24|.

$$T_{max} = T_o + T_f$$

$$T_f = 1.6 f p_o (U_1 - U_2) \sqrt{2b/(\pi K_1 \rho_1 C_1 U_1 + \sqrt{\pi K_2 \rho_2 C_2 U_2})}$$

où K_1, K_2, ρ_1, ρ_2, C_1 et C_2 sont respectivement les conductivités, les masses spécifiques et les chaleurs spécifiques des matériaux des massifs 1 et 2.

U_1 et U_2 sont les vitesses de roulement décrites précédemment,
p_o est la pression maximale hertzienne,
f le coefficient de frottement,
b est la demi-largeur du contact dans le sens des vitesses.

La difficultée essentielle est la connaissance ou l'appréciation du coefficient de frottement f réel. A ce jour, il n'existe pas de moyen théorique fiable pour calculer ce coefficient de frottement. Une expérimentation est donc indispensable. Cependant, pour un régime élasto-hydrodynamique des variations entre 0.02 et 0.06 sont caractéristiques d'un fonctionnement normal. Par ailleurs, à partir d'études très récentes, des valeurs de l'ordre de 0.12 à 0.15 sont le signe d'une défaillance de la composante hydrodynamique de la lubrification.

En résumé :

La modélisation du fonctionnement du contact conduit au classement des paramètres mécaniques en deux catégories :
- **les paramètres qui constituent l'état mécanique du contact,**
- **les paramètres de comportement du contact.**

Parmi les premiers, rappelons :
- **les géométries des massifs,**
- **les vitesses d'entraînement et de roulement,**
- **la charge normale transmise,**
- **les caractéristiques physiques du lubrifiant et des massifs.**

Parmi les seconds :
- le rapport de rugosité σ_c/h_m,
- le rayon moyen de courbure des aspérités β_c,
- le rapport d'échelle D_2/D_1,
- la vitesse de glissement U_1-U_2,
- la pression hertzienne maximale p_o,
- la température maximale T_M, ou simplement l'augmentation de température T_f.

IV - PARAMETRES SIGNIFICATIFS VIS-A-VIS DES AVARIES

IV.1. - Position du problème

Bien que les mécanismes d'avaries ne soient pas encore entièrement explicités, il est possible de définir l'effet de certains paramètres sur tel ou tel type d'avarie.

IV.2. - Fatigues superficielles

a) Ecaillage :

Il est bien connu que l'écaillage est fonction de la pression hertzienne maximale p_o, donc de la contrainte de cisaillement maximale en sous-couche. Toutefois, les initiations superficielles sont liées aux conditions de lubrification, donc au rapport de rugosité σ_c/h_m, |27,28|.

b) Micro-écaillage :

Le micro-écaillage est fonction uniquement du rapport de rugosité σ_c/h_m, |20|.

Il existe en effet, deux niveaux d'initiation des avaries de fatigue superficielle, le niveau profond ou hertzien classique et le niveau superficiel. Pour l'initiation profonde la contrainte de cisaillement maximale est le paramètre prépondérant. Pour l'initiation superficielle, le rapport de rugosité est le paramètre essentiel. Ces deux niveaux d'initiation génèrent respectivement les écailles et les micro-écailles. L'effet du rapport de rugosité sur l'écaillage est lié à l'intéraction des deux réseaux de fissuration.

Les bornes des paramètres p_o et σ_c/h_m ne sont pas clairement connues. Cependant, la pression hertzienne peut être judicieusement comparée à Hv/3 où Hv est la dureté de Vickers. En effet, le seuil de déformation plastique est obtenu pour une pression hertzienne maximale à Hv/3. En ce qui concerne σ_c/h_m, la valeur 1 signifie qu'en moyenne toutes les aspérités subissent une déflexion importante dans le contact et sont donc l'objet de surpressions de contact très élevées.

IV.3. Usures

Il n'existe pas de critère fiable concernant l'usure. Cependant, il est prouvé que c'est une fonction croissante de la vitesse de glissement U_1-U_2, du coefficient de frottement f et du rapport de rugosité σ_c/h_m, |6|.

IV.4. - Grippage

De même que pour l'usure, il n'existe pas de critères globaux pour le grippage. En effet, il faut considérer simultanément deux aspects : le fonctionnement mécanique et le comportement physico-chimique du contact.

a) Fonctionnement mécanique. Des études récentes, tant théoriques qu'expérimentales, |8,22,23|, montrent que la condition nécessaire au grippage est que le rapport d'échelle D_2/D_1 tende vers 1.

b) Comportement physico-chimique. Différentes études ont prouvé que l'action physico-chimique en surface et dans le lubrifiant sont liées à la température maximale dans le contact, convenablement représentée par l'approche de Blok |8,26|.

V - APPLICATION AUX AVARIES DE SURFACE DANS LES ENGRENAGES

L'application de la procédure ci-dessus aux surfaces de denture est tout à fait possible. Cependant, deux difficultés spécifiques doivent être surmontées : la variation de certains paramètres de l'état mécanique le long de l'engrènement et la nécessité de l'appréciation expérimentale de certains d'entre eux.

V.1. - Paramètres de l'état mécanique le long de l'engrenement

En chaque point de cet engrenement, les géométries et les vitesses des surfaces de dentures ainsi que la charge transmise varient. Il a été montré que pour des engrenages cylindriques à axes parallèles, on peut représenter un point donné de l'engrenement en régime permanent par le contact entre deux cylindres d'axes parallèles munis des mêmes charges, géométries et vitesses, |29|, Fig.11. Nous utiliserons cette simulation pour une analyse point par point.

Les paramètres de comportement du contact seront donc analysés pour un certain nombre de points de l'engrenement à partir de la connaissance en ces mêmes points des paramètres constituant l'état mécanique. Généralement, on choisit cinq points :

- T'_1 : premier point de l'engrenement en pied de pignon avec deux couples de dents en prise,
- T''_1 : point de transition entre pied de pignon et primitif,de deux à un couple de dents en prise, la charge normale étant supposée transmise par un seul couple de dents,
- I : point de contact confondu avec le primitif,
- T''_2 : point de transition entre primitif et sommet de pignon, de un à deux couples de dents en prise, ici encore la charge normale est supposée transmise par un seul couple de dents,
- T'_2: dernier point de l'engrenement au sommet du pignon avec deux couples de dents en prise.

Si les surfaces de denture présentent des corrections longitudinales, (bâteaux), le contact sera considéré comme elliptique.

V.2. - **Approche expérimentale**

L'état mécanique étant connu, deux difficultées demeurent : l'appréciation du coefficient de frottement f et du rapport d'échelle D_2/D_1 réels.

a) Dans un engrenement il est difficile de connaître le coefficient de frottement, en particulier à partir de la mesure de la puissance dissipée. Cependant, nous avons déjà noté qu'en régime élastohydrodynamique des variations entre 0.01 et 0.06 sont caractéristiques d'un fonctionnement normal, y compris pour des rapports de rugosités supérieur à 1, |22|. Au contraire, des valeurs de 0.12 à 0.15 sont typiques d'un mauvais fonctionnement hydrodynamique.

b) Le rapport d'échelle D_2/D_1 ne peut pas être connu à priori. Son appréciation nécessite une analyse fine de la micro-géométrie des surfaces et surtout de leur évolution au cours du fonctionnement, donc suppose une démarche expérimentale.

VI - Conclusions

1 - Les avaries de surface de contact élastohydrodynamique rugueux appartiennent à trois familles : les fatigues superficielles, les usures et le grippage. L'importance de l'échelle d'analyse est rappelée.

2 - Ces avaries sont associées à des effets normaux, tangentiels et thermiques dans le contact qui constituent les paramètres de comportement ou significatifs du contact. Les moyens pour les quantifier à partir de l'état mécanique sont présentés.

3 - Les relations entre ces avaries et ces paramètres sont rappelées. Plus particulièrement l'importance du rapport d'échelle est notée. En bref, des liens sont établis entre :
- le rapport de rugosité et le micro-écaillage,
- la pression hertzienne maximale et l'écaillage et la déformation plastique,
- le rapport d'échelle, l'augmentation de température et le grippage.

4 - Les difficultées pour appliquer cette analyse à l'engrenement sont soulignées.

5 - Le concepteur dispose alors de critères objectifs pour apprécier le comportement d'un contact élastohydrodynamique rugueux par exemple dans le cas des roulements et des engrenages.

VII - BIBLIOGRAPHIE

|1| - KU, P.M., "Gear failure mode. Importance of lubrication mechanics", A.S.L.E., Trans., vol.19.3, pp.239-249, 1976.

|2| - "Nomenclature of gear-tooth wear and failure", A.G.M.A. Standard, 110-03, 1962.

|3| - "Interpreting service damage in rolling type bearing", Publ. by the A.S.L.E., minth printing, 1980.

|4| - TALLIAN, T.E., "On compiting failure modes in rolling contact", A.S.L.E., 10, pp.418-439, 1967.

|5| - LITTMANN, W.E., WIDNER, R.L., "Propagation of contact fatigue from surface origin", A.S.M.E. J. of Basic Eng., series D, 88, pp.624-636, 1966.

|6| - ARCHARD, J.F., "Elastic deformation and laws of friction", Proc. Roy. Soc., London, 243 A, p.190, 1957.

|7| - BEGELINGER, A., DE GEE, A.W.J., "Boundary lubrication of sliding concentrated steel contacts", Wear, vol.22, n°3, pp.337-358, 1972.

[8] - DYSON, A.,"Scuffing - a review",Tribology, june 1975, pp.117-122.

[9] - DOWSON, D., HIGGINSON, G.R., "A numerical solution to the elastohydrodynamique problem". Jour. Mech. Eng. Sc., vol.1, p.6, 1959.

[10] - HAMROCK, B.J. et DOWSON, D., "Isothermal elastohydrodynamic lubrication of points contacts. Part III. Fully flooded results". Trans. A.S.M.E., J. Lub. Tech., series F, vol.99, pp.264-276, 1977.

[11] - CROOK, A.W., "The lubrication of rollers", II, Phil. Trans. Royal Society, A, Tome 254, p.223, 1961.

[12] - DALMAZ, G., GODET, M., "L'hydrodynamique du contact sphère-plan. 1ère partie : solution théorique, numérique exacte en régime équi et piézo visqueux". Revue Mécanique, Matériaux, Electricité, n°268, pp.32-41, 1972.

[13] - WEDEVEN, L.D., EVANS, D. et CAMERON, A., "Optical analysis of ball bearing starvation". Trans. A.S.M.E., series F, vol.93, pp.349-363, 1971.

[14] - CHENG, H.S. et STERNLICHT, B., "A numerical solution for the pressure, temperature and film thickness between two infinitely long lubricated rolling and sliding cylinders under heavy loads". Trans. A.S.M.E., Jour. of Basic Eng., series D, pp.695-707, 1965.

[15] - GUPTA, FLAMAND, L., BERTHE, D., GODET, M., "On the traction behaviour of several lubricant", A.S.M.E. Paper 80 C2, Lub. 15.

[16] - PATIR, CHENG, H.S., "An average flow model", A.S.M.E. Lub. Tech., vol.100, janv. 1978, pp.12-17.

[17] - BERTHE, D., FANTINO, B., FRENE, J., GODET, M., "Influence of the shape defects and surface roughness on the hydrodynamic of lubricated systems". Journ. of Mech. Eng. Sc., I.M.E., 1974.

[18] - HAMROCK, B.J. et DOWSON, D., "Isothermal elastohydrodynamic lubrication of points contacts. Part IV. Starvation results". Trans. A.S.M.E., J. Lub. Tech., series F, vol.99, pp.15-23, 1977.

[19] - MICHAU, B., BERTHE, D., GODET, M., "Influence of pressure modulation in a linear hertzian contact on the internal stress-field", Wear, vol.28, n°2, p.187, 1974.

[20] - BERTHE, D., FLAMAND, L., FOUCHER, D., GODET, M., "Micropitting in hertzian contact", A.S.M.E. Lub. Tech., vol.102, oct. 1980,pp.478-489.

[21] - JOHNSON, K.L., GREENWOOD, T.A., POON, S.Y., "A simple theory of asperity contact in elastohydrodynamic lubrication", Wear, 19, 1, pp.19-108, 1972.

[22] - AKL, E., "La méthode ferrographique, morphologie, avaries. Etude de la séparation, morphologie des particules dans un contact hertzien lubrifié. Applications aux mécanismes d'avaries", Thèse D.D.I., 1-8330, Lyon, 1983.

[23] - AKL, E., FLAMAND, L., BERTHE, D., "Séparation measurement in a rough E.H.D. contact", 10th Leeds-Lyon Symp., sept. 1983, à paraître.

[24] - PHAM, A., "Etude thermique du contact hertzien lubrifié", Thèse de Docteur 3° Cycle, spécialité Mécanique, Lyon, 1982.

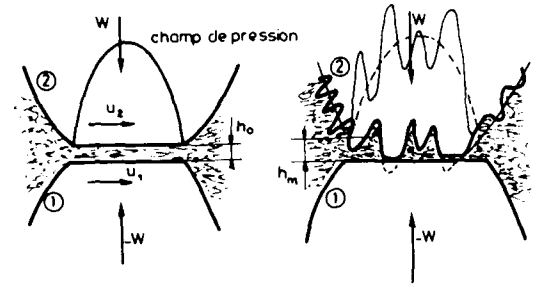
[25] - FLOQUET, A., "Températures de contact en frottement sec. Déterminations théorique et expérimentale", Thèse DDI, Lyon, 1978.

[26] - BLOK, H., "Theoritical study of temperature rise at surface of actual contact under oiliness lubricating conditions", Gen. Disc., Lub., Lust. Mech. Eng. 2, pp.222-235, 1937.

[27] - TALLIAN, T., "Rolling contact failure control through lubrication", I.M.E., vol.182, pp.205-236, 1967-1968.

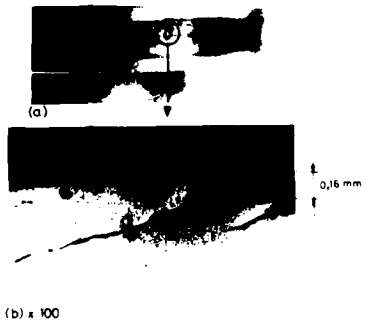
[28] - DAWSON, P.H., "Effect of metallic contact on the pitting of lubricated rolling surfaces", J. Eng. Sci., vol.4, pp.16-21, 1962.

[29] - FLAMAND, L., BERTHE, D., GODET, M., "Simulation of hertzian contacts found in spear gears with a high performance disk machine". A.S.M.E., Jl. of Mech. Des., vol.103, pp.204-209, janv.81.



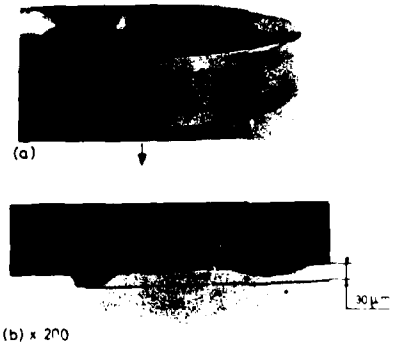
contact lisse - film complet contact rugueux - film partiel

Fig 1 Schématisation du contact hertzien lubrifié



(b) x 100

Fig. 2 Ecaillage, avarie "profonde"



(b) x 200

Fig. 3 : Microécaillage, avarie superficielle

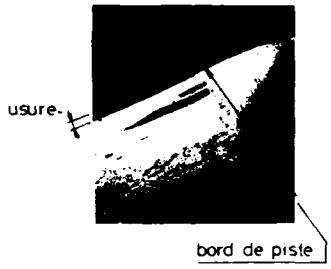


Fig. 4 : Caractérisation de l'usure

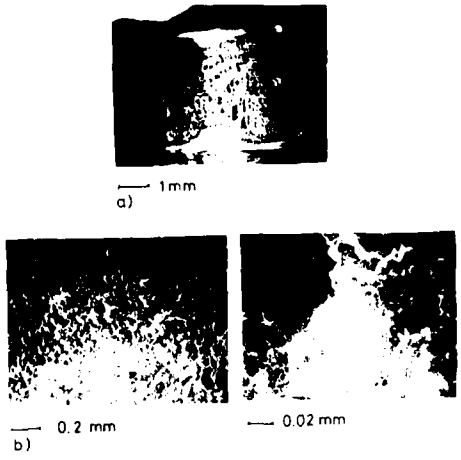


Fig.5 : Usure par micro-écaillage

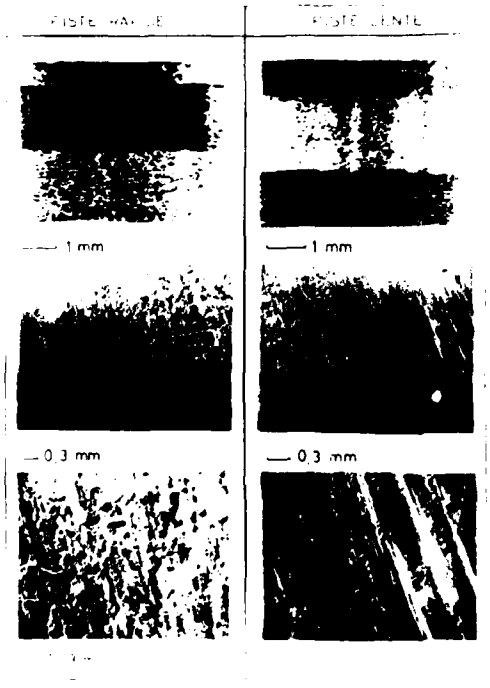


Fig.6 : Grippage, lubrifiant huile de base

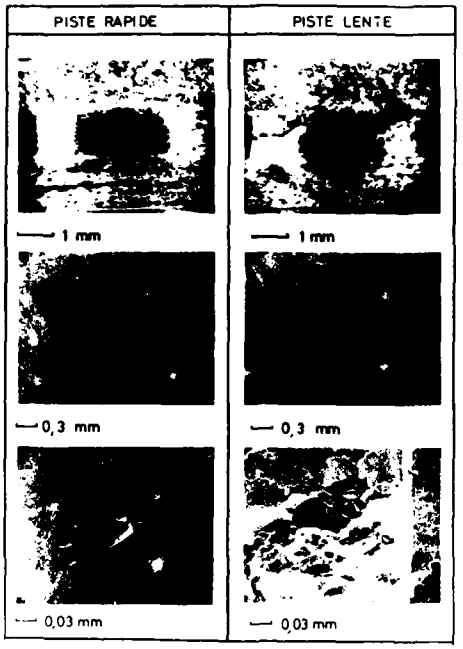
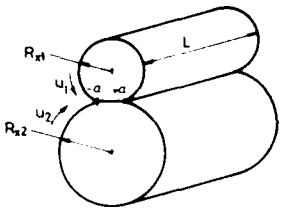
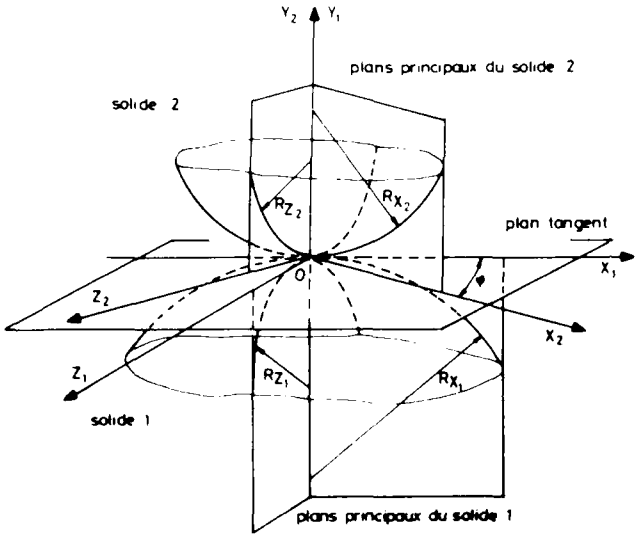


Fig. 7 : Grippage, lubrifiant avec additif DTPZn



a) contact cylindrique infiniment long



b) contact elliptique

Fig. 8 : Géométrie du contact hertzien cylindrique ou elliptique

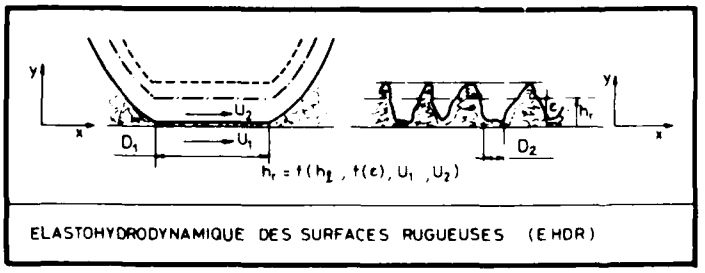
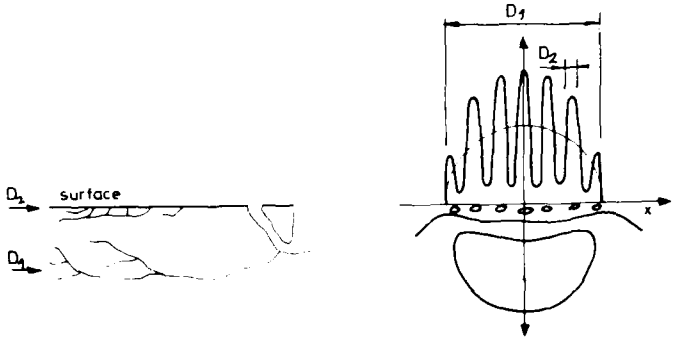


Fig. 9 : Longueurs caractéristiques du contact hertzien lubrifié rugueux



a) - les deux types de fissurations (figure tirée à partir d'une photo)

b) - les deux zones de contraintes maximales de cisaillement τ

Fig. 10 : Echelles d'analyse des contraintes dans le contact rugueux

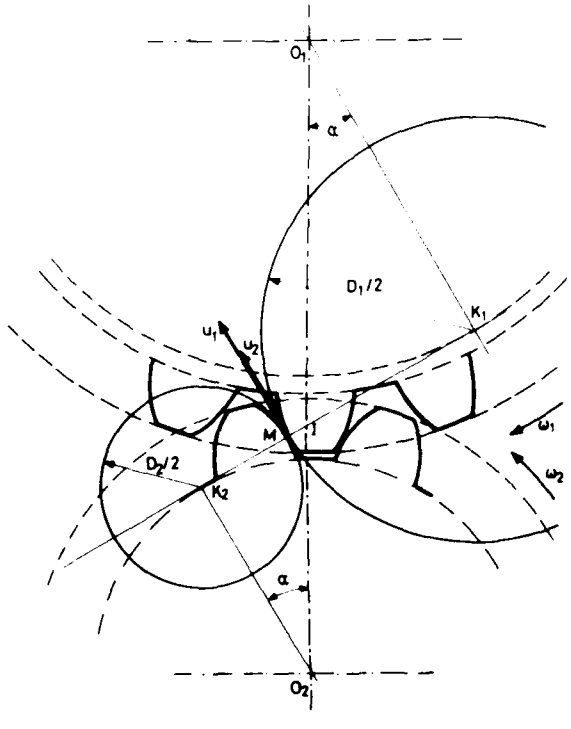


Fig. 11 : Simulation de l'engrènement

DISCUSSION

R.W.Snidle, U.K.

Various parameters have been mentioned in relation to scuffing failure: ratio of mean roughness to film thickness, flash temperature and micro-elastohydrodynamic lubrication. The work of Bell and Dyson casts doubt on the use of the first two parameters as the basis for a scuffing criterion. Do the authors favour an alternative model of scuffing? Our own work suggests that scuffing occurs when the mechanism of elastohydrodynamic lubrication of rough surfaces fails because of the rise in *bulk* temperatures of the surfaces. This tendency is offset to a greater or lesser extent by "running-in".

Author's Reply

In our approach to scuffing criteria, as we have mentioned in our paper, there is very strong experimental evidence that two phenomena must be present to lead to scuffing. First the failure of EHL film; second, the failure of physical-chemistry of the contact.

The paper you mentioned of Bell and Dyson (IME) has shown that a single criterion does not work. The later Cheng and Dyson paper proposes a condition for EHD film failure based on film formation in the rough contact.

In our approach similar to Cheng and Dyson's view:

EHD film failure is related to D_3-D_1 parameter

physics chemistry failure is related to T_{max}

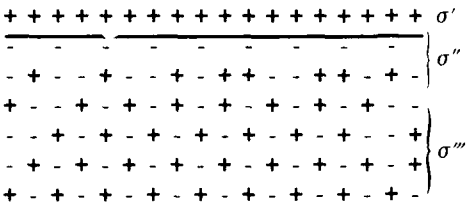


FIGURE 1. The Helmholtz-Gouy-Chapman charge distribution near the metal-electrolyte boundary.

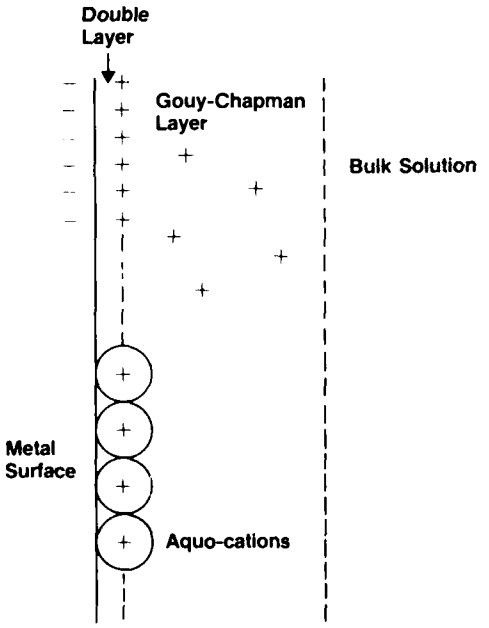


FIGURE 2

The case of diffusion of sulfur has also been experimentally observed [10] and it is stated that "both the maximum sulfur concentration and the degree of sulfur penetration increase with load." The effectiveness of the lubricants containing sulfur, in the sense of reducing wear and seizure of steel, has thus been correlated with the formation of surface layers of iron sulfide under loading.

The opposite of passivation could also occur as in hydrogen embrittlement by liquid-metal atoms (e.g., mercury) diffusing into the metal. Again we note that the initial defect structure of the surface plays a major role. A case in point is the observation* that pitting resulted only if there were defect structures on the surface to begin with. This observation supports the hypothesis that the chemostress effect is taking place at crack tips as well as in the diffusion of sulfur into a thin layer near the surface under stress. Whether passivation or crack propagation will occur is mainly determined by the chemical specificity of the diffusing ion or atom. Associated with this specificity are the volumetric changes that will occur in compound formation. Baskes and Holdbrook [13] have recently pointed out that volumetric changes should be taken into account in models for blistering. When the "compounds" formed within the metal are such that significantly large volumetric changes occur, this in turn intensifies the chemostress effect leading to an avalanche process. This picture is consistent with the rather controversial phenomenon of anomalously high rates of diffusion under mechanical stress [14].

CONCLUSIONS

We have shown that the migration of specific impurity ions in the lubricant to the metal-lubricant interface and into the metal are governed by the zeta potential, the Gouy effect, the chemostress effect, the initial defect structure of the metal surface layers and the nature of diffusion within these layers. The migration of these specific ions is always governed by the chemical potential gradient in the particular local environment. We have shown that the Gouy and chemostress effects can act synergistically to accelerate this migration process which leads to the reduction of cohesive forces in some instances depending upon the specific chemical bonds involved. Volumetric changes in the metal surface layers accompanying this process would then lead to blistering or pitting.

REFERENCES

1. G. Gouy, C. R. Acad. Sci., 114 (1892).
2. T. M. Riddick, Control of Colloid Stability Through Zeta Potential, Livingston, New York, 1968.
3. O. Stern, Z. Electrochem., 30 (1924) 508.
4. M. Ciftan and E. Saibel, The Chemostress Coefficient, Solid State Commun., 27 (1978) 435.
5. M. Ciftan, V. Ruck and E. Saibel, Stress Dependence of the Chemical Potential of Adsorbates, Solid State Commun., 27 (1978) 439.
6. The Chemostress Effect, Proc. 8th U. S Natl. Congr. of Applied Mechanics, Univ. California at Los Angeles, June 1978, Univ. California, Los Angeles, 1978, p. 67.
7. M. Ciftan and E. Saibel, 175-184 The Chemostress Effect, Int. Journ. Eng. Sci., 17 (1979).
8. G. P. Flynn, Point Defects and Diffusion, Oxford Univ. Press: Clarendon Press, Oxford, 1972, pp. 375-378.
9. T. L. Hill, An Introduction to Statistical Thermodynamics, Addison-Wesley, Reading, Mass., 1960, p. 321.
10. P. Kofstad, High-Temperature Oxidation of Metals, Wiley, New York, 1966, p. 116.
11. J. J. McCarroll, R. W. Mould, H. B. Silver and M. C. Sims, Auger Electron Spectroscopy of Wear Surfaces, Nature (London), 266 (1977) 519.
12. T. Solomon, Personal Communication, March 5, 1978.
13. M. I. Baskes and J. H. Hollbrook, Phys. Rev. B, 17 (1978) 422.
14. A. F. Brown, Diffusion Under Mechanical Stress. In J. n. Sherwood, A. V. Chadwick, W. M. Muir and F. L. Swinton (eds.), Diffusion Processes, Vol. 1, Gordon and Breach, New York, 1971, p. 219.
15. F. Powis Z. Phys Chem 89 (1915) 91.

*Solomon [12] states: "The most interesting case I had published dealt with a mandrel; severe pitting occurred in the zone of highest pressure (on the neck of the mandrel) when structure defect existed (owing to an incorrect heat treatment), whereas no damage was observed with mandrels from the same supplier without structure defects. This happened on the same machine under quite identical working conditions."

In all the above considerations we should distinguish between two types of impurity ions in the electrolyte solution: one that reduces the zeta potential to zero and one that migrates to the crack tip when the zeta potential is made zero, although in some cases the two types could be identical. This separation is not a mere convenience as we shall see when we discuss the physical forces that control the dynamics of the system. That the two are intertwined, however, was known by Stern [3] who assumed that apart from the electrostatic and thermal forces adsorptive forces were also acting on the ions. We now know that physisorptive (van der Waals) and chemisorptive forces act on these ions. There is also an augmentation of the adsorptive forces which has not been considered before and which we call the chemo-stress effect [4-7].

The central point is that the electrostatic forces between the ions are long range and therefore the presence of a given ion significantly affects the distribution of other ions. As a result virial-type expansions cannot be performed as in the case of imperfect gases. It was this point that led Debye and Huckel to develop a theory using the Poisson-Boltzmann equation. In fact, the virial expansion fails (divergences result) for potentials that fall off slower than the fourth power of the distance. In contrast, the van der Waals interaction falls off very rapidly, as $(\text{distance})^{-6}$, so that an Ursell-Mayer-type virial expansion, which is used for example to obtain the equation of state of a gas, does not create divergence problems. A significant point of this discussion for the present problem is that owing to the long range of the electrostatic forces there is a net repulsive force between two charged particles of like charge or between colloidal particles of the same type carrying the same charge since the halo of opposite charges that neutralizes the given charges on a given colloidal particle extends very far owing to the long range of the forces. There is thus a balance between the attractive van der Waals force and the repulsive electrostatic forces and agglomeration results. The same phenomenon would occur between adsorbate ions or colloidal particles and the metal surface when the zeta potential of the metal is reduced to zero. It can be shown in detail, using a theorem of electrostatics, that agglomeration results only when the zeta potential is zero and not when the zeta potential is either negative or positive. Thus a significant amount of ion migration to the metal surface and its subsequent diffusion into the metal occur only when the zeta potential is reduced to zero.

We have mentioned earlier that the fundamental quantity in our theory is the chemical potential of the second kind of impurity ion, such as an oxygen or a sulfur ion, and that this chemical potential will be position dependent and thereby cause migration. The fundamental quantity that causes diffusion is not the concentration gradient [8]. For weak electrolytes Debye-Huckel theory gives an explicit expression [9] for the chemical potential μ_i of an ion: $\mu_i = \mu_0 + RT \ln \gamma_i$

$$\ln \gamma_i \to \frac{z_i^2 e^2 \sqrt{I}}{2 \epsilon RT} \qquad I \to 0$$

where γ_i is the activity coefficient of the ith ion, I is twice the ionic strength, z_{ie} is the charge on the ith ion and e is the charge on a proton.

The activity coefficient γ_i thus depends upon the long-range interaction forces that act upon the ith ion and this makes the determination of μ_i for the more complicated charge distribution (which we are discussing) around the given ion rather difficult. In short this becomes a rather complex many-body problem. Beyond this complexity we shall need to consider the chemostress effect which complicates the theoretical determination of μ_i even further. It is for these reasons that at present an analytical formulation completely based on first principles and solution of the problem using quantum statistical mechanics is out of the question. Rather the problem must be broken down into coherent parts so that after the establishment of valid phenomenological parameters we could perhaps perform calculations of molecular dynamics to follow the migration and rearrangement of ions.

More specifically, the theoretical demonstration of the existence of a gradient toward the surface of the chemical potential of an ion in an electrolyte with and/or without the Helmholtz-Gouy-Chapman charge layer for the metal surface is a non-trivial problem of theoretical physics. Even so, the phenomenological description given earlier which is based on experimental findings, does provide a sufficient rational basis on which to build our model. The role of such a phenomenological theory becomes clear when it is realized that in the not so distant future molecular dynamics calculations could be performed to follow the actual migration of the ions utilizing the parameters that are arrived at by the phenomenological theory.

We now discuss the role of the second major effect, i.e., the chemostress effect. When an ion or a neutral atom or particle is sufficiently near the metal surface, i.e., of the order of a few atomic radii, near a crack tip, the chemostres effect becomes very strong owing to the high stress concentration factors of about 10^3 that exist there. We have shown [4, 5] that the chemical potential of the adsorbate changes appreciably; this change is given by $\frac{\Delta}{\mu} = 2 \frac{\Delta V}{V}$ where ΔV is the change in the local volume at the crack tips owing to change of stress in the solid per 10 kbar pressure change. Although the calculation was done for NaCl substrates, a similar result is obtained for metals. When the zeta potential is brought to zero by impurity ions, tenacious adsorptive binding to or agglomeration with the metal substrate results. However, the chemostress effect will ensure that the adsorbate is preferentially attracted to the crack tips and in addition it will also cause a stronger (because of a deeper potential) binding and may induce chemisorptive binding so that electron sharing would take place. It is therefore to be expected that the chemical bonds of the atoms of the metal near the surface would change resulting in a change in the cohesive forces and oxidation rates [10].

We now consider the diffusion of the impurity ion into the metal starting at the crack tip; it must be pointed out that the present argument is not necessarily confined to the existence of a crack tip at the surface of the solid, for indeed imperfections which have been well studied such as asperities, steps, voids, dislocations, and interstitials would also change the adatom-solid interaction potentials and high stress concentrations would exist in the vicinity of these imperfections.

least locally, bearing dissociated ions. It has been shown elsewhere* that electrostatic charges can exist in the lubricant.

In addition to these ions, particulate matter will be worn off in the form of the metal and its compounds such as oxides, and bubbles will also be present. All these additonal impurities can act as colloidal particles in the electrolyte solution. Once free ions are formed within the lubricant, they can migrate to the surface of the metal forming the well-known Helmholtz-Gouy-Chapman layer of electrical charge distribution at and near the lubricant-metal boundary, which is shown schematically in Fig. 1 in a simplified form (for a more detailed representation of this layer with specifically aosorbed ions see Figs. 2, 3, and 4).

The so-called "zeta potential" is the potential due to the outer diffuse layer of the distribution, i.e., the Gouy-Chapman layer. We note that there is a zeta potential for both the colloidal particles dispersed in the electrolyte, and those present at the metal-electrolyte interface. Furthermore, the zeta potential of the colloidal particles can be positive or negative, as Table 1 shows.

TABLE 1

Zeta potentials for colloidal particles dispersed in pure water

Dispersed phase	Zeta potential (V)
Fe_2O_3	+0.044
Iron	+0.028
Oil (emulsion)	-0.046
Air bubbles	-0.058

It is important to note that the zeta potentials for Fe_2O_3 and oil (emulsion) have about the same value but opposite signs so that it is possible that certain combination of colloidal particles when intermixed could give an effective overall zeta potential of zero at a distance from that combination of colloidal particles.

What is important for the present analysis is the experimental observation of Powis which showed that the zeta potential ζ of colloidal particles is dramatically affected by the addition of certain impurity ions (salts); the zeta potential of oil drops in water was measured by measuring the velocity of the colloidal particle (oil) under the influence of an externally applied electric field E, i.e., the electrophoretic velocity v given by $V = \alpha \frac{\zeta E \varepsilon}{\eta}$ where E is the applied electric field, ε is the dielectric constant, η is the viscosity and α a parameter which is $(4\pi)^{-1}$ for cylindrical colloidal particles and $(6\pi)^{-1}$ for spherical colloidal particles. The data of Powis which are shown in Fig. 5 combined with eqn. (1) indicate clearly that the zeta potential can be made zero by the addition of certain impurity ions.

The above observation becomes even more significant when combined with the following experimental observation by Gouy [1] that the maximum of the electrocapillary curve is reduced by the presence of certain ions in the electrolyte solution, as shown in Fig. 3 where γ is the surface tension and E is the applied electromotive force (the applied voltage). This is so since by the Lipmann-Helmholtz equation

$$\frac{\partial \gamma}{\partial E} = \sigma' \qquad (1)$$

where σ' is the charge on the metal near its surface. This equation implies that at the maximum of the electrocapillary curve $\sigma' = 0$ and therefore all the other charges are also neutralized or depolarized, i.e., the zeta potential is also zero. Before delving into an explanation of these observations we need to add to them a third observation: when the zeta potential of the colloidal particles is brought to a zero value (as measured by the electrophoretic velocity) agglomeration of the colloidal particles results. Numerous experiments, e.g., by Riddick [2], in recent years have reaffirmed this observation. We shall dwell on the physical forces which cause the agglomeration as it is an important part of our model but before doing that let us combine these three experimental observations. Since there is also a zeta potential for the charge distribution at the metal-electrolyte interface, the addition of impurity ions could bring this zeta potential to a zero value and agglomeration of certain ions or charged colloidal particles could then occur with the metal; at the same time σ' and the surface tension could be reduced to zero. In the case of a liquid metal, a reduction of surface tension is just the reduction of cohesive forces between the atoms of liquid metals such as mercury since it can be observed directly in an electrocapillary experiment. However, there is no doubt that the fundamental quantity, i.e., the cohesive force, does exist in both liquid and solid metals (of course of different magnitudes) leading in both cases to a surface free energy. In fact within metal alloys the surface tension at grain boundaries is perhaps the fundamental quantity determining the size of the grains and therefore the mechanical properties of the metal. Again if we were to go so far as to allow motion of ions as opposed to electrons in the metal as charge rearrangements occur owing to the reduction of the zeta potential to zero at the electrolyte side of the metal-electrolyte boundary, then it is not surprising to find that the surface free energy or the surface tension would be altered; thus it is intuitively clear that there is an analogue of the Gouy effect even for solid metals.

*Solomon [6] refers to "the Report of the Research team of the Boeing Company dealing with pitting observed on the outlet valve of the HP hydraulic systems in the Aircraft." He says "They had proven the existence of electrostatic charges . . .."

CHEMICAL-MECHANICAL INTERACTION IN GEARS

by
Edward Saibel
Chief Solid Mechanics Branch
U. S. Army Research Office
P. O. Box 12211
Research Triangle Park, NC 27709

SUMMARY

A theory of chemo-mechanical interaction is developed to explain several disparate phenomena in the field of tribology on a quantitative basis. The important new quantity in this theory is the variation of the Gibbs chemical potential with stress, a quantity formulated and calculated explicitly using statistical thermodynamics and many-body theory, called the chemo-stress coefficient. The theory gives the basis for quantitative explanation of stress corrosion, fretting corrosion, the Rehbinder effect, and enhanced chemical activity on solid surfaces. In particular it suggests methods of arresting corrosion by controlling the charge distribution of electrolytes near the surface of the solid. A mechanism for pitting corrosion observed on lubricated load bearing surfaces of mechanical components such as gears is proposed. This theory emphasizes the importance of specific ions in the lubricant which migrate to the tips of cracks and diffuse through near-surface layers of the metal thereby causing volumetric changes leading to blistering or pitting.

The migration of specific ions in the lubricant and in the metal is governed by a single fundamental quantity, the gradient of the chemical potential of the ion in the medium in which it is situated.

Gibbs introduced the concept of the chemical potential into mechanistic thermodynamics which had previously been developed by adding to the equation which expresses the first and second laws of thermo dynamics, namely $dE = TdS - pdV$, the term $\Sigma \mu_i dN_i$ where E, T, S, P, V are the internal energy, temperature, entropy, pressure and volume of the system; the new quantity μ_i is the chemical potential of the i- the component and N_i the number of atoms or molecules in the i- th component of the system. In a more general case the term pdV can be replaced by $\Sigma \sigma_{ij}\, de_{ij}$ where σ_{ij} is the stress and e_{ij} the strain, $i = 1, 2, 3$.

The gradient of the chemical potential in turn is modified and controlled by two fundamental effects. The first is the chemostress effect which is the change in the chemical potential of an adsorbate when the substrate solid is subject to a stress field due to externally applied stresses and/or residual internal stresses near its surface, e.g., at crack tips or defects. The second effect, called the Gouy effect is the change in the surface energy of a metal in contact with an electrolyte. These two effects can act synergistically to increase the rate of migration to the tips of cracks at the metal surface thereby providing the concentration and chemical gradients for anomalously high rates of diffusion into the near-surface bulk of the solid at defects.

The process leads to a reduction of the cohesive forces between the original bulk atoms, causing volumetric increases which in turn increase the stress concentration at the defects. Since increased stresses cause a further increase in the chemical potential of the impurity ions, the process becomes an avalanche which ultimately leads to an increase in the defect structures, the breaking of bonds, and the lifting of material such as a grain or a collection of atoms.

It was not until recently that the possibility of a chemical potential to carry detailed microscopic information on the state of stress in a solid or on the surface of a solid was considered. This possibility elucidates the coupling between chemical and mechanical interactions at the atomic-molecular level, particularly in situations where chemical reactions occur in heterogeneous systems such as at a gas-solid interface. This effect we have called the chemostress effect. It is represented by the dependence of the chemical potential μ on stress σ through the derivative $\frac{\partial \mu}{\partial \sigma}$ which we call the chemo-stress coefficient. The quantity σ is an abbreviation for σ_{ij} where $i, j = 1, 2, 3$ in the general case, so that the derivative is to be considered in the sense of Frechét.

The importance of chemical potential can be seen whenever phyisorption, chemisorption, diffusion, and chemical reactions are involved in a given phenomenon because it is this chemical potential that drives the process. In the case of diffusion for example, it is not Fick's law which is fundamental but the one that starts from the gradient of the chemical potential $\frac{\partial \mu}{\partial x}$ and in a stressed environment it is $\frac{\partial \mu}{\partial \sigma} \frac{\partial \sigma}{\partial x}$. Other dependences may be involved such as temperature, electric and magnetic fields, etc. Thus such quantities as $\frac{\partial \mu}{\partial T} \frac{\partial T}{\partial x}$, $\frac{\partial \mu}{\partial E} \frac{\partial E}{\partial x}$, $\frac{\partial \mu}{\partial H} \frac{\partial H}{\partial x}$ will be involved, where E and H are the electric and magnetic fields respectively. It is possible that in some cases $\frac{\partial \mu}{\partial E}$ and $\frac{\partial \mu}{\partial H}$ could be important but it is unlikely that these coefficients have ever been measured.

Another quantity that can play a significant role in the wear process is diffusion of certain species into the solid and under some stress conditions anomalously high rates of diffusion.

A lubricant between two metal components may at first be electrically non-conductive but as wear progresses its chemical components will decompose and it can become a weak electrolyte "solution," at

E Young modulus

υ Poisson modulus

υ_A, υ_B Poisson moduli of bodies A and B

η dynamic viscosity

$$E' = \frac{1}{2}\left(\frac{1-\upsilon_A^2}{E_A} + \frac{1-\upsilon_B^2}{E_B}\right)^{-1}$$

$H = h'/R$

$$M = \frac{w}{E'R}\left(\frac{E'R}{2\eta U}\right)^{1/2}$$

$R = R_A R_B/(R_A + R_B)$

$T = H/\sqrt{2U}$

$S = T A_{min}$

$U = \eta u/E' R$

$W = w h'/24 \upsilon R$

$X = x/\sqrt{2 R h'}$

$X_o = x/\sqrt{2 R h'}$

α = viscosity-pressure coefficient

$s = h^* /h'$

$\Delta v = v - v(0)$

REFERENCES

[1] Baronchelli, A., "Un metodo perturbativo nella lubrificazione elastoidrodinamica e sue applicazioni tecniche", *Tesi di Laurea* alla Facoltà di Ingegneria dell'Università di Pisa, 1 983.

[2] Dowson, D. and Higginson, G.R., "A Numerical Solution to Elastohydrodynamic Problem", J. Mech. Eng. Sci., e 1 (1), 7 - 15.

[3] Dowson, D. and Hamrock, B.J., "Numerical Evaluation of Surface Deformation of Elastic Solid Subjected to Hertzian Contact Stress", NASA TN TD 7774.

[4] Dowson, D. and Hamrock, B.J., "Elastohydrodynamic Lubrication of Elliptical Contacts for Materials of Low Elastic Modulus", Part I and II, J. Lubr. Technol. 100 (2), 236-245 and 101 (1), 92 - 98.

[5] Dowson, D. and Hamrock, B.J., "Minimum Film Thickness in Elliptical Contacts for Materials of Different Regimes of Fluid Film Lubrication", Mechanical Engineering Publications, Bury St. Edmunds, Suffolk, 22 - 27.

[6] Martin, H.M., "Lubrication of Gear Teeth", Engineering, London, 102, 199.

[7] Herrebrugh, K., "Solving the Incompressible and Isothermal Problem in Elastohydrodynamic Lubrication through an Integral Equation", J. Lubr. Technol., 90 (1), 262-270.

[8] Weber, C. a-d Saafeld, K., "Schmierfilm bei Walzen mit Verformung", Z. Angew. Math. Mech., 34 (Nos 1 - 2).

[9] Grubin, A.N., "Fundamentals of the Hydrodynamic Theory of Lubrication of Heavily Loaded Cylindrical Surfaces". In Investigation of the Contact Machine Components, Kh. F. Ketova, ed. Translation of Russian Book No 30, Central Scientific Institute for Technology and Mechanical Engineering, Moscow, Chap. 2.

[10] Ciulli, E., "Progetto di un'attrezzatura per esperienze sulla lubrificazione elastoidrodinamica", Tesi di Laurea alla Facoltà di Ingegneria dell'Università di Pisa, 1 984.

tacts such as those occurring between gear teeth and the rolling elements and raceways. Among the goals of current development programs are increased reliability, and power - to - weight ratio of power transmission systems. Considerable effort has been directed at improving the performance of spur gears with respect to these two criteria.

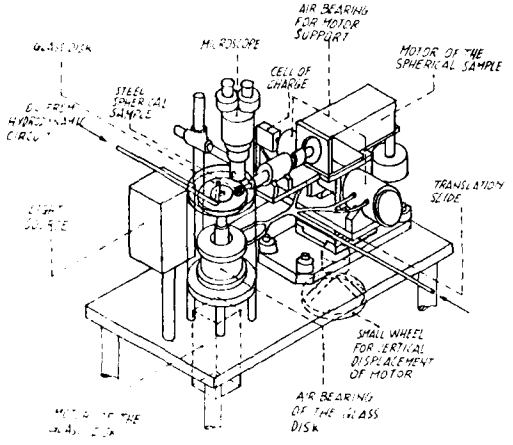


Fig. 9 - Advanced machine for lubrication film evaluation, Ref. 10.

The problem of lubrication in gear teeth is that the elasto-hydro-dynamic contact has to start and finish on every tooth. As the instantaneous line of contact moves over the oil wetted surface, an oil film becomes trapped between the surfaces due to the high viscosity that develops at the contact pressures existing between the teeth. Such condition has more to be investigated using disk machines which can maintain continuously the condition at one point during the action of two teeth. Although the central portion of the contact zone can be generating near perfect oil films, the edge discontinuities are still the regions where lubrication breakdowns most frequently occur.
Only if the true origin of a lubrication breakdown is recognized will it be possible to successfully modify future designs so that higher loads can be achieved.
One possibility for improving the performance of spur gears is to realize high contact ratio gearing without lubrication breakdowns.

Elastohydrodynamic lubrication may be viewed as one of the major needed developments in the field of tribology in the twentieth century, in order to improve helicopter transmission efficiency. The objective of the research is first to understand how thin-film lubrication works so that it can be fully utilized and second to formulate better lubricants.

SYMBOLS

h lubricant film thickness

h_{min} minimum film thickness

h_o film central thickness

$h' = h_o + v(0)$

$h^* = h(x_o)$

p pressure

$p^* = p\, h'^2/12 \eta u \bar{2} R h'$

u_A , u_B velocities of the bodies A and B along x

$u = (u_A + u_B)/2$

v deformation

$v(0)$ deformation at $x = 0$

w charge per unit length

$A = h/h'$

elasto-hydro-dynamic contact gives rise to a diffraction figure. In absence of lubricant, the monochromatic and coherent laser light establishes a relation in between film thickness, light wave length and distance among fringes in the diffraction figure. The image is distorted because of the lubricant, but Willis is able to carry out an empirical relation between the heights measured with and without fluid. Wedeven (1 975) proposes a machine analogue to the one of Foord, but with the possibility to evaluate the contact friction force. Jackson and Cameron (1 976) build another simple machine to measure film height and shape in not perfectly smooth contact. Wedeven, still in presence of not perfectly smooth surfaces, investigates the elasto-hydro-dynamics (1 978 and 1 982). Dalmaz (1 979) has recently used the interferometric method to detect contemporarely film height and shape, and friction force.
Among the recent realizations, the devices of Hartnett and Kennel (1 981), Safa and Others (1 982), and Dantu (1 983), still in the experimental phase, are to be mentioned, respectively investigating on the contact zone pressure behaviour, on the thickness, pressure and temperature, measurements, and on the lubricant film thickness trough radioactive fluids.

The most important parameters characterizing an elasto-hydro-dynamic contact, i.e. height and shape of the lubricant film, pressure, friction force and temperature, have been measured with various methods.
Summarizing, the methods for the lubricant thickness measurement are:

- electrical, electrical resistance (to show the presence of lubricant in the contact zone), electrical capacity (this depending upon thickness, lubricant dielectric constant, shape and surface area);
- x rays (thickness of the lubricant film measured by Geiger counter on the rays going across the contact zone);
- interferometric detection (suitable for elasto-hydro-dynamic film shape and size in point contacts; the best one until now);
- laser (interpretation of diffraction figures across laser coherent monochromatic light beam);
- mechanical technique (strain-gage for detecting, for example, the deformation of the ball bearing external ring during operation, from which deducing clearances and charges).

The only method suitable for pressure measurement is that one employing manganine, even though with problems to connect pressure and manganine resistance; however this experimental method is in agreement with theoretical and hertzian charge conditions.

To detect the friction force, there are various methods: moment measurement (on a disk of contact); force measurement (axial thrusts between the contact bodies).

The temperature is measured by thermocouples (average temperature between inlet and outlet of the contact zone), metallic films (electrical resistance variation of a very thin metallic film as function of the temperature gradient across the lubricant film), infrared ray measurement (suitable for real temperature behaviour on a point contact).

An advanced experimental machine is recently proposed, Ref. 10, for measuring lubricant film thickness and shape in a elasto-hydro-dynamic lubrication, suitable to simulate the commonly used mechanical contacts, e.g. that between sphere and rolling bearing racewas. The device is also able to measure friction force, pressure and temperature. The optical interferometric method is used for the thickness evaluation, in rolling and sliding tests between a metallic cylinder and glass disk, mutually perpendicular and pressed each other with a force up to 100 N in a peripheral velocity range variable from 0.1 to 6 m/s. Friction force developed in the contact may be in between 0.02 - 10 N. Oil, with density and viscosity, respectively, 8 000 - 20 000 N/m^3 at 293 K and 0.01 - 2.00 Pa - s, is admitted to the contact zone at flow adequate to the lubricant film formation between the bodies. An oil temperature of 293 - 343 K is not to be exceeded at the contact inlet, whose jet has to be opportunely screened in such a way to interest only the contact surfaces. A view of the machine is shown on figure 9.

FUTURE REQUIREMENTS

The emphasis in helicopter gearbox development has concentrated on those design innovations which will permit high temperature operation at increased speeds without degrading strength or weight goals. To provide high temperature capability, the main transmission housings are starting to be fabricated from a stainless steel alloy to replace the conventional magnesium alloy casing. In the coming decades there will be further advancements in all aspects of gearing development, with increased emphasis placed on such areas as: new gear materials with increased survivability traits, particularly running at higher temperatures; new gear designs with improved dynamic characteristics resulting in reduced noise generation; significant improvement on lubrication of non-conformal con-

provisions to collect and measure the heat generation due to mechanical power losses in the transmission. All the lubricants, near to the 5 - 7 centistoke range in viscosity, are tested for physical properties, contaminants, and wear particles prior to and after completion of all test runs. Efficiency test runs have to be made with the oil inlet temperature controlled to within less than one degree kelvin, at oil temperatures ranging from 350 to 370 K, at full power condition of the test transmission. After the tests are completed, the transmission is disassembled, cleaned and visually inspected for changes in the gear and bearing surfaces.

ADVANCED EXPERIMENTS ON ELASTO-HYDRO-DYNAMIC LUBRICATION

Devices with disks, spheres or oblique cylinders, have been realized, respectively for linear and point contacts, since 35 years ago, for measuring oil film thickness and simulating the actual operation of usual mechanical couplings. Even before, experiments were made with teeth wheels to demonstrate the lubricant presence at the contact zone, verifying, after the test, the operation signs or the superficial damage lack. So, in 1935 the Merrit disk machine was yet simulating teeth contact, to evaluate friction coefficient in absence of lubricant film. In 1 952, Lane and Hughes registered the lubricant film through the measurement of the electrical resistance difference, only some Ω for the lubricant layer in comparison to $10^9\ \Omega$ for metallic surfaces. Cameron (1 954) reveals that the lubricant electrical characteristics depend upon the current intensity, and Lewicki (1 955) verifies that such measuring method gives not satisfactory values of the lubricant thickness because of superficial asperities and eventual suspended particles. He builds a two lubricated disk machine through which the film thickness is evaluated from the electrical capacity difference, with acceptable values of 10^{-6} mm. In 1 958, Crook overcomes the difficulties due to the uncertinesses on the lubricant electrical characteristics connecting capacity to fluid flow, measuring the friction and the average film thickness. Misharin (1 958) and Smith (1 959), through steel disks extends experimental studies of friction at different rolling and sliding velocities as function of the lubricant charge and temperature. El-Sisi and Shawki (1 960) try to check the film height through a resistive method, adding additives to the oil for avoiding influence of the temperature on the electrical resistance, rather with unsatisfactory results. Another device for the lubricant film thickness, this being a little higher than the superficial asperities, was one utilizing a x ray beam (Sibley, Bell, Orcut and Allen, 1 960), in which the ray beam is subjected to diffraction in going across the crystal, obtaining a monochromatic collimated beam, whose shape and magnitude are registered through a variable wideness fissure. The x ray beam is impacting the contact zone and absorbed by the steel disks more than by the lubricant; the across passing beam is measured by a Geiger counter and used for deducing the film thickness, with values in agreement with Ref. 9, even though the measures heights resuted a little less than those theoretically computed. Archard and Kirk (1 961) show the persistence of the lubricant film even in condition of point contact. using a two mutual perpendicular cylinders device at variable approach (through a hydraulic piston) during the motion; adequate electrical insulation and particular Hg contacts giving the values of the height and friction force with a capacity method.
At early '60, the theory results start to be experimentally verified. In particular, regarding the lubricant film shape, they try to show the almost parallelism between the deformed surfaces at the contact central part and the outlet zone restriction. It is again Crook (1 961) to use a 4 disk device, with which he is able, for the first time, to experimentally deduce the film shape in the case of linear contact, through a capacitive method, even though with the uncertainess about the influence of the pressure.
During recent years the pressure behaviour in the lubricant film is considered. So, Higginson (1 962) investigates the pressure behaviour between a bronze cylinder and a plas block in mutual contact for a sufficiently wide surface, rather with negligible effect of the pressure on the viscosity. Dowson and Longfield (1 963) measure the pressure behaviour at the contact of 2 metallic surfaces, rather with too wide contact zone. Kennel, Bell and Allen (1 964) develop a method with manganine, a nickel, manganese and copper, alloy, whose electrical resistance is influenced by the pressure.
The first interferometric device is built by Cameron and Gohar (1 966), from which the film height and shape for a point contact is measured. Better results are obtained by Foord and Others (1 969) using the same principle, measuring the temperature through a thermocouple, studying the pure rolling but not rolling and sliding velocities together. Meyer and Wilson (1 971) use a charged ball bearing and a strain gauge for measuring the film thickness between balls and rolling race. A more detailed measure of the temperature at the contact zone is obtained by Turchina and Others (1 974). They use a new technique, later developed by Ashermann (1 976) and Magary (1 977), non interfering with the elasto-hydro-dynamic contact, and based on the lubricant capacity to release infrared rays in quantity dependent from the temperature. A further device for the film thickness evaluation is built by Willis and Others (1 975) exploiting the diffraction phenomenon of a laser beam. A light beam passing across a small fissure, in the case of

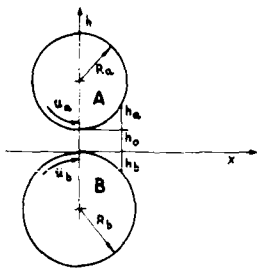


Fig. 1 - Rotating elastic bodies separated by variable viscosity fluid

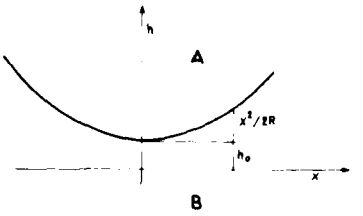


Fig. 2 - Rotating bodies approximate in shape around x = 0

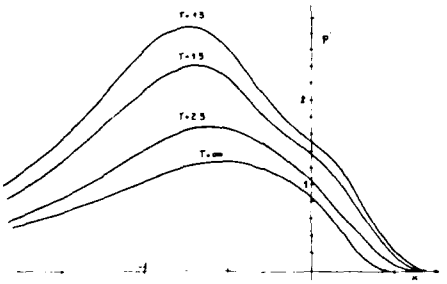


Fig. 3 - Adimensional pressure distribution in the lubricant film

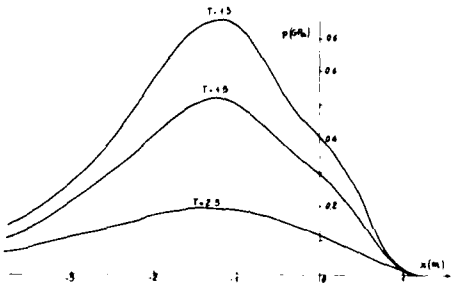


Fig. 4 - Dimensional pressure distribution in the lubricant film

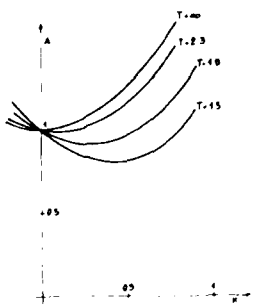


Fig. 5 - Adimensional film thickness in the lubricant film

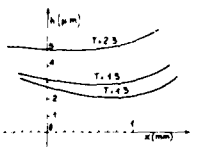


Fig. 6 - Dimensional film thickness in the lubricant film



Fig. 7 - Comparison between results of theories

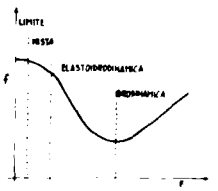


Fig. 8 - Friction coefficients between two oppositely moving surfaces

- the dimensional film thickness $A = h/h'$, for the same values of A, figure 5, and the dimensional thickness h for the above mentioned values of η, u, R, E', figure 6;
- the adimensional lift $W = w\,h'/24\,UR$, where w is the unit lenght charge as function of T. In the following Table are reported the values of A_{MIN}, $S = A_{MIN}\,T$ and $M = 12\,W/T$. In figure 7 the values of S and M, according the perturbation solution of Ref. 1, are compared with the ones of Ref. 6 (lubrication between rigid cylinders, Ref. 7 (iterative method), and Ref. 8.

In technical applications of the elasto-hydro-dynamic theory, the fundamental variable is the minimum lubricant film thickness, from the other hand so high to avoid contacts between superficial asperities.
The computation procedure for counter-rotating cylinders, roller bearings and gears, consists on:

- deducing the dimensional variables

$$R = R_A\,R_B/(R_A + R_B) \qquad u = (u_A + u_B)/2 \qquad 1/E' = \frac{1}{2}\left[\left(\frac{1-\nu_A^2}{E_A}\right) + \left(\frac{1-\nu_B^2}{E_B}\right)\right]$$

- computing the adimensional variables

$$U = \eta_o\,u/E'\,R \qquad W = w/E'\,R$$

- with the corresponding value of $M = w(E'\,R/2\,\eta\,U)^{1/2}/E'\,R$ is deduced S from the diagram S - M, from which $h_{min} = R\,S\sqrt{2\,U}$ to be sufficient high in relation to the average rugosities r_A and r_B of the surfaces. A correct operation from the elasto-hydro-dynamic point of view is commonly considered with $F = h_{min}/\sqrt{r_A^2 + r_B^2} = 1.2$. It has been experimentally shown that the life of a couple is significantly increasing for values F from 1.2 to 3.0, while for $F < 3$ fatigue resistance increases are not significant. The physical meaning of F is immediate: with low values of such parameter, the asperities of the surfaces enter frequently in contact causing wear; viceversa, beyond a certain limit, the distance is inadequate because pressures are transmitted through the fluid layer.
For a better understanding of the significance of F, it is shown on figure 8 how the friction coefficient f between two oppositely moving surfaces is related to F. There, high values of f are corresponding to low values of F, i.e. a limit lubrication with surfaces at direct contact. High values of F are corresponding to viscous fluid in hydrodinamic regime.

In conclusion, the present perturbation theory takes into account the relevant equations in elasto-hydro-dynamic lubrication, i.e.: Reynolds equation, viscosity variation, density variation for mineral oil, elasticity equation, and film thickness equation.
By using numerical procedures, the influence of the body shape and the dimensional speed, load, and materials parameters on minimum film thickness has been investigated. Equal consideration is given to the effects of both elastic deformation and pressure dependent viscosity in order, for the resulting film thickness equation, to adequately represent counterformal steel components lubricated with mineral oil.

The lubrication of non-conformal contacts such as those occurring between gear teeth and the rolling elements and raceways of rolling bearings is influenced by two major physical effects. These are the extent to which the lubricant viscosity is enhanced due to the pressures to which it is subjected and the degree of elastic distortion of the bounding surfaces. Now, the most typical elasto-hydro-dynamic contact between two approximately moving elements is the radial cylindrical roller bearing. For the case of a bearing with fixed external ring and moving internal ring, the fundamental cinematic relations are those of the angular velocities of the roller center and the roller around its center, from which the velocity u, to use in the formula, is deduced. From the charge on the bearing, the maximum charge on a roller and the above mentioned dimensional parameters and adimensional variables results. Deduced the minimum film thickness on the internal and external contacts of the roller, the corresponding values of the parameter F (at rugosities 0.2 and 0.1 respectively for roller and rings) indicate if the contact is correct from the elasto-hydro-dynamic point of view. Choosing an oil with higher viscosity, a significant increase of the couple life is insured by the corresponding higher film thickness and parameters F.

The behaviour of teeth wheels in proximity of the contact regions is equivalent to that one of two oppositely rotating cylinders.

In order to check the results of the theory in a helicopter transmission efficiency test, the measurement system has to be operated in a thermally insulated environment with

scribed as rigid-isoviscous, elastic-isoviscous, elasto-variable viscosity, and rigid-variable viscosity. For the case of line contacts, analytical or numerical solutions of each of these four lubrication regimes have been available. In the case of so called point contacts, where the boundary solids have curvatures in two principal directions, similar regimes of lubrication are possible and substantial computational effort has been directed towards obtaining numerical solutions predicting the film thickness. This is particularly true for the first three of the forms of lubrication mentioned above.

Other tentatives of solution were proposed by Dowson and Hamrock, Ref. 3, 4 and 5, through finite elements numerical procedure, considering more elastic moduli for both materials.

In the last years, the problem has had new experimental contributions due to reliable measuring methods of parameters, as pressure and temperature, on the elasto-hydrodynamic contact.

The general equations relative to a linear contact between two elastic infinite length cylindrical bodies separated by a variable viscosity fluid, figures 1, according Ref. 2, are

$$\frac{d}{dx}\left(\frac{h^3}{\eta}\frac{dp}{dx}\right) = 12\,u\,\frac{dh}{dx}$$

$$h = h' + \frac{x^2}{2R} + \Delta v(x) \qquad (1)$$

$$\Delta v(x) = -\frac{2}{\pi E'}\int_{-\infty}^{x_o} p(s)\,\ell n\left(\frac{x-s}{s}\right)^2 ds$$

with boundary conditions

$$p(-\infty) = 0 \qquad p(x_o) = 0 \qquad \frac{dp}{dx}(x_o) = 0$$

The rotating bodies, approximated in shape around $x = 0$ by a parabola, have the oil film height, figure 2

$$h = h_o + x^2/2R_A + x^2/2R_B = h_o + x^2/2R$$

considering: incompressible fluid, with viscosity η dependent upon the pressure p; Navier-Stokes equations, elastic deformation v.

The first equation of the system (1) may be simplified to $\frac{dp}{dx} = 12\,\eta\,u\,\frac{h-h^*}{h^3}$

So the system (1) may be linearized through a perturbation method, Ref. 1, obtaining, with adimensional variables

$$\frac{dp^*}{dX} = \frac{1 + X^2 - \beta}{(1 + X^2)^3} - \frac{24}{\pi}\,\frac{1}{T^2}\,\frac{3\beta - 2(1 + X^2)}{(1 + X^2)^4}\int_{-\infty}^{x_o} p^*(s)\,\ell n\left(\frac{X-s}{s}\right)^2 \cdot ds \qquad (2)$$

$$\Delta v(X) = \frac{24}{\pi}\,\frac{1}{T^2}\,h\int_{-\infty}^{x_o} p^*(S)\,\ell n\left(\frac{X-S}{S}\right)^2 \cdot dS \qquad (3)$$

The solution for p^* and $\Delta v(X)$ is consequence of a perturbation procedure and adequate boundary conditions.
The numerical results are as it follows:

- the distribution of the adimensional pressure $p^* = p\,h'^2/12\,\eta\,u\,\sqrt{2}\,R\,h'$, in which: $h' = h_o + v(0) = RT\sqrt{\eta u/E'R}$; $R = R_A\,R_B/(R_A + R_B)$; $\eta = \eta_o\,e^{\alpha p}$,is function of the parameter $T = H\sqrt{2U}$ in which: $H = h'/R$; $U = \eta u/E'R$; $E' = 1/2\left[(1 - \upsilon_A^2/E_A + (1 - \upsilon_B^2/E_B)\right]^{-1}$; υ = Poisson coefficient ; E = Young module.
  The elastic deformation is becoming progressively important, figure 3. The dimensional distributions of p are shown in figure 4 as function of dimensional $x = X\sqrt{2}\,R\,h'$ in order to give an idea of the behaviour of the normal elasto-hydro-dynamic contacts, for the following particular values: $u = 10$ m/s ; $\eta = 0.1$ Pa - s ; $E' = 2.2 \cdot 10^{11}$ N/m^2; $R = 0.5$ m;

exhibited by fluid-film journal bearings (with radial clearance, between the shaft and the bearing, about one-thousandth of the shaft diameter) and slider bearing (with inclination of the bearing surface to the runner corresponding to one part in a thousand).
From the other hand, the contact areas between non-conformal surfaces are very small in comparison to the contact areas between conformal surfaces, and the load must be carried with very high local pressure. While the load per unit area in non-conformal contacts, such as those that exist in ball bearings exceeds 700 MN/m^2, it is typically only 1 - 7 MN/m^2.
The maintenance of a fluid film of adequate magnitude is an essential feature of the correct operation of lubricated machine elements. The result of the elastic deformation of materials due to high contact pressures is a considerable increase in fluid viscosity. Equal consideration has to be given to the effects of both elastic deformation and pressure dependent viscosity in order for the resulting film thickness equation to adequately represent counter-formal steel components lubricated with mineral oil.

Important problems in elasto-hydro-dynamic lubrication arise both on fully flooded lubricated contacts, in which the film thickness is not significantly changed when the amount of lubricant is increased, and on the influence of lubricant starvation on film thickness and pressure in hard and soft elasto-hydro-dynamic contacts.

The examination of failed gears from many fields of operation, not only rotorcraft, has shown characteristics which suggest that there are several initiating mechanisms involved. However, damage to gear teeth attributable to lubrication lacking is an important failure mode. Lubrication breakdown can have its origin traced back to the tooth edges, eitner the endes or the tips, or to other factors as surface finish or surface treatments; tne nature of the gear materials, and the character of the speed and load spectra, having considerable influence.
The commonest time of damage initiation is during the early life of a gear set, when the surfaces are still changing because temperatures tend to increase and oil viscosity falls, rendering the generation of hydrodynamic oil film less efficient. However, not solely progressive loss of oil film thickness until intimate metallic contact is the process leading to breakdown, this one appearing frequently as sudden collapse to failure.
Long life lubrication breakdown can be associated with interruption in lubricant supply or fatigue of the metal surfaces. The combined effect of load and temperature frequently causes lubrication breakdown.
Since many lubricant breakdowns are associated with contact conditions, special teeth end profiles are used to alleviate adverse end stress conditions. Moreover, the surface finish on the boundary edges is important; its optimization being a difficult problem.

The lubricant itself is a link in the load carrying chain, but major improvements in load carrying performance can be reached without involving oil changes. The film thickness is generated at the ingoing edge of the Hertzian zone, and the radii of curvature of these approaching surfaces together with their velocities towards the conjunction will influence the magnitude of the film, according to the elasto-hydro-dynamic development process.

This paper has the purpose to investigate realistically the elasto-hydro-dynamic process and to improve the general understanding of the involved problems, suggesting the relative experimental equipment.

SOLUTION OF THE ELASTO-HYDRO-DYNAMIC GENERAL EQUATION

A realistic analysis of the elasto-hydro-dynamic lubrication must consider both the lubricant effect and the elastic deformation of bearing surfaces. The fundamental equations are at the same time those of dynamic lubrication and elasticity. Due to its complexity the problem is normally treated by numerical-iterative methods, but a proposed, Ref. 1, perturbation analytical procedure permits a better solution, suitable for transmission gear tooth contacts.
The method proposed by Dowson = Higginson, Ref. 2, was giving a satisfactory approach to the problem, because their model was taking into account the body elastic deformation, solving the elastic hydrodynamic linear contact between elastic surfaces separated by a viscosity pressure dependent fluid.

More sophisticated models were followed, considering ellipsoid bodies limiting the lubricant flow, being tridimensional the pressure distribution along the contact surfaces, with pressure and film thickness depending from more geometrical variables. The corresponding film thickness map enables the dominant physical action to be clearly identified based on the operating conditions, and also makes possible estimates of the appropriate minimum lubricant film thickness. The nature of the lubrication of a conjunction between two ellipsoid may be resolved by the degree to which two physical effects are influential. The variation of lubricant viscosity with pressure and local deformation of the solids under the action of high pressure may or may not be important, and this has prompted the recognition of four distinctive forms of fluid lubrication, normally de-

PROBLEMS OF ELASTIC HYDRODYNAMIC LUBRICATION OF HELICOPTER TRANSMISSION GEARS

Dino Dini
University of Pisa
Via Diotisalvi, 2 - 56100 Pisa - Italy

SUMMARY

In helicopter transmissions, it is to make every thing is possible to minimize power losses in order to extend the performance envelope. The reduction gear box and its components, from the engine to the main and tail rotors, contain epicyclic and bevel reduction gears, as taper thrust and cylindrical roller bearing, subjected to elasto-hydro-dynamic lubrication whose operation needs a better understanding in order to improve present efficiency. It is in fact known that a few tenths of one percent mechanical power loss can be equivalent to the loss of many kilowatts. Adequate fluid-film lubrication, where elastic deformation of bearing surfaces becomes significant, is vital. If non correct, it will lead sooner or later to failure of the main gear box and damage to gear teeth and bearings. Insufficient quantity of oil would produce, among other effects, increase of stresses on gears, bearing rollers and races which would be submitted to abnormal fatigue loads (leading to rupture), as well as increase of friction loads and therefore higher operating temperature which would, above certain value, quickly lead to bearing seizure.
Since the lubrication efficiency is depending upon the elastic deformation of the contact surfaces, a theory for a better physical interpretation of the mechanism is here discussed as a design means to alleviate adverse stress conditions during operations.
In the present paper, the author is trying to solve the problem of computing the pressure distribution in the contact and, at the same time, of allowing for the effects that this pressure has on the properties of the fluid and on the geometry of the elastic solids.
The solution also provides the shape of the lubricant film, particularly the minimum clearance between the solids.
Finally, it is proposed an experimental high performance equipment capable to simulate the behaviour of hertian contacts in elasto-hydro-dynamic lubrication.

LUBRICATION PROBLEMS IN HELICOPTER TRANSMISSIONS

An important step in development of the power transmission path in helicopters from engine to main rotor shaft, while reducing the output speed as it changes the direction of drive, is to do every thing possible to minimize power losses in order to extend the performance envelope. Range, payload, and operating ceiling can be increased if efficiency is increased. With large, high power, helicopter applications only a few tenths of one percent mechanical power loss can be equivalent to the loss of many kilowatts. There is a loss of 3 - 4% for a planetary stage, and 1 - 2% for a single gear mesh.
But the effect on the operating envelope may be more significant. Since all mechanical power losses must be dissipated as heat, improvements in transmission efficiency will permit smaller and higher weight cooling systems. This effect increases the payload capacity of the helicopter.
The transmission main box gears and bearings (planet and sun gears, bevel ring and oil pump gears, taper roller thrust bearing, cylindrical roller bearing), and the mast bearing are lubricated and cooled by pressurized oil. Lubrication of the main gear box is vital. If not correct, it will lead sooner or later to failure of the main gear box. Insufficient quantity of oil or use of unappropriate oil would have among other effects: increase of stresses on gears, bearing rollers and races, which will be submitted to abnormal fatigue loads; increase of friction loads and therefore higher operating temperature will, above a certain value, quickly lead to bearing seizure.
The role which bearings play in the performance and durability of transmissions has long been recognized. Even though advances have been made in bearing and lubrication technology during the past, there continue to be problems in performance limitations, manifest in the life and durability in current use and in the design of future transmissions.

The elasto-hydro-dynamic lubrication may be viewed as one of the major developments in the field of tribology. It is a form of fluid-film lubrication reducing friction where elastic deformation of bearing surfaces becomes significant; usually associated with highly stressed machine component such as gears and rolling-element bearings. The same mechanism of lubrication is also encountered with soft bearing materials (rubber seals and tires). In these applications asperity interaction is prevented by the coherent fluid films provided through local elastic deformation.
The surfaces fit smoothly into each other with a high degree of geometrical conformity, so that the load is distributed over a relatively large area. While the load is increased, the load-carrying surface area remains substantially constant. Conformal surfaces are

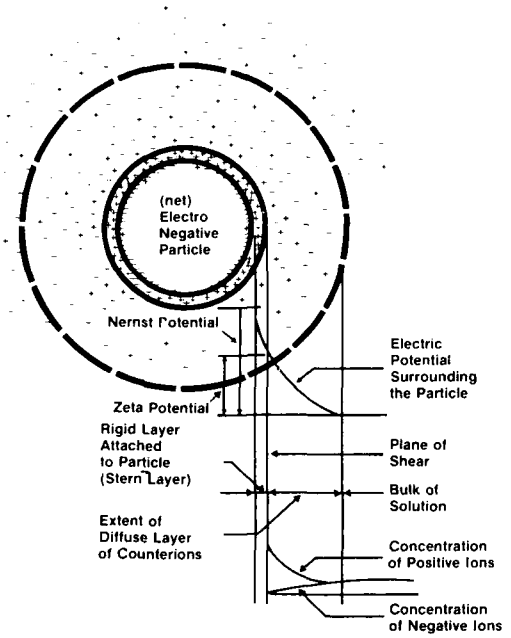


FIGURE 3

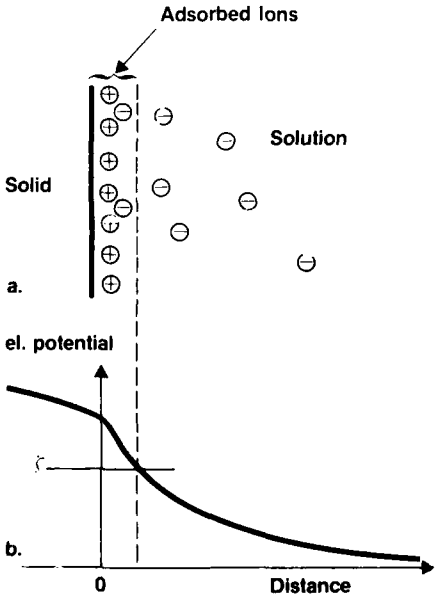


FIGURE 4

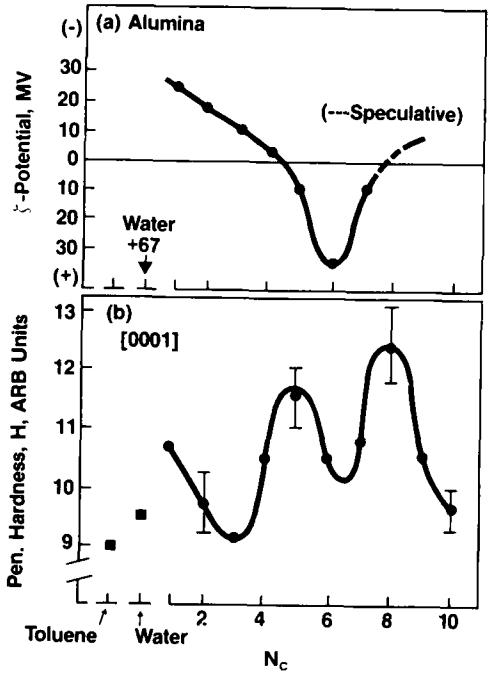


FIGURE 5

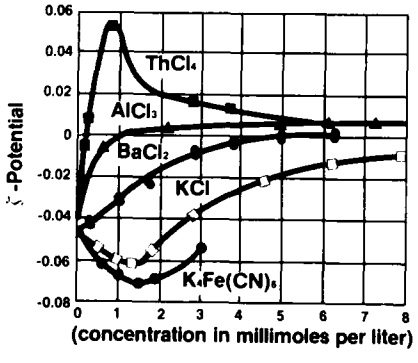


FIGURE 6. The effect of electrolyte concentrations upon the electrophoretic velocity of oil drops in water.

DISCUSSION

(Speaker not identified)

Since there will be temperature gradients in the lubricant, there will also be thermo-diffusion effects. Do you also account for those?

Author's Reply

We can and do account for the effect of thermal diffusion as well as the effect of temperature on the chemical potential, but the necessary physical data may not yet be available.

H.Blok, Ne

As you have pointed out, micro-cracks will as stress-raisers be affected either adversely or beneficially by the diffusion, or say the migration of the ions involved in your theory.

Will this theory, if only after extending it in some suitable way, account also for similar effects on kinds of defects other than micro-cracks, in particular for those on dislocations and inclusions of foreign material such as may, for instance, occur even in fairly clean ball-bearing steels? Especially in the case of inclusions the extension of the present theory may well prove a highly complicated affair, the reason being that in the course of time the foreign material concerned tends to diffuse in its turn and thus to leave an open hole.

Author's Reply

We have not specified the type of defect or micro-crack. The theory is applicable to any type or to inclusions. However, as these change shape or form, the effect naturally changes. While I think that it is possible to take these changes into account, we have not as yet done so.

REDUCTION DE L'USURE PAR LES LUBRIFIANTS DANS LES CONTACTS ETROITS

Ph. KAPSA : Chargé de recherche CNRS
M. BELIN : Ingénieur CNRS
Laboratoire de Technologie des Surfaces - UA 855 CNRS
Ecole Centrale de Lyon
B.P. 163
69131 - ECULLY Cedex

RESUME

La présence d'un lubrifiant et son activité chimique sont des paramètres importants pour le comportement en frottement et l'usure de solides en déplacement relatif. Dans le cas d'engrenages de transmission, le contact entre les deux solides est du type hertzien et le frottement se produit alors en absence d'un film d'huile épais : la lubrification est élastohydrodynamique, mixte ou limite. Dans les régimes de lubrification où des contacts solide-solide existent, la réduction de l'usure passe par la formation d'un film mince solide adhérent aux surfaces frottantes, créé par réaction chimique sous l'effet du frottement.

Les résultats d'expériences en présence d'additif anti-usure (dithiophosphate de zinc et tricrésylphosphate) montrent l'importance de la cinétique de formation de ces films sur l'usure. La pression apparente de contact et la vitesse de glissement ne modifient pas les phénomènes élémentaires d'usure mais jouent un rôle prépondérant sur l'usure globale des surfaces.

1 POSITION DU PROBLEME

Dans le domaine de la tribologie, il est admis qu'il existe plusieurs types de régimes de lubrification : les régimes hydrodynamique(HD) et élastohydrodynamique(EHD) qui se caractérisent par la présence d'un film de lubrifiant continu entre les surfaces et le régime limite qui correspond aux cas où les matériaux en glissement relatif ne sont plus séparés que par les molécules adsorbées. Dans les deux premiers régimes ce sont les propriétés mécaniques du fluide et des matériaux, et les conditions tribologiques qui gouvernent le fonctionnement alors qu'en lubrification limite ce sont les propriétés physicochimiques du fluide vis à vis des matériaux.

Selon les conditions tribologiques (cinématique, lubrifiant, température, propriétés des matériaux,...) un mécanisme en glissement fonctionnera dans un de ces trois régimes de lubrification.

Cependant, en partie en raison de la rugosité inévitable des surfaces, un mécanisme qui devrait théoriquement fonctionner en lubrification élastohydrodynamique fonctionnera souvent en régime mixte : on aura donc partiellement des contacts solide-solide, caractéristiques du régime limite.

Les études portant sur la lubrification limite et élastohydrodynamique sont nombreuses et visent à préciser l'influence des caractéristiques du lubrifiant, des matériaux et des conditions tribologiques sur le fonctionnement d'un contact glissant.

La détérioration des surfaces dûe au frottement apparait liée au régime de lubrification. En régime EHD, la fatique des matériaux est le phénomène prépondérant, d'où l'importance des caractéristiques métallurgiques des matériaux. L'usure est étudiée depuis très longtemps en lubrification limite. On peut noter l'existence de quatre types principaux d'usure : l'usure adhésive, abrasive, corrosive et par délamination.

Il a été montré que l'efficacité anti-usure d'un lubrifiant est liée à une modification du type d'usure présent [1]. En particulier en présence de dithiophosphate de zinc (DTPZn) et de tricrésylphosphate (TCP), additifs anti-usure très utilisés, l'effet anti-usure est dû à la formation, en cours de frottement d'une phase réactionnelle sur les surfaces frottantes [2,3]. L'usure, de nature abrasive et adhésive en début de frottement, devient de nature corrosive en présence de la phase réactionnelle appelée film réactionnel [1,4].

Différentes études ont été menées afin de cerner les conditions de formation de ces films réactionnels [2]. Actuellement, les travaux en cours dans ce domaine visent à connaître la structure et les propriétés mécaniques de ces films. Des observations en microscopie électronique à transmission ont récemment montré que les films réactionnels sont composés de petits cristaux (taille de l'ordre de 5 nm) en dispersion dans une matrice amorphe [5]. Par ailleurs, des mesures des caractéristiques élastiques des films montrent que ceux-ci ont un module d'élasticité très faible devant celui des métaux [6].

Le but de cet article est de donner certains éléments permettant de préciser l'influence de la vitesse de glissement et de la pression apparente de contact sur la formation du film réactionnel et sur l'usure.

Pour cela, on décrira l'évolution des surfaces et les phénomènes d'usure dans deux situations expérimentales où le frottement se produit en présence d'un lubrifiant contenant un additif anti-usure.

2 - DISPOSITIFS EXPERIMENTAUX

Les deux types d'essais que nous avons effectués correspondent à un régime de lubrification mixte pour la machine à disques et limite pour le tribomètre plan-plan.

2.1 Le tribomètre plan-plan

Le contact, sur le tribomètre utilisé, est du type surfacique. Les échantillons sont schématisés figure 1.

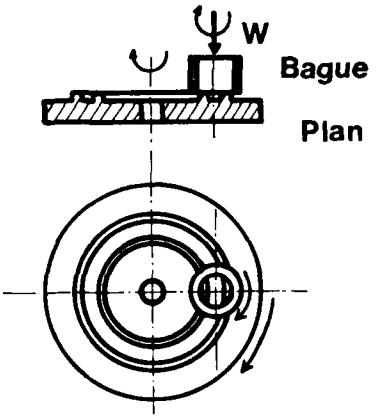


Figure 1 :

Représentation schématique des échantillons de frottement du tribomètre plan/plan.

La charge est appliquée sur la bague qui repose sur les deux couronnes concentriques du plan inférieur. Les deux échantillons sont entraînés en rotation autour de leurs axes propres. Le contact est immergé dans la solution lubrifiante. Le lubrifiant utilisé pour cette série d'essais est composé de dodécane pur additivé de 1 % de n-butyl dithiophosphate de zinc $(C_4H_9\text{-}O\rightarrow)_4P_2S_4Zn$.

La bague supérieure est en acier 100C6 traité de dureté Vickers 8 GPa, le plan inférieur est en fonte à graphite lamellaire de dureté 2 GPa.

Avant essais, les échantillons sont polis (Rt $<$ 0,1 µm) puis nettoyés par différents solvants avec agitation ultrasonore. Les essais ont été effectués dans les conditions suivantes :

- charge appliquée : 5 à 300 daN ce qui correspond à des pressions apparentes de contact de 5 à 300 MPa (aire apparente du contact : 10 mm).
- vitesses de rotation bague : 22 t/mn, plan : 14 t/mn ce qui produit une vitesse de glissement moyenne de 20 mm/s.
- la température est régulée à 80°C.

Dans ces conditions, le glissement se produit en lubrification limite et la surtempérature du contact dûe au frottement est négligeable. Le dispositif expérimental permet de mesurer la résistance électrique de contact (RC) entre les deux échantillons et donc de suivre la formation du film réactionnel sur les surfaces frottantes [7].

La mesure de hauteur usée est effectuée grâce à des mesures dimensionnelles d'une empreinte de microdureté Vickers effectuée sur la surface frottante.

2.2 La machine à disques

Le contact est du type cylindre-sphère. Il permet de reproduire les conditions variées de fonctionnement d'un contact dans une application de type dent d'engrenage : pression de contact élevée (1-2 GPa), vitesses de roulement et de glissement très variables [8] (voir figure n° 2).

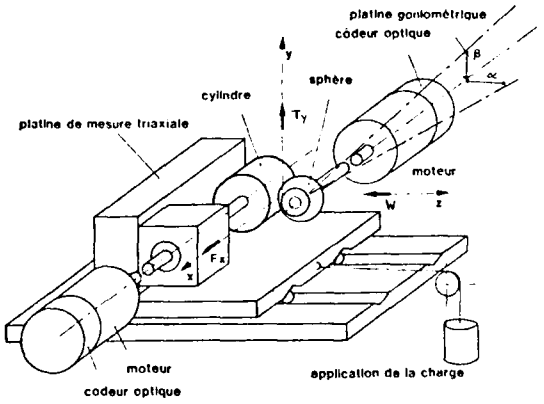


Figure 2 :

Schéma de principe de la machine à disques.

Dans cet essai, une sphère et un cylindre, entrainés en rotation indépendamment sont maintenus en appui avec une charge normale W. Elle provoque une déformation élastique des échantillons et conduit à une surface de contact elliptique.

Ses dimensions sont très proches de celles prévisibles par la théorie de Hertz, pour un contact statique. Dans ces essais, la charge W étant fixée à 135 N, le grand axe de l'ellipse vaut 550 µm , et la pression maximum de Hertz (qo) atteint 1,53 GPa.

Les deux échantillons sont entrainés en rotation indépendamment et leur vitesse U1 et U2 contrôlée avec une grande précision relative ($\simeq 10^{-5}$), par un système à vérouillage de phase.

Une platine de mesure permet de connaître la valeur instantanée :
- de l'effort normal W appliqué au contact
- des efforts tangentiels de cisaillement transmis par l'interface.

La mesure de la résistance électrique de contact Rc est effectuée durant chaque essai |9|.

Les échantillons métalliques sont en acier 100 C6 traité, avec une dureté Vickers de 7,5 GPa. Les surfaces de la sphère (rs = 12,5 mm) et du cylindre (rc = 17,5 mm) sont polies à la pâte diamantée puis nettoyées dans un bain de solvant sous ultrasons. La rugosité totale des surfaces reste inférieure à 50 nm.

Le lubrifiant utilisé est de l'hexadécane additivé à 1% en masse de métatricrésylphosphate (TCP).

3 - RESULTATS ET INTERPRETATION

3.1 Essais sur tribomètre plan/plan.

La charge appliquée sur un contact est un paramètre très important. En effet, l'aire réelle de contact, siège de l'usure est directement reliée à la charge. De ce fait, on admet que le taux d'usure varie linéairement avec la charge dans les cas où les phénomènes d'usure sont indépendants de la charge |10|. Ce dernier point est de plus en plus controversé en particulier lorsqu'on considère l'existence d'un troisième corps dans l'interface lié au phénomène d'usure |1,11,12|.

Des essais sur le tribomètre plan/plan ont été effectués afin d'étudier l'influence de la charge appliquée sur la formation de film réactionnel et sur l'usure en présence de DTPZn. L'aire apparente du contact est constante et le domaine de pression apparente du contact envisagé ici est compris entre 5 et 300 MPa ce qui correspond à H/400 et H/7 (H étant la dureté du corps le plus tendre : 2 GPa).

Des travaux expérimentaux antérieurs |1| ont montré que le contact, lors de ces essais peut être considéré comme discret (existence d'un nombre fini de jonctions entre les deux surfaces antagonistes) et que le nombre de jonctions existantes peut être estimé à partir de la théorie de la dureté (si on connait la taille des jonctions). Dans ces conditions, lorsque la charge augmente, la taille de chaque jonction et le nombre de jonctions augmentent. Cependant, il a été montré qu'on peut considérer en première approximation, que la taille est sensiblement constante et seul le nombre augmente |13|.

3.1.1 - Influence de la charge sur la formation du film réactionnel.

Les mesures de RC permettent de suivre l'évolution de l'interface car le film réactionnel est un bon isolant électrique.

Les évolutions de RC obtenues pour les différentes pressions sont reportées figure 3. Dans tous les cas, l'évolution présente trois périodes :

- la période d'induction I : la RC reste à une valeur très faible (< 0,1 Ohm),
- la période transitoire II pendant laquelle la RC fluctue autour d'une valeur moyenne qui augmente,
- la période stationnaire III pendant laquelle la RC fluctue autour d'une valeur moyenne stable égale à environ 10^5 Ohms. Pour la durée d'essai considérée, la période III n'a pas encore été atteinte pour les pressions de 5 et 30 MPa.

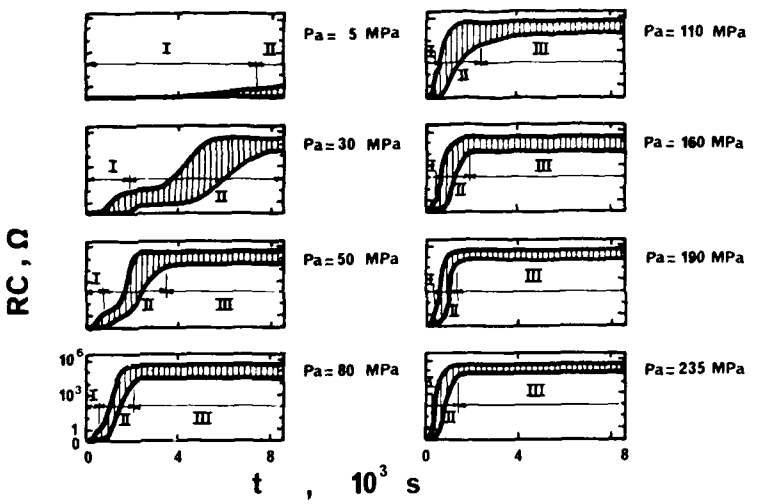


Figure 3 : Evolutions de la résistance électrique de contact RC en fonction du temps t pour différentes valeurs de pression.

L'examen des évolutions indique que la transformation de l'interface est rendue plus rapide par des pressions apparentes de contact plus élevées.

La durée de la période d'induction, qui peut caractériser la cinétique "globale" d'évolution du contact (formation de film réactionnel) varie avec la pression apparente de contact. Le temps d'induction qui est le temps nécessaire pour atteindre une valeur moyenne de RC égale à 0,1 Ohm varie avec la pression. L'évolution obtenue en fonction de la pression (voir figure 4) montre l'existence d'une valeur minimale au-dessous de laquelle il n'est pas possible de descendre lorsque la pression augmente.

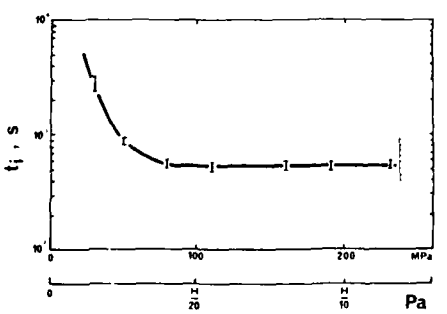


Figure 4 : Evolution du temps d'induction correspondant à une valeur de 0,1 Ohm en fonction de la pression apparente de contact.

Parallèlement à l'évolution de RC, des observations en microscopie optique permettent de suivre la formation du film sur les surfaces. Dans un premier temps (période I et partie de II), un film brun se forme sur les surfaces frottantes. Un film bleu se forme ensuite sur le brun (fin période II et période III). Le film bleu se présente sous la forme d'îlots, d'un diamètre moyen de 5 µm et recouvre environ 30% de la surface frottante. L'aspect des films apparait indépendant de la pression apparente de contact. Un exemple est montré sur la photographie prise en microscopie optique figure 5.

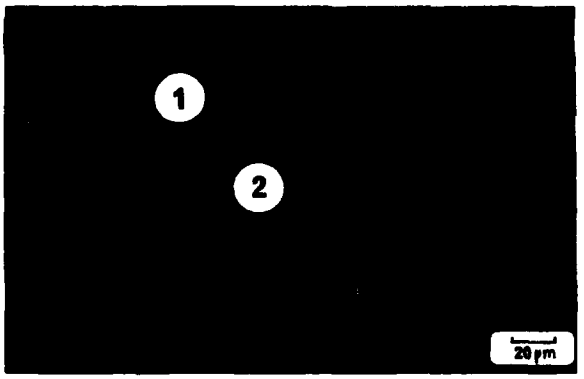


Figure 5 :

Aspect en microscopie optique du film recouvrant la surface de la bague (période III).
1 : îlot de film bleu
2 : film brun

Des analyses des surfaces après essais par spectrométrie AUGER ont montré que ces films sont composés des éléments provenant du lubrifiant et des surfaces (P, S, Zn, C, O, Fe). On note la présence de phosphate [14].

La théorie de la dureté permet d'estimer le nombre de jonctions correspondant à une pression donnée. Dans la période III, chaque jonction est du type métal/film/métal ce qui explique la valeur de RC élevée. Des calculs de la RC basés sur le nombre et la taille des jonctions, montrent alors que le fait que la valeur de RC soit indépendante de la pression correspond à une augmentation de l'épaisseur de film avec la pression.

L'examen des surfaces usées révèle que l'usure est du type adhésive et abrasive (à trois corps) avant et pendant la formation de film puis elle devient du type corrosive en présence de film réactionnel. Cette modification de type d'usure explique la diminution du taux d'usure qui accompagne la formation de film (facteur 100 environ).

Les mesures de hauteur usée en cours de frottement permettent de calculer le taux d'usure en présence de film. Son évolution est représentée figure 6. L'examen de cette évolution indique une augmentation de l'usure avec la pression.

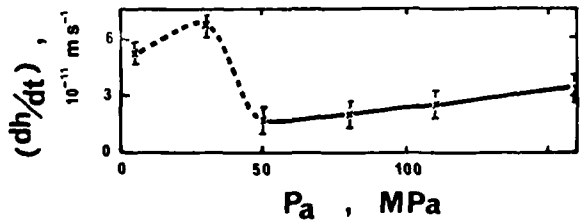


Figure 6 : Evolution du taux d'usure (dh/dt) en présence de film en fonction de la pression apparente de contact.
Les valeurs des essais sous 5 et 15 MPa ne correspondent pas à des films complets.

Ces différents résultats montrent donc que, pour toutes les pressions apparentes de contact testées, l'effet anti-usure associé à la présence du DTPZn correspond à la formation d'un film réactionnel dont l'apparence est sensiblement indépendante de la pression. Un film bleu sous la forme d'îlots se forme sur un film brun. Les îlots de film ont un diamètre sensiblement constant et l'épaisseur semble augmenter avec la pression.

Cet aspect de l'évolution de l'interface a pu être modélisé en considérant que le contact comprend des jonctions métal/métal et des jontions métal/film/métal (voir figure 7) et que les jonctions du premier type peuvent se transformer en jonctions du second type avec une certaine probabilité lorsqu'elles sont sollicitées [1]. Cette approche statistique du problème a permis de proposer des évolutions théoriques des grandeurs mesurées : résistance électrique du contact et hauteur usée et les évolutions obtenues sont apparues proches des évolutions expérimentales (figure 8) . De plus, il a été possible, grâce à cette modélisation, de quantifier l'usure avant la formation de film (grandeur inaccessible par des mesures classiques) et il est apparu que la présence d'additif anti-usure produit une augmentation du taux d'usure avant la formation de film.

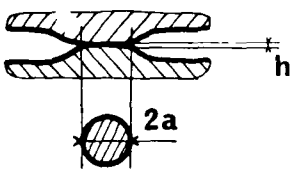


Figure 7 :

Représentation schématique d'une jonction,
a est de l'ordre de 5 µm.
Jonction sans film : h $\leq$ 5 nm
Jonction avec film : h $\geq$ 100 nm

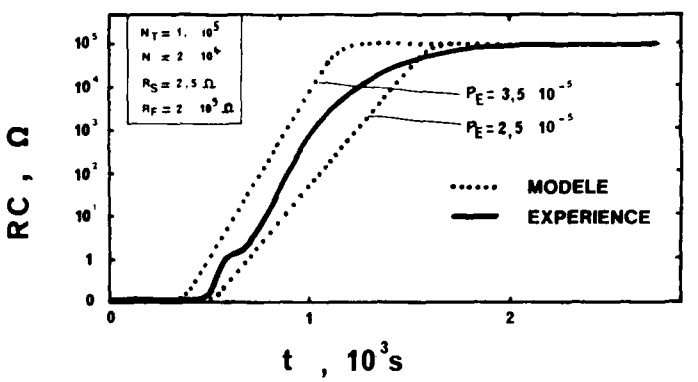


Figure 8 : Comparaison des évolutions de la résistance électrique du contact (RC) obtenues par l'expérience et par le modèle. PE est un paramètre du modèle qui représente la probabilité de transformation d'une jonction lorsqu'elle est sollicitée.
(N), (Nt), (Rs) et (Rf) sont des paramètres définissant le nombre de jonctions du contact et leurs propriétés électriques [1].

3.1.2. Effet du DTPZn sur la charge de grippage.

Lors d'un test de frottement, la charge est appliquée au contact dès le début. Le film réactionnel se forme sous l'effet du frottement et conduit à une baisse du taux d'usure. Des essais sous différentes charges montrent l'existence d'une charge maximum au-delà de laquelle le film ne se forme pas et le taux d'usure reste très élevé. Pour les conditions utilisées, cette charge de grippage correspond à une pression apparente de 235 MPa.

Lorsque la surface frottante est déjà recouverte de film réactionnel, la charge produisant un grippage apparaît plus élevée ; elle correspond alors à une pression de 340 MPa (augmentation d'environ 50 %). Ce phénomène montre donc un effet anti-grippage du film, effet que l'on peut attribuer sans doute aux propriétés mécaniques du film et à des possibilités de transformations physico-chimiques sous l'effet du frottement.

3.2 Essais sur machine à disques

Quand on introduit un lubrifiant dans le contact sur une machine à disques, il est possible d'entrainer le fluide dans l'interface, créant alors un film séparant les deux surfaces : le contact fonctionne donc en régime EHD.

De nombreux travaux ont permis d'établir que l'épaisseur h de ce film de fluide est liée aux différents paramètres de fonctionnement du contact : charge normale W , rayons de courbure, viscosité, vitesses ... Il a été établi [15] que h dépend fortement de la vitesse de roulement : $h = k.U^{0,7}$ ($U = 1/2(U1 + U2)$) et reste pratiquement indépendant de la vitesse de glissement DU ($DU = |U1 - U2|$).

Si on maintient h supérieur à la rugosité totale des surfaces, le cisaillement à l'interface se produit dans le film fluide. Dans le cas contraire , des contacts solide-solide apparaissent, pouvant provoquer l'endommagement des surfaces.

Dans des travaux précédents [9], il a été montré qu'en régime EHD, aucune dégradation des surfaces ne se produit. On n'observe pas la formation de film réactionnel et la seule cause d' usure des surfaces reste la fatique des matériaux.

Le but des essais présentés est de déterminer les paramètres de formation des phases réactionnelles dans un contact hertzien lubrifié en régime mixte.

3.2.1 Importance de la durée de sollicitation

On se propose d'observer l'évolution des surfaces en fonction du temps de fonctionnement d'un contact, les conditions cinématiques étant fixées : vitesse de roulement U = 1,0 m/s, glissement relatif DU/U = 5,0 %.

Lors du frottement, des films réactionnels apparaissent sur les surfaces. Ils se caractérisent optiquement par des colorations bleues-marron [9], réparties dans la trace de roulement (figure 9).

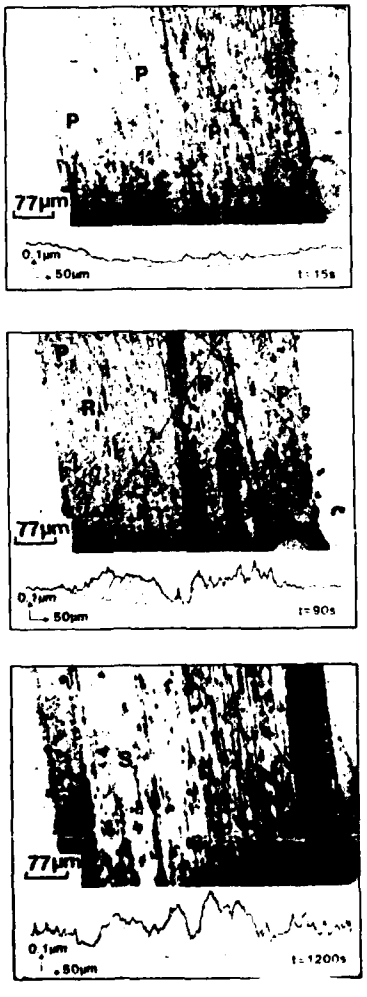


Figure 9 :

Aspect en microscopie optique de la piste de roulement du galet cylindrique après essai. (U = 1,0 m/s, DU/U = 5,0 %)
Différentes durées de test t = 5s, 90s, 1200s

Les zones sombres dans la piste sont recouvertes de film réactionnel en îlots.

Leur épaisseur moyenne peut être évaluée à l'aide des relevés profilométriques :
- trait plein : après essai, surface brute
- trait pointillé : après décapage du film.

[illegible] se présentent sous la forme de bandes orientées dans la direction du glissement. On peut déterminer l'épaisseur moyenne des produits formés (Et) en comparant le profil transversal de la trace de frottement avant et après décapage du film.

Sur [illegible], nous suivons l'évolution de Et avec le temps de fonctionnement t de l'essai. Les résultats ont été rassemblés pour trois valeurs de t : 15 s, 90 s, 1200 s.

Durée de l'essai (s)	Epaisseur moyenne de film Et(µm)
15	0.075
90	0.154
1200	0.886

On constate que Et est une fonction croissante du temps de sollicitation. Ce phénomène est analogue à celui observé en lubrification limite (paragraphe 3-1).

L'étude du signal de résistance électrique de contact apporte un résultat complémentaire en mettant en évidence une évolution de l'interface. En effet, si on suit l'évolution de la valeur moyenne de la résistance de contact avec le temps, on constate qu'elle augmente de façon significative, passant d'une valeur de 100 Ohms environ à plus de 1 MOhm (figure n° 9). Si on compare cette évolution à celle du même signal dans l'essai plan-plan en lubrification limite (figure n° 3), on constate qu'en début d'essai, dans un cas, la résistance de contact vaut environ 100 Ohms , et dans l'autre cas, reste inférieure à 0.1 Ohm .

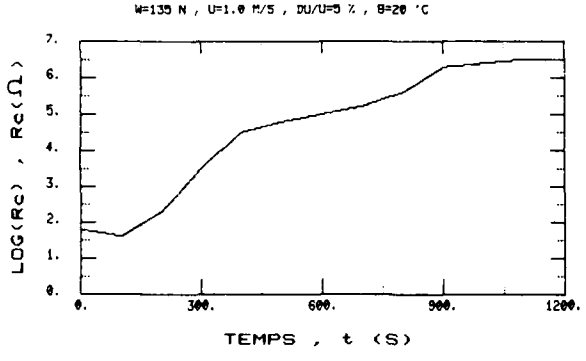


Figure 10 : Evolution de la valeur moyenne de la résistance électrique du contact en fonction du temps d'essai.
(U = 1,0 m/s, DU/U = 5,0 %)

Ce résultat s'explique en considérant que le contact en régime mixte est la contribution de deux phénomènes distincts pouvant exister simultanément :

- une partie du contact est en régime EHD (film continu de lubrifiant - épaisseur théorique : 0.05 µm), ce qui donne lieu à une résistance de contact très élevée : $Rc > 10^{14}$ Ohms
- une partie du contact est en régime limite (phénomène des jonctions, formation de film réactionnel) et donne lieu à des fluctuations de résistance de contact variant de 0,1 Ohm à 1 MOhm.

L'étude oscillographique détaillée du signal Rc confirme cette hypothèse [9].

En régime mixte, on constate donc l'apparition de film réactionnel sur les surfaces frottantes. Ce phénomène est fonction de la durée de sollicitation du contact. Une certaine analogie avec le régime limite apparait.

3.2.1. Influence de la vitesse de glissement

On se propose ici d'observer les dégradations de surface d'un contact fonctionnant dans différentes conditions de glissement relatif : DU/U valant 0 %, 2,5 %, 5,0 %, 10,0 %, en maintenant U fixe dans le contact.

Après essai, on détermine l'épaisseur moyenne de film réactionnel formé sur les deux surfaces (Et). L'évolution de Et avec le glissement relatif DU/U est portée sur la figure 10. La quantité de produit réactionnel formé dépend très fortement du glissement relatif appliqué aux surfaces.

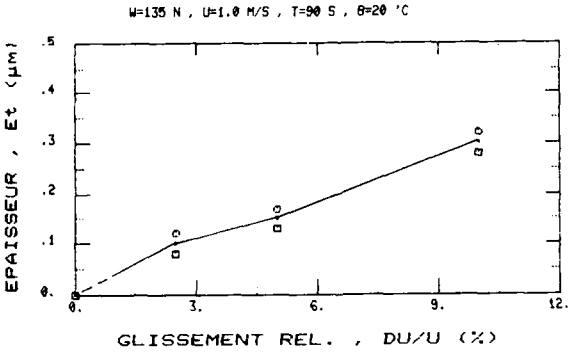


Figure 11 : Evolution de l'épaisseur moyenne du film réactionnel formé (Et) en fonction du glissement relatif (DU/U).
(U = 1,0 m/s, t = 90 s)

L'observation des traces de roulement après essai permet de déduire que :
- à glissement nul, aucune trace de film réactionnel n'apparait sur les surfaces (voir figure 12),
- le film réactionnel se développe par "îlots" distincts, ces îlots sont d'autant plus allongés que le glissement relatif est plus élevé.

Il faut noter aussi que la force tangentielle Ty transmise par l'interface n'est pas modifiée par la présence de film sur les surfaces (figure 12). On peut en conclure que dans ce régime mixte de lubrification, l'effort Ty est principalement dû au cisaillement du film fluide, la contribution du cisaillement des aspérités "solides" restant très faible.

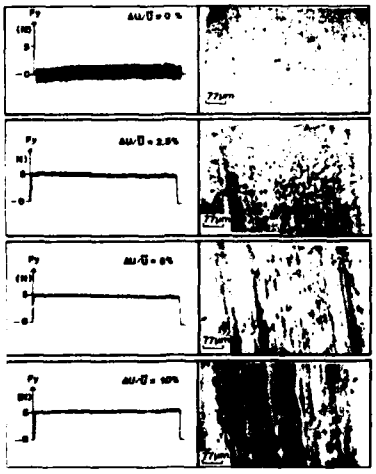


Figure 12 :

Evolution des surfaces de frottement en fonction du glissement relatif DU/U.
(U = .0 m/s, t = 90 s, W = 135 N)

A gauche, enregistrement de l'effort de cisaillement,
A droite, aspect en microscopie optique des surfaces.

A noter, l'allongement des îlots de film dans la direction de DU quand le glissement augmente.

La vitesse de glissement est donc un phénomène prépondérant dans la formation du film réactionnel en régime de roulement et glissement combinés.

Les phénomènes observés dans ces conditions sont analogies à ceux observés en glissement pur dans les essais plan-plan. On peut en déduire que ce dernier type de simulation est bien apte à reproduire les conditions de frottement variées d'un mécanisme réel comme un train d'engrenages par exemple.

4 - CONCLUSION

D'une manière générale, le frottement entre deux corps solides conduit à des transformations physico-chimiques superficielles. Cet effet existe aussi bien dans des conditions de frottement sec (formation de transferts...) que dans des conditions de frottement lubrifié (formation d'un troisième corps, de film réactionnel...).

Les résultats présentés nous ont permis de dégager l'influence des paramètres tribologiques sur la formation de film réactionnel dans un cas de frottement lubrifié en présence d'additif anti-usure.

Différents points ont été mis en évidence :

- la réduction de l'usure des matériaux est liée à la présence de film réactionnel. L'usure qui est de nature adhésive et abrasive en début de frottement devient de nature tribochimique en présence de film réactionnel.

- ces films réactionnels se présentent toujours sous une forme discontinue (présence d'îlots), indépendamment des conditions tribologiques.

- la pression apparente de contact accélère la cinétique globale de formation du film et de l'usure. Au niveau microscopique, on a montré que l'aspect des films n'est pas modifié, mais que leur épaisseur augmente avec la pression.

- en régime de lubrification mixte, la réduction de l'usure est aussi apparue liée à la formation de film réactionnel avec une cinétique analogue à celle observée en régime de lubrification limite.

- la vitesse de glissement accélère cette cinétique.

- l'effet bénéfique de la présence de film réactionnel se manifeste aussi par une augmentation importante de la charge de grippage.

REFERENCES

1. KAPSA Ph., Thèse d'Etat n° 8214, Lyon, France, (1982).

2. MARTIN J.M., Thèse d'Etat n° 7827, Lyon, France, (1978).

3. MONTES H., Thèse d'Etat n° 7915, Lyon, France, (1979).

4. GAC THIER A., Thèse docteur ingénieur n° 412, Lyon, France (1981).

5. MARTIN J.M., MANSOT J.L., BERBEZIER I., "Microstructural aspect of lubricated mild wear with zinc dialkyl phosphate". A paraître.

6. KAPSA Ph., TONCK A., SABOT J., "Propriétés mécaniques d'un film tribochimique formé en lubrification limite", C.R.A.S. A paraître (1984).

7. TONCK A., KAPSA Ph., MARTIN J.M., GEORGES J.M., Trib. Int., p. 209-213, (1979).

8. JOHNSON K.L., TEVAARWERK J.L., "Shear behavior of elastohydrodynamic oil films", Pr. R. Soc. Lond., Lond A 356, (1977), pp. 215-236.

9. GEORGES J.M., TONCK A., MEILLE G., BELIN M., "Chemical films and mixed lubrication", Trans. ASME, JOLT, vol. 26, 3, p 293-305 (1983).

10. ARCHARD J.F., Wear, 2, p. 438-455, (1959).

11. MATHIA T., Thèse d'Etat n° 7845, Lyon, France, (1978).

12. FORT M., Wear 77, p. 29-44, (1982).

13. TSUKIZOE T., HISAKADO T., ASME Trans., JOLT, p. 81-88, (1968).

14. KAPSA Ph., MARTIN J.M., BLANC C., GEORGES J.M., ASME Trans, JOLT, 103, p. 486- 496, (1981).

15. HAMROCK B.J., DOWSON D., "Isothermal elastohydrodynamic lubrication of point contacts". Trans. ASME, JOLT, vol. 99, p. 264-276, (1977).

REMERCIEMENTS

Les auteurs tiennent à remercier la Direction des Recherches et des Etudes Techniques et le Ministère de la Recherche et de l'Industrie pour l'aide financière apportée à cette étude.

DISCUSSION

H.A.Spikes, UK

I would like to congratulate the authors on a very interesting piece of work. Over the last two to three years we seem to be changing our views once more as to the nature of anti-wear and ep films and are coming to believe they can be quite thick, up to and over 1 micron thick. We have recently produced polymeric phosphate films several microns thick from phosphorate esters in pure rolling. How thick do the authors think that their films formed by TCP are?

Author's Reply

The authors thank Dr Spikes for his interesting remarks and for his questions. In our experiments, the TCP has produced in many types of contact, the formation of reactive films. The thickness of these films is approximately 0.1 to 0.2 microns in all cases. In the case of the tests on the roller test machine (machine à Galet) we have never observed the formation of films under conditions of pure rolling. The formation of reactive films has also been observed in the case of other additives (detergents, polymers, etc.) and it seemed to us that the thickness of these films was always sensibly about of the same order of magnitudes. Trials are also currently being made in our laboratory to measure certain mechanical characteristics of the film (particularly elastic modulus in shear). The first measurements show that the films have an elastic modulus of the order of 1 to GPa close to that obtained for high molecular mass polymers.

J.F.Chevalier, Fr

How can we assure ourselves of reproducibility in the feeding of the lubricant?

Author's Reply

In the case of the specimen tests, the feeding of the lubricant does not pose any problems since the specimens are submerged in the lubricant being studied.

In the case of the roller test machine (machine à galet) the tests are of relatively short duration and the feeding of the lubricant is done by injection at the entrance to the contact zone. The speed of injection, being governed by gravity, we have not observed any reproducibility problems related to the feeding of the lubricant.

B.A.Shotter, UK

The presence of non-metallic or polymeric films raises some interesting questions as to how the beneficial action of some additives may occur. In papermaking plant gearboxes, cellulose fibres in the oil can bring about plastic deformation of the steel gears and transport of the tooth contact surface layers. Perhaps the 0.1 mm thick polymeric films in the elastohydrodynamic contact environment act by promoting a mechanical process that allows the asperity contact stresses (including traction forces) to produce a plastic displacement of the asperities. Thus displacement, rather than wear or chemical erosion, may be the significant surface improvement mechanism in micropitting, plastic flow of the surface material is certainly observed. How the asperity fatigue and plastic displacement can be controlled is a much more difficult question

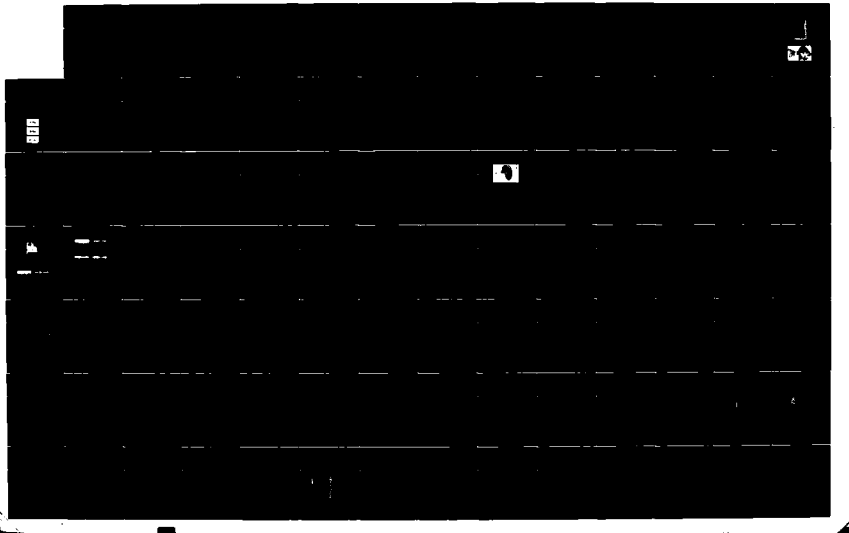
Author's Reply

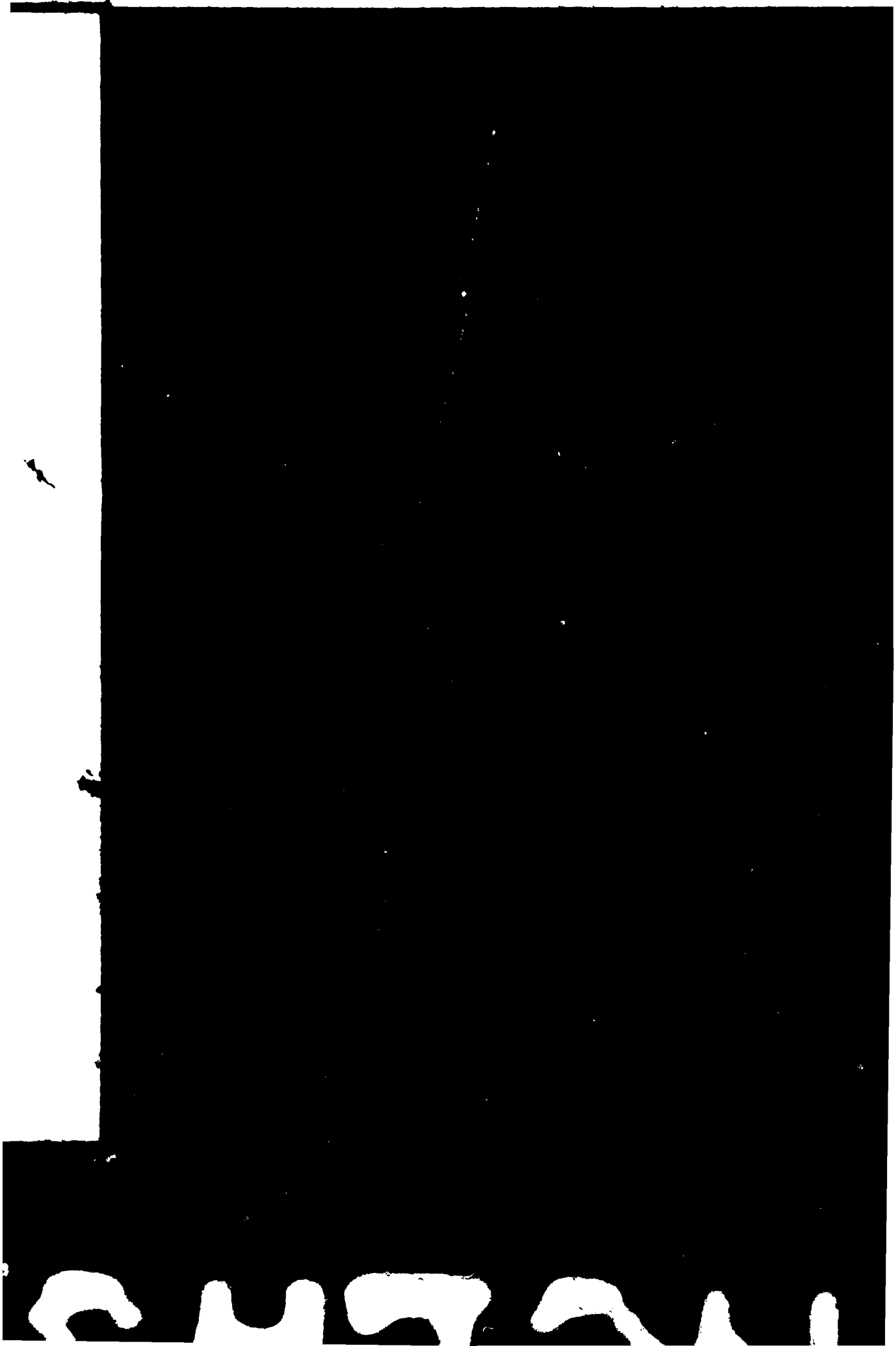
Asperity contacts can be catastrophic in the cases where the lubricant is not effective. One can in fact have adhesion between two materials followed by localized scoring at first and then generalized scoring if the conditions are severe. The presence of a reactive film on the asperities therefore permits that these asperities will deform plastically without the risk of introducing scoring. One effect of these films is also to reduce the friction forces.

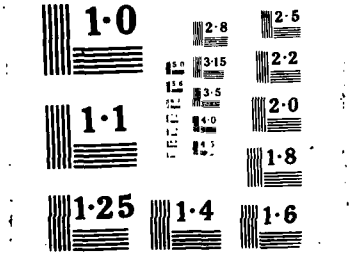
The phenomenon of fatigue, when it occurs at the level of the asperities, can therefore be reduced. However, in the case of certain combinations of materials and lubricants, the phenomena of "fragilisation" have been observed. Thus use of lubricants containing anti-wear additives must therefore always be considered in relation to the nature of materials which have to be protected, so that the desired effect is obtained.

AD-A152 673 GEARS AND POWER TRANSMISSION SYSTEMS FOR HELICOPTERS AND TURBOPROPS: CONF.. (U) ADVISORY GROUP FOR AEROSPACE RESEARCH AND DEVELOPMENT NEUILLY.. JAN 85 AGARD-CP-369 4/3

UNCLASSIFIED F/G 21/3 NL






1·0
1·1
1·25
1·4
1·6
2·8
3·15
3·5
4·0
2·5
2·2
2·0
1·8

"ROOT STRESSES IN CONFORMAL GEARS- STRAIN GAUGE AND PHOTOELASTIC INVESTIGATIONS"

BY

D.G. ASTRIDGE, B.R. REASON and D. BATHE

1. SUMMARY

This paper reviews the significant amount of analytical work on 'strong' gear tooth forms carried out since the classical papers of Shotter et al., and presents the results of a project which addresses a problem common to all three-dimensional photoelastic studies of root stresses in gears - that of maintaining an accurate delineation of the contact conjunction geometry throughout the stress-freezing cycle.

Photoelastic model results are compared with those measured by strain gauge methods on the definitive gears.

2. INTRODUCTION

The conformal tooth form has been successfully employed in the final reduction stage of the Westland Lynx helicopter main transmission and derivatives. Lynx has been in service for a decade now, uprated versions of its transmission are in service with Westland 30, and further development is in progress for growth versions of this commercial helicopter. The conformal tooth form lends itself particularly well to this high power application, where high power to weight ratio, large reduction ratio, and good tolerance of shaft alignment variations are required. The differences in tooth geometry between conformal and the more traditional involute are immediately apparent (see Figure 1), the conformal comprising constant curvature working flanks, 'all-addendum' convex teeth on the pinion, concave teeth on the wheel, and a helix angle necessary for conjugate action. The system is commonly known as Wildhaber-Novikov (W-N) gearing, after Wildhaber (1) who patented the system in the USA in 1926 and Novikov (2) in Russia in 1956. The more recent interest in the UK is attributed to an article appearing in the Manchester Guardian Newspaper in 1958 (3). The major advantage of conformals, anticipated at that time, was in overcoming the surface fatigue limitations of machineable steel gears and the AEI 'Circarc' gears successfully demonstrated this (4). However, it has been discovered from experience with Lynx gears that the W-N form can have advantages for case-hardened gears also, even though calculated maximum contact stresses exceed the normally accepted limits for involute gears, and high shear stresses can exist at the case/core interface and beyond (5). This is explained in terms of the radical differences in contact shape (Figure 2) - the relatively long, narrow ellipse of the involute form being more susceptible to localised defects or departures from the idealised form than the much lower aspect ratio ellipse of conformal gears and ball bearings. Rather more surprising at first sight is the apparent discrepancy between measured root stresses, and those calculated using involute procedures and normally-accepted root stress limits for high-quality, high-power gearing. Whilst work is continuing at Westland to determine the ultimate limits of conformal contacts (ie. surface stress and lubrication), this paper is concerned with root stress analysis and experimental validation. The sizing of conformal gear pairs at the project design stage is accomplished adequately using Specific Torque Capacity criteria determined from experience (an extension of the Lloyd's K factor concept derived by Shotter(5). The ability to go beyond this and determine contact and root stresses in detail is required for optimization of tooth geometry and refinement of life prediction.

3. ROOT STRESSES CALCULATION

The method generally used for calculating tooth root stresses in involute gears is based on the cantilever bending of an inscribed parabola (uniform strength beam), attributed to Lewis (6). Extensions of this to account for stress concentration arising from abrupt changes of curvature in the root region, tooth end effects, inclination of the load line in helical gears, and other factors have historically been generated by experimental methods (eg. the photoelastic studies of ref. 7) or by semi-empirical analyses (8), the results of which have been embodied in involute gear design standards (eg. 9). However, this approach is not reasonable for high strength tooth forms such as 'all-addendum' involutes or conformals in that St. Venant's Principle is violated - simple beam theory can only be used where there is a significant separation of load and support regions. The solution to this problem has been tackled analytically by Shotter and Fowle (10) with their 'isotropic wedge', and experimentally by strain-gauging (eg. 10), photoelastic modelling (eg. 11, 12, 14), and speckle pattern holography (14). 2D and 3D finite element analysis techniques have also been applied to the Lynx conformal tooth form (10, 13, 14). The two dimensional photoelastic study by Errichello (11) covered three tooth forms of greatly differing aspect ratio, characterised by pressure angle:- 14.5^0, 30^0 and 47.5^0. The results with large-scale models showed large discrepancies in root stress predictions for the stronger tooth forms using the AGMA method, but good agreement using the isotropic wedge provided that the latter results were factored by Dolan and Broghamer stress concentration factors (7). Application of the wedge theory to different conformal tooth designs has revealed the need for refinement to achieve acceptable accuracy in predicting the magnitude and location of minimum in-plane stresses, and to predict stress distribution in the transverse plane. The localised nature of the contact zone along the tooth produces fundamental limitations of analyses based on plane stress assumptions, as is revealed in the photoelastic results of Allison (15).

Three dimensional photoelastic modelling of a pair of conformal teeth loaded together also runs into difficulty, however, that of faithfully maintaining the correct contact geometry throughout the stress-freezing cycle. Significant differences in root stress results were obtained from a well executed 3-D photoelastic study commissioned by Westland, in which two different contact geometries were modelled. Another approach tried (15) was to model one component only, loaded by a metal ram. The study described in this paper addresses the problem of maintaining correct contact conditions in 3-D photoelastic modelling of conformal gears. Strain-gauge measurements made on static and dynamic gears at Westland are included for comparison.

4. CONTACT GEOMETRY IN CONFORMAL GEARS

French (16) produced an approximate analysis which predicted the contact shape to be an ellipse distorted towards a banana shape with major axis in the direction of rolling, ie. along the teeth. An exact analysis of Westland gears carried out recently (17), based on an earlier generalised analysis method (18) predicts that distortion of the contact ellipse is much less severe (Figure 3), having slight asymmetry about the major axis, and a small inclination of the major axis to the rolling direction. Figure 3, which relates to the Lynx conformal gears being modelled in this study, shows the gap contours for the unloaded contact. This data is being used by Snidle and Evans (19) in their subsequent elastohydrodynamic lubrication analysis of these contacts, but it is anticipated that the distortion of the contact ellipse will not be markedly different from the unloaded gap contours. There are other aspects of conformal gear technology that also depart from involute experience but space limitations prohibit discussion of them here. It is noteworthy, in passing, however, that good progress has been made in the difficult elastohydrodynamic lubrication analysis of this tooth form at high load conditions (19) and in the disc machine simulation of conformal contacts since earlier (eg. 20) published attempts.

5. STRAIN-GAUGE RESULTS ON LYNX CONFORMAL GEARS

The results of an extensive programme of strain-gauge measurements on full-scale gears in a 'four-square' arrangement at Westland were reported by Shotter (10). Whilst the tooth geometry was broadly that of the gears used in the Lynx transmission, there are differences in the precise tooth form and support structure which could influence the absolute stress - torque relationships sought in corroborating the results of this photoelastic study, but the comparison will be made as a first order check. The general form of the results from this earlier work is worth noting. Figure 4 shows the variation of stress measured at the bottom of a pinion tooth root in the mid-plane (single tooth contact) as pinion and wheel are barred round in small increments.

These results compared with those from strain gauges mounted at other positions, show that the bottom of the root experiences the largest total range of stress, but not quite the largest tensile stresses. The maximum compressive stress in this region is significantly greater than the maximum tensile stress experienced through the loading cycle, and thus there is a net compressive mean stress.

Whilst it was not attempted by strain-gauge placing to determine precisely the location of maximum stress range, and whilst it was appreciated that factors other than maximum range (eg. tensile mean stress results in lower fatigue life than stress cycles with a compressive mean), the criticality of the bottom region of the roots was demonstrated by the fatigue tests that preceeded the strain-gauge tests in this rig. The influence of centre distance variation was investigated and found to have a noticeable effect on stresses in the compressive region (Figure 5).

Subsequently, strain-gauge measurements were made on aircraft standard conformal gears in a complete Lynx main rotor gearbox in test rigs at quasi-static conditions, and at full speed. The gear configuration is shown in Figure 6. In these tests the pinions and wheel were strain-gauged in the bottom of the roots only, in a direction normal to the helix, at the mid-face and tooth extremities. A range of torques was investigated up to a maximum resulting in a range of ± 2450 microstrains. In the dynamic tests the strain-gauge signals were transmitted via a 12 channel slip ring, one channel of which was used for the pinion azimuth position indicator, a rotating potentiometer. The strain-gauge signals were amplified prior to recording, the amplifier having a flat response up to 2.2 KHz. Overall variation in output, assessed from duplicate strain gauges in adjacent tooth roots, and from the different torque settings was found to be ± 3% for the pinions and ± 5% for the wheel in the single-contact mid-plane positions. The results for these positions are summarised in Figure 7 in terms of average total stress range as a function of torque on the strain gauged conformal pinion. The differences between the results for pinion and wheel were within the variation quoted above, as were the differences for single and twin input drive to the gearbox, for different gearbox mounting arrangements, and for a 10^0 change in helix angle. The only signi icant difference was between static and running conditions, the results for full speed running being as much as 25% lower than static results at the highest torque condition. The frequency response of the strain-gauge system was more than adequate to resolve meshing frequency phenomena, and the lower values for running conditions are attributed to signal attenuation at the slip rings, or to inadequate temperature compensation. The static values are, therefore, used for comparison with results from the photoelastic study.

6. PHOTOELASTIC INVESTIGATION

6.1 Model Preparation

The models employed for the photoelastic studies were replicas of the conformal pinion and its integral shaft and mounting flange together with a segment of the conformal gear wheel. Both components were manufactured from "Araldite" CT200, silicone rubber mounds being produced from the original conformal gear pair.

Figure 9 shows the mould for the pinion mounted in the casting box, an aluminium core being employed to minimise thermal stress accumulation in the model upon cooling.

Casting was carried out in a heated oven (130°C) under a gradually increasing vacuum (1 in Hg/5 min), curing being over a 14 hour period. Slow cooling (2.5°C/hour) was employed to circumvent the danger of residual thermal stresses.

6.2 Conformal Contact Simulation

It had been established in previous experimental work that, because of the relatively large deflections occurring during a stress-freezing operation with conformal contacts (the strain must be large enough to generate an adequate fringe order), the resulting area of tooth contact on the model grossly exceeded that of the actual gear pair, with an inevitable reduction in the models' peak stresses.

To circumvent this difficulty a calculation of the elliptical profile in the Hertzian zone was carried out and a 0.004 ins. Beryllium Copper shim, photo-etched to this geometry, was cast into the surface of a wheel segment tooth. The geometry of the insert was produced under the assumption that the gear teeth were transmitting full load torque.

6.3 The Test Rig

Figure 10 shows the cast model components mounted in the rig prior to their mechanical testing.

Torque is applied by a simple dead-weight and lever system, the latter being bolted to the flange of the pinion shaft. The shaft itself is mounted in a rolling contact bearing simulating its location in practice.

The torque is reacted out through the wheel segment which, meshing with the pinion teeth, is bolted rigidly to a vertical pillar mounted in the bedplate. This carries slots allowing gear centre distances to be varied by moving the pillar in the plane of the bedplate.

A spherical bearing, clamped by a pinch-bolt to the pillar, allows adjustment of the wheel segment, thus providing accurate alignment of the tooth mesh.

6.4 Photoelastic Test Procedure

On initial testing a torque of 2.3 Nm (1.69 lbf.ft) was applied under ambient conditions to the model. The complete rig was then placed in a frozen stress oven and gradually heated (2.5°C/hour) to 135°C (the critical temperature of the "Araldite").

The temperature was held for one hour and cooling then commenced to 70°F at the rate of 2.5°C/hour. The rig was then unloaded and kept at 50°C for 24 hours to avoid any possibility of time edge effects.

The initial test, however, failed, since buckling of the segment flange occurred around the four set screws securing the model to its mounting block (Figure 10).

Using the same procedure a second specimen was tested but stresses on the model flange were relieved by interposing a wooden block between the new segment and the baseplate. This procedure successfully overcame the problem.

6.5 Slicing Procedure

Figure 11a shows the 'slicing-plan' the frozen stress model being cut with a diamond impregnated slitting wheel.

The initial slice, taken normal to the loaded tooth face, was positioned such that a whole tooth profile was produced on the adjacent tooth face. A 5 mm gap separated subsequent slices, each new surface representing the datum for the next slice, the loaded tooth being the datum length.

Upon cutting a new slice the pinion was indexed round by 2.5°. This kept the cutter normal to the loaded tooth flank (helix angle 15°-11') and produced a symmetrical profile for this tooth.

Slices were numbered according to Figure 11b, tooth "1" being the loaded tooth.

6.6 Analysis of Root Stresses

The purpose of the photoelastic investigation was to study the stress distribution around the tooth root arising from single point contact and to correlate the maximum value of the tensile and compressive stresses obtained with the values measured by strain gauging.

Stresses may be calculated by counting the number of fringe orders and converting this to a model stress by the relationship:

$$\sigma_m = \frac{f_o}{t} \times m.f.v.$$

where σ_m = model stress
f_o = number of fringe orders
m.f.v. = material fringe value ($N/f_o mm$)
t = slice thickness

The conversion of model stress to actual stress 'σ_p' requires the model stresses to be factored by the relationship:

$$\sigma_p = \sigma_m \times \frac{T_p}{T_m}$$

where 'T_p' and 'T_m' are the actual and model torques

6.7 Results

Figure 12 shows the isochromatic fringes of typical gear tooth sections. Since 't' and 'm f.v.' are known 'σ_m' can be calculated.

Sections 12a-c are purely arbitrary to illustrate the effect of changing Hertzian contact position. Unfortunately, subsequent to testing, defects were found in the batch of resin used. This had the minor effect of causing local perturbations in the fringe locii. The fringe orders however, were unaffected, these corresponding to other previous tests results under the same magnitude of applied torque.

Using the maximum value of prototype torque (253Nm (1866 lbf.ft)) and the model torque of 2.3Nm (1.696) the ratio T_p/T_m may be calculated. Calibration of the model material to establish the stress optic coefficient or material fringe value (m.f.v.) enabled the model stress to be determined from the fringe patterns, the thickness 't' of the slices being 2.54 mm.

Results from the photoelastic studies are shown as a graph (Fig. 13). This graph delineates the variation of root stresses (tensile and compressive) for the loaded tooth, along an axial locus traversing the tooth's helical flanks.

The maximum tensile stress established was 396 MP_a (57,400 lbf/in^2) the maximum compressive stress being 583 MP_a (84,500 lbf/in^2). It is seen that whilst the tensile root stress has a certain predisposition to symmetry about its maximum, the compressive stress displays a certain asymmetrical profile. The positions of the maxima do not, further, appear to be coincident.

7. DISCUSSION OF RESULTS

7.1 High Root Strength of Conformal Toothform

The high root strength established for conformal gears in fatigue tests on full-scale gears, and long experience with them in the Lynx transmission arises from the 'stubbiness' of the tooth form arising from 'all-addendum'pinion action. Clearly the strong root form is not subject to the bending action that occurs on unmodified involute teeth and the use of the term 'root bending' stress is, therefore, inappropriate to the stronger root forms.

The root stress analysis techniques derived for normal involutes are, therefore, unsatisfactory, and the isotropic wedge analysis has been shown to be more useful, although further refinement is necessary. The theory reasonably predicts the dominating compressive stress component of the overall root stress cycle, demonstrated by the strain-gauge and photoelastic results. The critical stress region in normal involute teeth occurs relatively high on the root fillet and is subject to a reversing tensile stress. In the conformal teeth studied here the critical stress region is much closer to the bottom of the roots and is subject to stress cycles with mean values well into the compressive region. Shotter (10) showed this root form to be capable of endurance limits with much greater stress cycle amplitudes than the normal involute, as indicated in the Goodman Diagram in Figure 8. The increasing upward trend of the alternating stress limit in the compressive mean stress region has been substantiated by extensive tests in the Westland Materials Laboratory on fully carburised steel push-pull test specimens designed to reproduce the conformal root geometry. The trend was confirmed up to the maximum mean compressive stress tested (200 MP_a).

7.2 Location of Critical Stress Region

From the photoelastic results for these gears from ref. 15 the maximum stress range extended over a region between 14^0 and 23^0 from the centre-line on the compressive side, the latter limit coinciding with the position of maximum compressive stress. However, the critical region relative to fatigue life is that for which the stress conditions (range and nature of mean stress) are closest to the Goodman limit line. Translating the results from ref. 15 for the Lynx conformal wheel to the Goodman Diagram of Figure 8, and measuring proximity to the limit line, the critical region appears to be between the centre-line and 30^0 on the tensile side. However, the margins on the compressive side are not much greater and in reality the critical region probably extends $\pm 30^0$ from the centre-line.

7.3 Nature of Stress Field in Roots

The photoelastic results from ref. 15 indicate large surface stresses in the transverse direction in the critical region. It is not safe, therefore, to base analysis on plane stress assumptions.

7.4 Comparison of Strain Gauge and Photoelastic Results

A comparison of the results obtained photoelastically with those obtained using strain gauge methods (Fig. 4) shows surprisingly close agreement for the tensile root stresses when the experimental divergence of the two approaches is contrasted.

The discrepancy between the compressive results, nevertheless, appears, on a cursory inspection, to be appreciable, the strain gauge results showing some 800 MP_a (116,000 lbf/in^2) against 583 MP_a (84,500 lbf/in^2) from the photoelastic approach (a difference of 27%).

7.5 Effect of Variation of Centre Distance on Root Stresses

A factor, however, which may have distinct relevance to this result is indicated in Fig. 5, which illustrates the effect of variation in centre distance on the peak stress values recorded by the root strain gauges.

In general, the magnitude of the peak tensile stress in the root of the loaded tooth is unaffected by variations in the true centre distance. On the compression side, however, the variation of centre distance produces a marked change in the magnitude of the peak compressive stress, a change of 0.127 mm (0.005 ins) on either side of the correct centre distance producing a variation of some 19% in the recorded peak to peak stress values. The applied torque in this case is, furthermore, some 22% less than that pertaining to Fig. 4, the inference being that changes in centre distance at higher torques produce a larger commensurate change than the 19% already indicated.

7.6 Change of Centre Distance in Photoelastic Model

Though every endeavour was made during the photoelastic investigations to simulate as far as possible the contact situation occurring in practice, the marked effect of centre distance on the magnitude of indicated peak compressive stress was certainly not realised. Undoubtedly, under the torque applied to the heated model an outward bowing of the pinion shaft took place (manifested by small angular movement of the pinion). The segment support pillar itself, must, additionally, deflect in the vertical plane. Both these movements would, essentially, produce the effect of an increased centre distance, a condition which, as shown in Fig. 5, reduces the recorded value of peak compressive stress to a marked degree. In the light of these findings the test rig has now been extensively modified, the segment support unit being redesigned both to allow a closely controlled adjustment of the centre distance (so that the effect of this may be monitored) and to minimise any flexural movement. Pinion shaft support diametrically opposite to the contact zone has also been incorporated.

7.7 Effect of Shim Implantation in Contact Zone of P.E. Model

The technique of shim implantation in the model, to simulate the contact geometry produced in practice, is considered to have been particularly successful. Fringe 'feeding' from the Hertzian zone undoubtedly influences the root stress on the compressive flank more than on the tensile (a probable factor in the peak stress magnitude differences shown in Fig. 13) and indicates the importance of closely modelling the geometry of the tooth conjunction during the stress-freezing process. Further work in this area will assist, additionally, in a better appreciation of the localised stress distribution in the Hertzian contact zone proper. A further factor, yet to be investigated, is the local effect of the high modulus shim material (in comparison with the lower modulus material of the P.E. model) on the general fringe distribution.

7.8 Influence of P.E. Results on Conformal Tooth Analysis

The variation in both magnitude and distribution of the stress field axially along the tooth, revealed by the photoelastic results, reinforces the belief that any two dimensional plane stress analysis is inappropriate to the conformal gear contact problem, not only for the Hertzian contact per se but for a delineation of the root stresses, since the two appear to be interconnected. This is, generally, not the case with the standard involute form. In the light of the results it would appear that a three dimensional analysis linking both localised Hertzian contact stress and root stress is required.

8. CONCLUSIONS

8.1 The experimental results (strain-gauge, photoelasticity, and holography) for the conformal tooth form used in the Lynx helicopter transmission and for other st·ong toothforms have demonstrated that:-

i) Cantilever beam theory used for normal involute toothforms is totallv inappropriate as is the associated terminology 'tooth bending'.

ii) The critical stress region in respect of fatigue failures lies within ± 30^0 of the root centreline.

iii) Within the critical stress region the material experiences in-plane stress cycles with tensile and compressive turning points, and compressive mean; plus significant stresses in the transverse plane.

8.2 Push-pull fatigue tests carried out on carburised gear steel specimens shaped to reproduce conformal root stress conditions have demonstrated that the fatigue limit continues upwards into the compressive mean stress region. Conformal tooth forms studied thus make better use of the material strength characteristics, and therefore offer benefits in root strength as well as surface strength relative to normal involutes.

8.3 The isotropic wedge theory (10) is much more appropriate to strong tooth forms than modified cantilever bending theory, but requires further refinement to obtain sufficient accuracy in predicting in-plane stresses. Analyses based upon plane stress assumptions cannot predict the significant transverse stresses measured. Three-dimensional finite-element analysis thus appears necessary at the present time in situations where the Specific Torque Capacity approach (5) is inadequate.

8.4 A technique has been developed for enhancing the accuracy of contact simulation in frozen stress photoelastic modelling. The results of the general three-dimensional stress distributions recorded indicate that localised stresses in the Hertzian contact influence both magnitude and distribution of the conformal tooth root stresses, particularly in the compressive flank. The modelling of the geometry of the contact conjunction further influences P.E. results, to a yet unknown degree.

9 RECOMMENDATIONS FOR FUTURE WORK

The complexity of the three-dimensional stress distribution in conformal tooth meshing revealed by this study indicates that, from the analytical standpoint, a 3D Finite Element approach could well provide an enhanced appreciation of the theoretical problem.

The correlation established between the separate strain gauge and photoelastic studies indicates their complementary nature. The importance of close integration between these two areas of experimental study cannot be over-emphasised, particularly in simulating working effects such as gear misalignment, deflections of shafts and gear teeth, centre distance effects and bearing support compliances in the experimental model itself. By a total approach such as this, the inherently high root stress capacity of the conformal gear may be optimised to its greatest advantage.

10 ACKNOWLEDGEMENTS

The authors would like to thank the Directors of Westland Helicopters and Hovercraft Limited for permission to publish this paper which reflects the views of the authors. They are also indebted to the many who have undertaken the strain-gauge tests and materials evaluations, expecially Mr. P. Sartin and Mr. A.V. Olver.

11. REFERENCES

(1) Wildhaber, E. "Helical Gearing", 1926, US Patent No. 1 601 750.

(2) Novikov, M.L., 1956, USSR Patent No. 109 750.

(3) Manchester Guardian, "Soviet Technology", 11th November 1958.

(4) Wells, C.F. and Shotter, B.A. "The Development of 'Circarc' Gearing", AEI Engineering March/April, 1962.

(5) Shotter, B.A. "Experiences with Conformal/W-N Gearing", EPIC World Conference on Gearing, Paris, June 1977 (printed in 'Machinery', 5th October, 1977).

(6) Lewis, W. "Investigation of the Strength of Gear Teeth", Proc. of the Engineers Club, Philadelphia, Pa 1893.

(7) Dolan, T.J. and Broghamer, E.L. "A Photoelastic Study of the Stresses in Gear Tooth Fillets", University of Illinois, Experimental Station Bulletin No. 335, 1942.

(8) Wellauer, E.J. and Seireg, A. "Bending Strengths of Gear Teeth by Cantilever Plate Theory" Jnl. of Engineering of Industry, Trans. ASME, August, 1960.

(9) AGMA Std. 221.02 "Rating the Strength of Helical and Herringbone Gear Teeth", July 1965/1970.

(10) Shotter, B.A., "A New Approach to Gear Tooth Root Stresses", ASME Paper No. 72-PTG-42, 1972.

(11) Errichello, R., "Bending Stress in Gear Teeth having Circular Arc Profiles" ASME Paper No. 77-DET-52, 1977.

(12) Lingaiah, K., and Ramachandra, K. "Photoelastic Optimisation of the Profiles of Wildhaber - Novikov Gears".

(13) Brighton, D.K., "Application of Finite Element Techniques to the Stressing and Improvement of Conformal Gearing", RAE Technical Report 77095, (1977).

(14) Lawson, T.T. "Static Analysis of Conformal Gear Teeth using NASTRAN Finite Element Analysis with Practical Verification by Holographic Techniques", Westland Internal Report RP602, 1979.

(15) Allison, I.M. "Photoelastic Study of Conformal Gear Stresses", University of Surrey, April, 1982.

(16) French, M.J. "Conformity of Circular-Arc Gears", J. Mech. Eng., Science 1965,7 (No. 2), P 220.

(17) Dyson, A., Snidle, R.W. and Evans, H.P., "Wildhaber-Novidov Circular Arc Gears, Part I: Geometry and Kinematics", University College, Cardiff, October 1983.

(18) Dyson, A. "A General Theory of the Kinematics and Geometry of Gears in Three Dimensions", Oxford University Press, 1969.

(19) Evans, H.P. and Sindle, R.W., "Analysis of Elastohydrodynamic Lubrication of Elliptical Contacts with Rolling Along the Major Axis", Journal of Mechanical Engineering Science. Proc. I.Mech.E, Vol. 197C, September, 1983.

(20) Astridge, D.G. and Longfield, M.D. "Capacitance Measurements and Oil Film Thickness in a Large Radius Disc and Ring Machine", Proc. I. Mech. E., (1967-1968) V 182, Pt. 3N.

(21) Bathe, D., "A Photoelastic Study of Stress Distributions in 'Novikov' Gears". MSc Thesis, School of Mechanical Engineering, Cranfield Institute of Technology, (1982-1983).

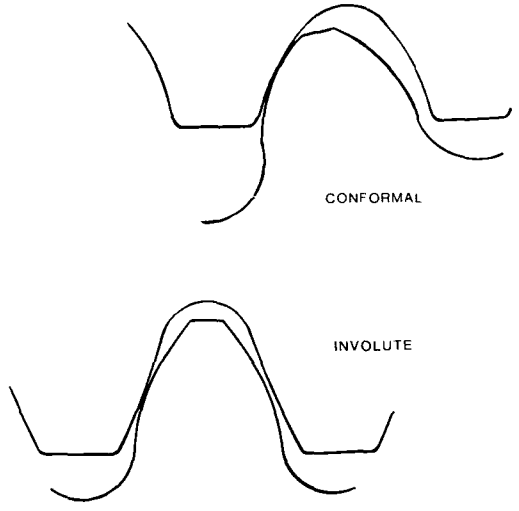


FIGURE 1 COMPARISON OF CONFORMAL AND INVOLUTE TEETH

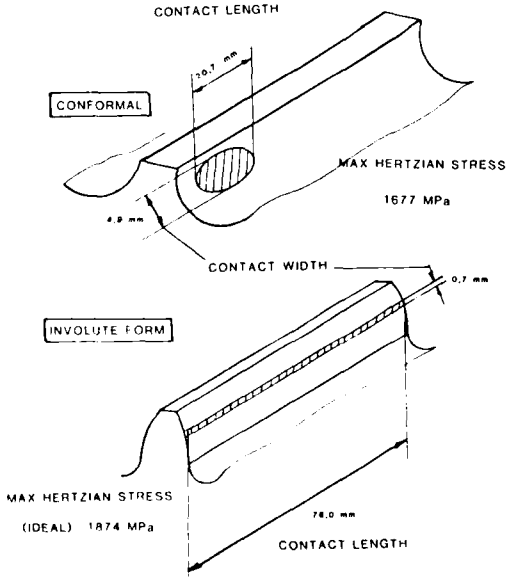
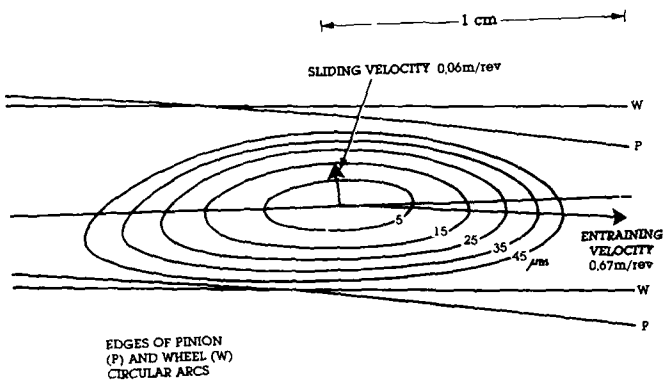


FIGURE 2 COMPARISON OF CONTACT AREAS AND STRESSES FOR INVOLUTE AND CONFORMAL GEARS OF SIMILAR PITCH CIRCLE DIAMETERS AND TANGENTIAL LOAD



EDGES OF PINION (P) AND WHEEL (W) CIRCULAR ARCS

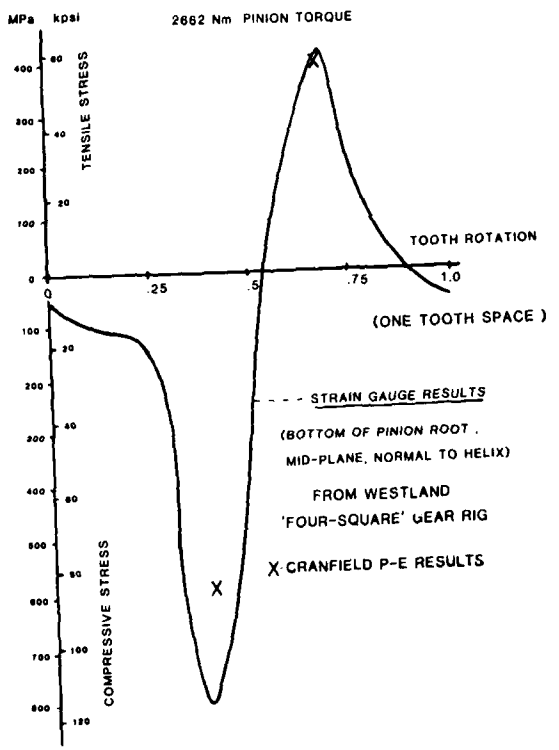


FIGURE 4 CONFORMAL PINION ROOT STRESS v ROTATION

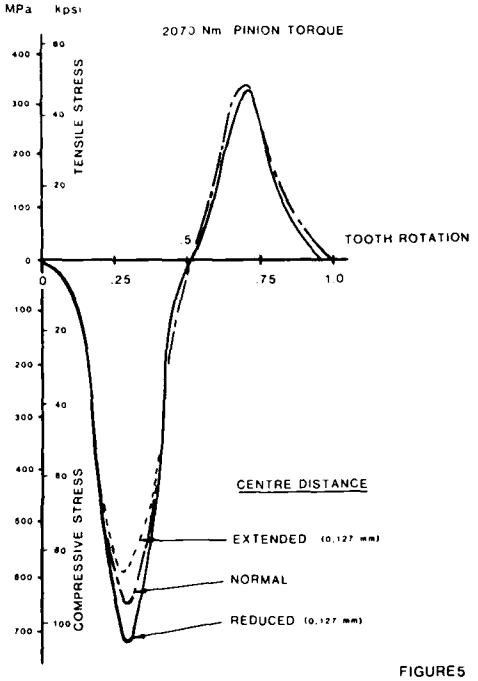


FIGURE5

INFLUENCE OF CENTRE-DISTANCE ON ROOT STRESSES
MEASURED IN WESTLAND 'FOUR-SQUARE ' RIG

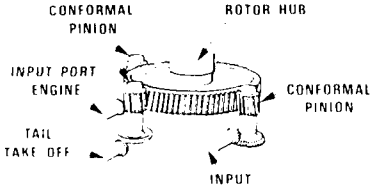


FIGURE 6 LYNX HELICOPTER - GEARBOX ARRANGEMENT

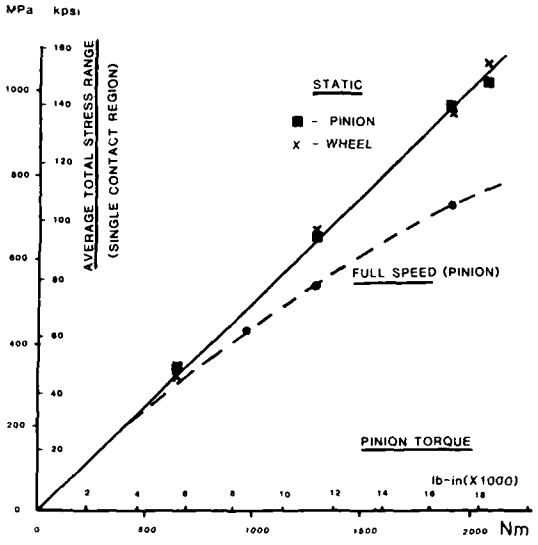


FIGURE 7 SUMMARY OF STRAIN-GAUGE RESULTS FOR CONFORMAL GEARS IN LYNX GEARBOX TESTS

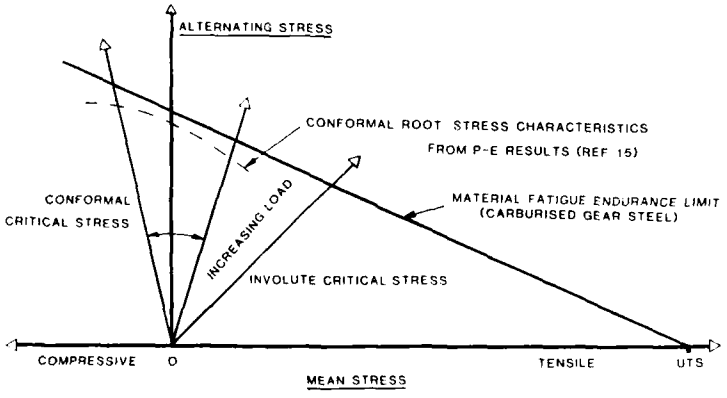


FIGURE 8 COMPARISON OF CRITICAL STRESS CHARACTERISTICS FOR CONFORMAL AND INVOLUTE TEETH IN RELATION TO MATERIAL STRENGTH



FIG.9. Cutaway of mould showing core



FIG.10 Test rig assembly

...ty of operation

...ty of operation is dependent upon the reliability of certain parts, the perfect running of which is ...tial to conclude the flight without accidents even if it is impossible to fulfill the mission.

To increase the safety of operation it is necessary to reduce the number of parts essential to the ...box survival and to increase the reliability of such parts.

Different ways to reach these targets are, at the moment, subject to *some* studies and tests. It is important to have a gearbox that can run long enough when a break-down puts completely out of service ...lubrication-cooling system. If we obtain this, then the reliability of the lubrication system is not ...be considered in the calculation of the reliability of the safety system. Most gearboxes are now ca-...ble of dry-run for, at least, 30 minutes.

A second point of remarkable interest is to *keep separate, as long as* possible, the kinematic chains ...transmit the power from the engines to the main rotor. In this case it is possible to have systems ...parallel. In addition, it is necessary to investigate what effects the failure of *one element in a* ...chain can cause on the elements of its chain and mainly on the elements of the other chain.

In the case of a gearbox for a twin engined helicopter, the failure of one element in a chain must ...prevent the good operation of the vital elements in the other chain or the good running of the vital ...ponents that are below the two chains mix-point.

...nerability

...nerability is mainly considered to be a military characteristic. For the helicopters designed for ...this use very detailed standards exist with all the requirements that must be satisfied. For example ...is required that the gearbox could run for a given period of time after it has been hit by a shell ...ed from a given distance.

...ver and above these requirements that are characteristic of each application and can therefore only ...satisfied individually, some general rules to reduce vulnerability can be listed.

A gearbox is not very vulnerable if it is small and has few external parts.

To achieve that, it is very important to have a gearbox that does not need an external cooling system, ...g. a radiator and some external piping. These parts are very vulnerable because of their dimensions and ...materials they are made of.

To do that it is necessary, on one hand, to reduce power losses (see [illegible]), and, on the other hand, ...find cooling systems that do not require a radiator.

We are investigating both these aspects. We consider, with great interest, the possibility to achieve ...cooling either inside the gearbox or using a very high efficiency exchanger. Very good results have ...been obtained during some tests of these solutions.

The results of this activity and the possibility for the gearbox to run at a temperature higher than ...present one, are likely to allow some significant modifications of the cooling system.

...wer losses

...e gearbox power loss reduction is a very important target for two reasons: first of all the power ...available for the rotor will be increased, and, secondly, the capacity of the cooling system will be ...duced.

The future aim will be the deletion of a vulnerable and heavy part such as the external oil cooling ...diator.

The gears (meshing losses and windage losses) and the rolling bearings are responsible for the gearbox ...wer losses.

In any case the power losses depend on the following factors:

- Bearing and gear geometric characteristics
- Main gearbox housing geometry
- Rotating speed
- Loads

...ese factors are determined by gearbox design considerations and cannot generally be modified to reduce ...wer losses.

Something, on the contrary, can be done with a proper design of the housing inner geometry in order ...improve the windage oil flow. An analysis of the ways to be followed by the oil to reach, after the [illegible] the designer to understand how to avoid a big ... of power losses mainly due to oil churning [illegible]. Keeping the gears far from the housing [illegible] a very significant increase of power ...transmission efficiency.

Another factor, [illegible] the gearbox efficiency, is the lube system [illegible].

Some tests that will allow a better knowledge of this effect are in progress. The main points to be investigated are the position and the direction of the oil jets and the oil flow amount. The results of [illegible] tests are [illegible] show the best way [illegible] efficiency increase.

a. Low Manufacturing Cost

Figure 12 shows the manufacturing costs of the main transmission components (gears and bearings) versus the reduction ratio of the last reduction stage for the four configurations considered. These values are scaled to the unit value of the cost of the typical gearbox.

The costs have been evaluated taking into account the direct costs of the gears and the purchase price of the bearings.

The use of the Value Analysis techniques allows to obtain considerable cost saving. Several projects have already been analyzed in FIAT AVIAZIONE using the above said techniques verifying cost reduction between 15 and 25 percent in terms of direct costs.

These results, of course, have been achieved without any performance penalties.

b. Noise Reduction

The gearbox noise level is affected by a few basic parameters: rotational speed, loads, rotating parts and housing mechanical properties and transmission errors. Each factor gives its different contribution, but all the effects are integrated.

The fight against gearbox noise can be carried out taking the following actions:

- Prevent noise generation
- Reduce noise amplification
- Attenuate noise transmission

During the gearbox design activity we can only consider the first two possibilities. Afterwards, during the gearbox development, we can also take into account the third possibility.

To prevent the excitation of vibrations that are responsible for noise generation there are a lot of different and well-known ways. We have no control over the rotational speeds and the loads since a gearbox is required to transmit a designed load at a set speed. On the contrary all the efforts must be directed towards the elimination of the causes of the transmission errors. (The transmission error is defined as the changes in reduction ratio in comparison with its theoretical value). These causes are tooth profile errors, tooth spacing errors, lead errors, teeth, shafts and bearings deformations under load.

We have taken the measures shown in the Table 5 to design the four gearbox configurations

Modified contact ratio	$\geqslant$ 1.30 Spur Gear $\geqslant$ 2 Bevel Gear
Tooth profile error	$\leqslant$ 0.012 mm with involute within 0.005 mm band
Tooth spacing error	$\leqslant$ 0.008 mm
Accumulated	$\leqslant$ 0.03 mm
Lead error	$\leqslant$ 0.005 mm/10 mm

TABLE 5

The noise reduction is related to a second aim, to reduce the gearbox noise and this is a responsibility of the design engineer. To reach this target it is necessary firstly to avoid resonances between the natural frequencies of the main gearbox components and the meshing frequencies or harmonics, and second to minimize the vibrations arising from the gears meshing.

A dynamic analysis of the transmission and gearbox casing, carried out with finite elements, allows the knowledge of both the natural frequencies and the displacements of the system. At this stage of the design it is then possible to deal with the vibration problem by stiffening the structure in order to raise the resonances and deformations responsible for the transmission errors.

Another point to be verified, that must still be well verified, is the use of materials of high damping capacity in place of the present materials and in addition coating, inserts ecc.). The present progress in the field of composite materials is likely to allow, in the future, their employment in the casing structure.

c. Low operating cost

The operating costs can be reduced by the following actions:

- Increasing the time between overhauls
- Decreasing the overhaul cost

The best way to increase the TBO is to improve the reliability of the equipment, see B.

To carry the second point during the design activity it is possible to take measures to reduce the maintenance cost. Bearing seats hardened in the shafts, cube nuts removable from the outside, generous radii in bushes at "O" ring seat, surfaces in order to make easier "O" ring assembly, etc.).

To attribute these costs are at the base of this paper.

Configuration	Number of stages	Number of gears	Number of bearings
A	2	7	14
B	2	7	14
C	2	7	14
D	3	11	18

TABLE 2

All the configurations have been designed without using epicyclic trains. This is the main difference in comparison with existing gearboxes: several considerations are responsible for such a choice and they will be analyzed later on.

For each design configuration we have considered several solutions obtained dividing the total reduction ratio in different manners between the single stages.

The evaluation of the four configurations will be carried out making a comparison with a typical main gearbox for a twin engined helicopter of the present generation.

In this activity all the appreciation functions are taken into account separately.

A. Weight

The graph of figure 10 shows the weights of the main transmission elements (gears, shafts and bearings), scaled to the unit value of the weight of the typical gearbox, for all the solutions taken into account. The weights are considered versus the reduction ratio of the last stage of the transmission.

B. Reliability

The graph of figure 11 shows the reliability calculated for the four design configurations on a Weibull's paper. These values have been obtained considering the main transmission elements only. The law versus time is exponential of the form $R(t) = \mathrm{Exp}\ (-A \times t/\theta)^{\beta}$ being $\beta=1.7$. As a comparison, the same graph shows the reliability of the typical gearbox.

The reliability increase shown is due both to the reduced number of components and to the increased reliability of some components.

Particularly for all the solution the following requirements have been set up:

- Minimum life for each bearing 6000h B10
- Minimum life for gears and splines: 20000h B01

Materials used and treatments to be performed are listed in Table 3 for all solutions.

Gears : AMS 6265 Carburized

Ring Gear : 32 CDV 13 Nitrided

Bearings : 100 C6 AISI 52100 (M50)

Shafts : AMS 6415 Hardened & Tempered

TABLE 3

The reliability and the costs have been calculated considering all the bearings made of 100 C6. If we foresee for the most critical bearings, the use of M50 we obtain for the main transmission chain, an increase of reliability (dotted lines in fig. 11) and an increase of cost (15 ÷ 17 percent). Table 4 shows the number of hours at which we have a reliability of 50% for each configuration and for the typical gearbox. In the first and in the second line there are the values obtained using bearings made of 100 C6 and M50 respectively.

	Typical GBX	A	B	C	D
Reliability of 50% (hours)	2800	4900 19000	4900 19000	4900 19000	4500 16000

TABLE 4

EVOLUTION OF THE DESIGN TECHNIQUES FOR HELICOPTER MAIN TRANSMISSION GEARBOXES

by
G. BENSI and L. TARRICONE
Direzione Progettazione
FIAT AVIAZIONE
Corso Ferrucci 122, 10100 Torino
Italy

SUMMARY

The paper shows the evolution of the design techniques adopted in FIAT AVIAZIONE for the helicopters main transmission gearboxes by means of the description of the mechanical units designed for the AEROSPATIALE helicopters: SA 321, SA 330, SA 360, SA 365.

The technical solutions have followed a development strictly related to the customer required specifications. Considering the past and present evolution we can foresee the future development trend.

As an explanatory example, an advanced main transmission gearbox for a medium twin engined helicopter is considered and some design solutions are shown.

INTRODUCTION

FIAT AVIAZIONE have acquired a long experience in the field of helicopter main transmission gearboxes.

In this activity it is of great importance the cooperation with the French Firm AEROSPATIALE which started in 1957 with the subcontract of mechanical groups for the SIKORSKY S 58 helicopter. Such cooperation continued with the design, the development and the manufacture of mechanical transmissions for the SA 321 Super Frelon, SA 330 Puma, SA 360 single engine Dauphin, SA 365/366 twin Dauphin helicopters.

The figures 1 to 4 show the main gearboxes of such helicopters. During the years of such activity the design techniques have shown a great evolution due to changes in user's requirements.

If we analyze an ordinary main transmission gearbox for helicopters in functional terms, we can identify three kinds of independent functions (see fig. 5).

1) Use functions: these are the functions which define the operating features of the gearbox.
2) Appreciation functions: these are the functions which define the appreciation of the gearbox by the user.
3) Imposed functions: these functions are imposed by the customer. It is a question of some requirements that must be taken into account during the design activity (e.g. interfaces, flange specifications, external dimensions etc.)

Leaving aside the imposed function requirements, the choice among the different design solutions that satisfy the use functions, depends upon the parameters defining the appreciation functions. Then the absolute and relative weights assigned to the appreciation functions during the design activity, are the reasons why in different times different configurations have been chosen.

Considering the more recent requirements we can foresee which design solutions will be valid for a gearbox to be made available in the late eighties.

As an example these considerations will be developed with reference to a hypothetic main gearbox for a medium twin engined helicopter. The main design requirements considered are listed below in the Table 1.

DESIGN REQUIREMENTS

Input power	2 x 650 HP
	1 x 1000 HP
Input speed	6000 RPM
Main rotor speed	385 RPM
Tail rotor drive speed	1700 RPM
Driven accessories	1 (or 2) Hydraulic pump
	1 A.C. generator
	2 Oil pumps
	1 Brake
	1 Cooler fan
Lubrication oil:	Synthetic oil conforming to MIL-L-23699

TABLE 1

Being the subject very general, all the considerations made later on will be about the main transmission chain. The conclusions of the analysis could be influenced by the characteristics of the considered example.

PROPELLER CONFIGURATION

Considering the requirements shown in Table 1 four different main gearbox configurations have been taken into account. In fig. 6, 7, 8, 9 solutions A, B, C, D are respectively shown and in the Table 2 their main characteristics are listed.

6. Berman, A., "A Generalized Coupling Technique for the Dynamic Analysis of Structural Systems," AHS J, 1980

7. Hurst, P.W., Berman, A., "DYSCO: An Executive Control System for Dynamic Analysis of Synthesized Structures," AIAA paper 83-0944-CP, 1983

8. Berman, A., "System Identification of Structural Dynamic Models-Theoretical and Practical Bounds," AIAA paper 84-0929, 1984

9. Nagy, E.G., "Improved Methods in Ground Vibration Testing," AHS J, 1983

10. Ibanez, P., Welding Research Council, New York, NY, Review of Analytical and Experimental Techniques for Improving Structural Dynamic Models, 1979, Bulletin 249

11. Bowes, M.A., Berman, A., "Prediction of Vibration and Noise of a Transmission Using a Dynamic Model Partially Derived From Test Data," Institute of Environmental Sciences, Proceedings, 1977

12. Berman, A., "System Identification of a Complex Structure," AIAA paper 75-809, 1975

13. Berman, A., Nagy, E.J., "Improvement of a Large Analytical Model Using Test Data," AIAA Journal, Vol. 21, 1984, pg. 1168-1173

DISCUSSION

R.Drago, US

Have you looked at the possibility of building a large, interconnected G/B Model using the Cray computer? How would this high speed machine impact your interesting approach?

***Author's* Reply**

High speed computers will allow more accurate computations such as time history analyses of non-linear systems. Otherwise they will not affect the considerations presented in the paper which will make the analysis more accurate (system identification) and more convenient (comparent synthesis).

D.G.Astridge, UK

I would like to pay tribute to Mr Berman and his colleagues at Kaman for demonstrating the need for analysis of the complete gearbox as a system, and for their useful work on analysis data compression and handling. His claim that finite element analysis techniques are not appropriate conflicts with our experience in carrying out a complete system analysis of our Lynx main transmission – but perhaps the simplicity of this gearbox configuration accounts for our successful application of FEA to the prediction of modal and forced response at frequencies up to 2.5 KHz. Using our WISDOM pre-post-processing facilities mounted on a DEC 11-45 computer and MSC/Nastran on our IBM 3081 main frame, we completed the analysis of 4 load cases using 14 minutes of CPU time on the latter. The model comprised 2000 grid points, producing 10,000 degrees of freedom, and was used to analyse the differences between the original configuration of this gearbox and the uprated 'power-sharing' version which contributed to the measured cabin noise reductions of up to 9 dB at the output stage meshing frequency (460 Hz).

Author's Reply

Your experiences are noteworthy and you are to be commended for their success. If your analyses truly represent the dynamics of the system, you should be able to optimize the configuration to obtain a true minimum of interior noise within the design constraints.

a repository for advanced technology related to all aspects of this problem. The program performs a generalized component synthesis function. A library of "technology modules," which is readily expandable, contains analytical representations of various components where each is treated as a free body. The library also contains force and solution

algorithms. A user of the system may develop a "model" consisting of an arbitrary set of component types, each augmented by the identification of the appropriate set of data and an arbitrary forcing function. The model then is formulated numerically and various solution methods may be applied to the resulting equations.

The general architecture is such that all the procedures described (and illustrated in Figure 1) may be incorporated. When a new or improved analysis method or component representation is formulated, it may be added to the technology library and becomes one of the available "modules" for use in executing a coupled analysis.

An overview of the program libraries is shown below in Figure 2. A more detailed description may be found in Ref. 7.

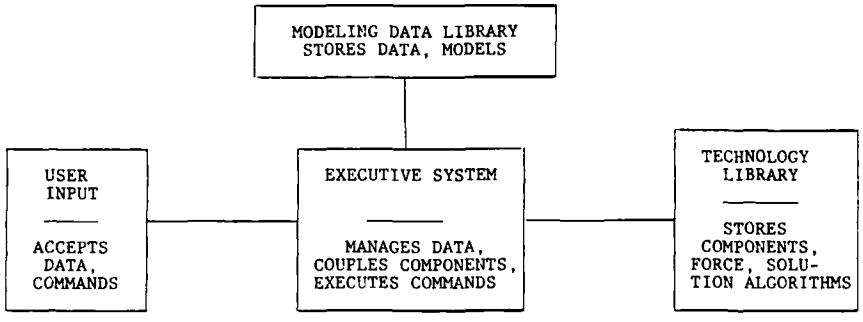


Figure 2. Overview of DYSCO Program

8. CONCLUDING REMARKS

In this paper, the problems associated with the prediction of resonant amplification of transmission gear noise is discussed. It is concluded that substantial practical and theoretical difficulties exist.

Certain techniques are suggested which can help to make the solution of this problem a practical reality. These include:

Independent component representations;

Use of test data to improve or develop analytical models;

Reduction of coordinates in the frequency domain;

Component coupling to evaluate various configurations and parameters;

Use of a generalized computer program to incorporate all the features of Figure 1 and serve as a repository for technology.

The problem is difficult, but not hopeless. Well directed research, and continuing improvements in the technology of analytical modeling and dynamic testing combined with advanced software to take advantage of new larger, faster, more economical computers will all help to bring this complex problem under control.

REFERENCES

1. Cremer, L., Heckl, M., Ungar, E.E., Structure - Borne Sound, New York, NY, Springer-Verlag, 1973

2. Sciarra, J.J., Howells, R.W., Lenski, J.W., Jr., Drago, R.J., Schaffer, E.G., Applied Technology Laboratory (AVRADCOM), Ft. Eustis, VA, Helicopter Transmission Vibration and Noise Reduction Program, 1978, USARTL-TR-78-2A

3. Hurty, W.C., Jet Propulsion Laboratory, Pasadena, CA, Dynamic Analysis of Structural Systems by Component Mode Synthesis, 1964, Technical Report 32-530

4. Berman, A., Giansante, N., "CHIANTI - Computer Programs for Parametric Variations in Dynamic Substructure Analysis," Shock and Vibration Bulletin, No. 47, 1977

5. Bowes, M.A., Giansante, N., Bossler, R.B., Jr., Berman, A., Eustis Directorate (USAAMRDL), Fort Eustis, VA, Helicopter Transmission Vibration and Noise Reduction Program, 1977, USAAMRDL-TR-77-14

points at which forces may be applied. This process can reduce the size of the problem to be solved by at least an order of magnitude or more.

The reduction process may be represented as follows. If the impedance matrix [Eq.(4)] is reordered so that the degrees of freedom to be retained are in the submatrix $(\ )_1$

$$Z(\omega) = \begin{bmatrix} Z_1 & Z_2 \\ Z_2^T & Z_4 \end{bmatrix} \tag{5}$$

then the reduced impedance matrix may be written

$$Z_R(\omega) = Z_1 - Z_2 Z_4^{-1} Z_2^T \tag{6}$$

Each of the reduced models at all necessary frequencies can be stored on a data base and will be directly available for use in the analyses of configurations.

The exact reduction process is only possible for frequency domain models and thus this formulation is suggested whenever it is technically appropriate. The relatively small number of discrete frequencies of interest also tends to make this an efficient procedure.

6. COMPONENT COUPLING

In the frequency domain or the time domain, the coupling of component analytical models to form the equations of the complete system can be quite straightforward.[3,6] Given a transformation matrix T_i, which relates the displacement vector of component i, X_i, to the displacement vector, ^iX, of the complete system:

$$X_i = T_i X \tag{7}$$

then the impedance matrix of the system can be written as:

$$Z(\omega) = \sum T_i^T Z_i(\omega) T_i \tag{8}$$

where the summation is over all the components. As shown in Ref. (6), the transformation matrix may be readily formed as long as the coupling of the components may be expressed in the form of a linear relationship between degrees of freedom of the components. In the simplest case where two displacements are equal (such as, a shaft displacement coordinate equals a specific bearing displacement) the relationship is of the form:

$$X_1 = X_2 \tag{9}$$

In a more complicated condition where a physical displacement interfaces a modal representation of a component, the relation will be of the form:

$$X_1 = \sum a_i q_i \tag{10}$$

where the q's represent modal amplitudes and the a's represent the mode shape displacements at the point of attachment. In either case the formation of the T_i matrix is a straightforward process which has been automated in existing computer programs, such as DYSCO [Ref. (6), (7)].

Given the equations of the components (e.g., the impedances), and information regarding the geometry of the coupling, such a program could automatically form the equations of the coupled system, retaining only a set of independent coordinates. The program then would have the capability to apply various solution algorithms, such as, computation of the forced response of the system at each frequency of interest. Individual components could then be modified or components such as vibration absorbers could be added and the coupling and solution could be repeated to assess the effectiveness of the changes.

It is also possible to provide a post processing feature to the program to allow the solution of each complete component of interest when each is treated as a free body acted upon by the interface forces determined in the coupled analyses. The interior vibration of the fuselage, for example, could then be obtained for each configuration of interest.

7. DISTRIBUTED TECHNOLOGY

The technologies involved in this problem may be classified as multidisciplinary. It is also true that specialists in the various areas are located in widely separated research organizations. In general, each researcher has an analysis method (computer program) that treats his area of specialization in detail, but may contain only a simplified representation of the related fields. What is required is a means of consolidating all the highest levels of the technologies into a single analysis method, and have that method available to all interested users.

The DYSCO program[6,7] is an example of a system that has such a capability. It is an executive control system that has a software architecture which will allow it to serve as

representation resulting from a prior finite element analysis. The rotor system may be represented by an analytical impedance formulation.

Another advantage is that the models of individual components may be separately modified or enhanced with increasing detail during various stages of the design and the development of the hardware.

A third benefit of the component synthesis form of analysis is that studies of modified designs may be conveniently carried out by changing only the analytical models of the components affected.

4. USE OF TEST DATA

When actual physical components are not available, the analysis represents the only known data and best use of it must be made. However, since the prediction of the dynamic behavior in the relevant frequency range is expected to be poor, analysis alone is unlikely to be adequate, except, possibly, for the prediction of trends. The formulation of such an analysis may be used as a base to be improved upon when additional data becomes available.

When the hardware of any components exists, there are several ways in which testing can be of great value. Suggestions are made below which should be considered depending on the specific conditions and structures involved.

Any component that interfaces with other components at a small number of locations may be modeled directly from test data. The most direct approach is as follows. The structure is excited at each of the degrees of freedom of the interfaces and the applied force and the responses are measured at all of these degrees of freedom. This procedure is repeated for each frequency of interest to form mobility matrices. The measured matrix elements $(\partial X_i/\partial f_i)$ form a mobility matrix, Y, where

$$Y(\omega)\ f(\omega) = X(\omega) \tag{3}$$

or, from Eq. (2)

$$Y(\omega)^{-1} = Z(\omega) = (K - \omega^2 M + i\omega C) \tag{4}$$

The inverses of the mobility matrices may be treated as an analytical model and may be directly coupled with other component representations. Great care must be exercised in this application, since measurement errors tend to be magnified in the matrix inversion. In addition, the measurement accuracy required increases very rapidly as the order of the matrices grows beyond a small number.[8]

In spite of the potential difficulties associated with this procedure, it can, under the proper circumstances, be quite useful. It may be possible to obtain a valid appropriate model of the entire airframe by the use of this technique. In order to simulate the appropriate boundary conditions, a soft suspension system must be used and care must be exercised to insure that the responses are in the linear range.[9]

Other components may also be candidates for such a procedure, such as, the tail rotor and tail rotor drive modeled at the transmission interface. Interfaces with other components must be taken into consideration, including drive shaft supports attached to the fuselage.

When a component has been represented by a derived mathematical analysis, testing can be used to confirm the validity by comparing the natural frequencies and modes of the component with those predicted by the analysis. If satisfactory agreement is not observed, the model may be modified by an iterative intuitive process until consistency is achieved.

More automated processes for model improvement are presently being researched under the general area known as "structural system identification." An excellent review of such procedures has been published by Ibanez.[10] Specific applications to a helicopter transmission housing are given in Ref. 11, 12 with a more advanced version of the technique given in Ref. 13. This specific procedure results in an analytical model which is still related to the structural characteristics but contains the precise natural frequencies and modes as measured on the structure.

5. REDUCTION OF DEGREES OF FREEDOM

For components which are analytically represented, considerable modeling detail is required in this frequency domain. The very large number of degrees of freedom of the coupled system will result in very large computational costs. Considerable economic benefits result from a procedure which can reduce the size of the problem without loss of accuracy.

Such a method, for frequency domain applications has been applied to transmission analyses.[4] This procedure allows the modeling of each component to be as detailed and complex as necessary. However, before use in a coupled analysis, the model is reduced so as to include only the interface degrees of freedom, plus any others necessary, such as,

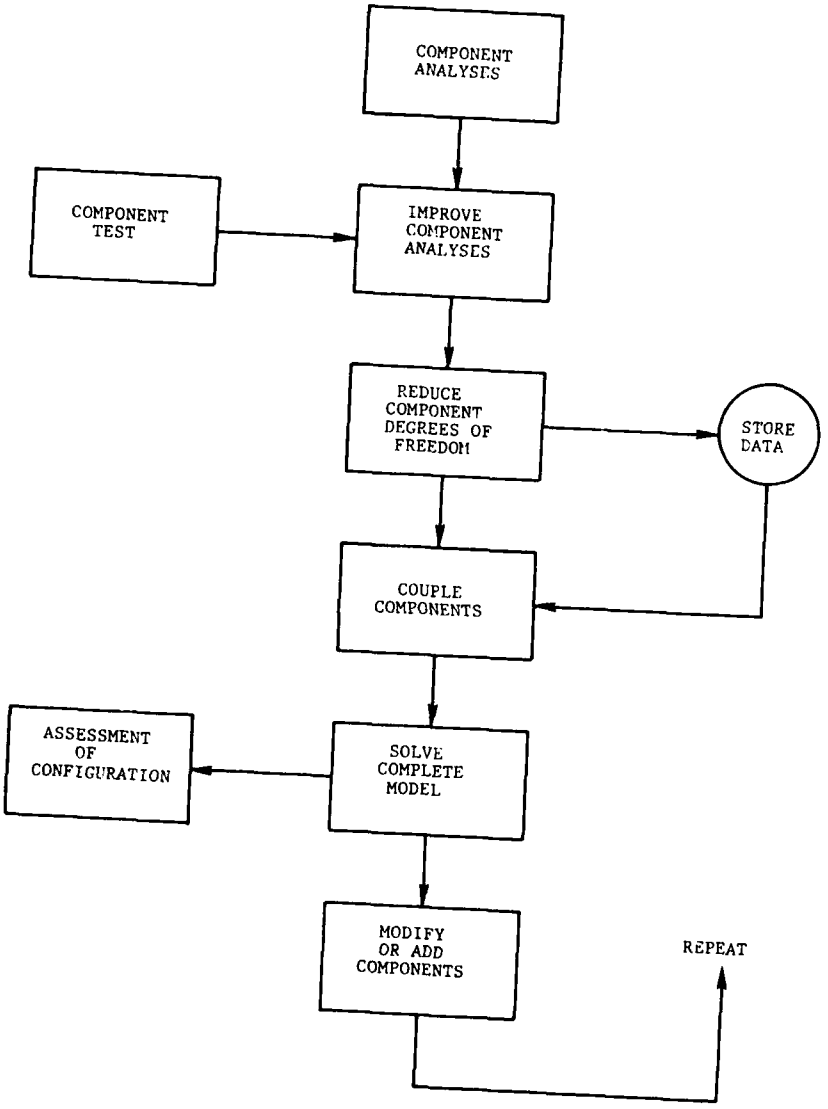


Figure 1. Procedure For Dynamic Analysis

frequency phenomena, it is unlikely to be so for acoustic range dynamics. Any physically attached component whose dynamics will influence the natural frequencies of the transmission system must be included in the analytical model. A priori assumptions regarding the validity of such special simplifying considerations are inappropriate.

Thus, it appears that the task required is to model in considerable detail: the entire drive system including all gears, shafts, bearings, housings; the fuselage and all its components; the rotor(s) and engine(s); and all shafts, couplings and other attachments. Not only would such a project be very expensive in terms of personnel and computer resources, but it is unlikely that sufficiently accurate predictions would be obtained.

The procedures suggested in the following sections will reduce the cost, increase the accuracy of the analysis, and will bring the solution of this aspect of the general problem into the realm of feasibility.

2. GENERAL APPROACH

Several concepts which can make the entire process more manageable, more efficient, and more accurate are defined in the following sections. They are briefly described below.

It is possible and convenient to treat portions of the dynamic system as separate entities or components. The components may be modeled using techniques appropriate to each. It is not necessary or desirable to model the entire system as a unit using a single type of analysis procedure, such as a finite element method.

Dynamic testing may be performed on each component, if the hardware is available, to improve the analytical model. Under certain circumstances, the test data may be used alone to represent the component's dynamics.

The number of degrees of freedom of individual component models may be greatly reduced with no loss of accuracy when working in the frequency domain. This also greatly reduces the size of the coupled analysis problem and is an important cost saving technique. The reduced models may be stored and later retrieved as required without repeating the prior analysis.

The component representations can be analytically combined into various configurations including modifications of particular components to assess the effects of structural changes.

This general procedure is illustrated in Figure 1.

3. COMPONENT ANALYSIS

The treatment of complex structures as a combination of components has become common practice since the important publication on the subject by Hurty.[3] Numerous related procedures have been used and specific applications to frequency domain transmission analysis were developed[4] and applied.[5] A general time domain software system for this purpose has been reported in References 6, 7.

The forms of the equations (for a linear, viscously damped system) of each component are as follows. The time domain representation is:

$$M\ddot{X} + C\dot{X} + KX = f(t) \tag{1}$$

and the frequency domain representation is:

$$(K - \omega^2 M + i\omega C)\, X(\omega) = f(\omega) \tag{2}$$

where M, C, K are real, symmetric nxn matrices representing mass, vicous damping, stiffness, n is the number of independent degrees of freedom, ω is the frequency of the applied force and $i = \sqrt{-1}$. f is a vector of applied forces at each degree of freedom and X is a vector of the displacement of each degree of freedom. The degrees of freedom may be physical displacements (and rotations) or generalized coordinates, such as, modal amplitudes. In Eq. (1), f and X are functions of time. In Eq. (2) f and X are complex amplitudes of $e^{i\omega t}$.

The equations of the complete coupled system are of precisely the same form as Eqs. (1), (2).

There are a number of advantages to using a synthesis method which will allow separate analyses types for components.

First, each component may be modeled in a most appropriate and effective manner. For example, a housing structure is likely best analyzed by a finite element method. A shaft component may more effectively be treated with a specially developed analysis which takes advantage of its beam characteristics and axial symmetry. The entire fuselage may be represented by a measured impedance matrix (at each forcing frequency) or by a modal

TRANSMISSION OF GEAR NOISE TO AIRCRAFT INTERIORS PREDICTION METHODS

by
Alex Berman
Kaman Aerospace Corporation
Post Office Box 2
Bloomfield, CT 06002-0002
U.S.A.

SUMMARY

Prediction of interior noise of helicopters due to drive train vibration ideally requires an analytical model of the entire dynamic system including airframe, transmission, and all attachments. The development of such a model is beset with numerous difficulties. This paper addresses the need for such a model and certain of the critical issues involved: the inadequacy of finite element modeling in the acoustic frequency range; the costs associated with assessment of parametric variations; the difficulty of incorporating new technology into existing computer programs. Potential solutions to these problems are discussed: use of combined test and analysis (system identification) to obtain better models; component synthesis using frequency domain reduced models; a computer program known as DYSCO. This program has a general capability to modify and couple components in the time or frequency domain and can act as a repository for the latest analytical developments.

PREFACE

The vibratory forces generated at gear meshes in helicopter power transmission systems often result in excessive noise in the aircraft interior. The high noise level may be due to large excitation forces or it may be the result of a mechanical resonance which amplifies the vibration. In the first instance, the problem may be corrected by reducing the forces of excitation through improved gear design. While this may require more costly manufacturing processes and the effect of wear lends some uncertainty to the process, there are few viable alternatives. The use of materials to block transmission of the vibration or to absorb the noise often results in excessive weight penalties and the effectiveness has not always been completely satisfactory.

In certain instances, the high noise level is due to a resonant amplification, in which case the problem may be treated by changing the structural characteristics of the dynamic system. Some changes may include: changes in mass, stiffness, or structural damping; modification of the geometry, such as, bearing or mount locations; or by installation of mechanical devices, such as vibration absorbers or isolators. The prediction of this condition and the evaluation of changes requires a detailed dynamic analysis. The problems associated with the development of an adequate analysis of the dynamics of the system are substantial and, optimistically, border on the edge of the present state of the art.

The discussion in this paper addresses the difficulties of the prediction of the resonant phenomena and the evaluation of candidate changes. Approaches are suggested which can improve the validity and cost effectiveness of such analyses. The topics of wave propagation, reflection of waves, elastic interlayers, blocking masses, and other similar phenomena[1] are not directly treated, however, the general concepts presented also have applications in these areas.

The problem of high interior noise due to transmission of gear noise is a difficult challenge and much research will be required before satisfactory solutions will be achieved.

1. MODELING DIFFICULTIES

Helicopter drive systems normally operate at a constant speed, thus there are generally a relatively small set of discrete frequencies of excitation. The frequencies of interest, however, are much higher than the low order natural frequencies of the structure. It is not uncommon for this range to include modes of order 30 to 60 and higher of a major component such as a transmission housing (see Ref. 2, p.90, for example). In order to make accurate predictions of this phenomena it is important that the natural frequencies of the dynamic system be known rather accurately.

The best methods of analyzing such a structure (e.g. transmission housing) are of the finite element category. The typical irregular shape, varying thickness, and numerous cutouts precludes any more analytical formulation. An analysis of adequate detail to predict such high frequency modes requires thousands of nodes and degrees of freedom. The cost of formulating and processing such an analysis will be very high. However, even with a very careful and detailed analysis, the likelihood of accurately predicting natural frequencies above the first few is extremely small.

There are certain very special circumstances when the local natural frequencies of individual components are meaningful in this context. The free-free frequencies of a shaft may fall in this category if the bearings are located precisely at the nodes of the modes. If the fuselage were very stiff with high inertia, the transmission could be considered as attached to ground. However, stiffness here is relative to the frequencies of interest. While such an approximation may be valid when considering very low

DISCUSSION

R.Drago, US

You noted that, for involute gears, the root tensile stress is much higher than the root compressive stress, but for conformals the compressive stress at root is higher than tensile. For thin RIM involutes, RIM bending predominates and the compressive stress becomes much higher than the tensile. This effect would be much worse on W—N gears and thus the alternating stress (i.e. comp.-tens.) would be much higher for W—N gears. Their bending strength would thus be low. Have you done any testing on realistic thin rimmed W—N gears? Either P—E or strain?

Author's Reply

The root stress variation shown in Figure 4 was found to apply to the bottom of the tooth root, single tooth contact region for the pinion (scatter ± 3%) and wheel (± 5%) in the 'dumb-bell' rig tests. In this rig the pinions were solid, and the wheel had a rim thickness to diameter ratio of approximately .02 — quite flexible. Subsequent results from strain gauge tests on the definitive gearbox in which pinion rim thickness to diameter ratios were approximately .2, also followed Figure 4 very closely. I am not aware of strain gauge measurements made on thin-rim involute gears, so I cannot comment. From our measurements it appears that the combination of the compressive peak stress arises from the strong tooth form and may also apply to all-addendum involute teeth. The conclusion from Figure 8 — that conformal teeth make better use of gear steel strength characteristics because of the compressive nature of the mean stress would apply to any geometry having this characteristic — provided that limiting stresses do not arise elsewhere — e.g. in the bore or body of the rim.

R.W.Snidle, UK

1. This study shows that, in high conformity gear tooth contacts, in which the area of contact can be of the same order as the tooth height, it may be necessary to consider non-Hertzian aspects of the contact stresses and deformations. The authors have made significant progress in this area, particularly in drawing attention to the interactions of the contact and root stress distributions.

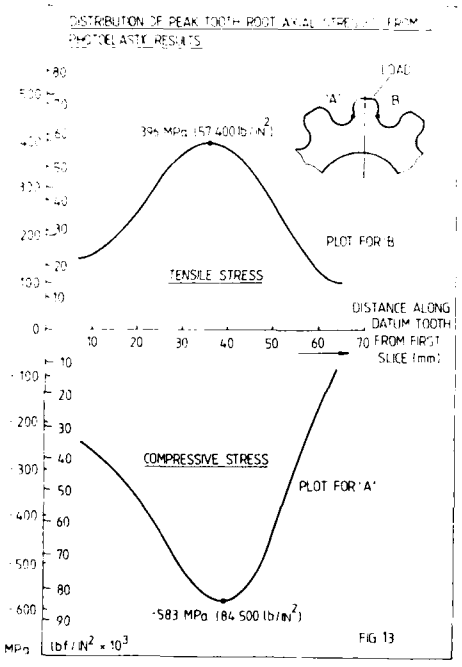
2. Analysis of elastohydrodynamic lubrication of these contacts is a very difficult problem. The contacts are, in EHL terms, very heavily loaded. Film thickness formulas which are based on the analysis of relatively lightly loaded contacts probably involve a significant extrapolation when applied to W-N conditions.

Author's Reply

The authors would concur with Dr Snidle's comments, and express appreciation for the valuable contributions that he and his co-workers are making to the analysis of the kinematics of conformal gears, and of elastohydrodynamic lubrication. Clearly the large relative areas of the conformal contact renders the applications of the basic Hertzian stress equations open to doubt, since these were erected to solve nominal point or line contact problems. Undoubtedly, on the basis of the photo-elastic results obtained, there is a marked interaction of the stress field from the contact area with that occurring in the tooth root on the compressive side. Since the stress fields themselves cannot be considered as planar this further complicates the analysis. It is felt, as the paper suggests, that an inductive approach employing experimental and analytical techniques in parallel is preferable to treating any approach.

These analytical problems occur with other machine elements also — in bearing balls the contact areas can be relatively large, and in rotating outer raceways the interaction of contact stress fields with tensile hoop stresses can be significant. Epicyclic ring gears have a conforming nature, and interaction between contact and root stress fields is quite common. It is important to continue the development of analysis methods for improved prediction of deflections, stresses, and surface separation in all forms of machine elements. The rapid growth of computing facilities, numerical methods, and improved experimental techniques are making a considerable impact on the most complex of problems. There is still much scope for progress with analytical tools in the sense that correlation of life or performance in service with magnitude of individual components of complex stress fields or classical failure criteria is lacking for many machine elements, but this is not surprising in view of the large number of possible failure modes and the complexity of stress fields and surface separation parameters (Paper 31 details some aspects of this problem).

In the meantime, however, gearbox designers are well served by empirical design criteria such as Lloyd's K factor or Specific Torque Capacity for gears, and Load Severity Criterion for bearings. These are based on nominal surface stress, and being simple to calculate have been used for a long time now for correlating service experience. Such experience factors have been particularly useful in the extension of designs within a given product range, which is a very common situation. This approach succeeds because many of the factors which have an impact on life remain relatively constant-environment, materials, and manufacturing parameters; and perhaps only speed or load intensity differ from previous experience — one is looking for performance 'deltas' rather than absolute levels. A heartening lesson from uprating activity, such as that described in this presentation for the Lynx conformal gears, is the way in which the hardware accepts higher duty conditions in spite of any pessimism engendered by calculated stress levels. This must be due at least in part to the cube root relationship between contact stress and load for elliptical contacts, a relationship that probably remains true despite any modification of absolute stress levels.


DISTRIBUTION OF PEAK TOOTH ROOT AXIAL STRESS FROM PHOTOELASTIC RESULTS
LOAD
'A'
B
396 MPa (57 400 lb/in²)
PLOT FOR B
TENSILE STRESS
DISTANCE ALONG DATUM TOOTH FROM FIRST SLICE (mm)
10 20 30 40 50 60 70
COMPRESSIVE STRESS
PLOT FOR 'A'
-583 MPa (84 500 lb/in²)
MPa
lbf/in² × 10³
FIG 13

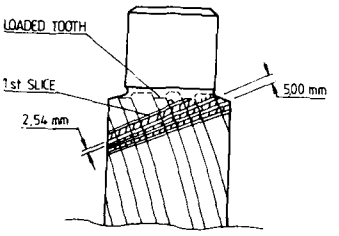


FIG 11a SLICING PLAN

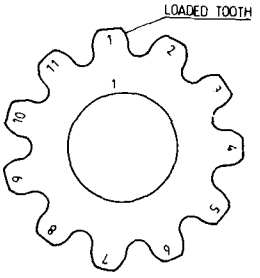


FIG 11b LABELLING SCHEME



FIG. 12 Isochromatic fringe patterns

1. Configuration Choice

The choice of the best configuration depends upon the priority and the weight we assign to the appreciation functions.

We take into account weight, direct costs and reliability. Using Value Analysis techniques and assigning suitable weights to the different functions it is possible to determine a general appreciation function for every configuration.

The analysis has been carried out considering that the weights assigned to the actions:

- Increase reliability
- Decrease manufacture cost
- Reduce weight

are in the ratio of 80 : 50 : 45 respectively.

The results of above analysis are shown in figure 13.

The configurations that achieve the best results are C and A with rather high reduction ratio in the last stage.

The main advantage of the A solution is its typical installation flexibility due to a configuration using bevel gears only.

The remarkable characteristic of the C configuration is the presence of an internal spur gear. A ring gear shows some advantages referred to lightness, reduced dimensions and quietness, but there are some problems of vibrations and displacements under load.

We are investigating the ring gear behaviour with theoretical and experimental methods.
Figure 14 shows a ring gear during a vibration test carried out by holographic technique.
Figure 15 shows the displacements of a ring gear under the loads due to the meshing with two pinions.
The shape has been calculated using finite elements method.

CONCLUSIONS

The evaluations of the four gearbox configurations has been carried out by assigning the right importance coefficient to three appreciation functions: reliability, cost and weight.

These coefficients take into account the different importance connected to the functions we have considered. Through the years the helicopter evolution has caused a great modification of the importance of the gearbox requirements. In the fifties the weight was the main factor. In the sixties we talked about reliability and in the seventies also the noise has assumed a great importance.

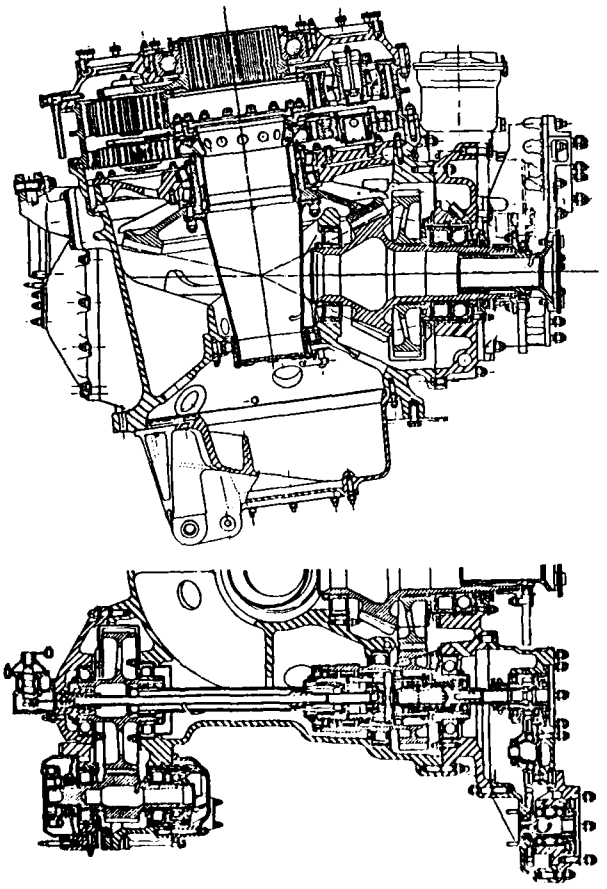
We can foresee that cost, reliability, safety and noise will still be the determinative factors for the choice of a gearbox in the late eighties.

From the results of our analysis we can draw some conclusions.

- In our range of reduction ratios the two-stage solution is quite preferable to the three-stage solution.
- The deletion of the epicyclic train results in remarkable advantages in so far as weight, cost and reliability are concerned.
- The ring gear solution is quite preferable to the solution using external spur gears.

A few of these conclusions are a matter of opinion as they depend upon the importance given to the appreciation functions. During the design activity, the imposed function requirements or some problems connected with accessory drive, tail rotor drive ect. could alter the above mentioned conclusions.

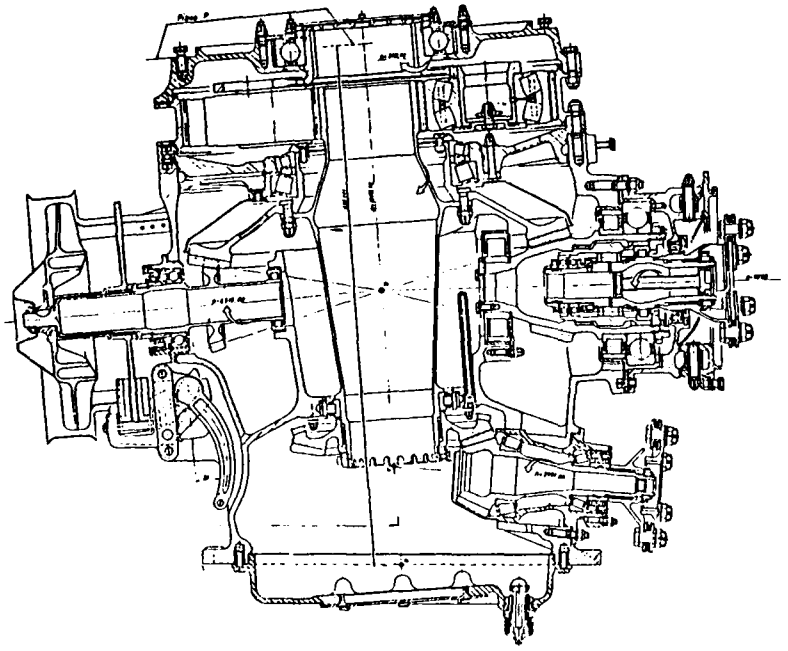
Main chain characteristics	Input speed	22841 RPM
	Output speed	265 RPM
	Number of stages	5
	Number of gears	30
	Number of bearings	38



SA 330 MAIN GEARBOX

FIGURE 2

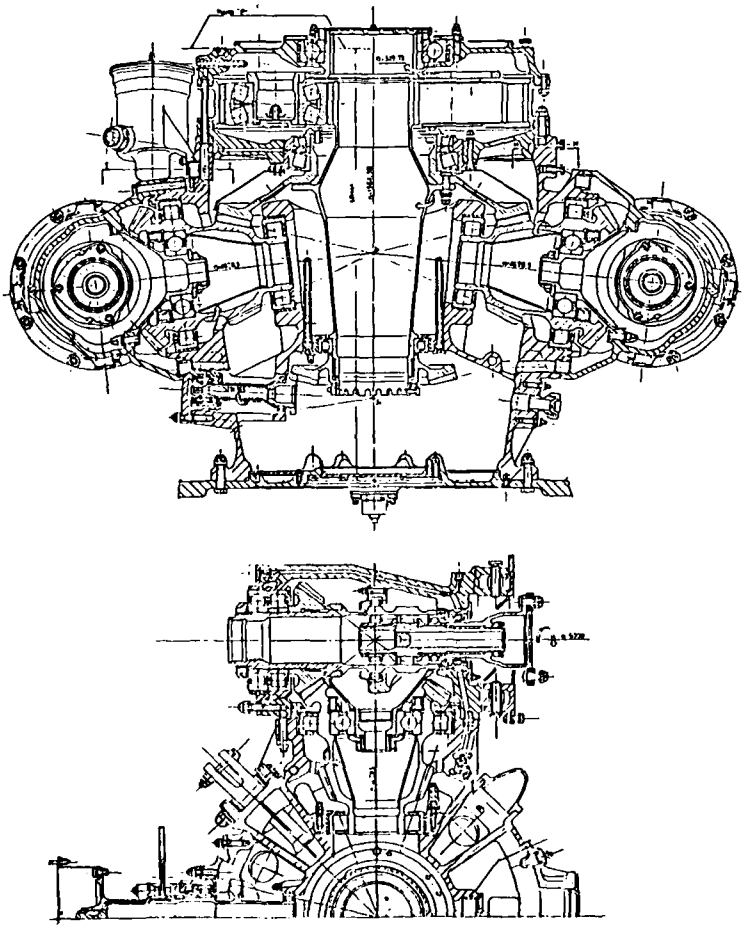
Main chain characteristics	Input speed	5830	RPM
	Output speed	349	RPM
	Number of stages	2	
	Number of gears	9	
	Number of bearings	12	



SA 360 MAIN GEARBOX

FIGURE 3

Main chain characteristics	Input speed	6000	RPM
	Output speed	350	RPM
	Number of stages	3	
	Number of gears	14	
	Number of bearings	20	



SA 365 MAIN GEARBOX

FIGURE 4

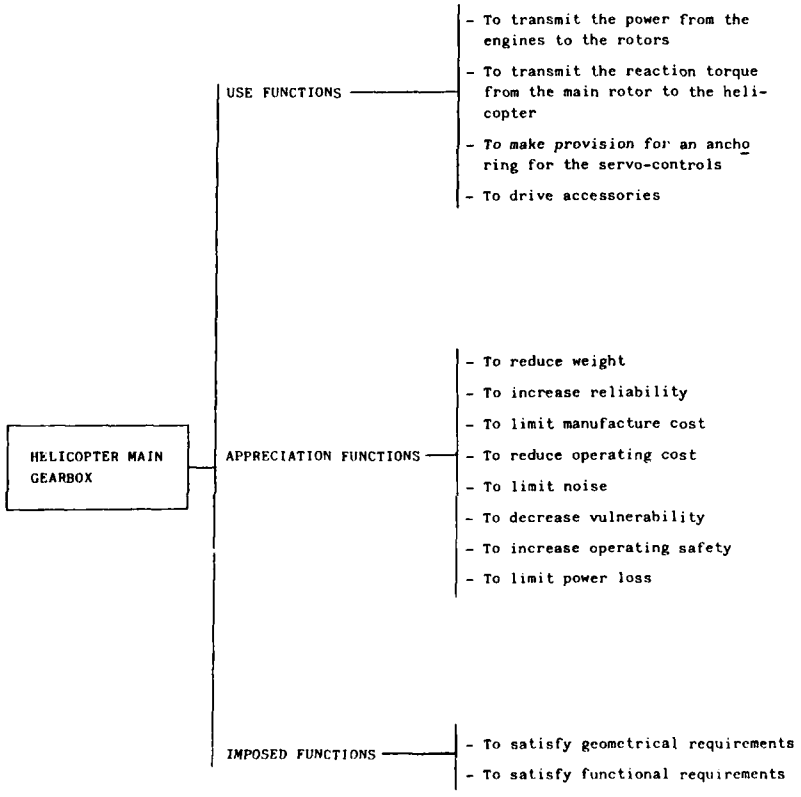

HELICOPTER MAIN GEARBOX
USE FUNCTIONS
- To transmit the power from the engines to the rotors
- To transmit the reaction torque from the main rotor to the helicopter
- To make provision for an ancho ring for the servo-controls
- To drive accessories
APPRECIATION FUNCTIONS
- To reduce weight
- To increase reliability
- To limit manufacture cost
- To reduce operating cost
- To limit noise
- To decrease vulnerability
- To increase operating safety
- To limit power loss
IMPOSED FUNCTIONS
- To satisfy geometrical requirements
- To satisfy functional requirements

FIGURE 5

CONFIGURATION "A"

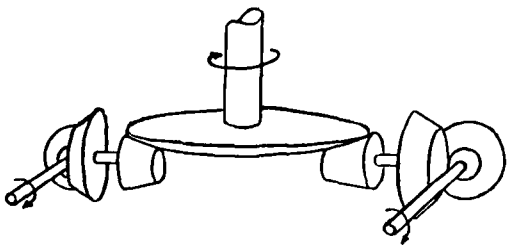


FIGURE 6

CONFIGURATION "B"

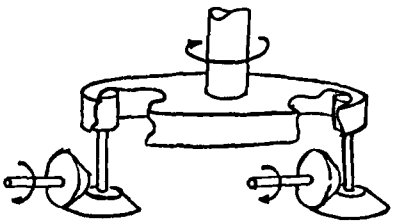


FIGURE 7

CONFIGURATION "C"

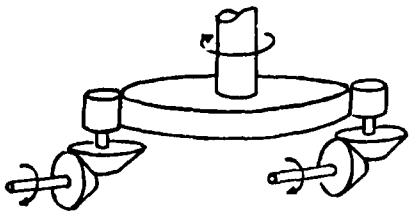


FIGURE 8

CONFIGURATION "D"

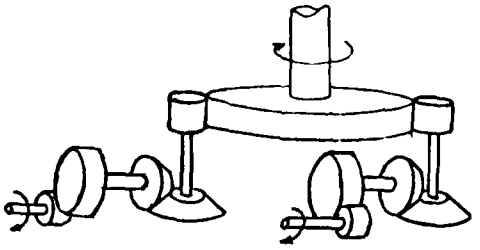


FIGURE 9

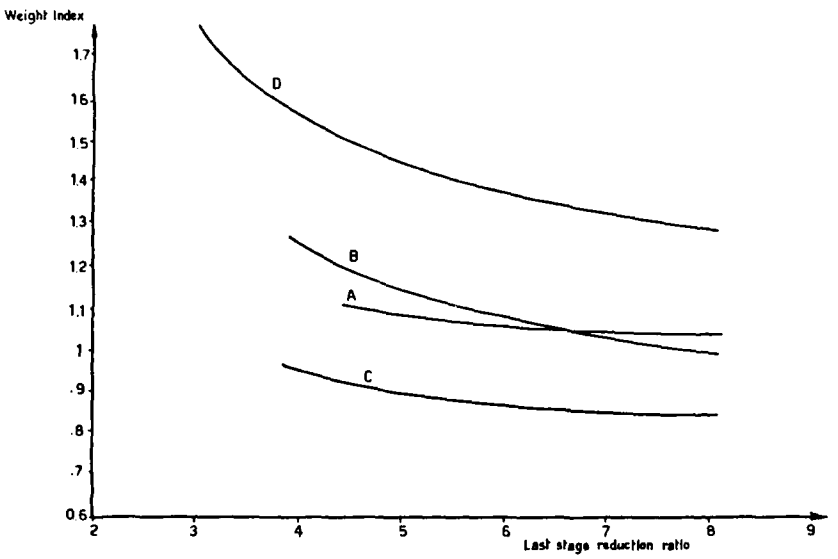


FIGURE 10

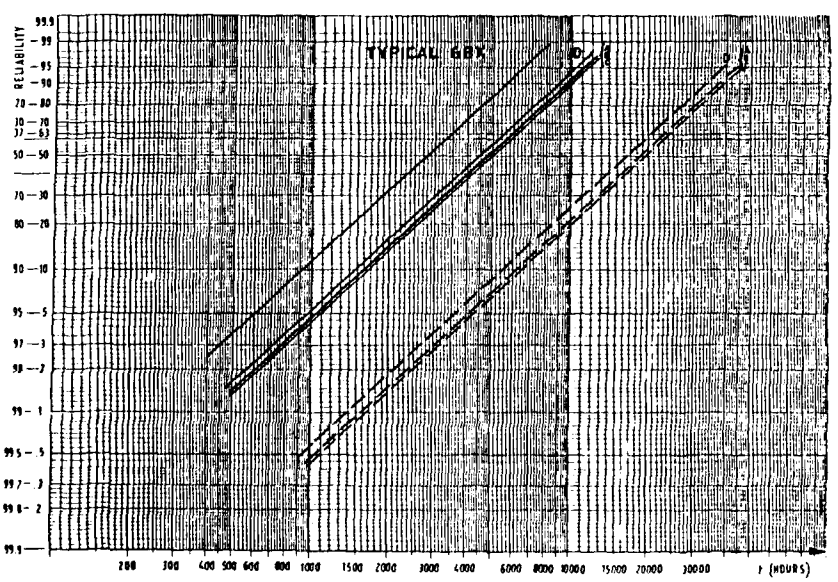


FIGURE 11

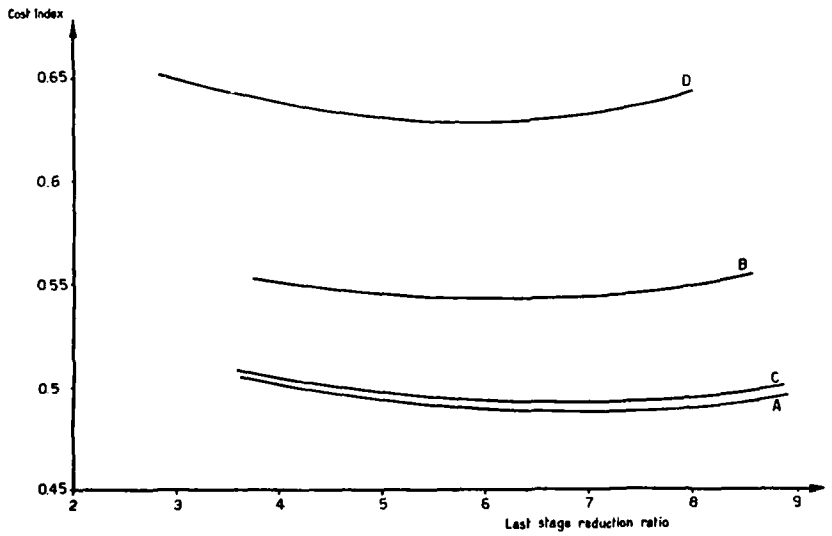


FIGURE 12

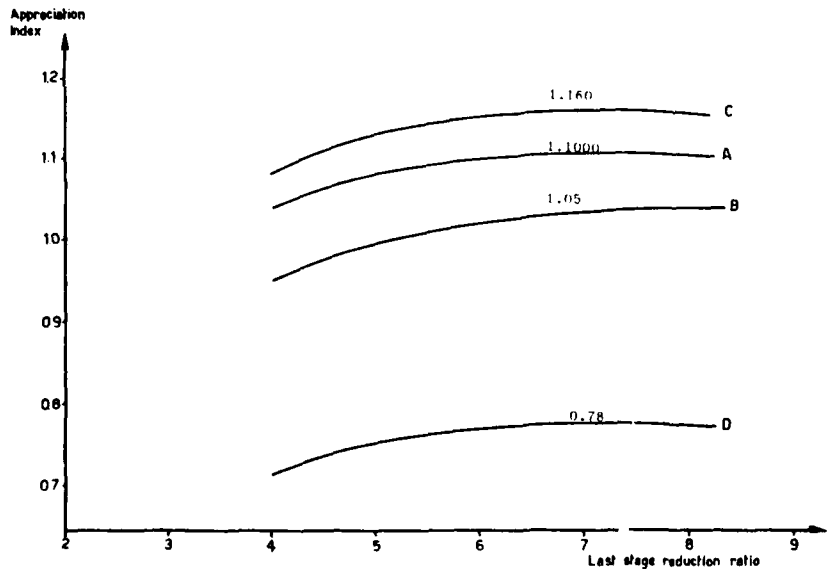


FIGURE 13

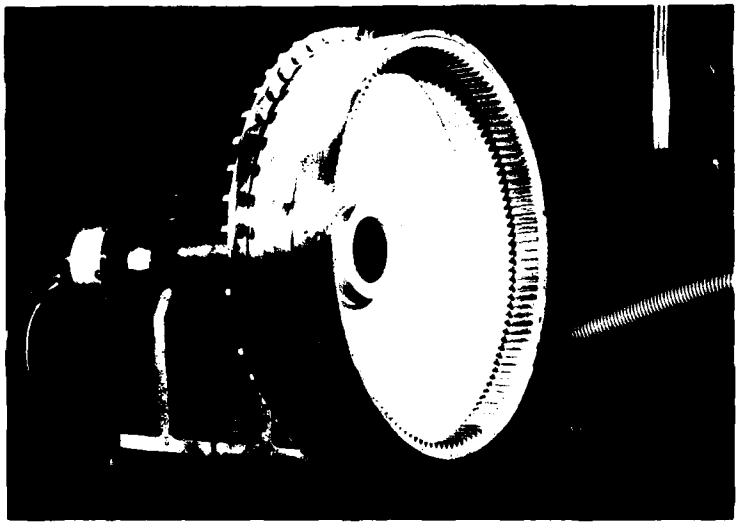
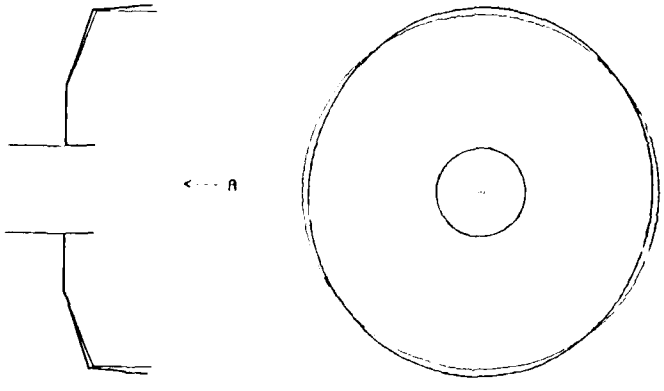


FIGURE 14



VISTA DA A

FIGURE 15

CONDITION MONITORING OF HELICOPTER GEARBOXES USING AUTOMATIC VIBRATION ANALYSIS TECHNIQUES

by

P.Gadd
Naval Aircraft Materials Labs.
RNAY Fleetlands
Gosport, Hants, UK

and

P.J.Mitchell
MOD Navy
DGA (N) St George Court
14 New Oxford Street
London WC1, UK

SUMMARY

Methods using enhanced signal averaging techniques have been developed to give early warning of the onset of a variety of gearbox failures. Prototype analysis equipment has been developed and tested which will permit the condition of components within helicopter dynamic systems (rotors, gearboxes, and powerplants) to be established.

The paper describes work carried out in the Fleet Air Arm to develop and prove the gearbox vibration techniques involved. Arrangements for data collection in flight and during ground runs are described. The signal processing methods, including the automatic techniques for secondary analysis which enable defined features to be extracted from the basic signatures, are discussed. Examples are given of the extent to which damage or malfunction of various internal components can be discerned by the techniques employed. The question of application to the widely dispersed fleet of naval aircraft is considered, and the prospects for achieving full on-condition maintenance of in-service gearboxes is assessed.

INTRODUCTION

1. The condition monitoring engineer must have in his armoury, a wide variety of techniques available for the monitoring of rotating assemblies. This paper addresses the background for Royal Navy operation of its helicopters and the role of vibration health monitoring for its helicopter gearboxes. The data analysis techniques which would complement existing monitoring methods are detailed. The basic premise is that the functioning of a rotating component can provide a vibration signature that is modified as the function or condition of the component changes. It is the task of the chosen signal processing methods to extract this pattern signature. These may then be further analysed by a selection of secondary analysis procedures to produce a series of numerical values which are designed to act as automatic fault descriptors. Finally the likely service application of vibration health monitoring for helicopter gearboxes is reviewed.

BACKGROUND

2. The Royal Navy's helicopter fleet consists mostly of Westland Lynx and Sea King (in ASW, AEW and Commando versions) together with a reducing number of the older Wessex and Wasp aircraft. At any one time more than half our active aircraft will usually be shore-based at naval air stations where extensive engineering support facilities are available. The aircraft at sea can be split into two groups: those on large ships such as the Invincible class where engineering support is also comprehensive, even if the facilities are rather cramped; and small ships which carry a single helicopter and are far less well equipped. The military value of aircraft at sea is so great that it is difficult nowadays to imagine any vessel of frigate size or larger not having a flight deck.

3. Just as successful aircraft have to achieve a satisfactory compromise between conflicting requirements, so warship designers have to achieve a balanced solution in their designs. Size and cost go up together and larger ships must, other things being equal, mean fewer of them. The design of the new T23 frigate has been under strict cost control from the outset with aviation facilities competing with accommodation, magazine, storage, weapon and propulsion systems for a limited amount of space. In single aircraft ships the space needed for a limited amount of space. In single aircraft ships the space needed for aviation workshops is usually not worthwhile because of the limited throughput of work that one aircraft generates. Generally it is better to carry spares and to replenish these when the ship is taking on other stores - a fairly frequent occurrence. This not only saves space even though additional line replaceable units (LRUs) may have to be held on the ships, it also economises on test and repair equipment and the highly trained manpower that would be needed to staff the workshops.

4. When we compare current aircraft with those such as the EH101 which will replace them in a few years time, a number of general trends can be recognised. Firstly in response to the increasing level of the threat posed by Warsaw Pact forces, future aircraft are going to be considerably more complex in terms of sensors and weapon systems. In order to be able to respond when needed they are also getting more complex as vehicles, with extensive de-icing systems, automatic deck handling and spreading arrangements, auxiliary power units, increased redundancy and sophisticated computer based systems management. These advanced future aircraft must, for operational reasons achieve higher levels of availability than their counterparts of today. They must also, for reasons mentioned earlier, be less man-power intensive and more frugal in their demands for storage space and workshop facilities in the small modern warship. Finally these much more capable aircraft are very expensive to develop and produce. In order to afford the numbers that are needed for operational reasons, there is a growing emphasis on reducing the cost of ownership to balance, at least in part, ever increasing acquisition costs. Table 1 lists some of our specific requirements for the EH101.

Table 1 ARM Requirements for EH101

Feature	Requirement
Overall availability	87%
Overall Failure rate	1 per 20 flying hours
Tx TBO	1000 flying hrs within 1 year
	3000 flying hrs within 5 years
Tx MTBR	800 flying hrs within 1 year
	2000 flying hrs within 5 years
Scheduled maintenance	2.5 man hrs/flying hr
Unscheduled maintenance	1.0 man hrs/flying hr
Component change time	2 hrs maximum
Avionic component change time	20 minutes

Meeting these requirements implies two separate things: high component reliability and rapid repair. On the avionic side this has led to the inclusion of sophisticated automatic built-in test equipment which will monitor system performance in flight and identify the causes of malfunctions so that LRU replacement can usually take place immediately the aircraft lands, without the need for further diagnosis. On the mechanical side, usage monitoring offers the prospect of extending the in-service lives of major components, and health monitoring may give sufficient advance warning of trouble so that a major component change can be planned in when convenient, either ashore or in a large ship. Vibration health monitoring offers us a new technique to add to the well established practices of magnetic plug examination, quantitive debris monitoring and spectrometric oil analysis. In conjunction with other techniques VHM offers the prospect of moving away from fixed, and necessarily very conservative, lives to a situation where individual gearboxes are removed at the appropriate time based on a knowledge of the mechanical condition of the particular gearbox. Avoiding unnecessary premature removals will increase the MTBR. This will produce a small direct improvement in overall aircraft availability, a reduction in overhaul costs due to a reduction in the annual number of overhauls needed, and a reduction in the number of spare units the customer needs to buy. Reducing the number of units in the repair loop can represent large financial savings. Another important benefit from introducing VHM would be, in the early life of a new aircraft, a much more rapid progression down the life extension road. The initial overhaul life of a new gearbox, based on endurance testing on ground rigs and early flying, is normally quite modest and commonly represents about 12 months service use - say around 300 flying hours. Extensions are based on a detailed examination of 3 lead gearboxes and increments of 100-200 flying hours are typical. With our modest flying rate and relatively small number of active aircraft, extensions can only come relatively slowly. VHM offers the prospect of being able to reduce the inspection requirement to only one lead gearbox and to move forward in somewhat larger steps to the point where it is possible to take the final step of removing the TBO and going "on condition" for removal.

TECHNIQUES

5. Whilst the major discussion is to be on gears and the methods of vibration analysis, equivalent analysis packages are being assessed for rolling element bearings and helicopter rotors. Briefly the proven faults sensitivity of the bearing package is at present limited to spalling of the tracks although in certain gas turbine applications the detection of oil starvation of the bearing has been deduced. Within the helicopter vibration monitoring work there has been an ambitious development plan to improve the efficiency of the fault diagnosis of the rotor system where much maintenance effort can be expended. Whilst

vibration measurements are taken, the work has been dependent on a twin 'beam' passive light tracker attached to the nose of the helicopter enabling timing of the blade tips passing above. This is translated into track and lag measurements and recent assessment has shown a stability of sensor readout approaching the as-specified performance even on a rev by rev basis. Evidence is accumulating from model work, theory and practice that by listing the track and vibration figures at various operating conditions, the faults are differently exercised and are thus identifiable.

6. Vibration spectra from complex gearboxes (Fig 1) exhibit many discrete frequency peaks which correspond to gear meshing, harmonic modulation and other effects. It is the variance

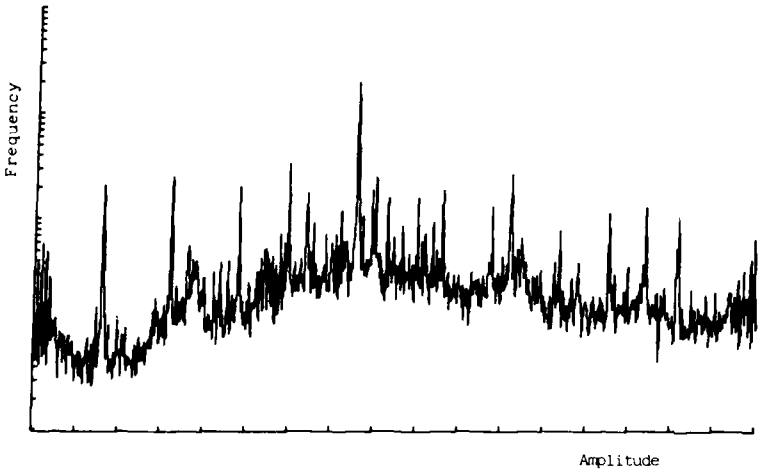


Fig 1: Typical Gearbox Vibration Spectrum

of the peak heights which appears to be relatively large when monitoring a gearbox over a period of time. Moreover a spectrum cannot yield diagnostic information on individual tooth problems. For these reasons, the Naval Aircraft Materials Laboratory was originally attracted to the method of signal averaging of vibration data in order to describe the dynamics of a gear.

7. For this analysis a synchronised repeating pulse is derived from a tachometer or rotating shaft and modified such that it gives a once per rev pulse for the gear under surveillance. That portion of the transducer output waveform pertaining to the gear is assumed identical from pulse marker to pulse marker and hence with numerous summations the average response will represent the mesh behaviour of the particular gear. The almost pictorial representation of the gear mesh allows an intuitive diagnosis to be made. Their origins may be considered as from a pinion rolling along the rack Fig 2a, which then allows the waveform to be directly compared to the teeth of the rack and shows how this signature is modified by the presence of a number of faults.

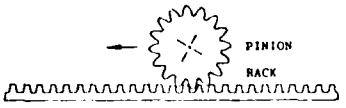


Fig 2(a) Pinion and Rack with Faults

Five separate situations are considered:

a. The 'perfect' gear (Fig 2b): this produces a regular sinusoidal waveform. No modulation of any kind is evident because by definition the teeth are identical and the gears rotate perfectly on centre.



Fig 2(b) The Nominally 'Perfect' Gear

c. The 'misaligned' gear (Fig 2c): when the direction of misalignment is such as to eliminate any backlash, the effect of it is to produce powerful once-per-rev modulation as shown. The fact that this covers one complete revolution of the pinion (for a true pair once-per-rev of the wheel would also be evident) indicates that the cause is related to motion of the gear as a whole rather than to individual teeth.

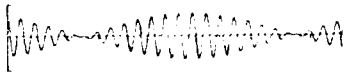


Fig 2(c) Gear Pair with Misalignment

d. The 'fractured' tooth (Fig 2d): as the tooth which has been fractured enters the mesh, it fails to transmit its due share of the load and the gear pair accelerates to engage the next pair. If in fact the whole tooth has been lost, a definite gap will need to be crossed and then upon engagement of the next pair, a significant impact will occur. In both instances the impulse that accompanies the acceleration or deceleration of the gear pair will excite the structural elements of the gear box and cause a pulse of vibration to occur. Depending on the contact ratio of the gearing, the Q-factors of the resonances, the frequency of the resonances and the power of the meshing tones, this vibration may either by weakly or strongly evident in the monitored signal. Furthermore, if the damaged gear mates with another gear other such pulses will be produced during the gear revolution. The multiple pulses will be strongly correlated ie occupy a fixed relationship to each other by the geometry of the gear layout.



Fig 2(d) Fractured Tooth on Pinion

e. The 'spalled' tooth produces a pulse that has the same basic origin as the fractured tooth signature, but is very much weaker.

f. The 'heavily worn' gear (Fig 2e): heavy wear on all, or a large number of teeth, produces a signature which is very much more random.

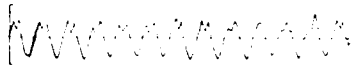


Fig 2e Heavy Wear and Light Load

3. From an understanding of how gears change their signature in response to faults, a general method of analysing the pattern content of signal averages was developed by Stewart Hughes Ltd Southampton, UK. This is referred to as the Figure of Merit (FOM) analysis package which currently produces values for a series of normalised parameters, using a number of different methods of analysis. The signal average is generally produced to include frequencies up to ½ times the gear mesh. Various parameters are extracted from the signal average prior to the FOM package including the level of the once-per-rev vibration (g rms) for detection and assessment of imbalance on shaft systems. The FOM methods of secondary analysis imposed upon the signal average are described below.

a. Figure of Merit FOM 0. This is the simplest parameter of them all and was designed to act as the general detector of significant faults. Referring to Fig 2b it can be seen that a dominant feature of the signal average or signature is its sinusoidal component at meshing frequency. Although this component is always present experience in general shows that as the condition of the gear changes so too does the meshing frequency component. Hence, by inference the perfect gear will generate a pure sinewave; in order to assess this the signal average is modified to look at 1.1 x mesh frequency or 1500 Hz ie the higher harmonics present may be eliminated by the low pass filtering. FM0 has been defined as:

$$FM0 = \frac{\text{peak-to-peak value of the signal average}}{\text{sum of rms levels of meshing frequencies}}$$

which for the 'perfect' gear will equal 2.0. Departures from this such as tooth breakage will produce local regions of resonance-excited transient activity and so cause the peak-to-peak to rise and hence also FM0 to rise. Alternatively, heavy wear of the gear will result primarily in a fall of meshing frequency components, again causing FM0 to rise.

b. Figure of Merit FOM 1. The purpose of this FOM set is to recognise modulations of the average ie its envelope shape, that signify misalignment, eccentricity and wobbling of the gear.

c. Figure of Merit FOM 2. This FOM is a measure of the number of zero crossings in the signal average compared to that expected of the gear mesh. The signal average for a gear can depict approximately one half, one third or one quarter the number of oscillations expected. This parametric excitation occurs when the meshing frequency equals an integer (normally 2) times the natural frequency eg shaft torsional resonance; then, and particularly if the loading is light, tooth separation and greatly accelerated tooth wear can result.

d. Figure of Merit FOM 4. FOM 4 was developed in order to create a level of greater sensitivity within the FOM analysis method for impulse quantification, viz tooth breakage. FOM 4 is derived by taking signal average and subtracting from it the expected and acceptable sinewave components. The residue should then describe the impulsive perturbations within the signal average, thus raising the detection efficiency for individual tooth faults.

(1) FOM 4A is a kurtosis judge of the spikiness of the residue, indicating localised tooth faults including spalling.

(2) FOM 4B. The standard deviation of the residue describes how well the configuration has generated the reconstruction. FOM 4B has been found useful in detecting distributed damage and as support to FOM 4A; for as the damage becomes greater eg occurs on an increasing number of teeth, so the vibration becomes more random, that is the non-sinusoidal portion of the signal average increases so the standard deviation of the residue, (FOM 4B) rises.

e. Figure of Merit FOM 5. This latest and most penetrating parameter enables a measure to be made automatically of the impulsive content of the signal average. After ranking the principal components of the signal average, a decomposition of the signal average into its impulsive and non impulsive components is achieved by a statistical judgement of the series of low pass filtered outputs of the heterodyned average. It has been found that FOM 5 is a necessary tool for examining singleton tooth defects in epicyclic gear trains.

TRIALS

9. The Service trials sought to demonstrate the feasibility of all aspects of condition monitoring/fault diagnosis for all assemblies of the helicopter. Whilst the algorithms of the gear analysis package have been highlighted, the feasibility of the fitting of transducers, aircraft looming and signal recording had also to be ascertained. This latter on-aircraft exercise established that the complexity of the loom and the number of transducers required the loom to be a permanent fit in the helicopter. Three Lynx aircraft underwent this first trials installation with accelerometers fitted as follows: engine-4, MGRB-6, IGB-1, TGB-1 plus a triaxial accelerometer in the cabin. Existing tachometer outputs were tapped without any undue difficulty. For the duration of the field trial the primary accelerometer chosen was the Bruel and Kjaer (B&K) type 4344. This particular accelerometer was chosen because of its small size (7 mm diameter x 10 mm high), minimal weight (2 grams), resonant frequency (70 KHz) and maximum operating temperature (250°C). Signal condition and recording equipment was fitted immediately prior to actual recording. The Racal Store 7 was found suitable to obtain satisfactory recordings in the helicopter. Its disadvantage for general future use is cost (£9K) weight 48lbs and size (19 x 6 x 19ins).

10. A Sea King transmission and rotor trial was proposed as a follow-up to the aforementioned Lynx work. The changes incorporated were cheaper transducers, more robust connectors, transducer sites unlikely to be disturbed by any anticipated servicing, and the utilisation of an already installed high quality airborne tape recorder. At present the transmission monitoring part of the exercise is underway; the rotor monitoring awaits the availability of suitable track sensors by the manufacturer.

11. The confidence to monitor the epicyclic gearing in the Sea King main rotor gearbox (MRGB) came after a series of tests with defects seeded into the epicyclic gears of the 'test' gearbox of the RAE Farnborough MRGB test rig. This proved invaluable in extending the hitherto fixed axis gearing signal averaging rules to epicyclic gearing. The epicyclic gear signatures tend to lack repeatability of the signal average because of the uncertain spatial relationship between transducer, gears, and faults. It is necessary to look at a number of independent averages of relatively short duration and then assess each FOM parameter from those produced from the averages. That is using the FOM to view a series of 'snapshots' and to assess the multiple sequential signal averages with their varying degree of fault visibility. The optimum transducer sites for gear damage were established as being on the ring gear for sun and planet damage but, for the ring gear itself, some distance away and lying as near to the gearbox centre line as possible.

12. The monitoring packages as envisaged by Stewart Hughes Ltd is necessary for the high level of diagnostic capability required by the target programme required the engineering of prototype equipment, the design of which was to incorporate all the essential hardware, both analogue and digital, found necessary for the realistic analysis of strings of operations after a number of years usage of large mil computer based systems. The Mechanical Systems Diagnostic Analyser (MSA) is shown in Fig 9.

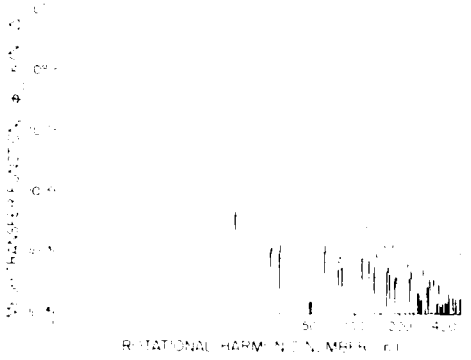


Fig. 10. Tooth spacing error (k=0, ℓ=0) mesh transfer function magnitude for a 50 tooth helical gear with Q_a = 3.19 and Q_t = 1.819.

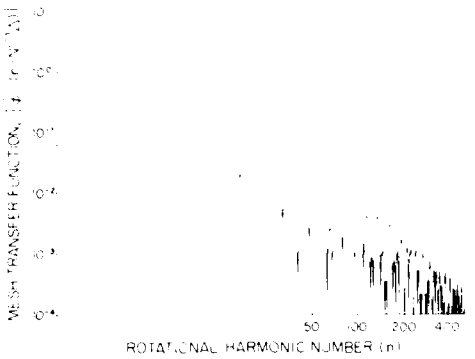


Fig. 11. Involute slope deviation (k=0, ℓ=1) mesh transfer function magnitude for a 50 tooth helical gear with Q_a = 3.19 and Q_t = 1.819.

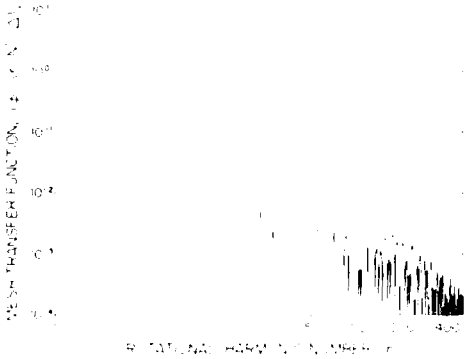


Fig. 12. Lead mismatch deviation (k=1, ℓ=0) mesh transfer function magnitude for a 50 tooth helical gear with Q_a = 3.19 and Q_t = 1.819.

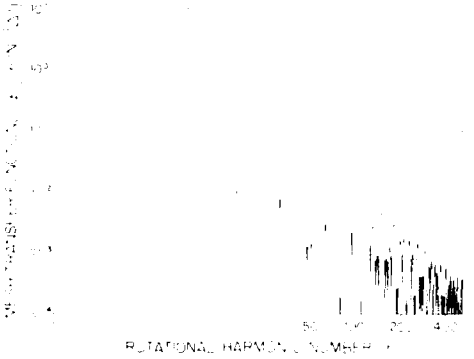


Fig. 13. Involute fullness deviation (k=0, ℓ=2) mesh transfer function magnitude for a 50 tooth helical gear with Q_a = 3.19 and Q_t = 1.819.

(2) the magnitudes of all other mesh transfer functions are small in comparison with unity in the region of the first few rotational harmonics

(3) the mesh transfer function for tooth-spacing errors [k = 0, ℓ = 0 (Fig. 10)] has nulls at the rotational harmonics $n = pN^{(*)}$, p = 0,1,2,... which are the locations of the tooth-meshing harmonics; moreover, these nulls are not infinitely sharp

(4) the other mesh transfer functions (k and ℓ not both zero) generally do not have nulls in the neighborhoods of the tooth-meshing harmonics

(5) when plotted on log-log coordinates, the envelopes of the magnitudes of all mesh transfer functions have an asymptotic slope of -12 dB per octave in the large harmonic number region in the case of helical gears and -6 dB per octave in the large harmonic number region in the case of spur gears.

Figure 14 shows the mesh transfer function for tooth-spacing errors (k = 0, ℓ = 0) for a spur gear with $N^{(1)}$ = 50 teeth and a transverse contact ratio of Q_t = 1.819 which was computed using Eq. (109) of reference 2. Comparison of Figs. 10 and 14 illustrates the different asymptotic slopes of -12 dB and -6 dB per octave, respectively, of the mesh transfer functions of helical gears and spur gears.

To illustrate the attenuating effect of the mesh transfer function in the case of a particular term in Eq. (23), the tooth-spacing error spectrum (k = 0, ℓ = 0) shown in Fig. 9 is plotted on a logarithmic frequency axis in Fig. 15. In Fig. 9, the lines representing the discrete harmonics are shown; however, in Fig. 15 only the envelope

$$a_{k\ell}^{(\bullet)} \triangleq \frac{1}{N^{(\bullet)}} \sum_{j=0}^{N^{(\bullet)}-1} c_{j,k\ell}^{(\bullet)} \tag{21a}$$

$$= B_{k\ell}^{(\bullet)}\{pN^{(\bullet)}\}' \ , \ p = 0,\pm1,\pm1,... \tag{21b}$$

where the second equality follows by setting $n = pN^{(\bullet)}$ in Eq. (18). All other rotational harmonics (i.e., except those occurring at the tooth-meshing harmonics $n = pN^{(\bullet)}$, $p = 0,\pm1, \pm2,...$) arise from the contributions

$$b_{j,k\ell}^{(\bullet)} \triangleq c_{j,k\ell}^{(\bullet)} - a_{k\ell}^{(\bullet)} \tag{22}$$

that come about from deviations of the individual tooth surfaces from the mean tooth surface whose expansion coefficients are $a_{k\ell}^{(\bullet)}$ - see Eq. 21a. All of the harmonics shown in Fig. 9 arise from such deviations $b_{j,00}^{(\bullet)}$.

7. THE ATTENUATING EFFECTS OF MULTIPLE TOOTH CONTACT

The tooth "error" spectra $B_{k\ell}^{(\bullet)}(n)'$ or their one-sided counterparts, such as that displayed in Fig. 9, contain none of the effects of the smoothing action of the multiple tooth contact illustrated in Fig. 2. In references 1-3, it is shown that these smoothing effects can be rigorously taken into account by multiplying each tooth error spectrum $B_{k\ell}^{(\bullet)}(n)'$ by an appropriate mesh transfer function $\hat{\phi}_{k\ell}(n/N^{(\bullet)}\Delta)$ that is a function of the design parameters of the mesh. The Fourier series coefficients of the contribution $\zeta^{(\bullet)}(x)$ of the deviations of the tooth surfaces of gear $(\bullet)$ from perfect involute surfaces are then obtained [1-3] by summation of the mesh-attenuated error spectra over all error types $k\ell$ - i.e.,

$$a_n^{(\bullet)} = \sum_{k=0}^{\infty} \sum_{\ell=0}^{\infty} B_{k\ell}^{(\bullet)}(n)'\hat{\phi}_{k\ell}(n/N^{(\bullet)}\Delta), \quad n = 0,\pm1,\pm2,... \tag{23}$$

where the $B_{k\ell}^{(\bullet)}(n)'$ are the error spectra defined by Eq. (18) and the $a_n^{(\bullet)}$ are the Fourier series coefficients of the contribution $\zeta^{(\bullet)}(x)$ to the static transmission error, $(\bullet) = (1)$ or (2) as in Eq. (4), arising from the deviations of the teeth of gear $(\bullet)$ from perfect involute surfaces. These Fourier series coefficients are defined [1-3] in terms of $\zeta^{(\bullet)}(x)$ by

$$a_n^{(\bullet)} \triangleq \frac{1}{N^{(\bullet)}} \int_{-N^{(\bullet)}\Delta/2}^{N^{(\bullet)}\Delta/2} \zeta^{(\bullet)}(x)e^{-i2\pi nx/(N^{(\bullet)}\Delta)}dx \ . \tag{24}$$

When the tooth pair stiffness per unit length of line of contact is assumed to be a constant, the mesh transfer functions $\hat{\phi}_{k\ell}(n/N^{(\bullet)}\Delta)$ can be evaluated for helical and spur gears, respectively, using Eqs. (95) and (110) of reference 2. For given values of k and ℓ, and a given number of teeth $N^{(\bullet)}$, the mesh transfer function $\hat{\phi}_{k\ell}(n/N^{(\bullet)}\Delta)$ depends on only two gear design parameters, the axial and transverse contact ratios Q_a and Q_t.

As we have mentioned earlier in the paper, the spectra $B_{k\ell}^{(\bullet)}(n)'$ in Eq. (23) contain the required description of the deviations of the individual gear teeth from perfect involute surfaces, and the mesh transfer functions $\hat{\phi}_{k\ell}(n/N^{(\bullet)}\Delta)$ in Eq. (23) describe the effects of the smoothing action of multiple tooth contact on the "error" spectra $B_{k\ell}^{(\bullet)}(n)'$. Since the behavior of the mesh transfer functions is controlled by the gear design parameters Q_a, Q_t, and $N^{(\bullet)}$, the attenuating effects on the error spectra of different gear mesh designs can be studied using the mesh transfer functions independently of the actual magnitudes of the deviations of the tooth surfaces from perfect involute surfaces.

Figures 10 through 13 display the absolute values of the mesh transfer functions computed by Eq. (95) of reference 2 for the different elementary error types described in Table 1 for the case of a helical gear with $N^{(1)} = 50$ teeth and axial and transverse contact ratios of $Q_a = 3.19$ and $Q_t = 1.819$, respectively. Certain features of these mesh transfer functions, which are common to all mesh transfer functions, are worthy of emphasis [2,3]:

(1) The mesh transfer function for tooth-spacing errors [$k = 0$, $\ell = 0$ (Fig. 10)] is approximately unity in the region of the first few rotational harmonics

The lower part of Fig. 8 displays a set of such accumulated tooth-spacing error measurements. Figure 8 is a computer plot of an original set of accumulated tooth-spacing error measurements modified by (a) removal of the overall slope which represents an instrumentation bias error in the measurements, and (b) removal of the mean value which represents an irrelevant rigid body rotation of the gear being measured. The abscissa in Fig. 8 is tooth number and the ordinate of the lower curve is the accumulated tooth-spacing error corrected as in (a) and (b) above, and measured in micro meters. This lower curve is $c^{(1)}_{j,00}$. The magnitude of the maximum accumulated tooth-spacing error of approximately 8 μm for this particular gear occurs on tooth number 32. The upper curve in Fig. 8 displays the differences in accumulated error between adjacent teeth. Gear (1), whose errors are displayed in Fig. 8, has $N^{(1)} = 50$ teeth.

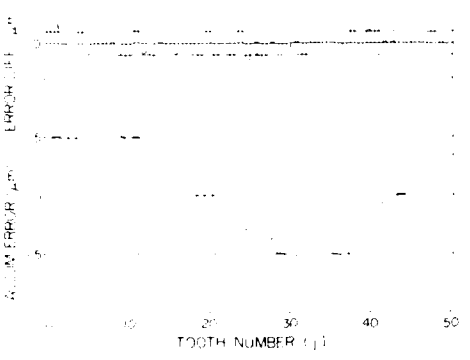


Fig. 8. Accumulated tooth spacing error coefficients $c^{(1)}_{j,00}$ (k=0, ℓ=0) for a 50 tooth gear.

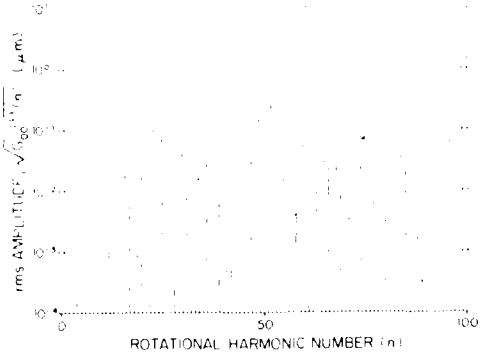


Fig. 9. Tooth spacing error spectrum $\sqrt{2}|B^{(1)}_{00}(n)|$ (k=0, ℓ=0) for a 50 tooth gear.

Figure 9 is a plot of the square-root of the one-sided discrete tooth-spacing error spectrum

$$G'^{(1)}_{00}(n) \triangleq 2\left|B^{(1)}_{00}(n)'\right|^2 , \tag{19}$$

where $B^{(1)}_{00}(n)'$ is defined by Eq. (18) for k = 0 and ℓ = 0 from the accumulated tooth-spacing error sequence $c^{(1)}_{j,00}$, j = 0,1,..., 49 shown in Fig. 8. The abscissa in Fig. 9 is rotational harmonic number n and the ordinate is the rms harmonic amplitude measured in micro meters. Notice that the spectrum shown in Fig. 9 is periodic in harmonic number with the period being equal to the number of teeth $N^{(1)} = 50$ on the gear. Also notice the symmetry about the harmonic number position $n = N^{(1)}/2$. Thus, the strong rotational harmonics in the neighborhoods of $n = N^{(1)}$, $n = 2N^{(1)}$, $n = 3N^{(1)}$, etc. contribute to the so-called sidebands in the neighborhoods of the tooth-meshing harmonics, which are located at rotational harmonic numbers that are integral multiples of the number of teeth on the gear. There is no contribution to the spectrum shown in Fig. 9 at the positions of these tooth meshing harmonics - i.e., at $n = N^{(1)}$ $n = 2N^{(1)}$, etc. - because the mean value of the accumulated error chart shown in Fig. 8 (which represents a rigid body rotation) has been removed.

Plots of the square-roots of the discrete one-sided spectra,

$$G^{(*)}_{k\ell}(n) \triangleq 2\left|B^{(*)}_{k\ell}(n)'\right|^2 , \tag{20}$$

where k and ℓ are not both zero, have the same general properties as shown in Fig. 9 except that, for k and ℓ not both zero, contributions will be present at the locations of the tooth-meshing harmonics $n = N^{(*)}$, $n = 2N^{(*)}$, $n = 3N^{(*)}$, etc. These contributions arise from the expansion coefficients $a^{(*)}_{k\ell}$ of the mean or average tooth surface on the gear - i.e., [2,3]

Equation (12) can be interpreted as an expansion of the tooth-surface deviation $\eta_{C_j}^{(\cdot)}(y,z)$ in a canonical set [3] of elementary errors

$$\psi_{yk}(y)\psi_{z\ell}(z) = [(2k+1)(2\ell+1)]^{1/2} P_k(2y/F)P_\ell(2z/D) \quad . \tag{17}$$

Each elementary error is designated by a pair of nonnegative integer indices k,ℓ where index k is associated with the lead (axial) direction and index ℓ is associated with the profile (radial) direction. From the definition (15) of the Legendre polynomials, we see that the low-order elementary errors possess the simple interpretations shown in Table 1 [3]. Figure 7 illustrates the terms k = 0, ℓ = 0,1,2,3 and ℓ = 0, k = 0,1,2. Thus, the normalized Legendre polynomials provide us with a convenient mathematical tool for representing tooth errors in a form closely allied with current gearing industry practice.

Table 1. Elementary Error Classifications [3].

k = 0, ℓ = 0	tooth-spacing deviations
k = 0, ℓ = 1	pure involute slope deviations
k = 1, ℓ = 0	pure lead mismatch deviations
k = 0, ℓ = 2	pure involute fullness deviations
k = 1, ℓ = 1	combined lead mismatch-involute slope deviations
k = 2, ℓ = 0	pure lead crowning deviations.

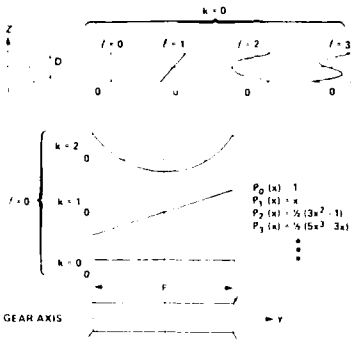


Fig. 7. Interpretation of elementary errors derived from the Legendre Polynomials $P_n(x)$, n=0,1,2,... .

For each fixed error component kℓ, we now consider the behavior of the expansion coefficients $c_{j,k\ell}^{(\cdot)}$ as a function of tooth number j, j = 0,1,...,$N^{(\cdot)}-1$ where $N^{(\cdot)}$ is the number of teeth on the gear under consideration. To obtain a description of the behavior of error type kℓ in the frequency domain, an analysis too involved [1-3] to be included here shows that the discrete Fourier transform of the sequence of coefficients $c_{j,k\ell}^{(\cdot)}$, j = 0,1,..., $N^{(\cdot)}-1$ is required, where this transform is taken with respect to tooth number j:

$$B_{k\ell}^{(\cdot)}(n)' \triangleq \frac{1}{N^{(\cdot)}} \sum_{j=0}^{N^{(\cdot)}-1} c_{j,k\ell}^{(\cdot)} e^{-i2\pi nj/N^{(\cdot)}} \quad , \; n=0,\pm1,\pm2,\ldots \; . \tag{18}$$

Harmonic number n counts the rotational harmonics of gear (·).

For each error type kℓ, the discrete spectrum $B_{k\ell}^{(\cdot)}(n)'$, n = 0,±1,±2,... characterizes for gear (·) the sequence of expansion coefficients $c_{j,k\ell}^{(\cdot)}$, j = 0,1,... $N^{(\cdot)}-1$ in the frequency domain. The set of all such sequences (for all elementary error types kℓ) completely characterizes in the frequency domain the deviations from perfect involute surfaces of all $N^{(\cdot)}$ teeth of gear (·).

6. THE ERROR SPECTRUM FOR TOOTH-SPACING ERRORS

From Eqs. (15) and (17), we can see that for k = 0 and ℓ = 0, we have $\psi_{y0}(y)\psi_{z0}(z) \equiv 1$. Thus, the elementary error given by Eq. (17) for k = 0, ℓ = 0 is readily interpreted as a pure tooth-spacing error - as is illustrated in Fig. 7. Since $\psi_{y0}(y)\psi_{z0}(z) = 1$, the expansion coefficient $c_{j,00}^{(\cdot)}$ in Eq. (12) measures the actual value of the (accumulated) tooth-spacing error of tooth j of gear (·), and for k = 0, ℓ = 0 $B_{00}^{(\cdot)}(n)'$ describes in the frequency domain the tooth-spacing errors of all teeth on gear (·).

For the purpose of illustrating a sequence of expansion coefficients $c_{j,k\ell}^{(\cdot)}$ and the associated error spectrum $B_{k\ell}^{(\cdot)}(n)'$, let us assume now that an ordinary set of accumulated tooth-spacing error measurements made with a point probe measures the sequence of tooth-spacing expansion coefficients $c_{j,00}^{(\cdot)}$, j = 0,1,..., $N^{(\cdot)}-1$. This assumption would be valid if all tooth surfaces on the gear being measured were identical except for tooth-spacing errors.

5. DECOMPOSITION OF TOOTH SURFACE DEVIATIONS INTO ELEMENTARY "ERRORS" AND THEIR SPECTRA

We turn now to prediction of the static transmission error contributions $\zeta^{(1)}(x)$ and $\zeta^{(2)}(x)$ in Eq. (4) arising from the deviations of the individual tooth surfaces of gears (1) and (2) from perfect uniformly spaced involute surfaces. Since, as the gears rotate, every point on the running surface of every tooth on a gear comes into contact with the teeth of the mating gear (see Fig. 3), it follows that prediction of the excitation spectrum arising from a gear requires, in principle, a description of the entire running surface of every tooth on that gear. The analysis of the effects of the deviations of the individual tooth surfaces from perfect uniformly spaced involute surfaces is greatly simplified [1-3] by decomposing these deviations into elementary "errors."

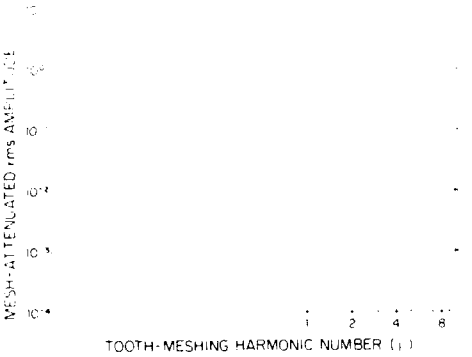


Fig. 5. Normalized contribution to static transmission error spectrum from elastic tooth deformations of a spur gear pair.

Let $\eta_{Cj}^{(\cdot)}(y,z)$ denote the deviation of the running surface of tooth j of gear $(\cdot)$, $(\cdot) = (1)$ or (2) as appropriate, measured as a function of the Cartesian coordinates y,z illustrated in Fig. 6. Such deviations are "measured" in a direction defined by the intersection of the plane of contact and a plane normal to the gear axes. An arbitrary "deviation surface" $\eta_{Cj}^{(\cdot)}(y,z)$ can be expanded [2,3] in a complete set of two-dimensional Legendre polynomials

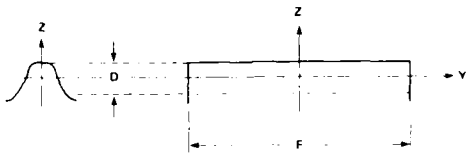


Fig. 6. Coordinate system used for description of tooth surface deviations $\eta_{Cj}^{(\cdot)}(y,z)$.

$$\eta_{Cj}^{(\cdot)}(y,z) = \sum_{k=0}^{\infty} \sum_{\ell=0}^{\infty} c_{j,k\ell}^{(\cdot)} \psi_{yk}(y) \psi_{z\ell}(z) \quad , \tag{12}$$

where the normalized Legendre polynomials $\psi_{yk}(y)$ and $\psi_{z\ell}(z)$ are defined [2,3] as

$$\psi_{yk}(y) \triangleq (2k+1)^{1/2} P_k(2y/F), \quad -(F/2)<y<(F/2) \tag{13}$$

$$\psi_{z\ell}(z) \triangleq (2\ell+1)^{1/2} P_\ell(2z/D), \quad -(D/2)<z<(D/2) \tag{14}$$

where the functions $P_n(x)$ are the usual Legendre polynomials:

$$\begin{aligned} P_0(x) &= 1 \\ P_1(x) &= x \\ P_2(x) &= \tfrac{1}{2}(3x^2-1) \\ P_3(x) &= \tfrac{1}{2}(5x^3-3x) \\ &\vdots \end{aligned} \tag{15}$$

and where the expansion coefficients $c_{j,k\ell}^{(\cdot)}$ in Eq. (12) are determined from the surface deviations $\eta_{Cj}^{(\cdot)}(y,z)$ by [2,3]

$$c_{j,k\ell}^{(\cdot)} = \frac{1}{FD} \int_{-D/2}^{D/2} \int_{-F/2}^{F/2} \eta_{Cj}^{(\cdot)}(y,z) \psi_{yk}(y) \psi_{z\ell}(z) \, dy \, dz \ . \tag{16}$$

the average number of teeth simultaneously in contact in the transverse plane (which is a plane cut normal to the gear axes). The parameters F, L, A, and Δ used to define Q_a and Q_t in Eqs. (8) and (9) are defined in Fig. 2. These parameters determine the geometrical properties of the meshing action.

If either the axial or transverse contact ratio $Q_a = FL/A\Delta$ or $Q_t = L/\Delta$, respectively, is an integer, it follows from Eqs. (6b) and (6d) that we have $a_{wp} = 0$, $p = \pm1, \pm2, \ldots$. This behavior is readily understood with the aid of Fig. 4 which shows for the cases $Q_a = FL/A\Delta = 3$ and $Q_t = L/\Delta = 2$ the zone of contact first introduced in Fig. 2. Careful examination of both sketches in Fig. 4 shows that, in each case, the total length of line of contact in each zone of contact will remain fixed as the gears rotate and the lines of contact move through the zone of contact. Since the total mesh stiffness $K_T(x)$ in Eq. (5) has been assumed to be proportional to the total length of line of contact, which is a constant if either Q_a or Q_t is an integer, we can see from Eq. (5) that $\zeta_w(x)$ must be a constant in these situations when W is constant. The behavior of Eqs. (6b) and (6d) is consistent with this observation.

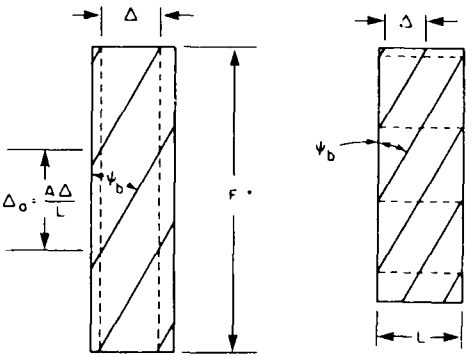


Fig. 4. Integral axial and transverse contact ratios.

In the case of real gears, the stiffness per unit length of line of contact is not exactly constant and the actual zone of contact is not the perfect rectangle shown in Figs. 2 and 4. Thus, integer axial or transverse contact ratios will not entirely eliminate fluctuations in the elastic deformation component $\zeta_w(x)$ of the static transmission error. Nevertheless, this basic idea undoubtedly has merit [8].

Equations (6b) and (6d) illustrate another important result. If we examine the envelopes of the maxima of the magnitudes of the right-hand sides of Eqs. (6b) and (6d) which are the loci of points where $|\sin(p\pi FL/A\Delta)| = 1$ and $|\sin(p\pi L/\Delta)| = 1$, then we have for helical gears

$$|a_{wp}|_{env} = \frac{W_0}{K_T} \frac{1}{p^2\pi^2 Q_a Q_t} , \tag{10a}$$

and for spur gears

$$|a_{wp}|_{env} = \frac{W_0}{K_T} \frac{1}{p\pi Q_t} , \tag{10b}$$

where subscript "env" denotes envelope and the definitions of Q_a and Q_t given by Eqs. (8) and (9) have been used. It follows [2,3] from Eqs. (10a) and (10b) that the envelope of the static transmission error spectrum contribution from the elastic deformation component depends only on a single mesh geometry design parameter, which in the case of helical gears is the product of the axial and transverse contact ratios Q_aQ_t, and in the case of spur gears is the transverse contact ratio, Q_t. This important single parameter has been named [3] the "aggregate contact ratio," ACR:

$$ACR \triangleq Q_aQ_t = \frac{FL}{A\Delta} \times \frac{L}{\Delta} , \text{ for helical gears} \tag{11a}$$

$$\triangleq Q_t = \frac{L}{\Delta} , \text{ for spur gears} . \tag{11b}$$

Equations (10a) and (10b) also show that the envelope of the contribution of the static transmission error spectrum arising from elastic deformation decays with tooth-meshing harmonic number p as p^{-2} in the case of helical gears and as p^{-1} in the case of spur gears. This behavior implies that the envelope of the spectrum of this component decreases with increasing harmonic number at a "rate" of 12 dB per octave in the case of helical gears and 6 dB per octave in the case of spur gears.

Figure 5 is a log-log plot of the elastic deformation component normalized rms harmonic amplitudes $\sqrt{2}\,|a_{wp}|/(W_0/K_T)$ computed from Eq. (6d) for a spur gear pair with transverse contact ratio $Q_t = 1.819$. The figure shows the linear decay of the envelope of the line spectrum with increasing harmonic number, which falls off at the rate of 6 dB per octave, as we have mentioned above.

$$x = R_b^{(1)}\theta^{(1)} = R_b^{(2)}\theta^{(2)} \quad , \tag{3}$$

which is common to both gears. The coordinate x is the independent variable used in our description of the static transmission error - i.e.,

$$\zeta(x) = \zeta_w(x) + \zeta^{(1)}(x) + \zeta^{(2)}(x) \quad , \tag{4}$$

which is the same as Eq. (2) except that in Eq. (4) the static transmission error components are expressed as functions of the independent variable x defined by Eq. (3).

4. ELASTIC DEFORMATION COMPONENT OF THE STATIC TRANSMISSION ERROR

If the instantaneous total stiffness of all meshing teeth of a gear pair is denoted by $K_T(x)$, then the component $\zeta_w(x)$ of the static transmission error arising from elastic deformation of the teeth and gear bodies of both gears of the meshing pair can be expressed [1] as

$$\zeta_w(x) = \frac{W}{K_T(x)} \quad , \tag{5}$$

where W is the total loading carried by the mesh as illustrated in Fig. 1. Since we use transfer function techniques in our structural response calculations, we require the frequency domain representation of $\zeta_w(x)$ - i.e., its Fourier series coefficients. If we assume (i) that W is a constant (independent of time) and (ii) that the tooth pair stiffness per unit length of line of contact is a constant (independent of the position of the line of contact on the tooth faces - see Fig. 3) then the Fourier series coefficients of $\zeta_w(x)$ are given approximately [2,3] <u>for helical gears</u> by

$$a_{wo} = \frac{W_0}{\bar{K}_T} \tag{6a}$$

$$a_{wp} = -\frac{W_0}{\bar{K}_T} \frac{\sin(p\pi FL/A\Delta)}{p\pi FL/A\Delta} \frac{\sin(p\pi L/\Delta)}{p\pi L/\Delta} \quad , \; p \neq 0 \quad , \tag{6b}$$

and <u>for spur gears</u> by

$$a_{wo} = \frac{W_0}{\bar{K}_T} \tag{6c}$$

$$a_{wp} = -\frac{W_0}{\bar{K}_T} \frac{\sin(p\pi L/\Delta)}{p\pi L/\Delta} \quad , \; p \neq 0 \quad , \tag{6d}$$

where W_0 is the constant loading transmitted by the mesh and p is the tooth meshing harmonic number. The Fourier series coefficients exhibited by Eqs. (6a) - (6d) are defined [1] by

$$a_{wp} \triangleq \frac{1}{\Delta} \int_{-\Delta/2}^{\Delta/2} \zeta_w(x) e^{-i2\pi px/\Delta} \, dx \quad , \tag{7}$$

where Δ is the tooth spacing interval in the plane of contact as illustrated in Fig. 2.

In addition to W_0 and p, Eqs. (6a) - (6d) contain the parameters $\bar{K}_T$,

$$Q_a \triangleq \frac{FL}{A\Delta} \quad , \tag{8}$$

and

$$Q_t \triangleq \frac{L}{\Delta} \quad . \tag{9}$$

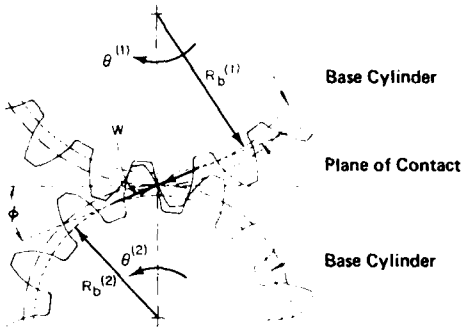
The parameter $\bar{K}_T$ is the average total mesh stiffness, as one might ascertain from the dc Fourier series coefficients given by Eqs. (6a) and (6c). The two other parameters Q_a and Q_t, defined by Eqs. (8) and (9), are the axial and transverse contact ratios: Q_a is the average number of teeth simultaneously in contact in an axial direction, and Q_t is

mission error is such that changes in the tooth surfaces of gears (1) or (2) that are "equivalent" to removal of material from perfect involute surfaces give rise to positive increments in the static transmission error ζ.

Since the static transmission error arises from elastic deformations of the teeth and gear bodies and from geometric deviations of the running surfaces of both gears (1) and (2) of a meshing pair, it is not surprising that the static transmission error can be decomposed [1-3] into three additive components,

$$\zeta = \zeta_w + \zeta^{(1)} + \zeta^{(2)} , \qquad (2)$$

where ζ_w is the component arising from the (loading dependent) elastic deformations of both gears and $\zeta^{(1)}$ and $\zeta^{(2)}$ are the components arising from the geometric deviations of the running surfaces of gears (1) and (2), respectively, from perfect uniformly spaced involute surfaces.



$$\zeta = R_b^{(1)}\delta\theta^{(1)} - R_b^{(2)}\delta\theta^{(2)}$$

Fig. 1. Definition of static transmission error.

3. GEAR MESHING GEOMETRY

The geometry of the temporally changing lines of contact between gear teeth is very important for both the physical and mathematical understanding of the vibratory excitation of gear systems. This geometry is illustrated in Fig. 2. In the upper portion of Fig. 2, the lines of contact are drawn on a fictitious belt that rides between the base cylinders of the two meshing helical gears. These lines of contact are drawn solid within the rectangular region (zone of contact) where the tooth contact actually takes place; they are drawn dashed elsewhere. As the gears rotate, the fictitious belt moves through the rectangular zone of contact shown in the figure, and the individual lines of contact drawn on this belt move through the fixed zone of contact. The geometry illustrated in Fig. 2 is an exact representation of the behavior of the lines of contact of perfect involute helical gears.

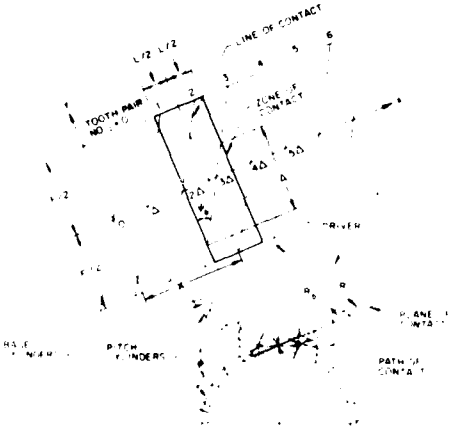


Fig. 2. Lines of contact and zone of contact in plane of contact.

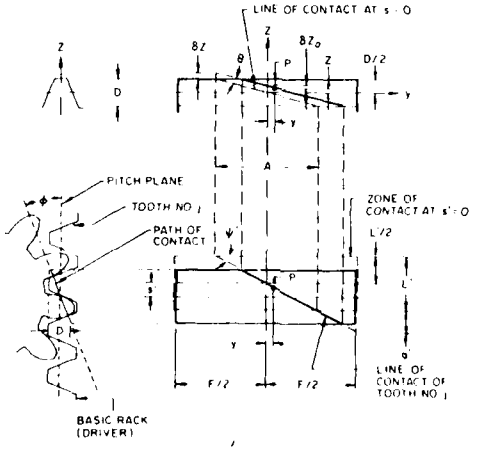


Fig. 3. Line of contact on tooth face.

The line of contact on a particular tooth is shown drawn on that tooth in the sketch in the upper right-hand corner of Fig. 3. As the two gears rotate, this line of contact sweeps across the tooth surface - always remaining at the constant angle θ shown in Fig. 3 as it moves across the tooth surface.

Returning to Figs. 1 and 2, we can see that the lineal position x of the center of the zone of contact measured from the tooth numbered j = 0 can be expressed [1-3] as

GEAR NOISE ORIGINS

by
William D. Mark
Principal Scientist
Bolt Beranek and Newman Inc.
10 Moulton Street
Cambridge, Massachusetts 02238
USA

SUMMARY

Each pair of meshing gears in a transmission gives rise to a source of vibratory excitation that can result in the radiation of sound. Each such source is most conveniently characterized as a displacement form of excitation generally referred to as the static transmission error of the gear pair. Contributions to the frequency spectrum of the static transmission error of spur and helical gears arising from tooth and gear body elastic deformations and from deviations of tooth surfaces from perfect involute surfaces are considered. Tooth surface deviations are decomposed into contributions giving rise to tooth meshing harmonic excitations and rotational harmonic or sideband excitations. Various types of gear tooth errors are defined and the contributions of these errors to different parts of the frequency spectrum are described. The attenuating effect on the static transmission error spectrum arising from the smoothing action of multiple tooth contact is explained.

1. INTRODUCTION

Each pair of meshing gears in a transmission is a source of vibratory excitation. Each such source gives rise to vibratory motions of the gearing elements, which excite the bearings and supporting structure, and eventually cause the radiation of sound by panels, beams, etc. In this paper, we describe a procedure for computing the vibratory excitation caused by a generic pair of meshing parallel-axis helical or spur gears of nominal involute design. The effects of gear design parameters, tooth elastic deformations, and machining errors are included in this procedure. The methodology reported on herein is a summary of some of the results obtained in references [1-4].

Consider the excitation from a generic pinion/gear pair. The most important source of vibratory excitation from this meshing pair arises from the nonuniformity in the transmission of angular motion between the pinion and the gear [5-10]. This nonuniformity in the transmission of angular motion has two causes: (i) elastic deformation of the teeth and gear bodies - which is a function of the loading transmitted by the gear mesh, and (ii) geometric deviations of the running surfaces of the pinion and gear teeth from perfect involute surfaces. In regard to (ii), it should be noted that perfect, uniformly spaced involute teeth with no elastic deformations transmit exactly uniform angular motion [11]. Since structural dynamics calculations are carried out very easily in the frequency domain, the vibratory excitation arising from the above causes will be described in the frequency domain.

In addition to the above-mentioned excitation source, the temporal variation in the total frictional force acting between the teeth also serves as an additional source of vibratory excitation. This latter source generally is believed to be small in comparison with the static transmission error source. Hence, the source arising from friction will be neglected in this paper.

2. STATIC TRANSMISSION ERROR

The excitation source arising from (i) elastic deformations of the teeth and gear bodies and (ii) geometric deviations of the tooth surfaces from perfrect involute surfaces is most conveniently described as a displacement type of excitation - rather than a force type of excitation. This composite excitation is characterized by the static transmission error [5,6], which can be defined loosely [1,3] as the deviation $\delta\theta$ from linearity of the angular position θ of a gear measured as a function of the angular position of the gear (or pinion) it meshes with when the gear pair is transmitting torque at low enough speed so that inertial effects are negligible. In [1-3], we have found it convenient to utilize a lineal form of the static transmission error. In order to give a precise definition of the static transmission error as it is used in [1-3], it is necessary to consider the idealized perfect, rigid, involute counterparts (of the same design) to the real gears under conside ation. Let $\delta\theta^{(1)}$ and $\delta\theta^{(2)}$ denote, respectively, the instantaneous deviations of the angular positions of real gears (1) and (2) of a meshing pair from the angular positions of their idealized perfect involute counterparts, and let $R_b^{(1)}$ and $R_b^{(2)}$ denote, respectively, the base circle radii of the two gears. Then, the precise definition of the static transmission error [1-3] is

$$\zeta = R_b^{(1)}\delta\theta^{(1)} - R_b^{(2)}\delta\theta^{(2)} , \qquad (1)$$

where the sign convention for the positive directions of $\delta\theta^{(1)}$ and $\delta\theta^{(2)}$ is indicated by the angles $\theta^{(1)}$ and $\theta^{(2)}$ shown in Fig. 1. The sign convention of the static trans-

DISCUSSION

H.Ferris, US

Vibration analysis for health monitoring has not been successfully applied in the past on commercial aircraft. The most effective diagnostic system has been chip detectors with pilot indicator lights. The latest state of the art is the use of fuzz burnoff (Zappers) to remove fine wear particles on heavily loaded gears and bearings, which eliminate nuisance warnings. When a cautionary or warning light comes on, it's from a large chip. In this case, you complete the mission with reduced power and investigate with maintenance action. What is your experience?

Author's Reply

In specific applications, simple vibration analysis is successful e.g. tracking filter readouts for detection of out of balance of gas turbine shafts. In other general applications, the analysis of vibration data has not been effective because the techniques used, e.g. overall level or spectrum analysis, gave poor repeatability of readings and this contributes to the lack of sensitivity in the detection of faults. The analysis approach described in our paper overcomes both these deficiencies for our work has shown the good repeatability of the derived FOM parameters and the excellent response to the faults listed in the paper.

The R.N. does employ electric chip detectors on the Sea King helicopters. They have a high incidence of spurious warnings and thus do not have a good reputation. Zappers would decrease these spurious incidents, but at present they have not found favour with the UK military. Magnetic plugs that merely collect debris from the lubricant (i.e. do not act as indicators) have a wide use in the UK for the monitoring of helicopters. Debris is removed at specified intervals, examined by a specialist and the record added to the aircraft file. In this system a diagnosis is made and leads directly to maintenance decisions. The diagnosis is made by optical particle recognition together with any knowledge of what is critical non-critical and experience of the system.

It would be stressed, however, that not all tribological manifestations yield large particles. They may not be magnetic and they may not increase the total number of equivalent sized particles being generated throughout the gearbox.

Hence the need is for a mix of techniques to provide the high overall efficiency in the detection diagnosis of faults coupled with the necessarily low spurious indications; vibration analysis of this paper and wear debris assessment techniques complement each other.

D.G.Astridge, UK

In response to Mr Ferris' comments:

(1) The type of vibration analysis techniques (enhanced signal averaging) described in this paper are applied on all Westland 30 helicopters (all gearboxes) in service in the UK and USA. Accelerometers and cables are permanently mounted and data is sampled using a portable tape recorder at intervals during short ground runs. The 'video format' tapes are expressed to Westland for rapid analysis (24 hour turnaround). In future this analysis will be carried out on board in the 300 Series growth version of this helicopter, using the Health and Usage Monitoring Computer described in Paper 81 of the Tenth European Rotorcraft Forum, The Hague, Aug. 1984.

(2) Virtually all the problems endemic to past generations of wear sensors or chip collectors are overcome by the *TEDECO QDM (Quantitative Debris Monitoring System)* described in the article on Advanced Gearbox Health Monitoring Techniques, published in the International Journal of Aviation Safety, Sept. 1984 p.165. This system is also a very important part of the armoury of health monitoring techniques applied to the Westland 30 transmission. We would concur wholeheartedly with Mr Gadd's comment at the beginning of his part of the presentation that no single health monitoring technique can detect all potential failure modes in a gearbox and that a collection of techniques is necessary, the precise constituents depending upon the particular gearbox design, lubrication and filtration system, and operation conditions.

an MTBR of appoximately 1000 hours and one in six reaching the current TBO, a 20% increase in TBO to 2400 hours would at best result in an improvement of 6% in the MTBR if every gearbox reaching 2000 hours were to survive the extra 400 hours. In reality the likely improvement in MTBR would be around 4%. To introduce VHM on a current aircraft would entail.

a. scheming, approval and fleet-wide fit of an aircraft modification to install accelerometers and a wiring harness.

b. purchase of sufficient high quality analogue tape recorders to meet the needs of a widely dispersed fleet.

c. establishing adequate analysis facilities (either centrally in the UK or, at greater expense, at major air stations and on large ships).

d. establishing a monitoring regime which would undertake routine data analysis, probably at 50 flying hour intervals.

A cost-benefit analysis showed that the break even point would be achieved with an MTBR improvement of around 15% (rather higher for the Sea King). It was reluctantly concluded that such gains were not likely and that the introduction of VHM to current aircraft was not warranted on cost-effectiveness grounds. A cheaper scheme where VHM would only be applied to UK shore based aircraft was also considered but was no more attractive on financial criteria, and had the added disadvantage of reducing the flexibility to reallocate individual aircraft. It is worth noting that being cost-effective is not in itself sufficient to ensure the adoption of VHM since there are many other competing improvement proposals, and insufficient funds to allow them all to be adopted. It is not uncommon, unfortunately, for us to be unable to introduce gearbox modifications to overcome known weaknesses despite the fact that they would extend MTBRs and are clearly cost effective. The Army and the Royal Air Force, who are also sponsoring this work, have come to the same conclusion regarding the cost-effectiveness of application to their current helicopter fleets.

18. The situation regarding future aircraft is rather more promising. Firstly the benefits to be gained from TBO extensions are far more significant in the early years in service when TBOs are low. Secondly the necessary installation can be incorporated during the development programme as part of a health and usage monitoring system, and the costs are lower and comparatively easily met. Thirdly the introduction of powerful computing facilities for general aircraft management purposes together with continuing advances in analysis techniques offer the prospect of overcoming on-aircraft analysis. This would be a major step forward removing many of the current practical drawbacks and providing valuable information at little extra cost. Advances in the aircraft using an already provided computer and recording high quality recording of raw data would [illegible] The recording of data could also become automated since we [illegible] engineering computing systems at air stations and [illegible] lower levices will be available to link these [illegible]

19. Although routine [illegible] VHM is not at present an [illegible] are being pursued. The first [illegible] well after gearboxes have [illegible] techniques for troubleshooting, [illegible] the aircraft. An example of this has been [illegible] under way to review our accident history [illegible] improving flight safety. The [illegible] of an aircaft could be sufficient [illegible] current aircraft.

20. Vibration health monitoring [illegible] effectiveness in diagnosing impending gearbox failures [illegible] trials. Routine monitoring is not being introduced [illegible] the advent of on-board analysis or a convincing flight safety argument would [illegible] carefully review the situation. Future HN aircraft can be expected to include a measure of VHM as part of their health and usage monitoring systems where they will make a useful contribution to meeting future requirements for high aircraft availability, low manpower requirements at first line and reduced life cycle costs.

ACKNOWLEDGEMENT

The contributions of Stuart Hughes Ltd and Westland Helicopters Ltd to the development and evaluation of these techniques is gratefully acknowledged by the authors. In addition there have been many valuable contributions from colleagues within the Ministry of Defence.

Copyright © Controller HMSO London 1984

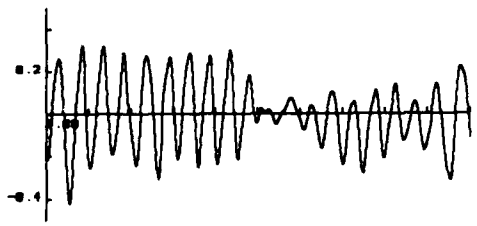


Fig 5. Sea King MRGB Lay Shaft Showing Apparent 20 Teeth (43 Teeth Actual)

b. A Wessex tail rotor gearbox persisted in generating high output shaft vibration when installed in numerous aircraft. Fig 6 shows the modulation of input gear mesh by the input shaft. Subsequent alignment checks on the input housing confirmed this diagnosis. On fitting another housing the modulation manifestation disappeared and after installation on an aircraft the vibration checks were well within the limits.

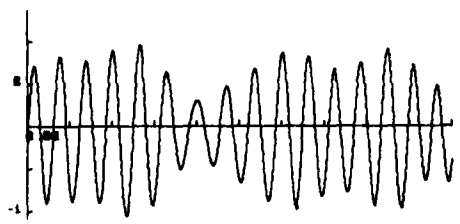


Fig 6. Signal Average of the Wessex Tail Gearbox 17 Teeth Input Pinion With Once-Per-Rev Modulation.

SERVICE APPLICATIONS

16. Having now described the techniques in detail and given some examples of their use, it is appropriate to look at how we are planning to exploit them. While our oldest aircraft, because of their reducing numbers and limited future are not good candidates for investment, we have had a careful look at the introduction of VHM to the Lynx and Sea King. Table 2 gives details of the current gearbox lives. The Lynx has been in squadron services for 7 years and the Sea King a great deal longer.

Table 2 Current RN Gearbox Lives

Gearbox	Lynx		Sea King	
	TBO (hrs)	% Lifex	TBO (hrs)	% Lifex
Main	900*	37	2000	16
Intermediate	1800	30	2500	33
Tail	1800	18	2500	26

* 2 pinion and 3 pinion

With the exception of the Lynx main gearbox, overhaul lives represent around 5 years actual flying at our modest rates. The Lynx figure is low because of problems with the early 2 pinion gearbox which is unlikely to get beyond the current figure. It will eventually be replaced with the more robust 3 pinion unit which is still in the early stages of TBO extension. However, partly by exploiting civil and Dutch naval experience with this gearbox, we hope to get up to 1200 hours shortly and then progress in stages to at least 2000 hours. It is also important to note that many gearboxes fail to reach their declared overhaul life since only these boxes stand to benefit from any further TBO extensions.

17. The scope for increasing the MTBR, and hence reducing the annual number of overhauls is therefore clearly limited. For example, with the Sea King main gearbox which is showing



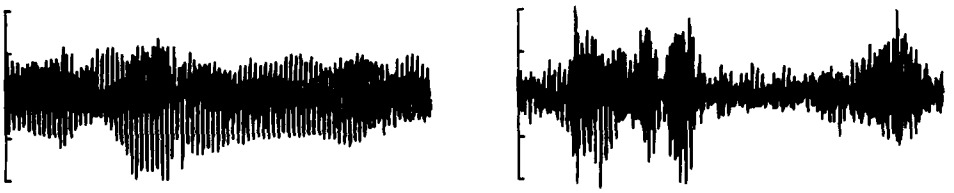
Raw Signal Average FOM 4 Residue

Fig 4B: Lynx MRGB Conformal Wheel Test - 110.15 Hrs

b. At 110.15 hours

(1) Signal Average - Nothing appears as obvious events.

(2) Residue - The tail and starboard pinion meshes are apparent as impulsive events and a burst of activity reveals in a general sense the position of the port pinion. FOM 4A rises from 5.1 to 6.3. FOM 4B rises from 0.12 to 0.19.



Raw Signal Average FOM 4 Residue

Fig 4C: Lynx MRGB Conformal Wheel Test - 118.25 Hrs

c. At 118.25 hours

(1) Signal Average - Some distortion of the signal average is apparent.

(2) Residue - The discrete nature of the events is obliterated by the increase in the noise. FOM 4A falls from 6.3 to 4.0. FOM 4B increases from 0.19 to 0.41.

14. The above example has been generated to illustrate a number of points:

a. The FOM 4 routine has to be used in order to achieve the required sensitivity for fault correction.

b. A mesh pattern character may become obscure as the tooth failure progresses, say into gear web.

c. FOM 4A has excellent sensitivity for discrete events but can fall away as the failure progresses as mentioned above.

d. FOM 4B, whilst sluggish to respond, quantifies the random energy 'leaking' into the residue, and can be expected to increase as the damage progresses.

Thus trend analysis, obviously an important element in any form of machinery monitoring, cannot be simple, particularly if done through a sampling programme. If the best diagnosis of faults is to be extracted automatically from the FOM package, some form of matrix of parameters will have to be constructed. This will allow for the fault to progress as a generally increasingly level, or for the fault to register only at some stage(s) of its development.

15. Further possibilities of fault data collection on gearbox (and other assemblies) occur from troubleshooting and test bench investigations. Two examples are quoted:

a. Following a pilot report of unusual vibration from a Sea King main rotor gearbox, an investigation was carried out. This revealed that the accessory free-wheel lay shaft when operating was in torsional resonance, hence the audible noise. The raw signal average for the shaft is shown in Fig 5. The apparent half number of teeth confirms the resonance phenomenon.

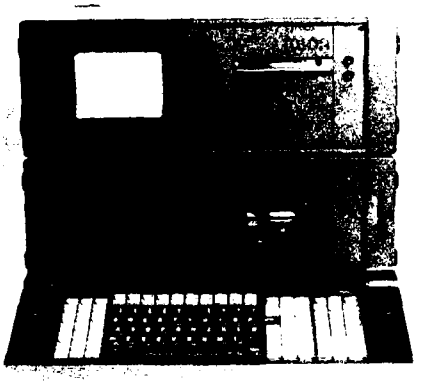
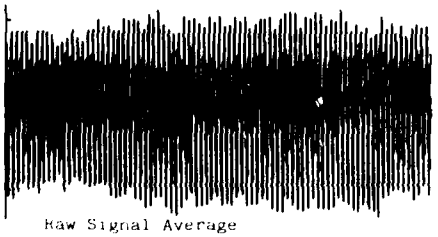


Fig 3: Mechanical System Diagnostic Analyser (MSDA)

RESULTS

13. For any monitoring programme the repeatability of the chosen parameters has to be good. Analysis of data from the Lynx main rotor gearbox gears has enabled values to be calculated for the FM procedures and the values have been shown to remain largely within close limits for a given gear on an aircraft when recordings are made on 2 or more occasions. The signature obtained from the 3 aircraft were also closely similar. This has enabled the bounds for a normal gearbox to be provisionally established. It is believed that the above repeatability is in no small way due to the non-dimensional form of the FOMs. The efficiency of gear fault detection for a variety of faults has been established by analysis of archival tapes, viz Westlands Helicopter fatigue substantiation gearbox trials where, in a number of high load tests, gear failure progression has been recorded. Fig 4 shows Lynx wheel tooth/web failure progression. In each revolution of the wheel the damage goes through 3 pinion meshes spaced 90°-90°-180°.



Raw Signal Average



FOM 4 Residue

Fig 4A: Lynx MRGB Conformal Wheel Test - 105.45 Hrs

a. At 105.45 hours

(1) Signal Average - Clearly an 84 tooth, gear appears good.

(2) Residue - A double event is obvious, the port pinion contribution is not readily seen probably because of the transducer siting. FOM 4A rises from 3.1 to 5.1 FOM 4B remains static.

connecting the tops of the lines is shown. In Fig. 15, a line component occurs at each discontinuity in slope, since the tops of the spectral lines have been connected there by straight line segments. The spectrum shown in Fig. 15 no longer appears periodic to the eye because it is plotted on a logarithmic axis of harmonic numbers; however, the positions of the tooth-meshing harmonics where the nulls and strong sidebands occur clearly are evident there.

The product of the tooth-spacing error spectrum $\sqrt{2}\left|B_{00}^{(1)}(n)'\right|$ [Eq. (20)] illustrated in Fig. 15 and the tooth-spacing error mesh transfer function $\left|\hat{\phi}_{00}(n/N^{(1)}\Delta)\right|$ illustrated in Fig. 14 is shown plotted on log-log coordinates in Fig. 16. The tops of the spectral lines are connected by straight lines in Fig. 16, just as in Fig. 15. Thus, Fig. 16 is a plot of the envelope of $\sqrt{2}\left|B_{00}^{(1)}(n)'\hat{\phi}_{00}(n/N^{(1)}\Delta)\right|$ which is the tooth-spacing error contribution from a single spur gear to the rms harmonic amplitudes of the static transmission error, which is the vibratory excitation.

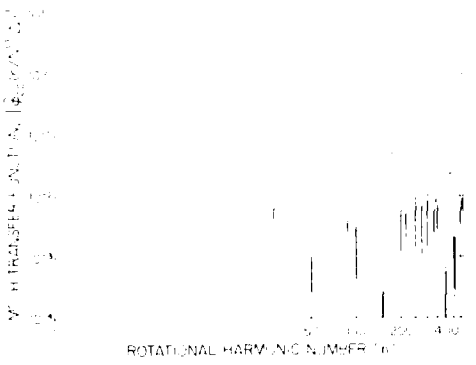


Fig. 14. Tooth spacing error (k=0, ℓ=0) mesh transfer function magnitude for a 50 tooth spur gear with Q_t = 1.819.

It is instructive to compare the mesh attenuated spectrum of tooth-spacing errors shown in Fig. 16 with the unattenuated spectrum of tooth-spacing errors shown in Fig. 15. In comparing the amplitudes of the first few rotational harmonics that occur at the discontinuities in slope, we see that there is negligible attenuation of these harmonics arising from the averaging action of the multiple tooth contact, since the tooth-spacing error mesh transfer function shown in Fig. 14 is approximately unity in this low-order harmonic number region. We also see that the strong sidebands that occur periodically in Fig. 15 in the neighborhood of each tooth-meshing harmonic are very strongly attenuated in Fig. 16 by the nulls in the tooth-spacing error mesh transfer function that are seen in Fig. 14 in the neighborhood of each tooth-meshing harmonic location. Finally, we see that the overall slope of the spectrum shown in Fig. 16 decays at a "rate" of 6 dB per octave in the high harmonic number region - which is the decay of the mesh transfer function shown in Fig. 14 in this same region.

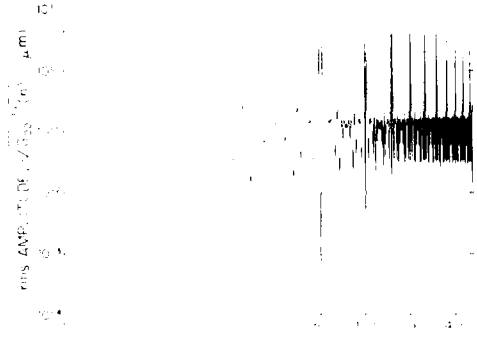


Fig. 15. Envelope of tooth spacing error spectrum $\sqrt{2}\left|B_{00}^{(1)}(n)'\right|$ (k=0, ℓ=0) on logarithmic harmonic number axis for a 50 tooth gear.

8. OVERALL BEHAVIOR OF THE EXCITATION SPECTRUM ARISING FROM A SINGLE PINION OR GEAR

By examining the large harmonic number asymptotic behavior of the dominant term in Eq. (95) of reference 2, one can show [2,3] that the envelopes of the magnitudes of the mesh transfer functions for helical gears are asymptotically equal to

$$\left|\hat{\phi}_{k\ell}(n/N^{(\cdot)}\Delta)\right|_{env} = \frac{[(2k+1)(2\ell+1)]^{1/2}}{\pi^2 Q_a Q_t}\left(\frac{n}{N^{(\cdot)}}\right)^{-2} \qquad (25a)$$

Similarly, by examining the large harmonic number behavior of the dominant term in Eq. (110) of reference 2, one can show [2,3] that the evelopes of the

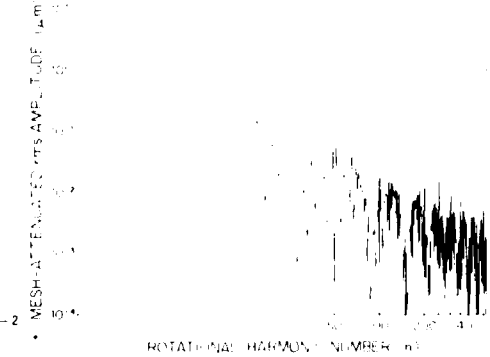


Fig. 16. Envelope of tooth spacing error contribution (k=0, ℓ=0) to the static transmission error spectrum for a 50 tooth spur gear with Q_t = 1.819.

magnitudes of the mesh transfer functions for spur gears are asymptotically equal to

$$\left|\hat{\phi}_{0_\ell}(n/N^{(\cdot)}\Delta)\right|_{env} = \frac{(2\ell+1)^{1/2}}{\pi Q_t}\left(\frac{n}{N^{(\cdot)}}\right)^{-1} \quad . \tag{25b}$$

Quantities Q_a and Q_t are the axial and transverse contact ratios defined by Eqs. (8) and (9). The decay in harmonic number n of the right-hand side of Eq. (25a) as n^{-2} yields the decay "rate" of 12 dB per octave in the large harmonic number region of the mesh transfer functions shown in Figs. 10 through 13. The decay in harmonic number n of the right-hand side of Eq. (25b) as n^{-1} yields the decay "rate" of 6 dB per octave in the large harmonic number region of the mesh transfer function shown in Fig. 14 and the mesh attenuated error spectrum shown in Fig. 16.

As we have mentioned earlier, the mesh transfer functions $\hat{\phi}_{k_\ell}(n/N^{(\cdot)}\Delta)$ describe the effects of the smoothing action of multiple tooth contact on the deviations of the tooth surfaces from perfect involute surfaces. From Eq. (25a), we see that in the large harmonic number region, the envelopes of the mesh transfer functions for helical gears depend on the axial and transverse contact ratios only through their product Q_aQ_t, which has been called [3] the aggregate contact ratio ACR - see Eq. (11a). This same dependence also has been found to be true of the loading dependent component, as can be seen from Eq. (10a). Similarly, from Eqs. (25b) and (10b) we see that the envelopes of the mesh transfer functions and loading dependent component for spur gears in the large harmonic region are inversely proportional to the transverse contact ratio Q_t which, according to Eq. (11b), is the aggregate contact ratio for spur gears. Thus, it follows that a single design parameter, the aggregate contact ratio, characterizes to a first approximation the gear mesh design parameters insofar as the vibratory excitation is concerned [2,3]. From Eqs. (10a,b) and (25a,b), it follows that doubling the ACR will decrease the excitation by about 6 dB in the general region of the tooth-meshing harmonics where the asymptotic approximations given by Eqs. (10a,b) and (25a,b) are valid. In Fig. 17, the axial and transverse contact ratios are related to fundamental gear-mesh design parameters, where F is the face width of a single helix, D is the tooth depth [3] illustrated in Fig. 3, $(Dia)_b^{(\cdot)}$ is the base cylinder diameter, $N^{(\cdot)}$ is the number of teeth, ϕ is the pressure angle, and ψ is the pitch cylinder helix angle.

To a First Approximation, Gear Design Parameters Influence Static transmission Error Spectrum as One Aggregate Parameter, ACR:

ACR = Aggregate Contact Ratio

$$= Q_a\, Q_t \text{ for Helical Gears}$$

$$= Q_t \text{ for Spur Gears}$$

Q_a = Axial Contact Ratio = FL/AΔ

$$= \frac{FN^{(\cdot)}\cos\phi\tan\psi}{\pi\,(Dia)_b^{(\cdot)}}$$

Q_t = Transverse Contact Ratio = L/Δ

$$= \frac{DN^{(\cdot)}\csc\phi}{\pi\,(Dia)_b^{(\cdot)}}$$

Fig. 17. Influence of gear design parameters on the static transmission error spectrum.

From the preceding material, we can conclude that the various components of the static transmission error from a single pinion or gear contribute to the vibratory excitation spectrum as shown in Fig. 18. The lighter spectral lines shown in Fig. 18 represent the rotational harmonics that arise from deviations of the individual tooth surfaces from the mean tooth surface [1-3]. The heavier spectral lines represent the tooth-meshing harmonics that arise from the deviation of the mean tooth surface from a perfect involute surface and from elastic deformations of the teeth and gear body.

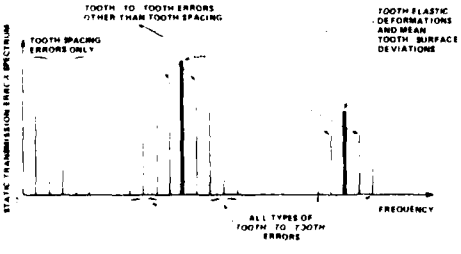


Fig. 18. Contributions to static transmission error spectrum from various types of tooth errors from a single pinion or gear.

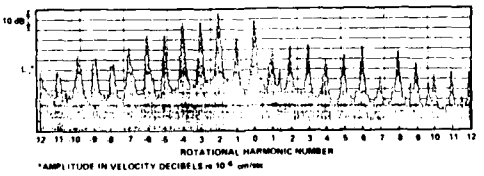


Fig. 19. Rotational harmonic structure of a hobbed and shaved gear (from Ref. 12).

Since the strengths of all mesh transfer functions except that for tooth-spacing errors are small in comparison with unity in the region of the first few rotational harmonics (see Figs. 10-13), the dominant contribution to the first few rotational harmonics will arise from tooth-spacing errors ($k = 0$, $\ell = 0$) as defined by Eqs. (12) through (17), Table 1, and Fig. 7. Furthermore, since the tooth-spacing error mesh transfer functions have nulls in the neighborhoods of the tooth-meshing harmonics, and since the other mesh transfer functions generally do not have nulls in the neighborhood of the tooth-meshing harmonics, the pairs of sidebands closest to the tooth-meshing harmonics should be dominated by error types other than tooth-spacing errors. Finally, contributions to the tooth-meshing harmonics arise from elastic deformations of the teeth and gear bodies and from the deviations of the mean tooth surface from a perfect involute surface, whose expansion coefficients are given by Eq. (21a). In the above discussion, it has been assumed that the stiffness characteristics of all teeth on a pinion or gear are the same.

The strengths of the rotational harmonics that surround the tooth-meshing harmonics are not necessarily negligible or small in comparison with the strengths of the tooth-meshing harmonics. Figure 19 shows on an expanded frequency scale a measured structureborne vibration velocity spectrum arising from vibration excitation by a hobbed and shaved helical gear. The amplitude scale is logarithmic and the frequency scale is linear. Only the portion of the frequency scale in the neighborhood of the tooth-meshing fundamental frequency $n = N$ is shown in Fig. 19. In this particular case, a few of the rotational harmonic levels are higher than the tooth-meshing fundamental.

To obtain the Fourier series representation of all contributions of the static transmission error spectrum from a meshing pair of gears, the mesh attenuated Fourier series coefficients given by Eq. (23) for each gear of the meshing pair are superimposed and added to the Fourier series coefficients arising from elastic deformations of the teeth and gear bodies given by Eqs. (6). Thus, the tooth-meshing harmonic contributions of this sum are given [1-3] by

$$\alpha_{mp} = \alpha_{wp} + \alpha_{pN^{(1)}}^{(1)}(1) + \alpha_{pN^{(2)}}^{(2)}(2) , \quad p = 0,\pm1,\pm2,... \tag{26}$$

where p denotes the tooth-meshing harmonic number, the α_{wp} are the elastic deformation contributions given by Eqs. (6), and $\alpha_{pN^{(1)}}^{(1)}(1)$ and $\alpha_{pN^{(2)}}^{(2)}(2)$ are the contributions given by Eq. (23) from gears (1) and (2) of the meshing pair for their respective tooth-meshing harmonics $n = pN^{(1)}$ and $n = pN^{(2)}$. Subscript m on the left-hand side of Eq. (26) denotes that the tooth-meshing harmonic contributions arise from the mean deviations of the loaded tooth surfaces from perfect involute surfaces. The remaining rotational harmonic contributions are given by the superposition of the remaining terms in Eq. (23) ($n \neq pN^{(\cdot)}$) from each gear of the meshing pair. These rotational harmonics from the two meshing gears generally occur at different frequencies due to the generally different numbers of teeth on the gears [1].

9. MEASUREMENT OF TOOTH SURFACES

To utilize Eq. (16) to compute the Legendre expansion coefficients, we require, in principle, the deviation $\eta_{C_j}^{(\cdot)}(y,z)$ of every point y,z of the running surface (Figs. 3 and 6) of every tooth j of gear $(\cdot)$. Measurement of the deviation $\eta_{C_j}^{(\cdot)}(y,z)$ at every point clearly is impossible to accomplish. However, a good approximation to the surface $\eta_{C_j}^{(\cdot)}(y,z)$ can be obtained by a kind of two-dimensional interpolation [4] between conventional lead and profile deviation measurements. If Gaussian quadrature is used to evaluate the double integral in Eq. (16), one can argue [4] that the lead and profile measurements should be located at the zeros of Legendre polynomials defined over the spans F and D shown in Fig. 6. Figure 20 shows the locations of four such lead measurements and three such profile measurements. For vibration excitation predictions, three lead measurements and three profile measurements on every tooth, located at the zeros of Legendre polynomials of degree 3, should provide excellent results.

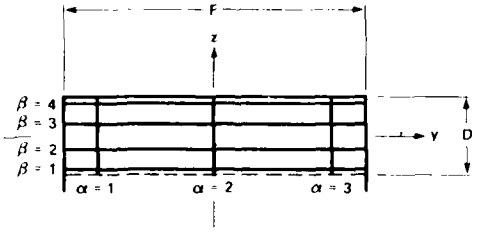


Fig. 20. Positions of 3 profile deviation measurements and 4 lead deviation measurements located at zeros of Legendre polynomials of degrees 3 and 4, respectively.

10. REFERENCES

1. W.D. Mark, "Analysis of the vibratory excitation of gear systems: Basic theory," J. Acoust. Soc. Amer., Vol. 63, 1978, pp. 1409-1430.

2. W.D. Mark, "Analysis of the vibratory excitation of gear systems. II: Tooth error representations, approximations, and application," J. Acoust. Soc. Amer., Vol. 66, 1979, pp. 1758-1787.

3. W.D. Mark, "Gear Noise Excitation," in Engine Noise: Excitation, Vibration, and Radiation, R. Hickling and M.M. Kamal, Eds., New York, Plenum Publishing Corp., 1982, pp. 55-93.

4. W.D. Mark, "Analytical Reconstruction of the Running Surfaces of Gear Teeth Using Standard Profile and Lead Measurements," ASME Journal of Mechanisms, Transmissions, and Automation in Design, Vol. 105, 1983, pp. 725-735, Vol. 106, 1984, p. 22.

5. S.L. Harris, "Dynamic Loads on the teeth of Spur Gears," Proc. Inst. Mech. Eng., Vol. 172, 1958, pp. 87-100.

6. R.W. Gregory, S.L. Harris, and R.G. Munro, "Dynamic Behavior of Spur Gears," Proc. Inst. Mech. Eng., Vol. 178, 1963-1964, pp. 207-218.

7. H.K. Kohler, A. Pratt, and A.M. Thompson, "Dynamics and Noise of Parallel-Axis Gearing," Proc. Inst. Mech. Eng., Vol. 178, 1963-1964, pp. 111-121.

8. G. Niemann and J. Baethge, "Drehwegfehler, Zahnfederhärte und Geräusch bei Stirnrädern," VDI-Z, Vol. 112, 1970, pp. 205-214 and pp. 495-499.

9. D.B. Welbourn, "Fundamental Knowledge of Gear Noise - A Survey," Conference on Noise and Vibrations of Engines and Transmissions, Cranfield Institute of Technology, The Inst. Mech. Eng., London, 1979.

10. J.D. Smith, Gears and Their Vibration: A Basic Approach to Understanding Gear Noise, New York, Marcel Dekker, Inc., 1983.

11. A. Sloane, Engineering Kinematics, New York, Macmillan, 1941 (Republished by Dover, New York, 1966).

12. G.W. Nagorny and R.A. Stutchfield, "Gear Noise - The Generation of Rotational Harmonic Frequencies in Marine Propulsion Gears," AGMA Paper P-299.06A, American Gear Manufacturers Association, Arlington, VA, 1981.

11. ACKNOWLEDGEMENTS

Mr. Charles E. Braddock of Bell Helicopter Textron supplied the original tooth spacing accuracy data shown in Fig. 8. The computer work shown in Figs. 5 and 8 through 16 was carried out by Mr. Raymond W. Fischer of BBN. Figure 3 was taken from Ref. 1, Figs. 4, 5, 8, 9, and 10 through 16 were taken from Ref. 2, Figs. 1, 2, 6, 7, 17, and 18 were taken from Ref. 3, Fig. 20 was taken from Ref. 4, and Fig. 19 was taken from Ref. 12.

DISCUSSION

B.A.Shotter, UK

Gear tooth spacing errors as measured on gear inspection machines can differ in character depending upon the way in which the gears have been produced. Some pitch errors are fixed in the rotational angular position, others travel around the gear with the tooth when it is helical. Have you considered the implication of these two types of spacing errors?

Author's Reply

The pitch errors that are fixed in rotational angular position will tend to produce the same error at progressively different values of axial location (Fig. 6) on successive helical gear teeth. The measurement method that we use (Fig. 20) to measure deviations of tooth surfaces from perfect involute surfaces is certainly capable of measuring such errors. However, the Legendre polynomial method that we use [Figs. 12–17 and Fig. 7] for representing the measurements illustrated in Fig. 20 would characterize such behaviour as a variation on successive teeth of pure lead mismatch deviations ($k = 1, l = 0$) pure lead crowning deviations ($k = 2, l = 0$) (Table 1).

On the other hand, the pitch errors that travel around the gear with a particular helical tooth will tend to show up in our Legendre polynomial method as a pure tooth spacing error of whatever tooth they are following.

F. da Silva, Po

Could you comment on the influence of the lubricant on your analysis as it seems to assume a dry contact?

Author's Reply

Our analysis assumes that as the line of contact sweeps across the tooth face (Fig. 3) there is negligible variation in the oil film thickness. If this assumption is true, there is no need to bring oil film considerations into the analysis.

E.Saibel, US

It seems to me that your method could be applied to the situation where wear is taking place and your system would become almost periodic.

Author's Reply

As long as there is negligible additional wear over the duration of a single revolution of a pinion or gear, we can retain all of the periodic assumptions used in the analysis. However, any long term wear components that are common to all teeth on a pinion or gear will change the levels of the tooth-meshing harmonics, whereas any long term wear components that differ among the teeth will change the rotational harmonic levels of that particular pinion or gear.

THE OBSERVATION AND INTERPRETATION OF GEAR TOOTH FAILURES

AUTHOR: B A SHOTTER

D C M D (TRANSMISSIONS)
WESTLAND HELICOPTERS AND HOVERCRAFT LIMITED
YEOVIL, ENGLAND

SUMMARY

Progress in transmission reliability can only come from a full understanding of what causes the limitation of tooth load carrying capacity. This paper will discuss the many aspects of tooth failure, the significance of various initiaion areas, possible approaches to improve the critical areas and other relevant factors.

INTRODUCTION

Whilst the text books usually classify tooth failures as surface fatigue (or pitting), root breakage, lubrication breakdown or scuffing, the minor details of any particular failure can often reveal a lot more useful information. Some failures are not always what they seem at first sight. The misinterpretation of failures can lead to conflict between the evidence from different tests. This reacts further into the design of new gear systems which cannot be as reliable as one would like unless the input data accurately relates to the design formulae being used. It is, therefore, extremely important to analyse all failure data, however obtained, very carefully indeed to extract the maximum amount of information that can be derived from the observable evidence.

Successful operation teaches one very little: catastrophic failure might occur with an extra five per cent load or gears might be fifty per cent heavier than they need to be. Only by testing to failure can one judge safety margins or attempt to make changes that will improve load capacity. The process of assessing any particular failure involves a large number of questions and answers. Some questions may be definable before any failure occurs, but others only appear in reaction to the particular set of circumstances that are relevant for this specific combination of observed facts. Although this may suggest that one cannot lay down any hard and fast rules that will be capable of general application, it is possible to indicate the basic guide lines that can be followed. In many ways one might say that the steps outlined in this paper are 'self-evident', however it is surprising how many times people only attempt to answer a part of a problem. Papers and reports often show examples of failures which raise questions that are not answered in the text. One can only assume that the authors never realised the possible significance of the evidence.

If one is attempting to analyse a specific failure case then it is important to start with a clearly defined objective, to understand the reason for the failure. Many reports have been produced that end with a statement defining the nature of the failure and do not attempt to investigate 'why it happened'.

This may happen because the investigation has been placed in the hands of people who only have limited information given to them. Metallurgists may be given a failed component and be asked to give the reason for the failure. They can usually define the type of failure and can help by investigating whether the metal is to the standard required by the drawings. However, they are often not in a position to comment on the actual operating condition in relationship to component accuracy or dynamic loading effects. A broad-minded approach is essential if one is to derive the maximum benefit from investigations into gear failures. This may well mean having failures investigated by a small team who contribute from their own individual disciplines. Testing to failure can be an expensive procedure, it is important to derive the maximum benefit from the results that are obtained.

Whilst it is often important to know what the ultimate failure mode might be for a full 'Failure Modes and Effects' analysis. It must also be stated that such tests can obscure the real origins of the initial failure. Early detection of possible failures can be very important in pin-pointing the true causes of failures. Such observations can often lead to minor modifications which may have very significant effects on the reliability or load capacity of the components. Thus 'Health Monitoring' techniques can play a very important part in the development of new transmissions as well as their more usual 'in-service' role.

As already mentioned it is impossible to lay down a simple logic procedure which will serve for the analysis of every failure case. Thus the approach offered starts from the three classical failure mechanisms and suggests some of the ways in which the basic failure should be considered. A further section considers the implications of micropitting on gear failures.

DISCUSSION ON TOOTH BREAKAGE QUESTIONS

When a gear tooth breakage occurs it can be of a single tooth with others showing little effect (a). This may mean a local material flaw or manufacturing damage at the root of that tooth alone. Alternatively there could have been a major shock load which caused the failure. The character of the fracture may help to distinguish these. If a gear were operating just in the finite life zone of its fatigue capability, then one would expect to find cracks at the roots of a lot of the teeth. The more teeth that are cracked, the more significant the result in terms of the definition of fatigue properties (b).

Sometimes one finds a pattern of failures such that teeth have failed or cracked in a symmetrical manner, say a four-fold symmetry. This can be due to a fundamental vibration of the gear itself or a cyclic loading pattern that may or may not be expected (c). When one tooth fails, the subsequent damage may be very considerable with extensive plastic deformation as teeth hit tip-to-tip or smash their way through others with impact failures. By carefully sorting through the debris it may be possible to find one or two fragements of teeth that clearly show fatigue fractures which are likely to be the initiation areas for the failure (d) (e). Fatigue, in its early stages, is usually recognisable by the smooth character of the fracture surface, rapid crack propagation is recognisable by its much rougher fracture surface.

TOOTH BREAKAGE QUESTIONS

CHART A

a) How many teeth have broken?

b) How many others show cracks?

c) Are the failures all adjacent or is there any significance in the grouping of the failures?

d) Which tooth failed first?

e) Was the failure by fatigue or excessive overload?

f) Was the failure origin at the tooth end or in the middle of the facewidth?

g) Did the failure originate from the contact area or from the root area?

h) If it starts on the root fillet area is its initiation point high up the fillet or down near the root diameter?

i) Having been initiated how does the crack develop?

j) Is the origin on the anticipated side of the tooth?

k) Are there any abnormal defects in the tooth root geometry?

l) Is the metal in the correct hardness condition near the origin?

m) Has the correct case depth been produced?

n) Does the fracture surface show changes in the crack propagation rate?

o) Can one detect any inclusions near the origin?

p) Were there any abnormalities in the unit operating characteristics?

q) Is the gear rim structure likely to contain stresses that could influence the failure?

r) Did the tooth fail as one single fragment or as a series of pieces breaking off?

s) Do any other parts of the transmission system show evidence of abnormal loading?

The position of a fatigue origin can be important. Was the loading uniform across the facewidth? If the crack originates at the tooth end it may be suggesting a heavy end loading. Failure sometimes start over a web where the relative tooth stiffness may be higher than at the ends of the facewidth (f).

Whilst the classical tooth breakage is expected to start from the root fillet area many failures don't seem to have read the text books. They may have started as a contact area failure with a crack that has propagated towards the tooth root. In this area the root bending stresses may take over, to continue the crack propagation and cause tooth breakage (g). The failed tooth fragment is often more helpful here than looking at the main body of the gear.

Even where the failure origin is away from the flank contact area the position of the origin may signify that factors other than simple bending are involved (h). For example, if a wheel rim is shrunk on a hub the high circumferential rim stresses can cause the cracks to initiate very low down in the root fillet. In this case the subsequent crack development may be almost radial through the rim as the crack tends to propagate across the line of tensile stressing (i). Material flaws can also affect the crack development. Such effects may cause a root fillet initiation on a helical gear to run axially along the gear only showing small deviations due to the root stresses when the crack progresses into adjacent root areas. Particularly in cases like this, one must check that the origin is from the normally loaded side of the teeth. Occasionally cases are found where the failure originate on the wrong side of the tooth (j)! These may indicate that braking torques are well in excess of the normal designed drive torques. Or sometimes that equipment has been operated in a manner for which it was not designed.

When only one tooth shows a failure and cracks cannot be detected at other roots one must suspect some local abnormality in that vicinity (k). This might be corrosion or some local machining defect or an inclusion in the metal (o). These defects may be characterised by very clear localised 'eyes' to fatigue crack where one would otherwise have expected the stress to be relatively uniform along the tooth root fillet.

The basic metallurgical characteristics of the metal are important but it is necessary to check the properties of the area adjacent to the failure as well as the bulk properties. Local hardness deviations have been found in a number of cases (l). Sometimes these may be difficult to explain but there are several mechanisms which recur more often than they should. The root surface may have been decarburised leaving a thin low fatigue strength layer ideal for initiating cracks. A second reason for low hardness material may be that the tooth grinding has removed a lot of the case depth (m). This has a double effect in that the material is intrinsically of lower fatigue strength and in addition the characteristic compressive stresses induced by the hardening process will also be reduced.

If the fracture surface shows changes in the propagation rate it may be possible to read a time history of crack development related to starting cycles perhaps. It is not infrequently found that electric motors exhibit very high accelerating torques which can be in excess of the fatigue limit torques (n). Other abnormal torque conditions might be important such as running on transmission system resonance conditions (p).

Whilst rim hoop stresses have been mentioned previously it is possible for gear rims to contain stresses for other reasons. There are probably many reasons for this but some are as follows (q):-

a) planet pinions where roller bearings act internally on the rim;

b) spoked gears where the twisting moment locally distorts the rim;

c) high speed gears where centrifugal stressing can become important.

When a tooth fails as a series of small fragments rather than as a single piece (r) it can be a sign of very bad face alignment, although there is also the possiblity that it may imply a failure from surface initiated damage.

It is always important to consider whether any other parts of a system show characteristics that could support particular hypothesis. If perhaps a single tooth has failed with no evidence of any other teeth being damaged on the same gear, one might suggest a sudden overload. In such cases the pitch checking of other gears in the system may show errors that were all caused by the same event (s). Some couplings and freewheel systems can also show overload evidence.

DISCUSSION ON TOOTH CONTACT FATIGUE QUESTIONS

One characteristic of tooth contact fatigue is that the damage to one surface can leave the other almost unmarked. Again the question of where the damage is observed may be significant in different ways. Gear alignment may cause the damage to be concentrated to one end of the facewidth. But this is not necessarily the only reason for damage at one end: cases have been known where the material hardness has differed significantly along the length of a pinion. Surface finish can differ across the facewidth with some production methods or there may be a considerable temperature gradient, either of which might provoke assymetric damage.

Circumferential variation of damage may also be found which can indicate hardness variation again, although a streak of inclusions due to dirty steel may give rise to a band of contact fatigue damage which can run axially across helical teeth.

Pitting tends to predominate as a failure mechanism on through-hardened materials but with harder clean steels there tends to be less of the classical pitting damage. Contact fatigue often becomes associated with local debris damage, perhaps due to local case cracking in case-hardened gears. Very bad surface finish can also provoke such damage, as can large sub-surface defects due to inclusions or high case-core interface stresses. The latter are usually associated with inadequate heat treatment procedures, these may also be associated with thin cases where case-crushing and exfoliation or removal of the surface-hardened layer may also be found.

The fatigue susceptability of a surface may be increased by local shear stressing caused by scuffing damage. This may have been relatively minor in the lubrication breakdown sense, but the local high traction forces associated with the minor contact welds subsequently fail by pitting. Another factor which can be a precursor to pitting is micropitting. Here a very fine scale

TOOTH CONTACT: FATIGUE QUESTIONS — CHART B

a) Are the pits in similar areas on each tooth?

b) Is there pitting damage on both wheel and pinion?

c) If the answer to (b) is "yes", are the damaged areas in contact with one another?

d) Are the pits in the dedenda only?

e) Is the apex of the pit in an area which has a modified surface appearance?

f) What was the original surface finish like?

g) Was the lubricant viscosity appropriate for the operating conditions?

h) Is there any evidence of water in the oil?

i) If the gear is case hardened, is the case depth adequate?

j) When a flake reaches the edge of a tooth does the crack tend to follow a case-core interface?

k) Does the fatigue development pattern originate from a sub-surface defect?

l) Are there many large non-metallic inclusions in the steel?

m) Is the pit size larger or smaller than the instantaneous Hertzian contact zone width?

n) Could the pits have developed from an earlier scuffing of the surfaces (look at both pinion and wheel)?

o) How long have the gears operated?

contact fatigue is involved where the size of the individual pits is too small to be easily resolvable by the naked eye. Such pits are usually an order of magnitude smaller than the width of the Hertzian contact zone or even less, whereas conventional pits are comparable in size to the Hertzian contact zone or even larger.

The lubricant can play a significant part in provoking pitting damage. The use of low viscosity oils where higher values should have been selected is a fairly common explanation. Another factor known to aggravate pitting damage in otherwise satisfactory lubrication conditions is the presence of water in the oil. A gearbox is frequently subject to quite wide temperature cycling and on cooling down can draw moisture laden air into the casing. This can condense on the cold metal and the water droplets so formed will run down under the oil into low recesses. Subsequent operation of the gears breaks up the globules but when they get between the gear teeth they do not have the pressure coefficient of viscosity that oil has and, in consequence, cannot form a separating film between the teeth. Such local areas may have high friction which provokes contact fatigue directly or they may give rise to minor scuffing areas which then fatigue in the the manner mentioned previously.

DISCUSSION ON TOOTH CONTACT MICROPITTING QUESTIONS

Micropitting is a surface fatigue failure which is also known by the names 'frosting' or 'grey staining'. It is characterised by the fact that the sizes of the pits are very small in comparison with the size of the Hertzian contact. They are usually associated with the peaks of the surface topography in their early stages but the pit depth is only a fraction of the peak-to-valley height.

In its own right the apparent improvement in surface finish might be thought to be beneficial, however, from this initiating damage can develop failures that look similar to any of the classical forms of tooth damage. It is, therefore, most important to recognise the true origin of a failure if design improvements are sought. The full understanding of the failure process is still under investigation but the observation of the failure characteristics can sometimes explain differences between successful and unsuccessful examples of the same gear design.

Where the damage is found (a) can show local 'edge of contact' area problems, perhaps inadequate tip relief. Although with correctly designed gears the damage is more usually found in the dedenda of the teeth. The pattern of damage can vary considerably from tooth to tooth or may be relatively consistent according to the characteristics of the mating surfaces. Sometimes it is only found on one of a meshing gear pair. This usually indicates a hardness differential between them. When it occurs on both members it seldom affects both parts of an instantaneous contact area (b).

Surface finish characteristics can vary from root to tip on a tooth flank and may be responsible for damage being confined to either addendum or dedendum. If a patch of damage bridges the pitch surface of the gears the appearance will change abruptly at the pitch line since the angle of the microcracks changes with the sliding direction. However, a bright or dull stained appearance can indicate active and developing damage or old and inert damage (d). Whilst

TOOTH CONTACT: MICROPITTING QUESTIONS

CHART C

a) Where is the damage found?

b) Is it on both pinion and wheel?

c) Does it occur in both addendum and dedendum?

d) Has the damage a bright or dull appearance?

e) What was the nature of the original surfaces?

f) Has any surface treatment been used?

g) At what temperature has the unit operated?

h) What type of lubricant was being used?

i) Which manufacturer produced the particular lubricant?

j) Had the lubricant been changed?

k) How long had the unit been operating?

l) Were the gears spur or helical?

m) Has significant erosion occurred?

n) What has happened to the debris?

i) Magnetic plugs.

ii) Filters.

iii) Magnetically active dark film.

arbox overhauls may observe the old stained appearance it is not unusual for assembly to initiate a reawakening of the damage process. Changes in inding wheel type or machine process can bring about variation in a design sceptability to this type of damage (e).

art from the basic manufacturing methods, surface treatments can lead to mage of this nature. Phosphate anti-scuffing processes are particularly one to render the surfaces more sensitive to micropitting (f). Shot peening tooth roots may cause scatter peening of the flanks and initiate areas of cropitting. Since surface roughening makes things worse it also follows that proved oil film thickness can reduce the damage. Thus changes in oil scosity may alter the characteristics. This may mean altering the type of l used or modifying the operating temperature which can be equally beneficial as far as film thicknesses are concerned (g/h). Whilst viscosity is the st obvious variable it has been found that oils produced to a common ecification by different manufacturers can have major differences in erational characteristics. Presumably the local asperity frictional forces n be modified by additive differences (i/j).

e types of damage developed can relate to whether the teeth are of spur or lical form. Spur gears are more prone to erosive wear damage by micropitting nce the motion errors produced by the damage increase dynamic loading and celerate the process further. With helical teeth significant erosive damage sometimes found but the helical characteristics preserve the motion iformity (l/m).

ilst most of our interest is concerned with the effect on the teeth emselves it is also important to consider what happens to the material moved from the tooth flanks (n). The very small size of the fragments often ly a few microns across by a fraction of a micron thick means that this bris can be easily transported by the oil. Many filters have pore sizes rough which it can pass. The particles are, however, often large enough to ldge the oil film generated in rolling contact bearings and may be sponsible for life reductions. Sometimes the debris is retained as a gnetically adherent film on other steel components. 'Magnetic sludge' can :en be micropitting debris.

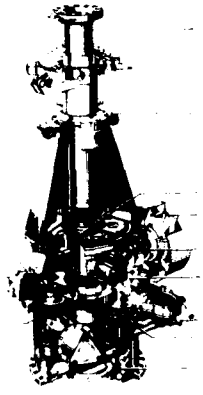
:CUSSION ON TOOTH CONTACT LUBRICATION FAILURE QUESTIONS

two previous sets of questions have related to relatively simple fatigue :cesses associated with gear tooth operation. The mechanism of oil film lure may be far more complex and is certainly less easily understood. Many ms of damage may be observed and attempts are sometimes made to subdivide damage by terms such as scuffing, scoring, ridging, rippling etc. This ses unnecessary difficulties in trying to identify which form of damage one on a particular set of components; demarcations between these effects are y indistinct. The first essential factor to look for is that both tacting areas will show similar damage effects (a). This may be influenced differential hardness so that sometimes friction-welded lumps of softer erial are smeared over the face of a harder tooth as ridges running up the th height. Correspondingly there will be grooves and perhaps evidence of n areas from which the metal has been plucked. The depth of damage can vary y considerably but the magnitude of the sliding-to-rolling action on the th and the material characteristics are probably the factors that most luence this.

New technologies which could be used were:

- Mg casting for the housing with a minimum thickness of 7 mm
- ESU steel for the gears
- Special aircraft bearings with vacuum degassed steel.

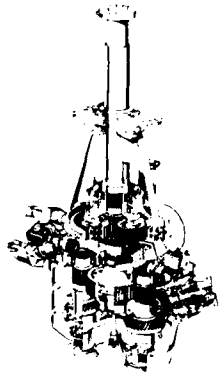
In 1977 this design has to be changed in order to allow higher power level and to increase the TBO (picture 3).



Picture 3:
FS 72 B Transmission

At that time only minor changes in the inner parts of the transmission were performed (bearings with higher capacity, the width of the bearings etc.) but the same technology was used.

MCP = 2 x 350 PS
OEI = 1 x 385 PS



Picture 4: FS 112 Transmission

In 1977 a redesign was necessary because the power level had to be increased drastically (picture 4). At that time new advantages in technology could be used:

- Mg castings with a minimum thickness of 5 mm
- New special aircraft bearings with integrated fixing devices, vacuum melted steel and optimized load carrying capacity
- Use of titanium for shafts and for the planetary carrier
- Dual oil lubrication systems-

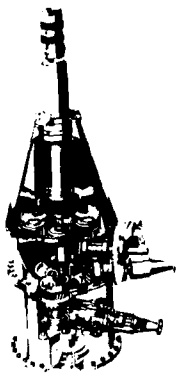
DEVELOPMENT OF DRIVE SYSTEMS

The introduction of new technologies in the past 20 years had a strong positive influence on the development of the drive systems, mainly on maintransmissions of helicopters.
This product improvement tendency is demonstrated in the following by the example of a light multi-purpose twin engined helicopter.
The development of the transmission for this two ton class helicopter began in 1962.
The design objectives for this program were:

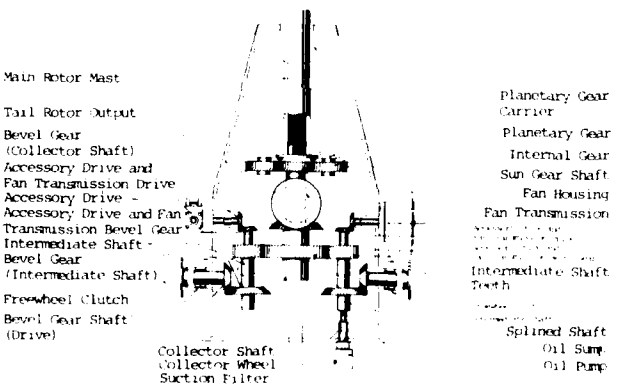
power ratings of MCP = 2 x 250 PS
OEI = 1 x 300 PS

Picture 1 shows technical details of the design, which uses all known technologies at that time, which were:

- Mg Alloy casting for the housing with a minimum thickness of 8 mm
- Standard bearings of the normal industry production with aircraft standard documentation
- Normal gear steel



Picture 1:
FS 72 Prototype Transmission



Picture 2:
Schematic drawing of the Transmission

Picture 2 shows schematically the function of this 3 stage transmission. The first stage is built up with bevel gears with a reduction rate of 1.5. The second stage is constructed as a spur gear which collects both input power trans (reduction rate: 1,71. The last stage is performed as planetary gearing with a reduction rate of 4. Additional drives for tail rotor, oil pump, hydraulic pumps and blower are activated via additional gears mounted on the 2 first stages.
In '86 the development of the production type transmission began. Besides other objectives the power level was increased by

MCP - 2 x 320 PS
OEI - 1 x 375 PS

DO NEW AIRCRAFT NEED NEW TECHNOLOGIES AND CERTIFICATION RULES?

by

Joachim Hartmann, Dipl. Ing.
Manager Drive System

and

Wolfgang Jonda, Dipl. Ing.
Manager Dynamic System

MESSERSCHMITT-BÖLKOW-BLOHM GMBH.
Helicopter and Military Aircraft Group
Postbox 80 11 40
8000 Munic 80, Germany

SUMMARY

With the example of the development steps, on a transmission usuable for a 2 ton dual engined multipurpose helicopter it could be demonstrated that new technologies improved drastically this product within approximately 15 years. From this result and from a preview on technologies in the future it could be shown, that transmissions will be further improved. The features which will be improved will change from weight reduction and life time increase to lower life cycle costs and higher safety. New technologies which will mainly influence the design are:

- New or improved manufacturing processes
- Use of computer calculation methods
- Use of testing procedure knowledge
- Use of new diagnosis systems

and to a smaller amount

- new materials.

New designs will use new technologies, but will also change the overall layout for example the available engine power. To avoid unnecessary disadvantages the certification rules should be updated.
From todays experience the area: dual engine with high power reserves, procedure for on condition establishing and certification testing should be improved. The optimum benefit will be achieved, when the certification rules could be standardized for all countries in the Western World.
It can be concluded, that new aircraft need new technologies and modified existing- or new certification rules.

INTRODUCTION

In the past 25 years the progress in aircraft development was very intensive. This fact is not only due to the advance in experience, but also because new technologies could be used step by step. If we consider the drive system of helicopters only, it can be proven that this component was major responsible for the general advantages.
If we look into the future and consider the enormous efforts in using new technologies all over the industry we can see a good potential that this trend will continue.
The existing certification rules, which have rising influence on the use of new technologies, were established in a time, when helicopters where mainly driven by reciprocating engines. With the experience of already certified helicopters these rules were continuously amended. This is one cause for relatively general rules. The load spectrum for example, which is important for the design and testing of the drive system, practiculary for the transmission, are specified in order to be valid for all helicopters.
The consequence is, that in practice, in most cases, drive systems will be either over- or undersized.
These discrepancies are well known to the certification authorities and they try to over come this by updating their regulations.

DISCUSSION

Comment: D.G.Astridge, UK

(1) The claim that motion of the localised contact region in conformal gears is a powerful source of noise generation is not borne out in our experience. Cabin noise measurements made in the Lynx helicopter show that the uprated or power-sharing version of the main gearbox is up to 9 dB quieter than the original design, whilst the conformal pinion support arrangements differ significantly in the two designs, and therefore any 'load-shuttling' influence might be expected, in fact, most of the difference is accounted for by tooth loading intensity, and follows the same relationship as involute teeth.

(2) In looking for a means of measuring TE at high frequency, a third alternative could be considered — that of short wave length FM telemetry. We have had very good experience of such torquemeters produced by EEL in the harsh operating environments of testings and helicopter main rotor gearboxes and tail rotor drive shafts. To date only mean torque has been extracted from these devices, but they have a very wide-frequency bandwidth and should be capable of extracting the high frequency T-E characteristics from this rugged and well proven hardware.

Comment: R.J.Willis, US

Hull distortion may be due to heavy sea states with the hull driving the gearbox when the thrust bearing is located near the propeller at the aft end of the ship. A different distortion mode occurs when the gearbox is charged to contain the thrust bearing and a cantilever type loading exists between the centre line of the propeller shaft (or hull gear) and the gearbox foundation.

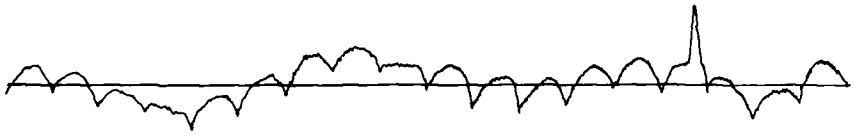


Fig. 4: Excitation with tooth damage. 1 revolution of 20 tooth gear.

giving accelerations of the order of 1 g, the vibration level at the bearing is likely to be only about 0.1% of this and to be lost in background noise. [There is an additional bonus in that background noise from the remainder of the system is likely to be lower on the gears than on the casing.] As yet this postulate has not been proven and it is, of course, very much more difficult practically to extract information from a rotating shaft than from a gearcase.

HIGH FREQUENCY TE MEASUREMENT

The practical frequency limit for gratings, as mentioned previously, is of the order of 1 kHz even when great care is taken with design. This limitation, combined with the necessity to have a free end on a gear shaft to avoid the 300 Hz limitation of a belt drive, has resulted in many attempts to devise systems which will extend the frequency range and work on a shaft to measure torsional vibration and hence TE.

Two types of system appear to have a chance of succeeding; they are:

(i) Magnetic track systems. These lay down a regular wave on either a magnetic film which is part of the gear or upon a separate magnetic tape which is then stuck on the gear. A tape head near the track should give a steady sine wave if the gear velocity is constant.

(ii) Accelerometer systems. These use two matched accelerometers mounted tangentially to measure torsional acceleration of a shaft or gear. Slip rings or telemetry are required to transmit the signal from the rotating shaft.

Although either system appears straightforward there are very great difficulties in practice and a satisfactory result has not yet been obtained but research is proceeding on this topic so that techniques should be available for the next generation of aircraft gearboxes.

It should however be observed that both systems are capable of giving false information since even if a system succeeds in measuring torsional vibration correctly, this is of little help if the system is accommodating TE principally by lateral vibration.

At the high frequencies of interest in condition monitoring, a gear pinion or wheel can no longer be considered as a rigid body. Under these circumstances, local deflections will be measured and there is a difference in that the magnetic track approach reads the local track movement at a fixed point in space whereas the accelerometers vary in position.

CONCLUSIONS

Measurement of TE is a very powerful weapon in any gearbox development where noise is of importance and can yield useful information on evenness of tooth loading and hence alignment accuracies and strength.

The use of TE or torsional vibration measurement for condition monitoring can be argued theoretically but has not been proven practically and presents difficulties.

The frequency and access limitations of existing grating systems restrict their use to helicopter gearboxes but the TE approach will extend to higher speeds for turboprop development eventually.

REFERENCES

1 Munro, R G, A review of the single flank method of testing gears. Annals of the CIRP, Vol. 28/1/79, pp. 325-329

2 Daly, K J and Smith, J D, Measurement with rotary gratings, JMES, 22, (6), 1980, pp 315-318

3 Smith, J D, Gears and their Vibration, Marcel Dekker/Macmillan, New York/London, 1983, Chs. 4 & 10

4 Daly, K J and Smith, J D, Using gratings in driveline noise problems, Conference on noise and vibrations of engines and transmissions, Inst. Mech. Eng. Aut. Div., Cranfield, 1979 (10), pp 15-20

5 Stewart, R M, Application of signal processing techniques to machinery health monitoring, Applications in time series analysis, ISVR, University of Southampton, April 1980, 16.1-16.23

length of line of contact between the teeth and by obtaining an even distribution of load along that line. The normal test for consistency and length of contact line is the bedding check but this is only reliable to about 5 micron and is usually carried out at light load only.

It is possible to have a gear drive which has good bedding and so a good low speed stress distribution but has a poor TE. Conversely it is possible to have a good TE with very high local stresses and a poor bedding pattern; this can occur with a helical mate which has good profile match but poor helix match.

Highly loaded gears in aircraft have, unlike marine gears, a facewidth of slightly over a single axial pitch with a relatively low helix angle. Such a drive, when in good alignment, will have an extremely low transmission error due to the averaging effects of the helix but the observed once per tooth error will increase as the gears are misaligned. Figure 3 shows an exaggerated case of this occuring in an automotive gearbox; at about one third of full load the alignment was good and excitation small but at higher or lower loads there were large increases in the once-per-tooth excitation component. There is correspondingly a link between the magnitude of the observed dynamic TE or vibration and the consistency of load intensity across the width of the gear. As the load moves towards either end of the teeth the TE will increase provided that the gear was originally designed well.

There is a paradox in testing helical meshes in this way because a badly designed gear will not show this effect but a gear designed for even loading across the facewidth will show it. If a gear has been crowned because of poor gearcase design or assembly uncertainties then TE will be very high, giving high vibration levels, and will not vary significantly with alignment. An even loading will give much lower vibration excitation which will vary with misalignment. Crowning, though used widely, carries penalties for both noise and increase of gearbox size and weight.

The method of testing in the case of a helical mesh is to establish the level of TE under full load and optimum alignment; this can be done by testing a 'good' gearbox or varying alignment in a test rig and should give a dynamic TE of well below 5 microns peak to peak. Once the target figure has been set, checking production gear drives is then very rapid and those which fail can be diverted for realignment.

Problems arise as in testing for noise purposes if operating speeds are high or if epicyclic load sharing systems allow movement.

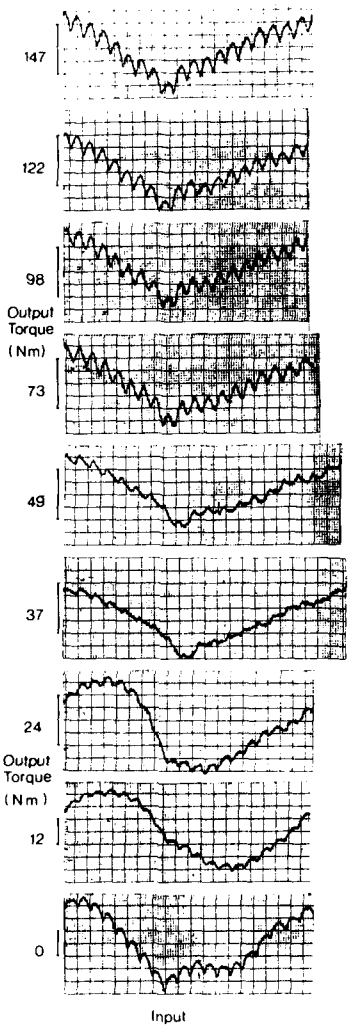


Fig. 3: Variation of TE with load torque

CONDITION MONITORING

Condition monitoring techniques for gear failure attempt to detect the initial stages of either progressive pitting or of cracking of teeth. In both cases the expectation is that the TE which is generating the 'normal' vibration will have an additional impulse imposed at the position corresponding to the faulty tooth. The resulting excitation may have the form sketched in Fig. 4 where there are pitch errors, a regular once-per-tooth and an additional high peak.

The standard procedure is to mount an accelerometer on a bearing housing and to analyse the vibration at this point. However vibration at the bearing housing has already been filtered mechanically in travelling from the mesh, which is the source of vibration, through the resonant system of gear inertias which are mounted on elastic shafts and bearings. These resonances are rarely above 1 kHz and so tend to filter out the high frequency components which are most likely to give information on small defects. In contrast the most effective monitoring techniques for rolling bearings use vibrations of the order of 20 kHz [5].

There is thus an argument to suggest that damage to gear teeth will be detected earlier or more effectively if vibration measurements are made on the gears near the source rather than on the gearcase. If we take a particular typical case and assume a tooth frequency of 1 kHz and a pinion mass of 10 kg on a combined lateral restraint stiffness of 2 10^8 N/m the important natural frequency (ignoring all other effects) will be of the order of 700 Hz. In more complex cases a full analysis can be used [3] but is rarely needed.

Damage to a single tooth, as in Fig. 4, is likely to be easiest detected at high frequencies of the order of 15 kHz and although the displacements involved at the tooth may be of the order of 0.001 micron,

Accuracy is high, effectively of the order of 0.2 seconds of arc at once per tooth frequencies corresponding to 0.25 micron at a radius of 0.25 m and is more than adequate for all but large marine gears. Speed limitations arise principally due to limitations of the electronics but these can be overcome relatively easily. Frequency limitations on the system arise principally from torsional oscillation of the grating on its shaft and flexible drive system and restrict the use of gratings to frequencies of the order of 600 Hz [2]. This assumes that there is a free shaft end from which the grating head may be driven on both input and output gear.

Ideally TE should be measured at low speed to eliminate dynamic resonance effects, with the gears in position in their casing and with full torque on the system so that all gear and box deflections are representative.

Once the gears are in position, measurement is rapid and all the information required is obtained in a minute or two, unlike conventional testing which takes a long time and uses skilled labour. Figure 2 shows a typical trace obtained.

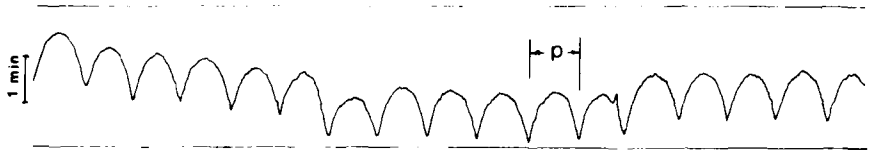


Fig. 2: TE trace. Full scale is 1 minutes of arc error, or 45 microns at 50 mm radius. p is one pitch, i.e. 1 tooth.

NOISE GENERATION

Transmission Error testing is of most direct use when noise and vibration are under investigation since in a well designed involute gear drive it is the vibrating part of the TE which is the major vibration source and reduction of TE will reduce vibration correspondingly. This does not apply for Wildhaber-Novikov gears where there is an additional powerful noise generation at once-per-tooth frequency and harmonics due to the transverse movements of the centre of pressure in the mesh [3]. This gives the effect of applying an oscillating torque to the gear and there is no effective way of compensating for this vibration excitation.

Helicopter final drives are traditionally very noisy and development of quieter drives can only be carried out by using TE checking. Conventional torque splitting drive systems and bevel drives usually have an end of each shaft "free" so that it is possible to circulate power through a back-to-back test rig and check TE under full torque over a range of speeds. This will give information on the mesh smoothness and on the internal dynamics of the gearbox [4]. The tooth frequencies involved are within the range of gratings and so information can be obtained up to full speed. In operation, loads vary very little so that the system does not have to cope with large variations of either speed or torque.

The alternative approach of measuring pitch, helix, profile, case accuracy and system distortion under load is subject to so many uncertainties that the end result is very inaccurate. Each of the 5 factors can contribute several microns to the final result at once per tooth of less than 5 microns.

A special case which presents problems occurs if the final drive unit is a conventional epicyclic gearbox since not only is space very limited within the gearbox but it is not usually possible to get access to the planets since they run on non-rotating shafts fixed to the planet carrier. Measurement of the TE from input to output of the drive as a whole is not very informative as the effects of several meshes are averaged and the gearbox is usually designed to distort dynamically to give even load distribution.

Turboprop reduction gearboxes run at higher speeds with tooth frequencies which are normally above 1 kHz so it is not possible to use gratings at full speed. On a test rig it is possible to run the gearbox at *full torque and low enough speeds to fall within the range of gratings but there are problems.* It is difficult to duplicate the engine restraint systems or the external loads imposed by a propellor and the tooth surfaces may scuff if run at high loads and low speeds. As in the case of helicopter gearboxes, epicyclic drives present problems due to rotation, lack of access and parallel paths. Any test rig must also be designed so that the return power path is torsionally much more flexible than the test gearbox to ensure that a measuring system is recording gearbox TE and not the TE of the return path.

Despite the rather taunting problems and limitations of TE measurements there is little doubt that they must be used more in the future as only measurement of TE will give an accurate and fundamental check on the cause of the gear noise.

GEAR STRENGTH

At first sight there is no valid reason for using TE measurement for checking or improving the torque capacity of a gear drive since it gives solely information on the smoothness of the drive. In contrast, neglecting dynamic effects, maximum torque from a given design is achieved by obtaining maximum

TRANSMISSION ERROR MEASUREMENTS IN GEARBOX DEVELOPMENT

J D Smith
University of Cambridge, Department of Engineering, Cambridge CB2 1PZ

SUMMARY

There is a requirement to test gears for initial development, for production monitoring and for condition monitoring in service. Traditionally the first two have been carried out by a combination of profile, helix, pitch and bedding checks and the third by measuring vibration at bearing housings.

Gear drives in aircraft applications present difficulties in checking due to high distortions in the light weight gear cases. The use of transmission error (single flank) checking can give useful information on accuracy of alignment in gearboxes as well as fundamental noise generation information. Problems arise with attempts to use grating systems in turboprops but helicopters have tooth frequencies in a suitable range.

INTRODUCTION

There are usually three stages in the production of gearboxes where it is advisable to check the characteristics of the gears. The first occurs during initial development of the prototype gearbox, the second as a routine check on the production line when it is mainly to control the consistency of manufacture and the third occurs when the vibration of a gearbox is monitored in flight as a safety check.

Until relatively recently the methods of gear checking were limited to measurements of the geometry of the individual gears, i.e. the classical measurements of profile, helix and pitch and a bedding check whose function was to confirm that contact occurred over the greater part of the tooth face. Transmission error is now used increasingly in all branches of gear work and is an extremely fast method of checking smoothness of drive; it is defined as the difference between the actual angular position of the output gear and the position it should have occupied if the drive were perfect and rigid.

Helicopter and turboprop gear drives differ from most industrial gearboxes in that, due to weight limitations, their gearcases are extremely flexible. This alters the balance of deflections under load so that whereas in a well designed "normal" gearbox it may be assumed that relative movements of the shaft centrelines are small compared with tooth deflections, this is not true for airborne gearboxes. Ships gearboxes may encounter similar problems but this is more likely to be due to hull distortion.

TRANSMISSION ERROR MEASUREMENT

Transmission error measurement (sometimes called single flank checking) is dominated by the use of circular gratings and is usually carried out at the manufacturing inspection stage. A gear may be mated with a master gear but for precision work, due to the effects of tolerance combinations, it is usual to test a gear with its mating gear.

An accurate grating with typically a line every minute of arc, i.e. 21,600 lines per revolution, is attached to the input gear which is driven at a steady speed of about 3 rpm. The sinusoidal light variation from the grating with its fixed matching index grating is converted to a string of pulses at exactly one per minute of arc. This string of pulses is then multiplied and divided electronically by the gear ratio to give the steady string of pulses that would be expected at the output if the gear drive were perfect.

Phase comparison of the actual and expected strings of pulses from the output gear grating gives the variation of phase and hence of the transmission error [1]. Figure 1 is a block diagram of the system.

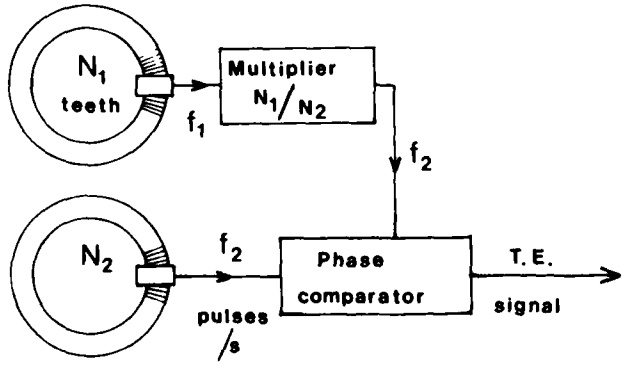


Fig. 1: Transmission error test system using gratings

problem of sharing the total losses between the two boxes. The solution presented envolves a calorimetric procedure with the sprinkling of cooling water and measurements of its flow rate and temperature rise. Assuming an error of ± 5% on the losses distribution between the two boxes and for the same referred numerical values Tournier reivindicates an improvement of four to five times over the accuracy of a single box test and the author also suggests its use for rear axles efficiency measurements. It is not clear how the referred value of ± 5% was obtained but if the previous statement is confirmed this was a possible solution for the problem, with the benefit of improved accuracy. Another efficiency analysis, but regarding helicopter transmission, was recently presented by Mitchell and Coy [5]. In this case the similarity with the procedure referred in [4] consists of the heat balance on the water running through an oil-water heat exchanger. In both cases the relevance of claimed results depend heavily on the degree of insolution actually achieved and accuracy of the referred balance.

4 CONCLUSIONS

Efficiency evaluation of gears has not been in the past a main concern probably because the values are very high compared with those of other mechanical systems. Rear axle gears have caught some general interest in this aspect because of recent automotive economy requirements. Worm gears are clearly at the bottom of the scale as regarding efficiency, but in this case it is not the economy factor that is of concern but to get a better knowledge of the actual available output.

From the brief exposition presented it is possible to conclude that some attention is needed in this field and the author would wellcome suggestions and experience contributions on this subject.

REFERENCES

[1] - Zak, P.S., Bogin Ya.I. and Goller, D.E. - "Fluid Friction in a Double-Enveloping Worm Drive" - Translation of HOBOE OCMA 3KE BMAW NHAX by ASME, Volume 18, 1964

[2] - Henriot - Traité Theorique et Practique des Engrenages, Chap VII, Paris, 1968

[3] - Merrit, H.E., "Gear Engineering"

[4] - Tournier, M - "Test Arrangement to Measure Accurately the Mechanical Losses of Gear-boxes" - "Performance and Testing of Gear Oils and Transmission Fluids", IP Symposium, October 1980

[5] - Mitchell, A. M. and Coy, I.I. - "Lubricant Effects on Efficiency of a Helicopter Transmission", Agard-CP-323, August 1982

PROBLEMS REGARDING THE PRACTICAL EVALUATION OF EFFICIENCY OF WORM GEARS

by

Prof. F.A.P. DA SILVA
CEMUL
Avenida Rovisco Pais
Lisbon 1096, Portugal

SUMMARY

Worm gears are often used in industry or domestic application (lifts) when a high transmission is required in a limited space, which prevents the option for multiple gear trains. Negative aspects of these gears are the complex geometry and high values of sliding during contact leading to low values of efficiency. For the other types of gear, spur, bevel and conical ones values are usually higher than 90% but in this case practical values of 50% may result. It is possible according to the choosen geometry to forecast the efficiency theoretically. However the lubricant behaviour is generally defined by a parameter, sometimes designated as lubricant factor, which is very difficult to ascertain with sufficient accuracy. Considerations regarding the practical determination of this factor and suggestions for testing are next presented for discussion.

1 INTRODUCTION

Geometry of worm gears are somehow complex if compared with other types of gears. Different types have been studied which mainly look for a better contact between the worm and the wheel.

Fluid friction has a major influence on the total friction but lack of lubricant or deformation of the worm axis due to loading or thermal distortion can cause the near metal to metal contact. The first situation may arise from the different positioning of the worm and the wheel relative to the sump. In the second case there is a strong influence of the worm supporting mountings, bearings clearance and allowable worm axial displacement.

Double-enveloping worm drive is probably one of the most interesting designs as it provides the better contact between teeth due to the convex surface of the worm spiral and the concave surface of the enveloping part of the wheel. It could also enligten other more simple situations. Data for geometric parameters regarding this design is presented in Ref. 1.

2 RELEVANT PREVIOUS RESULTS

The expressions for worm gears have been long established and discussed by, among others, Henriot [2].

An interesting early investigation on efficiency of worm drives was conducted by Zak and al [1], with experiments runned using a VN II PU glemash machine. In his conclusions it is mentioned that error in torque measurements at the worm shaft affects the accuracy of efficiency determination by a factor i times larger than an equal error at the wheel shaft with i being the transmission ratio. Because efficiency changes with the input choosen worm or the wheel, and the usual applications require the input at the worm, this is the bench arrangement for full use of the results. Zak mentions some precautions taken when recording the torques at worm shaft and the wheel shaft, which enable him an accuracy of efficiency determination of 0,45 per cent. He also compares the values of friction coefficient with those given by Merrit [3]. Merrit states that there is no coefficient of friction in the dry friction sense and that the term is used by him as the total viscous drag to the applied load. Whilst this work was published in 1971 there was already enough work on e.h.l. to enable him to say that this coefficient of friction should depend on pressure/temperature/viscosity of the lubricant. The coefficient of friction is influenced by the surface roughness and to some extent by the combination of materials for reasons not yet clear (sic). Today there is a better knowledge on the influence of these parameters. The rugosity parameter λ, is now established as a design variable to translate the effect of the rugosity.

A mean value of the coefficient of friction may be obtained from a mixed experimental theoretical approach from the tooth efficiency loss which is assumed to be determined in tests and geometry. This reverts us to the main necessity of bench testings.

3 GEAR BENCH TESTING

Measuring efficiency with worm gears has an inherent difficulty which results from the fact already referred that this variable assumes different values when the input element changes. In industry the input is usually made through the worm connected to an electric motor so that its high speed can be reduced to a more convenient value for mechanical applications. For industrial purposes and limited financial resources the most economical dynamometers available are of the water type. However it is necessary to go to highly oversized models so that sufficient braking torque is obtained at low speeds at which the wheel revs. The most evident solution is to use an extra train to multiply the output rotation speed but this obviously requires the previous knowledge of the efficiency of this group. A similar situation has been mentioned by Tournier [4] where two automative gear boxes have been coupled to achieve in this case a more accurate efficiency measurement. He bases his calculations on the assumption of a possible precision of $\pm$ 0,1% on speed measurements and $\pm$ 1% precision on torque evaluation. For a 95% efficiency value he concludes that with a single gearbox losses are determined with an accuracy of $\pm$ 45%. A double gearbox arrangement provides much better results but brings out the

DISCUSSION

P. de Castro, Po

I would be grateful to have the author's view of the possible application of fracture mechanics to this sort of problem (micro pitting).

Author's Reply

I think it would be difficult to consider applying fracture mechanics to micro pitting, since the nature of the applied forces are not known. The problem starts at asperity tips, so normal forces must be involved. But crack orientation is affected by the sliding direction, so traction forces are also involved. The contact zone is also subject to EHL pressures making the material properties even more uncertain. Work is being done to try to explain the mechanism of the phenomenon but not a lot has been published yet.

A.Watteeuw, Be

(1) Can "shot peening" be the original (cause) of initial "micro pitting"?

(2) Gear flanks resist this better, yes or no, against pitting (micro pitting) when they are "shot peened"?

(3) Is the case depth important with regard to micro pitting?

Author's Reply

Shot peening can make gear tooth flanks more susceptable to micro pitting. The cusps between the individual indentations are the areas where the damage initiates.

Whilst we have not seen any evidence that shot peening of flanks modifies the propagation of the micro pitting damage, there has been some evidence that it could affect the pitting limit of lower hardness machined gears.

The case depth is unlikely to affect the initiation of micro pitting. When the damage is propagating, the state of stress both within the case and at the case/pore interface can influence the way in which the subsequent damage progresses. Any surface decarburisation of the case is likely to be very important as this interacts directly with the asperity contact stresses.

There are some forms of damage which can be confused with oil film breakdown, in that they may affect both contacting surfaces (i). Sometimes low hardness materials may get into an application where the loading is too high although only for short periods. This can cause plastic deformation of the surfaces with a rippling developing in consequence. The material may often be workhardened considerably on the surface but the core material will still be soft. Typically the tips of the teeth will often show a burred edge where the plastically deformed metal has been carried over the edge. Transport of metal can also occur due to the rolling of hard particles between the teeth. Grains of sand may break down and cause abrasive wear, but in some slow speed cases they produce local plasticity which combined with the gear sliding motion can lead to a net displacement of metal over the contacting flanks. This can even happen with soft materials contaminating the lubricant. Cellulose fibres in oil can locally deform steel surfaces and again lead to plastic displacement of the surface layers.

The operational conditions may be significant when assessing a particular problem. Have there been any abnormal overloads (k)? When in the units life did the failure become apparent (m)? Early failures are often associated with a lack of running-in or fundamental inadequacies in design. But if the damage has happened well into the units life it may have been triggered off by some other form of failure. Scuffing can originate from the edge of pitting damage or even from micropitting (l). Units that have stood unused for long periods can be particularly susceptible to damage if the tooth surfaces are not well oiled before they are asked to carry load (n). The presence of water in the oil may also be a cause for breakdown occurring. Water unlike oil does not have a high pressure coefficient of viscosity and is unable to provide an adequate elastohydrodynamic lubricating film (q). In cold conditions oil jets may often not reach the gears where the oil is required and failures may be provoked by the period of running before an adequate oil flow is established.

This discussion may serve to illustrate why the scuffing load criteria used in gear design can be found to give such widely scattered results. A consistent set of results for a constant given gear design in a test rig operating under a given set of conditions will never explain all the examples of failure found in actual gear applications.

GENERAL CONCLUSIONS

I hope this paper has served to illustrate how complex the gear failure characteristics can be. Engineering text books usually suggest a much simpler situation and many people have been led astray by making simple assumptions about particular failure examples. Transmission testing is an expensive business and it is important to understand what the results really mean if progress is to be made to improve the load carrying characteristics of gearing.

It must be recognised that it is impossible for the whole surface to fail simultaneously. Sometimes some curious effects are associated with this fact: part of a facewidth only failed; perhaps only every fifth tooth damaged or diagonally striped markings. The first might indicate non-uniform load distribution (b) but this is not necessarily involved since it can be associated with blocked oil jets (o). If the gear pair has a common factor in their tooth numbers a failure can occur between two particular teeth and this will ususally transfer around the gears to each of the possible contacting teeth. Such damage may be initiated by some foreign object getting into the mesh and it may be possible to identify the tooth from which the damage started. Diagonal stripes of damage have been seen on very lightly damaged teeth where the rolling action appears to carry the generated debris up the tooth by the displaced oil where it becomes trapped and generates another welded area.

Sometimes lubricant failure is associated with heating effects (c) though it may be difficult to decide whether the oil breakdown was caused by the heating or whether the heating was caused as an after effect of the surface damage. Where the heat effects are most pronounced may be very significant. Perhaps only in the centre of the facewidth of high speed gearing is demonstrating the natural thermal gradient that can exist with such gears (e). When one end of a facewidth shows the heating effect with an adjacent bearing also showing heat problems, it is often the thermal conduction from the bearing that has caused the gear damage rather than the other way round. Heat marking on tooth tips or on unloaded flanks can be indicative of damage having occurred at an earlier stage but that subsequent running has polished off the normally contacting flank areas. Whilst it is usually denied, cases have been known where units were started up without being filled with oil. The difference in noise caused the operators to shut down quickly and fill the units again. However, the damage may have already been done which only became apparent after some thousands of hours of subsequent operation.

Apart from complete lack of oil, incorrect oils may be responsible (f). Too low a viscosity is often a cause, the selection of an oil may be difficult because of conflicting requirements in the same unit. The viscosity grade required by a gear pair is related to their pitch line velocity. But in a high ratio unit, the requirements of the high speed input stage and the low speed output stage are often very different. How to make the best compromise may often depend on different factors in different cases. For example a unit that carries high static torques such as in crane or winch duties would demand higher viscosity lubricants. If such units ran continuously they might well suffer from overheating due to the oil churning effects.

Metallurgical effects can influence the tendency towards lubrication breakdown. The use of similar hardness identical low alloy steels in the through-hardened state can be particularly susceptable to this type of failure (h). Differences in hardness between the contacting members can make significant improvements in the relative sensitivity to such breakdowns.

If it is possible to identify the areas where damage has started by early detection of metallic debris it is often possible to identify the real cause of a problem (j). In one case damage was found to start from a slight burr thrown-up by a deburring operation after grinding gear teeth. The hard edge was causing a local breakdown at the tooth end which often spread across the whole facewidth.

TOOTH CONTACT: LUBRICATION FAILURE QUESTIONS CHART D

a) Is every tooth similarly damaged on both pinion and wheel?

b) Does the damage extend across the full facewidth?

c) Has there been evidence of appreciable heating?

d) Is the damage associated with a tip/root contact?

e) Are there undamaged areas at the tooth ends?

f) Was the correct oil being used?

g) Can the gears experience torque without motion?

h) Are the contacting members of similar materials?

i) Is it really a lubrication failure?

   i) Low hardness effects.

   ii) Debris damage.

   iii) Wear.

j) Where did the failure start?

k) Have there been operational overloads?

l) Were there any previous failure mechanisms which initiated scuffing damage?

m) Where in the units life did the damage appear?

n) Had the unit stood for any appreciable period without reoiling of the tooth surfaces?

o) Has an oil jet been blocked?

p) Does the oil get to the teeth before they are asked to transmit significant torque?

q) Is there evidence of water in the oil?

Version	Specific Dual Engine Power Level (MCP) (PS/kg)	Improvement (%)	Specific OEI Power Level (PS/kg)	Improvement (%)	Time between Overhaul (h)	Improvement (%)
Prototype FS 72	4.0					
1. Production FS 72 A	4.8	BASIS	2.8	BASIS	1200	BASIS
1. Improvement FS 72B	5.2	+ 8	2.85	+ 2	1500	25
2. Improvement FS 730	5.9	+ 23	3.35	+ 20	2400 (on condition)	100

Picture 5:
Comparison of Specific Power Level on different Transmission Versions.

The usage of new technologies improved drastically the quality of the transmission as shown in picture 5, though the overall design could not be changed because the transmission was to be used in the same aircraft.

If we analyse the numbers with the first production transmission as a baseline, we can see that the first step from version FS 72 A to FS 72 B improves the specific power rate be 8 % (max.continuous power) respectively 2 % (One Engine Inoperative Power).
In the second step where new technology was used the improvements were 23 % and 20 %.
Beside the specific power increase the TBO could be drastically improved.

CERTIFICATION RULES (FAR-BCAR)

In the western world each country has its own bureaucracy for aircraft certification, which uses either the FAR- or the BCAR regulationes for civil an MIL-Specifications for military aircrafts as the baseline with small deviationes or amendments as well as different interpretationes of the paragraphs for their national certification procedure.

That means, that the tests, necessary for certification and their documentation has to be performed twice or at least in an unnecessary extended duration. This situation will hopefully be clarified on the civil side when the Joint Airworthiness Regulationes (JAR) for helicopters will be established. This is very important because cooperationes for new developments will be in the future the rule and not the exception.

Many existing helicopters use 2 engines, but the performance ratings are selected to be optimized for all engine operation, In this case the layout of the drive system has to be done for the maximum engine power level.

Modern twin engined helicopters use engines, which have a much higher power rating than necessary for the normal all engine operation, to allow to continue the flight in a large operational range by using the then existing power reserve of the remaining engine.

The existing regulations indeed consider a dual engine configuration, but is not sufficient to handle this subject, when high performance surplus for the normal dual engine operation is built in.

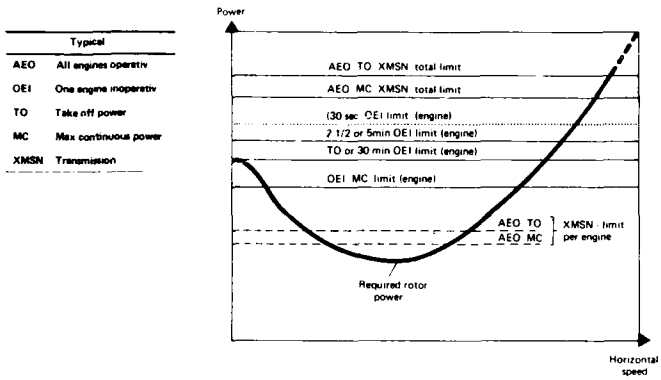
The regulations require, that the transmission has to be designed and tested to withstand the max.attainable torque. This requirement forces us to build transmissions, with power reserves, which are used only when one engine will fail and when the helicopter is operating under worst conditions regarding necessary power. Using statistics from the past, this case is only 1/3 of all engine failures.

Experience with twin engined helicopters show further, that the actual failure rate is low (approx. 1 per 1000 flight hours) depending on the engine used, power level etc. For training, maintenance actions, power assurance checks etc. it is not necessary and not allowed to use higher power ratings than the take off rating of the engines. The actual emergency case, where the max. power of the engine has to be used is so exceptional, that it can be handled, looking on the transmission layout, similar to static loads. All parts of the transmission are designed to have a safe life considering max. continuous power with one engine inoperative.

Based on actual values for gears, the stresses in this case are approx. 25 % of the static strength. The margin of 400 % is by far sufficient to handle the emergency case.

Over-sized transmission design does not influence the flight safety, but has negative effects on the [illegible] costs of the transmission.

Picture 6 showes that the main discrepancy is located between the max. continuous- and take off power of the transmission design and the intended use of the engine max. continuous, 2 1/2 min, take off or 30 min power from the view of type-testing.
With the existing regulations the test can be performed with loads from the transmission design. In this case the power loss is 50 %. If the design is performed to meet the engine performance ratings the transmission is oversized.



Picture 6:
Typical Performance Diagram of an Helicopter

NEW TECHNOLOGY

In a previous chapter it could be demonstrated that the introduction of new technologies in the past has improved the product transmission quite strongly.
The growth in specific power available shows also the effect of weight reduction possibilities, and the increase in TBO reduces to some extent the expenditure of the customers, respectively the life cycle costs (LCC). Beside of this, other features like safety, necessary spece, additional auxiliary drives etc. could be improved.
Looking in the future the trend will continue.
Special new technologies, which can be used for transmission developments, will be in the area of

- Materials
- Manufacturing process
- Diagnosis systems
- Calculation methods
- Testing procedures

Materials

New materials, such as Fibre Reinforced Plastics (FRP) which will strongly influence the configuration and design of all aircraft structures, will be of minor interest for transmissions.
Taking into account the existing knowledge, only the components housing, suspension system and to some extend the rotormast can probably be improved by this materials. But it will take a long time to get the same level of experience compared to today's standards.
For the other components like shafts, bearings and gears, which are the high cost and high weight parts, the now used steels and titanium will be used also in future designs. An overall improvment, which will be measurable cannot be seen at least for the near future.
Ceramics, which have some properties favoring them as bearing materials, need some further development steps. The optimum use of such bearings need a different overall design of transmissions, not allowing the use of metal bearings as back up solutions, which means a very high risk. The further development, currently done in this area for engines will show, if it is worth to use them.

Manufacturing process

Todays design needs a very high quality standard in the manufacturing processes (close tolerance work ISO 5 to ISO 4; surface roughness ≈ 1 µ). To achieve this in a series production line, a lot of series connected working and control cycles are necessary. With new automatically self sustaining manufacturing processes a cost reduction as well as closer tolerances may be possible.
This could improve the design, with respect to lower weight and smaller space.
Now available Mg alloy sand casting processes allow a minimum wall thickness of 5 mm. From the design requirements a minimum wall thickness of 2 mm will be sufficient to guarantee stiffness and a safe stress level. If the technology in casting processes will be improved similar to what was happened in the past, a quite attractive weight reduction can be achieved.
The application of HIP (Hot Isostatic Pressure) processes for bearings, gears and shafts is for the component maintransmission of helicopters with the knowledge of today not possible. Even for auxiliary drive pad the attainable quality standard is not sufficient.
Today's designs use titanium and steel for gears, where titanium is building the shaft and wheel body and steel the gear tooth. Both parts are connected via bolts or screws.
If new welding processes would allow the same level of safety for the connection of those parts, lower weight designs will be possible. Such welding processes could further enable designs which use gears with complicated shapes, which are not possible to be manufactured in one piece. This would allow designs with improved features such as weight, bearing distances etc.
The technology standard of bearings is relatively high. Further improvement which can be used in transmission design could be: integrated ball bearings similar to now used roller bearings, where the inner or outer bearing ring is an integrated part of the shaft or the gear. Another bearing development, where two or three different bearings are integrated to a common unit could improve the features of the transmissions.

Diagnosis systems

The powerful developments in electronics in the past have also influenced industry to develop components, which are usable for a condition monitoring and diagnoses system, in transmissions.
The last step to begin with the most difficult in this field, would be a system, which can show the condition, necessary maintenance actions, the rest of life time etc. at any time. This may be possible and payable in the far future, when the development in electronic and on other components like sensores will continue with the same speed.
In the near future the advance will take place only in small steps, because all new possibilities like vibration analysis, oil analysis, particle detection, boroscop informations etc. have to be tested very intensively before they can be used.

Calculation methods

Finite Element programs and other calculation software are used today similar to a slide rule 25 years ago. With these tools it is possible to check all deformations which results from inner and outer forces and to optimize the positions of gears, bearings and attachment points. This will reduce development-time and -costs and will provide a safer design.

Testing procedures

Since certification rules have been established valid for helicopter drive systems, the knowledge in testing and the safety in the interpretation of the results have been considerably improved. This will continue, because the development of the necessary software (application of computer systems) as well as of the hardware (sensors) will continue at least with the same speed.
To use the new information for the product transmission it is necessary to think about changes in the certification rules. The necessary tests are strongly recommended due to load spectrum and duration.
A consideration of the actual load spectrum cannot be incorporated in a simple way in the tests.
Further the certification rules require

ground tests
flight tests
overload tests.

Additional tests, for example in a test rig, which are necessary to assure the design in an early stage, cannot be used always for certification purpose. Though enough test information is available from such tests, additional tests, which do not give more information have to be performed. Also here a change in certification requirements could improve the situation.

TBO OR ON CONDITION OPERATION

With the certification of an Helicopter the manufacturer has to establish a list in which all parts responsible for flight safety are listed with data about their life time and about necessary maintenance actions. These instruction have an important influence on the operating costs of the helicopter. The manufacturer has therefore a strong interest to establish numbers which allows low cost procedures. This is contrary to the overall requirements within the certification rules. The procedure of today, to establish this data, is that in the beginning of the helicopter operation the transmissions have to be overhauled with fixed TBO's (Time Between Overhaul) and in addition to that with MTBR (Mean Time Between Removals) for life time restricted parts. To fix these TBO's and MTBR's the following steps are necessary

1. Fatigue test (with components and the total system)
2. Flight load results
3. Life time calculations.

The calculations with this information has to be performed very conservatively to stay within the limits for the worst case. Therefore the TBO development has to be started at a very low level and will be increased step by step after the availability of overhaul results up to the forecasted time. This is a very long procedure.

To shorten this establishing procedure and to cover all unknown load spectras the design of the drive system has to be done very conservatively. The result is that automatically the drive system weight and the operational costs for costumers which do not always operate on the limits are too high with no benefit due to flight safety.

To overcome this for existing designs and new designs in the future the TBO-idea will be dropped step by step and will be replaced by an "on condition system". The wording "on condition" means, that maintenance and overhauls or replacements have to be performed pending on the existing condition with its specific accumulated load spectrum in service. That requires, that the flight loads and the other conditiones of a drive system in service have to be recorded continuously.

For achieving this goal each helicopter manufacturer has its own philosophy. It shall not be discussed in this paper which philosophy or which technics is the optimum.

If an on condition concept will be created instead of a TBO from the beginning, more component testing is necessary. This additional testing could be compensated to a certain extent if the authorities would decrease their different requirements for the basic certification.

A proper working on condition system is the basis for reducing scheduled maintenance and overhauls as well as a too early part change and allows the optimized use of helicopters under different operational requirements, with an increased - or at least equal level of safety. But it requires a complete change in thinking from the manufacturer, the authorities and maintenance personal with new maintenance - and documentation technics.

ESTABLISHMENT AND MAINTENANCE OF CERTIFICATION STANDARDS FOR HELICOPTER AND TURBOPROP POWER TRANSMISSION SYSTEMS

by
Harold W. Ferris
Manager, Propulsion Branch, ACE-140C
FAA DOT
Chicago Aircraft Certification Office
2300 East Devon Avenue
Des Plaines, Illinois 60018
USA

SUMMARY

This paper discusses how the Federal Aviation Administration (FAA) develops qualification/certification safety standards for helicopter and engine turboprop drive systems. The rules are always generated in coordination with industry for a minimum of economic impact, and are worded to promote design innovation while maintaining adequate safety. The rules are periodically updated to account for service experience and advancements in the state-of-the-art.

A survey of the applicable Federal Aviation Regulations (FAR's) explains how all safety aspects of a new drive system are covered during the initial certification program. The FAR's also provide for continued airworthiness, as service experience is accumulated, such that inspection intervals may be increased to "on condition," or decreased, if service difficulties indicate that an area of redesign is required. As further testing continues, initial limitations on component replacement times are relaxed until operating costs decrease to a minimum as the design reaches maturity. The FAA role is to assist industry in the promotion of aviation without compromising safety.

Finally, a reference to the author's 1969 and 1979 papers on the subject of improving reliability and safety of drive systems is discussed with an update of additional concerns to the 1984 time frame. Some recent problems are listed.

PREFACE

The helicopter and turboprop drive system technology and arrangements are changing for higher power/weight ratios, reliability, operating cost, and new conceptual configurations like the tilt rotor XV-15. The FAA's rules and organization for the certification process and continued airworthiness activities are also changing. A new Helicopter and Engine Directorate organization is developing new rules and advisory material. The public is demanding a higher level of safety as helicopters are being deployed more and more for carrying people. The number of turboprop commuter operations is expanding at a high rate after deregulation of the airlines and higher fuel costs forced the pure jet aircraft to longer routes. Product liability litigation is causing great concern in the U.S. Congress as well as with manufacturers and operators.

The role of the FAA is to promote aviation while maintaining an adequate level of safety. Improved interface and better understanding is needed between the certifying agencies and the aviation community as we face an uncertain economic future.

This much needed paper, by an author with both industry and FAA certification experience, attempts to bridge the gap between the technical disciplines of the drive system designers and the certification engineers. We must understand each other's roles and missions and work together as a team to solve the problems before us.

THE WHY, WHAT, AND HOW OF CERTIFICATION STANDARDS

1. WHY RULES AND GUIDANCE

The qualification and certification procedures are in place to assure minimum safety standards for the intended use of the aircraft. They must be acceptable to the public and yet must also be economically attainable to assure healthy growth of the industry. No one applicant should be placed at a disadvantage with any others worldwide, hence the need for standardization of rules and interpretation.

The Federal Aviation Regulations (FAR's) are the U.S. equivalent of the European rules, such as the British Civil Airworthiness Requirements (BCAR's). Although the specific rules of the various countries which participate in the bilateral agreements are somewhat different in text and philosophy, they ensure equivalent levels of safety. Aircraft once certified via the bilateral agreements of any participating country can be exported to other countries and receive an airworthiness certificate for operation by that country's certification agency. Therefore, the free world has developed rules that are similar in scope and standardized for all their aircraft, propeller, and engine manufacturers.

The U.S. now has 12 geographically located aircraft certification offices (ACO's), including the European office in Brussels, and to ensure standardization of policy with uniform application of the Rules, 4 Directorates, each responsible for transport category airplanes, small airplanes, helicopters, or engine/propellers. Since 1982, all significant helicopter and engine certification programs are controlled through the ACO's by the Helicopter Directorate in Fort Worth, Texas and the Engine Directorate in Boston, Massachusetts. Sufficient staffs have been assembled in the directorates to assure technical and policy expertise needed to provide for rule changes and guidance material. Each

directorate is currently programmed to provide Advisory Circulars (AC's) that outline acceptable methods of compliance with all the certification FAR's. The engine rules (FAR 33) were recently updated by Amendment 10 to FAR 33, and the Helicopter Regulatory Review is a major activity reaching a conclusion at the Helicopter Directorate. Additionally, each major certification program has a directorate project officer to provide necessary policy to the ACO project engineers and to assist the U.S. and foreign ACO's when requested. The new FAA certification system is working well and is expected to be a great improvement over the previous understaffed Washington Headquarters organization with its now obsolete orders and directives system.

Since the FAR's do not normally specify how to design a drive system nor show compliance, guidance material is needed by both large and small companies with and without staffs of certification engineers. The large companies with certification experience and know-how must deal with new rules and policy for state-of-the-art developments. The small companies and modifiers with limited engineering staffs often need assistance and guidance from FAA specialists to complete a satisfactory certification program. Therefore, extensive AC's which are nonregulatory are being developed through public conferences so that inputs are received from all elements of the aviation community, both U.S. and overseas.

2. WHAT ARE THE DRIVE SYSTEM RULES

The FAA certification rules (FAR's) and Advisory Circular policy are contained in the documents shown in Fig. 1. Compliance with the pertinent FAR's is required by law prior to the issuance of a type and airworthiness certificate for an aircraft. The aircraft must be flown and maintained according to the operating FAR's which are not a subject of this paper.

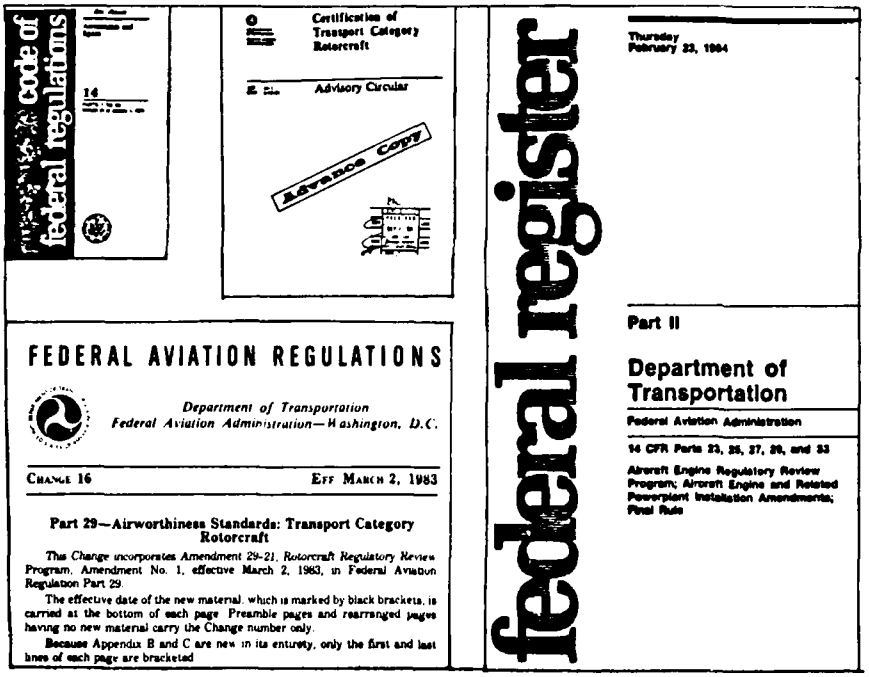


FIG. 1 THE CERTIFICATION FAR'S

A major certification program is conducted with close coordination between the applicant and the ACO project engineers through frequent contacts and the more formal Type Board Meetings. The purpose is to assure acceptable means of compliance for all the pertinent FAR's. A checklist or certification program plan is coordinated, early in the program, to properly address all requirements to assure a cost effective program. Considerations for a transport helicopter drive system certification plan follow (similar requirements exist in FAR 27).

Structural Analysis

FAR's 29.571, 29.923(m), and 29.907 Fatigue Evaluation
FAR's 29.301, 29.303, 29.305, 29.307, 29.309, and 29.361 Static Strength
FAR 29.901(b)(2) Assure Safe Operation Between Inspection Periods
FAR 29.927 Overtorque, Overspeed and other special tests

Compliance to the above rules requires tests and analysis. A stress report showing adequate static margins and safe fatigue life of all critical components is required. Such components as gears, driveshafts, gearshafts, bearings, flexible couplings, housings, and pylon support structure must be

included in the stress report. American Gear Manufacturers Association (AGMA) and Anti Friction Bearing Manufacturers Association (AFBMA) standards are acceptable for gear and bearing analysis. Fatigue Analysis Guidance is contained in Order 8110.9, January 1975, and AC 20-95, May 1976. Most applicants eventually develop their own fatigue methodology and obtain FAA approval. In all cases, the assumed loads and mission spectrums must be supported by flight strain surveys and a rational analysis of the assumed maneuver spectrum. The FAA is currently evaluating damage tolerance concepts but, so far, safe life has been the predominant philosophy for drive system components. Of course, all critical components must be analyzed to show a positive margin for design limit static loads. Some, such as castings, are specified in the rules (FAR 29.621).

A simplified and conservative common approach to the fatigue analysis is the Goodman Diagram as shown in Fig. 2. For analysis only, B = 1/3 A. A new drive system should be conservatively designed for future engine growth with few components showing a limited life.

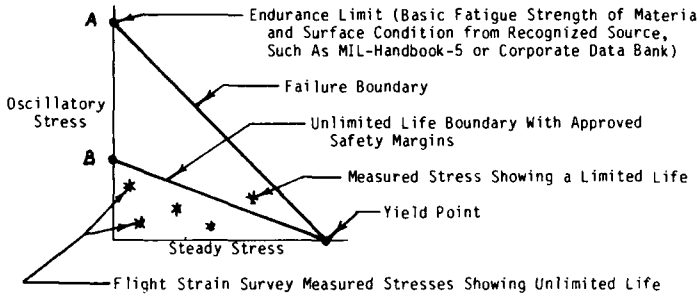


FIG. 2 GOODMAN DIAGRAM

Subpart D - Design and Construction

FAR's 29.601, 29.603, 29.605, 29.607, 29.609, 29.611, 29.613, 29.619, 29.621, 29.623, 29.625 Design Considerations

Although the above FAR's deal primarily with airframe design, they are also applicable to many drive system components, such as cast housings and their interface with aircraft structure. Of particular significance for drive shaft couplings is the 29.607 Fastener rule which requires double locking features for rotating fasteners. Advisory Circular 20-71 provides guidance material on acceptable methods of compliance.

Subpart E - Powerplant

This is the main section for drive system certification and includes the ground tie-down endurance tests.

FAR 29.901 Installation - stress reports

FAR 29.907 Engine Vibration - torsional vibration compatibility with the drive system and rotor inertia
- oscillatory stress evaluation of drive system components including engine

FAR 29.917 to 29.939 Rotor Drive System - These rules specifically deal with required testing for endurance, overspeed, transient torque, One Engine Inoperative (OEI) operation, shaft critical speeds, torsional stability and engine interface characteristics.

FAR 21.35 requires that the drive system, after the 200-hour endurance test teardown, be reassembled and used for Function and Reliability (F&R) Flight Tests. This rule is often overlooked which is a good reason for requiring the compliance checklist.

FAR 29.1163 Accessories - These components are installed on turboprop gearboxes and helicopter transmissions. The rule requires a method to prevent drive train damage in event of accessory seizure.

Subpart F - Equipment

R's 29.1301(a)&(d), 29.1305, 29.1322, 29.1337 and 29.1461 relate to environmental aspects (cold weather), instruments, markings, warning and caution lights, diagnostics and ECU/APU high energy rotors.

Subpart G - Operating Limitations

FAR's 29.1521, 29.1529, 29.1549, 29.1551, and 29.1581 relate to powerplant limitations, instrument markings, and Aircraft Flight Manual limitations. These sections become very important when the drive train is torque limited instead of the engine, and when OEI transients are tested and found to be higher than anticipated. The subpart now requires a maintenance manual in 29.1529, Instructions for continued airworthiness, in accordance with Appendix A, which outlines an Airworthiness Limitations Section approved by the Administrator. This section includes component mandatory replacement times and inspection intervals.

The FAA rules, described above, are complete as to general compliance requirements, and guidance material is provided describing acceptable, but not the only means, for showing compliance. The FAA does not provide a design guide nor get involved in dictating design. The U.S. Army, on the other hand, does provide design and test requirement standards as shown in Fig. 3. These very comprehensive documents, AMCP 706-201, 202, and 203, become part of the helicopter model specification and many chapters are devoted to drive system technology. The chapters were written for the U.S. Army by authors from industry who were regarded as experts in their fields. No drive system engineer should be without these safety oriented manuals. They may be obtained from National Technical Information Service, Dept. of Commerce, Springfield, Virginia 22151. The U.S. Army procures, qualifies, develops, operates, and maintains more helicopters than any other entity in the free world. Their mission spectrum, less the battlefield environment, is often similar to that of our civil fleets.

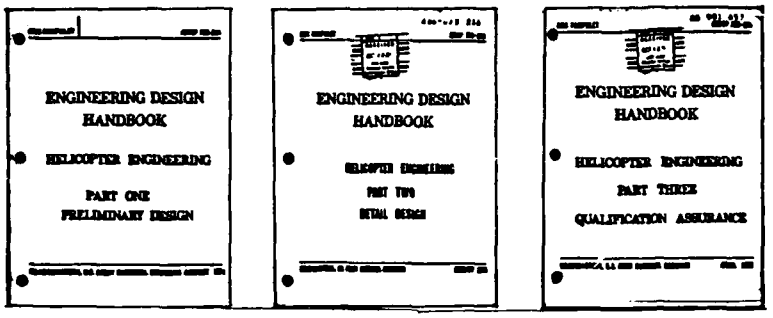


FIG. 3 U.S. ARMY STANDARDS

3. HOW ARE THE RULES DEVELOPED AND MAINTAINED

The FAA certification rules (FAR's), when formally issued, are legally enforceable as law, and all civil aircraft must comply prior to the issuance of a type and airworthiness certificate. These rules are related to safety of the public and have been developed over the years to enhance safety in a manner that promotes the growth of civil aviation. They are constantly being updated for clarity and improved safety as experience dictates. State-of-the-art developments require new or modified regulations. Amendments are thoroughly coordinated with industry, the public and world certification agencies. This section describes the complex procedure involved in promulgating a rule change.

The FAA periodically establishes formal Airworthiness Reviews by establishing a multiyear program initiated by a call for proposals. In 1978, industry requested a comprehensive reassessment of rotorcraft certification rules which resulted in the current Rotorcraft Regulatory Review Program and a call for proposals. Any individual or organization worldwide may submit proposals which are reviewed for compilation into an agenda for a public conference discussion. Figure 4 shows a typical proposal which was submitted by the author and compiled in one of the volumes presented at the Rotorcraft Regulatory Review Conference held in December 1979. The propulsion session FAA team of Messrs. Bud Wells and Hal Ferris discussed each drive system proposal with interested members of the audience until all comments were made and recorded. The FAA team later reviewed the notes and recordings to evaluate each proposal for a disposition of (1) proceed with no changes, (2) combine, expand, and revise, (3) defer for more information, or (4) drop for lack of support. The surviving proposals then had to pass a rigorous economic analysis to prove that the safety benefits outweighed any burden on the industry or public. The drive system proposals then become a Notice of Proposed Rulemaking (NPRM) inviting comments and are scheduled for publication in the Federal Register as Notice No. 3. All public comments will be analyzed and discussed. Proposals may be revised or deleted in acccordance with comments in the preamble of the Final Adopted Rule also published in the Federal Register. This amendment then becomes law and all applicants for a Type Certificate, after the published date, will be required to comply with the updated drive system rules.

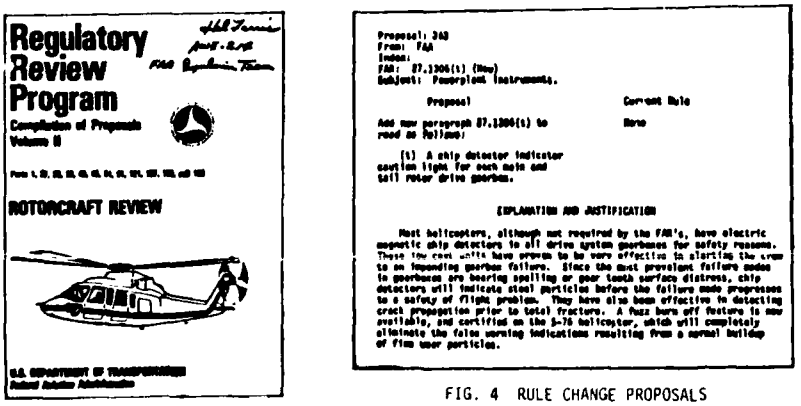


FIG. 4 RULE CHANGE PROPOSALS

It can be seen that the drive system certification rules are developed through a lengthy process with detailed coordination for all interested members of the public. Our philosophy is to provide standards that remain dynamic to changes in technology, yet do not stifle innovation in design, but retain a minimum level of safety. The system is working judged by the safety records and growth of the industry.

CONTINUED AIRWORTHINESS

The post certification life of the drive system may be a very difficult period, and the safety implications must be constantly monitored and addressed whenever a service difficulty is reported. On the other hand, the original Time Between Overhaul (TBO), a low time estimate based on limited testing, may be demonstrating all parts to be airworthy at overhaul after early fleet service evaluations. When the final design has matured, the TBO should eventually be increased in increments to perhaps "on condition" maintenance.

1. Service Difficulties - FAR 39 provides for a system of Airworthiness Directives (AD's) whenever an unsafe condition is discovered that may be repeatable for aircraft in service. FAR 21.99 requires a design change or inspection, if necessary to correct an unsafe condition, and the Type Certificate (TC) holder must provide a means to notify operators of corrective action, called Service Bulletins, Alert Notices, etc. An AD usually incorporates the Service Bulletin which, in effect, makes the contents of the Service Bulletin mandatory. Most service difficulties, however, do not warrant the rulemaking of an AD. The field maintenance activities may be advised of possible serious problems or trends by Service Bulletins and the FAA AC No. 43-16, "General Aviation Airworthiness Alerts," published monthly. Its purpose is to improve reliability and interchange service experience. The National Transportation Safety Board (NTSB), an independent branch of the government that investigates accidents, as a result of accident investigations, may recommend action to the Administrator. These recommendations must be satisfactorily answered by the FAA after its investigation and coordination with the TC holder. Sometimes accident prevention recommendations are received from FAA Flight Standards District Offices (FSDO's) and must be investigated by coordinated effort between FAA ACO project engineers and the TC holder. Accidents may require the drastic action of a Certification Review Team or Special Safety Team which could lead to grounding of aircraft.

Most of the service difficulties, however, are not so clearly defined. The FAA has established a computerized service difficulty reporting program whereby everyone in the field is encouraged to report Malfunction or Defect (M or D) Reports on special forms or cards which are mailed to FAA General Aviation District Offices (GADO's) for distribution through the system. The original cards end up with the Aircraft Certification Office project engineer assigned to the affected TC holder. These card inputs become agenda items for periodic service difficulty meetings with the manufacturer. Corrective action is usually coordinated for type design changes and/or service manual information via service letters or bulletins. If the difficulty is not an isolated case and further information is needed, up to a five-year computer run of all cards submitted may be easily obtained. This procedure is used where AD action may be indicated. Unfortunately, only a small percentage of problems are reported so they are used to supplement the problems already known by the TC holders Service Department. The exchange of this type of information is a two-way street, since FAR 21.3 requires the TC holder to inform the FAA within 24 hours certain prescribed failures, malfunctions, and defects. Of course, all accident reports are cooperatively investigated, and corrective action is developed.

2. Extension of Inspection Periods - A new transmission and drive system, at the time of the Type Certificate, will have a minimum of endurance and fatigue testing and no service experience. Therefore, the initial inspection intervals, and/or TBO's, and published mandatory replacement component lives may be low. As the design matures with service experience and additional fatigue test specimens, the TBO and lives will be increased.

The FAA, TC holder, and high time operators will establish a TBO escalation program where sample units will be carefully monitored and include engineering evaluation of teardown inspections. These post service evaluations and a close monitoring of the fleet performance will permit a continuous escalation of inspection intervals. As more fatigue specimen components are tested, lower reduction factors may permit an increase in the published replacement lives.

The design goals should provide margin for growth and an adequate diagnostic system to attain "on condition" maintenance. Fail-safe and damage tolerance concepts will improve safety and reduce cost of operations. Invariably, the drive system rated powers will increase as the next model engine is certified. The best method to increase ratings, aside from the required testing, is to have few life limited parts and a good record of service experience.

CONCLUSIONS AND SPECIAL CONSIDERATIONS

This paper has described the what, why, and how of the certification process and continued airworthiness after the Type Certificate is awarded. In these days of high product liability costs, your certification agency can be your best friend. A close working relationship and teamwork during and after the certification program will benefit all of us - especially the public.

To supplement the referenced papers of 1969 and 1979, the following case histories from the recent past are listed along with ways to avoid observed problem areas.

1. Lightening holes in gearshaft flanges presented unrecognized fatigue stress risers which led to an early fatigue failure and an accident.

2. One Engine Inoperative (OEI) torque transients to 140% were found in flight strain surveys which caused a reanalysis of the static support structure design limit load 125% margin.

3. Ground-Air-Ground (GAG) load cycles in the mission spectrum were fatigue damaging and may occur every five minutes in sling load operations.

4. Critical bearings should be consumable electrode vacuum remelt (CEVM), M-50 or equivalent material of high hot hardness, ABEC quality grade of 5 and should be 100% inspected as aircraft bearings. An L_{B10} bearing life calculation is insufficient for the high reliability requirements of helicopter transmissions or turboprop gearboxes.

5. Chip detector cautionary lights are necessary - one transmission uses five detectors, and a turboshaft engine uses three with a requirement for cockpit caution lights. The argument on false warnings is no longer appropriate with latest state-of-the-art chip detectors with fuzz burnoff features.

6. Tie-down loads during the FAR 29.923 endurance tests with full control travels exceeded design limit loads. Strain gage the output driveshafts and do not exceed design limit loads - reduced control travels may be adequate. (An AC is currently in work.)

7. With FAA approval, use overload (bench) testing, at high cubic mean average loads, to qualify alternate oils, design changes, and to supplement the FAR 29.923 minimum endurance test requirement.

8. Address operation in very cold weather and provide operating manual information if preheating is required because of clearance problems on bearings and gears.

9. Use flow-through oil on hardened free floating splines to avoid wear and fretting and avoid high stress riser keyways.

10. Provide oil system redundancy in critical oil lubrication areas and use 10 micron or lower filters with bypass indicators.

He who is ignorant of history is condemned to repeat it. (Santayana)

The views and opinions in this document are those of the author and may not represent the official position of the FAA.

REFERENCES

1. Ferris, H. W., "Development of the OH-6A Drive System for RVN Load Spectrums," 25th Annual National Forum Proceedings, American Helicopter Society, 217 N. Washington St., Alexandria, VA 22314, May 1969

2. Ferris, H. W., "Safety Considerations for Helicopter Drive Systems of the 1980s," Helicopter Propulsion System Specialists' Meeting, American Helicopter Society, November 1979

DISCUSSION

D.G.Astridge, UK

I welcome the author's opening comment that the FAA is the designer's friend. Certainly I can confirm that an extremely helpful relationship exists between our company, FAA, and CAA. The method of working with CAA – the design authority being devolved to the manufacturer, through the Chief Designer, and the CAA maintaining a monitoring function to ascertain that the design meets their airworthiness requirements – seems a good formula. The author's illustration of proposal 363 appears to indicate that the FAA is getting involved in detail design activity, usurping the Chief Designer's task – this is a disturbing trend in that it requires that the FAA be totally aware of all detail design technology – this is normally generated by the helicopter and engine manufacturers.

Author's Reply

We would not consider a requirement for a health monitoring system for engines and gearboxes any different to the current lesser important temperature and pressure indicators requirement. The proposal I submitted for chip detectors, or equivalent, as will be published as an NPRM in the Federal Register soon, will be worked to include, "other means," such as vibration detectors needed for gearboxes using grease where chip detectors would not be appropriate. The FAA does not dictate design details and the method used will be at the discretion of the applicant. We should mandate safety features when the state-of-the-art has been developed and the the system is obviously cost-effective and provides for an increased level of safety. I know of no helicopters or engines, when the proposal was submitted 6.3 years ago, that are not already equipped with chip detectors – most with cockpit indicator lights.

Through the certification process, the FAA does get involved with and understands the detail design process of each manufacturers's type data approval. We therefore keep up to date with the state-of-the-art for all of industry – not just one applicant. This process has been very successful in the free world certified aircraft and the safety record continues to improve.

Comment: E.Covert, USA

Comment for clarification of Mr Astridge's remark.
The CAA certification selects the designer and he is responsible for seeing to it that his design satisfies airworthiness. The FAA on the other hand allows the designer to design to standard but the design must be proved to FAA to meet standard by test or other means.

J.Worm, Ge

(1) Did you require to leave the chip detector light in the instrument panel, or is it possible to put the light outside of the cockpit on a panel right on the additional gearbox?

(2) Where more than one manufacturer who makes burn-off chip detector systems (Tedeco)?

Author's Reply

It would be our intent to have one caution light on the pilot's enunciator panel with a provision to determine which sensor (location) is showing evidence of a chip in the oil system. It is now apparent that a record should be kept of those indications that were burned off or "zapped" by the capacitive discharge – perhaps by a counter of actuations of a burn-off button. This is because on lightly loaded engine bearings where skidding is likely, the bearing can wear out to failure with only fine particles being generated. The heavily loaded gearbox bearings and gears will generate larger particles under the spall mode of failure and these must be investigated by an appropriate maintenance programme.

To my knowledge, the first Tedeco zapper was certified by our office on the S-76 helicopter. The other chip detector manufacturers have not developed the necessary burn-off feature to eliminate false alarms.

AGARD
NATO OTAN
7 RUE ANCELLE · 92200 NEUILLY SUR SEINE
FRANCE
Telephone 745.08.10 · Telex 610176

DISTRIBUTION OF UNCLASSIFIED AGARD PUBLICATIONS

AGARD does NOT hold stocks of AGARD publications at the above address for general distribution. Initial distribution of AGARD publications is made to AGARD Member Nations through the following National Distribution Centres. Further copies are sometimes available from these Centres, but if not may be purchased in Microfiche or Photocopy form from the Purchase Agencies listed below.

NATIONAL DISTRIBUTION CENTRES

BELGIUM
Coordonnateur AGARD – VSL
Etat-Major de la Force Aerienne
Quartier Reine Elisabeth
Rue d'Evere, 1140 Bruxelles

CANADA
Defence Scientific Information Services
Dept of National Defence
Ottawa, Ontario K1A 0K2

DENMARK
Danish Defence Research Board
Ved Idraetsparken 4
2100 Copenhagen O

FRANCE
O.N.E.R.A. (Direction)
29 Avenue de la Division Leclerc
92320 Châtillon

GERMANY
Fachinformationszentrum Energie,
Physik, Mathematik GmbH
Kernforschungszentrum
D-7514 Eggenstein-Leopoldshafen

GREECE
Hellenic Air Force General Staff
Research and Development Directorate
Holargos, Athens

ICELAND
Director of Aviation
c/o Flugrad
Reykjavik

ITALY
Aeronautica Militare
Ufficio del Delegato Nazionale all'AGARD
3 Piazzale Adenauer
00144 Roma/EUR

LUXEMBOURG
See Belgium

NETHERLANDS
Netherlands Delegation to AGARD
National Aerospace Laboratory, NLR
P.O. Box 126
2600 AC Delft

NORWAY
Norwegian Defence Research Establishment
Attn: Biblioteket
P.O. Box 25
N-2007 Kjeller

PORTUGAL
Portuguese National Coordinator to AGARD
Gabinete de Estudos e Programas
CLAFA
Base de Alfragide
Alfragide
2700 Amadora

TURKEY
Department of Research and Development (ARGE)
Ministry of National Defence, Ankara

UNITED KINGDOM
Defence Research Information Centre
Station Square House
St Mary Cray
Orpington, Kent BR5 3RE

UNITED STATES
National Aeronautics and Space Administration (NASA)
Langley Field, Virginia 23365
Attn: Report Distribution and Storage Unit

THE UNITED STATES NATIONAL DISTRIBUTION CENTRE (NASA) DOES NOT HOLD STOCKS OF AGARD PUBLICATIONS, AND APPLICATIONS FOR COPIES SHOULD BE MADE DIRECT TO THE NATIONAL TECHNICAL INFORMATION SERVICE (NTIS) AT THE ADDRESS BELOW.

PURCHASE AGENCIES

Microfiche or Photocopy
National Technical
Information Service (NTIS)
5285 Port Royal Road
Springfield
Virginia 22161, USA

Microfiche
ESA/Information Retrieval Service
European Space Agency
10, rue Mario Nikis
75015 Paris, France

Microfiche or Photocopy
British Library Lending
Division
Boston Spa, Wetherby
West Yorkshire LS23 7BQ
England

Requests for microfiche or photocopies of AGARD documents should include the AGARD serial number, title, author or editor, and publication date. Requests to NTIS should include the NASA accession report number. Full bibliographical references and abstracts of AGARD publications are given in the following journals:

Scientific and Technical Aerospace Reports (STAR)
published by NASA Scientific and Technical
Information Branch
NASA Headquarters (NIT-40)
Washington D.C. 20546, USA

Government Reports Announcements (GRA)
published by the National Technical
Information Services, Springfield
Virginia 22161, USA

Printed by Specialised Printing Services Limited
40 Chigwell Lane, Loughton, Essex IG10 3TZ

ISBN 92-835-0372-4

AGARD Conference Proceedings No.369
Advisory Group for Aerospace Research and Development, NATO
GEARS AND POWER TRANSMISSION SYSTEMS FOR HELICOPTERS AND TURBOPROPS
Published January 1985
396 pages

The Conference Proceedings contain 32 papers presented at the Propulsion and Energetics 64th Symposium on Gears and Power Transmission Systems for Helicopters and Turboprops, which was held 8–12 October 1984 in Lisbon, Portugal.

The Technical Evaluation Report is included at the beginning of the Proceedings. Questions and answers of

P.T.O.

AGARD-CP-369

Gears
Power transmission systems
Helicopters
Turboprops
Tooth failures
Transmission systems
Drive trains
Roller bearings
Tribology
Lubrication

AGARD Conference Proceedings No.369
Advisory Group for Aerospace Research and Development, NATO
GEARS AND POWER TRANSMISSION SYSTEMS FOR HELICOPTERS AND TURBOPROPS
Published January 1985
396 pages

The Conference Proceedings contain 32 papers presented at the Propulsion and Energetics 64th Symposium on Gears and Power Transmission Systems for Helicopters and Turboprops, which was held 8–12 October 1984 in Lisbon, Portugal.

The Technical Evaluation Report is included at the beginning of the Proceedings. Questions and answers of

P.T.O.

AGARD-CP-369

Gears
Power transmission systems
Helicopters
Turboprops
Tooth failures
Transmission systems
Drive trains
Roller bearings
Tribology
Lubrication

AGARD Conference Proceedings No.369
Advisory Group for Aerospace Research and Development, NATO
GEARS AND POWER TRANSMISSION SYSTEMS FOR HELICOPTERS AND TURBOPROPS
Published January 1985
396 pages

The Conference Proceedings contain 32 papers presented at the Propulsion and Energetics 64th Symposium on Gears and Power Transmission Systems for Helicopters and Turboprops, which was held 8–12 October 1984 in Lisbon, Portugal.

The Technical Evaluation Report is included at the beginning of the Proceedings. Questions and answers of

P.T.O.

AGARD-CP-369

Gears
Power transmission systems
Helicopters
Turboprops
Tooth failures
Transmission systems
Drive trains
Roller bearings
Tribology
Lubrication

AGARD Conference Proceedings No.369
Advisory Group for Aerospace Research and Development, NATO
GEARS AND POWER TRANSMISSION SYSTEMS FOR HELICOPTERS AND TURBOPROPS
Published January 1985
396 pages

The Conference Proceedings contain 32 papers presented at the Propulsion and Energetics 64th Symposium on Gears and Power Transmission Systems for Helicopters and Turboprops, which was held 8–12 October 1984 in Lisbon, Portugal.

The Technical Evaluation Report is included at the beginning of the Proceedings. Questions and answers of

P.T.O.

AGARD-CP-369

Gears
Power transmission systems
Helicopters
Turboprops
Tooth failures
Transmission systems
Drive trains
Roller bearings
Tribology
Lubrication

the discussions follow each paper. The Symposium was arranged in seven sessions: Review of Current Transmission Technology (4); Helicopter and Turboprop Transmission Technology Needs and Design (4); Component Design Technology and Manufacturing Considerations (8); Tribological Aspects of Transmission Components (6); Diagnostics, Measurements, and Noise (5); Problems and Failures in Gearing Applications (3); and Qualification Standards and Specifications (2).

The purpose of the Symposium was to exchange and disseminate information on research and development conducted on gears and transmission systems in order to introduce new technologies for improvements in weight, performance, and life-cycle costs. The achievements were listed in the Technical Evaluation Report. The Symposium could not cover the whole area; the gaps left will be discussed in an AGARDograph to be published in 1987.

ISBN 92-835-0372-4

the discussions follow each paper. The Symposium was arranged in seven sessions: Review of Current Transmission Technology (4); Helicopter and Turboprop Transmission Technology Needs and Design (4); Component Design Technology and Manufacturing Considerations (8); Tribological Aspects of Transmission Components (6); Diagnostics, Measurements, and Noise (5); Problems and Failures in Gearing Applications (3); and Qualification Standards and Specifications (2).

The purpose of the Symposium was to exchange and disseminate information on research and development conducted on gears and transmission systems in order to introduce new technologies for improvements in weight, performance, and life-cycle costs. The achievements were listed in the Technical Evaluation Report. The Symposium could not cover the whole area; the gaps left will be discussed in an AGARDograph to be published in 1987.

ISBN 92-835-0372-4

the discussions follow each paper. The Symposium was arranged in seven sessions: Review of Current Transmission Technology (4); Helicopter and Turboprop Transmission Technology Needs and Design (4); Component Design Technology and Manufacturing Considerations (8); Tribological Aspects of Transmission Components (6); Diagnostics, Measurements, and Noise (5); Problems and Failures in Gearing Applications (3); and Qualification Standards and Specifications (2).

The purpose of the Symposium was to exchange and disseminate information on research and development conducted on gears and transmission systems in order to introduce new technologies for improvements in weight, performance, and life-cycle costs. The achievements were listed in the Technical Evaluation Report. The Symposium could not cover the whole area; the gaps left will be discussed in an AGARDograph to be published in 1987.

ISBN 92-835-0372-4

the discussions follow each paper. The Symposium was arranged in seven sessions: Review of Current Transmission Technology (4); Helicopter and Turboprop Transmission Technology Needs and Design (4); Component Design Technology and Manufacturing Considerations (8); Tribological Aspects of Transmission Components (6); Diagnostics, Measurements, and Noise (5); Problems and Failures in Gearing Applications (3); and Qualification Standards and Specifications (2).

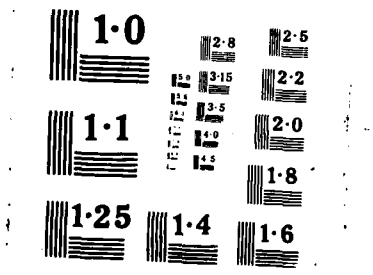
The purpose of the Symposium was to exchange and disseminate information on research and development conducted on gears and transmission systems in order to introduce new technologies for improvements in weight, performance, and life-cycle costs. The achievements were listed in the Technical Evaluation Report. The Symposium could not cover the whole area; the gaps left will be discussed in an AGARDograph to be published in 1987.

ISBN 92-835-0372-4

AD-A152 673 GEARS AND POWER TRANSMISSION SYSTEMS FOR HELICOPTERS AND TURBOPROPS: CONF..(U) ADVISORY GROUP FOR AEROSPACE RESEARCH AND DEVELOPMENT NEUILLY.. JAN 85 AGARD-CP-369 5/3

UNCLASSIFIED F/G 21/3 NL




1·0
1·1
1·25
1·4
1·6
1·8
2·0
2·2
2·5
2·8
3·15
3·5

DISCUSSION

D.G.Astridge, UK

I welcome the author's opening comment that the FAA is the designer's friend. Certainly I can confirm that an extremely helpful relationship exists between our company, FAA, and CAA. The method of working with CAA — the design authority being devolved to the manufacturer, through the Chief Designer, and the CAA maintaining a monitoring function to ascertain that the design meets their airworthiness requirements — seems a good formula. The author's illustration of proposal 363 appears to indicate that the FAA is getting involved in detail design activity, usurping the Chief Designer's task — this is a disturbing trend in that it requires that the FAA be totally aware of all detail design technology — this is normally generated by the helicopter and engine manufacturers.

Author's Reply

We would not consider a requirement for a health monitoring system for engines and gearboxes any different to the current lesser important temperature and pressure indicators requirement. The proposal I submitted for chip detectors, or equivalent, as will be published as an NPRM in the Federal Register soon, will be worked to include, "other means," such as vibration detectors needed for gearboxes using grease where chip detectors would not be appropriate. The FAA does not dictate design details and the method used will be at the discretion of the applicant. We should mandate safety features when the state-of-the-art has been developed and the the system is obviously cost-effective and provides for an increased level of safety. I know of no helicopters or engines, when the proposal was submitted 63 years ago, that are not already equipped with chip detectors — most with cockpit indicator lights.

Through the certification process, the FAA does get involved with and understands the detail design process of each manufacturers's type data approval. We therefore keep up to date with the state-of-the-art for all of industry — not just one applicant. This process has been very successful in the free world certified aircraft and the safety record continues to improve.

Comment: E.Covert, US

Comment for clarification of Mr Astridge's remark:
The CAA certification selects the designer and he is responsible for seeing to it that his design satisfies airworthiness. The FAA on the other hand allows the designer to design to standard but the design must be proved to FAA to meet standard by test or other means.

J.Worm, Ge

(1) Did you require to leave the chip detector light in the instrument panel, or is it possible to put the light outside of the cockpit on a panel right on the additional gearbox?

(2) Is there more than one manufacturer who makes burn-off chip detector systems (Tedeco)?

Author's Reply

It would be our intent to have one caution light on the pilot's enunciator panel with a provision to determine which sensor (location) is showing evidence of a chip in the oil system. It is now apparent that a record should be kept of those indications that were burned off or "zapped" by the capacitive discharge — perhaps by a counter of actuations of a burn-off button. This is because on lightly loaded engine bearings where skidding is likely, the bearing can wear out to failure with only fine particles being generated. The heavily loaded gearbox bearings and gears will generate larger particles under the spall mode of failure and these must be investigated by an appropriate maintenance programme.

To my knowledge, the first Tedeco zapper was certified by our office on the S-76 helicopter. Theother chip detector manufacturers have not developed the necessary burn-off feature to eliminate false alarms.

REPORT DOCUMENTATION PAGE			
1. Recipient's Reference	**2. Originator's Reference**	**3. Further Reference**	**4. Security Classification of Document**
	AGARD-CP-369	ISBN 92-835-0372-4	UNCLASSIFIED

5. Originator	Advisory Group for Aerospace Research and Development North Atlantic Treaty Organization 7 rue Ancelle, 92200 Neuilly sur Seine, France
6. Title	GEARS AND POWER TRANSMISSION SYSTEMS FOR HELICOPTERS AND TURBOPROPS
7. Presented at	the Propulsion and Energetics Panel 64th Symposium, held in Lisbon, Portugal, 8—12 October 1984.

8. Author(s)/Editor(s)	**9. Date**
Various	January 1985
10. Author's/Editor's Address	**11. Pages**
Various	396

12. Distribution Statement	This document is distributed in accordance with AGARD policies and regulations, which are outlined on the Outside Back Covers of all AGARD publications.

13. Keywords/Descriptors

Gears	Transmission systems
Power transmission systems	Drive trains
Helicopters	Roller bearings
Turboprops	Tribology
Tooth failures	Lubrication

14. Abstract

The Conference Proceedings contain 32 papers presented at the Propulsion and Energetics 64th Symposium on Gears and Power Transmission Systems for Helicopters and Turboprops, which was held 8—12 October 1984 in Lisbon, Portugal.

The Technical Evaluation Report is included at the beginning of the Proceedings. Questions and answers of the discussions follow each paper. The Symposium was arranged in seven sessions: Review of Current Transmission Technology (4); Helicopter and Turboprop Transmission Technology Needs and Design (4); Component Design Technology and Manufacturing Considerations (8); Tribological Aspects of Transmission Components (6); Diagnostics, Measurements, and Noise (5); Problems and Failures in Gearing Application (3); and Qualification Standards and Specifications (2).

The purpose of the Symposium was to exchange and disseminate information on research and development conducted on gears and transmission systems in order to introduce new technologies for improvements in weight, performance, and life-cycle costs. The achievements were listed in the Technical Evaluation Report. The Symposium could not cover the whole area; the gaps left will be discussed in an AGARDograph to be published in 1987.

END

DATE
FILMED

11-86

DTIC